Università degli Studi di Ferrara

DOTTORATO DI RICERCA IN "SCIENZE CHIMICHE"

CICLO XXVIII

COORDINATORE Prof. Carlo Alberto BIGNOZZI

Chemical characterization of atmospheric aerosol for air quality evaluation in Emilia Romagna region

Settore Scientifico Disciplinare CHIM/01

Dottorando

Marco Visentin

Tutore

Prof. Maria Chiara Pietrogrande

Cotutore

Prof. Vanes Poluzzi

Anni 2013/2015

Sezioni

Dottorati di ricerca

Il tuo indirizzo e-mail

vsnmrc@unife.it

Oggetto:

Dichiarazione di conformità della tesi di Dottorato

Io sottoscritto Dott. (Cognome e Nome)

Visentin Marco

Nato a:

Rovigo

Provincia:

Rovigo

Il giorno:

26/01/1987

Avendo frequentato il Dottorato di Ricerca in:

Scienze Chimiche

Ciclo di Dottorato

28

Titolo della tesi:

Chemical characterization of atmospheric aerosol for air quality evaluation in Emilia Romagna region

Titolo della tesi (traduzione):

Caratterizzazione chimica dell'aerosol atmosferico per la valutazione della qualità dell'aria in Emilia Romagna

Tutore: Prof. (Cognome e Nome)

Pietrogrande Maria Chiara

Settore Scientifico Disciplinare (S.S.D.)

CHIM/01

Parole chiave della tesi (max 10):

Wood burning, Atmospheric aerosol, Oxidative potential, Po valley, GC/MS

Consapevole, dichiara

CONSAPEVOLE: (1) del fatto che in caso di dichiarazioni mendaci, oltre alle sanzioni previste dal codice penale e dalle Leggi speciali per l'ipotesi di falsità in atti ed uso di atti falsi, decade fin dall'inizio e senza necessità di alcuna formalità dai benefici conseguenti al provvedimento emanato sulla base di tali dichiarazioni; (2) dell'obbligo per l'Università di provvedere al deposito di legge delle tesi di dottorato al fine di assicurarne la conservazione e la consultabilità da parte di terzi; (3) della procedura adottata dall'Università di Ferrara ove si richiede che la tesi sia consegnata dal dottorando in 2 copie, di cui una in formato cartaceo e una in formato pdf non modificabile su

idonei supporti (CD-ROM, DVD) secondo le istruzioni pubblicate sul sito : http://www.unife.it /studenti/dottorato alla voce ESAME FINALE – disposizioni e modulistica; (4) del fatto che l'Università, sulla base dei dati forniti, archivierà e renderà consultabile in rete il testo completo della tesi di dottorato di cui alla presente dichiarazione attraverso l'Archivio istituzionale ad accesso aperto "EPRINTS.unife.it" oltre che attraverso i Cataloghi delle Biblioteche Nazionali Centrali di Roma e Firenze. DICHIARO SOTTO LA MIA RESPONSABILITA': (1) che la copia della tesi depositata presso l'Università di Ferrara in formato cartaceo è del tutto identica a quella presentata in formato elettronico (CD-ROM, DVD), a quelle da inviare ai Commissari di esame finale e alla copia che produrrà in seduta d'esame finale. Di conseguenza va esclusa qualsiasi responsabilità dell'Ateneo stesso per quanto riguarda eventuali errori, imprecisioni o omissioni nei contenuti della tesi; (2) di prendere atto che la tesi in formato cartaceo è l'unica alla quale farà riferimento l'Università per rilasciare, a mia richiesta, la dichiarazione di conformità di eventuali copie. PER ACCETTAZIONE DI QUANTO SOPRA RIPORTATO

Dichiarazione per embargo

6 mesi

Richiesta motivata embargo

1. Tesi in corso di pubblicazione

Liberatoria consultazione dati Eprints

Consapevole del fatto che attraverso l'Archivio istituzionale ad accesso aperto "EPRINTS.unife.it" saranno comunque accessibili i metadati relativi alla tesi (titolo, autore, abstract, ecc.)

Firma del dottorando

Ferrara, li _16/02/2016_____ (data) Firma del Dottorando

_Visentin Marco_____

Firma del Tutore

Visto: Il Tutore Si approva Firma del Tutore _____

Publications

1. Pietrogrande M.C., Bacco D., Visentin M., Ferrari S., Poluzzi V., 2014. *Polar organic marker compounds in atmospheric aerosol in the Po Valley during the Supersito campaigns d Part 1: Low molecular weight carboxylic acids in cold seasons.* Atmospheric Environment 85, 164-175.

2. Pietrogrande M.C., Bacco D., Visentin M., Ferrari S., Casali P., 2014. *Polar organic marker compounds in atmospheric aerosol in the Po Valley during the Supersito campaigns d Part 2: Seasonal variations of sugars.* Atmospheric Environment 97, 215-225.

3. Visentin M., Pietrogrande M.C., 2014. *Determination of polar organic compounds in atmospheric aerosols by gas chromatography with ion trap tandem mass spectrometry.* Journal of Separation Science 37, 1561-1569.

4. Pietrogrande M.C., Bacco D., Ferrari S., Kaipainen J., Ricciardelli I., Riekkola M.L., Trentini A., Visentin M., 2015. *Characterization of atmospheric aerosols in the Po valley during the supersito campaigns d Part 3: Contribution of wood combustion to wintertime atmospheric aerosols in Emilia Romagna region (Northern Italy).* Atmospheric Environment 122, 291-305.

5. Pietrogrande M.C., Bacco D., Ferrari S., Ricciardelli I., Scotto F., Trentini A., Visentin M. *Characteristics and major sources of carbonaceous aerosols in PM2.5 in Emilia Romagna Region (Northern Italy) from four-year observations.* Science of the Total Environment, in press.

6. Gilardoni S., Massoli P., Costabile S., Gobbi G., Fuzzi S., Facchini M.C., Paglione M., Rinaldi M., Giulianelli L., Carbone C., Decesari S., Sandrini S., Pietrogrande M.C., Visentin M., Scotto F. *Direct observation of aqueous secondary organic aerosol from biomass burning emissions.* Proceedings of the National Academy of Sciences, submitted for publication.

Oral presentations

1. <u>M. Visentin</u>, M.C. Pietrogrande. *Determination of oxidative potential of particulate matter by spectrophotometric techniques*. XV Giornata della Chimica dell'Emilia Romagna, Modena, 18 dicembre 2015.

2. <u>N. Zanca</u>, S. Decesari, M. Paglione, M. Rinaldi, S. Gilardoni, M.C. Pietrogrande, M. Visentin. *Organic source apportionment by NMR and GC/MS techniques at two Po Valley sites in the cold season during the SUPERSITO campaign in 2013*. European Aerosol Conference 2015, Milano, 6-11 settembre 2015.

3. <u>M.C. Pietrogrande</u>, M. Visentin. *Spectrophotometric cell-free assays for measurement of the oxidative potential of atmospheric aerosol*. Giornata di Bioanalitica 2015, Firenze, 26 giugno 2015.

4. <u>M. Visentin</u>, M.C. Pietrogrande. *Sviluppo di un metodo GC-MS e GC-MSMS per la determinazione di marker organici polari nell'aerosol atmosferico*. Incontri di Scienza delle Separazioni 2014, Roma, 12 dicembre 2014.

5. <u>M.C. Pietrogrande</u>, D. Bacco, M. Visentin, S. Ferrari, V. Poluzzi. *Caratterizzazione degli acidi organici nell'aerosol atmosferico della Pianura Padana durante le stagioni fredde*. PM2014, Genova, 20-23 maggio 2014.

6. <u>M. Visentin</u>, M.C. Pietrogrande. *Determination of polar organic markers in atmospheric aerosols by gas chromatography-ion trap tandem mass spectrometry*. PM2014, Genova, 20-23 maggio 2014.

7. <u>S. Gilardoni</u>, M. Rinaldi, M. Paglione, N. Zanca, P. Massoli, M.C. Pietrogrande, M. Visentin, F. Costabile, V. Poluzzi, S.Ferrari, C. Facchini. *Contributo della combustione di biomassa all'aerosol carbonioso della Pianura Padana*. PM2014, Genova, 20-23 maggio 2014.

Poster presentations

1. <u>M.C. Pietrogrande</u>, D. Bacco, S. Ferrari, M. Visentin. *Impact of residential wood combustion on wintertime atmospheric aerosol in Emilia Romagna region (Northern Italy)*. European Aerosol Conference 2015, Milano, 6-11 settembre 2015.

2. <u>M.C. Pietrogrande</u>, D. Bacco, C. Colombi, M. Visentin, E. Cuccia, V. Gianelle, P. Lazzeri. *Intercomparison of chromatographic methods used for quantification of levoglucosan in ambient aerosol filters*. European Aerosol Conference 2015, Milano, 6-11 settembre 2015.

3. <u>M.C. Pietrogrande</u>, D. Bacco, S. Ferrari, I. Ricciardelli, A. Trentini, M. Visentin. *Sources and processes affecting carbonaceous aerosol in urban and rural areas in Emilia-Romagna region (Northern Italy)*. European Aerosol Conference 2015, Milano, 6-11 settembre 2015.

4. S. Ferrari, F. Scotto, D. Bacco, I. Ricciardelli, A. Trentini, M.C. Pietrogrande, M. Visentin, P. Ugolini, T. D'Alessandro, V. Poluzzi. *Organic characterization of PM2.5 in the Emilia-Romagna region (I).* European Aerosol Conference 2015, Milano, 6-11 settembre 2015.

5. M. Visentin, D. Bacco, M. Forini, M.C. Pietrogrande. *Contribution of wood combustion to wintertime atmospheric aerosol in Emilia Romagna region.* XIV Giornata della Chimica dell'Emilia Romagna, Parma, 18 dicembre 2014.

6. M. Visentin, M.C. Pietrogrande. *Determination of alkyl phenols in atmospheric aerosol by gas chromatography-ion trap mass spectrometry.* European Aerosol Conference 2013, Praga, 1-6 settembre 2013.

7. M.C. Pietrogrande, M. Visentin, D. Bacco, S. Ferrari, V. Poluzzi. *Chemical characterization of polar organic markers in $PM_{2.5}$ during intensive campaigns of Supersito Project in Po Valley (Italy).* European Aerosol Conference 2013, Praga, 1-6 settembre 2013.

8. M.C. Pietrogrande, D. Bacco, M. Nassi, M. Visentin. *GC-MS method for simultaneous analysis of dicarboxylic acids and sugars in atmospheric aerosol: response surface methodology for optimizing solvent extraction.* XXIII Congresso Nazionale di Chimica Analitica, Isola d'Elba, 16-20 settembre 2012.

INDEX

PREFACE

The main topic of the present work is the chemical characterization of PM composition in order to monitoring air quality.

Among the different pollutants that lead to a worsening of air quality, particulate matter (PM) is the most debated topic because it can influence the global climate and, above all, it has been linked to adverse health effect. Thus, in the last years, a growing number of studies have been carried out on this environmental matrix.

The analysis of chemical composition of PM is a challenge for analytical chemistry due to the extreme complexity of aerosol matrix that contains thousands of chemical compounds. Despite this difficulty, the chemical characterization is mainly focused on some specific molecules called markers. They can give important information regarding sources and processes PM undergoes and such molecules can provide information that are important for institutions to decide strategies in order to reduce atmospheric pollution.

The first part of the thesis is devoted to the development of analytical procedures for polar organic compounds determination in PM. The central part is a description of the results obtained in eight $PM_{2.5}$ sampling campaigns in the framework of the Supersito project, set up by ARPA Emilia Romagna in collaboration with national and international institutions. The campaigns were performed in different seasons in the period 2011-2014 in two sites in Bologna province. The last part is devoted to the study of PM toxicity in terms of oxidative potential and some preliminary results are given.

Chapter 1 provides some basic information about PM, its composition and some toxicological effects.

Chapter 2 describes the analytical procedure used and some improvements made in terms of sensitivity and analytical performance. Moreover a comparison among different procedures was done.

Chapter 3 presents the results obtained during eight sampling campaigns while Chapter 4 is a more detailed study on the contribution of wood combustion, the main PM emission source.

Finally, in Chapter 5 some preliminary results on PM toxicity assays are presented.

This thesis is an overview on PM chemical analyses and information that can be deduced, in particular from the point of view of atmospheric pollutants sources.

It should be underline that, even if very useful information are provided from these kind of studies, a completely knowledge of atmospheric particulate matter is still far, thus is important to push research forward in this direction.

1. INTRODUCTION

1.1 Overview on PM

Particulate matter (PM) or atmospheric aerosol is one of the most studied and controlled pollutant in the last years, due to the increasing awareness of public opinion and institution on environmental problems.

PM is a combination of solid and liquid particles dispersed in the atmosphere which can have a broad range of diameters, from few nanometres to hundreds of micrometres.

Due to their irregular shapes, particles size is described using the equivalent aerodynamic diameter: it is define as the diameter of a sphere of unit density that has aerodynamic behaviour identical to that of the particle in question.

Using this classification, atmospheric aerosol can be divided in three main classes: ultrafine particles (D_p < 100nm), fine particles (0.1 < D_p < 2.5µm) and coarse particles (D_p > 2.5µm). In this work $PM_{2.5}$ was considered, thus particles with an aerodynamic diameter lower than 2.5 µm

PM is a very complex matrix composed of a large number of different species both organic and inorganic.

The sources of airborne particulate matter can be divided into two broad categories: primary and secondary. Primary sources include combustion sources (heavy and light duty vehicles, wood smoke, and industries), soil resuspension and biogenic activity. The particles emitted from these primary sources may undergo photochemical processing in the presence of various atmospheric oxidants (such as ozone and radical OH and NO_3) to yield secondary particles. The physical and chemical characteristics of these secondarily formed particles are distinctly different compared to their primary precursors [Kawamura et al. 1996, Ho et al. 2006, Rompp et al. 2006, Yang et al. 2008a,b].

Composition, origin and abatement of atmospheric aerosol are topics of a large number of studies in order to extend the knowledge about this environmental matrix and to limit the problems linked to it.

High concentrations of PM can cause both environmental and health problems.

Regarding environment, PM is able to decrease visibility and to change the energetic budget of earth by reflecting or absorbing solar radiation. Aerosol could scatter solar radiation back to space and exert a negative (cooling) radiative forcing effect on climate

while black carbon aerosol exert a positive (warming) radiative forcing effect on climate [Chung et al. 2002, Monks et al. 2012] .

Moreover, PM also act indirectly by modifying the radiative properties of clouds. Particles act as cloud condensation nuclei, increasing droplet number concentrations and decreasing the average droplet size in clouds [Haywood et al. 2000, Shilling et al. 2007]. This process affects the ability of the clouds to scatter radiation. The precipitation efficiency from the clouds is also reduced, so that their lifetime is increased [Facchini et al. 1999]. Overall, the aerosol indirect effect is cooling; its magnitude is highly uncertain.

Both epidemiological and clinical researches have demonstrated strong links between atmospheric aerosol and adverse health effects, including premature deaths and respiratory and cardiovascular diseases [Dockery et al. 1994, Schwartz 1994, Schwarze et al. 2006, Perrone et al. 2013].

In fact, PM can easily penetrate in the respiratory system and ultrafine particles can reach alveolus and, from here, the circulatory system.

Epidemiological study results highlight that both physical (surface area, dimension) and chemical (absorbed substances) characteristics of inhaled particles are involved in toxic and carcinogenic effects concerning especially the respiratory tract [Harrison et al. 2000].

The mechanisms through which PM elicits toxic effects are not clearly understood but some transition metals, polycyclic aromatic hydrocarbons (PAHs) and oxoPAHs seem to be the main responsible of health problems [Kelly 2003, Janssen et al. 2014].

In light of these results, legal limit for PM_{10}, $PM_{2.5}$ and some chemical species in PM_{10} fraction have been set by Directive 2008/50/CE (Table 1.1), the most recent directive regarding air pollution.

To notice that these limits are higher than the guideline values suggested by World Health Organization (WHO) to reduce cardiopulmonary and lung cancer mortality (20 and 10 $\mu g/m^3$ annual average for PM_{10} and $PM_{2.5}$ respectively and 50 and 25 $\mu g/m^3$ daily average for PM_{10} and $PM_{2.5}$ respectively).

PM$_{10}$	Averaging period	Note	From	Concentration
Limit value	One day	not to be exceeded more than 35 times a calendar year	2010	50 µg/m^3
Limit value	Calendar year		2010	40 µg/m^3
PM$_{2.5}$	**Averaging period**	**Note**	**From**	**Concentration**
Limit value	Calendar year		2015	25 µg/m^3
PAH and metals	**Averaging period**	**Note**	**From**	**Concentration**
Lead	Calendar year	in PM$_{10}$ fraction	2010	0.5 ng/m^3
Arsenic	Calendar year	in PM$_{10}$ fraction	2013	6 ng/m^3
Cadmium	Calendar year	in PM$_{10}$ fraction	2013	5 ng/m^3
Nickel	Calendar year	in PM$_{10}$ fraction	2013	20 ng/m^3
Benzo (a) pyrene	Calendar year	in PM$_{10}$ fraction	2013	1 ng/m^3

Table 1.1. Directive 2008/50/CE legal limit for some pollutants.

1.2 PM chemical composition

Chemical composition of PM is influenced by several factors, in particular it depends on the emission source and the residence time in the atmosphere.

The natural sources that have the greatest impact on PM include suspended terrestrial dust, sea salt spray, volcanoes, forest fires and natural gaseous emissions.

The major sources of anthropogenic, i.e., man-made, particles include transportation, stationary combustion, residential heating, biomass burning, and industrial and traffic-related fugitive emissions (street dust). Urban PM from man-made sources is a complex mixture, since the majority of sources emit both primary particles and precursor gases for the formation of secondary particles.
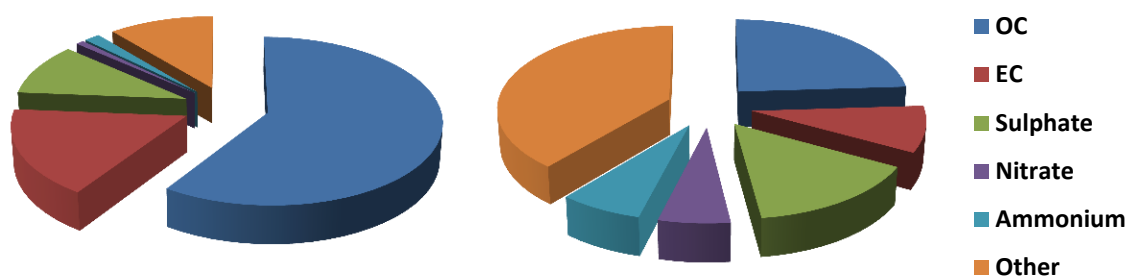
Figure 1.1. PM composition in remote and urban site [Li et al. 2012].

Air samples of particulate matter from urban areas from around the world typically show the same major components, although in considerably different proportions according to the sampling location [Vallius 2005, Alves 2008]. These major components are typically:

- Sulphate - derived predominantly from sulphur dioxide oxidation in the atmosphere;
- Nitrate - formed mainly from oxidation of nitrogen oxides (NO and NO_2) to nitrate; NO_2 oxidizes much more rapidly than SO_2;
- Ammonium - atmospheric ammonia forms ammonium salts in neutralization reactions with sulphuric and nitric acids;
- Chloride - main sources are sea spray and de-icing salt during winter; also from ammonia neutralization of HCl gas from incineration and power stations;
- Elemental carbon (EC) is a highly polymerized dark fraction that is generated by incomplete combustion of organic material from traffic, residential heating, industrial activities and energy production using heavy oil, coal or biofuels;
- Organic carbon (OC) - can have both anthropogenic and biogenic origin and comprises thousands of different chemical species emitted as primary pollutants or produced by reactions in the atmosphere. In urban aerosol it usually account from 20 to 50% of PM mass;

- Crustal materials - soil dusts and wind-blown crustal material; are quite diverse in composition reflecting local geology and surface conditions; their concentration is dependent on climate as the processes which suspend them into the atmosphere tend to be favoured by dry surfaces and high winds; these particles reside mainly in the coarse particle fraction;
- Biological materials - bacteria, spores, pollens, debris and plant fragments; generally coarse in size, considered as part of the organic carbon component in most studies rather than as a separate biological component.

The greater fraction of airborne organic particulate matter is undoubtedly presents in the respirable particle size range [QUARG 1993].

There is a general consensus that the organic composition of atmospheric aerosol should be understood to correctly describe the chemical mechanisms and models concerning the multiphase atmospheric system and to evaluate its environmental and health effects. Despite the progress made in elucidating the source types, their relative importance and contribution to certain particulate components, the organic composition of aerosols and particle formation processes are still scarcely known. This is probably due to analytical difficulties, complexity of phenomena and huge number of compounds that are present [Zhang et al. 2005, Alves 2008].

Therefore, the study of polar organic fraction of PM is usually devoted to the investigation of specific molecular markers. They are molecules or molecule classes emitted only from certain sources so, the determination of these species provides indications on the origin and processes that PM undergoes in the atmosphere.

1.3 The Supersito project

Most of the work described in this thesis has been done in the framework of the Supersito project, a research project supported and financed by Emilia Romagna region and ARPA (Regional Agency for Prevention and Environment) during the 2011-2015 period. The aim of the project is a detailed study of some chemicals, physical and toxicological parameters of atmosphere. The project rose from the necessity to improve knowledge about environmental and health aspects of fine and ultrafine particulate, in primary and secondary components, in atmosphere.

Po Valley, the most industrialized and populated region of Italy, is recognized as one of the worst air quality zones in whole Europe (Figure 1.2), where high air pollution may cause serious risks for human health. There is evidence that low wind speed and stable

atmospheric stratification are meteorological factors leading to air pollution episodes [Larsen et al. 2012, Perrone et al. 2013]. Under this complicated meteorological conditions in Po Valley, it is worthy of interest to improve knowledge on chemical characteristics and sources of atmosphere particulate material and its effects on human health, in order to decide effective abatement strategies.

Several research institutes have collaborated to the project in addition to the University of Ferrara: CNR-ISAC, University of Bologna (Department of Pathology and Department of Statistical Science), University of Ferrara (Department of Chemistry), University of Helsinki (Department of Physic), University of Eastern Finland (Department of Applied Physics), Finnish Meteorological Institute and Department of Epidemiology Lazio Regional Health Service.
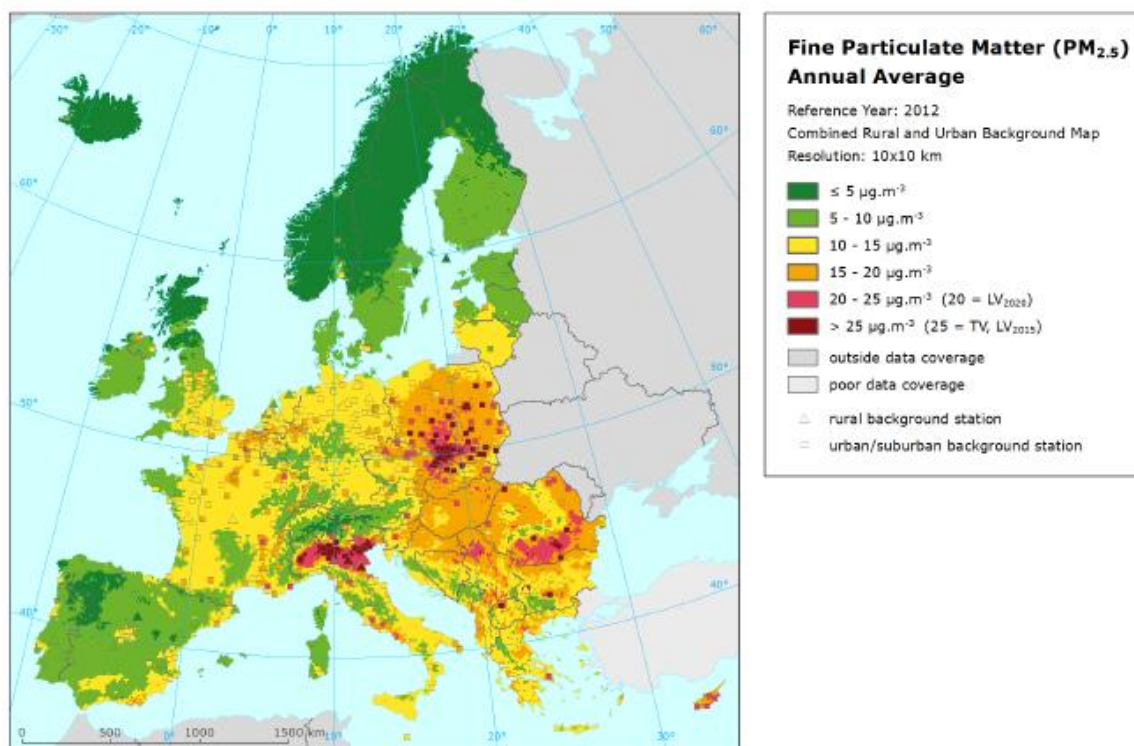
Figure 1.2. Annual average concentration of $PM_{2.5}$ over Europe [Horálek et al. 2015].

The project, structured in seven work packages, is organized in two measures programs: the routine one that have a time resolution principally daily and the intensive one with high time resolution and an increase of chemical speciation respect to the routine one.

The project main value is the close integration among environmental data and health and epidemiological information. Many epidemiological studies have already demonstrated the correlation between air particulate and higher morbidity and mortality. Therefore it is necessary to improve the knowledge about atmospheric aerosol to achieve a better governance of themes related to atmospheric and health protection.

The seven work packages are:

LP1: sampling, chemical analysis and size distribution of PM;

LP2: physical measurement and air quality models;

LP3: atmospheric intensive measurement campaigns;

LP4: predictive toxicology;

LP5: indoor intensive measurement campaigns;

LP6: long and short term epidemiological analysis;

LP7: environmental data analysis.

This work is mainly comprised in LP3. The strategy of LP3 is to concentrate complex measurements which need long analysis time in intensive observation periods (IOPs) during different intervals along the year in order to obtain the most comprehensive information under certain environmental conditions.

The sampling sites chosen were two: the first in Bologna (MS), the main city of the region, and the second in San Pietro Capofiume (SPC), situated in a rural zone 30 km north-east of urban site. The different characteristics of the sites could give information about regional aerosol background and transport phenomena PM undergoes.

Among the different activities in LP3, this thesis is focused on the quantification of polar organic micropollutants in $PM_{2.5}$, such as sugars, low molecular weight (LMW) carboxylic acids and phenols, typical markers emitted from combustion sources.

The obtained data have been integrated with data from other research groups: in particular PAHs, long chain alkanes, OC and EC were considered.

Moreover, meteorological parameters have been related to chemical data to improve knowledge about emission sources and fate of organic components in atmospheric aerosol in a polluted area as the Po plain.

1.4 Molecular markers

Although an accurate apportionment of the carbonaceous aerosol would require detailed knowledge of characteristic source emission profiles and atmospheric processes, molecular tracers can provide qualitative and quantitative estimate of the different contributions to carbonaceous PM. In this work low molecular weight carboxylic acids were investigated to differentiate between primary emissions and secondary organic aerosol, sugars to discriminate between primary emissions from biomass burning and

from the ecosystem and polycyclic aromatic hydrocarbons (PAHs) to differentiate among different combustion emissions.

Furthermore, to have a better view of atmospheric pollution in the region, phenols and n-alkanes were also considered. These two classes of compounds can provide helpful information about biomass burning and traffic or biogenic related emissions.

1.4.1 Carboxylic acids

Carboxylic acids are one of the most abundant classes in organic fraction of atmospheric aerosol.

Various studies have been carried out on dicarboxylic acids, oxo-hydroxycarboxylic acids and low molecular weight aromatic acids. Usually, the concentration decreases increasing carbon chain length and ramifications of the chain. Unsaturated acids result less abundant than the corresponding saturated ones: the only exception is maleic acid. Aromatic acids have usually very low concentrations [Kawamura et al. 1996].

Dicarboxylic acids are an important part of water soluble organic carbon (WSOC) in particulate matter [Rogge at al. 1993, Jacobson et al. 2000, Kawamura et al. 2005].

Most part of these molecules is produced from photochemical reactions in the atmosphere and therefore they are considered as marker for secondary organic aerosol (SOA) [Lough et al. 2006, Alves 2008].

The precursors could be a wide range of molecules both anthropogenic and biogenic (Figure 1.3).

Smog chamber experiments have shown that the main precursors are cyclic olefins, alkanes, fatty acids and high molecular weight dicarboxylic acids. Biogenic precursors could derive from plant wax [Oliveira et al. 2007, Bi et al. 2008, Huang et al. 2012,].

It is possible they can be originated from aqueous chemistry in fog and clouds [Blando et al. 2000].

Malonic acid, for example, is produced by the oxidation of aromatic hydrocarbons but also from photo oxidation of succinic acid.

Aromatic acids descend mainly from aromatic hydrocarbons while pinonic acid is produced from the oxidation of α-pinene, a terpene emitted from plants. It could be used as a marker for secondary processes of biogenic precursors [Glasius et al. 2000, Oliveira et al. 2007, Cheng et al. 2011].
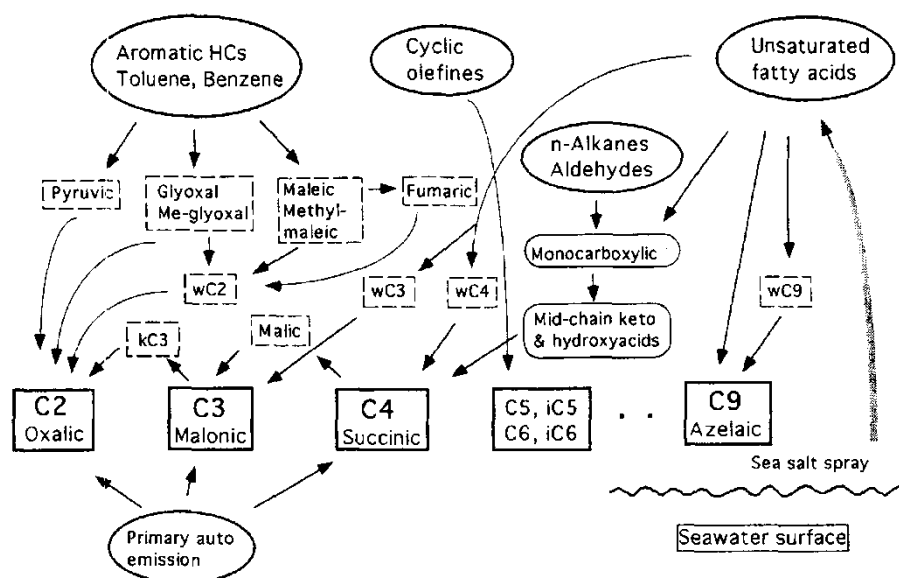
Figure 1.3. Possible photochemical production of some low molecular weight carboxylic acids [Kawamura et al. 1996].

The use of dicarboxylic acids as SOA indicators is made difficult by the presence of some primary sources, both anthropogenic and biogenic.

Such polar species are emitted directly into the atmosphere by a multiplicity of sources including power plants, vehicular circulation, biomass burning and meat cooking operations [Ray et al. 2005, Rogge et al. 2006, Hsieh et al. 2008, Giannoni et al. 2012, Wang et al. 2011].

The biogenic activity of plants and microorganisms could release these species in the atmosphere or in the soil, even if some studies indicate that the amount of carboxylic acids from biological activities is very low in comparison to anthropogenic emissions [Kawamura et al. 1987].

Great attention is devoted to these molecules due to their possible role in climate change. Their low vapour pressure and high solubility in water affect the physico-chemical characteristics of PM. They are considered the main responsible of cloud condensation nuclei phenomenon: the conversion of hydrophobic molecules such as hydrocarbons in hydrophilic ones, increases the possibility of water vapour condensation with the consequence formation of water droplets, the first step in cloud formation [Blando et al. 2000, Rompp et al. 2006, Shilling et al. 2007].

1.4.2 Sugars

Another important component of organic aerosol is the class of sugars. It can be divided in three main groups: primary sugars (mono and disaccharides), polyols or sugar alcohols and anhydrosugars [Simoneit et al. 2004, Medeiros et al. 2006].

Anhydrosugars, mainly levoglucosan with minor quantities of its isomers mannosan and galactosan, are primarily produced during biomass combustion as the pyrolytic decomposition products of cellulose and hemicellulose [Simoneit et al. 2002].

A cellulose molecule is a long-chain, linear polymer made up of 7000–12,000 D-glucose monomers and individual cellulose molecules organize to form bundles (elementary fibrils), which are associated into larger parallel fibre structures [Crawford 1981].

In contrast, hemicelluloses are a mixture of polysaccharides derived mainly from glucose, mannose galactose, xylose, and arabinose. Hemicellulose molecules consist of only about 100–200 sugar monomers, are less structured than cellulose and their sugar composition varies widely among different tree species [Simoneit et al. 1999].

No traces of anhydrosugars have been found during the combustion of fossil fuels (except some types low rank brown coal) [Fabbri et al. 2009] or food cooking [Simoneit et al. 2007, Alves et al. 2008].

Therefore, they are key tracers for biomass burning to estimate the contribution of both open and residential biomass combustion to fine particle.

To notice that yield of anhydrosugars during combustion processes is influenced by combustion conditions and moisture amount in the fuel.

The moisture content of wood varies considerably and the optimal content, in terms of minimizing particulate emissions during wood combustion, is between 20 and 30% [Simoneit et al. 2000, 2002].

If the moisture content is too high, an appreciable amount of energy is necessary to vaporize the water, reducing the heating value of the wood as well as decreasing combustion efficiency, which in turn increases smoke formation. This is a phenomenon often observed with campfires and wildfires. On the other hand, wood with low moisture content burns faster eventually causing oxygen-limited conditions that lead to incomplete combustion with increased smoke particle formation [Core et al. 1982].

Also combustion temperature is an important parameter that influence anhydrosugars yield. In fact, the emission levels of levoglucosan and its isomers increase with increasing combustion temperature, reaching maxima around 250-300°C and diminishing at higher temperatures [Kuo et al. 2011].

An important characteristic of these anhydrosugars is the strong stability in the atmosphere [Ma et al. 2009] even if some studies highlight that under certain conditions they can undergo oxidation [Hoffmann et al. 2010, Zhao et al. 2014].

Some diagnostic ratios of anhydrosugars have been proposed as useful tools for identifying combustion sources. For example, differences in the levoglucosan/mannosan (L/M) and levoglucosan/mannosan+galactosan ratios in smokes from softwoods and hardwoods/grasses can help discriminate between inputs from these combustion sources to the atmosphere [Ward et al. 2006, Schmidl et al. 2008, Louchouarn et al. 2009, Alves et al. 2010] .

However, the broad ranges of the values of L/M and L/(M + G) ratios from different sources [Engling et al. 2009; Fabbri et al. 2009; Alves et al. 2010] show some overlaps which make the source apportionment difficult.

Polyols and primary sugars are common in primary biological particles, including microorganisms, pollen, vegetative debris, bacteria and viruses, since sugars represent the major form of photosynthetically assimilated carbon in the biosphere [Simoneit et al. 2004, Medeiros et al. 2006].

Glucose, sucrose and mycose (trehalose), as the most common saccharides present in vascular plants and microorganisms, have been proposed as source-specific tracers for soil biota released into the atmosphere by farmland soil suspension and natural soil erosion [Rogge et al. 2007, Jia et al. 2010, Tominaga et al. 2011, Fu et al. 2012, Tsai et al. 2013].

Sugar alcohols, including mannitol and eritrhytol, have been used as biomarkers to estimate atmospheric fungal spore abundance [Medeiros et al. 2006, Jia et al. 2010].

Small amount of polyols and mono and disaccharides could also derive from primary emissions of biomass burning [Simoneit et al. 2004].

Size partitioning of sugars showed that the emissions from primary bio aerosols and soil resuspension are generally most associated with coarse fraction, whereas those from biomass burning present higher concentrations in the fine mode range [Medeiros et al. 2006, Yttri et al. 2007, Bauer et al. 2008, Ma et al. 2009, Jia et al. 2011, Wang et al. 2011, Tominaga et al. 2011].

Although the comprehensive apportionment of biogenic emissions would require investigation of coarse and fine PM samples [Bauer et al. 2008, Tominaga et al. 2011], the concentration and seasonal variation of major saccharides in $PM_{2.5}$ samples may give helpful information to track aerosols of biologically derived origin [Jia et al. 2010,2011].

The main purpose of this study is to investigate the abundances and temporal variations of primary sugars, sugar alcohols and anhydrosugars in atmospheric $PM_{2.5}$, in order to isolate the sources of biological and anthropogenic origins, as a part of the general study for characterize primary emissions and secondary processes that contribute to the ambient $PM_{2.5}$ levels in Emilia Romagna region.

1.4.3 Phenols

Lignin, an essential and major biopolymer of woody tissue together with cellulose, is derived primarily from three aromatic alcohols, namely p-coumaryl, coniferyl and sinapyl alcohol.

Burning of lignin in wood yields the breakdown products of the biopolymers as phenols, aldehydes, ketones, acids and alcohols, generally with the retention of the original substituents on the phenyl ring [Simoneit 2002].

The proportions of these bio monomers vary considerably among the major plant classes.

Vascular plants combustion yields specific lignin phenol signatures that are representative of different taxonomic and tissue sources. For example, angiosperm (hardwood) tissues are characterized by substantial amounts of syringyl structural units (S), while these units are nearly absent in lignin of gymnosperms (softwood). Similarly, cinnamyl structural units (C) are abundant in most herbaceous and soft tissues (i.e. leaves and needles) but almost absent from woods. Vanillyl structural units (V), however, are found in both angiosperms and gymnosperms [Simoneit 2002, Kuo et al. 2011].

Most of these compounds have been identified in soot and smoke condensate from residential wood stoves and were proposed as tracers for this fugitive source [Mazzoleni et al. 2007, Schmidl et al. 2008, Kuo et al. 2011, Caseiro et al. 2012].

Thus, in environmental samples, syringyls to vanillyls (S/V) and cinnamyls to vanillyls (C/V) ratios have been used extensively to identify specific compositional signatures of vascular plant tissues [Kuo et al. 2011].

However, the above ratios are also susceptible to the effects of combustion conditions as indicate for anhydrosugars.

1.4.4 PAHs

The polycyclic aromatic hydrocarbons (PAHs) represent an organic class more investigated than any other, because they are believed to be carcinogenic and/or mutagenic [Crimmins et al. 2006, Alves 2008].

The European Community and the U.S. Environmental Protection Agency have listed them as priority pollutants. Benzo[a]pyrene (BaP), is notable for being the first carcinogen chemical to be discovered.

Fossil fuels combustion is the main anthropogenic activity responsible for the introduction of PAHs into the urban atmospheres. Stationary sources such as domestic heating, various industrial processes, incineration and energetic production systems are also responsible for the imprint of polyaromatics [Liu et al. 2006, Cincinelli et al. 2007]. The natural sources responsible for the release of PAHs comprise forest fires, microbiological processing of detritus (e.g. fossil fuel) and mechanisms of biosynthesis carried out by algae, plants and bacteria [Cincinelli et al. 2007, Wang et al. 2007].

Because of their low vapour pressure, some PAHs are present at ambient temperature in air, both as gas and associated with particles. The lightest PAHs, such as phenanthrene, are found almost exclusively in gas phase whereas the heaviest PAHs, such as BaP, are almost totally adsorbed onto particles [Ravindra et al. 2008].

PAHs are always emitted as a mixture, and the relative molecular concentration ratios are considered to be characteristic of a given emission source. Most diagnostic ratios involve pairs of PAHs with the same molar mass and similar physicochemical properties so they ought to undergo similar environmental fate processes [Mackay et al. 2006, Tobiszewski et al. 2010].

A particular class of PAHs is nitro-PAHs which are recognize to be more dangerous for human health in comparison to unsubstituted PAHs, even if the atmospheric concentration of this class is usually 1-2 orders of magnitude less than unsubstituted PAHs [Bamford et al. 2003].

Nitro-PAHs are emitted from the same sources of PAHs but could also be produced from photochemical reactions in the atmosphere [Bamford et al. 2003, Perrini et al. 2005].

1.4.5 Alkanes

Aliphatic hydrocarbons, particularly normal alkanes, represent ubiquitous organics which are released into the atmosphere by many sources, rendering difficult the association between the levels of different compounds and their origin.

Usually, the homologous compound distributions of n-alkanes in atmospheric aerosols range from C_{12} to C_{40} [Alves 2008].

Anthropogenic sources of n-alkanes typically include the combustion of fossil fuels, wood and agricultural debris or leaves. Biogenic sources include particles shed from the epicuticular waxes of vascular plants and from direct suspension of pollen, microorganisms (e.g., bacteria, fungi and fungal spores), and insects [Yassaa et al. 2001]

The highest molecular weights with an odd carbon number represent typical alkanes from natural plant waxes [Xie et al. 2009].

CPI (carbon preference index) is defined as the ratio of odd carbon numbered n-alkanes to the amount of even carbon numbered ones [Kotianová et al. 2008].

This is a useful parameter to determine the biogenic or anthropogenic origin of alkanes in PM. In fact, combustion sources emitted random odd and even alkanes with a CPI ≈ 1, while plant emissions have CPI >1 [Pietrogrande et al. 2010a].

1.5 Oxidative potential to evaluate PM toxicity

There is extensive epidemiological evidence associating ambient particulate pollution with adverse health effects in humans [Schwartz et al. 2002]. Nevertheless, fundamental uncertainty and disagreement persist regarding what physical and chemical properties of particles can impact health risks.

From a toxicological perspective, much of the mass of PM consists of biologically inert material: sodium chloride, crustal dust, ammonium, sulphates, nitrates, etc., whilst, the content of relatively low masses of transition metals and organic species are likely to contribute significantly to the health effects [Mudway et al. 2009].

The mechanisms of PM related health effects are still incompletely understood, but a hypothesis under investigation is that many of the adverse health effects may derive from oxidative stress.

Oxidative stress results when the generation of reactive oxygen species (ROS), or free radicals, exceeds the available antioxidant defences [Janssen et al. 2014]. It is a disturbance in the prooxidant-antioxidant balance in favour of the former, leading to potential damage.

Free radicals are potentially very dangerous since they can react indiscriminately with neighbouring molecules. This process of "electron stealing" leads to oxidation, and

often inactivation of target molecules. If these reactions are numerous they can cause extensive cellular damage [Kelly 2003].

The general consensus does indicate that the mechanism of air pollution-induced health effects involves an inflammation related cascade and oxidation stress both in lung, vascular, and heart tissue [Ghio et al. 2001, Schafer et al. 2001, Hirano et al. 2003, Wold et al. 2006]. Inflammation is initially a protective mechanism which removes the injurious stimuli and produces reactive oxygen species (ROS) able to induce cell killing. In the early phase of inflammation, oxidant stress does not directly cause cell damage and can induce the transcription of stress defence genes including antioxidant genes.

This preconditioning effect of ROS enhances the resistance against future inflammatory oxidant stress and promotes the initiation of tissue repair processes. The additional release of cell contents amplifies the inflammatory process and consequently can induce tissue injury [Jaeschke 2011].

In the oxidative stress paradigm, inhaled particles generate oxidative stress through two major pathways:

- by direct introduction of ROS or other radicals in the respiratory system;
- by the introduction of oxidizing species into the lung, including redox catalysts absorbed onto the particle surface.

Oxidative potential (OP) is defined as a measure of the capacity of PM to oxidise target molecules. It has been proposed as a metric that is better related to biological responses to PM exposures and thus could be more informative than mass alone [Borm et al. 2007].

To provide the rapid read out of the oxidative potential of PM, acellular assays are employed due to their low price and practicality, when compared to cellular assays.

The only analytical method that provides direct quantification of radical species in the samples is electron spin resonance (ESR). However, ESR is an expensive and complicated instrument which has low sensitivity due to low steady state concentration and short radical's lifetimes [Hedayat et al. 2014].

Other assays examining the capacity of particle suspensions to oxidise antioxidants from models of human respiratory tract lining fluids (RTLFs). The RTLFs, represent the first physical interface encountered by inhaled materials and has been shown to contain high concentrations of the antioxidants ascorbate (vitamin C), urate and reduced glutathione (GSH) [Zielinski et al. 1999, Ayres et al. 2008]. A simplified RTLFs model uses only ascorbate [Mudway et al. 2011, Janssen et al. 2014, Hedayat et al. 2014].

Another common method for the determination of OP of particulate matter measures the oxidation of dithiothreitol (DTT), a strong reducing agent [Cho et al. 2005, Charrier et al. 2012, Yang et al. 2014, Janssen et al. 2014].

Some studies on oxidative potential of atmospheric aerosol make use of fluorescent (2',7'- dichlorofluorescin diacetate, profluorescent nitroxide probes, dihydrorhodamine) or chemiluminescent (acridinium ester) reagents which emit after chemical reactions with ROS [Hedayat et al. 2014, Yang et al. 2014].

2. ANALYSIS OF POLAR ORGANIC FRACTION OF PM$_{2.5}$

A large part of the work has been devoted to the development of the proper procedure suitable for chemical analysis of polar organic fraction of PM$_{2.5}$.

A variety of methods have been used to typify the organic composition of atmospheric aerosols, but separative techniques are the most utilized. In particular, gas chromatography coupled with mass spectrometry has been extensively used because it provides high separation resolution, identification capability, and sensitivity compatible with PM monitoring [Alves 2008].

Starting from literature methods, new procedures have been developed in order to achieve the best possible sensitivity and to minimize the procedure time for samples preparation.

2.1 Sampling

The samples were collected in two sites with different characteristics in Emilia Romagna region.

The urban background site MS is located in the city of Bologna which is the most populous city in the region (~400,000 inhabitants) characterized by significant agricultural and industrial activities and the presence of main arterial roads. The field station of San Pietro Capofiume (SPC) is a rural background site located about 30 km northeast from the city of Bologna and it is not directly influenced by human activities (Figure 2.1).

Eight sampling intensive campaigns were performed from 2011 to 2014 to represent different meteorological scenarios throughout the year:

- from 18th November to 6th December 2011 (W11);
- from 14th June to 11th July 2012 (Su12);
- from 23rd October to 10th November 2012 (A12);
- from 30th January to 17th February 2013 (W13);
- from 7th May to 27 May 2013 (Sp13);
- from 27th September to 25th October 2013 (A13);
- from 28th January to 27th February 2014 (W14);

- from 13th May to 11th June 2014 (Su14).

Figure 2.1. Sampling sites location.

PM$_{2.5}$ samples were collected on quartz fibre filters (Whatman, 47 mm diameter) by low volume automatic outdoor samplers (Skypost PM, TCRTECORA Instruments, Corsico, Milan, Italy) at an airflow rate of 38.3 L min^{-1} for 24 h (~55 m^3 day^{-1}). In Spring 2013, Autumn 2013 and Summer 2014, higher air volumes (~283 m^3 day^{-1}) were sampled on quartz fibre filters (Munktell, 100 mm diameter) using an Hi-Vol sampler (Echo Hi-Vol, TECORA Instruments, Corsico, Milan, Italy) operating at a flow rate of 11.7 m^3 h^{-1} for 24 h. This choice was motivated by the need of assuring PM amounts compatible with the analytical sensitivity, since the target analytes are expected at low concentration levels in the investigated region [Bigi et al. 2011, Pietrogrande et al. 2013a, Perrone et al. 2013].

After sampling, the procedure outlined in European Standard EN 12341 [CEN 1998] was applied for equilibration and weighing. The filters were stored in a freezer at -20 °C before analysis.

Meteorological data were collected at the meteorological stations of San Pietro Capofiume and Bologna by Hydro-Meteo- Climate Service of ARPA-ER. Mixing layer height at both sites was estimated using the pre-processor CALMET by ARPA Emilia-Romagna [Deserti et al. 2001].

2.2 Standards and analytes

Individual standard stock solutions were prepared for each analyte by weighting pure standards (Fluka, Sigma Aldrich, Acros, Carbosynth) at concentrations varying from 0.5 to 2 μg μL^{-1} using HPLC grade methanol as solvent.

These solutions were diluted serially with methanol to prepare composite standard solutions to determine retention times and to compute calibration curves. Calibration curves were computed for each campaign.

As said previously, three polar organic compound classes were analysed in this work: low molecular weight carboxylic acids, sugars and phenols.

Seven linear dicarboxylic acids with 3-9 carbon atoms as well as maleic and phthalic acids were analysed in all the campaigns. In addition, five hydroxycarboxylic acids, namely glycolic, malic, 3- and 4-hydroxy benzoic and mandelic acids, and four oxocarboxylic acids, pinonic, 2-ketoglutaric, pyruvic and glyoxylic acids, were investigated in this study.

Moreover, seventeen sugars were considered in this work: three anhydrosugars, levoglucosan, mannosan and galactosan, four polyols, namely erythritol, xylitol, ribitol and mannitol, four monosaccharides – arabinose, mannose, glucose and galactose – and six disaccharides – maltose, mycose, lactose, lactulose, sucrose and melibiose.

Finally, thirteen phenols were analysed, vanillin, vanillic acid, acetovanillone, syringol, syringaldehyde, syringic acid, acetosyringone, cathecol, pyrogallol, guaiacol, eugenol, p-coumaric acid and ferulic acid.

Literature data shown that these compounds are the most relevant markers identified in PM samples [Jacobson et al. 2000, Simoneit et al. 2004, Wang et al. 2004, Medeiros et al. 2006, Oliveira et al. 2007, Alves 2008, Ma et al. 2009, Balducci et al. 2010, Kumagai et al. 2010, Goncalves et al. 2011, Kuo et al. 2011, Fu et al. 2012, Pietrogrande et al. 2013a].

Structures of the analytes are shown in Appendix A.

2.3 GC/MS analysis of polar organic compounds

In the present work the analytical procedure was developed previously by Pietrogrande [Pietrogrande et al. 2010b, 2011, 2013b].

2.3.1 Extraction

Most of the analytical procedures for determining polar organic compounds in PM samples are based on solvent extraction using different solvents, including water, organic solvents, or their mixtures. In this case, PM samples were extracted for 15 min in an ultrasonic bath with 15 mL of methanol:dichloromethane, 9:1 solvents mixture. The mixture used combines extraction efficiency and short solvent evaporation time [Pietrogrande et al. 2013b]. Solvent evaporation is very important to avoid problems during next procedure steps. Moreover short time evaporation is desirable to prevent the loss of analytes.

The extracts were then filtered using a syringe PTFE filter (25 mm, 0.45 μm, Supelco, Bellefonte, PA) to remove insoluble particles and the filtrates were evaporated to dryness in a centrifugal vacuum concentrator (miVac Duo Concentrator, Genevac Ltd, Ipswich, UK) at 40°C.

The samples were reconstituted with 500 μL of the extraction solvents mixture, transferred in close tubes and centrifuged at 14000 rpm for 15 minutes. This procedure allows the removal of solid particles formed during solvent evaporation which can create problems throughout GC analysis.

The liquid was then transferred to 2 mL glass vials and dried under gently nitrogen flow.

2.3.2 Derivatization

Due to their high polarity, hydrophilicity and low volatility, the considered analytes have to be converted into volatilizable and stable derivatives to allow GC analysis.

In fact, the analysed molecules contain in their structure carboxylic and hydroxyl groups which can easily form hydrogen bonds.

The most common reactions used to modify compounds containing acidic hydrogens are alkylation, acylation, and silylation [Wang et al. 2002, Jaoui et al. 2004, Bi et al. 2008, Koutchev et al. 2008, Schummer et al. 2009, Becker et al. 2013].

Among the different reactions, silylation with N, O-bis-(trimethylsilyl)trifluoroacetamide (BSTFA) was preferred because it provides lower detection limits and higher reproducibility [Pietrogrande et al. 2010b].

The silylation reaction converts the hydroxyl groups into their corresponding trimethylsilyl (TMS) derivatives via a substitution reaction, which yields one main product for each compound and with high conversion efficiency (Figure 2.2) [Schummerer et al. 2009].

The BSTFA reaction is moisture sensitive, hence is very important to completely dry the solvent that is composed for 90% of methanol which could react instead of the compounds of interest. Moreover, the reaction requires mild conditions to complete the derivatization in order to achieve GC/MS detection at very low concentrations.
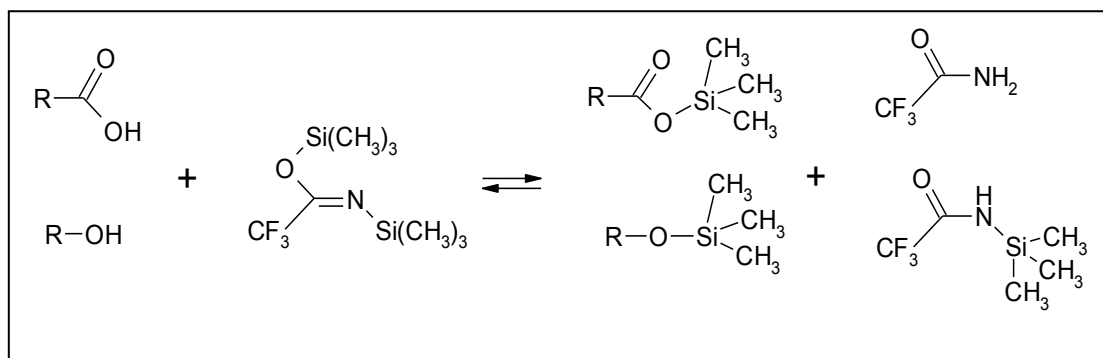
Figure 2.2. Derivatization reaction.

Mass spectra of acids and sugars derivatized with BSTFA usually display characteristic mass fragments at m/z=73, corresponding to $[Si(CH_3)_3]^+$, and m/z=75, attributable to $[OH=Si(CH_3)_2]^+$, which derives from the substitution of a hydroxyl hydrogen with a trimethylsilyl group. When the molecule of interest contains two or more hydroxyl hydrogens, other two common fragments appear in the mass spectra: m/z=147 and m/z=149 corresponding to $[(CH_3)_2Si=Si(CH_3)_2]^+$ and to its hydrogenated homologous respectively [Pietrogrande et al. 2005, Schummerer et al. 2009].

Regarding sugars, in addition to the aforementioned fragments, other three abundant ions are obtained from the fragmentation of pyranose structures at m/z=191, 294 and 217.

They correspond to $[(CH_3)SiO-CH-OSi(CH_3)]^+$, $[(CH_3)SiO-(CH)_2-OSi(CH_3)]^+$ and $[(CH_3)SiO-(CH)_3-OSi(CH_3)]^+$, respectively [Petersson 1974].

Typical ions for phenols fragmentation correspond usually to M-15. Characteristic fragments used for qualification and quantification of analytes are reported in Appendix A.

The derivatization reaction was performed at 75°C for 70 minutes: 40 µL of BSTFA containing 1% of trimethylchlorosilane (TMCS) and 15 µL of pyridine were added to 5 µL of Internal Standard (the deuterated $C_{12}H_{26}$) and 40 µL of isooctane.

23

Then, 2 μL of the derivatized solutions were analysed by GC/MS.

2.3.3 GC/MS analysis

The GC/MS system was a Scientific Focus-GC (Thermo-Fisher Scientific, Milan, Italy) coupled to PolarisQ Ion Trap Mass Spectrometer (Thermo-Fisher Scientific, Milan, Italy). The column used was a DB-5MS column (L = 30 m, I.D. = 0.25 mm, df = 0.25 mm film thickness; J&W Scientific, Rancho Cordova, CA, USA). High purity helium was the carrier gas with a flow rate of 1.5 ml min^{-1}. Temperature program conditions were optimized for analysis of a wide range of target polar organic compounds.

The temperature program used is reported in Table 2.1:

	Slope (°C/min)	Temperature (°C)	Time (min)
Initial conditions		70	0.00
Ramp 1	2.5	125	7.00
Ramp 2	2	145	5.00
Ramp 3	2.5	170	0.00
Ramp 4	7.0	300	1.00

Table 2.1. GC temperature program used for polar organic fraction analysis.

Due to the low concentration of the analysed compounds, all samples were injected in splitless mode (splitless time: 60 s); the injector temperature was 250 °C.

The mass spectrometer operated in Electron Ionization mode (positive ion, 70 eV). Ion source and transfer-line temperatures were 250°C and 280°C, respectively. The mass spectra were acquired in full scan mode from 50 to 650 m/z in 0.58 s. For identification and quantification of the target analytes, the extracted ions chromatograms (EICs) were recovered from the entire data set for each chromatographic run by selecting either the base peak ion or the most abundant characteristic fragments.

Quality assurance and quality control were assessed by precision, accuracy and sensitivity for polar organic tracers. The procedure provides low detection limits (1.3-4.9 ng m^{-3} using low volume air sampler) and good reproducibility (RSD% < 7%) suitable for applicability in environmental monitoring. Good procedure recoveries ranging from 78 to 104% were evaluated on PM samples spiked with surrogate standards [Pietrogrande et al. 2013b].

2.4 Complementary analytical data

To have a better understanding about PM$_{2.5}$ emission sources, other markers in the apolar organic fraction were considered: n-alkanes homologs to assess the contribution of biogenic signatures of epicuticular plant waxes and PAHs to differentiate among different combustion emissions.

Furthermore, OC and EC were determined as generic indicators of air quality and source apportionment since they are related to several sources in urban and rural environments.

2.4.1 Analytical procedure for apolar organic fraction

The analysis of n-alkanes homologs and polycyclic aromatic hydrocarbons were carried out in the ARPA laboratory in Ravenna, as a part of the Supersito project activities.

PM samples were extracted in an ultrasonic bath for 20 minutes with 15 mL of dichloromethane. Before extraction, 5-α-androstane (C$_{19}$H$_{32}$, 200 mL of a standard solution at 10 ng mL^{-1}) were spiked into all samples for recovery determination. Interfering compounds were removed by solid/liquid chromatography using a glass column (0.6 x 10 cm) packed with 3 g of deactivated silica gel and eluting with 25 mL of n-hexane, following the procedure of the EPA 3630C method. The elution solvent was evaporated until dryness under a gentle stream of nitrogen, and then the residue was dissolved in 200 mL of isooctane.

The instrument used was a Thermo Scientific DFS High Resolution GC/MS system. The gas chromatograph was equipped with a TR-5MS capillary column ((L = 60 m, I.D. = 0.25 mm, df = 0.25 mm film thickness). The mass spectrometer was a high resolution magnetic sector.

The initial oven temperature was set at 100 °C for 1 min, raised to 300 °C at a rate of 10 °C min^{-1} and then held for 50 min. Isotope labelled (deuterated) PAH standards were used for quantification.

2.4.2 Analytical procedure for carbonaceous aerosol

Carbonaceous aerosol fractions were quantified in the ARPA laboratory in Ferrara using the thermal-optical transmission method, as a common procedure widely used for the determination of OC and EC [Lonati et al. 2007, CEN 2011].

The instrument used was a thermo-optical-transmission analyser by Sunset Laboratory Inc.

The punched filters (1.5 cm^2) were submitted to volatilization using the EUSAAR2 thermal protocol [Cavalli et al., 2010; Chiappini et al., 2014]. According to this protocol, the carbonaceous material (OC) is initially thermally desorbed in an inert atmosphere (99.999% pure He) at relatively low temperature in four steps (200 °C for 120 s; 300 °C for 150 s; 450 °C for 180 s; 650 °C for 180 s). Then desorption is performed to evolve the EC component at higher temperature in four steps (500 °C for 120 s; 550 °C for 120 s; 700 °C for 70 s; 850 °C for 80 s) in an oxidizing atmosphere (2% oxygen/98% helium final mixture in the sample oven).

2.5 GC/MSMS development

The original procedure was further developed to improve specificity and sensitivity by using MSMS detection. Such a method decreases LODs and improves signal to noise ratio due to the effective exclusion of interfering matrix compounds [Garrido Frenich et al. 2008, Walser et al. 2008, Medina et al. 2009, Botitsi et al. 2011, Lv et al. 2013].

Tandem-in-space MS approach with triple quadrupole, tandem quadrupole/time of flight (QqTOF) or sector MSMS instruments is used in the most analytical applications to environmental samples, since it provides excellent quantification and unambiguous identification of the detected analytes [Garrido Frenich et al. 2008, Medina et al. 2009]. On the other hand, these kinds of instruments are very expensive.

Tandem-in-time technique with ion trap detector (ITD-MS/MS) system has been shown to be a valuable, user-friendly and cost-effective alternative, in particular using instruments with internal source that allows switching between full-scan and MSMS detection modes during the same chromatographic run [Szmigielski et al. 2007, Walser et al. 2007, Botsisi et al. 2011].

In light of the normally low concentration levels of polar organic tracers in aerosol and the complexity of the environmental matrix, the potential of GC/MSMS using ion trap for the sensitive and reliable determination of 28 compounds was investigated.

These compounds belong to two categories: low molecular weight carboxylic acids and phenols.

GC and MS parameters were the same as described in paragraph 2.3.3. Farther, in the multiple reaction monitoring mode, the isolation window was set at 1.5 m/z. Precursor ions were stored with a Paul stability parameter (qz) of 0.30 and fragmented by collision-induced dissociation (CID) using a resonant excitation mode.

2.5.1 Optimization of IT-MS/MS parameters

The operative key parameters were investigated in order to select proper precursor and product ions and to optimize collision energies for the best responses.

One precursor ion was selected for each compound from EI full-scan spectra at 70 eV and an emission current of 40 mA. The choice was based on selectivity rather than on signal intensity.

For each analyte, the precursor ion was subjected to further fragmentation under different collision energies to give different fragments in product scan mode. Product ions were selected from such fragment ions on the criteria of peak sensitivity and the likelihood of potential interference from other compounds.

At least two product ions with high responses were chosen for each target analyte: product ions with highest abundance were used for quantification while those with lowesty abundance for qualification.

Once selected qualification and quantification ions, collision CID energy was optimized in order to obtain the highest abundance of product ions and minimizes interference during the analysis.

A series of CID energies were tested for each analyte in the range of 0.5-2.5 V and the response was measured (Figure 2.3).
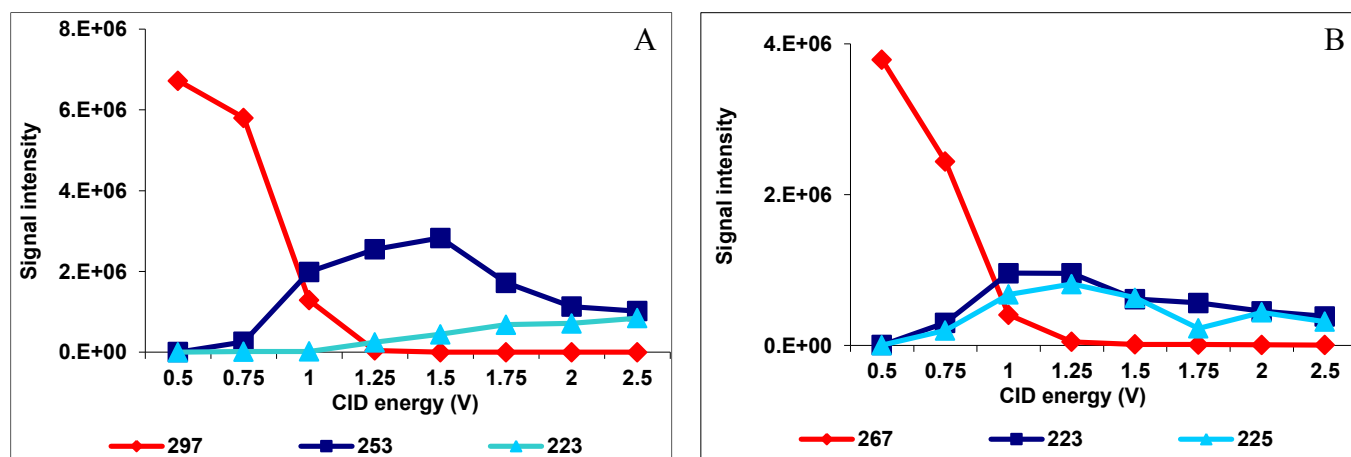
Figure 2.3. Optimization of the CID energy for (A) syringic acid; (B) 3-hydroxybenzoic acid [Visentin et al. 2014].

As a general pattern, the parent ion gradually fragmented, and peak intensity of the product ions obtained increased with the voltage. However, when the voltage was too high, the product ion intensities sharply reduced. The optimal CID voltages were in the range of 0.75-1.5 V for all the considered compounds.

2.5.2 Method validation

Using these IT-MS/MS optimized operating conditions, the method was validated by determining the linearity and LODs on standard solutions of the target compounds.

The calibration curves were developed using working solutions composed of mixed 28 target standards.

The obtained limits of detection were in the range 0.2-0.7 ngm^{-3} using a low volume air sampler. This sensibility is comparable with that provided by more advanced systems that require high capital and operating costs, such as high-resolution mass spectrometers or direct thermal desorption method followed by GC and TOF MS [Dong et al. 2011, Orasche et al. 2011, Ruiz-Jimenez et al. 2012, Zangrando et al. 2013,] .

The detection limits achieved with MSMS procedure were compared with those obtained for the same standard solutions using the GC/MS method with EIC procedure.

The results clearly show that the hyphenation with MSMS method effectively improves method sensitivity by a factor of six.

2.5.3 Method for real-life samples

The developed method was then applied to real PM$_{2.5}$ samples. As an example is reported a sample collected with low volume sampler ($\sim$55 m^3 day^{-1}) in winter 2011 at the urban site of Bologna.

The total ion current (TIC) chromatogram was acquired. As shown in Figure 2.4, the complex TIC signal contains several visible peaks due to original and derivatized components of the real sample that may interfere the GC/MS analysis.

The lower enlarged details show the EICs for vanillin, 3- and 4-hydroxybenzoic acids and syringic acid. The EIC strongly enhances selectivity but various interferences and high noise still remain.

The MSMS method (upper enlarged detail) further improves detection performance due to the effective exclusion of interfering matrix compounds.

The results obtained reveal that the implementation with MSMS detection permits the quantification of most part of the target tracers at concentration levels below the detection limits of the EIC detection (Table 2.2).

No sugars were analysed in MSMS mode because of their similar mass spectra that did not allow the choice of a characteristic parent ions for each analyte. Moreover various sugars were isomers with very close retention times and multiple peaks which resulted in complex chromatogram.
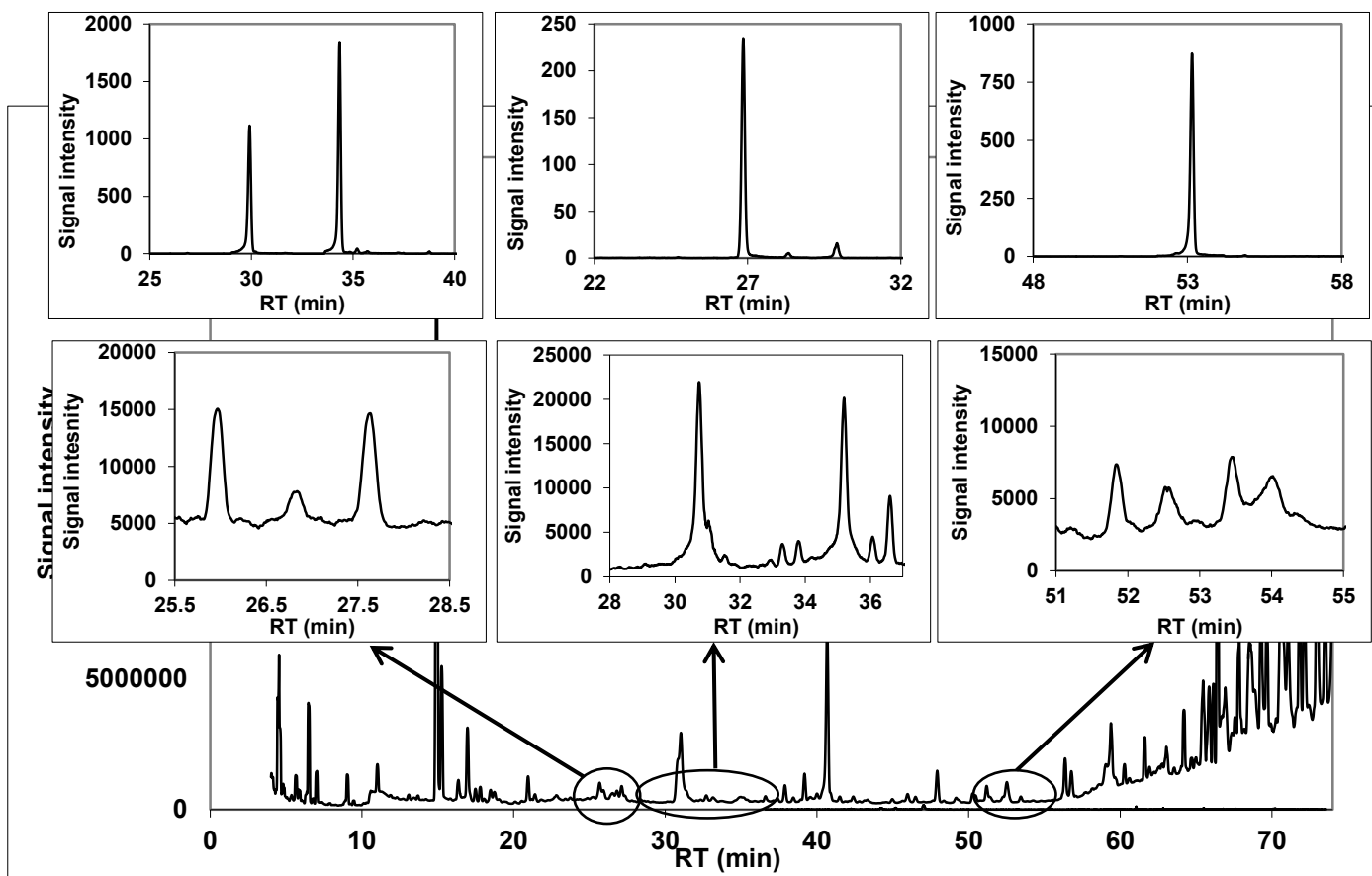
Figure 2.4. GC/MS chromatogram (TIC signal) of the real PM$_{2.5}$ sample collected in winter. Enlarged details: signals for four selected compounds using SIM detection (bottom) and MS/MS detection (top). m/z 165, 137: Vanillin, m/z 193, 223, 225: 3-and 4-OH-benzoic acids, m/z 223, 253: syringic acid [Visentin et al. 2014].

For these reasons we choose to focus our attention on LMW carboxylic acids and phenols.

These two groups of compounds together with anhydrosugars, those are usually present in concentration levels that do not need MSMS detection, are the most useful markers to study anthropogenic contribution to PM, the main purpose of Supersito project.

The possibility of combining full-spectrum mode and MSMS detection in a single chromatographic acquisition run is a very useful tool to give information on contribution of primary emission sources and secondary processes on air quality of the investigated sites.

	EIC (ng/m^3)	MS/MS (ng/m^3)
Acids		
Glycolic acid	12,4	
Malonic acid	n.d.	2.1
Glyoxylic acid	n.d.	n.d.
Maleic acid	27.6	
Succinic acid	32.8	
Glutaric acid	2.6	
Malic acid	n.d.	n.d.
Pyruvic acid	n.d.	<LOD
Adipic acid	<LOD	0,6
Pinonic acid	n.d.	n.d.
3-OH benzoic acid	<LOD	0,7
Pimelic acid	n.d.	n.d.
2-ketoglutaric acid	n.d.	1,2
4-OH benzoic acid	<LOD	1,1
Phthalic acid	5,0	
Suberic acid	n.d.	n.d.
Azelaic acid	n.d.	3,9
Phenols		
Cathecol	<LOD	<LOD
Syringol	n.d.	<LOD
Vanillin	n.d.	0,6
Pyrogallol	n.d.	<LOD
Acetosyringone	n.d.	n.d.
Syringaldehyde	<LOD	1,3
Acetovanillone	<LOD	<LOD
Vanillic acid	n.d.	<LOD
Syringic acid	n.d.	0,7
p-coumaric acid	n.d.	<LOD
Ferulic acid	n.d.	n.d.

Table 2.2. Concentrations of the polar markers in a real PM$_{2.5}$ samples [Visentin et al. 2014].

2.6 Derivatization procedure improvement

The original procedure developed and optimized by Pietrogrande [Pietrogrande et al. 2011] for the simultaneous analysis of sugars and LMW carboxylic acids has been further developed.

This research is actually in progress: preliminary results are reported in the following. First, the method was extended to methoxyphenols, thus, part of the research activity was devoted to the study of optimal derivatization conditions that maximize the response for all the compounds of interest. Moreover, the method has been improved in order to reduce reaction time, amount of derivatizating agent used and reaction temperature.

2.6.1 Sonication

"Classical" derivatization procedure was conducted in a water bath for 70 minutes at 75°C. The energy used for the reaction was therefore provided by heating. Another common method to supply energy to chemical reaction is sonication that allows reactions to occur at lower temperature. This is in line with the 6th principle of Green Chemistry called design for energy efficiency: energy requirements of chemical processes should be recognized for their environmental and economic impacts and should be minimized. If possible, synthetic methods should be conducted at ambient temperature and pressure [Anastas et al. 1998].

Ultrasound are sound waves that can be transmitted through any substance, solid, liquid or gas, possessing elastic properties. Sound waves movement produces compression and expansion cycles on medium molecules and, in the case of a liquid, expansion cycles produce negative pressures pulling the molecules away from one another. If this negative pressure exceeds the tensile strength, then a cavity can forms. A bubble irradiated with ultrasound continually absorbs energy from alternating compression and expansion cycles of the sound wave. Over many cycles the cavities will grow slowly. The growing cavity can eventually reach a critical size where it will most efficiently absorb energy from the ultrasound. Without this energy input the cavity can no longer sustain itself [Suslick 1989].

The implosion of cavities establishes an unusual environment for chemical reactions. The gases and vapours inside the cavity are compressed, generating intense heat that raises the temperature of the liquid immediately surrounding the cavity and creates a local hot spot with pressure up to 2000 atm and temperature of about 5000 K [Suslick 1989, Luque de Castro et al. 2011]. Even though the temperature of this region is

extraordinarily high, the size of the bubbles is very small relative to the total liquid volume, so the heat they produce is rapidly dissipated with no appreciable change in the environmental conditions [Suslick 1989, Luque de Castro et al. 2011, Delgado-Povedano et al. 2013].

Various studies used ultrasound to accelerate chemical reactions and in particular derivatization [Luque de Castro et al. 2011, Delgado-Povedano et al. 2013].

Considering silylation reactions, triterpenes derivatization time decreases from two hours using heating to five minutes using ultrasound [Sánchez Ávila et al. 2007], while for sterols and some alcohols from two hours to ten minutes [Orozco-Solano et al. 2011].

Therefore sonication seems to be a better alternative than heating, thus the attention was focused on some parameters affecting derivatization yield, mainly solvent polarity, reaction time, reaction temperature and BSTFA volume.
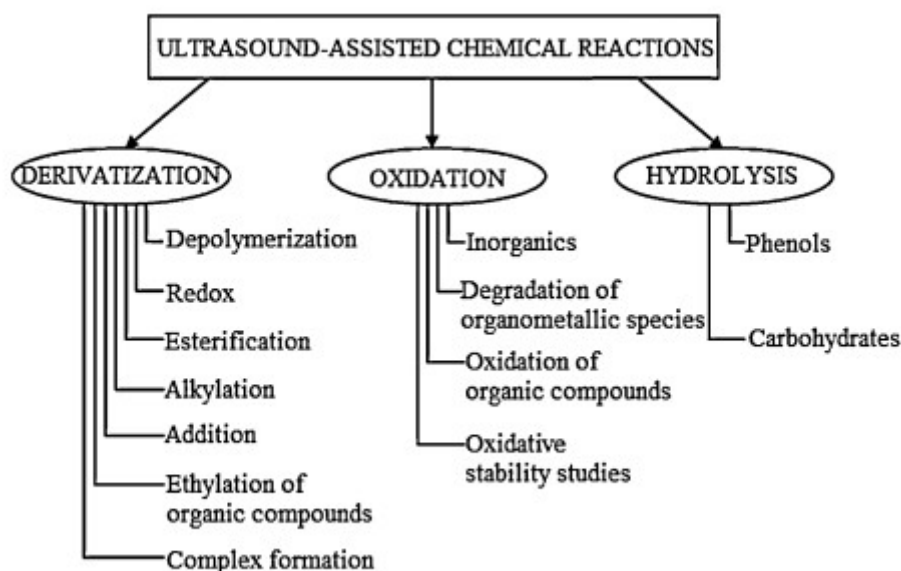
Figure 2.5. Scheme of ultrasound-assisted chemical reactions of analytical interest involving liquid samples [Delgado-Povedano et al. 2013].

2.6.2 Preliminary experiments

Before performing the optimization study, some preliminary tests were performed on a standard solution containing various compounds representative of the three classes of polar organic species considered in this study, to evaluate the experimental conditions that mostly influence derivatization reaction i.e., solvent polarity, reaction time, reaction temperature and BSTFA amount.

As arbitrary starting point, the reactions were performed using the same reagent amounts of previously developed procedure (40 µL BSTFA, 40 µL solvent, 15 µL pyridine and 5 µL internal standard), room temperature and ten minutes as sonication time. The ultrasonic bath used was an Elmasonic 100H (Elma Schmidbauer GmbH, Singen, Germany) with an ultrasonic frequency of 37 KHz and an effective power of 150 W.

Regarding solvent polarity, five different solvents were considered: acetonitrile (P^I =5.8), acetone (P^I =5.1), ethyl acetate (P^I =4.4), dichloromethane (P^I =3.1) and isooctane (P^I =0.1). P^I is the solvent polarity index introduced by Snyder.

Important information obtained from such preliminary experiments is that reaction temperature does not seem to condition reaction yield. Experiments conducted at 6.5, 25, 45 and 60°C gave very similar results, thus all subsequent experiments were performed at room temperature. Working at room temperature has permitted the use of a major number of different solvents: solvents as acetone, and dichloromethane could not be used in the previous derivatization procedure because of their boiling point that is lower than the reaction temperature. In fact derivatization was performed at 75°C while acetone boiling point is 56°C and dichloromethane boiling point is around 40°C.

2.6.3 Optimization

To systematically investigate the derivatization parameters that mostly affect the analytical response the response surface methodology was used.

A response surface is a graph of a system response plotted as a function of one or more system factors. Response surface offers a convenient means of visualizing how various factors affect the considered system [Massart et al. 1988].

To have a good description of the data, a mathematical model is need.

In many systems, the effect of one factor will depend upon the value of another factor. This phenomenon is called factor interaction.

Among the various models that can be used to represent a system response where factor interactions exist, full second-order polynomial model is the most used. Such equations are exceptionally versatile for use as empirical models in many systems over a limited domain of the factors [Box et al. 1951].

2.6.4 Design of experiment (DOE)

To explore the response surface, a series of designed experiments have to be performed. Supposing that the considered factors can assume discrete values in a certain interval,

central composite design can be used. Central composite designs (CCD) are very useful for obtaining data that can be used to fit a full second order polynomial model [Box et al. 1960]. They are a combination of a star design with 2k+1 factor combinations and a two-level k-factor factorial design with 2^k factor combinations to give a total of $2^k + 2k + 1$ factor combinations (Figure 2.6). While factorial points distance from the centre is ± 1, the star points are at coordinates $\pm\alpha$, which value depends on the desired properties of experimental design. The centre point of CCD is usually replicated to estimate experimental uncertainty [Massart et al. 1988].

The experimental parameters that most greatly affected analytical response were optimized: sonication time, solvent polarity and BSTFA amount. Thus a three-factor CCD was used.
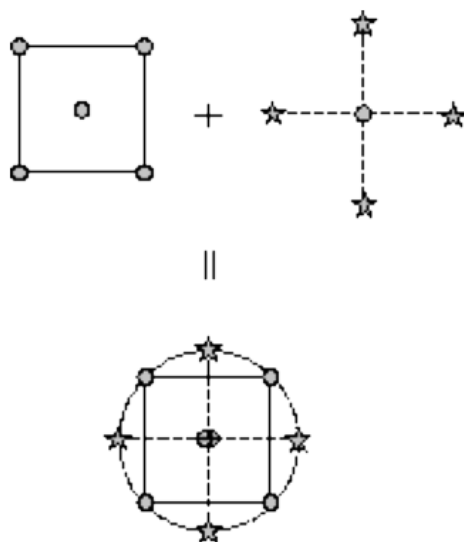
Figure 2.6. A two-factor central composite design.

The experiments were carried out on a composite standard solution containing forty five species belonging to the three polar organic compounds classes considered in the work and usually determined in $PM_{2.5}$ in the Bologna area. In addition to LMW carboxylic acids, sugars and phenols, also two fatty alcohols, 1-hexadecanol and 2-octadecanol were present in the composite solution. They are mainly emitted from plants and, in minor amounts from microorganism [Mudge 2005]. Fatty alcohols were also found in vegetal biomass burning emissions [Simoneit 2002, Fu et al. 2008].

Each independent variable was investigated in the range +1 and -1, inside the exploited domain defined by the limits chosen on the basis of the experimental constraints (BSTFA volume not larger and reaction time not longer than previous derivatization procedure) as well as data from preliminary experiments (the coded values of

independent variables are given in Table 2.3). The limits were 5-70 minutes for sonication time, 5-40 μL for BSTFA volume and acetonitrile (P^I =5.8) and isooctane (P^I =0.1) as solvent polarity.

A three-factors, five-level Central Composite Design with a quadratic model was employed (Figure 2.7). It generates a total 24 different combinations (including ten replicates of the centre point) that were experimentally measured in duplicate in random order.

Independent variables	Coded units	Coded variable levels
BSTFA volume	-1, -0.59, 0, +0.59, +1	5, 12, 22.5, 33, 40 μL
Sonication time	-1, -0.59, 0, +0.59, +1	5, 18, 38, 57, 70 minutes
Solvent polarity	-1, -0.59, 0, +0.59, +1	0.10, 1.18, 2.90, 4.62, 5.80

Table 2.3. Data of the central composite design: coded values of the independent variables investigated with 15 full-factorial design and optimized values estimated for each variable.

Solvent polarities that did not correspond to a pure solvent were obtained by mixing in exact proportions different solvents.

Due to the great difference in solvent polarities, a common internal standard soluble in the same manner in all the solvents was impossible to use. Thus the absolute value of peaks area was considered in this phase of the study.
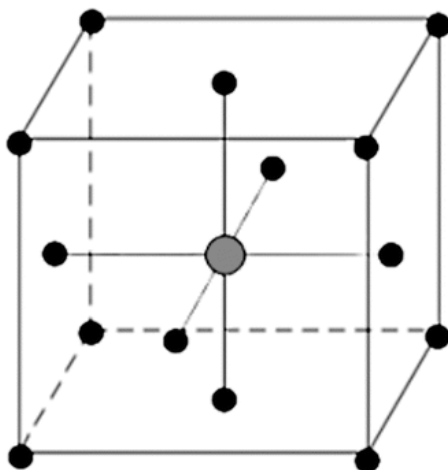
Figure 2.7. A five-level three factor central composite design.

2.6.5 Response surface methodology

To describe the response surface, the experimental data were fitted by a second polynomial equation containing quadratic terms explaining the non-linear nature of the response, according to the general equation:

$$Y = b_0 + b_1X_1 + b_2X_2 + b_3X_3 + b_4X_{1,2} + b_5X_{1,3} + b_6X_{2,3} + b_7X_1^2 + b_8X_2^2 + b_9X_3^2 \qquad \mathbf{1}$$

        Y: studied response;

        X_1: BSTFA volume;

        X_2: sonication time;

        X_3: solvent polarity;

        b_0: response mean value;

        $b_1 - b_3$: parameters of the isolated variables;

        $b_4 - b_6$: parameters of interaction;

        $b_7 - b_9$: quadratic terms of the studied variables.

2.6.6 Multivariate optimization on target compounds

Five different models have been investigated by selecting acids (A), sugars (S), phenols (P) and fatty alcohols (FA) separately or including all the compound classes.

The results were fitted by equation 1 and a statistical evaluation of the estimate of the parameters was made by using the Student's t-test: parameters with significance levels (p) lower than 5% were considered relevant (bold values in Table 2.4). The R^2 and calculated F values - in comparison with fixed F parameters - were used to verify the significance or not of the model. Finally, the goodness-of-fit statistics are described by the root mean squared error (rmse) in order to estimate standard error [Massart et al. 1997].

Although the coefficients of determination are low (R^2% 0.6), the p values - i.e., statistically significant fit with p $<$0.1 for the three models - and the low rmse values implied that the equations found can adequately predict the experimental results.

To better visualize the effect that each parameter displays on the derivatization yield, the fitted models were plotted separately as a function of a single variable between its low and high boundary levels, holding all other factors at a fixed level (center levels) (Figure 2.8). The direction of the line slope gives the direction of the effect of each parameter and the slope is proportional to this effect: in fact, the higher the slope, the greater the influence. In order to compare response values of the different classes, responses are expressed as relative values compared to maximum response.

	∑ Acids	∑ Phenols	∑ Sugars	∑ Fatty alcohols	∑ Total
Intercept	74.04	95.73	-5.99	2.51	170.32
BSTFA	-0.16	2.20	**2.71**	0.09	4.63
Time	-0.07	0.16	0.12	**0.06**	0.18
Polarity	**-8.48**	**-15.62**	2.12	-0.60	-23.54
BSTFA*Time	**-0.02**	**-0.03**	-0.01	**-0.002**	**-0.07**
BSTFA*Polarity	0.089	0.12	0.05	0.006	0.26
Time*Polarity	**0.09**	0.10	-0.01	0.0009	0.17
BSTFA*BSTFA	0.006	-0.02	**-0.04**	-0.0009	-0.05
Time*Time	0.002	0.007	0.005	-0.0002	0.01
Polarity*Polarity	**0.47**	**1.84**	0.02	0.06	2.55
R^2	0.82	0.66	0.62	0.58	0.61
p	0.002	0.04	0.08	0.12	0.09
F	0.69	2.81	2.33	2.04	2.28
rmse	2.31	7.8	7.24	0.36	15.7

Table 2.4. Coefficients and statistical parameters of second-order polynomial equations calculated on experimental results from CCD models.

For each class of compounds, BSTFA volume (X_1) displays similar effect on the response, except for acids. For acids, a quasi-linear, negative effect is seen suggesting that acid derivatization is favoured by decreasing this parameter; on the other hand, a parabolic pattern was found for the other compounds classes where the highest response occurred close to the centre level. This last pattern prevails when the four classes of compounds are investigated simultaneously (Figure 2.8A)

Regarding the effect of sonication time (X_2), it is apparent that increasing the time bring about a slight increase in derivative yield, so that the maximum response is obtained at 100% value for all the classes except acid. Maximum yield for acids is reached at minimum sonication time. Despite this exception, the general trend has indicated in 70 minutes the optimum sonication time (Figure 2.8B).

Considering the last parameter, solvent polarity (X_3), a parabolic patters is observed for near all classes of compounds but maximum and minimum values were registered at different X_3 values The only exception are sugars which show a liner increase of yield increasing solvent polarity. Acids and fatty alcohols display similar effect of solvent polarity with maximum response registered at the low-end of he considered range. On

the contrary, phenols reached the maximum yield when X_3 is maximum. The trend shown by phenols and sugars is predominant, thus considering the total response given by the four classes, the optimal value for X_3 is 5.8, that is the maximum exploited value polarity corresponding to acetonitrile (Figure 2.8C).
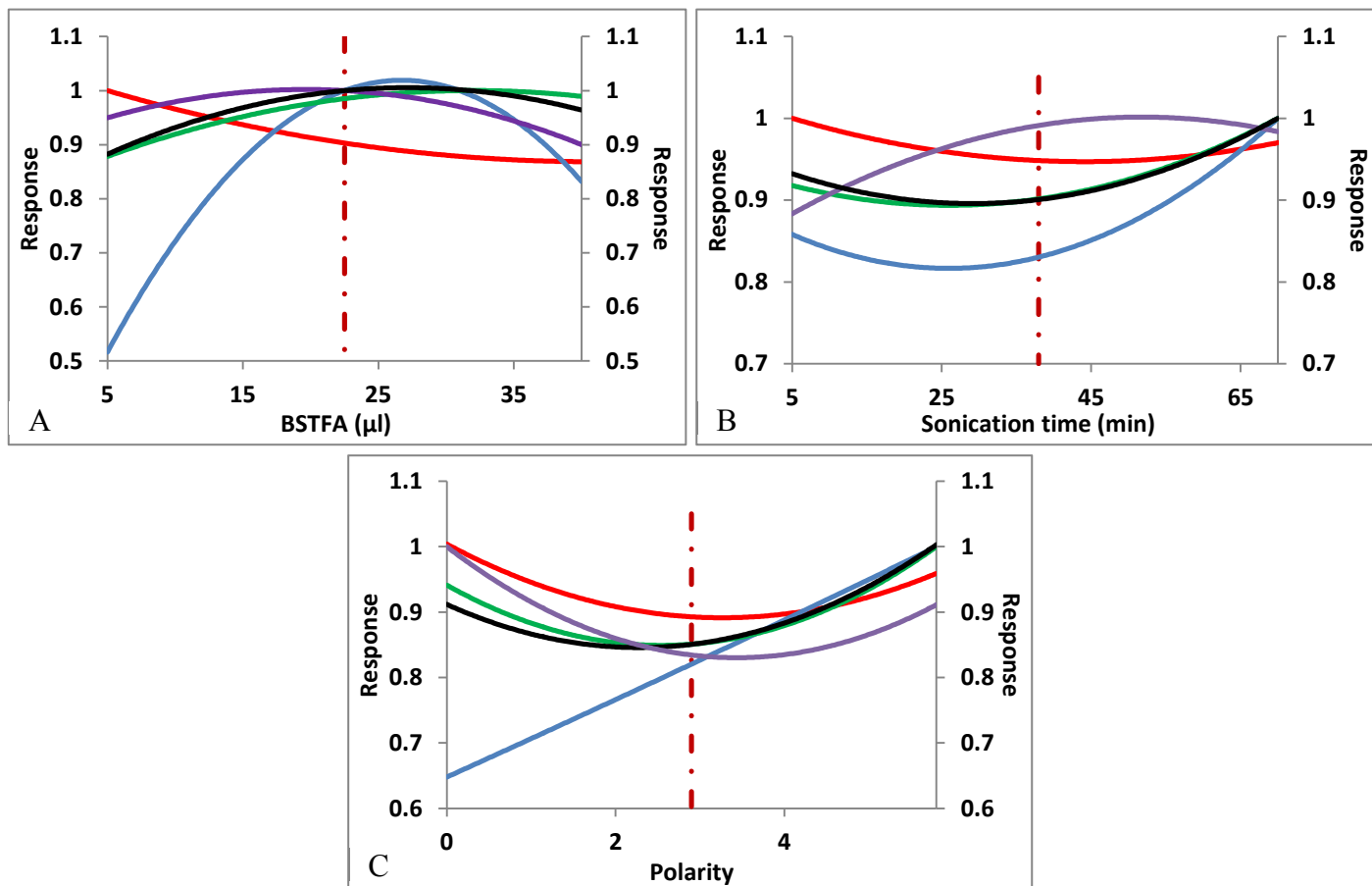
Figure 2.8. Reaction response plotted as a function of a single variable, set between its lower and upper boundaries (other parameters constant at their center levels). Five fitted models (Eq. (1)) are reported: acids (red line), sugars (blue line), phenols (grren line), fatty alcohols (purple line) and their combination (black line). A) Effect of the BSTFA volume (X_1); B) effect of sonication time (X_2); C) effect of solvent polarity (X_3).

The combination of two effects for the total test mixture can be investigated by reporting the response in a 3-dimentional plot (3D) as a function of two factors at one time (the other factor at centre level). The interaction between BSTFA amount and solvent polarity can be understood by observing Figure 2.9A. It shows that optimum conditions are located in the area described by maximum solvent polarity and BSTFA volume around the centre value of the explored interval. The plot of solvent polarity versus sonication time clearly shows two maxima at the intervals extremity but the maximum response is reached for the highest ends of both the intervals.
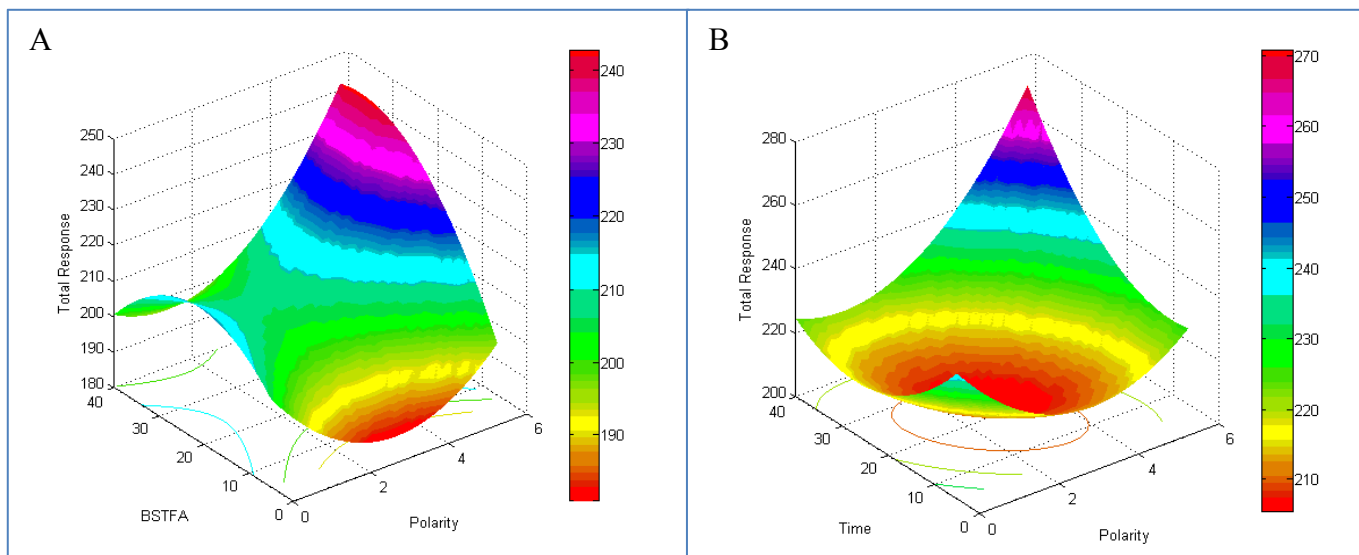
Figure 2.9. 3-D surface plots showing the interacting effects of two derivatization parameters (other parameters constant at their center level) on derivatization yield. A) Interferacting effects of BSTFA volume and solvent polarity (X_1 and X_3); B) Interacting effects of sonication time and solvent polarity (X_2 and X_3).

An important remark about these experiments is that sugars derivatization seems to be strongly influenced by solvent. In fact, as shown in Figure 2.10, peaks number for sugars derivatives in the chromatogram change with solvent polarity. As general trend, increasing solvent polarity leads to a decreasing in peaks number.

39
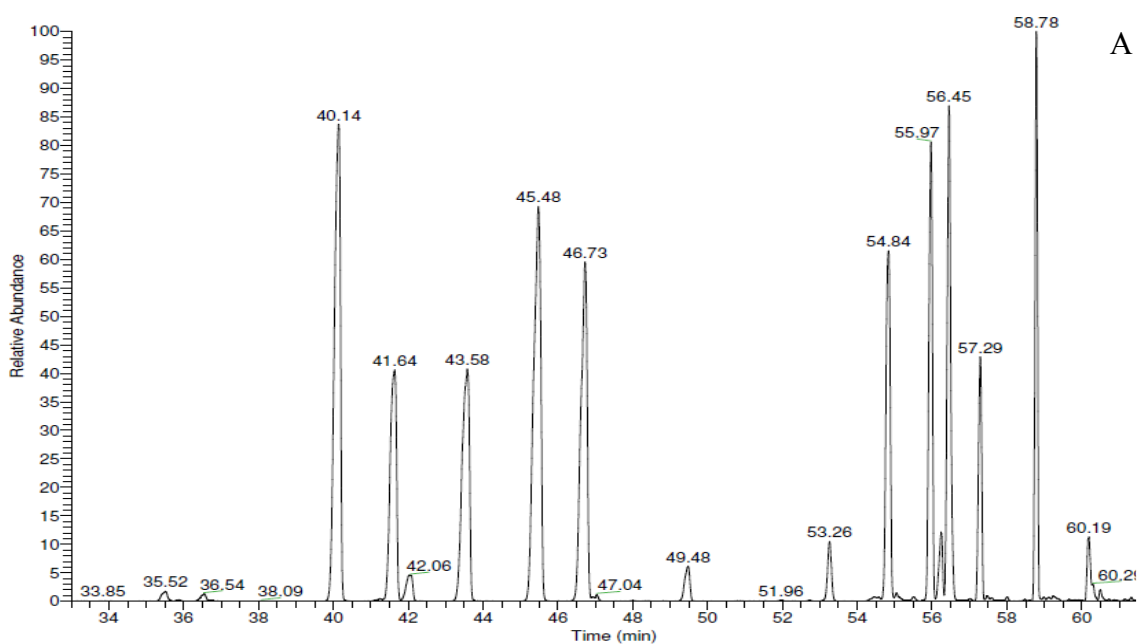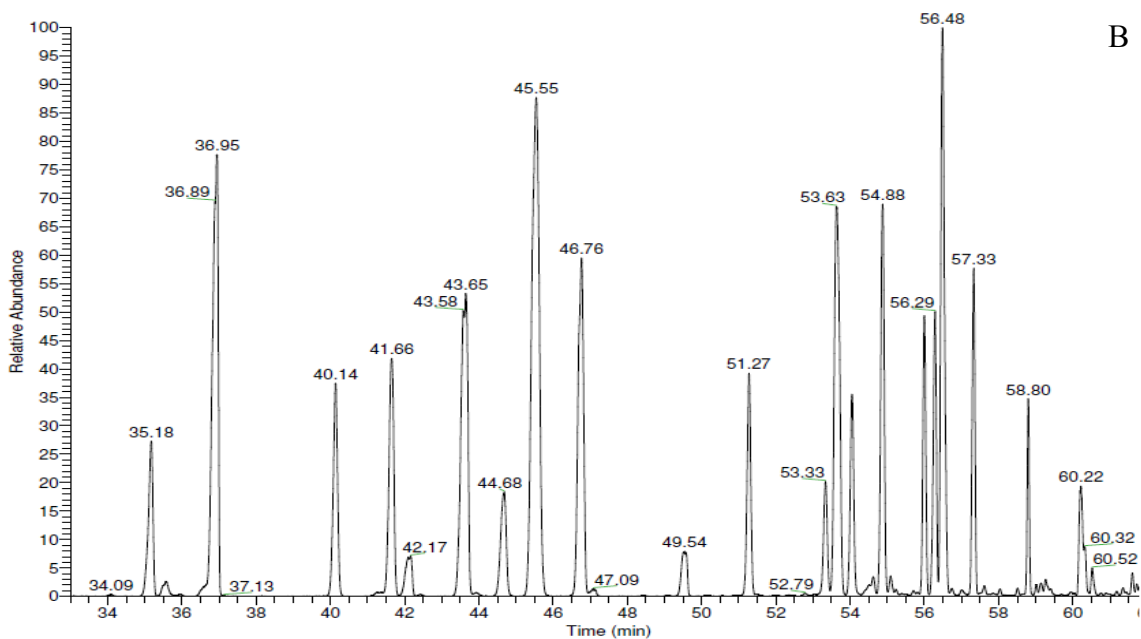
Figure 2.10. Galactosan, mannosan, levoglucosan, xylitol, ribitol, galactose, glucose and mannitol signals in A) acetonitrile and B) isooctane.

2.6.7 Evaluation of analytical performance

The new developed procedure was finally applied to some PM$_{2.5}$ real samples.

One of the main purpose of the work was to decrease derivatization time. Unfortunately, results from experimental design showed that the maximum response was obtained at 70 minutes sonication time with no advantages in comparison to the previous procedure. Wishing to fulfil the aim of this study, the reaction was performed in the optimized conditions reducing the reaction time to 40 minutes of sonication i.e., 22.5 µL of BSTFA and acetonitrile as solvent. The reliability for quantitative determination was investigated using some real world PM$_{2.5}$ samples and the performances were compared with that of the original method.

The obtained results show that the two methods are comparable in terms of sensibility as shown in Figure 2.11.

Moreover, the stability of BSTFA derivatives was studied by injecting samples 24 hours after derivatization. Stability in time of derivatives is a fundamental requirement in an analytical chemistry laboratory where a large number of samples are analysed in a day using an autosampler. In fact, samples are usually prepared in the morning and loaded on autosampler to automate as much as possible the analyses. Thus, several hours could pass between derivatization and injection and no modification in samples during this time is desirable.
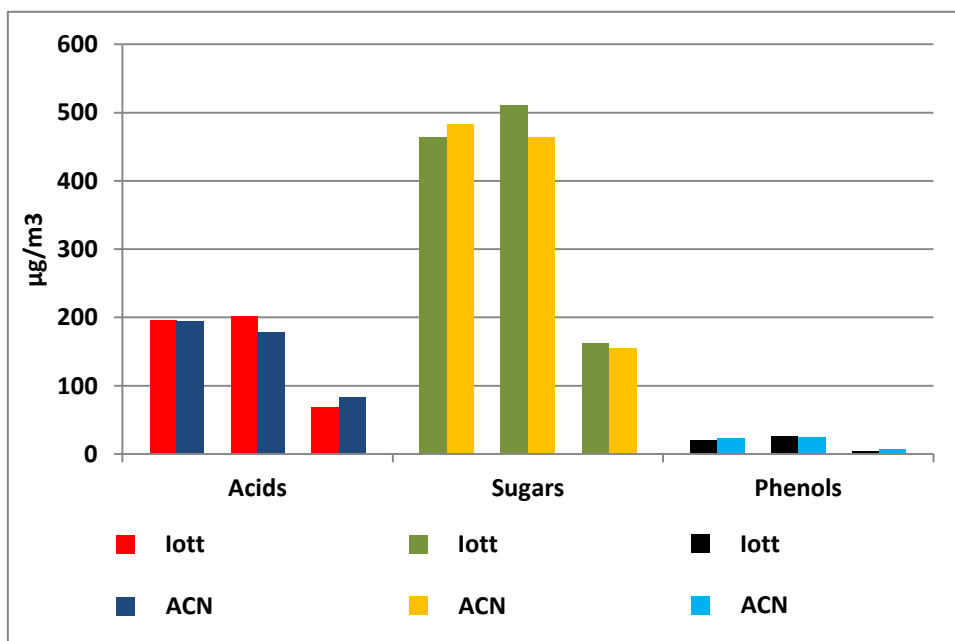
Figure 2.11. Response of acids, sugars and phenols in three real sample of PM$_{2.5}$ to "classic" derivatization in water bath using isooctane and to new method using sonication and acetonitrile as solvent.

As reported in Figure 2.12, derivatives in acetonitrile seem to be slightly more stable than those in isooctane, especially regarding sugars.

In conclusion, the modified procedure provided comparable results in terms of response together with several improvements. Smaller amount of BSTFA used, lower reaction temperature and greater stability of derivatives confirm that the developed procedure could be an effective and cheaper alternative to the classical derivatization procedures which make use of long heating times for the reaction to occur.

The obtained results can be considered promising also in light of the used sonication device. In fact, the Elmasonic 100H is an ultrasonic cleaning unit with fixed parameters that cannot be adjusted by the operator. This is a limit of the developed procedure since ultrasound action is influencing by several factors as the applied ultrasound frequency and intensity, two parameters that can be regulated in ultrasound devices studied to perform chemical reactions [Sánchez Ávila et al. 2007, Luque de Castro et al. 2011, Orozco-Solano et al. 2011]. Thus, future further improvements are possible in order to obtain a real decrease in sample preparation time.
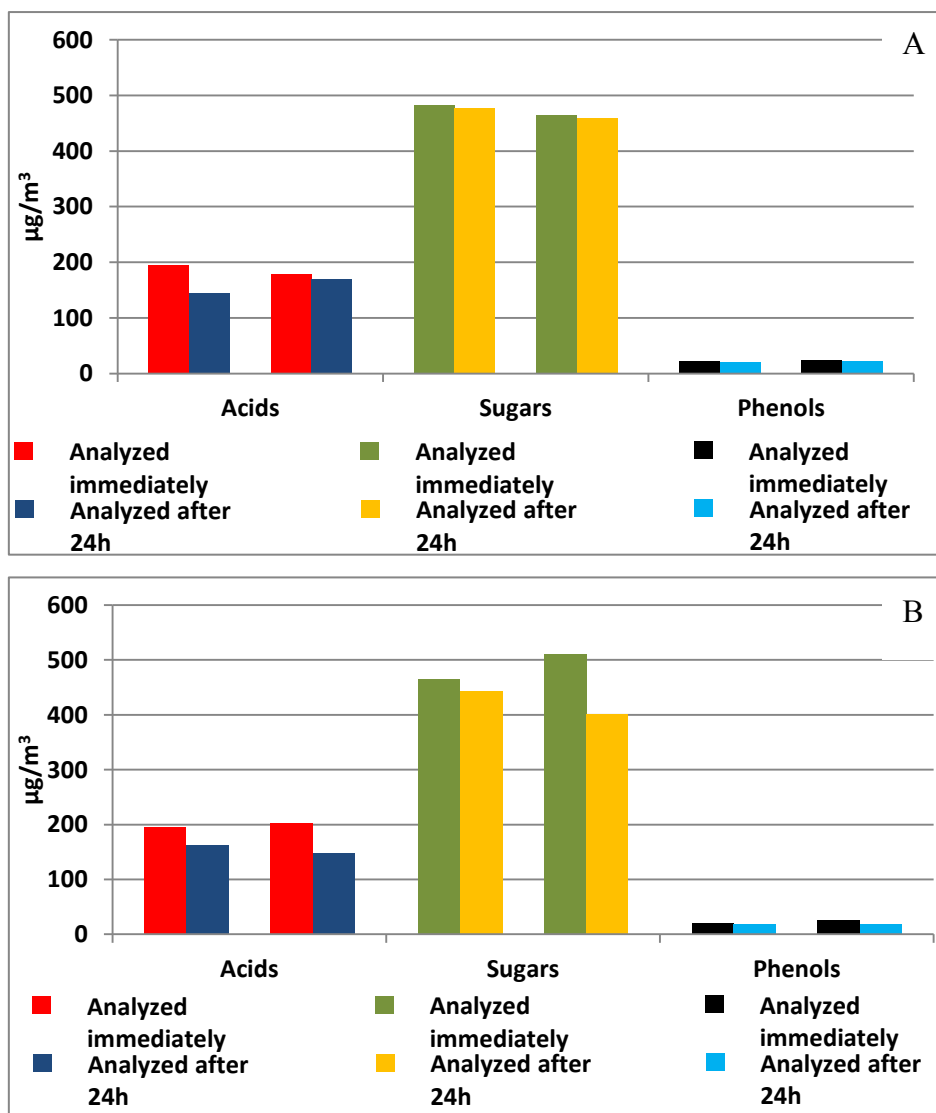
Figure 2.12. Response of acids, sugars and phenols in phenols in two real sample of PM$_{2.5}$ immediately after derivatization and after 24 hours from derivatization for A) derivatization in acetonitrile and B) derivatization in isooctane.

2.7 Intercomparison study of sugars analysis in PM

Finally, the analytical methods for measuring sugars in PM samples are under investigation by performing an intercomparison study involving ten laboratories.

Sugars, and in particularly anhydrosugars, are often linked to biomass burning emissions in the atmosphere. Several studies in recent years have demonstrated that emissions from biomass combustion in domestic appliances are significant contributors of the total PM$_{2.5}$ and PM$_{10}$ emitted especially in the Po valley [Belis et al. 2011, Bernardoni et al. 2011, Larsen et al. 2012, Perrone et al. 2012, 2013, Piazzalunga et al. 2013]. Thus, increasing efforts have been put into sugars quantification during the last

decade using different analytical methods. Gas chromatography-mass spectrometry (GC/MS), high-performance liquid chromatography coupled with mass spectrometry (HPLC/MS) and high-performance anion-exchange chromatography (HPAEC) are the most commonly used methods for sugars determination in ambient aerosol [Yttri et al. 2015].

The study was organized at national level in the WG2 working group of IAS (Italian Aerosol Society) with the purpose of evaluating the comparability of the different methods used in Italian laboratories and to compare the obtained results to ensure the use in extensive campaigns of control/monitoring of air pollution.

The work presents preliminary results for three anhydrosugars, galactosan, mannosan and levoglucosan.

The laboratories participated in the intercomparison exercise use methods with different characteristics: six of them used HPAEC, two used GC/MS, one liquid chromatography-mass spectrometry (UHPLC-HQOMS) and one nuclear magnetic resonance (^{1}HNMR) without preliminary separation. All HPAEC systems were coupled with a pulsed amperometric detector except one that used a mass spectrometer as detector. A short description of analytical methods is given in Table 2.5.

To validate the analytical procedures, three synthetic quartz filter samples were prepared at known concentrations of the considered sugars using an aerosol generator. Moreover, the study was extended to twenty six real samples of $PM_{2.5}$ sampled in Milan and Trento between winter and spring. The two sites represent two urban backgrounds in different geographical contexts in order to consider particles with different composition and with a large range of analytes concentration. Some punches of the filters were submitted to the participating laboratories.

All ten laboratories reported levels for levoglucosan, whereas seven reported also data for mannosan and galactosan.

The results are presented in terms of the percentage error (PE) that was calculated for each of the participating laboratories for each of the filter samples according to the following equation:

$$ PE \ = \frac{measured - theoretical}{theoretical} \times 100 $$

where measured is the value of the analyte reported by the actual laboratory and theoretical is the median value of the analytes based on the values reported by all

participating laboratories. The arithmetic mean PE for each laboratory, accounting for all filters, was then subsequently calculated.

Lab no.	Instrument	Solvent	Derivatization
1	HPAEC-PAD	Water	No
2	HPAEC-PAD	Water	No
3	HPAEC-PAD	Water	No
4	HPAEC-PAD	Water	No
5	HPAEC-PAD	Water	No
6	HPAEC-MSQ	Water	No
7	GC-QMS	Acetonitrile	Yes
8	GC-ITMS	Methanol/Dichloromethane	Yes
9	UHPLC-HQOMS	Water	No
10	^{1}HNMR	Water	No

Table 2.5. Overview of the analytical methods used by the participating laboratories.

From the obtained calculated data, the mean PE for levoglucosan ranged from -63 to 47%, for mannosan from -14 to 18% and for galactosan from -23 to 76%. Regarding levoglucosan, the mean PE was within ±25% for seven of the ten laboratories, whilst mannosan shows the smaller PE with all laboratories below 20%. Finally, galactosan shows a narrow PE range among laboratories within ±25% excluding one laboratory that exhibited a PE of about 80% (data in Figure 2.13).

The data reported in Figure 2.13 do not show significant differences among the different methods used. Hence, the results obtained by most analytical methods currently used to quantify monosaccharide anhydrides in ambient aerosol filter samples provide comparable results as assert also by Yttri [Yttri et al. 2015].

The only remark that can be done, excluding the three laboratories with higher PE values, is that HPAEC-PAD and LC methods exhibit a slightly lower PE in comparison to other methods and that GC based procedures tend to underestimate anhydrosugars. This last observation could be explained considering that derivatization is need prior to GC analyses and a loss of analytes may occur.
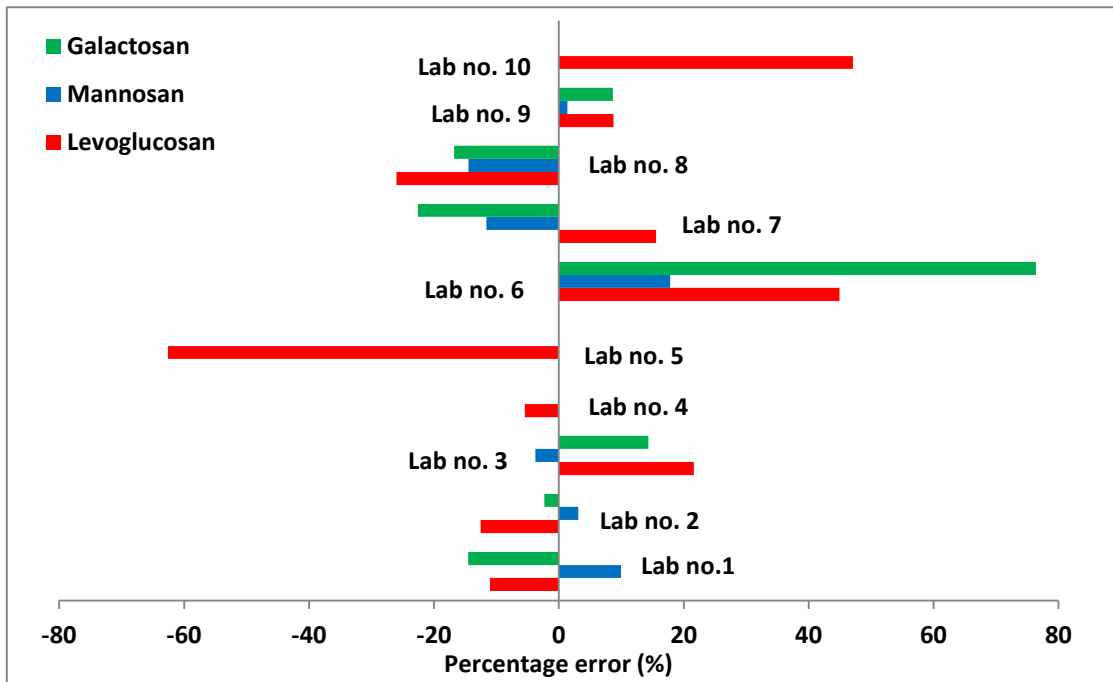
Figure 2.13: Calculated mean percentage error for each of the ten laboratories reporting levels of the three anhydrosugars.

3. AIR QUALITY OF EMILIA ROMAGNA REGION: THE SUPERSITO PROJECT

The results obtained in the framework of the Supersito project are reported in Appendix B, in four published papers [Pietrogrande et al. 2014a,b, 2015, 2016] and summarized in the following.

3.1 Meteorological conditions

During the monitoring campaigns, large differences concerning meteorological conditions occurred. Fall/winter periods were characterized by atmospheric stability with shallow Planetary Boundary Layer (PBL) depths (H_{mix} mean values ~300 m), rather low temperatures (3-12°C), low solar irradiance (mean values ~75 W m^{-2}) and weak amount of wet depositions. Exceptions are winter 2014 with maximum deposition at Main Site (~140 mm during the sampling period) and very dry winter 2011 with almost no precipitations (maximum 5 mm at San Pietro Capofiume during the three weeks campaign).

On the contrary, spring/summer periods are characterized by high PBL depths (H_{mix} mean values >900 m), high temperatures (16-28 °C), large solar irradiance (mean values ~270 W m^{-2}), weak amount of wet depositions (maximum precipitations ~65 mm during May 2013).

	Main Site				San Pietro			
	Temperature (°C)	Solar irradiance (W/m^2)	PBL height (m)	Precipitations (mm)	Temperature (°C)	Solar irradiance (W/m^2)	PBL height (m)	Precipitations (mm)
W11	6.5 ± 1.8	61 ± 23	229 ± 81	1.0	3.9 ± 1.8	65 ± 30	169 ± 43	5.2
Su12	27.5 ± 2.6	295 ± 27	974 ± 132	3.8	25.7 ± 2.6	324 ± 32	854 ± 109	12.4
A12	12.0 ± 2.6	71 ± 35	376 ± 107	65.0	10.6 ± 2.7	86 ± 44	263 ± 77	74.8
W13	3.9 ± 1.6	78 ± 33	398 ± 83	49.4	2.6 ± 1.0	89 ± 47	296 ± 103	40.4
Sp13	17.6 ± 2.3	228 ± 64	954 ± 204	64.6	16.5 ± 2.4	240 ± 79	786 ± 160	53.0
A13	15.7 ± 2.5	97 ± 52	468 ± 188	131.6	15.0 ± 2.5	105 ± 62	402 ± 133	118.6
W14	8.3 ± 2.1	72 ± 44	411 ± 140	141.6	7.3 ± 1.8	80 ± 52	302 ± 86	117.0
Su14	21.0 ± 3.3	258 ± 57	974 ± 171	24.4	19.4 ± 2.8	286 ± 55	876 ± 160	49.0

Table 3.1. Average values and standard deviations of meteorological parameters.

Among the investigated periods, the atmospheric conditions of October 2013 were intermediate between cold and warm seasons with temperatures higher than 15°C and PBL deeper than 400 m.

It should be noted that temperatures and PBL height values are higher at Main Site in all the campaigns while solar irradiance is always higher at the rural site. This behaviour is probably due to the different anthropization level between the two sites.

3.2 PM concentration

The $PM_{2.5}$ concentration in the investigated periods shows a clearly seasonal trend with higher amount of particles in the cold seasons.

A peculiarity of the obtained data is the close similarity between the PM levels of the urban and rural sites, reflecting the regional nature of the emission sources and their similar impact across the air shed.

$PM_{2.5}$ levels were close 10 μg m^{-3} in spring-summer and around 30 μg m^{-3} during autumn-winter. Winter 2011 exhibits the highest concentration of particles with an average value twice respect to the other cold period and daily maxima close to 100 μg m^{-3}.

	Main Site	San Pietro
	$PM_{2.5}$ (μg/m^3)	$PM_{2.5}$ (μg/m^3)
W11	59.2 ± 1.4	46.3 ± 17.8
Su12	15.1 ± 4.3	17.8 ± 4.3
A12	31.1 ± 17.3	26.7 ± 16.6
W13	33.1 ± 14.0	35.2 ± 19.5
Sp13	8.5 ± 2.4	8.0 ± 4.8
A13	21.6 ± 10.2	16.5 ± 10.3
W14	19.3 ± 11.7	16.3 ± 8.0
Su14	10.0 ± 3.6	10.5 ± 4.3

Table 3.2. Average values and standard deviations of $PM_{2.5}$ concentrations.

This is consistent with the meteorological data registered during the sampling campaigns which display the lowest PBL among all the sampling periods (229 m MS and 169 m SPC) and almost no precipitations (1 mm Main Site and 5.2 mm San Pietro Capofiume). Such atmospheric conditions favoured the accumulation of pollutants in

the first hundred meters of the atmosphere and condensation of semi-volatile species, causing high PM episodes as shown in Figure 3.1. In addition, the low solar irradiance (~60 W m^{-2}) limited atmospheric photochemical processing of the accumulated organic precursors [Balducci et al. 2010, Belis et al. 2011, Pietrogrande et al. 2013a, Paglione et al. 2014].

These high PM values found in winter are coherent with other data registered in the Po Valley, because of the enhanced anthropogenic emissions, mainly road traffic exhausts and domestic heating, combined with stagnant atmospheric conditions characterized by low vertical mixing and cold temperatures [Bigi et al. 2011, Larsen et al. 2012, Perrone et al. 2012].
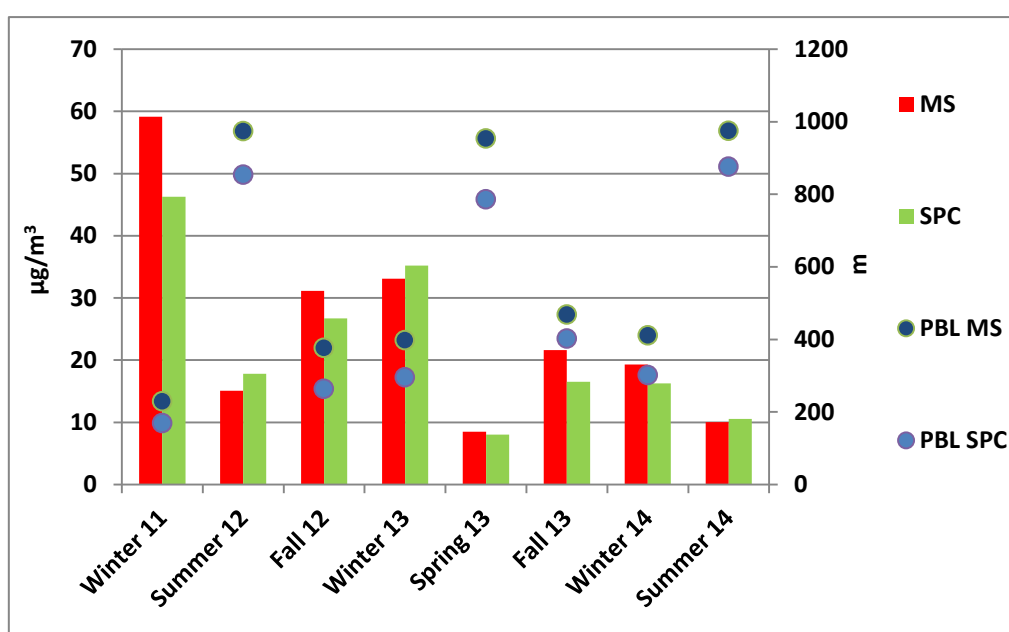
Figure 3.1. Concentrations of PM$_{2.5}$ related to PBL heights.

3.3 Polar organic fraction

3.3.1 Low molecular weight carboxylic acids

Most of the considered acids were determined in all the campaigns [Pietrogrande et al. 2014a].

It must be underlined that oxalic acid is not detectable with the used analytical procedure, and malonic acid may be somewhat underestimated because of the volatility of silyl derivatives.

The total sum of acid concentrations (total carboxylic acid concentration, TCA) was computed from the values of each analysed acid. The measured carboxylic acids (CAs)

show similar concentrations in the two sampling sites in all the campaigns (Table 3.3). They also follow the seasonal trend as for PM: higher concentrations were found during cold seasons when PBL height is minimum with concentrations ~5 times higher in fall/winter (mean value ~200 ng m^{-3}, maximum value 308 ng m^{-3} at San Pietro in winter 2011) in comparison with spring/summer (mean value ~40 ng m^{-3}, minimum value 14 ng m^{-3} at San Pietro in spring 2013).

The results obtained in fall 2013 were more similar to those obtained in spring/summer (average temperature in fall 2013 were higher than 15°C).

In June 2012, acid concentrations were ≤ LOD since low-volume air sampler (55 m^3 in a day) was used.

These results were comparable with those reported in atmospheric aerosols collected from different cities in the world (Milan, Algiers) but significantly lower than those from other megacities (Tokio, Hong Kong) [Kawamura et al. 2005, Ho et al., 2006, 2011, Ladji et al. 2009, Perrone et al. 2012].

		Main Site					San Pietro				
	oxCAs (ng/m^3)		Other CAs (ng/m^3)		%oxCAs		oxCAs (ng/m^3)		Other CAs (ng/m^3)		%oxCAs
W11	84.5 ± 41.4		177.6 ± 72.9		31.7 ± 6.0		70.2 ± 31.7		238.1 ± 205.5		25.8 ± 8.4
Su12	n.d.		n.d.		n.d.		n.d.		n.d.		n.d.
A12	74.8 ± 50.4		92.6 ± 60.0		44.0 ± 4.7		61.1 ± 47.8		53.7 ± 43.2		53.1 ± 5.3
W13	83.4 ± 43.1		165.9 ± 84.5		34.4 ± 9.9		87.7 ± 55.7		160.1 ± 90.1		34.2 ± 9.3
Sp13	11.6 ± 8.6		5.8 ± 3.5		66.0 ± 9.7		8.5 ± 4.1		5.4 ± 2.1		59.4 ± 14.8
A13	18.3 ± 8.8		31.7 ± 18.9		38.7 ± 10.1		23.0 ± 12.1		32.5 ± 23.1		45.1 ± 8.8
W14	41.5 ± 41.5		76.5 ± 57.4		36.8 ± 9.2		41.2 ± 14.4		62.4 ± 21.6		39.9 ± 5.7
Su14	58.9 ± 58.9		34.1 ± 43.0		60.9 ± 14.3		62.2 ± 57.2		36.6 ± 27.1		59.9 ± 15.1

Table 3.3. Average values and standard deviations of acids concentrations and relative contribution of oxoacids to total CA concentration.

A detailed investigation of CAs distribution profile may provide information on the origin and fate of organics in the atmosphere. In general, chain length distributions of dicarboxylic acids show a decrease of the concentration of the individual species with the increase in carbon chain length, as reported in most cities [Kawamura et al. 2005, Ho et al. 2006, Hyder et al. 2012].

Accordingly, the highest concentrations were observed for C3-C4 dicarboxylic acids with the most abundant succinic, malic, maleic and malonic as average mean for all the campaigns.

To give insight into the origin of CAs, the correlation among carboxylic acids was studied since strong correlation coefficients among these compounds may suggest a similar source or involvement in the same photo oxidation processes.

Most of the values obtained during warm periods are nicely correlated (R^2 >0.7), suggesting that the concentrations of these species are mainly controlled by the same atmospheric processes in this period. Otherwise, only a limited number of acid pairs measured in colder periods show significant correlations, which strongly suggested the combined contribution of primary emissions and secondary reactions.

As a general trend, in the seven considered campaigns, among the acids detected, succinic acid was the most correlated with the others, especially with malic, azelaic and 3- and 4-hydroxybenzoic acids (R^2 ~0.8). Only during warm period succinic acid is also strongly correlated with glutaric and adipic acid (R^2 ~0.9) and glycolic acid (R^2 ~0.8).

These results are consistent with the finding that succinic acid is originated from different sources, like the direct emissions from fuel burning and the oxidation of precursors emitted from both anthropogenic and biogenic sources.

The limited correlation between succinic (C4) and malonic (C3) acids observed in all the campaigns (R^2 =0.3-0.6) suggests that malonic acid is only in part produced from oxidation atmospheric processes, with succinic as a precursor. Even if the correlation coefficient between the two acids is low, it shows greater values in warm periods and at San Pietro. This is coherent with the higher solar irradiance in spring/summer, particularly at the rural site.

Significant amounts of azelaic acid (~9 ng m^{-3}) were found during fall/winter. This acid is believed to be produced from photo oxidation of unsaturated carboxylic acids, such as oleic and linoleic acids having unsaturation at carbon 9 position (OH oxidation should be involved in the production of C9 diacid) [Ho et al. 2006, 2011, Hyder et al. 2012]. The presence of this acid is consistent with the emission of biogenic unsaturated fatty acids from the vegetation activity, although it is limited in the cold seasons. In warmer period the concentrations of azelaic acid were often below detection limit even if vegetation activities should be favoured. This is probably due to the dilution effect given by a high planetary boundary layer.

Phthalic acid has been proposed as a surrogate for the contribution of SOA to an environmental sample, since it mainly derives from the oxidation of naphthalene and

other polycyclic aromatic hydrocarbons or phthalates. In minor quantities, it may also have origin from primary sources like biomass burning or vehicle exhaust [Oliveira et al. 2007, Ho et al. 2011].

Also adipic acid (C6) has been suggested as a product of atmospheric oxidation of anthropogenic hydrocarbons, in particular cyclohexene derivatives [Ho et al. 2006, Zhang et al. 2010, Hyder et al. 2012].

For these reasons the phthalic/C9 and C6/C9 ratios have been proposed as indicators of the impact of anthropogenic and biogenic precursors to SOA production [Ho et al. 2006, Zhang et al. 2010].

The ratios are usually larger in winter than in warm periods suggesting a higher contribution of biogenic secondary aerosol in summer/spring.

Among the oxo and hydroxyl carboxylic acids, malic acid was found the dominant marker followed by 2-ketoglutaric and glycolic.

During all the campaigns, the concentrations of malic and succinic acids as well as glutaric and 2-ketoglutaric acids showed similar temporal trend, indicating their involvement in common photochemical reactions. In fact, because of the similarity between their molecular structures, malic acid and 2-ketoglutaric acid were thought to be produced by the oxidation reaction of succinic and glutaric acid in the atmosphere [Kawamura et al. 2005].

Glycolic acid, the smallest LMWCA determined in this study, shows a great correlation with C3-C5 acids in warm periods, correlation that decreases but not disappears during winter. Since glyoxylic acid has been recognize as SOA tracer [Ho et al. 2006, Bikkina et al. 2015], this suggests that oxidation of longer chain acids and production of SOA are important phenomena all year long.

As useful markers to discriminate between primary and secondary origin of the investigated carboxylic acids, the separated contribution of hydroxyl/oxo carboxylic acids was computed as absolute (oxCAs) and relative (%oxCAs) to TCAs values.

Although the absolute data are ~2.6 times higher in fall/winter (mean value ~68 ng m^{-3}) in comparison with spring/summer (mean value ~23 ng m^{-3}), the relative values are higher in the warm seasons (%oxCAs ~62%) than in colder months (%oxCAs ~38%), with similar values at both sites.

This clear seasonal trend is consistent with enhanced photochemical oxidation in spring/summer with increasing solar radiation, as supported by the significant positive correlation ($R^2 = 0.72$) between %oxCAs and solar irradiance.

These findings highlight that the strong correlations among acids in warmer period is due to the same atmospheric oxidation they undergo. Such a trend suggests that the higher temperature and the larger solar irradiance facilitate the conversion of oxidized acids into smaller dicarboxylic acids.
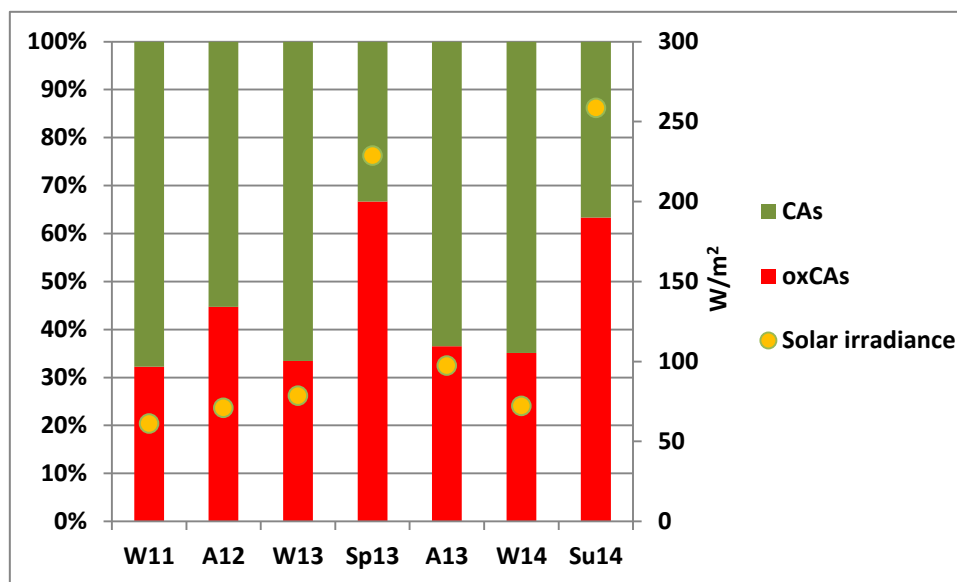
Figure 3.2. Relative contribution of polyoxidated LMW carboxylic acids related to solar irradiance.

The weekly trends of carboxylic acid concentrations was also studied in order to have a better view about the impact of various emission sources and photochemical transformations on atmospheric pollutant concentrations. In fact, day-of-week trends can be directly related to contribution of different sources from human activities, since no weekly trends were seen in meteorological properties, which usually played a major role in environment PM concentrations [Lough et al. 2006, Oliveira et al. 2007]. Since each campaign went on in general for three weeks, samples were composited by day of week at each site and three-week averages were used to investigate day-of-week trends.

As an example, in Fall 2012 a clearly dependence of CAs concentration on the day of week was observed. It increased from Monday through Friday and fell over the weekend to the lowest levels on Monday (Figure 3.3A).

This behaviour might be explained by the emission of CAs from sources with a weekly activity patterns, such as motor vehicle traffic, that are higher on weekdays [Lough et al 2006, Bigi et al. 2011].

On the contrary, in Winter 2013, the concentration of CAs showed a random pattern during the week (Figure 3.3B): this behaviour suggests that in the colder winter periods the main contribution to CAs concentration derived from civil heating that is an anthropogenic source without clear weekly pattern.

For each monitored periods, the same weekly trends were found in urban and rural sites, which further confirmed the homogeneous impact of the different sources all over the investigated area.
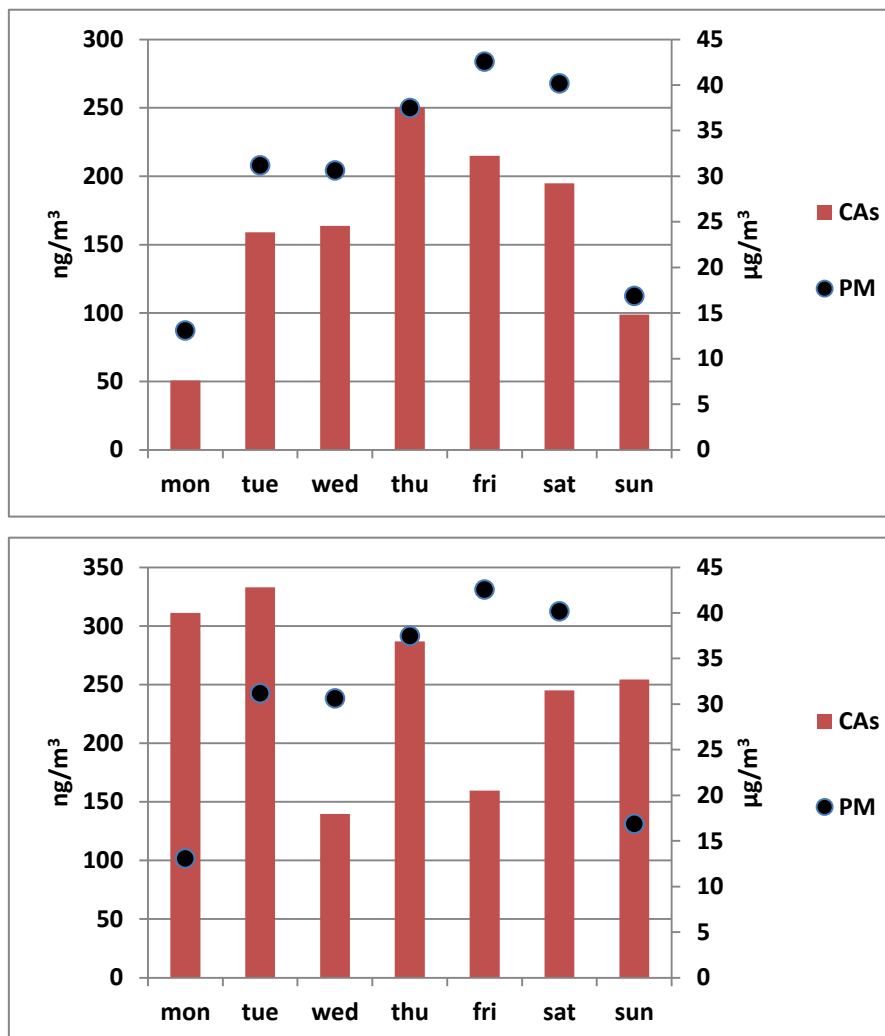
Figure 3.3. Day-of-week pattern of carboxylic acids (left axis) and PM$_{2.5}$ (right axis) concentrations in the urban MS site during fall 2012 and winter 2013 respectively [Pietrogrande et al. 2014a].

3.3.2 Sugars

Sugars were determined in PM$_{2.5}$ samples to give insight into the relative contribution of biomass burning and biogenic emissions [Pietrogrande et al. 2014b].

The individual sugar concentrations were overall summed to compute the total sugar concentrations, and separately to compute the contribution of sugars emitted by biomass burning (levoglucosan, mannosan and galactosan) and the total concentration of the primary sugars emitted by the ecosystem.

As for acids, also for sugars no great differences in concentration were registered between the urban and rural sites during the campaigns except in summer 2012 when

the amount of sugars was seven times higher at San Pietro in comparison to Bologna site.

In general, total concentration of sugars was one order of magnitude higher in cold seasons than those in summer/spring.

In fact, the highest levels were found in November 2011 with an average concentration of 1288 ng m^{-3} at MS, while the lowest concentration was observed in June 2012 still at MS with an average value of 7 ng m^{-3}.

Due to the particular meteorological conditions of winter 2011 (no precipitations and very low PBL), this campaign reached a sugar concentration values three times higher than the other colder periods (~1200 ng m^{-3} compared to 370 ngm^{-3} in autumn 2012 and winter 2013 and 400 ng m^{-3} in winter 2014).

Seasonality is evident also in sugar concentration profiles, providing information on the relative contributions of different emission sources.

Anhydrosugars were by far the dominant sugars in fall and winter (excluding fall 2013), both on a relative and absolute basis: higher levels were found for levoglucosan in fall/winter with a mean value of 454 ng m^{-3}, followed by mannosan and galactosan (mean values 65 and 31 ng m^{-3} respectively). These data specifically indicate that anhydrosugars are nearly the only source for particulate saccharides in fall/winter, comprising nearly 94% of the total sugars at both sites, while their impact strongly decreases in spring/summer when the average concentration was 24 ng m^{-3} and the relative contribution to total sugars was ~30%.

As anhydrosugars are key tracers for smoke emissions from both open and residential biomass combustion, these results indicate the relevance of biomass burning emissions as a source of atmospheric particles. This may be mainly related to wood combustion occurring in household stoves, since the use of biomass as a fuel for residential purposes is increasing in recent years, not only in rural areas but also in urban environments, as a consequence of increasing oil prices and economic crisis. This conclusion is consistent with other studies carried out in Lombardia region which demonstrated that wood burning for domestic heating is a diffuse regional source during fall and winter [Perrone et al. 2012].

Low levels and homogeneous distribution between urban and rural sites in warmer periods likely excludes a significant contribution of smoke emissions from open fires [Mazzoleni et al. 2007, Gelencser et al. 2007, Kourtchev et al. 2011, Vassura et al. 2014].

Similar anhydrosugars levels (300-500 ng m^{-3}) were measured in urban and rural areas in Central and Northern Europe and in other urban-background sites in Italy, where residential wood combustion has been identified as an important source of air pollution [Oliveira et al. 2007, Piazzalunga et al. 2011, Caseiro et al. 2012, Giannoni et al. 2012, Viana et al. 2013,].

The ambient concentration, seasonal variation, and urban/rural comparison of primary sugars were separately investigated to single out the contribution of emissions associated with primary biological particles. They have been proposed as source-specific tracers for soil biota released into the atmosphere by farmland soil suspension and natural soil erosion - glucose, sucrose and mycose - and for atmospheric fungal spore abundance, i.e., mannitol and erithrytol [Medeiros et al. 2006, Rogge et al. 2007, Tominaga et al. 2011, Jia et al. 2011, Fu et al. 2012]. In addition, these sugars are released as uncombusted materials from the biomass burning processes, emitted through direct volatilization from vascular plant saccharides or formed from the breakdown of polysaccharides i.e., glucose is commonly present at higher levels in vascular plants, while arabinose and galactose are predominant sugars in pectin, a polysaccharide contained in non-woody tissues [Medeiros et al. 2006, Jia et al. 2010, Fu et al. 2012].

Some of the sugars may also be produced by hydrolysis of the corresponding anhydrosugars under the acidic atmospheric conditions created by biomass burning [Simoneit et al. 2004, Medeiros et al. 2006].

It must be underlined that these contributions could be influenced by the fact that primary biosugars are generally more represented by the coarse than by the fine particles of atmospheric aerosol [Simoneit et al. 2004, Yttri et al. 2007, Pio et al. 2008]. Therefore, their concentrations in the present study may represent only a fraction of the total primary biologically derived carbon present in atmospheric PM.

In general, these primary sugars show nearly constant value close to 35 ng m^{-3} through the year at both the urban and rural sites.

Over all the sampling periods, sucrose was the most abundant primary sugars (9 ng m^{-3}) followed by mannitol and glucose (~6 ng m^{-3}).

The monosaccharides galactose, mannose and arabinose, the disaccharide mycose and the polyols ribitol and erythritol were also present in lower concentrations in most samples

Mannitol, ribitol, mannose, mycose are the only primary sugars that increase their concentration in warm periods in comparison to colder ones. This suggest a main biogenic origin of these sugars, likely reflecting the enhanced biogenic activity of plants

and microorganisms and agricultural activities that release soil biota from farmland soils [Simoneit et al. 2004, Tsai et al. 2013].

Mannitol has been found as the major sugar polyol in bacteria, fungi, lower plants and invertebrates, serving as storage or transport carbohydrate and cell protectant against external stresses [Elbert et al. 2007]. The highest concentration of mannitol in summer has been explained by the increased emissions from vegetation detritus and fungal spores as a result of external stress of heat [Medeiros et al. 2006, Burshtein et al. 2011]. Concentration of mannitol is strongly covaried with that of ribitol, the pentose alcohol formed by the reduction of ribose.

Mycose is the most common disaccharide in symbiotic fungal tissues, is present in a large variety of microorganisms (fungi, bacteria, yeast), higher plants and invertebrates [Simoneit et al. 2004].

Sucrose and glucose show only a slight decreasing in concentration from cold periods to warmer ones while the decreasing for erythritol, arabinose and galactose is more evident.

This suggests that the last three sugars could be mainly emitted by biomass burning which is most abundant in fall/winter while arabinose and galactose are predominant sugars in pectin, a polysaccharide contained in non-woody tissues, such as leaves and needles. Similar results were found in smoke-impacted samples in many other locations in the world [Simoneit et al. 2004, Medeiros et al. 2006, Pio et al. 2008].

The presence of not negligible amount of sucrose and glucose in winter may be related to direct volatilization during the combustion, since they are predominant sugars present at higher levels in vascular plants [Wang et al. 2011].

The obtained results highlight that wood burning is the most important source of sugars during the year.

Important correlations were identified among anhydrosugars and some carboxylic acids. Succinic and malic acids, which were the most abundant acids detected, are very well correlated with biomass burning sugars, especially during winter periods with a R^2 >0.85.

Succinic acid has been found specifically originated from wood burning, as well as the other C3-C4 diacids with similar molecular structures that are involved in common photochemical reactions of the burning products [Oliveira et al. 2007, Mazzoleni et al. 2007, Hyder et al. 2012, Alves et al. 2010].

Another surprisingly high correlation was found among biomass burning sugars and 3- and 4-hydroxybenzoic acids in cold periods with values close to 0.95 since they are produced during the pyrolysis of polysaccharides [Medeiros et al. 2006].

The data are in a good agreement with the results recently obtained by Paglione at the same site San Pietro indicating that biomass burning aerosol includes a non-negligible fraction of secondary origin, rich of carbonylic compounds and acids, in addition to a primary oxygenated component, rich of phenols and polyols [Paglione et al. 2014].

Overall, only a scattered correlation (R^2 ~0.6) was found between the concentrations of anhydrosugars and the total CAs concentration. This suggests that acids are emitted by a combination of different sources and are involved in secondary oxidation of several biogenic gases or volatile precursors, in addition to those related to biomass burning.

		Main Site				San Pietro			
	Anhydrosugars (ng/m^3)		Primary sugars (ng/m^3)		%anhydrosugars	Anhydrosugars (ng/m^3)		Primary sugars (ng/m^3)		%anhydrosugars
W11	1215.6 ± 552.8		72.3 ± 24.1		93.7 ± 2.5	1064.5 ± 443.4		65.3 ± 18.9		93.7 ± 2.0
Su12	2.3 ± 2.1		4.4 ± 5.0		46.0 ± 27.3	6.9 ± 14.2		35.6 ± 49.7		19.1 ± 18.5
A12	382.2 ± 198.7		23.9 ± 12.9		93.1 ± 4.4	303.9 ± 153.3		23.0 ± 13.8		92.3 ± 4.7
W13	354.6 ± 133.3		20.0 ± 7.5		94.6 ± 0.9	346.3 ± 151.3		18.4 ± 5.3		94.6 ± 1.2
Sp13	15.7 ± 22.3		34.5 ± 38.6		30.7 ± 14.1	4.9 ± 3.0		25.7 ± 21.3		20.4 ± 13.5
A13	47.9 ± 31.1		29.3 ± 18.7		57.8 ± 23.2	50.1 ± 33.0		25.6 ± 12.5		59.8 ± 23.0
W14	342.1 ± 140.4		30.9 ± 14.8		91.1 ± 5.3	390.4 ± 154.3		31.1 ± 15.5		92.5 ± 2.4
Su14	8.7 ± 4.3		49.9 ± 27.5		18.4 ± 14.7	7.1 ± 5.0		67.0 ± 76.4		15.7 ± 8.2

Table 3.4. Average values and standard deviations of sugars concentrations and relative contribution of biomass burning sugars to total sugars concentration.

3.3.3 Phenols

In addition to the most abundant anhydrosaccharides, a number of aromatic species carrying hydroxyl, carbonyl and carboxyl functional groups have been identified as lignin breakdown products and proposed as tracers for wood smoke pollution. They are mostly constituted by methoxyphenols arising from pyrolysis of wood lignin that is an important constituent of the macromolecular matter in wood.

The concentrations of individual considered compounds were added together to obtain the total concentration of all the investigated phenols.

Overall, each methoxylated phenol occurred at low level in the 0.1-5.8 ngm^{-3} range, yielding a total average level of ~9 ng m^{-3} through the campaigns. As a trend,

concentrations of total phenols in wintertime are two times higher yhan in warmer periods.

It must be underlined that the concentration levels of several target phenols were close to the detection limit of the analytical procedure, yielding large measurement uncertainties.

	Main Site	San Pietro
	Tot phenols (ng/m^3)	Tot phenols (ng/m^3)
W11	13.3 ± 6.2	9.7 ± 4.9
Su12	n.d.	0.4 ± 0.1
A12	14.1 ± 4.9	8.1 ± 4.1
W13	17.3 ± 9.7	18.5 ± 11.8
Sp13	1.1 ± 0.5	0.6 ± 0.4
A13	1.0 ± 0.8	0.6 ± 0.4
W14	10.9 ± 4.2	12.4 ± 6.5
Su14	11.6 ± 15.0	9.3 ± 11.1

Table 3.5. Average values and standard deviations of phenols concentrations.

For this reason the more sensible GC/MSMS method was applied after Fall 2013 campaign to assure the accurate quantification of the less abundant target tracers.

Although with much lower concentration values, the methoxylated phenols data resemble closely those of sugars, even if relative abundances of methoxy phenols were not found to have good correlation with those of biomass burning sugars. Only vanillic acid shows a notable correlation (R^2 ~0.8) in wintertime. This observation is not surprising since the two classes of biomarkers originate from distinct biopolymers - hemicellulose/cellulose and lignin -with different combustion processes [Mazzoleni et al. 2007, Kuo et al. 2011].

3.4 Apolar fraction

To further investigate pollutants present in particulate phase in the considered sites and to have a better estimation of emission sources, data obtained from polar organic fraction were integrated with those from apolar organic fraction and with carbonaceous aerosol OC and EC obtained from other laboratories participating at Supersito project [Pietrogrande et al. 2016].

3.4.1 PAHs

PAHs were investigated in $PM_{2.5}$ samples in order to elucidate the composition of the combustion emission sources, as they are emitted into the atmosphere from incomplete combustion of different fuels, such as fossil (e.g. traffic emission) as well as biomass (e.g. wood combustion emissions) and they have been frequently found in Northern Italy during the cold seasons [Piazzalunga et al. 2013, Gianelle et al. 2013, Vassura et al. 2014].

Once emitted into the atmosphere, PAHs distribute between gas and particle phases, depending on their volatile properties, with five and six ring PAHs mainly adsorbed on the particulate matter, depending on ambient temperatures [Schmidl et al. 2008, Van Drooge et al. 2012, Jedinska et al. 2014].

19 individual PAHs were quantified, including the US EPA PAH priority pollutants: naphthalene, acenaphthene, acenaphthylene, fluorene, phenanthrene, anthracene, fluoranthene, pyrene, benzo[a]anthracene, cyclopenta(cd)pyrene, chrysene (Chr), benzo[b]fluoranthene (BbF), benzo[k]fluoranthene (BkF), benzo[e]pyrene (BeP), benzo[a]pyrene (BaP), perylene, indeno[1,2,3-c,d]pyrene (IcdP), dibenzo[a,h]anthracene and benzo[g,h,i]perylene (BghiP).

As expected, PAHs showed the strong seasonal trend experienced by the other trace organics with atmospheric levels nearly 10 times higher during colder periods in comparison with the warmer months. In general, PAHs were more abundant at the urban than at the rural site that is consistent with larger direct emissions in the more populated urban location. In November-February, the total PAHs concentration was 5.7 ng m^{-3} and 4.0 ng m^{-3} at MS and SPC sites respectively with a maximum of ~13ng m^{-3} in November 2011.

In May-October, concentrations were 0.6 ng m^{-3} and 0.3 ng m^{-3} at the MS and SP sites respectively.

The higher PAHs levels in colder seasons could be explained by higher PAHs emissions, mainly related to domestic heating, and more stagnant atmospheric

conditions, resulting in atmospheric PAHs accumulation. However, besides these ambient factors, physicochemical properties, such as volatility related to the gas/particle partitioning, and reactivity with oxidants, influence the PAHs concentration.

In the present dataset, the particulate-phase PAHs distribution profiles are similar for all the samples. They are dominated by five to six ring compounds, such as benzo[b] and benzo[k]fluoranthenes and benzo[ghi]perylene followed by BaP, IcdP and Chr. In addition, fluoranthene and pyrene were among the most abundant PAHs in warmer seasons. Such PAHs distribution profiles indicate that road transport and biomass burning are the most important sources of primary emissions in the studied area, as found in other sites in the Po valley [Larsen et al. 2012, Perrone et al. 2012, Piazzalunga et al. 2013].

	Main Site	San Pietro
	Tot PAHs (ng/m^3)	Tot PAHs (ng/m^3)
W11	13.4 ± 4.9	8.0 ± 4.4
Su12	0.2 ± 0.1	0.2 ± 0.1
A12	3.8 ± 2.2	2.0 ± 1.4
W13	3.6 ± 2.5	4.3 ± 2.9
Sp13	0.3 ± 0.1	0.1 ± 0.1
A13	0.6 ± 0.5	0.6 ± 0.3
W14	2.1 ± 1.2	1.7 ± 1.1
Su14	0.1 ± 0.1	0.1 ± 0.2

Table 3.6. Average values and standard deviations of PAHs.

The set of individual PAHs showed a strong collinearity with intercorrelation values ranging from 0.7 to values higher than 0.9, especially in wintertime and at the urban site, which indicated a single dominant source for these compounds. Exception are lighter PAHs such as naphthalene, acenaphthene, acenaphthylene, fluorene, phenanthrene and anthracene that have no or very poor correlation with other heavier PAHs.

To obtain more information from this class of compounds various diagnostic ratios have been proposed to attempt source reconciliation [Alves 2008, Tobiszewski et al. 2011].

BaP/BeP and BaP/BaP+BeP ratios have been proposed as indicators of aerosol age, since both compounds are normally emitted in similar amounts by combustion sources but BaP is more reactive than BeP in the atmosphere [Oliveira et al. 2011]. It is for this

reason that a BaP/BeP ratio <1 and a BaP/BeP+BaP ratio <0.5 indicate an aged aerosol. The values obtained during sampling campaigns are usually lower than the reference values especially during spring/summer (minimum value 0.16 in spring 2013). This highlights that a certain fraction of SOA is always present in atmospheric PM even in wintertime.

Other ratios have been used more specifically to obtain information about combustion processes that originate PAHs.

IcdP/IcdP+BghiP could be useful to discriminate between fossil fuels and biomass burning. Literature values of the IcdP/IcdP+BghiP ratio are above 0.50 for grass combustion, wood soot, creosote, almost all wood and coal combustion aerosols while combustion products of gasoline, kerosene, diesel and crude oil all have ratios below 0.50, with vehicle emissions falling between 0.24 and 0.40 [Yunker et al. 2002, Tobiszewski et al. 2011]. In all sampling campaigns the calculated values are around 0.4, a value that indicates mainly a contribution from fossil fuel combustion.

On the other hand, ∑benzofluoranthenes/BghiP, another ratio proposed for combustion sources discrimination, indicates that wood burning is the major source of aerosol. A ratio of 2.18 is characteristic for wood burning, while a value of 1.6 and 0.3 are indicative for diesel and gasoline combustion respectively [Alves 2008, Li et al. 1993]. The ratio obtained for the sampling campaigns are in most part higher than 2 (lowest value 1.4 in summer 2012), therefore closer to wood combustion values.

The information deduced from PAHs ratios seem to provide conflicting results that are not very useful to understand the origin of such compounds. For these reasons another approach was developed.

In order to apportion atmospheric PAHs sources, a profile-based source apportionment was applied by comparing the abundance distributions of the measured PAHs to those of the dominant emissions, i.e., traffic and wood combustion found in literature. Although simplicity and ease of application make this approach appealing, uncertainty may affect the obtained results, since PAHs relative distribution can be greatly modified by atmospheric removal and transformation processes.

	Main Site				San Pietro			
	$\dfrac{BaP}{BaP+BeP}$	$\dfrac{BaP}{BeP}$	$\dfrac{IcdP}{IcdP+BghiP}$	$\dfrac{BFs}{BghiP}$	$\dfrac{BaP}{BaP+BeP}$	$\dfrac{BaP}{BeP}$	$\dfrac{IcdP}{IcdP+BghiP}$	$\dfrac{BFs}{BghiP}$
W11	0.52	1.10	0.44	2.19	0.47	0.93	0.46	3.05
Su12	0.42	0.73	0.34	1.45	0.38	0.63	0.41	1.42
A12	0.50	1.02	0.42	2.37	0.44	0.83	0.45	2.93
W13	0.45	0.86	0.43	2.81	0.46	0.89	0.46	3.54
Sp13	0.40	0.71	0.32	2.25	0.35	0.54	0.41	4.91
A13	0.47	0.91	0.38	2.91	0.42	0.73	0.48	3.53
W14	0.47	0.90	0.40	1.98	0.40	0.68	0.41	2.91
Su14	0.36	0.57	0.33	1.92	0.40	0.59	0.41	2.48

Table 3.7. Calculated PAHs ratios.

Concerning the contribution of traffic source, the chemical profiles of emissions from gasoline and diesel powered vehicles have been found largely influenced by several factors, including different fleet compositions, driving patterns, climate conditions and fuels composition [Saarnio et al. 2008, Jedynska et al. 2014]. A traffic profile that closely describes actual fleets of on-road vehicles in the investigated area is desirable but given the lack of such experimental profile for Emilia Romagna region, a traffic source profile derived from literature data considering several urban areas was used [Miguel et al. 1998, Marr et al. 1999, Wingfors et al. 2001, Perrone et al. 2012]. The calculated traffic profile showed a prevailing contribution of lighter PAHs as fluoranthene and pyrene but also high amount of indeno[1,2,3-cd]pyrene.

Regarding PAHs profiles from biomass combustion sources, a large variability was found potentially related to differences in the type of wood combusted and stove used as well as in the burning conditions, i.e., rates, air dilution, and moisture content in the fuel [Szidat et al. 2006, Mazzoleni et al. 2007, Herich et al. 2014, Goncalves et al. 2011].

Therefore, as for traffic, site-specific source profiles are needed for an accurate description of local emissions, taking into account both the wood species burnt and the type of appliances in use. Unfortunately, this information was unknown for Emilia Romagna region, thus, a representative profile derived from several literature sources was utilized [Rogge et al. 1998, Schauer et al. 2001, Fine et al. 2001, 2004, Hays et al. 2003, Orasche et al. 2012]. The profile is dominated by benzofluoranthenes and benzo[a]pyrene.

In order to investigate the impact of the two main sources to ambient PAHs, the correspondence between the experimental PAHs distribution and source profile was estimated by intercorrelation values (Figure 3.4).

In most campaigns, the measured PAHs show a significant collinearity ($R^2 \geq 0.7$) with wood burning emissions profile, excluding summer 2012 and summer 2014 ($R^2 < 0.5$).

The PAHs more specifically related to traffic source demonstrate poor correlation with data obtained during the sampling campaigns but the correlation slightly increase in warmer periods up to an R^2 value of ~0.5 in summer 2012. The higher correlation values were found at the urban site, consistently with the direct impact of traffic emissions, associated with vehicles transport inside Bologna city and close to major roads. The contribution of such a local source decreases and combines with other emission sources by moving away from the city to SPC (30 km far).

Not surprisingly, these findings suggest that measured PAHs distributions are composite profiles of the two investigate sources, with higher contribution of biomass burning, mainly during winter.
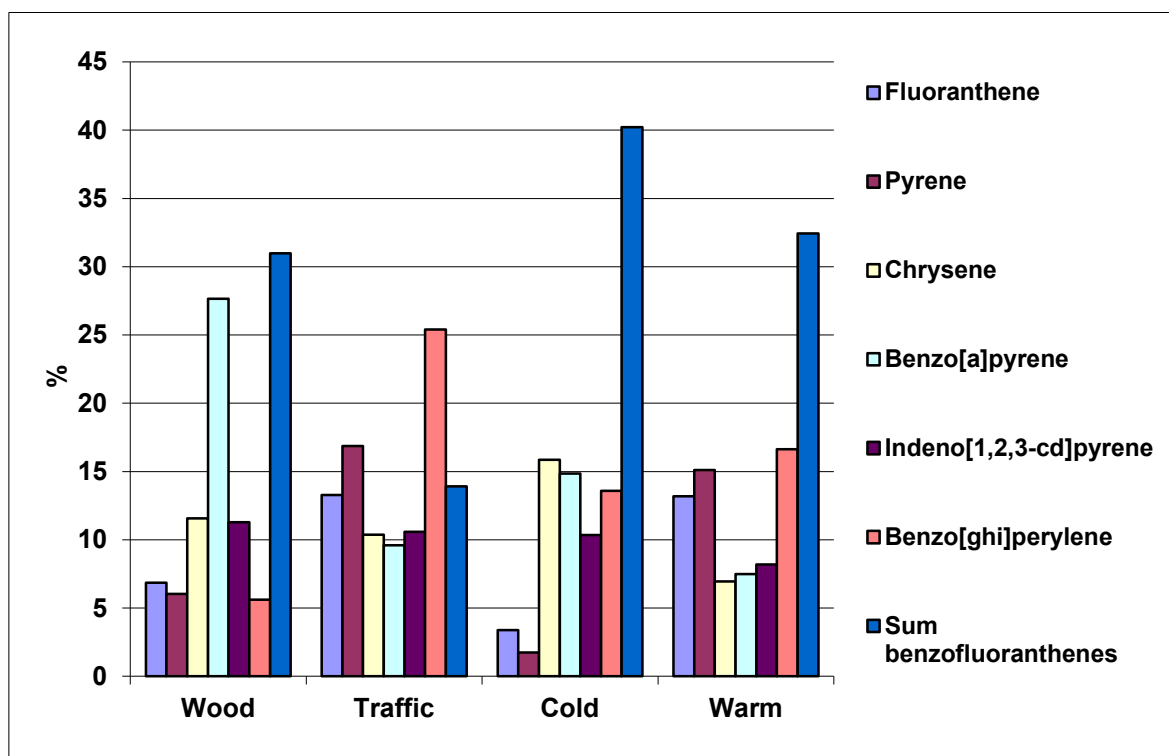
Figure 3.4. Comparison among PAHs sources and registered profiles at the two sampling sites [Pietrogrande et al. 2016].

3.4.2 n-alkanes

In order to further investigate the contribution of biogenic emissions, the study was extended to n-alkane homologous series, suited for discriminating between the contribution of biogenic and anthropogenic sources [Zheng et al. 2002, Jia et al. 2010, Pietrogrande et al. 2010].

These compounds are emitted into the atmosphere by a large variety of sources, including biogenic sources from epicuticular waxes of vascular plants, anthropogenic combustion of fossil fuels and resuspension of deposited material from these sources. A specific bio signature can be identified for n-alkanes emitted from primary biogenic sources, since they reflect the biochemical specificity of the biosystem metabolism characterized by higher concentrations of C_{29}-C_{31} terms with a strong odd carbon number predominance [Standley et al. 1987].

In this study the C_{14}-C_{40} terms of n-alkane series were investigated, as the most commonly found in atmospheric PM [Standley et al. 1987, Zheng et al. 2002, Jia et al. 2010].

The concentrations of each C_{14}-C_{40} term were added together to obtain the total alkanes content in $PM_{2.5}$ samples. It must be underlined that the reported values may represent only a fraction of the total n-alkanes, since the n-alkanes emitted from biological sources may concentrate more in the coarse than in the fine fraction of atmospheric aerosol [Simoneit et al. 2004, Wang et al. 2011, Fu et al. 2012].

The most aboundant alkanes were in the range C_{22}-C_{33} with higher and lower mass compounds concentrations usually below 1 ng m^{-3}.

Considering all the sampling campaigns, the average concentration was similar at both sites (~40ng m^{-3} at the rural site and ~44ng m^{-3} at the urban site) but seasonal trends were different. While concentrations at MS showed only slight different between warm and cold periods (40 and 48 ng m^{-3} respectively), at rural site winter concentration is five time higher than summer/spring concentration (60 ng m^{-3} versus 12 ng m^{-3} respectively).

The CPI parameter was computed using the traditional procedure that considers C_{20}-C_{33} n-alkane to describe their abundance distribution [Bray et al. 1961].

All the campaigns show a CPI index higher than unity except in summer 2014 at the urban site which exhibits a very low index of 0.23.

Excluding this value, the CPI ranges from 1 registered in winter 2014 at main site to ~15 at San Pietro in spring 2013.

Mean values in fall/winter periods and spring/summer periods were 1.6 and 2.3 at urban site respectively and 2.0 and 7.0 at rural site respectively.

The large difference between CPI values in warm periods between the two sites could be explained by the major biogenic activity of plants at San Pietro which yields maximum emissions during the vegetative season.

This conclusion is also supported by the predominance of C_{29} and C_{31} terms at the rural site, typical alkanes originated from plant wax.

The pronounced plant wax signature is a good indication of the predominance of biogenic sources from terrestrial higher plants and supports the results obtained from primary sugars on the dominating role of primary biogenic emissions during warm periods.

At urban site no predominance alkanes were identified highlighting that anthropogenic emissions have a major impact in Bologna city.

In conclusion, alkanes data show that anthropogenic emissions are dominant in almost all the considered periods since CPI is usually below 3, reference value to discriminate biogenic emissions from combustion emissions.

	Main Site				San Pietro			
	Sum alkanes (ng/m^3)		CPI		Sum alkanes (ng/m^3)		CPI	
W11	100.6 ± 44.5		1.8 ± 0.2		86.3 ± 45.3		1.7 ± 0.2	
Su12	10.4 ± 5.1		1.3 ± 0.4		27.1 ± 19.2		1.8 ± 0.5	
A12	27.0 ± 17.7		2.0 ± 0.5		112.1 ± 367.0		3.6 ± 3.4	
W13	40.5 ± 19.4		1.3 ± 0.3		29.6 ± 27.2		1.4 ± 0.5	
Sp13	15.8 ± 3.4		5.7 ± 3.2		4.8 ± 1.0		15.3 ± 9.1	
A13	96.1 ± 72.7		1.0 ± 0.6		15.8 ± 11.3		2.2 ± 0.5	
W14	23.7 ± 16.6		1.1 ± 0.4		18.0 ± 16.0		1.1 ± 0.4	
Su14	7.5 ± 3.5		0.2 ± 0.1		14.2 ± 14.2		3.7 ± 2.9	

Table 3.8. Average values and standard deviations of n-alkanes concentrations and CPI.

3.5 Carbonaceous aerosol

In the framework of the Supersito project, the characterization of the carbonaceous aerosol into organic (OC), elemental (EC) and total carbon (TC) was performed, as generic indicator of air quality and source apportionment. Data concerning EC and OC characterization are reported in Pietrogrande et al. 2016. For the first campaign in November 2011, only TC values are available, due the lack of unbiased discrimination between OC and EC [Costa et al. 2016].

As expected, at both sites, the carbonaceous components show the highest levels during the November-March periods that decrease in the May-June months. In fall/winter, TC values ranged from a highest of 11.9 μg m^{-3} in November 2011 at MS to a lowest of 5.5 μg m^{-3} in February 2014 at SP, with an average of 9.1 μg m^{-3} and 7.6 μg m^{-3} at MS and SP respectively. In spring/summer, TC values ranged from 4.8 μg m^{-3} in June 2012 at the urban site to 1.8 μg m^{-3} in May 2013 at San Pietro, with an average of 3.6 μg m^{-3} and 2.9 μg m^{-3} at MS and SP respectively.

Accordingly, OC and EC concentrations exhibit the same seasonality. The highest concentrations of OC are in all cases observed during the cold periods (an average of 6.2 μg m^{-3} and 5.9 μg m^{-3} at Bologna and San Pietro respectively) and the lowest in the warm months (an average of ~2.7 μg m^{-3} at both sites). The highest EC levels were in fall/winter (average values of 1.9 μg m^{-3} and 1.1 μg m^{-3} at urban site and rural site respectively) in comparison with spring/summer (average values of 0.8 μg m^{-3} and 0.4 μg m^{-3} at Bologna and San Pietro, respectively). In October 2013, the values for TC, EC and OC show halfway values between warm and cold periods (6.0, 4.3 and 1 μg m^{-3} respectively), accordingly to meteorological conditions.

Although the spatial homogeneity of OC data, significant differences were found for EC values with higher levels at the urban site MS than at San Pietro. The mean enrichment factor ranges from 1.6 in fall/winter up to 2.1 in spring/summer.

This behaviour reflects the strong impact on EC of primary emissions from local traffic or residential heating, in contrast to OC, which is emitted by a much larger number of source types [Szidat et al. 2006, Kourtchev et al. 2011, Sandrini et al. 2014]. The same urban/rural discrimination of EC levels was observed in other sites in the Po valley, with high levels encountered at urban background sites decreasing when moved to rural areas [Sandrini et al. 2014].

	Main Site			San Pietro		
	TC (µg/m³)	OC (µg/m³)	OC (µg/m³)	TC (µg/m³)	OC (µg/m³)	OC (µg/m³)
W11	11.9 ± 3.0	n.d.	n.d.	8.6 ± 3.2	n.d.	n.d.
Su12	4.8 ± 1.0	3.7 ± 0.8	1.0 ± 0.4	4.4 ± 1.0	3.8 ± 1.0	0.7 ± 0.2
A12	9.6 ± 4.2	6.9 ± 3.8	2.4 ± 1.2	6.0 ± 1.4	4.9 ± 1.2	1.1 ± 0.2
W13	9.2 ± 2.7	7.2 ± 2.0	1.9 ± 0.8	10.2 ± 3.9	8.3 ± 3.6	1.4 ± 0.3
Sp12	2.9 ± 0.9	2.0 ± 0.6	0.9 ± 0.4	1.9 ± 0.5	1.5 ± 0.4	0.3 ± 0.1
A13	6.3 ± 2.9	3.7 ± 1.9	1.1 ± 0.4	5.7 ± 1.4	4.9 ± 1.3	0.8 ± 0.2
W14	5.9 ± 2.4	4.6 ± 2.1	1.3 ± 0.5	5.5 ± 2.1	4.6 ± 1.8	0.9 ± 0.4
Su14	3.1 ± 1.7	2.6 ± 1.5	0.6 ± 0.3	2.5 ± 1.1	2.3 ± 1.0	0.3 ± 0.1

Table 3.9. Average values and standard deviations of TC, OC and EC.

The relationship between OC and EC was evaluated to give useful information to discriminate between different sources and processes of PM. In fact, significant correlation of OC vs. EC commonly indicates dominance of the primary carbon emissions compared with photochemical activity, since EC is mainly representative of primary OC [Alves et al. 2010, Bautista et al. 2014].

In general, the whole dataset shows significant correlation between OC and EC measured values, with good correlation for data collected at the rural site (R^2 ~0.75), but only weak (R^2 ~0.5) for those at the urban site (Figure 3.5).

More scattered data in the more populated site may be related to the occurrence of concomitant contribution of different local emission sources and also by the lower accuracy of the OC/EC discrimination using the TOT measurement of the highly loaded PM filters collected in the urban area [Costa et al. 2016].

The OC to EC ratio was computed and compared to some literature data in order to obtain information about emission sources. The OC/EC ratios range from 2.55 in spring 2013 at Main Site to 9.11 obtained in summer 2014 at San Pietro. A clear spatial discrimination is observed, with OC/EC values in general higher at the rural site, which is less impacted by EC emission sources, in particular related to traffic.

OC/EC ratio from fossil fuel burning is frequently lower than 1 (OC/EC ~0.7), while residential wood burning is expected to release more organics (OC/EC ≥ 9) [Alves et al. 2010, Pio et al. 2011; Giannoni et al. 2012; Bautista et al. 2014].
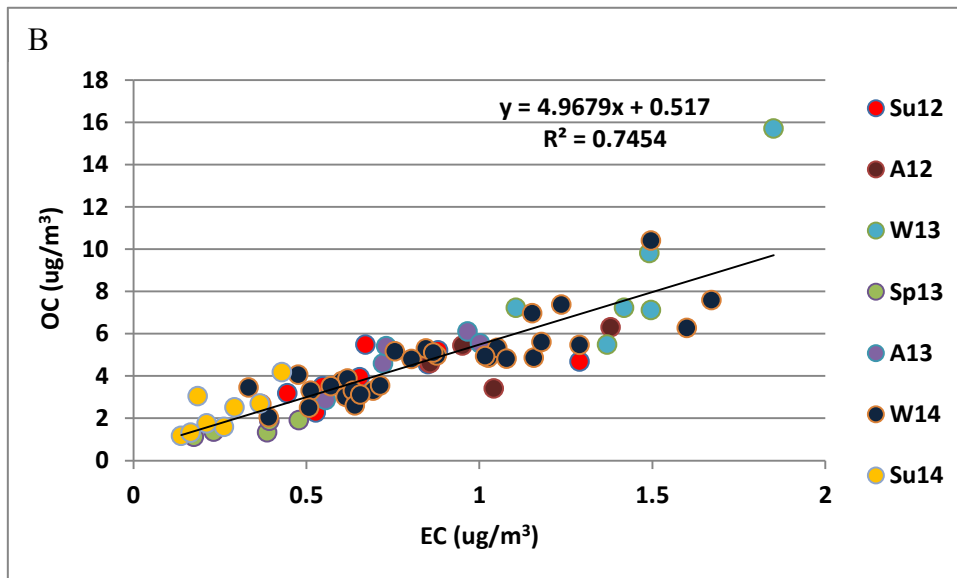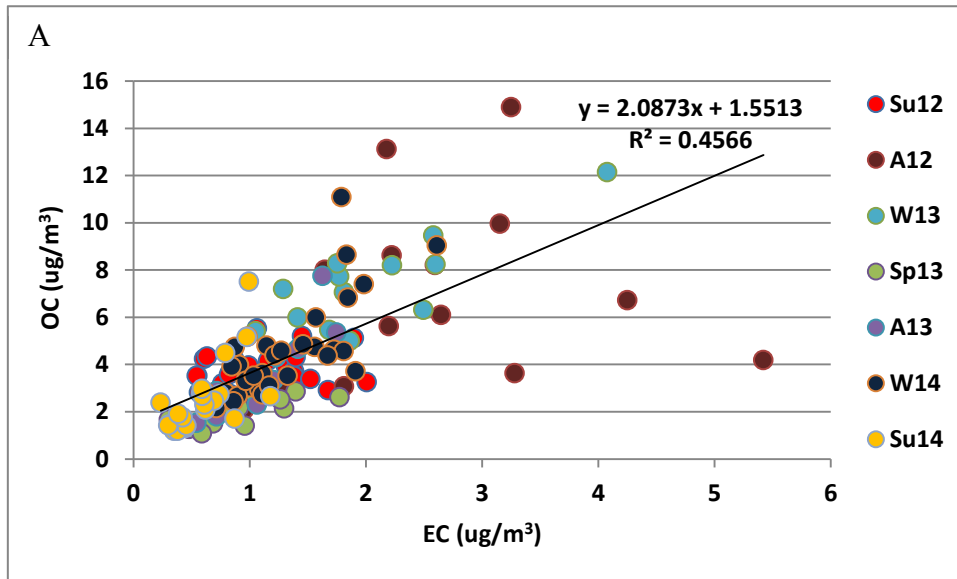
Figure 3.5. Correlation between OC and EC at A) urban site and B) rural site [Pietrogrande et al. 2016].

The obtained results, with OC/EC always above 1, highlight that traffic slightly affects the two sites in comparison with other sources, especially at rural site. This result may indicate that in the investigated atmosphere there is a constant input of OC added to the fossil fuel transport emission, presumably generated by biomass burning during winter and biogenic activity in warmer periods.

3.5.1 Secondary OC estimation

To give deeper insight into carbonaceous fraction knowledge, the discrimination between primary (OC_{prim}) and secondary OC (OC_{sec}) was attempted. The issue is a difficult task because of the still limited knowledge of OC molecular composition,

atmospheric processes and characteristic emission profiles [Szidat et al. 2006, Gelencester et al. 2007, Gentner et al. 2012]. With the current lack of an experimental method to directly measure OC_{prim} and OC_{sec} fractions, indirect methods are usually employed based on the observed concentrations of total OC and EC. A common and very simple method to estimate secondary OC is based on the assumption that the minimum OC/EC ratio of the dataset represents samples containing exclusively primary OC and only negligible secondary OC from atmospheric oxidation processes [Cabada et al. 2004, Pio et al. 2011, Day et al. 2015]. This minimum ratio is then multiplied with individual EC value (that is emitted exclusively as primary pollutant) to get primary OC and this value is then subtracted from the corresponding total OC to determine OC_{sec} value, according to the following equation:

$$OC_{sec} = OC - EC \left(OC/EC \right)_{min}$$

In order to reduce subjectivity in the fitting and removal of outliers, data are grouped by season and location. At the urban site the computed $(OC/EC)_{min}$ values were 1.6 and 1.8 in cold and warm periods, respectively and at San Pietro were 3.2 and 4.4 in the two periods.

Secondary OC values were estimated for each campaign both as absolute and relative basis (OC_{sec}%). Although the absolute OC_{sec} values show the same seasonal trend of the other carbonaceous components, with higher values in fall/winter than in spring/summer (on average, ~2.9 µg m^{-3} and ~1 µg m^{-3} respectively), the percentage contribution OC_{sec}% is nearly constant across the year: 47% at MS and 30% at SP (Table 3.10).

The obtained results are unexpected and in contrast with those obtained from carboxylic acids since a seasonal trend would be expected with higher OC_{sec}% contribution in spring/summer, as a consequence of the stronger solar irradiance and higher temperatures that lead to increasing oxidation. Another surprising result concerns spatial distribution, since secondary processes are presumed stronger at the rural site that is less impacted by local emission sources, mainly traffic.

It is noteworthy that the computed values may be affected by the large uncertainty of the used approach, which was found to overestimate the OC_{prim} and underestimate OC_{sec} components, as a consequence of bias in estimating $(OC/EC)_{min}$ ratios from open air measurements of OC and EC. In fact, data from LMW carboxylic acids highlight that secondary components are always present in atmosphere even in wintertime when solar irradiance and thus photo oxidation are limited.

	Main Site		San Pietro	
	OC_{sec} $(\mu g/m^3)$	$OC_{sec}\%$	OC_{sec} $(\mu g/m^3)$	$OC_{sec}\%$
W11	n.d.	n.d.	n.d.	n.d.
Su12	2,1 ± 0,8	57,5 ± 13,2	1,5 ± 0,7	38,5 ± 10,4
A12	5,3 ± 3,7	73,4 ± 9,9	2,0 ± 0,3	36,6 ± 7,5
W13	2,3 ± 1,1	32,1 ± 14,6	3,5 ± 2,9	33,6 ± 14,9
Sp13	0,7 ± 0,4	37,2 ± 19,6	0,5 ± 0,1	31,7 ± 14,6
A13	1,4 ± 1,2	31,7 ± 12,7	1,0 ± 0,5	18,6 ± 9,6
W14	2,1 ± 1,5	42,8 ± 13,1	1,3 ± 0,9	28,1 ± 14,0
Su14	1,5 ± 1,2	51,8 ± 15,4	0,8 ± 0,6	32,5 ± 14,7

Table 3.10. Average values and standard deviations of calculated OC_{sec} and relative contribution to OC.

For these reasons, the use of LMW carboxylic acids seems to be a proper parameter suitable for estimating the relative contribution of SOA production, providing more reliable data than $OC_{sec}\%$ based on $(OC/EC)_{min}$.

3.6 Source apportionment using PCA

To summarize the huge amount of data obtained in the framework of the Supersito project, Principal Component Analysis (PCA) was applied as a descriptive tool for source apportionment, even if Positive Matrix Factorization (PMF) could be used as quantitative tools. Principal component analysis is a way to represent multidimensional data, identifying patterns among them and expressing them in order to highlight their similarities and differences. Since patterns in data of high dimension can be hard to display, PCA is a powerful tool for analysing data.

It is a statistical procedure used to represents an n-dimensional data structure in a smaller number of dimensions, usually two or three. A reduction to a smaller number of dimensions means the determination of some axes in which the data points must be projected from the n-dimensional space. In practice, PCA consists of a rotation of original data in order to obtain new axes that preserve as well as possible the data structure originally presents in the n-dimensional space and this means that they must maximize variation along the lines and minimize variation around them. So, first principal component is selected in order to explain as much variation as possible, the

second one must be orthogonal to the first and must explain as much variation as possible of that left unexplained by the first principal component and so on [Todeschini 1998].

Principal components are thus a linear combination of variables of the original dataset. The coefficients of the original variables for a principal component are called loadings. The higher the loading of a variable on a principal component, the more the variable has in common with this component. The loadings can be interpreted as correlations between the variables and the components. Small values indicate a weak contribution of a variable to a principal component. The value taken by an object for a principal component is called the score of the object for this principal component.

It is theoretical possible to determine a number of principal components equal to the number of original variables but usually the first few principal components explain an important part of the total variations [Massart et al. 1988].

PCA of the data from Supersito project is in progress, thus data presented afterwards are just preliminary. The whole dataset of eight monitoring campaigns was grouped seasonally due to the strong dependence on meteorological conditions found for the data. Each parameter was normalized by the PM amount in order to retain only information on chemical composition independently of concentration level. From the total number of parameters some were selected as descriptive for different specific amission sources and atmospheric processes. Thus, PCA was performed with 13 parameters. Some carboxylic acids were considered as representative for SOA contribution, sugars were classified in anhydrosugars, which account for biomass burning, and primary sugars mainly emitted from biogenic activities. Moreover, BaP and PAHs wereconsidered as parameters representative for combustion sources while lighter alkanes (C_{14}-C_{24}) are representative for traffic sources and even alkanes for higher plant emissions.

The results of PCA applied to data collected in winter campaigns are reported in Figure 3.6A. The first Principal Component (PC1 in Figure 3.6A), that explains more that 30% of the total variance, is mainly loaded by variables representing traffic, biomass burning and SOA, with different trends between the two sites. Anyway, the considered carboxylic acids representing SOA show a very good correlation with anhydrosugars at both sites, suggesting that SOA is mainly originated from emissions from wood burning. The second Principal Component (PC2 in Figure 3.6A), that explain more that 21% of the total variance, is mainly loaded by PAHs and traffic, with similar pattern at both sites. In general, these 2 PCs don't show a net discrimination among the different

campaigns winters, as it is shown by the overlapping pattern of score values of the different campaings, i.e., W4 (January-February 2013) and W7 (February 2014), in the score plot of PC2 vs. PC1 reported in Figure 3.6A.

Figure 3.6B shows PCA results for fall campaigns. The first Principal Component explains about 40% of the variance and is characterized by high loads of variables representing biomass burning and traffic sources with minor amount of carboxylic acids and it is similar between the two sites. PC2, that explain around 20% of the total variance, is mainly loaded by SOA and traffic indicators, with different patterns at the two sites. In fact, it is dominated by lighter alkanes and some derived SOA (2-ketoglutaric acid) at main sites while at rural site the main contribution is given by glycolic and malic acid, tipically SOA indicators. In fall periods PCs display some differences among the campaigns. F1 data (November-December 2011) have high scores on PC1, indicating high contribution of biomass burning. On the contrary F6 (October 2013) shows high scores on PC2 due to a major contribution of secondary aerosol. In fact, this period was more similar to a late summer with respect to colder periods, considering meteorological parameters. F3 data (October-November 2012) show an halfway behaviour between the other autumn periods.

Considering summer periods, PC1 explain around 40% of the total variance and is highly loaded by carboxylic acids, primary sugars and alkanes and the trends are similar at both sites. On the contrary, PC2 is characterized mainly by BaP and PAHs and account for more than 20% of the variance. This PC shows different trends between the two sites since at San Pietro some SOA indicators display high loads in addition to PAHs. The PC1 vs PC2 score plot (Figure 3.6C) shows that S8 data (May-June 2014) with higher PC1 scores suggesting a major contribution of SOA with respect to S2 (June-July 2012) and S5 (May 2013) that have a similar behaviour.

In conclusion, a strong seasonality of different sources was seen with a major contribution of biomass burning as primary (anhydrosugars) and secondary (carboxylic acids) emissions in colder periods and an increasing importance of secondary aerosol and biogenic activities in warmer months.
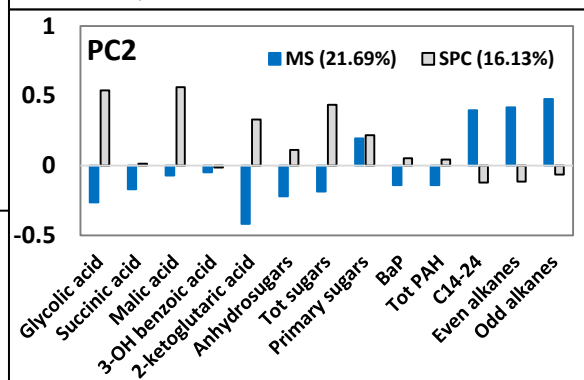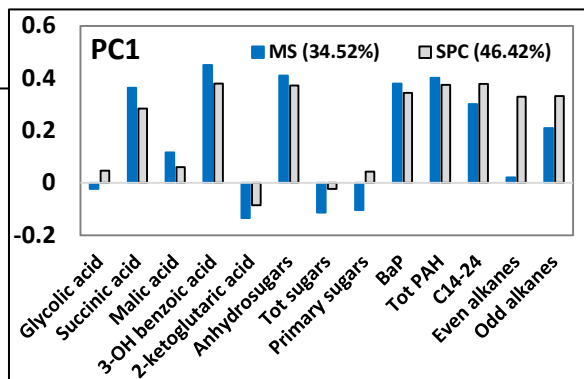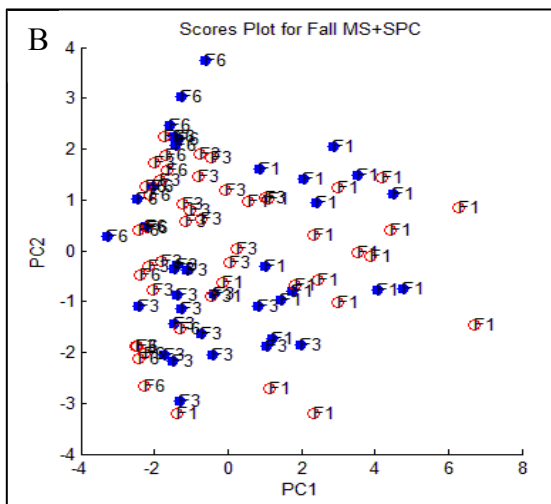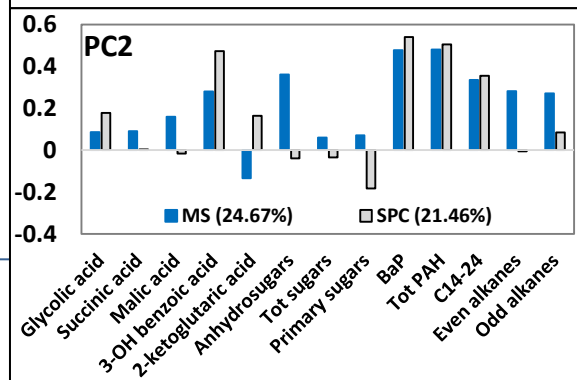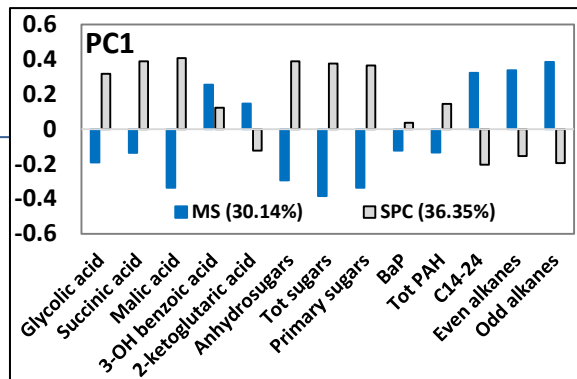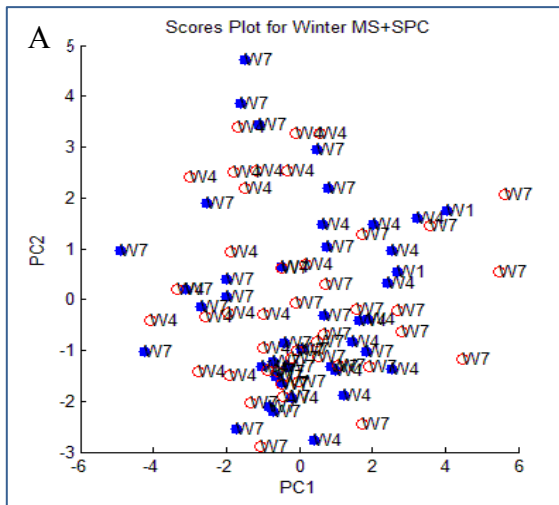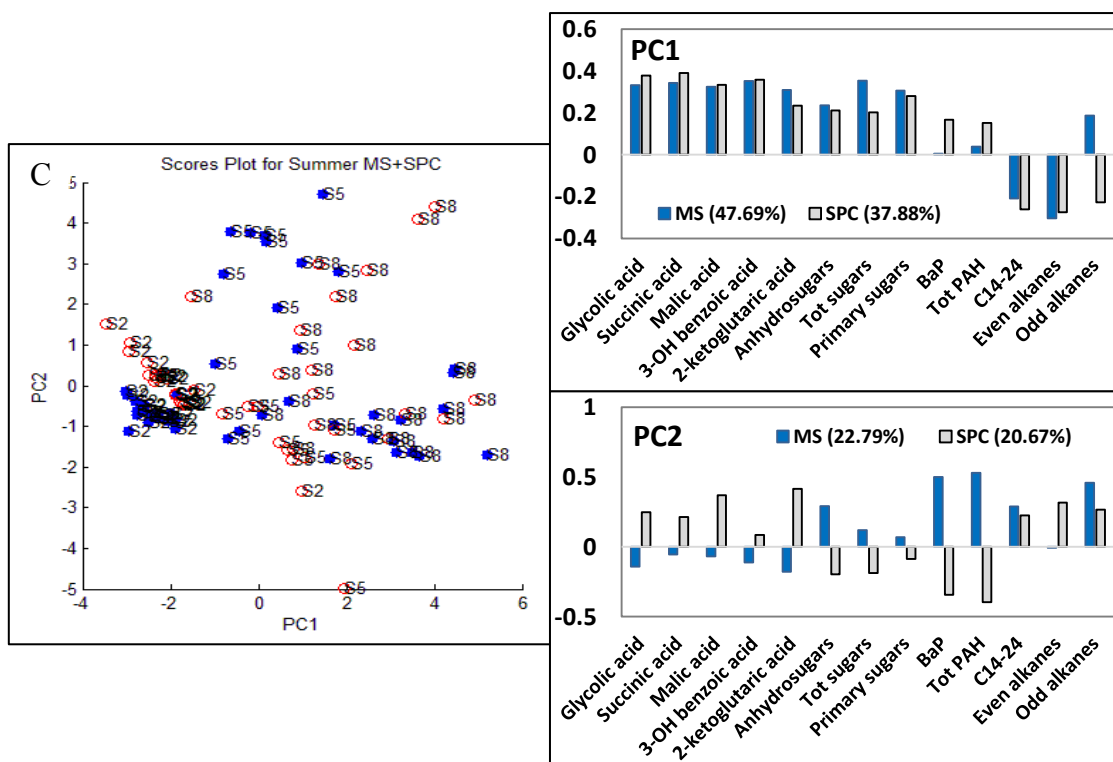
Figure 3.6. Scores and loadings plots for the datasets of A)Winter (W), B) Autumn (F) and C) Summer (S) campaigns at both sites. W4 January-February 2013; W7 February 2014; F1 November-December 2011; F3 October-Novembre 2012; F6 October 2013; S2 June-July 2012; S5 May 2013; S8 May-June 2014.

3.7 Summary

More than one hundred compounds were taken into account to estimate sources and origin of particulate matter.

Even if a great number of substances were determined, they represent only 7% in mass of OC. This means that a very large part of organic fraction of PM is still unknown.

Seasonal concentration trends of all compounds are directly linked to meteorological conditions, mainly planetary boundary layer height and precipitations.

Low PBL depths and weak amount of wet depositions favour pollutants accumulation as can be clearly seen during winter 2011. A large increment in wet depositions and a slightly increase of PBL height lead to a reduction of pollutants level of approximately three times (Fall 2012, Winter 2013 and Winter 2014 in comparison to Winter 2011).

In spring/summer periods, the enhancement of PBL height together with the decreasing emissions from domestic heating cause a sharp decrease in analytes concentrations.

Regarding the relative contribution of each class to the total amount of determined compounds, cold periods are dominated by anhydrosugars that represent at least 50% of the total mass (Figure 3.7).
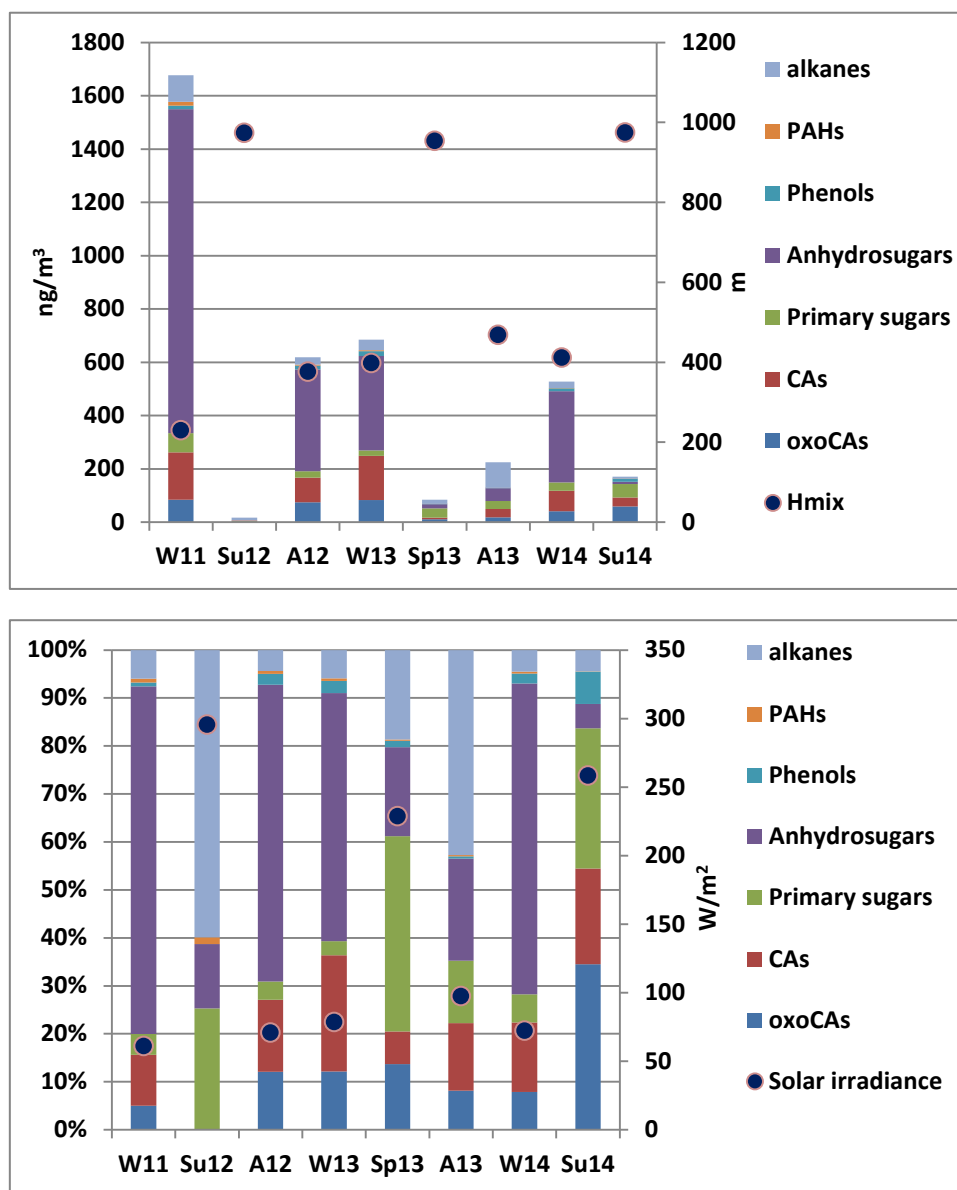
Figure 3.7. Concentrations and relative distributions of each class of compounds related to meteorological parameters.

Primary sugars contribution is related to temperature and solar irradiance, probably due to the enhanced biogenic activity stimulated by these two factors. In fact, in warmer periods they account for about 30% of the determined compounds at Main Site and for about 50% at rural site.

Also polyoxidated carboxylic acids show an increasing contribution in spring/summer periods likely due to the oxidizing conditions of the atmosphere.

Among the many information extracted from the whole dataset of analysed compounds, the most impressive is that wood combustion seems to be the major source of organic compounds during cold periods.

This finding is in agreement with data found in neighbouring regions [Gilardoni et al. 2011, Piazzalunga et al. 2013] and point out that the impact of residential wood combustion is globally much higher than assumed in the past, especially during winter season, when the domestic burning of wood logs, briquettes, chips and pellet represents an important renewable energy source [Bernardoni et al. 2011, Perrone et al. 2012, Viana et al. 2013, Fountoukis et al. 2014]. In fact, numerous studies have demonstrated that emissions from biomass combustion in domestic appliances are significant contributors of the total $PM_{2.5}$ and PM_{10} emitted, and these particles may contain numerous toxic/carcinogenic components with a potentially high impact on human health [Oliveira et al. 2007, Perrone et al. 2013, Piazzalunga et al. 2013].

In light of these results a more detailed study on wood combustion contribution to wintertime atmospheric aerosols in Emilia Romagna region was carried out.

4. CONTRIBUTION OF WOOD COMBUSTION

Among the huge amount of data collected in the framework of the Supersito project, specific attention has been focused to investigate the contribution of wood combustion to atmospheric emissions. In fact, in recent years, the use of biomass as energy source has become increasingly important thanks to the assumption of carbon neutrality. Biomass and in particular wood used as fuel are considered renewable energy sources and CO_2 neutral combustibles. Global warming has point out the need to reduce greenhouse gases emitted from human activities. Under this light, biomass has a special appeal since it does not contribute to the net emission of CO_2. During the combustion it emits only CO_2 fixed by photosynthesis during it life so that lifecycle of carbon dioxide released by biomass combustion is of some years. On the contrary, fossil fuels emit carbon dioxide fixed in remote geological ages and thus lifecycle of this kind of CO_2 could potentially be of millions of years.

Furthermore, the economic crisis began in 2008 has moved people habits regarding residential heating toward the use of cheaper fuels as wood. Another important perspective regarding biomass is the tax treatment it undergoes. In fact, while fossil fuels and electric energy are subject to manufacture taxes and VAT (22%), biomass is not susceptible to excises and for domestic heating the VAT value is 10% excluding pellet VAT recently increased to 22%. These considerations are valid only for "formal" sales but, as shown in Figure 4.1, they represent only the minor part of the total market.

In the framework of the European policy related to climate change contrast, Directive 2009/28/CE considers as a priority the increase in renewable energy sources use. Regarding biomass, the main legislative instruments to support the use of this kind of fuel contemplate incentives for biomass stoves, fireplaces and boilers (D.M. 28 December 2012).

This has led to a significant increase in the consumption of woody biomass.

The results obtained highlight that biomass burning is one of the main anthropogenic emission sources of PM and chemical compounds in the atmosphere.

Policy assessments and energy-environmental goals prescribed by European Union neglect the contribution of biomass burning to the emission of pollutants different from CO_2 and the consequent effects on air quality.
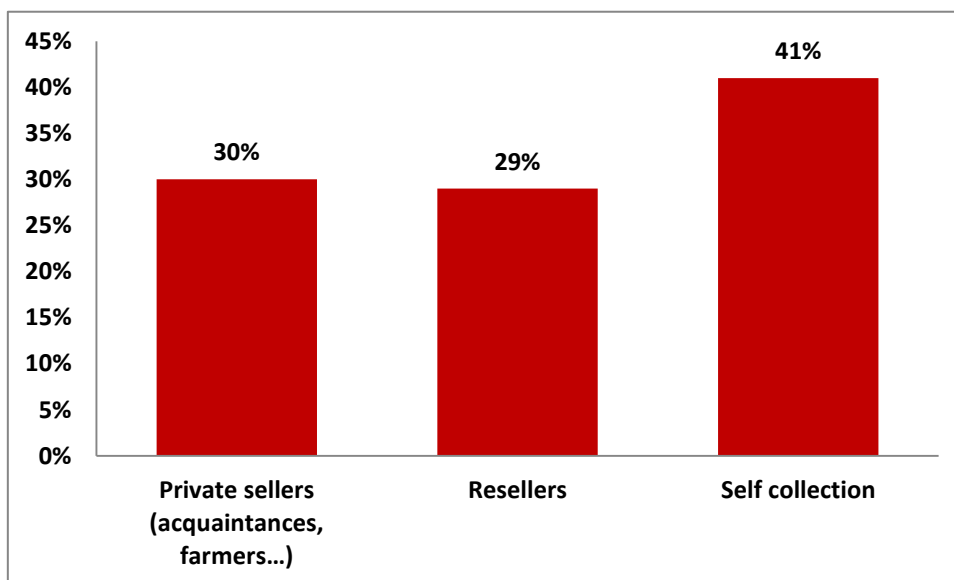
Figure 4.1. Firewood supply mode [Deserti et al. 2011].

4.1 Type of burned wood

4.1.1 Anhydrosugars

Dehydrated monosaccharides such as levoglucosan and its isomers (mannosan and galactosan) are of particular interest because they are exclusive thermal degradation products of cellulose/hemicellulose and have been found in significant level in chars and smokes from combustion of different plant species [Simoneit et al. 1999, 2002]. The proportional yield of levoglucosan to its isomers further permits combustion source discrimination (e.g. softwoods vs. hardwoods) [Ward et al. 2006, Schmidl et al. 2008, Fabbri et al. 2009]. These anhydrosugars have been widely used as qualitative markers of biomass combustion in atmospheric particulate matter [Caseiro et al. 2009, Mochida et al. 2010]. The ratios between the concentrations of anhydrosugars (L/M and M/G) have been utilized as useful diagnostic indicators for the possible biomass burning categories [Ward et al. 2006, Puxbaum et al. 2007, Fabbri et al. 2009, Alves et al. 2010, Kuo et al. 2011, Piazzalunga et al. 2011]. For example, differences in the L/M ratio in smokes from softwoods and hardwoods/grasses can help discriminate between inputs from these combustion sources to the atmosphere. It has been found that generally smoke samples from conifer wood have an average L/M ratios in the range of 2-6, while emissions from hardwoods exhibit ratio values higher than 10 and the L/M ratios of some herbaceous tissues may reach as high as 50 [Fine et al. 2001, 2002, 2004, Ward et

al. 2006, Puxbaum et al. 2007, Engling et al. 2009, Fabbri et al. 2009, Alves et al. 2010, Kuo et al. 2011, Piazzalunga et al. 2011].
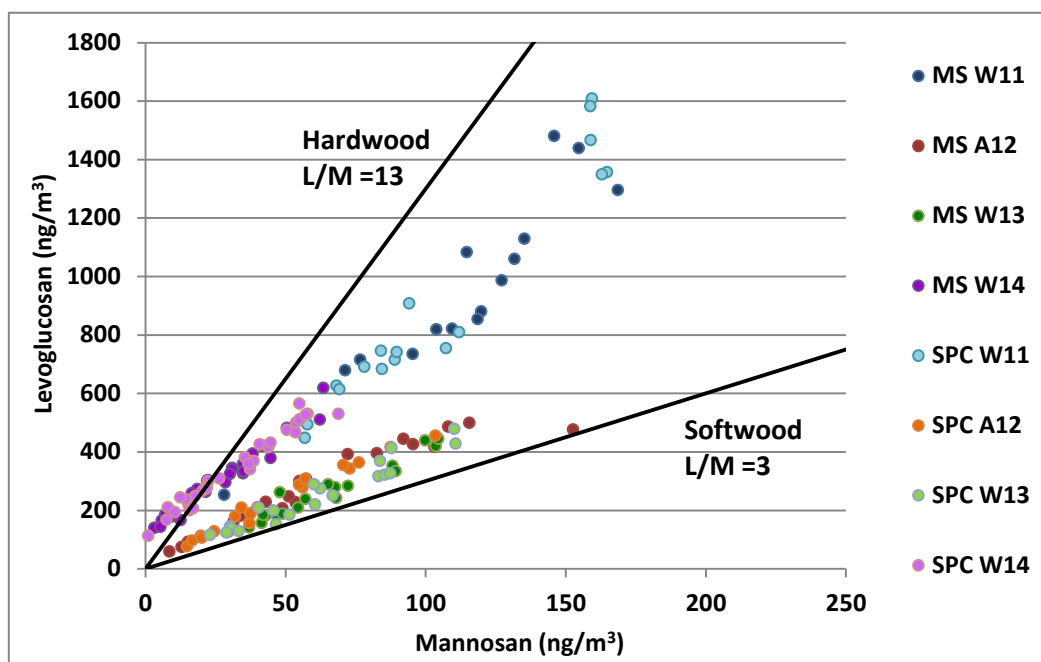
Figure 4.2. Levoglucosan versus mannosan concentrations during cold periods monitoring campaigns at urban and rural sites [Pietrograndé et al. 2015].

The measured L/M ratios cover a wide range, from 4 to 15, with a mean value of ~8. These are intermediate values between wood types from which we can infer that in the investigated region wood smoke is produced by combustion of a mixture of hard and softwood (Figure 4.2). The limit cases are maximum values (on average 15) measured in winter 2014 indicating nearly exclusive combustion of hard wood type (oak, beech and walnut), and minimum values in winter 2013 (on average 4) suggesting an increased contribution of softwood.

The proportion of soft and hardwood to ambient wood smoke level can be estimated from the L/M ratios in ambient PM by applying a simple equation derived by Schmidl on the basis of the data obtained for the combustion of common hardwoods (beech and oak) and softwoods (spruce and larch) in wood stoves in Austria [Schmidl et al. 2008]. When the Austrian approach is transferred to Emilia Romagna region, it can be estimated that wood fuel used in the investigated seasonal periods is generally formed by 70% softwood and 30% hardwood mixture, with lower percentages of softwood in winter 2014.

Information on the wood types burnt in the region during the sampling periods is lacking. The only available information is an inventory of the wood consumption,

compiled in 2010 by the Emilia Romagna Regional Agency for Environmental and Sustainable Development [Deserti et al. 2011]. They reported that 90% of the wood burnt in domestic heating systems is common firewood, mainly collected in the local woodland or bought by farmers and acquaintances (Figure 4.1 and 4.3).
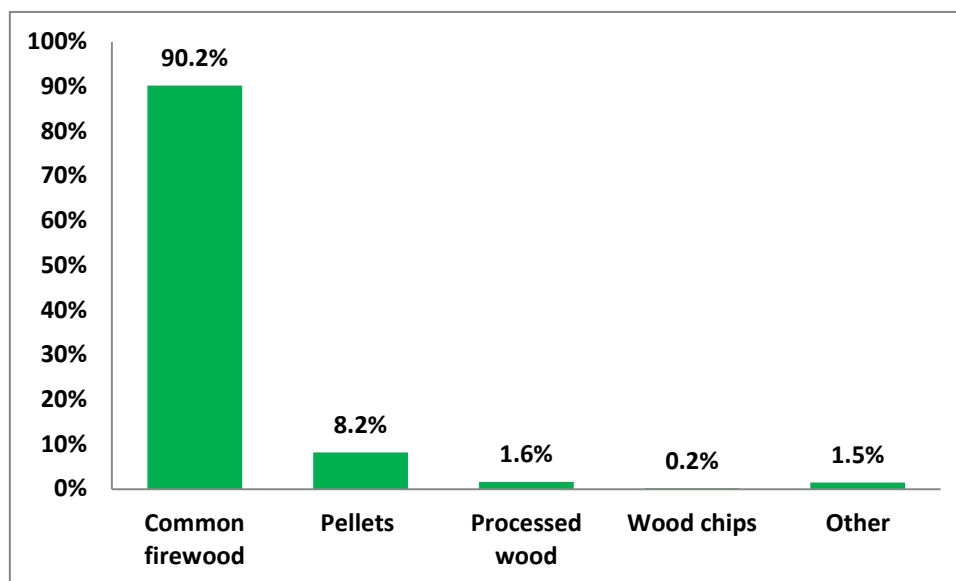
Figure 4.3. Fuel type burned.

As a consequence, the prevalence of hardwood combustion would be likely expected, due to the highest local availability of these kinds of wood types in Emilia Romagna, such as poplar, beech, hornbeam, black locust, ash and oak.

However, caution should be taken when anhydrosugars ratios are exploited in the interpretations, since the strong dependence of anhydrosugars yields on combustion conditions.

Such variability could be explained by the observations made by Kuo [Kuo et al. 2011]. Higher combustion temperature and longer combustion duration result in higher L/M ratio, regardless of plant species. This effect is probably due to the higher thermal lability of mannosan and galactosan compared to that of levoglucosan. Under such circumstances, the power of the anhydrosugars ratios for source discrimination is seriously weakened because of potential overlaps between hardwood, softwood, and grass chars.

4.1.2 Methoxylated phenols

Methoxylated phenols are another group of biomarkers linked to plant combustion.

These solvent-soluble phenolic compounds are degradation products from oxidation and/or pyrolysis of lignin, a major biopolymer in vascular plants [Simoneit 2002, Kuo et al. 2011].

The lignin derivatives may be categorized into syringyls (S) and vanillyls (V), according to the relative distribution of OH/OCH3 substituents. Such S/V ratios have been shown to be a useful indicator for the class of plants that is burnt and have been used by atmospheric scientists for source apportionment of biomass combustion in atmospheric aerosols [Schauer et al. 2000, Bari et al. 2010].

For example, hardwood tissues are characterized by substantial amounts of syringyl structural units (S), while these units are almost absent in lignin of softwoods. Vanillyl structural units (V), however, are found in both angiosperms (hardwoods) and gymnosperms (softwoods) [Simoneit 2002, Kuo et al. 2011]. Thus, high S/V ratio values in burning smoke prove the presence of angiosperms while typical ratios representative of softwoods are below 0.5 [Fine et al. 2001, 2002, 2004 Mazzoleni et al. 2007, Kuo et al. 2011].

The measured S/V values cover the range from 0.4 to 4, indicating that these smoke particles were emitted from a heterogeneous mix of combustion conditions. However, for most of the samples S/V ratios fall in range 0.4-2.5 yielding a general mean value of 1.1 that is characteristic for chars from hardwood. This is confirmed by the average values computed for each campaign that are >1, thus confirming the predominant contribution of smoke from hardwood combustion, with the only exception of unexpected lower value in November 2011 (S/V ≈0.3).

However, the above ratio is also susceptible to the effects of combustion conditions. A significant decrease of S/V ratio was observed by Kuo at elevated combustion temperatures and this finding suggests that syringil phenols are more susceptible to thermal degradation than vanillyl phenols [Kuo et al. 2011].

4.1.3 Combined use of anhydrosugars and lignin phenols in source characterization

The influence of combustion conditions on the yields and diagnostic ratios of anhydrosugars and lignin phenols complicates their application towards the characterization of biomass combustion residues. However, even though these two

classes of biomarkers are derived from distinct precursors, they respond similarly to the changes in combustion conditions [Kuo et al. 2011].

For this reason, a property–property plot using diagnostic ratios from these two biomass combustion biomarkers was used, as an improved tool for the source characterization of biomass combustion residues.
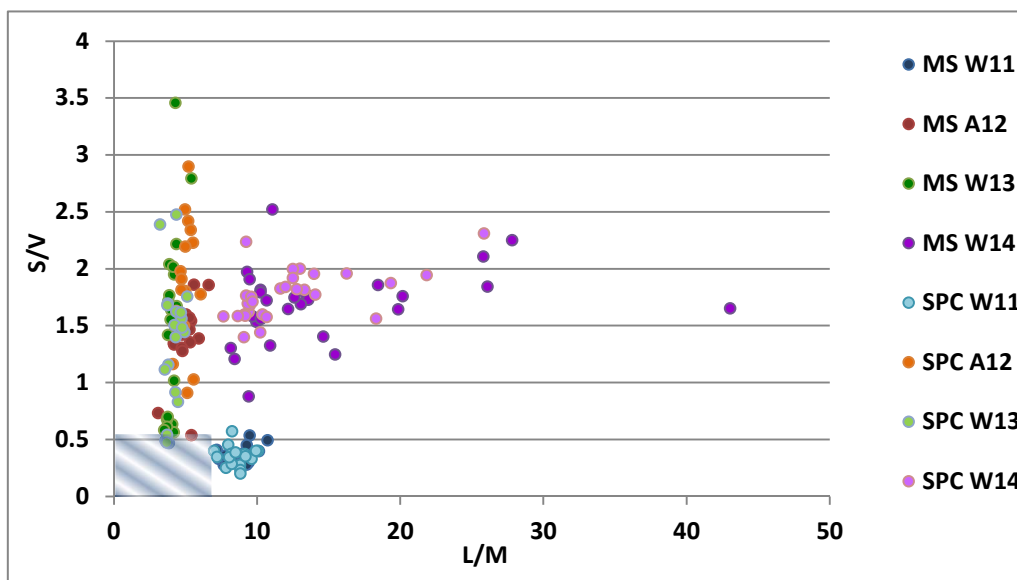
Figure 4.3. Property-property plot of diagnostic ratios: levoglucosan to mannosan (L/M) ratio vs. syringyl to vanillyl phenols (S/V) ratios. Dashed area is representative for softwood. Data of fall/winter campaigns (excluding fall 2013).

The plot in Figure 4.3 shows that only few samples are comprise in the area described by typical softwood values (dashed area) but a not negligible number of points lie very close to this area. This behaviour suggests a mixture of wood type burned with a predominance of hardwood combustion.

4.2 Contribution of wood combustion to benzo[a]pyrene

Among the target PAHs, benzo[a]pyrene was investigated in detail, as it is regulated in the European Union (EU) by the 4th Air Quality Daughter Directive (2004/107/EC) and it is among the 17 priority PAHs that The United States Agency for Toxic Substances and Disease Registry has considered based on their toxicological profile.

BaP is notable for being the first carcinogec chemical to be discovered.

The average concentrations ranged from values lower than 0.1 ng m^{-3} in warmer periods to 1.2 ng m^{-3} in November 2011. In general, BaP levels were lower than those detected

in cold seasons at other urban sites in Northern Italy [Perrone et al. 2012] and also below the EU annual target value for the protection of human health of 1 ng m^{-3}.

The measured BaP data show a linear increase with levoglucosan and the other two anhydrosugars concentrations, following a statistically significant correlation through all the campaigns (R^2 ~0.75).

The relationship between levoglucosan and BaP is the basis for computing the BaP to levoglucosan ratio giving the estimation for the source contribution of biomass burning to the measured BaP concentration (BaP_{bb}). [Belis et al. 2011, Piazzalunga et al. 2013].

The value of 0.0011 proposed by Belis [Belis et al. 2011] as average of various literature data was used.

The relative contribution of wood combustion to BaP in colder periods was estimated to be close to 70% for most of the campaigns, nearly 50% in warmer October 2013, but unrealistically higher than 100% in February 2014 campaign. This may be due to the low accuracy of this single tracer method associated with the intrinsic uncertainty of the emission factors, since emissions of BaP and levoglucosan in wood smoke are largely influenced by several experimental conditions [Szidat et al. 2006, Orasche et al. 2012, Viana et al. 2013]. In fact, literature data show a very wide range of BaP/levoglucosan ratios depending on the type of wood burnt and the device used.

In general, higher ratios were found for softwoods and woodstoves (up to 0.025), while lower ratios were found for hardwoods and pellet stoves [Schauer et al. 2001, Oros et al. 2001a, b, Fine et al., 2001, 2002, 2004, Orasche et al. 2012].

Although the approximation of the present approach, the obtained results clearly prove that wood burning for residential heating is the main source for ambient BaP during the colder months. Such a contribution is in general lower at the urban site MS, which is strongly impacted also by traffic source, and more relevant at the rural site, where BaP emissions from traffic are lower.

4.3 Contribution of wood combustion to PM

As for BaP, the estimation of wood burning contribution to PM can be achieved through the quantification of specific markers like levoglucosan. The main problem in applying this method is the choice of suitable emission factors. The PM/levoglucosan ratio measured at the source, in fact, depend on many factor: type of wood combusted and appliance used as well as to burning rates, air dilution, and moisture content in the fuel.

As a matter of fact, the apportionment methods are often based on partially known parameters like the wood consumption or the appliances used in the investigated area.

Not much information were available on wood species combusted in the domestic heating systems in the sampling zone and, at present, burning tests conducted on plants and types of wood in Europe are still scarce.

To calculate the percentage contribution of wood combustion to PM, Szidat [Szidat et al. 2006] proposed to use as emission factor the average value of data present in the literature.

Considering various works [Schauer et al. 2001, Fine et al. 2001, 2002, 2004, Schmidl et al. 2008, Bari et al. 2009, Orasche et al. 2012], the calculated value for levoglucosan/PM ratio was 0.036. Using this value, the relative contribution of wood combustion to PM was around 40% during wintertime with the maximum value of ~65% in winter 2014, while it decrease of one order of magnitude in warmer periods. No great differences were observed between the two sites, indicating that wood burning is a regional scale phenomenon.

4.4 Contribution of wood combustion to the carbonaceous fraction

4.4.1 Levoglucosan approach

The mono-tracer approach based on the ambient concentrations of levoglucosan was used to estimate the contribution of OC generated by wood burning, as levoglucosan is the key tracer for biomass combustion.

The relationship between levoglucosan and OC was studied for each cold period campaign.

The measured values yield highly variable levoglucosan to OC emission factors which are mostly included in the $0.06 - 0.2$ range reported in literature for the residential burning of softwood-hardwood mixtures [Szidat et al. 2006, Schmidl et al. 2008, Kourtchev et al. 2011, Herich et al. 2014]. Such a large degree of variation may be ascribed to the variability of factors that influence emissions from wood combustion, meanly the type of wood combusted and the appliance used as well as to burning rates, air dilution, and moisture content in the fuel [Mazzoleni et al. 2007, Alves et al. 2010, Piazzalunga et al. 2011, Holden et al. 2011].

As suggested by Caseiro [Caseiro et al. 2009], an accurate estimate of wood burning contribution to OC in a region could be achieved using site-specific emission factors, taking into account both the wood species actually burnt and the type of appliances in use. As this information was unknown for Emilia Romagna region, the emission factor of 0.15 proposed by Szidat as suitable for European areas was used [Szidat et al. 2006]. Such a factor has been calculated from literature data considering combustion for domestic heating of a wood fuel consisting of a mixture of hard and softwood and has been recently used in a study carried out at another Emilia Romagna site [Perrino et al. 2014]. With this assumption, it was estimated the amount of OC derived from wood smoke as absolute concentrations (OC_{bb}) as well as relative contributions of OC_{bb} to total OC ($OC_{bb}\%$). The absolute concentrations of OC_{bb} in cold periods at both the sites were on average ~3 $\mu g\ m^{-3}$ in all the campaigns, excluding the exceptionally low values in October 2013. Not surprisingly, primary organic aerosol emission from wood burning established a significant contribution ($OC_{bb}\%$, ~33%) at both sites in fall/winter with higher values of about 50% during winter 2014, whilst in warmer periods only a small impact was registered ($OC_{bb}\%$, ~3%).

4.4.2 Radiocarbon approach

As highlighted previously, mono-tracer approach suffers of limited atmospheric lifetimes of molecular tracers considered due to their chemical reactivity and highly variable emission factors.

For these reasons, Currie [Currie 2000] proposed a method for source apportionment of carbonaceous aerosol particles based on radiocarbon (^{14}C). This isotopic method enables a direct distinction of contemporary and fossil carbon in ambient aerosols, because ^{14}C has decayed in fossil materials.

Following the procedure used by Szidat [Szidat et al. 2006], the evaluation of carbonaceous particulate matter origin was attempted. It is based on a parameter called f_M that represents a $^{14}C/^{12}C$ ratio of a sample related to that present in the reference year 1950 and on the concentrations of OC and EC recorded in the sampling sites.

The f_M values proposed by Szidat are reported in Table 4.1 and used for the calculation.

For source apportionment of OC, EC originating from biomass burning (EC_{bb}) is need and were deduced from $f_M(EC)$.

$$EC_{bb} = EC_{tot} \cdot \frac{f_M(EC)}{f_{M,bb}}$$

The biomass burning fraction of OC (OC_{bb}) was estimated from EC_{bb} using an average literature EC/OC emission ratio typical for biomass burning $(EC/OC)_{ER, bb}$.

$$OC_{bb} = \frac{EC_{bb}}{\dfrac{EC}{OC}_{ER,bb}}$$

With this method is also possible to calculate OC fraction due to biogenic activity (OC_{bio}) and to fossil fuel combustion (OC_{ff}) in order to have a completely view of the main sources of organic carbonaceous aerosol.

$$OC_{bio} = \frac{OC_{tot} \cdot f_{M}\ OC\ - OC_{bb} \cdot f_{M,bb}}{f_{M,bio}}$$

$$OC_{ff} = OC_{tot} - OC_{bb} - OC_{bio}$$

	$f_{M}(EC)$	$f_{M}(EC)$	$f_{M,ff}$	$f_{M,bb}$	$f_{M,bio}$	$(OC/EC)_{ER,bb}$
Summer	0.07	0.76				
Winter	0.31	0.79	0	1.24	1.072	0.16
Springlike	0.14	0.81				

Table 4.1. f_{M} ratios from different sources and average OC/EC literature emission ratio for biomass burning.

In addition to the absolute amount, the relative contribution of each source was determined.

The computed results show a clearly trend through different seasons, with an increasing contribution of biomass burning to OC during colder period (average contribution 44% at Main Site and 31% at San Pietro) and major contribution of biogenic activity in warmer periods (average contribution 65% and 56% at the rural and urban site respectively).

OC_{ff} exhibits only small changes during the different seasons with an average constant value around 30% (Table 4.2).

The results highlight that anthropogenic activities (fossil fuel and biomass combustion) in wintertime dominate OC emissions, being responsible of nearly 80% of OC released in the atmosphere at urban site.

Natural activity is stronger at rural site with a contribution of approximately 50% of OC through the year.

	Mains Site			San Pietro		
	$OC_{bb}\%$	$OC_{ff}\%$	$OC_{bio}\%$	$OC_{bb}\%$	$OC_{ff}\%$	$OC_{bio}\%$
W11	n.d.	n.d.	n.d.	n.d.	n.d.	n.d.
Su12	10,1	30,7	59,2	6,3	30,1	63,6
A12	41,8	32,9	25,4	34,6	31,7	33,7
W13	43,3	33,1	23,6	28,1	30,7	41,2
Sp13	15,6	26,9	57,5	7,6	25,6	66,8
A13	23,2	28,1	48,7	11,7	26,3	62,1
W14	46,8	33,6	19,6	29,0	30,9	40,1
Su14	9,1	30,5	60,3	4,2	29,8	66,1

Table 4.2. Relative contribution of biomass burning, fossil fuel combustion and biogenic activity to OC.

The calculated data are in very good agreement with those reported in other studies performed in Zurich and Milan [Szidat et al. 2006, Gilardoni et al. 2011].
Considering only OC_{bb}, the values obtained with the radiocarbon method and those obtained from levoglucosan approach display only slight differences, therefore, the two methods could potentially provide the same information.

4.5 Wood residential heating impact in Emilia Romagna

The amount of woody biomass used as energetic source is not well known because the supply of such a material often occurs outside the "formal" economy (Figure 4.1), hence this problem gave rise to some statistical investigation both at national [Istat 2014] and regional level [Deserti et al. 2011].

Data reported from these statistical studies have been cross-checked with data obtained in this work and with those reported by INEMAR (INventario EMissioni ARia), a database projected from Lombardia region and used from several Italian regions to estimate the emissions of various pollutants separated by activities and type of fuel.

The extrapolation of data regarding Bologna province from INEMAR database highlights that about 50% of $PM_{2.5}$ mass and more than 80% of PAHs are emitted from

non-industrial combustion plants and, within this category, more than 90% of both PM$_{2.5}$ and PAHs derives from residential plants.
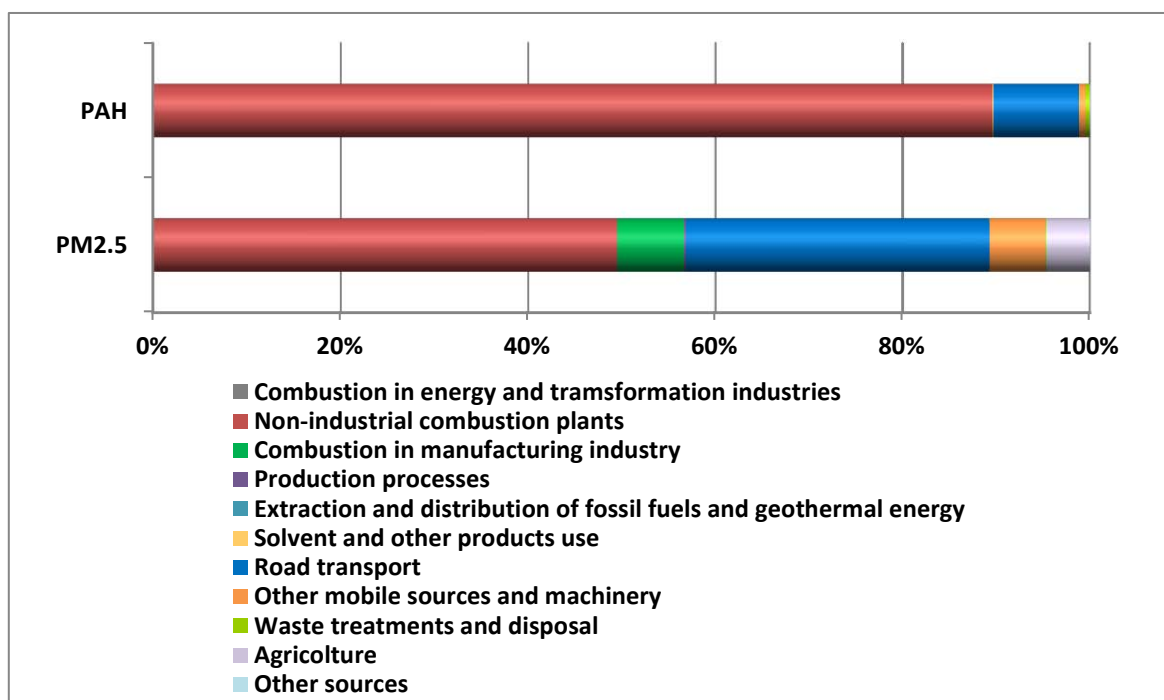
Figure 4.4. Contribution of different sources to PAHs and PM$_{2.5}$ emissions in Bologna province [ISPRA].

A study conducted by Deserti [Deserti et al. 2011] reports that the most common fuel used in Emilia Romagna region for domestic heating is by far natural gas and that biomass is used only from 7% of the families as shown in Figure 4.5.

4.5.1 Regional consumption and emissions from wood

In the present work it was found that around 30% of PM$_{2.5}$ as annual average is emitted from biomass burning. Approximately the same amount of particles are emitted from traffic sources but traffic is an emission source nearly constant all year long while wood burning from residential heating is mainly concentrated during winter. In fact, the estimated contribution of wood burning to PM$_{2.5}$ accounts up to about 70% in colder periods (Appendix B).

This means that, even if biomass burning for residential heating is not a very common phenomenon (Figure 4.5), its impact on PM emission is not negligible.

Considering BaP and other common PAHs usually found in particle phase, the same considerations as to PM are valid. Unfortunately, no data for single PAHs are available neither for Bologna province nor for Emilia Romagna region. Thus, data from a neighbouring region such as Lombardia, with geographic and anthropogenic characteristics similar to Emilia Romagna, were considered.
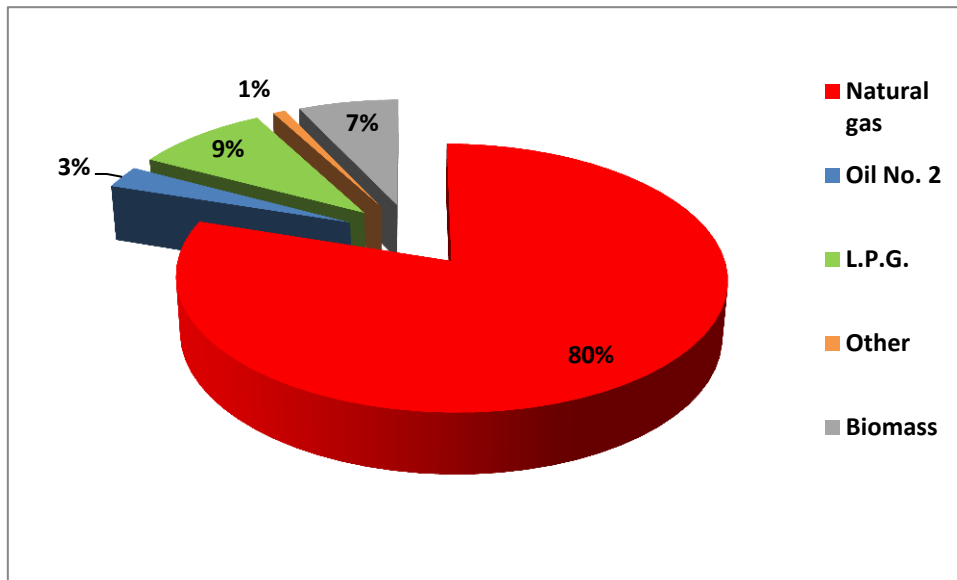
Figure 4.5. Relative distribution of fuel type for residential heating in Bologna province [Deserti et al. 2011].

The data extrapolated by INEMAR clearly show that IcdP, BkF, BbF and, above all, BaP are emitted in a large part by residential heating (Figure 4.6) and, according to the data calculated in the present work, wood combustion is responsible for about 60% of the total emission of BaP during the year although only 7% of the families in Bologna province use wood as fuel for residential heating.

To give further inside into wood combustion phenomenon, the devices used for residential heating were considered.

Deserti [Deserti et al. 2011] reported that the most widespread devices are traditional fireplaces and woodstoves, accounting for 55 and 28% respectively. Modern devices such as closed fireplaces and pellet stoves are not still common in the studied area (Figure 4.7).

It is easy to understand why wood combustion is the main responsible for both $PM_{2.5}$ and BaP emissions in atmosphere. In fact, emissions factors from traditional appliances are much more higher than that from modern devices which in turn are higher than those from No. 2 oil (residential heating diesel) and natural gas fired devices (Figure 4.8) [Rogge et al. 1998, Schauer et al. 2001, Fine et al. 2004, McDonald 2009, Pettersson et al. 2011, Boman et al. 2011, Meyer 2012, Gianelle et al. 2013].
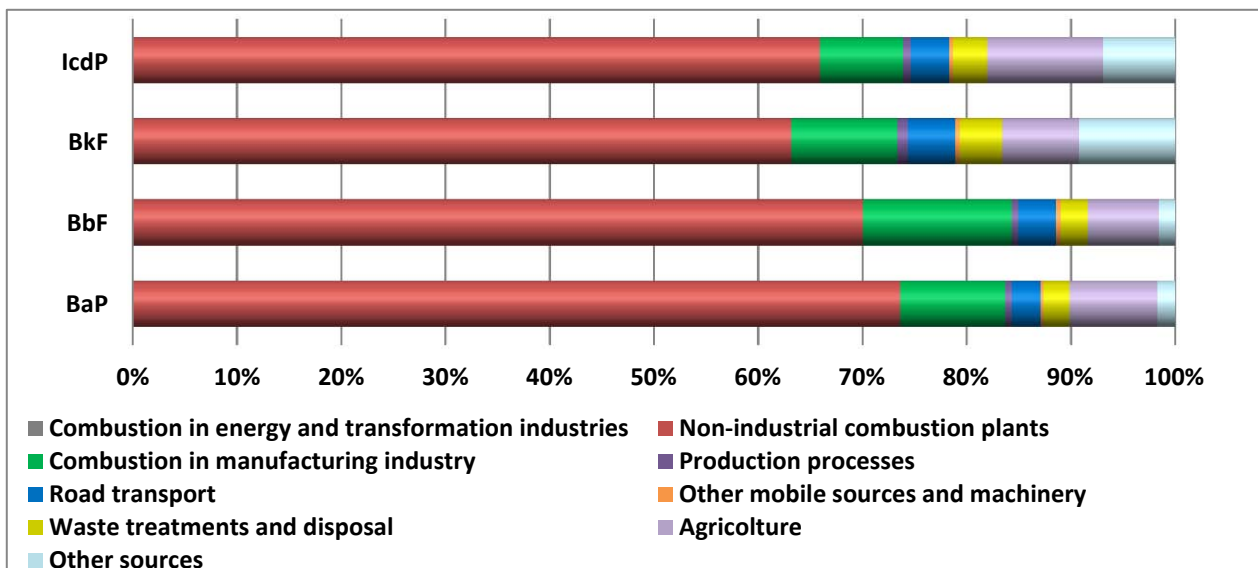
Figure 4.6. Contribution of different sources to single PAH emission in Lombardia region [INEMAR-Regione Lombardia].
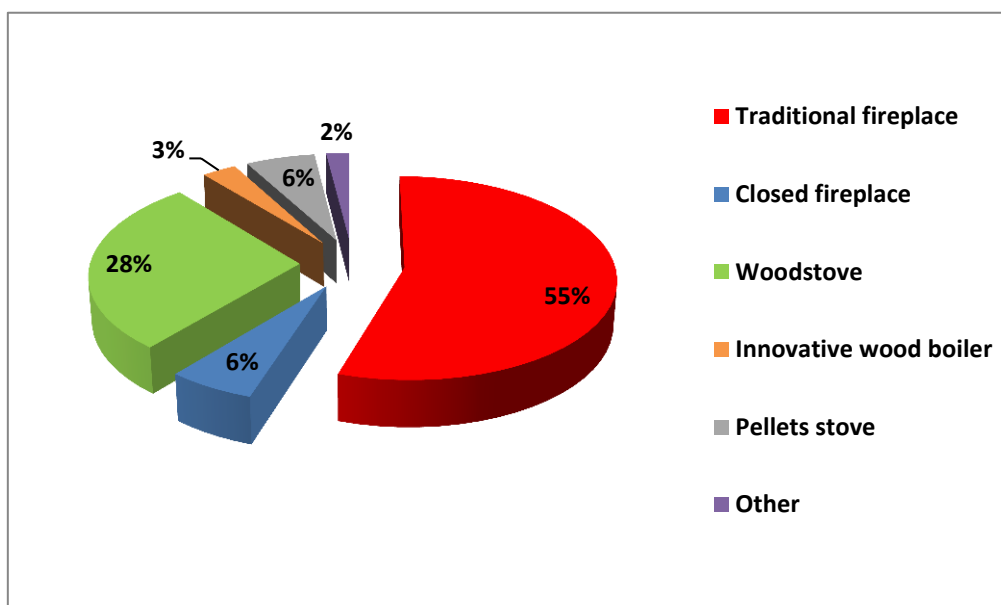
Figure 4.7. Relative distribution of wood burning devices for residential heating in Bologna province [Deserti et al. 2011].

In conclusion, the obtained results indicate that wood burning for domestic heating is the dominating emission source at both the investigated sites especially in cold seasons when pollution episodes are more frequent.

92
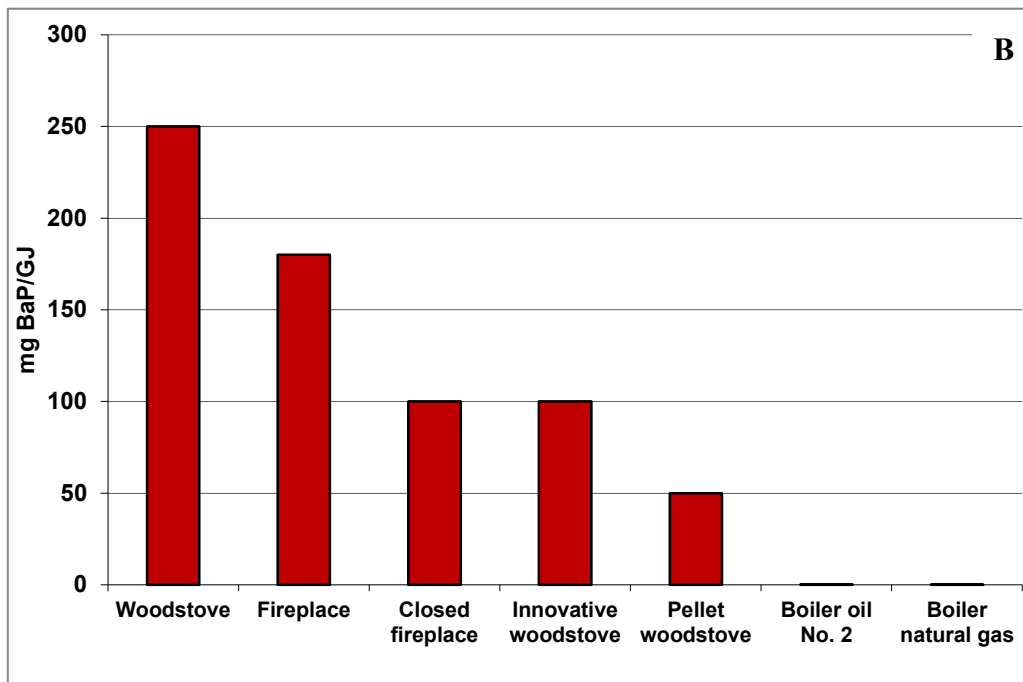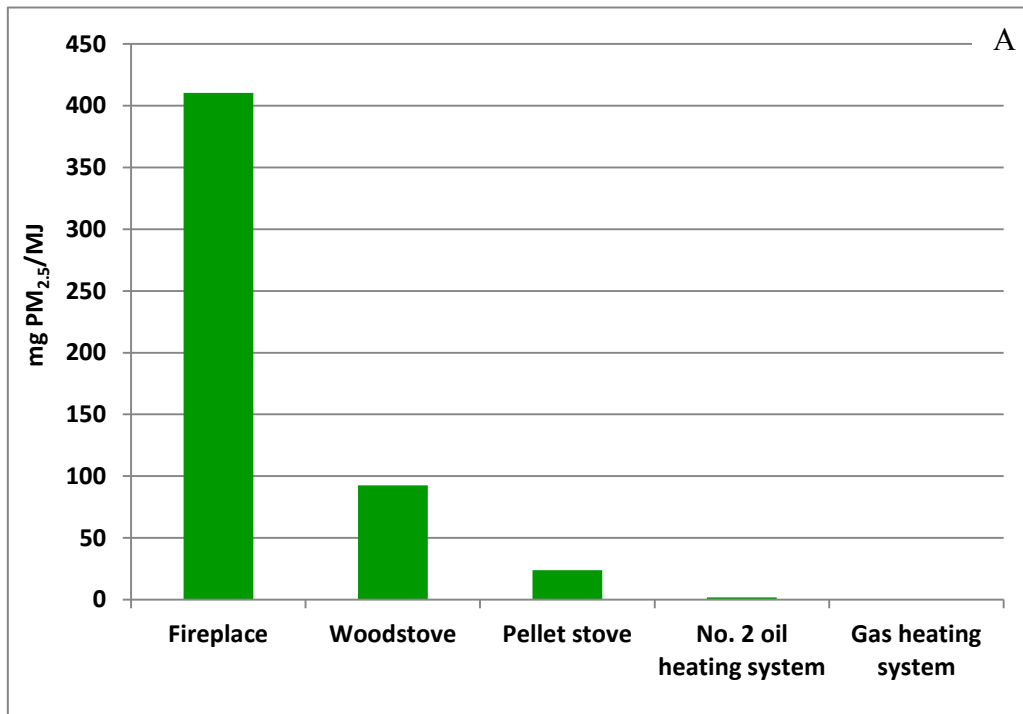
Figure 4.8. Emission factors of A) $PM_{2.5}$ and B) BaP from different residential heating appliances.

4.6 Conclusions and perspectives

The information obtained would lead to increased understanding and better management of emissions in both urban and rural areas of the region. In particular, the dangerous implications of biomass combustion sources highlight the need for the regulation of the emissions of such particulates.

In fact, if biomass can be considered an environmental friendly fuel regarding greenhouse gases emissions, it cannot be considered, using the technologies currently widespread, a clean fuel from human health point of view.

Policy appears to give conflicting signals about this problem: from one hand it is trying to limit PM emissions with some measures while, from the other hand, encourages the installation of wood burning appliances for residential heating.

Moreover DPR 74/2013 imposes periodic checks to thermal plants to control energy efficiency but, among the considered parameters, particulate matter determination is not contemplated. This law excludes from the definition of "thermal plants", woodstoves, fireplaces and all devices for local heating using radiative energy. Thus only boilers are subjected to these controls but they represent no more than 5% of wood burning devices for residential heating.

The measures implemented for reducing PM and potentially toxic compounds related to it are thus not enough. Traffic blocks or limitations that are usually proposed as a manner to reduce PM, seldom lead to desired results.

In fact, in the last years, PAHs emissions from vehicular traffic show a slight increase, while PM exhibits a decreasing trend. These results are probably due to the increasingly stringent parameters imposed by Euro standards on exhaust vehicle emissions.

On the contrary, PM and PAHs emissions from residential heating systems are strongly increased in the last twenty years and this trend is due exclusively to biomass burning appliances since emissions from No. 2 oil, natural gas and L.P.G. devices show a constant reduction.
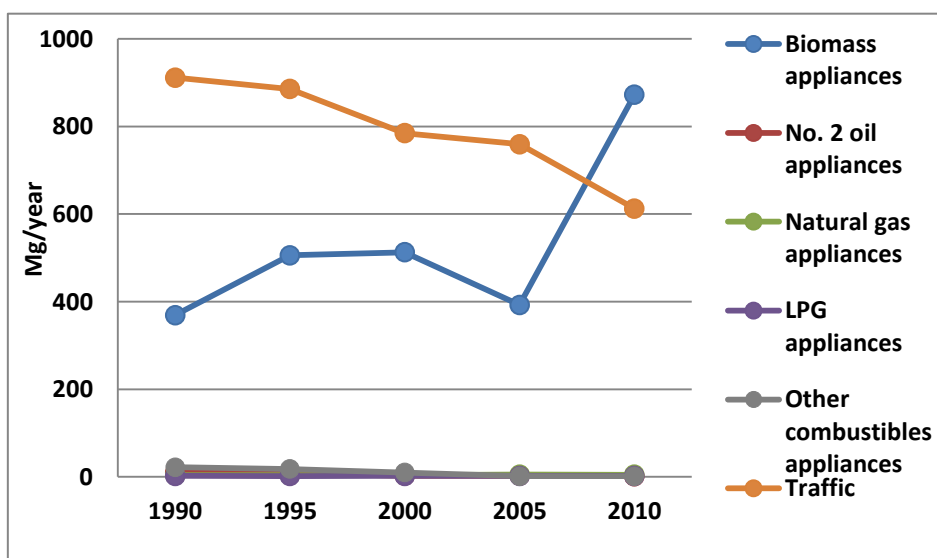
Figure 4.9. Temporal trend emissions from some residential heating appliances and vehicular traffic [ISPRA].

ENEA and Board of Health studies indicate harmful effects on environment and health of wood combustion because of particulate emissions.

To have a real abatement of pollutants in atmosphere, more controls and restrictions on wood burning residential heating devices emissions are need, although traffic restrictions could be useful to the purpose. The use of particulate matter abatement technologies, as occurs in industrial chimneys, may be desirable. The practice of biomass burning for residential heating does not bring the expected benefits and, indeed, due to the emissions of particulate matter ($PM_{2.5}$), increases air pollution and causes health damage.

One of the biggest risks in existing policies that support the use of biomass is to reduce the positive results related to the improvement of air quality, achieved through the policies of containment of transport, electricity generation plants and industry emissions [Virdis et al. 2015].

Health aspects have been highlighted by a study of the Centre for Diseases Control of Board of Health, VIIAS (Integrated Assessment of Air Pollution Impact on Environment and Health). Regarding Italy, VIIAS has evaluated in 30000 deaths a year the impact of fine particles, 7% of natural deaths, and more than 65% of deaths occur in Northern Italy with the maximum rate in Lombardia region (164 per 100000 inhabitants) and a rate of 124 deaths per 100000 inhabitants in Emilia Romagna region [VIIAS]. Moreover life expectancy loss due to $PM_{2.5}$ exposition has been estimated in about 10 months.

This work has also highlighted that no significant differences in $PM_{2.5}$ amount and composition were found between the urban area of Bologna, which is strongly anthropized, and the rural area of San Pietro Capofiume, not directly affected from anthropogenic source of PM.

Thus, adopted policies of pollution management cannot be decided only at local level, as often happens nowadays, but on a larger scale, provincial or regional, since atmospheric pollution is not a problem confined only in the pollutants emission zones.

5. EVALUATION OF PM TOXICITY

For a comprehensive characterization of air quality, finally, PM toxicological impact has been evaluated with the aim to relate it to PM chemical composition. This part of the work is still in progress, thus some preliminary results are presented below.

5.1 Oxidative potential

Measuring the levels of pollution in the air provides a measure of exposure that is used as a surrogate for risk. The closer the metric is to the actual harmful component of the exposure, the better the risk management and the relationship to adverse health effects in epidemiological studies are likely to be [Ayres et al. 2008].

In recent decades, the mass of particulate matter measured by the PM_{10} or $PM_{2.5}$ has been the metric of choice for ambient particles. It can however be argued that PM_{10} and $PM_{2.5}$ mass are not ideal because much of the ambient particle mass consists of low toxicity components. In contrast, relatively tiny masses of transition metals and organic species may make a major contribution in worsen human health [Mudway et al. 2009].

Directive 2008/50/CE contemplate PM mass measurement and the determination of some metal ions (Pb, Ni, Cd and As) and benzo[a]pyrene in PM_{10} fraction since they are recognized to affect human health.

In fact:

- Pb may damage fertility and unborn child and may cause damages to organs;
- Ni is suspected to cause cancer and cause damages to organs;
- Cd may cause cancer, is suspected of causing genetic defects, is suspected of damaging fertility or the unborn child and is fatal if inhaled;
- As is toxic if inhaled;
- benzo[a]pyrene may cause genetic defects, may cause cancer, may damage the unborn child and is suspected of damaging fertility.

These parameters are certainly important but they are not the only parameters related to health diseases.

Thus, in the last years, other characteristics of PM have been extensively studied for linking them to its toxicity response. Among the various property of PM, oxidative potential has been proposed as a metric that is better related to biological responses to

PM exposures and thus could be more informative than mass alone [Borm et al. 2007, Yang et al. 2014].

It is a measure of the ability of PM to generate oxidative stress at the air-lung interface initiated by the formation of reactive oxygen species (ROS) within affected cells.

In light of trend, parallel to the chemical characterization of PM, another characteristic as oxidative potential was studied since it has been proposed as a metric that may potentially serve as a biologically pertinent index of PM toxicity and thus could be more informative than parameters normed in Directive 2008/50/CE

Among the various assays developed for measuring OP, in this study two common cell free methods were investigated. They are spectrophotometric kinetic methods based on ascorbic acid and dithiothreitol (DTT) as target molecules miming PM-lung interface. Some preliminary results are reported below.

5.1.1 Dithiothreitol assay

Dithiothreitol is a strong reducing agent which forms six membered ring with an internal disulphide bond when oxidized. It is commonly used as a cell-free measure of the oxidative potential of particles because it simulates cysteine residues in proteins present in respiratory tract.

Oxidation of DTT from metals and quinones is a catalytic process. This oxidation process forms ROS which can subsequently oxidize DTT [Kumagai et al. 2002]. The contribution of generated ROS to DTT depletion during the assay is not yet well understood and different conclusions are reported in literature [Ayres et al. 2008, Charrier et al. 2012]

The assay is based on a two-step reaction. In the first step, redox active chemicals in particulate matter oxidize DTT to its disulphide form and then donate an electron to dissolved molecular oxygen, forming superoxide [Kumagai et al. 2002], which can subsequently form other reactive oxygen species (ROS) such as hydrogen peroxide and, in the presence of metals, hydroxyl radicals (Figure 5.1). When this reaction is monitored under conditions of excess DTT, the rate of DTT consumption is proportional to the concentration of the catalytically active redox-active species in the sample [Cho et al. 2005].

The redox cycle catalysed by PM species is similar to cycles that occur in living cells. Typically, ROS are formed in cells through the reduction of oxygen by biological reducing agents such as NADH and NADPH, with the catalytic assistance of electron transfer enzymes and redox-active chemicals [Cho et al. 2005].
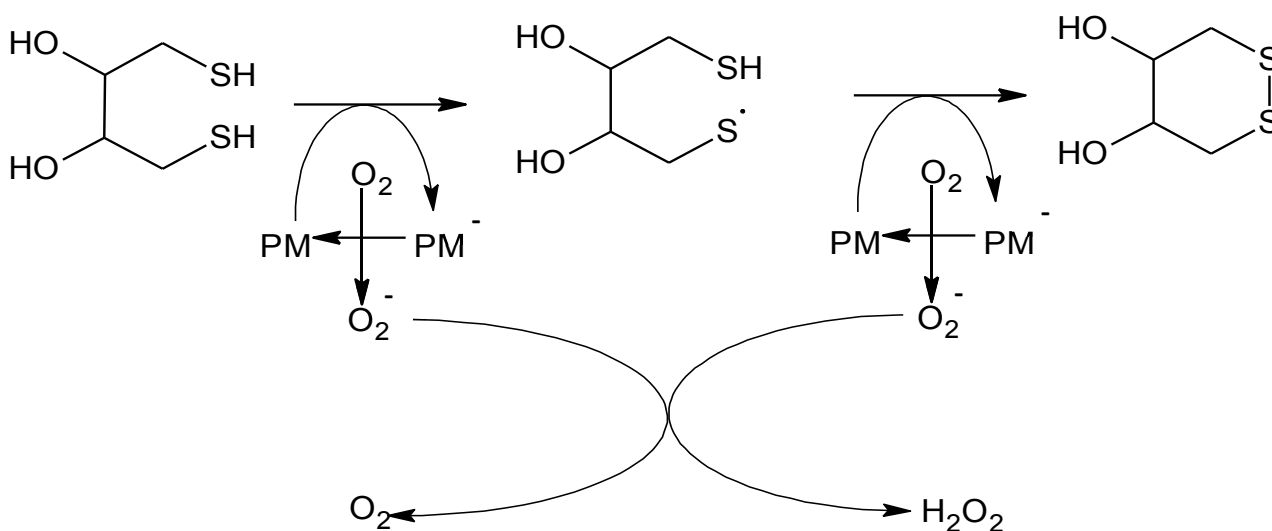
Figure 5.1. Chemical reaction between DTT and oxygen with PM as a catalyst.

A diagram of the redox cycling of quinones generating ROS in vivo is shown in Figure 5.2. Comparing the cycling of DTT method with the redox cycling of quinones generating ROS in vivo shows that they share elements of the same mechanism of ROS generation [Li et al 2009].

In the second step (Figure 5.3), the remaining DTT is reacted with DTNB (Ellman's Reagent) to generate DTT-Disulfide and 2-nitro-5-thiobenzoic (TNB). TNB is the "coloured" species produced in this reaction and has a high molar extinction coefficient ($14150 \ M^{-1} cm^{-1}$ at 412 nm) in the visible range.

While the DTT assay provides a quantitative measure of oxidation, it does not measure the production of specific ROS, which is significant since the different ROS have very different reactivity [Charrier et al. 2012].

The particulate species responsible for DTT oxidation are typically examined by correlating DTT activity with PM composition. These analyses often identify carbonaceous species, i.e., elemental carbon, water soluble organic carbon and/or polycyclic aromatic hydrocarbons (PAHs), as most strongly correlated with DTT loss. However, correlations do not show causation, especially since particulate species are often highly covariate. For example, PAHs levels often strongly correlate with DTT loss from particles, but PAHs are not redox active.

Typically compounds which react in this assay are organic species, mainly quinones [Kumagai et al. 2002, Cho et al. 2005], but some studies have shown that transition metals can also oxidize DTT [Lin et al. 2011, Charrier et al. 2012].
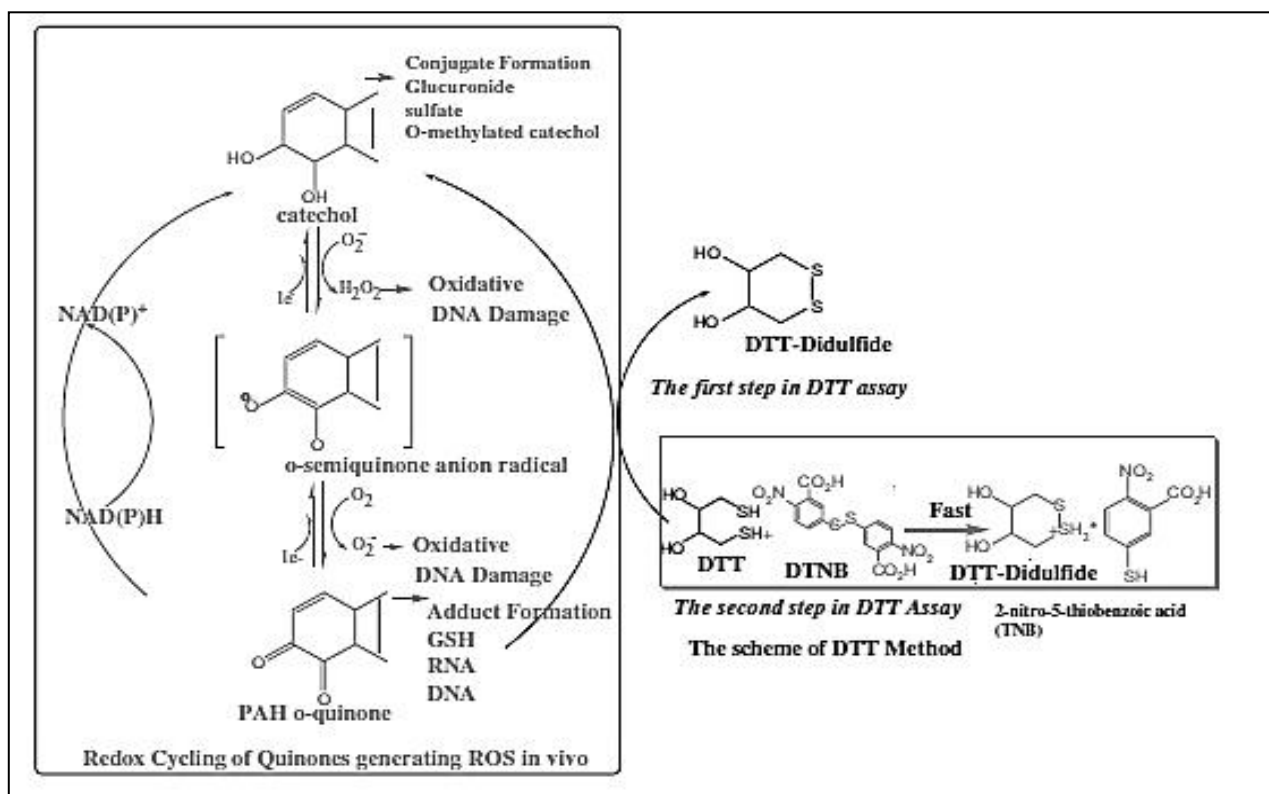
Figure 5.2. The redox cycling of quinones generating ROS in vivo, and the similar cycling in DTT assay [Li et al. 2009].
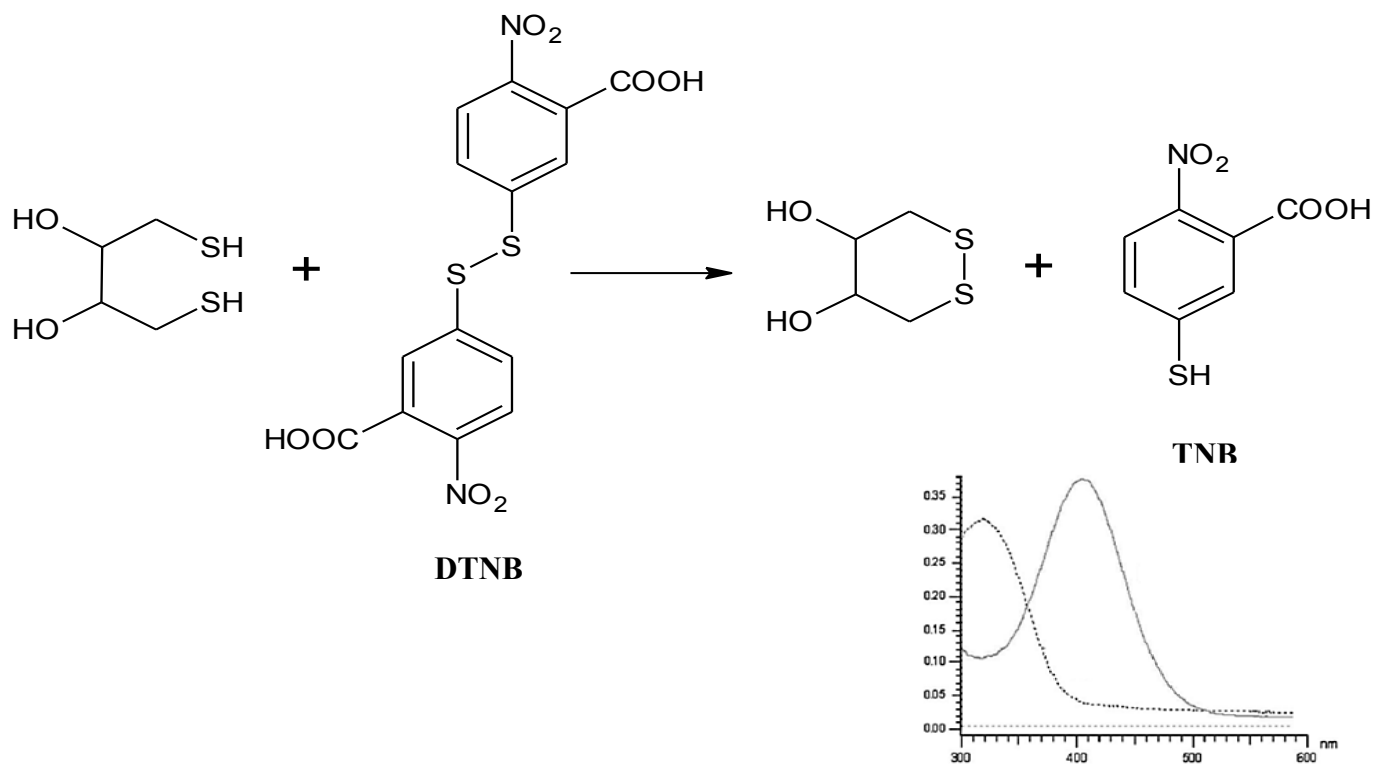
Figure 5.3. DTT revelation with Ellman's reagent and UV/Vis spectra of species involved in the reaction.

5.1.2 Ascorbate assay

The respiratory tract lining fluid (RTLF), represents the first physical interface encountered by inhaled materials and has been shown to contain high concentrations of the antioxidants ascorbate (vitamin C), urate and reduced glutathione.

The oxidative capacity of PM samples has been determined by their ability to oxidize a range of protective antioxidant molecules present at the surface of the lung using a validated in vitro model [Zielinski et al. 1999, Mudway et al. 2011].

The AA assay is a simplified version of the synthetic respiratory tract lining fluid (RTFL) assay, where only ascorbic acid is used.

The reaction mechanism is similar to the first step of DTT reaction: ascorbic acid is oxidized to dehydroascorbic acid while redox active species in PM are reduced (Figure 5.4). These reduced species can then transfer an electron to oxygen molecules promoting the formation of ROS.

The depletion of ascorbate by PM in acellular assays has been linked to metals, especially copper [Ayres et al. 2008], but has also shown to be sensitive to quinones [Roginski et al. 1999].
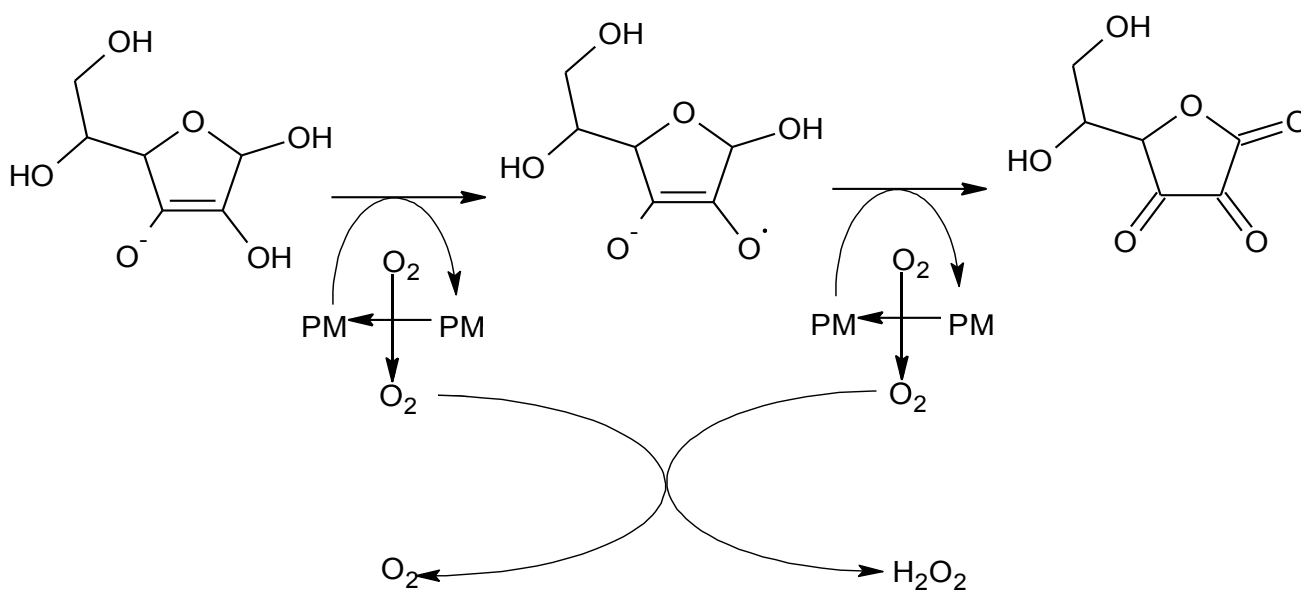
Figure 5.4. Chemical reaction between ascorbic acid and oxygen with PM as a catalyst.

5.2 Study of oxidative potential of PM samples

5.2.1 Methods

The goal of this work is to better understand the chemical species in PM that are able to oxidize DTT and ascorbic acid and to quantify their redox activity with respect to the two reagents. Thus, the two assays were tested on standard solutions of compounds commonly present in ambient PM.

Moreover, the oxidative potential of some real $PM_{2.5}$ samples collected in the area of Bologna were quantified.

Standards and reagents

Fifteen compounds representative of different chemical classes were considered for this study: four quinones namely 9,10-phenantrenequinone (9,10-PQN), 1,2-naphthoquinone (1,2-NPQ), 1,4-naphthoquinone (1,4-NPQ) and anthraquinone, three PAHs (naphthalene, phenanthrene and anthracene), two oxo-PAH (1,8-naphthalic anhydride and xanthone) and six metals (copper (II), manganese (II), Nickel (II), chromium (III), zinc (II) and iron (III)).

Quinones and metals are often indicate as redox active species [Roginsky et al. 1999, Kumagai et al. 2002, Cho et al. 2005, Lin et al. 2011, Charrier et al. 2012, Hedayat et al. 2014], while the activity of PAHs and oxo-PAHs is somewhat controversial [Cho et al. 2005, Lodovici et al. 2011, Charrier et al. 2012].

Individual standard stock solutions were prepared for each analyte by weighting pure standards (Acros Organics, Sigma Aldrich, Dr. Ehrenstorfer, Carlo Erba Reagenti) at a concentration of 10^{-2} M in acetonitrile for quinones, PAHs and oxo-PAHs and MilliQ water for metal ions. The solutions were stored in amber glass vials in the dark at -20°C. DTT solution was made at a concentration of 10 mM in a 0.1 M phosphate buffer (Na_2HPO_4 and NaH_2PO_4) at pH 7.4, while ascorbic acid solution was made at the same concentration as DTT but in MilliQ water. Aqueous solutions of the reagents are unstable at room temperature and DTT solutions are also sensible to light, thus they were preserved in amber glass vials in the dark and at -20°C.

Phosphate buffer was treated with Chelex 100 resin (Sigma Aldrich), a cation exchange resin, to remove trace metals. The resin was poured into an acid-rinsed glass chromatographic column that had a permanent glass frit to contain the resin. The phosphate solution was allowed to drip through the resin at 4°C and the resulting treated phosphate buffer was collected into a clean, acid washed, PTFE bottle.
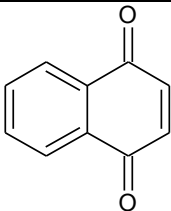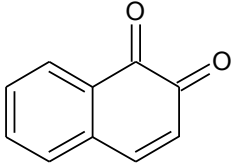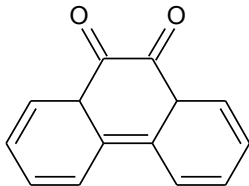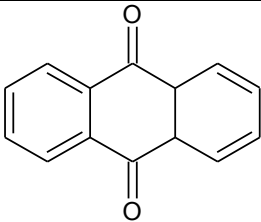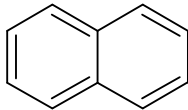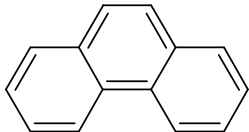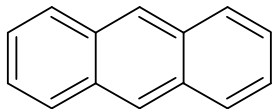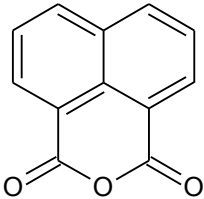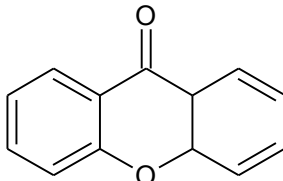
1,4-naphthoquinone	1,2-naphtoquinone	9,10-phenanthrenequinone
Anthraquinone	Naphthalene	Phenanthrene
Anthracene	1,8-naphthalic anhydride	Xanthone

Table 5.1. Organic species considered.

Analyses of standard solutions: DTT

For DTT, the method proposed by Charrier [Charrier et al. 2012] was followed. A small volume (< 30µL) of stock solution of the compound of interest was added to an amber vial containing 3 mL of phosphate buffer at pH 7.4 and the obtained solution was heated at 37°C using a dry bath.

Once the temperature reached 37°C, at time zero 30 µL of the DTT solution 10 mM were added to the vial. At known times, a 0.50 mL aliquot of the reaction mixture was removed and added to 0.50 mL of 10 % trichloroacetic acid to stop the reaction. When all time points were quenched, 50 µL of 10.0 mM DTNB in phosphate buffer at pH 7.4 were added, mixed well, and allowed to react for 2 minutes. Then 2.0 mL of 0.40 M Tris-HCl buffer at pH 8.9 with 20 mM of EDTA was added. It is important to increase pH value because the protonated form of TNB (Figure 5.3) show only a slight absorbance in contrast with the mercaptide ion (TNB^{2-}, thiol group pKa =4.53 at 25 °C) which has a higher absorbance (ε =14150 M^{-1} cm^{-1} at 412 nm) [Li et al. 2009].

Charrier suggests to add the DTNB before the Tris buffer to ensure the sample remains quenched until DTT has reacted with DTNB, even if the DTNB and DTT reaction is very fast [Li et al. 2009, Charrier et al. 2012].

Because both DTT and TNB are sensitive to light, the reactions were performed in dark vials covered with aluminium foil and store in the dark when not in use.

TNB was quantified using a 1 cm path length PS cell in a Varian Cary 50 UV-Vis spectrophotometer.

The reactions were performed at pH 7.4 and 37°C to simulate biological conditions that normally occur in a human body.

Analyses of standard solutions: AA

Most of the ascorbate assay studies in literature are performed in a 96 well plates equipped with a plate reader [Mudway et al. 2011, Janssen et al. 2014, Yang et al. 2014].

In this study, the method was adapted to a classical spectrophotometer and the reaction occurred directly into the spectrophotometric quartz cuvette. The procedure is similar to that used for DTT assay. Briefly, an aliquot of stock solutions of analytes were diluted in 3 ml phosphate buffer and heated at 37°C. At time zero, 30 μL of ascorbic acid solution were added to the cuvette and at known time the absorbance of the solution was read at 265 nm.

At pH 7.4, vitamin C is present almost totally as ascorbate ion [Buettner et al. 1993] that has a molar extinction coefficient of about 14500 M^{-1} cm^{-1} at the considered wavelength.

Data analysis

Rates of DTT and ascorbate loss were determined from a linear regression of five points of reagents concentration versus time (5, 10, 15, 25, 40 minutes). The blank consists of a 100 μM solution with no redox active species added. The rate of DTT or ascorbate loss in each standard was calculated from the slope of the linear regression and then blank corrected by subtracting the average blank rate. In almost cases the rate of loss was linear over the entire experiment but in few experiments last point of the kinetic (40 minutes) was rejected due to the not linearity of the loss.

5.2.2 DTT response from individual organic species and transition metals

The rate of DTT consumption was measured in the presence of different chemical compounds and transition metals to identify species that contribute most to oxidative stress (Table 5.2).

Among the four quinones tested, 9,10-PQN showed the highest reactivity while 1,2-NQN and 1,4-NQN also oxidized DTT with a remarkable rate. This is consistent with previous studies which indicate quinones as very reactive species in DTT oxidation [Kumagai et al. 2002, Cho et al. 2005, Chung et al. 2006, Li et al. 2009, Charrier et al. 2012]. In contrast, anthraquinone showed only a very slight redox activity.

The three considered PAHs are the not oxidized homologs of the tested quinones. All three PAHs caused no loss of DTT. This finding is in line with other studies [Cho et al. 2005, Charrier et al.2012] that indicate PAHs as not redox active species in the DTT assay even if the assay response could sometimes be correlated with PAHs concentration. This is likely due to the reactions PAHs can undergo; in fact, they can be oxidized to more polar compounds including quinones which have demonstrated a very strong redox activity.

	Conc. (µM)	Depletion rate (µM/min)
Reagents blank		-0.59
9,10-PQN	0.17	-3.81
1,2-NPQ	1.0	-5.79
1,4-NPQ	1.0	-2.81
Anthraquinone	1.0	-0.70
Cu^{2+}	1.0	-1.64
Mn^{2+}	1.0	-1.51
Ni^{2+}	1.0	-0.99
Cr^{3+}	1.0	-0.92
Zn^{2+}	1.0	-0.87
Fe^{3+}	1.0	-0.87

Table 5.2. DTT assay response to stock solutions.

In addition to the aforementioned organic species, two oxo-PAHs with a similar molecular formula to other considered species were tested since they were found in PM samples in the investigated area. Both 1,8-naphthalic anhydride and xanthone did not demonstrate redox activity in the DTT assay.

The tested metals shown a DTT depletion rate lower than that found for quinones (excluding anthraquinone). Cu (II) and Mn (II) were the most reactive ions followed by Ni (II), Cr (II), Fe (III) and Zn (II). Results are reported in Table 5.2.

DTT oxidation from metals seems to be slower in comparison to that obtained from some organic species but ambient concentrations of metals are often high and thus they might be important in DTT loss of real PM samples as shown in Figure 5.5.
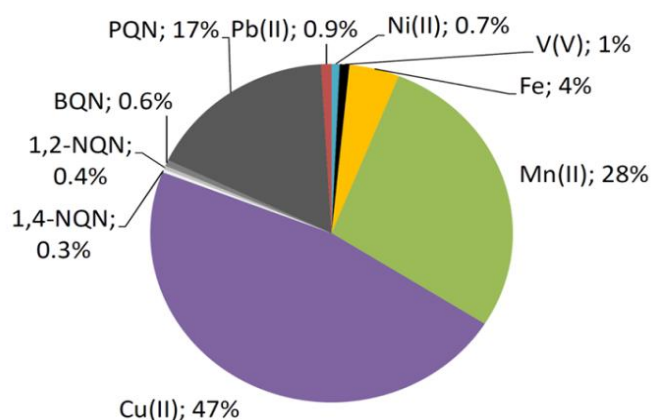
Figure 5.5. Calculated contributions of soluble metals and quinones to DTT loss in a hypothetical typical PM$_{2.5}$ sample [Charrier et al. 2012].

5.2.3 AA response from individual organic species and transition metals

The ascorbate assay sensitivity was tested using the same species as for DTT assay and different results were obtained.

Both quinones and metal ions are reported in literature as species able to oxidize ascorbic acid [Taqui Khan et al. 1967, Xu et al. 1990, Strizhak 1994, Anusevičius et al. 1998, Ayres et al. 2008].

Cu (II) was by far the most redox active species in this assay. In general, also the other considered metal ions have demonstrated good reactivity except Mn (II) that showed a depletion rate close to blank values.

Among quinones, 1,2-NPQ showed very high activity in the depletion of ascorbate while 9,10-PQN and 1,4-NPQ have demonstrated a redox capacity similar to metals. Anthraquinone did not cause measurable ascorbate oxidation.

As for DTT assay, PAHs and oxo-PAHs have highlighted their redox inactivity. Results are reported in Table 5.3.

The results obtained demonstrate that the two assays respond to the same chemical species but with different sensitivity, thus they could potentially provide complementary information on oxidative potential characteristic of PM. This behaviour is confirmed by some other studies [Mudway et al. 2011, Janssen et al. 2014, Yang et al. 2014] even if only few inter assay comparison have been published.

	Conc. (µM)	Depletion rate (µM/min)
Reagents blank		-0.43
1,2-NPQ	0.17	-1.80
1,4-NPQ	1.0	-1.07
9,10-PQN	1.0	-0.83
Cu^{2+}	0.17	-3.95
Cr^{3+}	1.0	-1.45
Fe^{3+}	1.0	-1.19
Zn^{3+}	1.0	-1.08
Ni^{2+}	1.0	-0.91
Mn^{2+}	1.0	-0.50

Table 5.2. Ascorbate assay response to stock solutions.

5.3 Analysis of ambient particulate matter

The investigated assays were applied to some real samples of $PM_{2.5}$ collected onto quartz filters in the Bologna area. The $PM_{2.5}$ samples on filters were stored at −20 °C in the dark prior to use. The response of reagents blank and of blank filters were determined to take into account the effect of reagents and sampling support on sample DTT and AA loss.

5.3.1 Results

A quarter of quartz filter (Whatman, 47 mm diameter, low volume sampler, ~55 m^3 day^{-1}) of $PM_{2.5}$ particles was extracted for 15 minutes in an ultrasonic bath using the Chelex

treated phosphate buffer 0.1 M at pH 7.4. Suspended solid particles from filter extracts were removed using a regenerate cellulose syringe filter (13 mm, 0.22 µm, Kinesis). Then 3 mL of the extracts were submitted to the analyses.

Data reported are only preliminary results that need further detailed studies.

As an example, the results obtained from filters with different PM loads are reported.
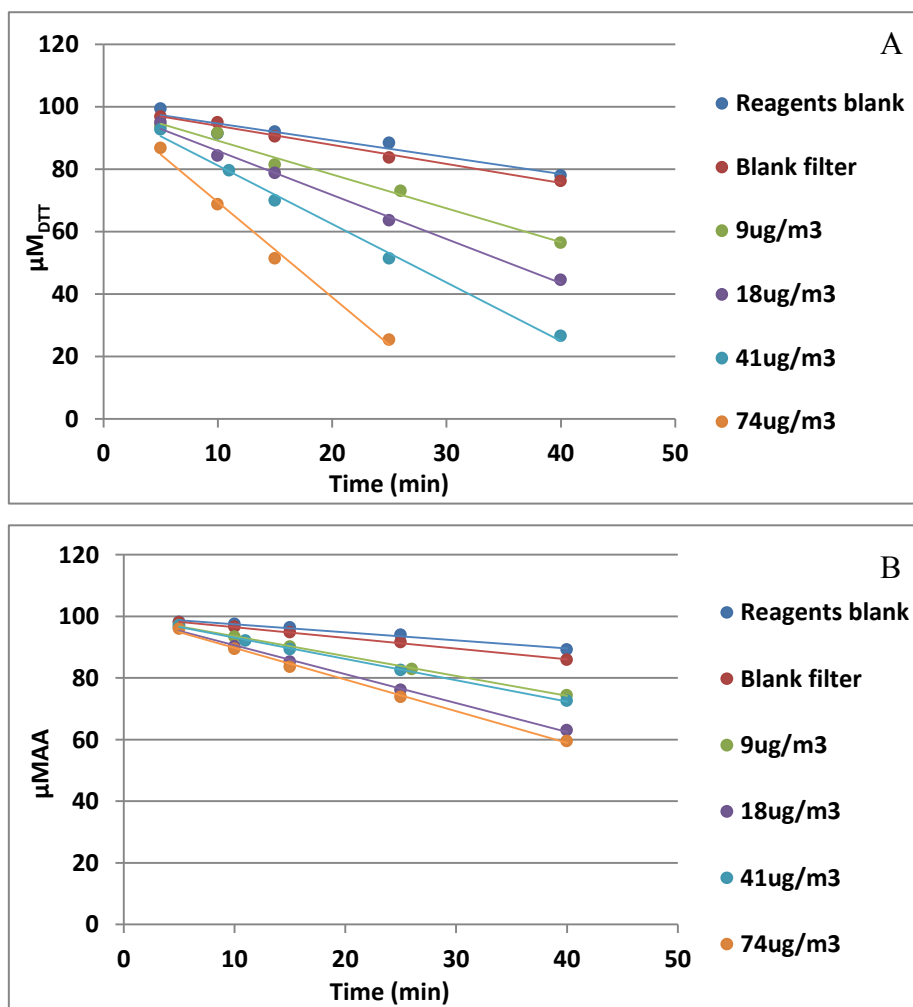
Figure 5.6. Response of A) DTT and B) AA assays to real samples with different PM concentrations.

Blank filter does not contribute much to assay response while sampled filters shown different sensibility to the two assays, as shown in Figure 5.6.

The most important thing to note is that the response magnitude is not always linked to the amount of particles on the filter. This found highlights that other parameters as well as PM mass concentration should be taken into account to evaluate aerosol effects on human health.

Usually, results are expressed per cubic meter of sampled air that is probably the best unit of measure to link results with biological effects since it is representative of the amount of air inhaled.
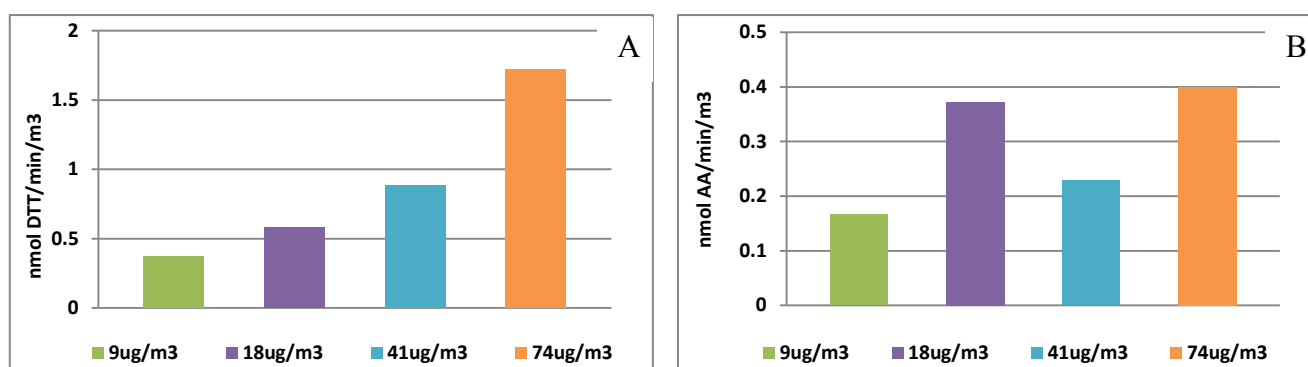
Figure 5.7. Response of A) DTT and B) AA assays to real samples with different PM concentrations expressed on volume basis.

Metals analysis

To better understand real sample responses, the concentrations of Cu, Zn, Cr, Fe, Ni and Mn were determined by atomic absorption spectroscopy.

The instrument used was an AAnalyst 800 by Perkin Elmer equipped with a THGA (transverse heating graphite atomizer) graphite furnace. Zeeman correction was applied to minimize matrix effect.

Briefly, one half of the filter was extracted in 10 mL of Chelex treated phosphate buffer, the solution was the filtered on regenerated cellulose syringe filter and finally submitted to the analysis.

PM concentration	Cu (ng/m^3)	Zn (ng/m^3)	Cr (ng/m^3)	Fe (ng/m^3)	Ni (ng/m^3)	Mn (ng/m^3)
Blank filter	1.0	3.0	2.3	28.8		1.0
9 $\mu g/m^3$	1.9	9.5	2.8	25.0		2.1
18 $\mu g/m^3$	2.6	10.8	4.7	28.1	<LOD	2.6
41 $\mu g/m^3$	2.8	11.5	9.2	37.5		2.1
74 $\mu g/m^3$	7.5	16.1	25.5	39.3		5.5

Table 5.4. Metals concentration in analysed $PM_{2.5}$ filters.

As a general trend, the higher PM concentration is, the higher metals concentration on the filter becomes.

Considering that AA assay is very sensible to copper and that quinones concentration is usually lower than those of metals [Walgraeve et al. 2010, Charrier et al. 2012], a much higher response of the most concentrated filter was expected.

This is not the case, highlighting that probably other species not considered in the study contribute in a not negligible amount to OP.

5.4 Conclusions and perspectives

Expressing the results on mass basis shows that less concentrated samples demonstrate higher OP. These less concentrated filters were sampled during summertime, suggesting that they may contain higher abundance of strong oxidized species. Emerging evidences suggest that photochemical aging and secondary sources may as well significantly impact the overall toxicity and redox activity of the ambient aerosols. Moreover, it was demonstrated higher summer-time cell-based ROS activities compared to winter in multiple urban areas of the world, again suggesting the potential enhancement of PM-induced redox activity and toxicity through secondary aerosol formation [Saffari et al. 2015].
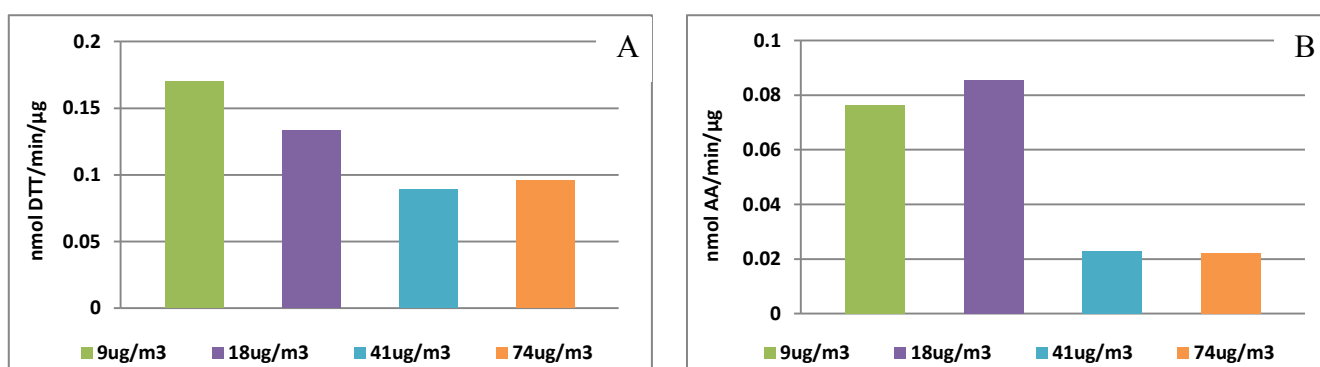
Figure 5.8. Response of A) DTT and B) AA assays to real samples with different $PM_{2.5}$ concentrations expressed on mass basis.

As aforementioned, further studies are needed to confirm the obtained results and to have a better knowledge on oxidative potential phenomenon. Future perspectives are to carry out monitoring campaigns to examine physico-chemical properties that mainly affect OP of aerosol and to test the real efficiency of acellular assays in simulating in vivo oxidative stress by perform in parallel to acellular assay, epidemiological studies on cellular lines in collaboration with ARPA Emilia Romagna.

The preliminary data presented underline once again the importance of an in-depth chemical speciation of particulate matter as even small amounts of some species that act as catalysers could give important effects on human health.

6. CONCLUSIONS

The present work is focused on the study of chemical composition of particulate matter (PM), as environmental matrix commonly connected to both human health problems and phenomena related to climate change.

There is a growing interest of authorities on properties and origin of PM, in particular, it is becoming increasingly important to be able to characterize the direct emission sources of aerosols or substances that can lead to the formation of PM into the atmosphere. In this way, specific information can be supplied to the competent authorities to establish future environmental and health protection policies in order to minimize the effects of air pollution, especially in the Po plain that is recognized as one of the worst air quality areas in Europe.

Sources and processes PM undergoes in the atmosphere can be derived from its chemical composition. The study its composition is a particularly complex challenge for analytical chemistry because particulate is composed of thousands of substances, both organic and inorganic. The analytical methods used for PM analysis are subjected to continuous evolutions in order to provide an increasing amount of information.

In light of these considerations, a part of the present work was devoted to the development and improvement of analytical techniques based on GC/MS analyses for the determination of polar organic compounds in atmospheric particle phase.

Gas chromatography coupled with mass spectrometry is a suitable technique for the analysis of very low concentrated compounds in an extremely complex matrix such as PM because of its great sensitivity and separative power.

Even if GC/MS techniques are very sensitive, the compounds of interest have often ambient concentrations below the detection limit of the methods. In order to further increase the analytical sensitivity, a mass tandem acquisition method was developed by exploiting the potential of the available detector, i.e. the ion trap.

The results obtained have shown that the signal acquisition in MSMS mode decreases drastically the interferences of the matrix and the background noise. This implementation has permitted to decrease the detection limit of an average of 6 times for many of the considered molecules with consequent benefits in analytes determination.

Furthermore, two other aspects of interest are actually under investigation. One concerns derivatization reaction: a reduction of energy and reagent consumption, and a

decrease in reaction time was desirable. The aim was achieved using ultrasound as energy supplier and optimizing the parameters that mostly affect reaction yield by response surface methodology.

The other aspect concerns a detailed investigation of the analytical procedure for the determiantion of sugars in PM samples as typical biomass combustion markers. In particular, an intercomparison study on anhydrosugars among ten laboratories is in progress to assess the comparability among different commonly used analytical techniques (gas chromatography-mass spectrometry, liquid chromatography-mass spectrometry, ion exchange chromatography and nuclear magnetic resonance). The study showed that in most cases the results obtained are comparable. The main activity of the work was devoted to air quality monitoring in Emilia Romagna region in the framework of the Supersito project. The developed techniques have been applied to the analysis of more than 100 markers in about one thousand samples of $PM_{2.5}$ filters collected in eight sampling campaigns carried out in different seasons between 2011 and 2014 at two sites in province of Bologna (Bologna located in an urban city and one rural San Pietro Capofiume, about 30 km northeast of Bologna).

The results have been integrated with data on the apolar organic fraction (polycyclic aromatic hydrocarbons and alkanes) and carbonaceous fraction (elemental carbon and organic carbon) acquired by other research groups within the Supersito project.

Using molecular markers, it was possible to identify that anthropogenic PM is mainly due to urban transport and domestic heating. Residential heating is by far the dominant source of PM and pollutants in winter periods, while traffic displays a constant contribution during the year.

Moreover, it was found that meteorological conditions play a key role regard the concentration of analytes in the atmosphere and their relative contribution. Much higher PM and pollutants concentration were in fact recorded in winter months when the limited planetary boundary layer height confines the considered substances in the first hundred meters of the atmosphere. In spring/summer periods, when solar irradiance and temperatures reach high values, a major contribution of secondary fraction of PM was registered together with an enhanced biogenic activity. In particular, the combustion of biomass has been recognize as one of the main sources of PM and other pollutants in winter periods, when heavy air pollution phenomena occurs. Thus, part of the work was specifically focused on a more detailed study on wood as domestic fuel. The obtained data have shown that up to 70% of PM is derived from biomass combustion and almost all benzo[a]pyrene is emitted from the same source during colder periods. The problem
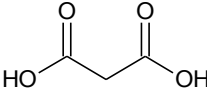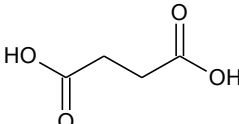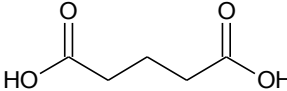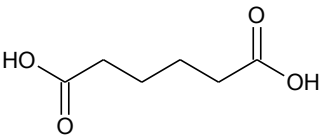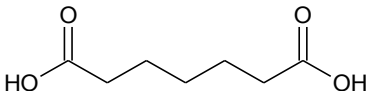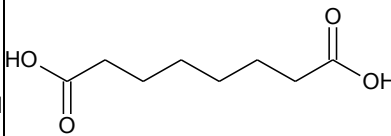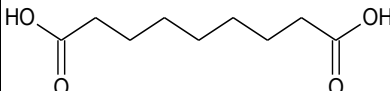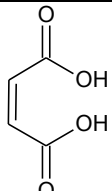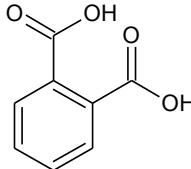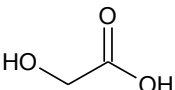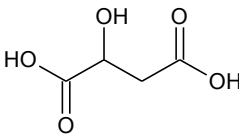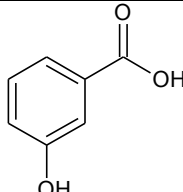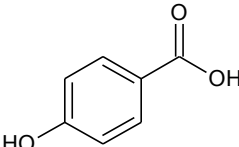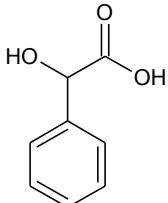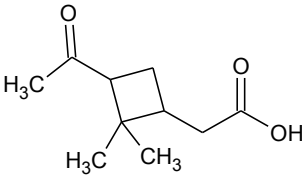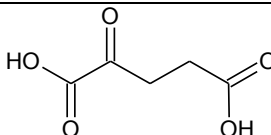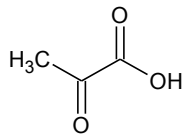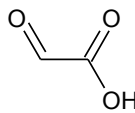
of biomass burning became more evident considering that heating plants using wood as fuel represent only a minority of the total.

The main perspective of this study is to relate PM chemical composition to toxicological effect of atmospheric aerosol. Therefore, part of the doctoral project has been devoted to the study of oxidative potential (OP) of particulate. In fact, many studies have described this property as more closely linked to adverse effects of PM on human health than its concentration. The work is still in progress by using two kinetic cell-free methods for the determination of OP: one uses ascorbic acid (AA) while the other uses dithiothreitol (DTT). The preliminary results highlight that the response is not always related to the concentration of PM in the atmosphere. This suggests that other parameters in addition to the concentration of PM should be taken into account in assessing the effects on human health.
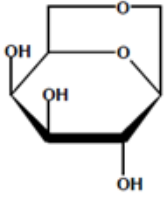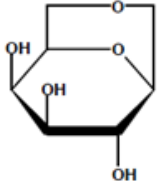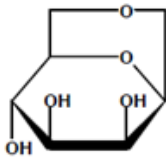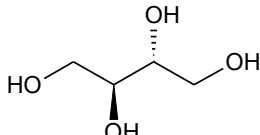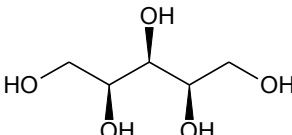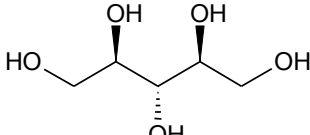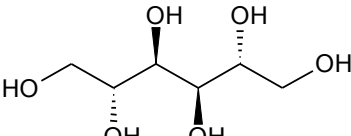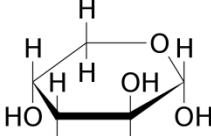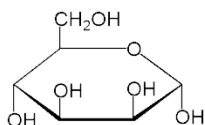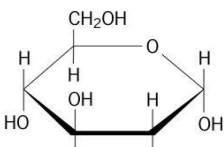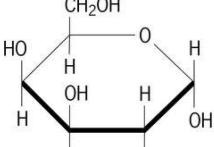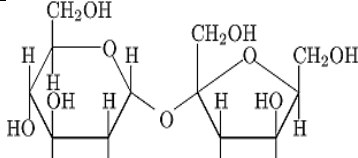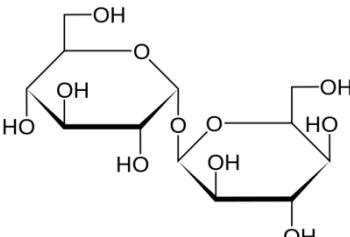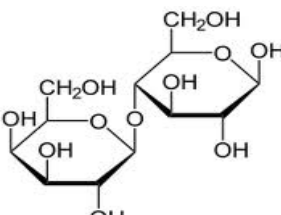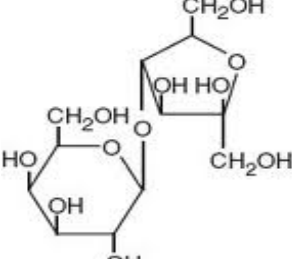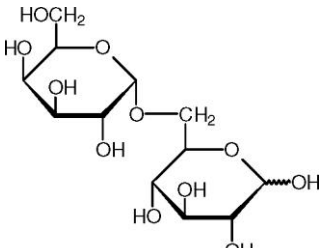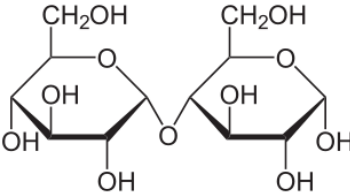
APPENDIX A

A.1 - Molecular formula
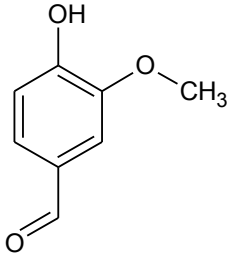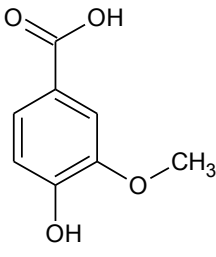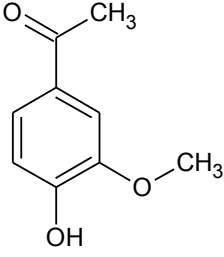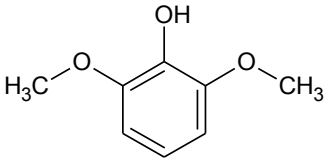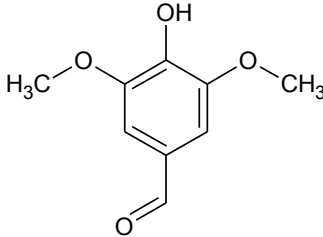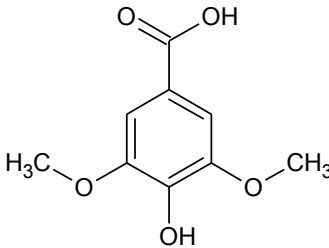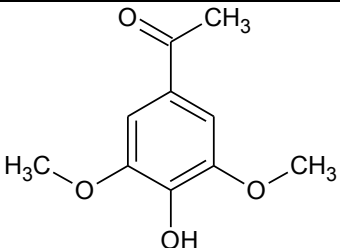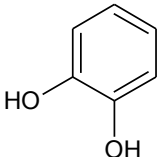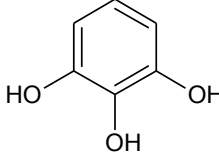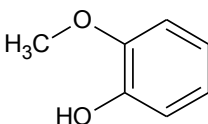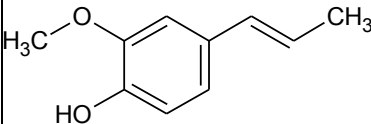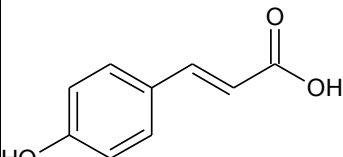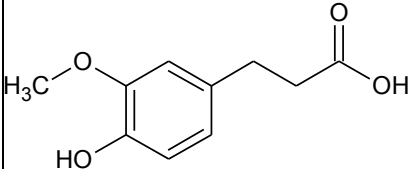
Acids

Malonic acid	Succinic acid	Glutaric acid
Adipic acid	Pimelic acid	Suberic acid
Azelaic acid	Maleic acid	Phthalic acid
Glycolic acid	Malic acid	3-hydroxybenzoic acid
4-hydroxybenzoic acid	Mandelic acid	Pinonic acid
2-ketoglutaric acid	Pyruvic acid	Glyoxylic acid

Sugars

Levoglucosan	Mannosan	Galactosan
Erythritol	Xylitol	Ribitol
Mannitol	Arabinose	Mannose
Glucose	Galactose	Sucrose
Mycose	Lactose	Lactulose
Melibiose	Maltose	

116

Phenols

Vanillin	Vanillic acid	Acetovanillone
Syringol	Syringaldehyde	Syringic acid
Acetosyringone	Cathecol	Pyrogallol
Guaiacol	Eugenol	p-coumaric acid
Ferulic acid		

A.2 - Analytical parameters

Acids

Name	Characteristic fragments (m/z)	MS/MS precursor ion	CID energy (V)	Product ions (m/z)	Ions intensity ratio
Malonic acid	73, 147, 149	233	1,00	147, 149, 217	1 : 1 : 4
Succinic acid	73, 147, 149	247	1,00	147, 149	2 : 1
Glutaric acid	73, 147, 149	233	1,25	147, 149	2 : 1
Adipic acid	111, 141, 185	141	0,75	75, 99	32 : 1
Pimelic acid	125, 155, 199	125	1,0	69, 79, 97	1 : 3,5 : 1
Suberic acid	169, 185, 303	169	1,0	75, 93, 141	21 : 1 : 1
Azelaic acid	133, 225, 317	225	1,5	143, 167, 169	3 : 8 : 1
Maleic acid	73, 147, 149	245	1,0	147, 149, 217	2,5 : 1,5 : 1
Phthalic acid	219, 265, 295	295	1,0	147, 149	2.5 : 1
Glycolic acid	73, 147, 149				
Malic acid	73, 147, 149	245	1,25	147, 149, 217	2,5 : 1 : 1,5
3-hydroxybenzoic acid	193, 223, 267	267	1,25	193, 223, 225	1 : 3 : 2
4-hydroxybenzoic acid	193, 223, 267	267	1,25	193, 223, 225	1 : 17 : 6
Mandelic acid	179, 253				
Pinonic acid	83, 109, 125, 171	109	1,0	79, 81, 91	3 : 2 : 1
2-ketoglutaric acid	113, 291, 347	113	1,25	69, 85, 95	1,5 : 1 : 1
Pyruvic acid	215, 258, 281	215	1,25	147, 149	2 : 1
Glyoxylic acid	133, 191, 221, 265	191	1,0	73, 147, 149	1,5 : 1,5 : 1

Phenols

Name	Characteristic fragments (m/z)	MS/MS precursor ion	CID energy (V)	Product ions (m/z)	Ions intensity ratio
Vanillin	193, 194, 209	194	1,5	137, 165	1 : 1
Vanillic acid	223, 267, 297	267	1,25	223, 225	1 : 3
Acetovanillone	223, 238, 253	238	1,0	223, 238	18 : 1
Syringol	181, 196, 211	196	1,25	153, 167, 181	2 : 1 : 3,5
Syringaldehyde	223, 224, 239	224	1,25	137, 167, 195	1,5 : 1 : 1,5
Syringic acid	253, 297, 312, 327	297	1,5	223, 253	1 : 6
Acetosyringone	193, 208, 223	193	1,25	137, 165	1 : 1,5
Cathecol	166, 239, 254, 327	254	1,0	166, 239	1 : 49
Pyrogallol	239, 240, 342	239	1,25	133, 151, 211	3,5 : 1 : 4,5
Guaiacol	151, 166, 181				
Eugenol	205, 206, 221				
p-coumarc acid	219, 249, 293	293	1,5	219, 233, 249	1 : 1 : 6
Ferulic acid	249, 293, 323	293	1,5	219, 233, 249	1 : 1 : 5,5

Sugars

Name	Characteristic fragments (m/z)
Levoglucosan	191, 204, 217
Mannosan	191, 204, 217
Galactosan	191, 204, 217
Erithrytol	191, 204, 217
Xylitol	191, 204, 217
Ribitol	191, 204, 217
Mannitol	191, 204, 217
Arabinose	191, 204, 217
Mannose	191, 204, 217

Name	Characteristic fragments (m/z)
Glucose	191, 204, 217
Galactose	191, 204, 217
Sucrose	169, 361
Mycose	169, 361
Lactose	169, 361
Lactulose	169, 361
Melibiose	169, 361
Maltose	169, 361

APPENDIX B - Results

Mean values ± standard deviation (SD) of the concentrations of determined analytes and calculated parameters. n.d. means not detected, more than 90% of the measured values were below the detection limit; <LOD means below detection limit; empty space means not determined; * means unrealistic values.

B.1 - Winter 2011

18th November – 6th December

Meteorological Conditions

		Main Site				San Pietro Capofiume			
		Min	Max	Average	S.D.	Min	Max	Average	S.D.
Average temperature	°C	2.1	9.0	6.5 ±	1.8	1.9	7.0	3.9 ±	1.8
Solar irradiance	W/m^2	17	88	61 ±	23	17	117	65 ±	30
PBL height	m	135	516	229 ±	81	88	248	169 ±	43
Precipitations	mm	1.0				5.2			

PM

		Main Site				San Pietro Capofiume			
		Min	Max	Average	S.D.	Min	Max	Average	S.D.
PM	μg/m^3	33.2	97.6	59.2 ±	17.4	22.3	85.2	46.3 ±	17.8
PM$_{bb}$	μg/m^3	7.0	68.8	29.0 ±	13.6	12.4	44.7	25.4 ±	10.8
PM$_{bb}$%		12.4	100*	52.0 ±	25.1	16.1	100*	60.8 ±	27.0

Carbonaceous fraction

For the first campaign, only TC values were available, due the lack of unbiased discrimination between OC and EC [Costa et al. 2016].

		Main Site				San Pietro Capofiume			
		Min	Max	Average	S.D.	Min	Max	Average	S.D.
TC	μg/m^3	8.1	18.0	11.9 ±	3.0	5.3	12.6	8.6 ±	3.2

Acids

		Main Site					San Pietro Capofiume				
		Min	Max	Average		S.D.	Min	Max	Average		S.D.
Malonic acid	ng/m^3	<LOD	77.4	21.7	±	24.1	<LOD	130.6	41.5	±	37.5
Succinic acid	ng/m^3	60.9	172.4	112.1	±	36.4	44.1	218.1	110.7	±	44.1
Glutaric acid	ng/m^3	8.8	31.6	18.4	±	7.2	6.3	30.3	17.4	±	7.8
Adipic acid	ng/m^3										
Pimelic acid	ng/m^3										
Suberic acid	ng/m^3										
Azelaic acid	ng/m^3										
Maleic acid	ng/m^3	<LOD	107.3	22.1	±	25.9	<LOD	661.5	65.3	±	156.6
Phthalic acid	ng/m^3	2.6	4.6	3.3	±	0.5	2.5	5.1	3.2	±	0.7
Glicolic acid	ng/m^3	7.6	42.6	20.1	±	8.3	5.9	37.0	19.0	±	8.1
Malic acid	ng/m^3	5.4	92.5	40.9	±	24.2	<LOD	63.3	31.8	±	18.6
3-hydroxybenzoic acid	ng/m^3	3.1	13.4	6.9	±	2.4	3.5	10.3	6.0	±	2.2
4-hydroxybenzoic acid	ng/m^3	4.3	25.7	9.3	±	4.9	3.5	12.1	7.1	±	2.9
Pinonic acid	ng/m^3										
2-ketoglutaric acid	ng/m^3	<LOD	15.4	7.2	±	4.0	<LOD	13.3	6.3	±	4.1
TCAs	ng/m^3	126.8	525.6	262.0	±	111.2	84.1	1010.0	308.3	±	220.2
OxCAs	ng/m^3	20.4	184.0	84.5	±	41.4	16.2	124.8	70.2	±	31.7
Other CAs	ng/m^3	89.4	341.6	177.6	±	72.9	52.9	931.3	238.1	±	205.5
% oxCAs		13.2	36.6	31.7	±	6.0	7.8	37.1	25.8	±	8.4
C3/C4		0.07	0.45	0.21	±	0.13	0.15	0.74	0.43	±	0.18
C6/C9											
Ph/C9											

Phenols

		Main Site					San Pietro Capofiume				
		Min	Max	Average		S.D.	Min	Max	Average		S.D.
Vanillin	ng/m^3			n.d.					n.d.		
Vanillic acid + Acetovanillone	ng/m^3	1.9	18.7	8.6	±	3.9	1.6	12.4	6.4	±	3.3
Syringaldehyde	ng/m^3										
Syringic acid	ng/m^3	0.7	4.8	2.1	±	0.9	0.0	2.9	1.5	±	0.8
Acetosyringone	ng/m^3	<LOD	5.0	1.3	±	1.1	0.1	2.0	0.8	±	0.6
Tot phenols	ng/m^3	3.0	31.1	13.3	±	6.2	3.5	17.6	9.7	±	4.9
S/V		0.27	0.53	0.36	±	0.08	0.20	0.57	0.35	±	0.09

Sugars

		Main Site					San Pietro Capofiume				
		Min	Max	Average	±	S.D.	Min	Max	Average	±	S.D.
Galactosan	ng/m^3	11.3	99.8	52.0	±	20.0	21.3	69.7	42.8	±	16.5
Mannosan	ng/m^3	28.2	230.2	120.7	±	45.1	56.9	164.8	105.7	±	39.6
Levoglucosan	ng/m^3	251.1	2477.3	1042.9	±	490.4	446.4	1607.8	916.0	±	389.3
Erithrytol	ng/m^3	3.2	7.9	5.2	±	1.4	1.2	9.6	4.2	±	2.1
Xylitol	ng/m^3										
Ribitol	ng/m^3	<LOD	8.0	4.2	±	2.0	<LOD	6.0	3.5	±	1.6
Mannitol	ng/m^3	<LOD	7.3	5.3	±	1.7	<LOD	7.8	4.4	±	2.1
Arabinose	ng/m^3	<LOD	6.5	3.2	±	1.8	<LOD	9.8	3.2	±	2.4
Mannose	ng/m^3	<LOD	11.7	4.9	±	2.4	<LOD	12.2	4.1	±	2.6
Glucose	ng/m^3	<LOD	53.9	9.4	±	12.1	<LOD	9.2	6.0	±	2.3
Galactose	ng/m^3	<LOD	7.2	4.6	±	1.7	<LOD	6.1	3.7	±	1.2
Sucrose	ng/m^3	<LOD	65.2	35.4	±	15.6	<LOD	49.7	36.1	±	12.3
Mycose	ng/m^3										
Tot sugars	ng/m^3	329.8	2880.4	1287.9	±	559.6	550.2	1918.0	1129.8	±	452.1
Anhydrosugars	ng/m^3	290.6	2807.3	1215.6	±	552.8	524.6	1832.9	1064.5	±	443.4
Primary sugars	ng/m^3	33.5	124.6	72.3	±	24.1	23.1	95.7	65.3	±	18.9
% anhydrosugars		88.1	97.5	93.7	±	2.5	90.6	95.6	93.7	±	2.0
% primary sugars		2.5	11.9	6.3	±	2.5	4.4	9.4	6.3	±	2.0
L/M		7.19	10.76	8.54	±	1.09	7.02	10.09	8.59	±	0.87

Alkanes

		Main Site					San Pietro Capofiume				
		Min	Max	Average	±	S.D.	Min	Max	Average	±	S.D.
C22	ng/m^3	1.29	15.99	5.89	±	3.88	0.48	10.75	4.21	±	2.50
C23	ng/m^3	3.86	18.52	9.65	±	4.20	2.38	15.93	7.53	±	3.35
C24	ng/m^3	5.02	21.50	11.06	±	4.15	3.66	18.02	8.83	±	3.71
C25	ng/m^3	3.90	20.80	10.46	±	4.41	2.14	18.15	8.19	±	4.23
C26	ng/m^3	2.60	14.12	7.13	±	3.03	1.48	13.72	5.68	±	3.43
C27	ng/m^3	4.05	26.24	11.00	±	5.69	1.61	20.13	8.34	±	5.39
C28	ng/m^3	1.32	10.33	4.70	±	2.37	0.33	10.84	3.93	±	2.82
C29	ng/m^3	4.80	32.19	15.45	±	7.13	2.20	29.38	11.59	±	7.64
C30	ng/m^3	0.62	7.07	3.20	±	1.76	0.00	7.42	2.36	±	2.02
C31	ng/m^3	2.77	21.73	10.59	±	5.03	0.86	17.84	6.84	±	4.79
C32	ng/m^3	0.51	4.05	1.83	±	0.99	0.02	4.21	1.37	±	1.15
C33	ng/m^3	<LOD	8.19	3.24	±	2.41	0.44	5.38	2.45	±	1.48
Tot alkanes	ng/m^3	34.78	200.45	100.64	±	44.47	29.04	199.60	86.29	±	45.34
CPI		1.44	2.30	0.21	±	0.13	1.41	2.20	1.71	±	0.19

123

PAHs

		Main Site					San Pietro Capofiume				
		Min	Max	Average		S.D.	Min	Max	Average		S.D.
Phenanthrene	ng/m^3	0.03	0.23	0.13	±	0.06	0.01	0.29	0.06	±	0.07
Anthracene	ng/m^3	<LOD	0.03	0.01	±	0.01	<LOD	0.04	0.005	±	0.008
Fluoranthene	ng/m^3	0.23	1.46	0.73	±	0.32	0.04	1.02	0.41	±	0.29
Pyrene	ng/m^3	0.26	1.83	0.67	±	0.40	0.01	0.92	0.34	±	0.27
Benzo (a) anthracene	ng/m^3	0.32	2.07	1.11	±	0.49	0.11	2.11	0.69	±	0.50
Chrysene	ng/m^3	0.39	2.34	1.18	±	0.52	0.15	1.50	0.62	±	0.36
Benzo (b+j) fluoranthene	ng/m^3	0.90	4.41	2.36	±	0.77	0.48	4.18	1.82	±	0.95
Benzo (k) fuoranthene	ng/m^3	0.23	0.99	0.58	±	0.19	0.11	0.86	0.40	±	0.21
Benzo(e)pyrene	ng/m^3	0.45	1.94	1.00	±	0.37	0.19	1.56	0.72	±	0.36
Benzo(a)pyrene	ng/m^3	0.30	2.11	1.12	±	0.48	0.09	1.68	0.72	±	0.45
Perylene	ng/m^3	0.05	0.34	0.20	±	0.08	0.00	0.29	0.11	±	0.08
Indeno (1,2,3-c,d,) pyrene	ng/m^3	0.39	2.21	1.15	±	0.50	0.14	1.40	0.65	±	0.33
Benzo (g,h,i) perylene	ng/m^3	0.57	2.47	1.44	±	0.58	0.16	1.46	0.75	±	0.36
Tot PAHs	ng/m^3	4.95	22.59	13.43	±	4.86	1.72	16.75	8.01	±	4.36
BaP/(Bap+BeP)		0.36	0.58	0.52	±	0.05	0.31	0.55	0.47	±	0.07
BaP/BeP		0.57	1.41	1.10	±	0.20	0.44	1.23	0.93	±	0.23
IcdP/IcdP+BghiP		0.37	0.48	0.44	±	0.03	0.39	0.53	0.46	±	0.04
∑BFs/BghiP		1.05	3.57	2.19	±	0.65	2.03	4.39	3.05	±	0.60
BaP$_{bb}$	ng/m^3	0.20	1.98	0.83	±	0.39	0.36	1.29	0.73	±	0.31
BaP$_{bb}$%		14.3	100*	79.7	±	69.1	45.5	100*	81.3	±	24.1

B.2 - Summer 2012

14th June – 11th July

Meteorological conditions

		Main Site				San Pietro Capofiume			
		Min	Max	Average	S.D.	Min	Max	Average	S.D.
Average temperature	°C	20.4	31.9	27.5	± 2.6	18.6	29.6	25.7	± 2.6
Solar irradiance	W/m^2	213	328	295	± 27	221	366	324	± 32
PBL height	m	756	1252	974	± 132	668	1120	854	± 109
Precipitations	mm	3.8				12.4			

PM

		Main Site				San Pietro Capofiume			
		Min	Max	Average	S.D.	Min	Max	Average	S.D.
PM	μg/m^3	8.4	26.6	15.1	± 4.3	10.6	24.9	17.8	± 4.3
PM$_{bb}$	μg/m^3	0.01	0.17	0.06	± 0.05	0.02	1.58	0.16	± 0.33
PM$_{bb}$%		0.05	1.56	0.46	± 0.46	0.08	15.0	1.19	± 3.13

Carbonaceous fraction

		Main Site				San Pietro Capofiume			
		Min	Max	Average	S.D.	Min	Max	Average	S.D.
TC	μg/m^3	3.1	7.0	4.8	± 1.0	2.8	6.1	4.4	± 1.0
OC	μg/m^3	2.5	5.5	3.7	± 0.8	2.3	5.5	3.8	± 1.0
EC	μg/m^3	0.4	2.0	1.0	± 0.4	0.4	1.3	0.7	± 0.2
OC/EC	μg/m^3	1.6	7.0	4.0	± 1.5	3.6	8.2	5.9	± 1.2
Oc$_{sec}$	μg/m^3	0.2	3.8	2.1	± 0.8	0.4	3.1	1.5	± 0.7
Oc$_{sec}$%		27.0	76.7	57.5	± 13.2	15.8	55.6	38.5	± 10.4
Oc$_{bb(levo)}$	μg/m^3	0.003	0.040	0.014	± 0.013	0.007	0.071	0.039	± 0.079
Oc$_{bb(levo)}$%		0.05	1.43	0.40	± 0.42	0.15	1.81	0.53	± 0.49
Oc$_{bb(radio)}$	μg/m^3	0.2	0.7	0.4	± 0.1	0.2	0.5	0.2	± 0.1
OC$_{fossil}$	μg/m^3	0.8	1.7	1.1	± 0.2	1.4	3.6	2.5	± 0.6
Oc$_{bio}$	μg/m^3	1.4	3.5	2.2	± 0.5	0.7	1.6	1.2	± 0.3
Oc$_{bb(radio)}$%		5.1	21.7	10.1	± 4.2	4.3	9.7	6.3	± 1.4
OC$_{fossil}$%		29.9	32.5	30.7	± 0.7	59.7	65.9	63.6	± 1.7
OC$_{bio}$%		45.7	65.0	59.2	± 4.8	29.8	30.6	30.1	± 0.2

Acids

Acid concentrations were ≤ LOD since low-volume air sampler (55 m^3 in a day) was used.

Phenols

Phenol concentrations were ≤ LOD since low-volume air sampler (55 m^3 in a day) was used.

Sugars

		Main Site					San Pietro Capofiume				
		Min	Max	Average		S.D.	Min	Max	Average		S.D.
Galactosan	ng/m^3			n.d.					n.d.		
Mannosan	ng/m^3	<LOD	0.8	0.1	±	0.2	<LOD	11.1	0.9	±	2.3
Levoglucosan	ng/m^3	<LOD	5.9	2.1	±	1.9	<LOD	57.0	5.4	±	11.5
Erithrytol	ng/m^3			n.d.			<LOD	3.3	0.5	±	1.0
Xylitol	ng/m^3			n.d.			<LOD	0.6	0.03	±	0.13
Ribitol	ng/m^3	<LOD	1.7	0.3	±	0.5	<LOD	26.4	4.3	±	7.1
Mannitol	ng/m^3	<LOD	12.8	3.0	±	3.9	<LOD	150.7	25.8	±	35.4
Arabinose	ng/m^3			n.d.			<LOD	2.2	0.3	±	0.5
Mannose	ng/m^3			n.d.			<LOD	3.4	0.4	±	0.9
Glucose	ng/m^3	<LOD	2.7	0.8	±	0.8	<LOD	22.2	3.3	±	4.6
Galactose	ng/m^3			n.d.			<LOD	7.8	0.8	±	1.8
Sucrose	ng/m^3			n.d.					n.d.		
Mycose	ng/m^3			n.d.					n.d.		
Tot sugars	ng/m^3	0.6	18.2	6.7	±	6.0	0.9	228.1	41.9	±	59.3
Anhydrosugars	ng/m^3	0.4	6.7	2.3	±	2.1	0.6	68.1	6.9	±	14.2
Primary sugars	ng/m^3	0.2	16.2	4.4	±	5.0	0.3	199.8	35.6	±	49.7
% anhydrosugars		11.3	89.3	46.0	±	27.3	3.7	61.7	19.1	±	18.5
% primary sugars		10.7	88.7	54.0	±	27.3	38.3	96.3	80.9	±	18.5
L/M		7.44	19.23	14.74	±	4.94	5.08	11.00	7.66	±	2.18

Alkanes

		Main Site					San Pietro Capofiume				
		Min	Max	Average		S.D.	Min	Max	Average		S.D.
C22	ng/m^3	0.46	1.34	0.75	±	0.24	0.53	4.34	1.15	±	0.72
C23	ng/m^3	<LOD	1.78	0.86	±	0.41	0.95	4.60	1.56	±	0.70
C24	ng/m^3	0.20	1.71	0.60	±	0.38	0.26	3.90	1.18	±	0.80
C25	ng/m^3	0.09	2.59	1.08	±	0.53	0.77	7.14	2.05	±	1.25
C26	ng/m^3	0.44	1.69	0.79	±	0.34	0.60	5.07	1.54	±	1.14
C27	ng/m^3	0.51	3.20	1.20	±	0.55	1.06	7.05	2.70	±	1.60
C28	ng/m^3	0.31	2.11	0.67	±	0.43	0.44	10.62	1.79	±	2.22
C29	ng/m^3	0.11	2.65	0.91	±	0.58	1.35	19.85	4.17	±	3.57
C30	ng/m^3	<LOD	2.07	0.30	±	0.49	0.18	16.43	1.68	±	3.22
C31	ng/m^3	0.07	2.97	0.76	±	0.65	0.86	15.00	2.93	±	2.81
C32	ng/m^3	0.05	2.68	0.31	±	0.49	0.00	7.53	0.93	±	1.61
C33	ng/m^3	0.07	2.47	0.36	±	0.44	0.22	3.15	0.88	±	0.79
Tot alkanes	ng/m^3	4.06	26.28	10.37	±	5.08	11.83	90.98	27.10	±	19.23
CPI		0.47	2.51	1.32	±	0.43	0.87	2.79	1.77	±	0.48

PAHs

		Main Site					San Pietro				
		Min	Max	Average		S.D.	Min	Max	Average		S.D.
Phenanthrene	ng/m^3	<LOD	0.03	0.01	±	0.01	<LOD	0.03	0.01	±	0.01
Anthracene	ng/m^3	<LOD	0.01	0.001	±	0.002	<LOD	0.01	0.001	±	0.002
Fluoranthene	ng/m^3	<LOD	0.04	0.02	±	0.01	<LOD	0.03	0.01	±	0.01
Pyrene	ng/m^3	0.01	0.05	0.02	±	0.01	<LOD	0.03	0.01	±	0.01
Benzo (a) anthracene	ng/m^3	<LOD	0.04	0.01	±	0.01	<LOD	0.01	0.004	±	0.001
Chrysene	ng/m^3	<LOD	0.06	0.02	±	0.01	<LOD	0.02	0.008	±	0.003
Benzo (b+j) fluoranthene	ng/m^3	<LOD	0.10	0.03	±	0.02	<LOD	0.10	0.02	±	0.02
Benzo (k) fuoranthene	ng/m^3	<LOD	0.02	0.01	±	0.01	<LOD	0.02	0.004	±	0.005
Benzo(e)pyrene	ng/m^3	<LOD	0.05	0.02	±	0.01	<LOD	0.05	0.01	±	0.01
Benzo(a)pyrene	ng/m^3	<LOD	0.04	0.02	±	0.01	<LOD	0.02	0.007	±	0.003
Perylene	ng/m^3	<LOD	0.01	0.002	±	0.001	<LOD	0.01	0.001	±	0.002
Indeno (1,2,3-c,d,) pyrene	ng/m^3	0.01	0.04	0.02	±	0.01	<LOD	0.06	0.01	±	0.01
Benzo (g,h,i) perylene	ng/m^3	0.01	0.05	0.03	±	0.01	0.01	0.05	0.01	±	0.01
Tot PAHs	ng/m^3	0.13	0.57	0.24	±	0.09	0.00	0.40	0.16	±	0.07
BaP/(Bap+BeP)		0.36	0.53	0.42	±	0.05	0.09	0.49	0.38	±	0.07
BaP/BeP		0.56	1.11	0.73	±	0.14	0.10	0.96	0.63	±	0.15
IcdP/IcdP+BghiP		0.22	0.46	0.34	±	0.05	0.32	0.54	0.41	±	0.05
∑BFs/BghiP		0.85	2.60	1.45	±	0.40	0.40	2.48	1.42	±	0.52
BaP$_{bb}$	ng/m^3	0.0003	0.0048	0.0017	±	0.0015	0.0004	0.0029	0.0047	±	0.0095
BaP$_{bb}$%		1.7	52.4	13.7	±	13.9	6.8	72.9	30.6	±	19.7

B.3 - Fall 2012

23rd October – 10th November

Meteorological conditions

		Main Site				San Pietro Capofiume			
		Min	Max	Average	S.D.	Min	Max	Average	S.D.
Average temperature	°C	6.7	16.0	12.0	± 2.6	4.7	14.1	10.6	± 2.7
Solar irradiance	W/m^2	23	120	71	± 35	22	149	86	± 44
PBL height	m	261	695	376	± 107	161	462	263	± 77
Precipitations	mm	65.0				74.8			

PM

		Main Site				San Pietro Capofiume			
		Min	Max	Average	S.D.	Min	Max	Average	S.D.
PM	μg/m^3	6.2	71.0	31.1	± 17.3	5.8	64.6	26.7	± 16.6
PM$_{bb}$	μg/m^3	1.6	13.8	8.0	± 4.0	2.1	12.6	6.5	± 3.2
PM$_{bb}$%		6.1	59.2	28.6	± 12.4	11.9	56.8	27.0	± 13.2

Carbonaceous fraction

		Main Site				San Pietro Capofiume			
		Min	Max	Average	S.D.	Min	Max	Average	S.D.
TC	μg/m^3	3.0	18.1	9.6	± 4.2	4.5	7.7	6.0	± 1.4
OC	μg/m^3	2.1	14.9	6.9	± 3.8	3.4	6.3	4.9	± 1.2
EC	μg/m^3	0.7	5.4	2.4	± 1.2	0.9	1.4	1.1	± 0.2
OC/EC	μg/m^3	0.8	6.0	2.9	± 1.5	3.3	5.7	4.7	± 1.1
Oc$_{sec}$	μg/m^3	1.1	12.4	5.3	± 3.7	1.8	2.3	2.0	± 0.3
Oc$_{sec}$%		54.6	87.2	73.4	± 9.9	28.3	42.6	36.6	± 7.5
Oc$_{bb(levo)}$	μg/m^3	0.4	3.3	1.9	± 1.0	0.5	3.0	1.6	± 0.8
Oc$_{bb(levo)}$%		7.0	90.1	36.2	± 24.2	14.7	37.4	23.0	± 10.0
Oc$_{bb(radio)}$	μg/m^3	1.5	8.5	4.1	± 1.9	1.3	2.2	1.7	± 0.4
OC$_{fossil}$	μg/m^3	0.8	4.7	2.5	± 1.1	0.6	2.3	1.7	± 0.8
Oc$_{bio}$	μg/m^3	0	5.7	0.4	± 3.4	1.2	2.0	1.6	± 0.4
Oc$_{bb(radio)}$%		26.0	61.1	41.8	± 12.2	27.4	47.7	34.6	± 9.2
OC$_{fossil}$%		30.4	35.9	32.9	± 1.9	18.5	42.0	33.7	± 10.6
OC$_{bio}$%		3.0	43.7	25.4	± 14.1	30.6	33.8	31.7	± 1.4

Acids

		Main Site				San Pietro Capofiume			
		Min	Max	Average	S.D.	Min	Max	Average	S.D.
Malonic acid	ng/m^3	<LOD	100.8	26.7 ±	32.6	<LOD	65.0	12.3 ±	22.2
Succinic acid	ng/m^3	5.7	52.1	26.8 ±	14.3	6.2	49.8	22.2 ±	12.6
Glutaric acid	ng/m^3	3.9	35.9	17.1 ±	9.0	<LOD	13.2	5.9 ±	3.9
Adipic acid	ng/m^3	1.3	7.1	3.5 ±	1.9	1.3	7.3	3.0 ±	1.7
Pimelic acid	ng/m^3	1.0	7.9	3.2 ±	1.6	0.9	4.0	2.0 ±	1.1
Suberic acid	ng/m^3	n.d.				n.d.			
Azelaic acid	ng/m^3	2.7	25.3	10.0 ±	7.1	<LOD	22.4	5.7 ±	6.2
Maleic acid	ng/m^3	n.d.				n.d.			
Phthalic acid	ng/m^3	1.7	11.4	5.3 ±	3.0	<LOD	5.0	2.7 ±	1.6
Glicolic acid	ng/m^3	3.7	43.4	16.3 ±	12.4	3.9	42.9	13.6 ±	11.7
Malic acid	ng/m^3	1.8	66.9	25.7 ±	22.5	5.2	56.1	22.1 ±	17.1
3-hydroxybenzoic acid	ng/m^3	<LOD	2.9	1.2 ±	0.9	<LOD	2.7	0.8 ±	0.8
4-hydroxybenzoic acid	ng/m^3	<LOD	5.3	2.2 ±	1.3	<LOD	3.1	1.5 ±	0.8
Pinonic acid	ng/m^3	<LOD	5.1	2.1 ±	1.4	<LOD	3.4	0.7 ±	1.3
2-ketoglutaric acid	ng/m^3	4.8	67.7	27.4 ±	19.2	4.5	91.8	22.3 ±	22.4
TCAs	ng/m^3	35.5	330.3	167.4 ±	109.6	29.8	316.3	114.8 ±	89.5
OxCAs	ng/m^3	15.5	156.4	74.8 ±	50.4	16.3	165.7	61.1 ±	47.8
Other CAs	ng/m^3	20.1	191.7	92.6 ±	60.0	13.5	165.2	53.7 ±	43.2
% oxCAs		36.4	56.3	44.0 ±	4.7	44.5	61.1	53.1 ±	5.3
C3/C4		0.13	2.87	0.92 ±	0.8	0.32	1.75	0.95 ±	0.62
C6/C9		0.20	0.78	0.40 ±	0.1	0.26	3.04	0.65 ±	0.73
Ph/C9		0.41	0.87	0.59 ±	0.1	0.60	2.27	0.61 ±	0.54

Phenols

		Main Site				San Pietro Capofiume			
		Min	Max	Average	S.D.	Min	Max	Average	S.D.
Vanillin	ng/m^3	1.3	2.4	1.8 ±	0.3	1.0	1.7	1.2 ±	0.2
Vanillic acid	ng/m^3	1.1	6.1	2.3 ±	1.1	0.9	1.3	1.1 ±	0.1
Acetovanillone	ng/m^3	<LOD	9.7	1.9 ±	2.1	<LOD	3.4	0.7 ±	0.9
Syringaldehyde	ng/m^3	2.6	7.3	4.2 ±	1.5	<LOD	4.9	2.4 ±	1.7
Syringic acid	ng/m^3	1.8	6.1	3.6 ±	1.2	<LOD	5.3	2.7 ±	1.5
Acetosyringone	ng/m^3	n.d.				n.d.			
Tot phenols	ng/m^3	7.0	22.3	14.1 ±	4.9	2.0	15.7	8.1 ±	4.1
S/V		0.53	1.86	1.41 ±	0.31	0.91	2.90	1.88 ±	0.55

Sugars

				Main Site					San Pietro Capofiume			
		Min	Max	Average		S.D.		Min	Max	Average		S.D.
Galactosan	ng/m³	3.4	62.1	29.8	±	18.3		6.7	49.4	23.7	±	13.8
Mannosan	ng/m³	8.6	152.7	63.5	±	38.4		14.9	103.6	47.0	±	25.6
Levoglucosan	ng/m³	57.4	498.1	288.9	±	143.9		75.1	454.1	233.2	±	114.6
Erithrytol	ng/m³	<LOD	3.6	1.7	±	1.1		<LOD	2.0	0.9	±	0.6
Xylitol	ng/m³			n.d.						n.d.		
Ribitol	ng/m³			n.d.						n.d.		
Mannitol	ng/m³	<LOD	10.4	3.4	±	3.8		<LOD	23.2	4.3	±	6.0
Arabinose	ng/m³	<LOD	5.9	2.4	±	1.6		<LOD	5.4	2.4	±	1.4
Mannose	ng/m³			n.d.						n.d.		
Glucose	ng/m³	2.0	12.4	6.9	±	2.9		1.7	8.6	4.9	±	1.9
Galactose	ng/m³	1.0	5.1	2.8	±	1.2		1.0	6.6	2.6	±	1.4
Sucrose	ng/m³	<LOD	15.8	4.6	±	4.3		<LOD	46.1	6.2	±	11.0
Mycose	ng/m³	1.2	4.9	2.1	±	0.9		0.9	2.8	1.6	±	0.6
Tot sugars	ng/m³	89.8	729.4	406.1	±	208.2		105.5	636.8	327.0	±	158.7
Anhydrosugars	ng/m³	69.4	675.9	382.2	±	198.7		96.6	607.1	303.9	±	153.3
Primary sugars	ng/m³	7.4	53.5	23.9	±	12.9		7.2	58.0	23.0	±	13.8
% anhydrosugars		77.3	97.7	93.1	±	4.4		80.3	97.2	92.3	±	4.7
% primary sugars		2.3	22.7	6.9	±	4.4		3.8	19.7	7.7	±	4.7
L/M		3.11	6.64	4.91	±	0.77		4.14	6.07	5.09	±	0.46

Alkanes

				Main Site					San Pietro Capofiume			
		Min	Max	Average		S.D.		Min	Max	Average		S.D.
C22	ng/m³	<LOD	2.90	1.18	±	0.81		<LOD	2.29	0.43	±	0.61
C23	ng/m³	<LOD	4.58	2.26	±	1.32		0.64	5.49	2.29	±	1.19
C24	ng/m³	1.28	5.31	3.25	±	1.32		<LOD	5.59	1.88	±	1.59
C25	ng/m³	1.46	7.96	4.04	±	2.07		1.37	15.02	4.78	±	3.25
C26	ng/m³	<LOD	4.39	2.16	±	1.26		<LOD	25.64	3.19	±	5.60
C27	ng/m³	<LOD	7.05	3.09	±	2.20		0.64	68.03	7.41	±	14.52
C28	ng/m³	<LOD	3.75	1.04	±	1.16		<LOD	154.73	9.05	±	34.33
C29	ng/m³	<LOD	11.72	4.23	±	3.50		1.01	277.33	18.95	±	60.91
C30	ng/m³	<LOD	2.84	0.61	±	0.95		<LOD	331.71	17.25	±	74.02
C31	ng/m³	<LOD	10.71	3.23	±	3.01		<LOD	353.04	21.10	±	78.18
C32	ng/m³	<LOD	2.01	0.28	±	0.61		<LOD	241.53	12.20	±	53.98
C33	ng/m³	<LOD	4.21	0.94	±	1.18		<LOD	122.41	6.94	±	27.21
Tot alkanes	ng/m³	3.21	64.07	27.01	±	17.74		5.95	1669.45	112.13	±	366.98
CPI		1.04	2.76	1.99	±	0.46		1.01	15.00	3.59	±	3.41

PAHs

		Main Site					San Pietro Capofiume				
		Min	Max	Average		S.D.	Min	Max	Average		S.D.
Phenanthrene	ng/m^3	<LOD	0.10	0.03	±	0.02	<LOD	0.03	0.01	±	0.01
Anthracene	ng/m^3	<LOD	0.02	0.003	±	0.006	<LOD	0.10	0.004	±	0.002
Fluoranthene	ng/m^3	0.02	0.35	0.15	±	0.09	<LOD	0.14	0.05	±	0.04
Pyrene	ng/m^3	0.01	0.42	0.15	±	0.12	<LOD	0.08	0.03	±	0.02
Benzo (a) anthracene	ng/m^3	0.03	0.69	0.22	±	0.20	0.01	0.30	0.08	±	0.07
Chrysene	ng/m^3	0.06	0.69	0.28	±	0.19	0.01	0.26	0.13	±	0.08
Benzo (b+j) fluoranthene	ng/m^3	0.12	1.87	0.79	±	0.47	0.08	1.27	0.48	±	0.34
Benzo (k) fuoranthene	ng/m^3	0.04	0.50	0.23	±	0.13	0.02	0.33	0.12	±	0.09
Benzo(e)pyrene	ng/m^3	0.08	0.86	0.37	±	0.19	0.04	0.62	0.24	±	0.16
Benzo(a)pyrene	ng/m^3	0.07	1.17	0.40	±	0.16	0.02	0.70	0.21	±	0.19
Perylene	ng/m^3	0.01	0.14	0.06	±	0.04	0.01	0.31	0.06	±	0.08
Indeno (1,2,3-c,d,) pyrene	ng/m^3	0.05	0.64	0.32	±	0.17	0.03	0.42	0.18	±	0.12
Benzo (g,h,i) perylene	ng/m^3	0.09	0.85	0.44	±	0.23	0.04	0.49	0.22	±	0.14
Tot PAHs	ng/m^3	0.88	8.66	3.83	±	2.16	0.34	5.18	2.02	±	1.41
BaP/(Bap+BeP)		0.39	0.58	0.50	±	0.05	0.05	0.57	0.44	±	0.11
BaP/BeP		0.65	1.36	1.02	±	0.20	0.06	1.34	0.83	±	0.29
IcdP/IcdP+BghiP		0.35	0.46	0.42	±	0.03	0.42	0.50	0.45	±	0.02
∑BFs/BghiP		0.80	3.56	2.37	±	0.64	1.49	7.52	2.93	±	1.83
BaP$_{bb}$	ng/m^3	0.05	0.40	0.23	±	0.11	0.06	0.36	0.19	±	0.09
BaP$_{bb}$%		20.0	98.2	61.7	±	22.4	50.7	232.2	88.5	±	48.0

B.4 - Winter 2013

30th January – 17th February

Meteorological conditions

		Main Site				San Pietro Capofiume			
		Min	Max	Average	S.D.	Min	Max	Average	S.D.
Average temperature	°C	0.4	7.4	3.9	± 1.6	1.0	4.7	2.6	± 1.0
Solar irradiance	W/m^2	14	121	78	± 33.3	9	144	89	± 47
PBL height	m	243	560	398	± 83.1	110	444	296	± 103
Precipitations	mm	49.4				40.4			

PM

		Main Site				San Pietro Capofiume			
		Min	Max	Average	S.D.	Min	Max	Average	S.D.
PM	µg/m^3	12.6	73.0	33.1	± 14.0	9.5	86.9	35.2	± 19.5
PM$_{bb}$	µg/m^3	3.5	12.3	7.2	± 2.8	3.2	13.3	7.0	± 3.1
PM$_{bb}$%		12.7	43.0	23.4	± 8.4	9.1	46.2	22.8	± 9.6

Carbonaceous fraction

		Main Site				San Pietro Capofiume			
		Min	Max	Average	S.D.	Min	Max	Average	S.D.
TC	µg/m^3	6.2	16.2	9.2	± 2.7	6.9	17.5	10.2	± 3.9
OC	µg/m^3	4.8	12.1	7.2	± 2.0	5.5	15.7	8.3	± 3.6
EC	µg/m^3	1.0	4.1	1.9	± 0.8	0.9	1.9	1.4	± 0.3
OC/EC	µg/m^3	2.5	5.6	3.8	± 0.9	4.0	8.5	5.9	± 1.6
Oc$_{sec}$	µg/m^3	0.3	3.9	2.3	± 1.1	1.1	8.3	3.5	± 2.9
Oc$_{sec}$%		5.7	54.6	32.1	± 14.6	15.8	52.8	33.6	± 14.9
Oc$_{bb(levo)}$	µg/m^3	0.8	2.9	1.7	± 0.7	0.8	3.2	1.7	± 0.7
Oc$_{bb(levo)}$%		15.6	58.9	26.2	± 12.4	11.9	30.2	20.3	± 7.1
Oc$_{bb(radio)}$	µg/m^3	1.6	6.4	3.1	± 1.2	1.7	2.9	2.3	± 0.4
OC$_{fossil}$	µg/m^3	1.6	4.2	2.4	± 0.7	1.6	8.2	3.8	± 2.4
Oc$_{bio}$	µg/m^3	0.1	3.0	1.7	± 0.9	1.8	4.6	2.7	± 1.0
Oc$_{bb(radio)}$%		28.0	61.7	43.3	± 10.1	18.4	39.0	28.1	± 7.5
OC$_{fossil}$%		30.7	36.0	33.1	± 1.6	28.6	52.4	41.2	± 8.6
OC$_{bio}$%		2.4	41.3	23.6	± 11.7	29.2	32.4	30.7	± 1.2

Acids

		Main Site				San Pietro Capofiume			
		Min	Max	Average	S.D.	Min	Max	Average	S.D.
Malonic acid	ng/m³	4.3	76.2	26.8 ±	21.1	<LOD	92.0	23.1 ±	26.1
Succinic acid	ng/m³	13.3	49.4	32.3 ±	12.6	11.1	61.2	35.1 ±	14.5
Glutaric acid	ng/m³	<LOD	52.6	18.5 ±	13.2	<LOD	52.6	23.1 ±	17.8
Adipic acid	ng/m³	<LOD	9.6	3.8 ±	2.4	<LOD	8.5	4.2 ±	2.1
Pimelic acid	ng/m³	<LOD	4.7	1.1 ±	1.9	<LOD	7.6	3.2 ±	2.3
Suberic acid	ng/m³			n.d.				n.d.	
Azelaic acid	ng/m³	<LOD	34.1	9.9 ±	10.1	<LOD	29.0	10.4 ±	9.5
Maleic acid	ng/m³	<LOD	158.6	64.2 ±	39.9	<LOD	134.2	51.7 ±	41.1
Phthalic acid	ng/m³	<LOD	28.5	9.3 ±	7.7	<LOD	35.5	9.4 ±	9.0
Glicolic acid	ng/m³	5.9	32.0	14.2 ±	6.5	4.3	34.4	16.9 ±	9.5
Malic acid	ng/m³	3.9	38.8	20.3 ±	11.5	<LOD	46.2	21.4 ±	15.4
3-hydroxybenzoic acid	ng/m³	<LOD	3.9	1.8 ±	1.0	<LOD	5.1	1.8 ±	1.4
4-hydroxybenzoic acid	ng/m³	0.9	5.3	2.8 ±	1.5	0.6	7.5	3.0 ±	1.9
Pinonic acid	ng/m³			n.d.		<LOD	6.4	1.4 ±	2.0
2-ketoglutaric acid	ng/m³	<LOD	97.0	44.3 ±	29.6	2.3	137.8	43.3 ±	34.2
TCAs	ng/m³	51.6	458.3	249.3 ±	122.3	44.0	524.6	247.9 ±	139.0
OxCAs	ng/m³	15.5	149.0	83.4 ±	43.1	15.6	202.7	87.7 ±	55.7
Other CAs	ng/m³	23.2	346.2	165.9 ±	84.5	28.4	371.8	160.1 ±	90.1
% oxCAs		12.7	54.9	34.4 ±	9.9	18.7	50.3	34.2 ±	9.3
C3/C4		0.14	1.99	0.81 ±	0.52	0.15	2.30	0.87 ±	0.64
C6/C9		0.12	0.43	0.29 ±	0.09	0.20	0.78	0.38 ±	0.17
Ph/C9		0.32	1.90	0.87 ±	0.50	1.53	2.13	0.96 ±	0.62

Phenols

		Main Site				San Pietro Capofiume			
		Min	Max	Average	S.D.	Min	Max	Average	S.D.
Vanillin	ng/m³	<LOD	1.7	0.6 ±	0.7	<LOD	1.6	1.0 ±	0.5
Vanillic acid	ng/m³	2.1	8.7	4.2 ±	1.9	1.3	10.9	4.5 ±	2.9
Acetovanillone	ng/m³	<LOD	6.5	2.2 ±	2.1	<LOD	12.4	2.6 ±	3.3
Syringaldehyde	ng/m³	<LOD	12.5	4.2 ±	4.3	<LOD	14.7	4.5 ±	4.8
Syringic acid	ng/m³	2.1	11.1	5.8 ±	2.8	1.8	11.3	5.3 ±	3.1
Acetosyringone	ng/m³			n.d.				n.d.	
Tot phenols	ng/m³	4.2	38.6	17.3 ±	9.7	3.3	37.2	18.5 ±	11.8
S/V		0.56	3.45	1.52 ±	0.81	0.47	2.47	1.33 ±	0.58

Sugars

		Main Site					San Pietro Capofiume				
		Min	Max	Average		S.D.	Min	Max	Average		S.D.
Galactosan	ng/m³	7.9	50.9	31.6	±	12.3	8.7	57.0	32.0	±	15.4
Mannosan	ng/m³	29.8	104.6	63.6	±	23.7	23.2	110.7	61.5	±	27.2
Levoglucosan	ng/m³	125.5	442.7	259.4	±	98.9	114.4	477.3	252.9	±	110.7
Erithrytol	ng/m³	<LOD	10.2	2.8	±	2.4	<LOD	7.3	2.1	±	1.9
Xylitol	ng/m³			n.d.					n.d.		
Ribitol	ng/m³			n.d.					n.d.		
Mannitol	ng/m³	<LOD	4.3	1.4	±	1.1	<LOD	3.1	1.0	±	0.9
Arabinose	ng/m³	<LOD	6.1	3.2	±	1.5	1.5	6.7	3.2	±	1.6
Mannose	ng/m³			n.d.					n.d.		
Glucose	ng/m³	3.6	11.2	5.6	±	1.7	3.6	8.7	5.4	±	1.4
Galactose	ng/m³	1.8	6.0	3.0	±	1.1	1.6	6.4	3.1	±	1.3
Sucrose	ng/m³	<LOD	14.0	3.1	±	3.0	<LOD	4.9	2.6	±	1.2
Mycose	ng/m³	<LOD	2.5	1.0	±	0.7	<LOD	2.1	1.0	±	0.6
Tot sugars	ng/m³	179.3	639.8	374.6	±	139.8	159.3	661.8	364.7	±	155.9
Anhydrosugars	ng/m³	169.5	598.2	354.6	±	133.3	149.3	637.1	346.3	±	151.3
Primary sugars	ng/m³	9.8	41.6	20.0	±	7.5	10.0	28.2	18.4	±	5.3
% anhydrosugars		93.1	96.6	94.6	±	0.9	92.4	96.3	94.6	±	1.2
% primary sugars		3.4	6.9	5.4	±	0.9	3.7	7.6	5.4	±	1.2
L/M		3.53	5.43	4.09	±	0.41	3.24	5.15	4.18	±	0.52

Alkanes

		Main Site					San Pietro Capofiume				
		Min	Max	Average		S.D.	Min	Max	Average		S.D.
C22	ng/m³	0.92	6.42	3.31	±	1.53	0.46	4.22	2.37	±	1.18
C23	ng/m³	0.73	8.34	3.97	±	2.14	0.88	6.60	2.96	±	1.53
C24	ng/m³	1.01	7.61	4.08	±	1.78	0.73	5.69	2.69	±	1.47
C25	ng/m³	1.19	8.34	4.16	±	1.89	<LOD	5.87	2.49	±	1.82
C26	ng/m³	0.55	8.52	3.44	±	1.87	<LOD	5.68	1.66	±	1.61
C27	ng/m³	1.52	6.23	3.68	±	1.27	<LOD	11.19	2.38	±	2.88
C28	ng/m³	<LOD	4.12	1.50	±	1.20	<LOD	11.74	1.38	±	3.04
C29	ng/m³	1.21	8.07	4.50	±	1.83	<LOD	17.05	3.08	±	4.15
C30	ng/m³	<LOD	4.67	2.09	±	1.43	<LOD	16.32	1.45	±	4.05
C31	ng/m³	<LOD	7.70	3.48	±	1.98	<LOD	15.40	2.23	±	3.75
C32	ng/m³	<LOD	3.94	1.63	±	1.40	<LOD	8.44	0.75	±	2.01
C33	ng/m³	<LOD	3.48	1.56	±	1.36	<LOD	7.89	0.71	±	1.89
Tot alkanes	ng/m³	9.72	74.15	40.50	±	19.42	4.40	118.56	29.64	±	27.17
CPI		0.92	6.42	3.31	±	1.53	0.46	4.22	2.37	±	1.18

PAHs

		Main Site					San Pietro Capofiume				
		Min	Max	Average		S.D.	Min	Max	Average		S.D.
Phenanthrene	ng/m^3	<LOD	0.05	0.01	±	0.01	<LOD	0.33	0.08	±	0.09
Anthracene	ng/m^3			n.d.			<LOD	0.03	0.005	±	0.009
Fluoranthene	ng/m^3	<LOD	0.32	0.09	±	0.09	<LOD	0.63	0.31	±	0.18
Pyrene	ng/m^3	<LOD	0.19	0.05	±	0.05	<LOD	0.42	0.21	±	0.12
Benzo (a) anthracene	ng/m^3	0.04	0.84	0.28	±	0.22	<LOD	0.80	0.18	±	0.22
Chrysene	ng/m^3	0.12	1.48	0.42	±	0.32	0.01	0.95	0.32	±	0.32
Benzo (b+j) fluoranthene	ng/m^3	0.28	2.99	0.84	±	0.62	0.09	2.29	0.98	±	0.69
Benzo (k) fuoranthene	ng/m^3	0.07	0.83	0.22	±	0.17	0.02	0.65	0.28	±	0.20
Benzo(e)pyrene	ng/m^3	0.13	1.42	0.39	±	0.29	0.02	1.02	0.44	±	0.31
Benzo(a)pyrene	ng/m^3	0.05	2.20	0.39	±	0.48	0.01	1.17	0.47	±	0.41
Perylene	ng/m^3	0.01	0.15	0.05	±	0.04	0.00	0.16	0.06	±	0.05
Indeno (1,2,3-c,d,) pyrene	ng/m^3	0.11	0.69	0.27	±	0.14	0.02	0.75	0.30	±	0.22
Benzo (g,h,i) perylene	ng/m^3	0.17	0.90	0.36	±	0.18	0.02	0.98	0.37	±	0.27
Tot PAHs	ng/m^3	1.14	11.58	3.57	±	2.51	0.28	10.11	4.29	±	2.92
BaP/(Bap+BeP)		0.26	0.61	0.45	±	0.09	0.24	0.58	0.46	±	0.10
BaP/BeP		0.35	1.56	0.86	±	0.31	0.32	1.36	0.89	±	0.31
IcdP/IcdP+BghiP		0.40	0.47	0.43	±	0.02	0.39	0.68	0.46	±	0.06
∑BFs/BghiP		1.69	4.27	2.81	±	0.62	1.54	4.45	3.54	±	0.73
BaP$_{bb}$	ng/m^3	0.10	0.35	0.21	±	0.08	0.09	0.38	0.20	±	0.09
BaP$_{bb}$%		15.2	108.6	68.6	±	27.3	10.3	96.2	52.9	±	28.5

B.5 - Spring 2013

7th May – 27th May

Meteorological conditions

		Main Site				San Pietro Capofiume			
		Min	Max	Average	S.D.	Min	Max	Average	S.D.
Average temperature	°C	10.8	21.8	17.6 ±	2.3	9.8	20.6	16.5 ±	2.4
Solar irradiance	W/m²	113	312	228 ±	64.0	87	342	240 ±	79
PBL height	m	679	1348	954 ±	204	566	1145	786 ±	160
Precipitations	mm	64.6				53.0			

PM

		Main Site				San Pietro Capofiume			
		Min	Max	Average	S.D.	Min	Max	Average	S.D.
PM	μg/m³	5.2	13.3	8.5 ±	2.4	2.8	19.4	8.0 ±	4.8
PM_{bb}	μg/m³	0.01	1.9	0.3 ±	0.5	0.02	0.2	0.1 ±	0.1
$PM_{bb}\%$		0.2	23.5	4.3 ±	5.8	0.3	6.7	1.8 ±	2.1

Carbonaceous fraction

		Main Site				San Pietro Capofiume			
		Min	Max	Average	S.D.	Min	Max	Average	S.D.
TC	μg/m³	1.7	4.4	2.9 ±	0.9	1.3	2.4	1.9 ±	0.5
OC	μg/m³	1.1	2.9	2.0 ±	0.6	1.1	1.9	1.5 ±	0.4
EC	μg/m³	0.3	1.8	0.9 ±	0.4	0.5	0.4	0.3 ±	0.1
OC/EC	μg/m³	1.5	5.5	2.6 ±	1.1	3.5	6.4	4.9 ±	1.2
Oc_{sec}	μg/m³	0.001	1.2	0.7 ±	0.4	0.2	0.6	0.5 ±	0.1
$Oc_{sec}\%$		0.04	72.9	37.2 ±	19.6	12.9	45.5	31.7 ±	14.6
$Oc_{bb(levo)}$	μg/m³	0.002	0.5	0.1 ±	0.1	0	0.04	0.03 ±	0.02
$Oc_{bb(levo)}\%$		0.0	21.2	4.5 ±	5.6	0	4.8	1.5 ±	1.9
$Oc_{bb(radio)}$	μg/m³	0.1	0.6	0.3 ±	0.1	0.1	0.2	0.1 ±	0.1
OC_{fossil}	μg/m³	0.3	0.8	0.5 ±	0.2	0.8	1.3	1.0 ±	0.2
Oc_{bio}	μg/m³	0.6	1.6	1.2 ±	0.3	0.3	0.5	0.4 ±	0.1
$Oc_{bb(radio)}\%$		6.5	23.9	15.6 ±	5.1	5.5	10.2	7.6 ±	1.9
$OC_{fossil}\%$		25.5	28.2	26.9 ±	0.8	63.8	69.2	66.8 ±	2.2
$OC_{bio}\%$		47.9	68.1	57.5 ±	5.9	25.4	26.0	25.6 ±	0.3

Acids

		Main Site				San Pietro Capofiume			
		Min	Max	Average	S.D.	Min	Max	Average	S.D.
Malonic acid	ng/m^3	<LOD	2.0	0.9 ±	0.6	<LOD	2.0	0.9 ±	0.6
Succinic acid	ng/m^3	<LOD	4.7	1.9 ±	1.4	<LOD	5.3	2.6 ±	1.5
Glutaric acid	ng/m^3	<LOD	1.7	0.4 ±	0.5	<LOD	1.4	0.5 ±	0.4
Adipic acid	ng/m^3	<LOD	1.3	0.4 ±	0.4	<LOD	1.1	0.4 ±	0.4
Pimelic acid	ng/m^3	n.d.				n.d.			
Suberic acid	ng/m^3	<LOD	2.0	1.0 ±	0.6	<LOD	1.3	0.6 ±	0.5
Azelaic acid	ng/m^3	<LOD	2.0	0.5 ±	0.7	<LOD	1.5	0.1 ±	0.4
Maleic acid	ng/m^3	<LOD	0.8	0.2 ±	0.3	<LOD	1.0	0.2 ±	0.4
Phthalic acid	ng/m^3	<LOD	1.2	0.3 ±	0.4	<LOD	0.9	0.1 ±	0.3
Glicolic acid	ng/m^3	1.0	7.7	4.2 ±	2.0	<LOD	10.6	4.3 ±	2.6
Malic acid	ng/m^3	<LOD	29.1	6.5 ±	7.1	<LOD	7.6	3.1 ±	1.8
3-hydroxybenzoic acid	ng/m^3	n.d.				n.d.			
4-hydroxybenzoic acid	ng/m^3	n.d.				n.d.			
Pinonic acid	ng/m^3	<LOD	0.7	0.3 ±	0.3	<LOD	1.6	0.8 ±	0.6
2-ketoglutaric acid	ng/m^3	<LOD	1.0	0.2 ±	0.3	<LOD	1.1	0.1 ±	0.3
TCAs	ng/m^3	6.0	54.5	17.4 ±	11.9	5.3	24.1	13.9 ±	4.7
OxCAs	ng/m^3	4.1	38.9	11.6 ±	8.6	2.2	16.4	8.5 ±	4.1
Other CAs	ng/m^3	1.0	15.6	5.8 ±	3.5	1.3	8.5	5.4 ±	2.1
% oxCAs		46.6	84.8	66.0 ±	9.7	41.0	90.5	59.4 ±	14.8
C3/C4		0.07	0.64	0.39 ±	0.17	0.12	0.77	0.30 ±	0.18
C6/C9		0.43	0.70	0.57 ±	0.12	0.39	2.87	1.22	0.99
Ph/C9		0.37	0.73	0.53 ±	0.14	0.35	2.27	1.36	0.84

Phenols

		Main Site				San Pietro Capofiume			
		Min	Max	Average	S.D.	Min	Max	Average	S.D.
Vanillin	ng/m^3	n.d.				<LOD	0.3	0.2 ±	0.1
Vanillic acid	ng/m^3	<LOD	0.4	0.2 ±	0.1	<LOD	0.3	0.1 ±	0.1
Acetovanillone	ng/m^3	<LOD	0.4	0.1 ±	0.2	<LOD	0.3	0.1 ±	0.2
Syringaldehyde	ng/m^3	<LOD	0.3	0.2 ±	0.1	<LOD	0.2	0.1 ±	0.1
Syringic acid	ng/m^3	<LOD	0.3	0.2 ±	0.1	<LOD	0.3	0.1 ±	0.1
Acetosyringone	ng/m^3	n.d.				n.d.			
Tot phenols	ng/m^3	0.5	2.0	1.1 ±	0.5	0.2	1.4	0.6 ±	0.4
S/V		0.41	2.27	0.89 ±	0.56	0.31	0.71	0.53 ±	0.14

Sugars

		Main Site					San Pietro Capofiume				
		Min	Max	Average		S.D.	Min	Max	Average		S.D.
Galactosan	ng/m³	<LOD	10.6	1.3	±	2.6	<LOD	0.8	0.4	±	0.2
Mannosan	ng/m³	<LOD	12.4	1.8	±	3.0	<LOD	1.7	0.7	±	0.4
Levoglucosan	ng/m³	<LOD	69.3	12.6	±	16.9	<LOD	8.1	3.8	±	2.5
Erithrytol	ng/m³	<LOD	3.4	0.6	±	0.8	<LOD	0.6	0.3	±	0.1
Xylitol	ng/m³			n.d.					n.d.		
Ribitol	ng/m³			n.d.					n.d.		
Mannitol	ng/m³	<LOD	72.1	13.7	±	17.4	<LOD	15.7	6.3	±	4.9
Arabinose	ng/m³	<LOD	3.4	0.5	±	0.8	<LOD	0.5	0.3	±	0.1
Mannose	ng/m³	<LOD	35.6	3.8	±	8.9	<LOD	18.0	4.6	±	6.1
Glucose	ng/m³	<LOD	40.4	6.2	±	9.7	<LOD	29.0	7.3	±	9.2
Galactose	ng/m³	<LOD	9.4	1.1	±	2.3	<LOD	2.2	0.7	±	0.7
Sucrose	ng/m³	<LOD	7.0	1.7	±	1.8	<LOD	4.2	0.9	±	1.1
Mycose	ng/m³	<LOD	15.8	6.9	±	5.1	<LOD	21.4	5.3	±	5.6
Tot sugars	ng/m³	4.4	256.6	50.2	±	60.2	8.2	81.2	30.5	±	22.3
Anhydrosugars	ng/m³	0.6	92.3	15.7	±	22.3	1.1	10.4	4.9	±	3.0
Primary sugars	ng/m³	1.6	164.3	34.5	±	38.6	6.6	73.1	25.7	±	21.3
% anhydrosugars		12.2	62.7	30.7	±	14.1	4.7	55.5	20.4	±	13.5
% primary sugars		37.3	87.8	69.3	±	14.1	44.5	95.3	79.6	±	13.5
L/M		2.16	11.31	6.98	±	2.84	2.86	7.42	5.40	±	1.58

Alkanes

		Main Site					San Pietro Capofiume				
		Min	Max	Average		S.D.	Min	Max	Average		S.D.
C22	ng/m³	<LOD	0.50	0.25	±	0.16			n.d.		
C23	ng/m³	0.23	0.73	0.38	±	0.16	<LOD	0.21	0.09	±	0.07
C24	ng/m³	0.13	0.85	0.34	±	0.20	<LOD	0.24	0.14	±	0.06
C25	ng/m³	0.67	1.43	1.00	±	0.30	0.10	0.38	0.25	±	0.09
C26	ng/m³	0.11	1.06	0.42	±	0.30	<LOD	0.11	0.02	±	0.04
C27	ng/m³	1.34	2.97	2.15	±	0.60	0.51	1.38	0.88	±	0.27
C28	ng/m³	<LOD	0.79	0.34	±	0.25	<LOD	0.26	0.05	±	0.10
C29	ng/m³	1.45	3.94	2.73	±	0.72	0.82	1.93	1.44	±	0.38
C30	ng/m³	<LOD	0.91	0.38	±	0.24	0.00	0.20	0.06	±	0.09
C31	ng/m³	1.75	3.95	2.60	±	0.63	0.53	2.02	1.22	±	0.41
C32	ng/m³	0.21	0.66	0.36	±	0.13	<LOD	0.19	0.07	±	0.08
C33	ng/m³	1.52	3.98	2.41	±	0.85	<LOD	0.32	0.22	±	0.09
Tot alkanes	ng/m³	16.58	21.14	15.78	±	3.43	2.55	6.62	4.78	±	1.00
CPI		2.35	14.34	5.69	±	3.17	3.15	26.36	15.26	±	9.07

PAHs

		Main Site					San Pietro Capofiume				
		Min	Max	Average		S.D.	Min	Max	Average		S.D.
Phenanthrene	ng/m^3	<LOD	0.02	0.006	±	0.003	n.d.				
Anthracene	ng/m^3	<LOD	0.02	0.002	±	0.005	n.d.				
Fluoranthene	ng/m^3	0.02	0.04	0.02	±	0.01	<LOD	0.01	0.004	±	0.002
Pyrene	ng/m^3	0.01	0.06	0.02	±	0.01	<LOD	0.01	0.004	±	0.002
Benzo (a) anthracene	ng/m^3	0.01	0.03	0.01	±	0.01	n.d.				
Chrysene	ng/m^3	0.01	0.03	0.02	±	0.01	<LOD	0.01	0.002	±	0.002
Benzo (b+j) fluoranthene	ng/m^3	0.02	0.08	0.05	±	0.02	<LOD	0.13	0.02	±	0.03
Benzo (k) fuoranthene	ng/m^3	0.01	0.02	0.01	±	0.01	<LOD	0.03	0.01	±	0.01
Benz(e)pyrene	ng/m^3	0.01	0.05	0.03	±	0.01	<LOD	0.06	0.01	±	0.02
Benzo(a)pyrene	ng/m^3	0.01	0.05	0.02	±	0.01	<LOD	0.04	0.01	±	0.01
Perylene	ng/m^3	<LOD	0.01	0.003	±	0.002	n.d.				
Indeno (1,2,3-c,d,) pyrene	ng/m^3	0.01	0.03	0.01	±	0.01	<LOD	0.01	0.004	±	0.001
Benzo (g,h,i) perylene	ng/m^3	0.01	0.05	0.03	±	0.01	<LOD	0.01	0.006	±	0.002
Tot PAHs	ng/m^3	0.13	0.49	0.26	±	0.11	0.02	0.31	0.08	±	0.08
BaP/(Bap+BeP)		0.32	0.54	0.40	±	0.06	0.25	0.42	0.35	±	0.05
BaP/BeP		0.47	1.16	0.71	±	0.18	0.65	0.72	0.54	±	0.11
IcdP/IcdP+BghiP		0.23	0.41	0.32	±	0.04	0.37	0.47	0.41	±	0.03
∑BFs/BghiP		1.77	2.98	2.25	±	0.35	1.01	22.11	4.91	±	5.81
BaP$_{bb}$	ng/m^3	0	0.06	0.01	±	0.01	0	0.01	0.003	±	0.002
BaP$_{bb}$%		8.3	96.1	39.7	±	34.2	0	100*	34.7	±	33.0

B.6 - Fall 2013

27th September – 25th October

Meteorological conditions

		Main Site					San Pietro Capofiume				
		Min	Max	Average		S.D.	Min	Max	Average		S.D.
Average temperature	°C	13.1	23.1	15.7	±	2.5	12.4	22.4	15.0	±	2.5
Solar irradiance	W/m^2	13	176	97	±	52	156	205	105	±	62
PBL height	m	225	930	468	±	188	200	652	402	±	133
Precipitations	mm	131.6					118.6				

PM

		Main Site					San Pietro Capofiume				
		Min	Max	Average		S.D.	Min	Max	Average		S.D.
PM	μg/m^3	7.6	38.7	21.6	±	10.2	3.7	40.2	16.5	±	10.3
PM$_{bb}$	μg/m^3	0.004	2.7	1.0	±	0.7	0.1	2.7	1.1	±	0.7
PM$_{bb}$%		0.01	14.3	4.9	±	3.4	2.2	26.8	7.3	±	6.0

Carbonaceous fraction

		Main Site					San Pietro Capofiume				
		Min	Max	Average		S.D.	Min	Max	Average		S.D.
TC	μg/m^3	2.1	12.1	6.3	±	2.9	3.4	7.1	5.7	±	1.4
OC	μg/m^3	1.5	7.8	3.7	±	1.9	2.9	6.1	4.9	±	1.3
EC	μg/m^3	0.5	1.7	1.1	±	0.4	0.7	1.0	0.8	±	0.2
OC/EC	μg/m^3	2.2	4.8	3.2	±	0.8	5.2	7.4	6.1	±	0.9
Oc$_{sec}$	μg/m^3	0.3	4.2	1.4	±	1.2	0.4	1.6	1.0	±	0.5
Oc$_{sec}$%		13.9	54.4	31.7	±	12.7	6.7	30.3	18.6	±	9.6
Oc$_{bb(levo)}$	μg/m^3	0.001	0.653	0.231	±	0.158	0.02	0.64	0.26	±	0.17
Oc$_{bb(levo)}$%		2.0	14.4	5.2	±	3.6	2.7	6.4	5.0	±	1.4
Oc$_{bb(radio)}$	μg/m^3	0.4	1.2	0.8	±	0.3	0.4	0.7	0.6	±	0.1
OC$_{fossil}$	μg/m^3	0.4	2.1	1.0	±	0.5	1.7	3.8	3.1	±	0.8
Oc$_{bio}$	μg/m^3	0.7	4.5	1.9	±	1.1	0.8	1.6	1.3	±	0.3
Oc$_{bb(radio)}$%		14.8	32.5	23.2	±	5.1	9.5	13.7	11.7	±	1.6
OC$_{fossil}$%		26.8	29.5	28.1	±	0.8	59.7	64.5	62.1	±	1.9
OC$_{bio}$%		38.0	58.4	48.7	±	5.9	26.4	26.6	26.3	±	0.3

Acids

		Main Site				San Pietro Capofiume			
		Min	Max	Average	S.D.	Min	Max	Average	S.D.
Malonic acid	ng/m^3	<LOD	26.8	10.3 ±	8.8	<LOD	29.4	10.5 ±	9.5
Succinic acid	ng/m^3	2.1	19.4	8.6 ±	5.3	2.8	23.0	10.7 ±	6.5
Glutaric acid	ng/m^3	<LOD	4.8	2.3 ±	1.3	<LOD	6.6	3.0 ±	1.9
Adipic acid	ng/m^3	<LOD	2.4	1.3 ±	0.7	<LOD	3.2	1.4 ±	0.8
Pimelic acid	ng/m^3	<LOD	1.4	0.8 ±	0.4	<LOD	1.9	0.9 ±	0.5
Suberic acid	ng/m^3								
Azelaic acid	ng/m^3	<LOD	4.7	2.4 ±	1.4	<LOD	4.5	2.6 ±	1.2
Maleic acid	ng/m^3	<LOD	24.5	3.6 ±	6.6	<LOD	18.0	3.1 ±	4.6
Phthalic acid	ng/m^3	<LOD	12.4	1.5 ±	3.3	<LOD	5.6	0.9 ±	1.8
Glicolic acid	ng/m^3	1.0	11.1	5.7 ±	3.0	<LOD	15.7	7.0 ±	3.9
Malic acid	ng/m^3	1.3	17.9	9.5 ±	4.4	<LOD	21.2	10.7 ±	5.5
3-hydroxybenzoic acid	ng/m^3	<LOD	0.5	0.1 ±	0.2	<LOD	0.4	0.1 ±	0.1
4-hydroxybenzoic acid	ng/m^3	<LOD	4.7	0.7 ±	1.1	<LOD	0.7	0.3 ±	0.3
Pinonic acid	ng/m^3	<LOD	1.6	0.4 ±	0.5	<LOD	2.8	1.5 ±	1.1
2-ketoglutaric acid	ng/m^3	<LOD	5.2	1.8 ±	1.7	<LOD	6.9	2.7 ±	2.0
TCAs	ng/m^3	8.4	102.8	50.0 ±	25.9	2.5	135.6	55.5 ±	34.3
OxCAs	ng/m^3	2.8	34.9	18.3 ±	8.8	1.4	49.5	23.0 ±	12.1
Other CAs	ng/m^3	5.6	67.9	31.7 ±	18.9	1.1	86.2	32.5 ±	23.1
% oxCAs		19.1	54.3	38.7 ±	10.1	27.1	62.3	45.1 ±	8.8
C3/C4		0.42	2.17	1.27 ±	0.59	0.31	1.99	1.08 ±	0.55
C6/C9		0.26	13.28	1.35 ±	3.30	0.24	0.77	0.53 ±	0.14
Ph/C9		0.02	7.84	0.89 ±	1.94	0.02	2.21	0.43 ±	0.75

Phenols

		Main Site				San Pietro Capofiume			
		Min	Max	Average	S.D.	Min	Max	Average	S.D.
Vanillin	ng/m^3	<LOD	0.4	0.1 ±	0.1	<LOD	0.3	0.1 ±	0.1
Vanillic acid	ng/m^3	<LOD	1.2	0.3 ±	0.3	<LOD	0.5	0.2 ±	0.2
Acetovanillone	ng/m^3	<LOD	0.5	0.2 ±	0.1	<LOD	0.3	0.1 ±	0.1
Syringaldehyde	ng/m^3	<LOD	0.2	0.10 ±	0.05	<LOD	0.1	0.08 ±	0.01
Syringic acid	ng/m^3	<LOD	0.9	0.3 ±	0.3	<LOD	0.6	0.1 ±	0.2
Acetosyringone	ng/m^3	n.d.				n.d.			
Tot phenols	ng/m^3	0.3	2.7	1.0 ±	0.8	0.0	1.8	0.6 ±	0.4
S/V		0.18	0.96	0.52 ±	0.2	0.1	0.7	0.4 ±	0.18

Sugars

		Main Site					San Pietro Capofiume				
		Min	Max	Average		S.D.	Min	Max	Average		S.D.
Galactosan	ng/m^3	0.8	9.9	5.0	±	3.2	<LOD	9.5	4.3	±	2.9
Mannosan	ng/m^3	<LOD	28.9	8.3	±	8.5	<LOD	16.1	6.9	±	5.6
Levoglucosan	ng/m^3	<LOD	98.1	34.6	±	23.8	2.9	97.5	38.8	±	25.9
Erithrytol	ng/m^3	<LOD	1.1	0.6	±	0.4	<LOD	1.0	0.5	±	0.3
Xylitol	ng/m^3	<LOD	1.4	0.3	±	0.5	<LOD	2.0	0.4	±	0.6
Ribitol	ng/m^3	<LOD	10.4	4.1	±	2.6	<LOD	8.3	3.8	±	2.7
Mannitol	ng/m^3	<LOD	21.1	7.3	±	5.6	<LOD	12.7	6.9	±	4.3
Arabinose	ng/m^3	<LOD	1.9	0.6	±	0.6	<LOD	1.8	0.7	±	0.6
Mannose	ng/m^3	1.7	8.5	4.2	±	1.7	<LOD	6.7	3.1	±	1.6
Glucose	ng/m^3	1.7	8.5	4.2	±	1.7	1.2	10.5	4.3	±	2.3
Galactose	ng/m^3	n.d.					n.d.				
Sucrose	ng/m^3	<LOD	25.3	4.2	±	6.0	<LOD	7.2	2.9	±	1.9
Mycose	ng/m^3	<LOD	11.2	3.9	±	3.0	<LOD	7.4	3.1	±	2.2
Tot sugars	ng/m^3	20.6	133.1	77.2	±	29.8	11.3	136.0	75.7	±	32.0
Anhydrosugars	ng/m^3	6.8	119.0	47.9	±	31.1	3.9	118.3	50.1	±	33.0
Primary sugars	ng/m^3	13.4	85.4	29.3	±	18.7	7.4	45.1	25.6	±	12.5
% anhydrosugars		11.5	89.4	57.8	±	23.2	26.2	87.0	59.8	±	23.0
% primary sugars		10.6	88.5	42.2	±	23.2	13.0	73.8	40.2	±	23.0
L/M		1.38	21.70	7.12	±	5.1	2.88	16.73	7.43	±	3.82

Alkanes

		Main Site					San Pietro Capofiume				
		Min	Max	Average		S.D.	Min	Max	Average		S.D.
C22	ng/m^3	0.10	11.62	4.10	±	3.06	<LOD	0.95	0.33	±	0.36
C23	ng/m^3	0.17	10.26	4.30	±	2.97	<LOD	2.32	0.83	±	0.63
C24	ng/m^3	0.17	16.07	6.09	±	4.55	<LOD	2.56	0.89	±	0.75
C25	ng/m^3	0.32	15.85	6.31	±	4.75	0.25	4.91	1.56	±	1.19
C26	ng/m^3	0.18	30.26	10.10	±	9.40	0.24	3.12	1.21	±	0.84
C27	ng/m^3	0.49	15.39	6.33	±	4.82	0.42	6.23	2.01	±	1.41
C28	ng/m^3	0.17	39.50	11.19	±	12.02	0.22	2.28	0.94	±	0.60
C29	ng/m^3	0.61	13.01	5.82	±	4.03	0.55	8.86	2.64	±	2.07
C30	ng/m^3	0.00	45.09	10.67	±	12.64	0.14	1.45	0.55	±	0.38
C31	ng/m^3	0.48	12.31	5.16	±	3.81	0.36	7.36	2.16	±	1.89
C32	ng/m^3	<LOD	14.96	5.46	±	4.73	<LOD	0.82	0.33	±	0.25
C33	ng/m^3	0.17	12.38	4.07	±	3.59	0.14	2.42	0.65	±	0.59
Tot alkanes	ng/m^3	3.91	257.76	96.11	±	72.72	2.71	46.49	15.85	±	11.29
CPI		0.50	2.73	1.01	±	0.62	1.44	3.20	2.23	±	0.49

PAHs

		Main Site				San Pietro Capofiume			
		Min	Max	Average	S.D.	Min	Max	Average	S.D.
Phenanthrene	ng/m^3	<LOD	0.02	0.01 ±	0.01	<LOD	0.04	0.01 ±	0.01
Anthracene	ng/m^3	n.d.				n.d.			
Fluoranthene	ng/m^3	0.02	0.03	0.04 ±	0.02	0.01	0.16	0.05 ±	0.04
Pyrene	ng/m^3	0.01	0.07	0.03 ±	0.02	0.01	0.12	0.04 ±	0.04
Benzo (a) anthracene	ng/m^3	<LOD	0.12	0.03 ±	0.03	<LOD	0.03	0.02 ±	0.01
Chrysene	ng/m^3	0.01	0.14	0.04 ±	0.03	0.01	0.06	0.03 ±	0.02
Benzo (b+j) fluoranthene	ng/m^3	0.02	0.63	0.15 ±	0.15	0.02	0.26	0.13 ±	0.07
Benzo (k) fuoranthene	ng/m^3	<LOD	0.12	0.03 ±	0.03	<LOD	0.07	0.03 ±	0.02
Benzo(e)pyrene	ng/m^3	0.01	0.23	0.07 ±	0.05	0.01	0.13	0.06 ±	0.03
Benzo(a)pyrene	ng/m^3	0.01	0.28	0.07 ±	0.07	0.01	0.12	0.05 ±	0.03
Perylene	ng/m^3	<LOD	0.03	0.01 ±	0.01	<LOD	0.02	0.005 ±	0.004
Indeno (1,2,3-c,d,) pyrene	ng/m^3	0.01	0.13	0.04 ±	0.03	0.01	0.09	0.04 ±	0.02
Benzo (g,h,i) perylene	ng/m^3	0.01	0.12	0.06 ±	0.03	0.01	0.09	0.04 ±	0.02
Tot PAHs	ng/m^3	0.09	2.16	0.63 ±	0.51	0.11	1.12	0.58 ±	0.33
BaP/(Bap+BeP)		0.40	0.55	0.47 ±	0.05	0.32	0.49	0.42 ±	0.05
BaP/BeP		0.68	1.24	0.91 ±	0.18	0.48	0.95	0.73 ±	0.14
IcdP/IcdP+BghiP		0.29	0.52	0.38 ±	0.05	0.44	0.53	0.48 ±	0.03
∑BFs/BghiP		1.94	6.35	2.91 ±	1.06	2.20	4.52	3.53 ±	0.72
BaP$_{bb}$	ng/m^3	0	0.08	0.03 ±	0.02	0	0.08	0.03 ±	0.02
BaP$_{bb}$%		0	100*	50.9 ±	31.7	0	100*	56.0 ±	28.8

B.7 - Winter 2014

28th January – 27th February

Meteorological conditions

		Main Site				San Pietro Capofiume			
		Min	Max	Average	S.D.	Min	Max	Average	S.D.
Average temperature	°C	2.1	11.2	8.3 ±	2.1	0.9	10.6	7.3 ±	1.8
Solar irradiance	W/m²	15	155	72 ±	44	13	179	80 ±	52
PBL height	m	180	752	411 ±	140	154	488	302 ±	86
Precipitations	mm			141.6				117.0	

PM

		Main Site				San Pietro Capofiume			
		Min	Max	Average	S.D.	Min	Max	Average	S.D.
PM	µg/m³	7.0	52.0	19.3 ±	11.7	4.0	35.0	16.3 ±	8.0
PM_{bb}	µg/m³	3.9	17.1	8.4 ±	3.3	3.1	15.6	9.5 ±	3.6
PM_{bb}%		20.2	100*	50.6 ±	22.3	32.5	100*	65.6 ±	28.6

Carbonaceous fraction

		Main Site				San Pietro Capofiume			
		Min	Max	Average	S.D.	Min	Max	Average	S.D.
TC	µg/m³	2.9	12.9	5.9 ±	2.4	2.4	11.9	5.5 ±	2.1
OC	µg/m³	2.2	11.1	4.6 ±	2.1	2.0	10.4	4.6 ±	1.8
EC	µg/m³	0.6	2.6	1.3 ±	0.5	0.3	1.7	0.9 ±	0.4
OC/EC	µg/m³	1.9	6.2	3.5 ±	1.0	3.9	10.4	5.6 ±	1.4
Oc_{sec}	µg/m³	0.6	7.6	2.1 ±	1.5	0.1	4.5	1.3 ±	0.9
Oc_{sec}%		21.3	68.6	42.8 ±	13.1	3.7	62.3	28.1 ±	14.0
$Oc_{bb(levo)}$	µg/m³	0.9	4.1	2.0 ±	0.8	0.7	3.8	2.3 ±	0.9
$Oc_{bb(levo)}$%		22.7	66.2	43.8 ±	12.4	27.3	100*	52.7 ±	21.3
$Oc_{bb(radio)}$	µg/m³	1.0	4.1	2.1 ±	0.7	0.5	2.6	1.3 ±	0.6
OC_{fossil}	µg/m³	0.6	3.4	1.5 ±	0.6	0.8	5.0	1.9 ±	0.8
Oc_{bio}	µg/m³	0	4.9	1.1 ±	1.1	0.6	3.1	1.4 ±	0.5
$Oc_{bb(radio)}$%		25.2	80.5	46.8 ±	12.1	15.1	39.9	29.0 ±	5.8
OC_{fossil}%		30.3	38.9	33.6 ±	1.9	27.6	56.3	40.1 ±	6.8
OC_{bio}%		0	44.5	19.6 ±	14.0	28.7	32.6	30.9 ±	0.9

Acids

		Main Site					San Pietro Capofiume				
		Min	Max	Average		S.D.	Min	Max	Average		S.D.
Malonic acid	ng/m^3	<LOD	15.3	2.0	±	3.1	<LOD	9.7	2.9	±	2.4
Succinic acid	ng/m^3	3.0	56.6	22.4	±	13.7	7.5	57.9	25.9	±	12.3
Glutaric acid	ng/m^3	2.7	13.9	6.3	±	3.5	1.1	13.1	6.1	±	2.9
Adipic acid	ng/m^3	<LOD	4.9	1.0	±	1.4	<LOD	2.9	0.9	±	1.1
Pimelic acid	ng/m^3	n.d.					n.d.				
Suberic acid	ng/m^3	n.d.					n.d.				
Azelaic acid	ng/m^3	<LOD	15.6	7.7	±	3.5	3.0	14.0	8.0	±	2.4
Maleic acid	ng/m^3	7.8	191.2	34.6	±	45.2	6.4	29.9	15.1	±	6.3
Phthalic acid	ng/m^3	<LOD	10.1	2.5	±	2.8	<LOD	10.6	3.5	±	2.9
Glicolic acid	ng/m^3	3.1	20.5	8.5	±	4.7	2.0	23.8	8.7	±	4.4
Malic acid	ng/m^3	0.0	50.4	22.5	±	12.6	6.8	48.0	24.4	±	10.8
3-hydroxybenzoic acid	ng/m^3	<LOD	1.5	0.5	±	0.4	<LOD	1.6	0.6	±	0.6
4-hydroxybenzoic acid	ng/m^3	<LOD	3.2	0.8	±	0.9	<LOD	3.1	1.1	±	1.0
Pinonic acid	ng/m^3	n.d.					n.d.				
2-ketoglutaric acid	ng/m^3	<LOD	47.6	9.2	±	13.4	<LOD	24.1	6.3	±	8.2
TCAs	ng/m^3	55.5	339.4	118.0	±	72.4	36.8	181.5	103.6	±	34.0
OxCAs	ng/m^3	14.2	110.4	41.5	±	22.5	16.4	76.1	41.2	±	14.4
Other CAs	ng/m^3	37.9	270.2	76.5	±	57.4	20.4	112.1	62.4	±	21.6
% oxCAs		15.4	48.7	36.8	±	9.2	27.1	51.5	39.9	±	5.7
C3/C4		0.06	5.05	0.41	±	1.24	0.03	0.40	0.12	±	0.08
C6/C9		0.09	2.90	0.70	±	0.91	0.25	0.39	0.30	±	0.05
Ph/C9		0.22	11.05	1.64	±	2.94	0.36	1.82	0.67	±	0.32

Phenols

		Main Site					San Pietro Capofiume				
		Min	Max	Average		S.D.	Min	Max	Average		S.D.
Vanillin	ng/m^3	1.0	3.8	1.8	±	0.5	1.0	2.9	1.8	±	0.5
Vanillic acid	ng/m^3	<LOD	1.9	0.7	±	0.6	<LOD	3.1	0.9	±	1.0
Acetovanillone	ng/m^3	0.7	3.1	1.6	±	0.7	0.6	4.8	1.8	±	1.2
Syringaldehyde	ng/m^3	2.2	7.6	4.2	±	1.2	2.8	8.2	4.4	±	1.5
Syringic acid	ng/m^3	<LOD	5.5	1.8	±	1.6	<LOD	6.8	2.3	±	2.2
Acetosyringone	ng/m^3	<LOD	2.1	0.7	±	0.7	<LOD	1.4	1.1	±	0.3
Tot phenols	ng/m^3	5.0	22.0	10.9	±	4.2	5.1	26.5	12.4	±	6.5
S/V		0.88	2.52	1.68	±	0.33	1.40	2.31	1.78	±	0.22

Sugars

		Main Site				San Pietro Capofiume			
		Min	Max	Average	S.D.	Min	Max	Average	S.D.
Galactosan	ng/m^3	7.0	31.5	14.9 ±	6.2	6.0	30.3	16.3 ±	6.5
Mannosan	ng/m^3	3.2	63.5	26.4 ±	16.8	1.0	68.9	32.1 ±	18.8
Levoglucosan	ng/m^3	138.9	616.9	300.7 ±	117.8	111.8	563.3	341.9 ±	129.6
Erithrytol	ng/m^3	<LOD	1.8	0.9 ±	0.5	<LOD	5.3	1.0 ±	1.0
Xylitol	ng/m^3	<LOD	19.4	3.2 ±	3.9	<LOD	9.4	4.7 ±	2.6
Ribitol	ng/m^3	<LOD	9.1	0.6 ±	2.2	n.d.			
Mannitol	ng/m^3	2.1	9.3	5.1 ±	1.9	2.4	13.5	5.3 ±	2.4
Arabinose	ng/m^3	<LOD	4.5	1.5 ±	1.0	<LOD	3.5	1.8 ±	0.9
Mannose	ng/m^3	<LOD	6.2	1.4 ±	1.5	<LOD	3.3	0.5 ±	0.8
Glucose	ng/m^3	1.4	26.6	8.2 ±	4.6	3.9	13.9	8.0 ±	2.4
Galactose	ng/m^3	<LOD	2.5	0.1 ±	0.5	n.d.			
Sucrose	ng/m^3	<LOD	44.1	8.5 ±	9.6	<LOD	46.9	9.6 ±	9.4
Mycose	ng/m^3	<LOD	13.7	1.4 ±	2.8	<LOD	1.6	0.3 ±	0.5
Tot sugars	ng/m^3	172.0	773.8	373.0 ±	147.4	129.3	736.1	421.5 ±	165.6
Anhydrosugars	ng/m^3	149.5	711.9	342.1 ±	140.4	118.8	648.5	390.4 ±	154.3
Primary sugars	ng/m^3	13.2	75.5	30.9 ±	14.8	10.4	87.6	31.1 ±	15.5
% anhydrosugars		67.3	95.3	91.1 ±	5.3	83.2	95.2	92.5 ±	2.4
% primary sugars		4.7	32.7	8.9 ±	5.3	4.8	16.8	7.5 ±	2.4
L/M		8.17	43.06	14.98 ±	7.92	7.68	108.90	15.59 ±	18.12

Alkanes

		Main Site				San Pietro Capofiume			
		Min	Max	Average	S.D.	Min	Max	Average	S.D.
C22	ng/m^3	0.46	3.94	1.80 ±	0.77	<LOD	2.66	1.06 ±	0.72
C23	ng/m^3	1.02	6.70	2.84 ±	1.33	0.46	4.68	2.43 ±	0.93
C24	ng/m^3	0.82	9.96	3.85 ±	1.88	<LOD	8.80	3.45 ±	1.67
C25	ng/m^3	0.73	10.80	3.29 ±	2.09	<LOD	6.05	2.88 ±	1.30
C26	ng/m^3	0.46	9.12	2.60 ±	1.69	<LOD	6.97	1.93 ±	1.45
C27	ng/m^3	<LOD	8.65	2.23 ±	1.80	<LOD	3.57	1.39 ±	1.01
C28	ng/m^3	<LOD	5.86	1.01 ±	1.29	<LOD	5.68	0.61 ±	1.13
C29	ng/m^3	<LOD	7.63	1.76 ±	2.13	<LOD	9.72	0.90 ±	2.09
C30	ng/m^3	<LOD	3.54	0.34 ±	0.85	<LOD	11.28	0.46 ±	2.07
C31	ng/m^3	<LOD	4.75	1.05 ±	1.29	<LOD	12.65	0.65 ±	2.34
C32	ng/m^3	<LOD	2.20	0.20 ±	0.57	<LOD	11.19	0.44 ±	2.05
C33	ng/m^3	<LOD	3.30	0.32 ±	0.80	<LOD	9.08	0.35 ±	1.67
Tot alkanes	ng/m^3	4.58	73.33	23.72 ±	16.61	1.01	91.68	18.02 ±	16.04
CPI		0.46	3.94	1.80 ±	0.77	<LOD	2.66	1.06 ±	0.72

PAHs

		Main Site					San Pietro Capofiume				
		Min	Max	Average		S.D.	Min	Max	Average		S.D.
Phenanthrene	ng/m^3	<LOD	0.16	0.03	±	0.03	<LOD	0.06	0.01	±	0.02
Anthracene	ng/m^3	<LOD	0.01	0.001	±	0.003	<LOD	0.02	0.002	±	0.004
Fluoranthene	ng/m^3	<LOD	0.24	0.09	±	0.06	0.01	0.20	0.09	±	0.05
Pyrene	ng/m^3	0.01	0.27	0.10	±	0.07	0.01	0.25	0.09	±	0.06
Benzo (a) anthracene	ng/m^3	<LOD	0.40	0.12	±	0.10	<LOD	0.30	0.05	±	0.08
Chrysene	ng/m^3	0.01	1.31	0.22	±	0.23	<LOD	0.41	0.09	±	0.10
Benzo (b+j) fluoranthene	ng/m^3	<LOD	1.24	0.39	±	0.28	0.05	1.20	0.42	±	0.28
Benzo (k) fuoranthene	ng/m^3	<LOD	0.34	0.11	±	0.08	0.01	0.31	0.11	±	0.07
Benzo(e)pyrene	ng/m^3	0.08	0.54	0.22	±	0.11	0.02	0.58	0.20	±	0.13
Benzo(a)pyrene	ng/m^3	0.04	0.73	0.21	±	0.14	0.02	0.68	0.15	±	0.14
Perylene	ng/m^3	<LOD	0.25	0.04	±	0.04	<LOD	0.08	0.03	±	0.02
Indeno (1,2,3-c,d,) pyrene	ng/m^3	0.04	0.37	0.18	±	0.09	0.02	0.84	0.15	±	0.15
Benzo (g,h,i) perylene	ng/m^3	0.08	0.58	0.27	±	0.14	0.03	0.95	0.21	±	0.17
Tot PAHs	ng/m^3	0.69	5.71	2.12	±	1.16	0.21	5.27	1.71	±	1.07
BaP/(Bap+BeP)		0.32	0.57	0.47	±	0.06	0.26	0.54	0.40	±	0.07
BaP/BeP		0.48	1.35	0.90	±	0.21	0.36	1.17	0.68	±	0.20
IcdP/IcdP+BghiP		0.30	0.45	0.40	±	0.03	0.38	0.48	0.41	±	0.02
∑BFs/BghiP		0.27	3.02	1.98	±	0.68	0.13	6.09	2.91	±	1.15
BaP$_{bb}$	ng/m^3	0.11	0.49	0.24	±	0.09	0.09	0.45	0.27	±	0.10
BaP$_{bb}$%		42.6	100*	77.6	±	25.0	50.0	100*	100*	±	435.3

B.8 - Summer 2014

13th May – 11th June

Meteorological conditions

		Main Site				San Pietro Capofiume			
		Min	Max	Average	S.D.	Min	Max	Average	S.D.
Average temperature	°C	16.3	28.3	21.0 ±	3.3	15.2	25.9	19.4 ±	2.8
Solar irradiance	W/m^2	153	321	258 ±	57	187	350	286 ±	55
PBL height	m	425	1153	974 ±	171	348	1048	876 ±	160
Precipitations	mm	24.4				49.0			

PM

		Main Site				San Pietro Capofiume			
		Min	Max	Average	S.D.	Min	Max	Average	S.D.
PM	µg/m^3	5.2	19.4	10.0 ±	3.6	3.9	18.8	10.5 ±	4.3
PM$_{bb}$	µg/m^3	0.05	0.38	0.18 ±	0.10	0.05	0.32	0.17 ±	0.07
PM$_{bb}$%		0.3	7.3	2.1 ±	1.7	0.4	5.2	1.9 ±	1.3

Carbonaceous fraction

		Main Site				San Pietro Capofiume			
		Min	Max	Average	S.D.	Min	Max	Average	S.D.
TC	µg/m^3	1.5	8.5	3.1 ±	1.7	1.3	4.6	2.5 ±	1.1
OC	µg/m^3	1.2	7.5	2.6 ±	1.5	1.2	4.2	2.3 ±	1.0
EC	µg/m^3	0.2	1.2	0.6 ±	0.3	0.1	0.4	0.3 ±	0.1
OC/EC	µg/m^3	2.0	10.2	4.4 ±	1.8	6.1	16.3	9.1 ±	3.1
Oc$_{sec}$	µg/m^3	0.4	5.6	1.5 ±	1.2	0.3	1.9	0.8 ±	0.6
Oc$_{sec}$%		13.3	80.8	51.8 ±	15.4	18.0	62.9	32.5 ±	14.7
Oc$_{bb(levo)}$	µg/m^3	0.01	0.09	0.04 ±	0.02	0.01	0.08	0.04 ±	0.02
Oc$_{bb(levo)}$%		0.2	7.6	2.2 ±	1.8	0.7	5.6	2.1 ±	1.7
Oc$_{bb(radio)}$	µg/m^3	0.1	0.4	0.2 ±	0.1	0.05	0.15	0.09 ±	0.04
OC$_{fossil}$	µg/m^3	0.4	2.2	1.6 ±	1.0	0.8	2.8	1.5 ±	0.7
Oc$_{bio}$	µg/m^3	0.7	4.9	0.8 ±	0.5	0.3	1.2	0.7 ±	0.3
Oc$_{bb(radio)}$%		3.5	18.0	9.1 ±	3.4	2.2	5.8	4.2 ±	1.0
OC$_{fossil}$%		29.6	31.9	60.3 ±	3.9	64.2	68.4	66.1 ±	1.2
OC$_{bio}$%		50.0	66.9	30.5 ±	0.5	29.4	30.0	29.8 ±	0.2

Acids

		Main Site				San Pietro Capofiume			
		Min	Max	Average	S.D.	Min	Max	Average	S.D.
Malonic acid	ng/m^3	<LOD	90.9	13.4 ±	24.4	<LOD	25.1	8.7 ±	8.8
Succinic acid	ng/m^3	1.6	43.5	8.5 ±	10.2	<LOD	46.0	11.9 ±	10.8
Glutaric acid	ng/m^3	<LOD	16.0	5.1 ±	3.9	<LOD	21.1	5.5 ±	5.3
Adipic acid	ng/m^3	1.2	27.1	5.1 ±	6.4	1.2	21.0	5.2 ±	4.8
Pimelic acid	ng/m^3		n.d.				n.d.		
Suberic acid	ng/m^3		n.d.				n.d.		
Azelaic acid	ng/m^3		n.d.				n.d.		
Maleic acid	ng/m^3	<LOD	15.7	2.0 ±	4.1	<LOD	30.1	5.2 ±	7.1
Phthalic acid	ng/m^3								
Glicolic acid	ng/m^3	1.1	60.4	15.8 ±	14.6	4.5	48.6	15.5 ±	14.1
Malic acid	ng/m^3	<LOD	140.1	23.3 ±	33.8	<LOD	78.5	21.4 ±	20.3
3-hydroxybenzoic acid	ng/m^3	1.2	1.3	1.2 ±	0.1	1.1	19.4	2.4 ±	4.3
4-hydroxybenzoic acid	ng/m^3		n.d.				n.d.		
Pinonic acid	ng/m^3		n.d.				n.d.		
2-ketoglutaric acid	ng/m^3	<LOD	135.0	18.6 ±	32.4	<LOD	72.2	23.0 ±	28.4
TCAs	ng/m^3	8.6	514.4	93.0 ±	120.4	10.9	271.2	98.8 ±	79.4
OxCAs	ng/m^3	2.8	336.9	58.9 ±	79.2	8.4	201.6	62.2 ±	57.2
Other CAs	ng/m^3	5.6	177.5	34.1 ±	43.0	2.5	105.4	36.6 ±	27.1
% oxCAs		32.2	81.7	60.9 ±	14.3	31.4	81.0	59.9 ±	15.1
C3/C4		0.03	5.19	1.27 ±	1.43	0.06	2.14	0.73 ±	0.60
C6/C9									
Ph/C9									

Phenols

		Main Site				San Pietro Capofiume			
		Min	Max	Average	S.D.	Min	Max	Average	S.D.
Vanillin	ng/m^3	1.0	2.0	1.2 ±	0.4	<LOD	8.4	1.3 ±	1.8
Vanillic acid	ng/m^3	<LOD	1.1	0.4 ±	0.3	<LOD	0.4	0.1 ±	0.1
Acetovanillone	ng/m^3		n.d.				n.d.		
Syringaldehyde	ng/m^3	<LOD	0.6	0.54 ±	0.04	<LOD	8.6	1.0 ±	1.9
Syringic acid	ng/m^3	<LOD	0.2	0.1 ±	0.1	<LOD	1.4	0.2 ±	0.3
Acetosyringone	ng/m^3	<LOD	0.2	0.03 ±	0.08	<LOD	3.6	0.4 ±	0.8
Tot phenols	ng/m^3	2.9	63.8	11.6 ±	15.0	2.8	47.4	9.3 ±	11.1
S/V		0.23	0.73	0.52 ±	0.18	0.76	1.63	1.04 ±	0.30

Sugars

		Main Site				San Pietro Capofiume			
		Min	Max	Average	S.D.	Min	Max	Average	S.D.
Galactosan	ng/m³	0.8	2.1	1.1 ±	0.3	0.8	9.7	1.5 ±	2.0
Mannosan	ng/m³	<LOD	2.8	1.1 ±	0.6	<LOD	2.5	1.0 ±	0.5
Levoglucosan	ng/m³	1.7	13.6	6.5 ±	3.6	1.7	11.4	6.2 ±	2.6
Erithrytol	ng/m³	<LOD	3.5	0.9 ±	0.7	<LOD	3.3	1.1 ±	0.8
Xylitol	ng/m³	n.d.				n.d.			
Ribitol	ng/m³	<LOD	24.4	4.4 ±	6.3	<LOD	23.6	6.8 ±	6.0
Mannitol	ng/m³	3.3	33.1	10.5 ±	6.7	1.1	72.5	13.1 ±	15.6
Arabinose	ng/m³	<LOD	3.9	0.9 ±	0.8	<LOD	6.5	1.0 ±	1.4
Mannose	ng/m³	<LOD	8.5	1.6 ±	2.1	<LOD	5.7	2.3 ±	1.4
Glucose	ng/m³	0.9	9.2	4.0 ±	2.2	<LOD	15.6	4.8 ±	3.2
Galactose	ng/m³	<LOD	8.5	2.6 ±	2.3	<LOD	9.7	1.5 ±	2.4
Sucrose	ng/m³	<LOD	48.4	20.1 ±	15.0	<LOD	206.4	30.5 ±	45.8
Mycose	ng/m³	<LOD	12.1	5.6 ±	3.5	<LOD	22.1	6.0 ±	5.1
Tot sugars	ng/m³	14.2	136.0	58.5 ±	28.2	8.0	380.2	75.8 ±	79.7
Anhydrosugars	ng/m³	3.0	17.2	8.7 ±	4.3	<LOD	20.5	7.1 ±	5.0
Primary sugars	ng/m³	10.1	118.8	49.9 ±	27.5	4.9	359.7	67.0 ±	76.4
% anhydrosugars		6.2	59.2	18.4 ±	14.7	5.4	38.5	15.7 ±	8.2
% primary sugars		40.8	93.8	81.6 ±	14.7	61.5	94.6	84.3 ±	8.2
L/M		1.73	9.26	6.25 ±	2.19	3.34	29.67	8.32 ±	7.50

Alkanes

		Main Site				San Pietro Capofiume			
		Min	Max	Average	S.D.	Min	Max	Average	S.D.
C22	ng/m³	<LOD	0.42	0.18 ±	0.16	<LOD	3.54	0.56 ±	0.92
C23	ng/m³	<LOD	0.39	0.19 ±	0.15	<LOD	2.66	0.51 ±	0.62
C24	ng/m³	0.28	0.78	0.54 ±	0.14	<LOD	2.50	0.40 ±	0.68
C25	ng/m³	0.00	0.67	0.29 ±	0.14	0.28	6.64	1.11 ±	1.27
C26	ng/m³	0.25	1.30	0.65 ±	0.30	<LOD	5.76	0.86 ±	1.25
C27	ng/m³	<LOD	0.70	0.35 ±	0.14	0.35	9.30	1.90 ±	1.78
C28	ng/m³	0.67	4.68	1.49 ±	1.06	<LOD	7.53	0.96 ±	1.69
C29	ng/m³	<LOD	0.60	0.18 ±	0.23	0.42	10.19	2.48 ±	1.99
C30	ng/m³	0.92	4.30	1.73 ±	0.91	<LOD	6.20	0.77 ±	1.42
C31	ng/m³	<LOD	0.46	0.02 ±	0.10	<LOD	7.53	1.82 ±	1.62
C32	ng/m³	0.74	2.43	1.30 ±	0.48	<LOD	2.78	0.26 ±	0.63
C33	ng/m³	n.d.				<LOD	1.83	0.26 ±	0.47
Tot alkanes	ng/m³	3.66	16.20	7.52 ±	3.50	1.51	62.44	14.16 ±	14.15
CPI		0.07	0.43	0.23 ±	0.1	0.6	9.9	3.7 ±	2.9

PAHs

		Main Site				San Pietro Capofiume			
		Min	Max	Average	S.D.	Min	Max	Average	S.D.
Phenanthrene	ng/m^3	<LOD	0.02	0.01 $\pm$	0.01	<LOD	0.06	0.004 $\pm$	0.012
Anthracene	ng/m^3			n.d.				n.d.	
Fluoranthene	ng/m^3	<LOD	0.04	0.01 $\pm$	0.01	<LOD	0.31	0.02 $\pm$	0.07
Pyrene	ng/m^3	<LOD	0.04	0.01 $\pm$	0.01	<LOD	0.26	0.02 $\pm$	0.06
Benzo (a) anthracene	ng/m^3	<LOD	0.01	0.003 $\pm$	0.003	<LOD	0.01	0.002 $\pm$	0.002
Chrysene	ng/m^3	<LOD	0.02	0.01 $\pm$	0.01	<LOD	0.12	0.01 $\pm$	0.02
Benzo (b+j) fluoranthene	ng/m^3	<LOD	0.04	0.02 $\pm$	0.01	<LOD	0.03	0.02 $\pm$	0.01
Benzo (k) fuoranthene	ng/m^3	<LOD	0.01	0.006 $\pm$	0.004	<LOD	0.03	0.01 $\pm$	0.01
Benzo(e)pyrene	ng/m^3	<LOD	0.02	0.01 $\pm$	0.01	<LOD	0.02	0.008 $\pm$	0.004
Benzo(a)pyrene	ng/m^3	<LOD	0.02	0.01 $\pm$	0.01	<LOD	0.01	0.005 $\pm$	0.003
Perylene	ng/m^3			n.d.				n.d.	
Indeno (1,2,3-c,d,) pyrene	ng/m^3	<LOD	0.01	0.008 $\pm$	0.005	<LOD	0.03	0.01 $\pm$	0.01
Benzo (g,h,i) perylene	ng/m^3	<LOD	0.03	0.02 $\pm$	0.01	<LOD	0.03	0.01 $\pm$	0.01
Tot PAHs	ng/m^3	<LOD	0.24	0.12 $\pm$	0.08	0.03	0.96	0.13 $\pm$	0.19
BaP/(Bap+BeP)		0.11	0.45	0.36 $\pm$	0.08	0.29	1.00	0.40 $\pm$	0.15
BaP/BeP		0.13	0.81	0.57 $\pm$	0.16	0.40	1.00	0.59 $\pm$	0.15
IcdP/IcdP+BghiP		0.27	0.38	0.33 $\pm$	0.03	0.34	1.00	0.41 $\pm$	0.14
$\sum$BFs/BghiP		0.76	2.77	1.92 $\pm$	0.48	1.17	7.83	2.48 $\pm$	1.55
BaP$_{bb}$	ng/m^3	0.001	0.011	0.005 $\pm$	0.003	0.001	0.009	0.005 $\pm$	0.002
BaP$_{bb}$%		33.2	100*	55.9 $\pm$	27.4	25.0	100*	61.1 $\pm$	26.5

REFERENCES

Alves C.A., 2008. *Characterisation of solvent extractable organic constituent in atmospheric matter: an overview*. Anais da Academia Brasileira de Ciencias 80, 21-82.

Alves C.A., Goncalves C., Evtyugina M., Pio C.A., Mirante F., Puxbaum H., 2010. *Particulate organic compounds emitted from experimental wildland fires in a Mediterranean ecosystem*. Atmospheric Environment 44, 2750–2759.

Anastas P.T., Warner J.C., 1998. *Green Chemistry: Theory and Practice*. Oxford University Press: New York.

Anusevičius Ž., Ramanavičius A., Šarlauskas J., 1997. *Some aspects of electron-transfer reaction of ascorbate with quinones*. Chemical Papers 58, 643-649.

Ayres J.G., Borm P., Cassee F.R., Castranova V., Donaldson K., Ghio A., Harrison R.M., Hider R., Kelly F., Kooter I.M., Marano F., Maynard R.L., Mudway I., Nel A., Sioutas C., Smith S., Baeza-Squiban A., Cho A., Duggan S., Froines J., 2008. *Evaluating the toxicity of airborne particulate matter and nanoparticles by measuring oxidative stress potential—A workshop report and consensus statement*. Inhalation Toxicology 20, 75-99.

Balducci C., Cecinato A., 2010. *Particulate organic acids in the atmosphere of Italian cities: Are they environmentally relevant?*. Atmospheric Environment 44, 652-659.

Bamford H.A., Baker J.E., 2003. *Nitro-polycyclic aromatic hydrocarbon concentrations and sources in urban and suburban atmospheres of the Mid-Atlantic region*. Atmospheric Environment 37, 2077–2091.

Bari M.A., Baumbach G., Kuch B., Scheffknecht G., 2009. *Wood smoke as a source of particle-phase organic compounds in residential areas*. Atmospheric Environment 43, 4722-4732.

Bari M.A., Baumbach G., Kuch B., Scheffknecht G., 2010. *Temporal variation and impact of wood smoke pollution on a residential area in southern Germany*. Atmospheric Environment 44, 3823-3832.

Bauer H., Schueller E., Weinke G., Berger A., Hitzenberger R., Marr I.L., Puxbaum H., 2008. *Significant contributions of fungal spores to the organic carbon and to the aerosol mass balance of the urban atmospheric aerosol*. Atmospheric Environment 42, 5542-5549.

Bautista A.T.VII, Pabroa P.C.B., Santos F.L., Racho J.M.D., Quirit L.L., 2014. *Carbonaceous particulate matter characterization in an urban and a rural site in the Philippines*. Atmospheric Pollution Research 5, 245-252.

Becker M., Liebner F., Rosenau T., Potthast A., 2013. *Ethoximation-silylation approach for mono- and disaccharide analysis and characterization of their identification parameters by GC/MS*. Talanta 115, 642-661.

Belis C.A., Cancelinha J., Duane M., Forcina V., Pedroni V., Passarella R., Tanet G., Dous K., Piazzalunga A., Bolzacchini E., Sangiorgi G., Perrone M.G., Ferrero L., Fermo P., Larsen B.R., 2011. *Sources for PM air pollution the Po Plain, Italy: I. Critical comparison of methods for estimating biomass burning contributions to benzo(a)pyrene*. Atmospheric Environment 45, 7266-7275.

Bernardoni V., Vecchi R., Valli G., Piazzalunga A., Fermo P., 2011. *PM$_{10}$ source apportionment in Milan (Italy) using time-resolved data*. Science of the Total Environment 409, 4788-4795.

Bi X., Simoneit B. R. T., Sheng G., Ma S., Fu J., 2008. *Composition and major sources of organic compounds in urban aerosols*. Atmospheric Research 88, 256-265.

Bigi A., Ghermandi G., 2011. *Particle number size distribution and weight concentration of background urban aerosol in a Po Valley site*. Water Air & Soil Pollution 220, 265-278.

Blando J.D., Turpin B.J., 2000. *Secondary organic aerosol formation in cloud and fog droplets: a literature evaluation of plausibility*. Atmospheric Environment 34, 1623-1632.

Boman C., Pettersson E., Westerholm R., Boström D., Nordin A., 2011. *Stove performance and emission characteristics in residential wood log and pellet combustion, Part 1: pellet stoves*. Energy & Fuels 25, 307-314.

Borm P.J.A., Kelly F., Künzli N., Schins R.P.F., Donaldson K., 2007. *Oxidant generation by particulate matter: from biologically effective dose to a promising, novel metric*. Occupational and Environmental Medicine 64, 73-74.

Botitsi H.V., Garbis S.D., Economou A., Despina F., Tsipi, D.F, 2011. *Current mass spectrometry strategies for the analysis of pesticides and their metabolites in food and water matrices*. Mass Spectrometry Reviews 30, 907-939.

Box G.E.P., Wilson K.B., 1951. *On the experimental attainment of optimum conditions*. Journal of the Royal Statistical Society, series B 13, 1-45.

Box G.E.P., Behnken D.W., 1960. *Some new three level designs for the study of quantitative variables*. Technometrics 2, 455-475.

Bray E.E., Evans E.D., 1961. *Distribution of n-paraffins as a clue to recognition of source bed*. Geochimica et Cosmochimica Acta 22, 2-15.

Buettner G.R., Jurkiewicz B.A., 1993. *Catalytic Metals, Ascorbate and Free Radicals: Combinations to Avoid*. Radiation Research 145, 532-541.

154

Burshtein N., Lang-Yona N., Rudich Y., 2011. *Ergosterol, arabitol and mannitol as tracers for biogenic aerosols in the eastern Mediterranean*. Atmospheric Chemistry and Physics 11, 829-839.

Cabada J.C., Pandis S.N., Subramanian R., Robinson A.L., Polidori A., Turpin B., 2004. *Estimating the secondary organic aerosol contribution to PM2.5using the EC tracer method*. Aerosol Science and Technology 38, 140-155.

Caseiro A., Bauer H., Schmidl C., Pio C.A., Puxbaum H., 2009. *Wood burning impact on PM10 in three Austrian regions*. Atmospheric Environment 43, 2186-2195.

Caseiro A., Oliviera C., 2012. *Variations in wood burning organic marker concentrations in the atmospheres of four European cities*. Journal of Environmental Monitoring 14, 2261-2269.

Cavalli F., Viana M., Yttri K., Genberg J., Putaud J., 2010. *Toward a standardized thermal-optical protocol for measuring atmospheric organic and elemental carbon: the EUSAAR protocol*. Atmospheric Measurement Techniques 3, 79–89.

CEN, 1998. *Cen 12341: Air quality-determination of the PM₁₀ fraction of suspended particulate matter-reference method and field test procedure to demonstrate reference equivalence of measurement methods*. European Committee for Standardization, Brussels, Belgium.

CEN, 2011. *Cen/tr 16243: Ambient air quality - guide for the measurement of elemental carbon (EC) and organic carbon (OC) deposited on filters*. European Committee for Standardization, Brussels, Belgium.

Charrier J.G., Anastasio C., 2012. *On dithiothreitol (DTT) as a measure of oxidative potential for ambient particles: evidence for the importance of soluble transition metals*. Atmospheric Chemistry and Physics 12, 11317-11350.

Cheng Y., Brook J. R., Li S. M., Leithead A., 2011. *Seasonal variation in the biogenic secondary organic aerosol tracer cis-pinonic acid: enhancement due to emissions from regional and local biomass burning*. Atmospheric Environment 45, 7105-7122.

Chiappini L., Verlhac S., Aujay R., Maenhaut W., Putaud J.P., Sciare J., Jaffrezo J.L., Liousse C., Galy-Lacaux C., Alleman L.Y., Panteliadis P., Leoz E., Favez O., 2014. Clues for a standardized thermal-optical protocol for the assessment of organic and *elemental carbon within ambient air particulate matter*. Atmospheric Measurement Techniques 7, 1649–1661.

Cho A.K., Sioutas C., Miguel A.H., Kumagai Y., Schmitz D.A., Singh M., Eiguren-Fernandez A., Froines J.R., 2005. *Redox activity of airborne particulate matter at different sites in the Los Angeles Basin*. Environmental Research 99, 40-47.

Chung M.Y., Lazaro R.A., Lim D., Jackson J., Lyon J., Rendulic D., Hassom A.S., 2006. *Aerosol-borne quinones and reactive oxygen species generation by particulate matter extracts*. Environmental Science & Technology 40, 4880-4886.

Chung S.H., Seinfeld J.H., 2002. *Global distribution and climate forcing of carbonaceous aerosols*. Journal of Geophysical Research 107, AAC 14-1-AAC 14-33.

Cincinelli A, Bubba M., Martellini T., Gambaro A., 2007. *Gas-particle concentration and distribution of n-alkanes and polycyclic aromatic hydrocarbons in the atmosphere of Prato (Italy)*. Chemosphere 68, 472–478.

Core J.E., Cooper J.A., DeCesar R.T., Houck J.E., 1982. *Residential wood combustion study*. EPA 910/9-9-82-089a.

Costa V., Bacco D., Castellazzi S., Ricciardelli I., Vecchietti R., Zigola C., Pietrogrande M.C., 2016. *Characterization of Carbonaceous Aerosol in Emiliaromagna during the Supersito Project: Influences of the Thermal-Optical Measurement Protocols*. Atmospheric Research 167, 100-107.

Crawford L.R., 1981. *Lignin biodegradation and transformation*, Wiley.

Crimmins B.S, Baker J.E., 2006. *Improved GC/MS methods for measuring hourly PAH and nitro-PAH concentrations in urban particulate matter*. Atmospheric Environment 40, 6764–6779.

Currie L.A., 2000. *Evolution and multidisciplinary frontiers of ^{14}C aerosol science*. Radiocarbon 42, 115– 126.

Day M.C, Zhang M., Pandis, S.N., 2015. *Evaluation of the ability of the EC tracer method to estimate secondary organic carbon*. Atmospheric Environment 112, 317-325.

Delgado-Povedano M.M., Luque de Castro M.D., 2013. *Ultrasound-assisted extraction and in situ derivatization*. Journal of Chromatography A 1296, 226-234.

Deserti M., Savoia E., Cacciamani C., Golinelli M., Kerschbaumer A., Leoncini G., Selvini A., Paccagnella T., Tibaldi S., 2001. *Operational meteorological pre-processing at Emilia-Romagna ARPA Meteorological Service as a part of a decision support system for Air Quality Management*. International Journal of Environment and Pollution 16, 571-582.

Deserti M., Tugnoli S., 2011. *Risultati dell'indagine sul consumo domestico di biomassa legnosa in Emilia-Romagna e valutazione delle emissioni in atmosfera*. ARPA Emilia Romagna.

Dockery D.W., Pope C.A., 1994. *Acute respiratory effects of particulate air pollution*. Annual Review of Public Health 15, 107-132.

Donaldson K., Stone V., Borm P.J, Jimenez L.A, Gilmour P., Schins R.P., Knaapen A.M., Rahman I., Faux S.P., Brown D.M., MacNee W., 2003. *Oxidative stress and calcium signaling in the adverse effects of environmental particles (PM10)*. Free Radical Biology & Medicine 34, 1369–1382.

Dong J., Pan U.X., Lv J.X., Sun J., Gong X.M., Li K., 2011. *Multiresidue Method for the Determination of Pesticides in Fruits and Vegetables Using Gas Chromatography-Negative Chemical Ionization-Triple Quadrupole Tandem Mass Spectrometry*. Chromatographia 74, 109-119.

Elbert W., Taylor P.E., Andreae M.O., Poschl U., 2007. *Contribution of fungi to primary biogenic aerosols in the atmosphere: wet and dry discharged spores, carbohydrates, and inorganic ions*. Atmospheric Chemistry and Physics 7, 4569-4588.

Engling G., Lee J., Tsai Y.W., Lung S.C., Chou C.K., Chan C.Y., 2009. *Size resolved anhydrosugar composition in smoke aerosol from controlled field burning of rice straw*. Aerosol Science & Technology 43, 662–672.

Fabbri D., Torri C., Simoneit B. R. T., Marynowski L., Rushdi A. I., Fabianska M.J., 2009. *Levoglucosan and other cellulose lignine markers in emissions from burning of Miocene lignites*. Atmospheric Environment 43, 2286-2295.

Facchini M.C., Mircea M., Fuzzi S., Charlson R.J., 1999. *Cloud albedo enhancement by surface-active organic solutes in growing droplets*. Nature 401, 257-259.

Fine P.M., Cass G.R., Simoneit B.R.T., 2001. *Chemical characterization of fine particle emissions from fireplace combustion of woods grown in the Northeastern United States*. Environmental Science & Technology 35, 2665-2675.

Fine P.M., Cass G.R., Simoneit B.R.T., 2002. *Chemical Characterization of Fine Particle Emissions from the Fireplace Combustion of Woods Grown in the Southern United States*. Environmental Science & Technology 36, 1442-1451.

Fine P.M., Cass G.R., Simoneit B.R.T., 2004. *Chemical characterization of fine particle emissions from the wood Stove combustion of prevalent United States tree species*. Environmental Engineering Science 21, 387-409.

Fountoukis C., Butler T., Lawrence M.G., Denier van der Gon H.A.C., Visschedijk A.J.H., Charalampidis P., Pilinis C., Pandis S.N., 2014. *Impacts of controlling biomass burning emissions on wintertime carbonaceous aerosol in Europe*. Atmospheric Environment 87, 175-182.

Fu P., Kawamura K., Okuzawa K., Aggarwal S.G., Wang G., Kanaya Y., Wang Z., 2008. *Organic molecular compositions and temporal variations of summertime mountain aerosols over Mt. Tai, North China Plain*. Journal of Geophysical Research: Atmospheres 113, D19.

Fu P., Kawamura K., Kobayashi M., Simoneit B.R.T., 2012. *Seasonal variations of sugars in atmospheric particulate matter from Gosan, Jeju Island: significant contributions of airborne pollen and Asian dust in spring*. Atmospheric Environment 55, 234-239.

Garrido Frenich A., Plaza-Bolaños P., Martínez Vidal J.L., 2008. *Comparison of tandem-in-space and tandem-in-time mass spectrometry in gas chromatography determination of pesticides: Application to simple and complex food samples*. Journal of Chromatography A 1203, 229-238.

Gelencser A., May B., Simpson D., Sanchez-Ochoa A., Kasper-Giebl A., Puxbaum H., Caseiro A., Pio C., Legrand M., 2007. *Source apportionment of PM2.5 organic aerosol over Europe: primary/secondary, natural/anthropogenic, and fossil/biogenic origin*. Journal of Geophysical Research:Atmospheres 112.

Gentner D.R., Isaacman G., Worton D.R., Chan A.W.H., Dallmann T.R., Davis L., Liu S., Day D.A., Russell L.M., Wilson K.R., Weber R., Guha A., Harley R.A., Goldstein A.H., 2012. *Elucidating secondary organic aerosol from diesel and gasoline vehicles through detailed characterization of organic carbon emissions*. Proceedings of Natural Academy of Sciences U. S. A. 109, 18318-18323.

Ghio A.J., Kim C., Devlin R.B., 2001. *Concentrated ambient air particles induce mild pulmonary inflammation in healthy human volunteers*. American Journal of Respiratory and Critical Care Medicine 162, 981-988.

Gianelle V., Colombi C., Caserini S., Ozgen S., Galante S., Marongiu A., Lanzani G., 2013. *Benzo(a)pyrene air concentrations and emission inventory in Lombardy region, Italy*. Atmospheric Pollution Research 4, 257-266.

Giannoni M., Martellini T., Del Bubba M., Gambaro A., Zangrando R., Chiari M., Lepri M., Cincinelli A., 2012. *The use of levoglucosan for tracing biomass burning in $PM_{2.5}$ samples in Tuscany (Italy)*. Environmental Pollution 167, 7-15.

Gilardoni S., Vignati E., Cavalli F., Putaud J., Larsen B., Karl M., Stenström K., Genberg J., Henne S., Dentener F., 2011. *Better constraints on sources of carbonaceous aerosols using a combined ^{14}C–macro tracer analysis in a european rural background site*. Atmospheric Chemistry and Physics 11, 5685–5700.

Glasius M, Lahaniati M., Calogirou A., Di Bella D., Jensen N.R., Hjorth J., Kotzias D., Larsen B.R., 2000. *Carboxylic acids in secondary aerosols from oxidation of cyclic monoterpenes by ozone*. Environmental Science & Technology 34, 1001-1010.

Goncalves C., Alves C., Fernandes A. P., Monteiro P., Tarelho L., Evtyugina M., Pio C., 2011. *Organic compounds in $PM_{2.5}$ emitted from fireplace and woodstove combustion of typical Portuguese wood species*. Atmospheric Environment, 45, 4533-4545.

Harrison, R.M., Yin, J., 2000. *Particulate matter in the atmosphere: which particle properties are important for its effects on health?*. Science of the Total Environment 249, 85-101.

Hays M.D., Smith N.D., Kinsey J., Dong Y., Kariher P., 2003. *Polycyclic aromatic hydrocarbon size distributions in aerosols from appliances of residential wood combustion as determined by direct thermal desorption-GC/MS*. Journal of Aerosol Science 34, 1061-1084.

Haywood, J., Boucher, O., 2000. *Estimates of the direct and indirect radiative forcing due to tropospheric aerosols: A review*. Reviews of Geophysics 38, 513-543.

Hedayat F., Stevanovic S., Miljevic B., Bottle S., Ristovski Z.D., 2014. *Review-evaluating the molecular assays for measuring the oxidative potential of particulate matter*. Chemical Industry and Chemical Engineering Quarterly 21, 201-210.

Herich H., Gianini M.F.D., Piot C., Mocnik G., Jaffrezo J.L., Besombes J.L., Prévôt A.S.H., Hueglin C., 2014. *Overview of the impact of wood burning emissions on carbonaceous aerosols and PM in large parts of the Alpine region*. Atmospheric Environment 89, 64-75.

Hirano S., Furuyama A., Koike E., Kobayashi T., 2003. *Oxidative-stress potency of organic extracts of diesel exhaust and urban fine particles in rat heart microvessel endothelial cells*. Toxicology 187, 161-170.

Ho K.F., Lee S.C., Cao J.J., Kawamura K., Watanabe T., Cheng Y., Chow J.C., 2006. *Dicarboxylic acids, ketocarboxylic acids and dicarbonyls in the urban roadside area of Hong Kong*. Atmospheric Environment 40, 3030-3040.

Ho K.F., Ho S.S.H., Lee S.C., Kawamura K., Zou S.C., Cao J.J., Xu H.M., 2011. *Summer and winter variation of dicarboxylic acids, fatty acids and benzoic acid in PM2,5 in Pearl Delta River Region, China*. Atmospheric Chemistry and Physics 11, 2197-2208.

Hoffmann D., Tilgner A., Iinuma Y., Herrmann H., 2010. *Atmospheric stability of levoglucosan: a detailed laboratory and modeling study*. Environmental Science & Technology 44, 694-699.

Horálek., J., de Smet, P., Kurfürst, P., de Leeuw, F., Benešová, N., 2015. *European air quality maps of PM and ozone for 2012 and their uncertainty*. ETC/ACM Technical Paper 2014/4.

Hsieh L.Y., Chen C.L., Wan M.W., Tsai C.H., Tsai Y.I., 2008. *Speciation and temporal characterization of dicarboxylic acids in $PM_{2.5}$ during a PM episode and a period of non-episodic pollution*. Atmospheric Environment 42, 6836-6850.

Huang X.F., He L.Y., Hu M., Zhang Y.H., 2006. *Annual variation of particulate organic compounds in $PM_{2.5}$ in the urban atmosphere of Beijing*. Atmospheric Environment 40, 2449-2458.

Hyder M., Genberg J., Sandahl M., Swietlicki E., Jonsson J.A., 2012. *Yearly trend of dicarboxylic acids in organic aerosols from south of Sweden and source attribution*. Atmospheric Environment 57, 197-204.

Istat, 2014. *I consumi energetici delle famiglie*.

Jacobson M.C., Hansson H.C., Noone K.J., Charlson R.J., 2000. *Organic atmospheric aerosols: Review and state of the science*. Reviews of Geophysics 38, 267-294.

Jaeschke H., 2011. *Reactive oxygen and mechanisms of inflammatory liver injury: present concepts*. Journal of Gastroenterology and Hepatology 26, 173-179.

Janssen N.A.H., Yang A., Strak M., Steenhof M., Hellack B., Gerlofs-Nijland M.E., Kuhlbusch T., Kelly F., Harrison R., Brunekreef B., Hoek G., Cassee F., 2014. *Oxidative potential of particulate matter collected at sites with different source characteristics*. Science of The Total Environment 472, 572-581.

Jaoui M., Kleindienst T.E., Lewandowski M., Edney E.O., 2004. *Identification and Quantification of Aerosol Polar Oxygenated Compounds Bearing Carboxylic or Hydroxyl Groups. 1. Method Development*. Analytical Chemistry 76, 4765-4778.

Jedynska A., Hoek G., Eeftens M., Cyrys J., Keuken M., Ampe C., Beelen R., Cesaroni G., Forastiere F., Cirach M., 2014. *Spatial variations of PAH, hopanes/steranes and EC/OC concentrations within and between European study areas*. Atmospheric Environment 87, 239-248.

Jia Y., Bhat S., Fraser M.P., 2010. *Characterization of saccharides and other organic compounds in fine particles and the use of saccharides to track primary biologically derived carbon sources*. Atmospheric Environment 44, 724-732.

Jia Y., Fraser M.P., 2011. *Characterization of saccharides in size-fractionated ambient particulate matter and aerosol sources: the contribution of primary biological aerosol particles (PBAPs) and soil to ambient particulate matter*. Atmospheric Environment 45, 930-936.

Kawamura K., Kaplan I.R., 1987. *Motor exhaust emissions as primary source for dicarboxylic acids in Los Angeles ambient air*. Environmental Science & Technology 21, 105-110.

Kawamura K., Kasukabe H., Barrie L.A., 1996. *Source and reaction pathways of dicarboxylic acids, ketoacids and dicaronyls in arctic aerosols: one year of observations*. Atmospheric Environment 30, 1709-1722.

Kawamura K., Yasui, O., 2005. *Diurnal changes in the distribution of dicarboxylic acids, ketocarboxylic acids and dicarbonyls in the urban Tokyo atmosphere*. Atmospheric Environment 39, 45-60.

Kelly F.J., 2003. *Oxidative stress: its role in air pollution and adverse health effects*. Occupational and Environmental Medicine 60, 612-616.

Kotianová P., Puxbaum H., Bauer H., Caseiro A., Marr I.L., Čík G., 2008. *Temporal patterns of n-alkanes at traffic exposed and suburban sites in Vienna*. Atmospheric Environment 42, 2993-3005.

Kourtchev I., Warnke J., Maenhaut W., Hoffmann T., Claeys M., 2008. *Polar organic markers compounds in $PM_{2.5}$ aerosol from a mixed forest site in western Germany*. Chemosphere 73, 1308-1314.

Kourtchev I., Hellebust S., Bell J.M., O'Connor I.P., Healy R.M., Allanic A., Healy D., Wenger J.C., Sodeau J.R., 2011. *The use of polar organic compounds to estimate the contribution of domestic solid fuel combustion and biogenic sources to ambient levels of organic carbon and $PM_{2.5}$ in Cork Harbor, Ireland*. Science of the Total Environment 409, 2143-2155.

Kumagai K., Iijima A., Shimoda M., Saitoh Y., Kozawa K., Hagino H., Sakamoto K., 2010. *Determination of Dicarboxylic Acids and Levoglucosan in Fine Particles in the Kanto Plain,*

Japan, for Source Apportionment of Organic Aerosols. Aerosol and Air Quality Research 10, 282-291.

Kumagai Y., Koide S., Taguchi K., Endo A., Nakai Y., Yoshikawa T., Shimojo N., 2002. *Oxidation of Proximal Protein Sulfhydryls by Phenanthraquinone, a Component of Diesel Exhaust Particles*. Chemical Research in Toxicology 15, 483-489.

Kuo L.J., Louchouarn P., Herbert B.E., 2011. *Influence of combustion conditions on yields of solvent-extractable anhydrosugars and lignin phenols in chars: Implications for characterizations of biomass combustion residues*. Chemosphere 85, 797-805.

INEMAR-Regione Lombardia:
http://inemar.arpalombardia.it/inemar/webdata/elab_standard_reg.seam;jsessionid=A4BAAA

ISPRA: http://www.sinanet.isprambiente.it/it/sia-ispra/inventaria/disaggregazione-dellinventario-nazionale-2010/disaggregazione-dell2019inventario-nazionale-2013-versione-completa/view

ISTAT, 2014. I consumi energetici delle famiglie.

Ladji R., Yassaa N., Calducci C., Cecinato A., Meklati B.Y., 2009. *Annual variation of particulate organic compounds in PM10 in the urban atmosphere of Algiers*. Atmospheric Research 92, 258-269.

Larsen B.R., Giraldoni S., Stenstrom K., Niedzialek J., Jimenez J., Belis C.A., 2012. *Sources for PM pollution in the Po Plain, Italy. II. Probabilistic uncertainty characterization and sensitivity analysis of secondary and primary sources*. Atmospheric Environment 50, 203-213.

Li C.K., Kamens R.M., 1993. *The use of polycyclic aromatic hydrocarbons as source signatures in receptor modelling.* Atmospheric Environment 27, 523-532.

Li J.J., Wang G.H., Wang X.M., Cao J.J., Sun T., Cheng C.L., Meng J.J., Hu T.F., Liu S.X., 2012. *Abundance, composition and source of atmospheric $PM_{2.5}$ at a remote site in the Tibetan Plateau, China*. Tellus B 65, 1-16.

Li Q., Wyatt A., Kamens R.M., 2009. *Oxidant generation and toxicity enhancement of aged-diesel exhaust.* Atmospheric Environment 43, 1037-1042.

Lin P., Yu J.Z., 2011. *Generation of reactive oxygen species mediated by humic-like substances in atmospheric aerosols*. Environmental Science & Technology 45, 10362-10368.

Liu Y., Sklorz M., Schnelle-Kreis J., Orasche J., Ferge T., Kettrup A., Zimmermann R., 2006. *Oxidant denuder sampling for analysis of polycyclic aromatic hydrocarbons and their oxygenated derivates in ambient aerosol: Evaluation of sampling artefact*. Chemosphere 62, 1889–1898.

Lodovici M., Bigagli E., 2011. *Oxidative Stress and Air Pollution Exposure*. Journal of Toxicology 2011, Article ID 487074.

Lonati G., Ozgen S., Giugliano M., 2007. *Primary and secondary carbonaceous species in $PM_{2.5}$ samples in Milan (Italy)*. Atmospheric Environment 41, 4599-4610.

Louchouarn P., Kuo L.J., Wade T.L., Schantz M., 2009. *Determination of levoglucosan and its isomers in size fractions of aerosol standard reference materials*. Atmospheric Environment 43, 5630–5636.

Lough G. C., Schauer J. J., Lawson D. R., 2006. *Day-of-week trends in carbonaceous aerosol composition in the urban atmosphere*. Atmospheric Environment 40, 4137-4149.

Luque de Castro, M.D., Priego-Capote F., Peralbo-Molina A., 2011. *The role of ultrasound in analytical derivatizations*. Journal of Chromatography B 879, 1189-1195.

Lv Q., Zhang Q., Li W., Li H., Li P., Ma Q., Meng X., Qi M., Bai H, 2013. *Determination of 48 fragrance allergens in toys using GC with ion trap MS/MS*. Journal of Separation Science 36, 3534-3549.

Ma S.X., Wang Z.Z., Bi X.H., Sheng G.Y., Fu J M., 2009. *Composition and source of saccharides in aerosols in Guangzhou, China*. Chinese Science Bulletin 53, 4500-4506.

Mackay D., Shiu W.Y., Ma K.C., Lee S.C., 2006. *Handbook of Physical-Chemical Properties and Environmental Fate for Organic Chemicals*. CRC Press.

Marr L.C., Kirchstetter T.W., Harley R.A., Miguel A.H., Hering S.V., Hammond S.K., 1999. *Characterization of Polycyclic Aromatic Hydrocarbons in Motor Vehicle Fuels and Exhaust Emissions*. Environmental Science & Technology 33, 3091-3099.

Massart D.L., Vandenginste B.G.M., Deming S.N., Michotte Y., Kaufman L., 1988. *Chemometrics: a textbook*. Elsevier Science Publishers B.V., Amsterdam.

Massart D.L., Vandeginste B.G.M., Buydens L.M.C., De Song S., Lewi P.J., Smeyers-Verbeke J., 1997. Handbook of Chemometrics Qualimetrics (Part A), Elsevier Science Publisher B.V., Amsterdam.

Mazzoleni L.R., Zielinska B., Moosmüller H., 2007. *Emissions of levoglucosan, methoxy phenols, and organic acids from prescribed burns, laboratory combustion of wildland fuels, and residential wood combustion*. Environmental Science & Technology 41, 2115-2122.

McDonald R., 2009. *Evaluation of gas, oil and wood pellet fueled residential heating system emissions characteristics*. Brookhaven National Laboratory, Energy Sciences and Technology Department, Report No. BNL-91286-2009-IR.

Medeiros P.M., Conte M.H., Weber J.C., Simoneit B.R.T., 2006. *Sugars as source indicators of biogenic organic carbon in aerosols collected above the Howland Experimental Forest, Maine*. Atmospheric Environment 40, 1694-1705.

Medina C.M., Pitarch E., Portolés T., Lopez F.J., Hernandez F., 2009. *GC-MS/MS multi-residue method for the determination of organochlorine pesticides, polychlorinated biphenyls and polybrominated diphenyl ethers in human breast tissue*. Journal of Separation Sciences 32, 2090-2102.

Meyer N.K., 2012. *Particulate, black carbon and organic emissions from small-scale residential wood combustion appliances in Switzerland* Biomass & Bioenergy 36, 31-42.

Miguel A.H., Kirchstetter T.W., Harley R.A., Hering S.V., 1998. *On-Road Emissions of Particulate Polycyclic Aromatic Hydrocarbons and Black Carbon from Gasoline and Diesel Vehicles*. Environmental Science & Technology 32, 450-455.

Mochida M., Kawamura K., Fu P., Takemura T., 2010. *Seasonal variation of levoglucosan in aerosols over the western North Pacific and its assessment as a biomass-burning tracer*. Atmospheric Environment 44, 3511-3518.

Monks P., ApSimon H., Carruthers D., Carslaw D., Derwent D., Harrison R., Laxen D., Stedman J., 2012. *Fine particulate matter (PM$_{2.5}$) in the United Kingdom*. UK Department for Environment, Food & Rural Affair.

Mudge, S.M., 2005. *Fatty Alcohols – a review of their natural synthesis and environmental distribution*. School of Ocean Sciences, University of Wales–Bangor, The Soap and Detergent Association.

Mudway I.S., Fuller G., Green D., Dunster C., Kelly F.J., 2011. *Quantifying the London specific component of PM$_{10}$ oxidative activity*. UK Department for Environment, Food & Rural Affair.

Oliveira C., Pio C., Alves C., Evtyugina M., Santos P., Goncalves V., Nunes T., Silvestre A.J.D., Palmgren F., Wahlin P., Harrad S., 2007. *Seasonal distribution of polar organic compounds in the urban atmosphere of two large cities from the North and South of Europe*. Atmospheric Environment 41, 5555-5570.

Oliveira C., Martins N., Tavares J., Pio C., Cerqueira M., Matos M., Silva H., Oliveira C., Camões F., 2011. *Size distribution of polycyclic aromatic hydrocarbons in a roadway tunnel in Lisbon, Portugal*. Chemosphere 83, 1588-1596.

Orasche J., Schnelle-Kreis J., Abbaszade G., Zimmermann R., 2011. *Technical Note: In-situ derivatization thermal desorption GC-TOFMS for direct analysis of particle-bound non-polar and polar organic species*. Atmospheric Chemistry and Physics 11, 8977-8993.

Orasche J., Seidel T., Hartmann H., Schnelle-Kreis J., Chow J.C., Ruppert H., Zimmermann R., 2012. *Comparison of emissions from wood combustion. Part 1: emission factors and characteristics from different small-scale residential heating appliances considering particulate matter and polycyclic aromatic hydrocarbon (PAH)-related toxicological potential of particle-bound organic species*. Energy & Fuels 26, 6695-6704.

Oros D.R., Simoneit B.R.T., 2001. *Identification and emission factors of molecular tracers in organic aerosols from biomass burning Part 1. Temperate climate conifers*. Applied Geochemistry 16, 1513-1544.

Oros D.R., Simoneit B.R.T., 2001. *Identification and emission factors of molecular tracers in organic aerosols from biomass burning Part 2. Deciduous tree*. Applied Geochemistry 16, 1545-1565.

Orozco-Solano, M., Ruiz-Jiménez J., Luque de Castro M., 2010. *Ultrasound-assisted extraction and derivatization of sterols and fatty alcohols from olive leaves and drupes prior to determination by gas chromatography–tandem mass spectrometry.* Journal of chromatography A 1217, 1227-1235.

Paglione M., Saarikoski S., Carbone S., Hillamo R., Facchini M.C., Finessi, E., Giulianelli L., Carbone C., Fuzzi S., Moretti F., Tagliavini E., Swietlicki E., Stenstrom K.E., Prevot A.S.H., Massoli P., Canaragatna M., Worsnop D., Decesari S., 2014. *Primary and secondary biomass burning aerosols determined by proton nuclear magnetic resonance (H-1-NMR) spectroscopy during the 2008 EUCAARI campaign in the Po Valley (Italy)*. Atmospheric Chemistry and Physics 14, 5089-5110.

Perrini G., Tommasello M., Librando V., Minniti Z., 2005. *Nitrated PAHs in the environment: formation, occurrence and analysis*. Annali di Chimica 95, 567–577.

Perrino C., Catrambone M., Dalla Torre S., Rantica E., Sargolini T., Canepari S., 2014. *Seasonal variations in the chemical composition of particulate matter: a case study in the Po Valley. Part I: macro-components and mass closure*. Environmental Science and Pollution Research 21, 3999-4009.

Perrone M.G., Larsen B.R., Ferrero L., Sangiorgi G., De Gennaro G., Udisti R., Zangrando R., Gambaro A., Bolzacchini E., 2012. *Sources of high PM$_{2.5}$ concentrations in Milan, Northern Italy: molecular marker data and CMB modeling*. Science of the Total Environment 414, 343-355.

Perrone M.G., Gualtieri M., Consonni V., Ferrero L, Sangiorgi G., Longhin M., Ballabio D., Bolzacchini E., Camatin M., 2013. *Particle size, chemical composition, seasons of the year and urban, rural or remote site origins as determinants of biological effects of particulate matter on pulmonary cells*. Environmental Pollution 176, 215-227.

Petersson G., 1974. *Gas chromatography-mass spectrometry of sugars and related hydroxyl acids as trimethylsilyl derivates.* Chalmers University of Technology, Department of Engineering Chemistry, Goteborg.

Pettersson E., Boman C., Westerholm R., Boström D., Nordin A., 2011. *Stove performance and emission characteristics in residential wood log and pellet combustion, Part 2: wood stoves*. Energy & Fuels 25, 315-323.

Piazzalunga A, Belis C., Bernardoni V., Cazzuli O., Fermo P., Valli G., Vecchi R., 2011. *Estimates of wood burning contribution to PM by the macro-tracer method using tailored emission factors*. Atmospheric Environment 45, 6642-6649.

Piazzalunga A., Anzano M., Collina E., Lasagni M., Lollobrigida F., Pannocchia A., Fermo P., Pitea D., 2013. *Contribution of wood combustion to PAH and PCDD/F concentrations in two urban sites in northern Italy*. Journal of Aerosol Science 56, 30-40.

Pietrogrande M.C., Zampolli M.G., Dondi F., Szopa C., Sternberg R., Buch A., Raulin F., 2005. *In situ analysis of the Martian soil by gas chromatography: Decoding of complex chromatograms of organic molecules of exobiological interest*. Journal of Chromatography A 1071, 255-261.

Pietrogrande M.C., Mercuriali M., Perrone M.G., Ferrero L., Sangiorgi G., Bolzacchini E., 2010a. *Distribution of n-alkanes in the Northern Italy Aerosols: Data Handling of GC/MS Signals for Homologous Series Characterization*. Environmental Science & Technology 44, 4232-4240.

Pietrogrande M.C., Bacco D., Mercuriali M., 2010b. *GC-MS analysis of low-molecular-weight dicarboxylic acids in atmospheric aerosol: comparison between silylation and esterification derivatization procedures*. Analytical Bioanalytical Chemistry 396, 877-885.

Pietrogrande M.C., Bacco D., 2011. *GC-MS analysis of water-soluble organics in atmospheric aerosol: Response surface methodology for optimizing silyl-derivatization for simultaneous analysis of carboxylic acids and sugars*. Analytica Chimica Acta 689, 257-264.

Pietrogrande M.C., Bacco D., Rossi M., 2013a. *Chemical characterization of polar organic markers in aerosols in a local area around Bologna, Italy*. Atmospheric Environment 75, 279-286.

Pietrogrande M.C., Bacco D., Chiereghin S., 2013b. *GC/MS analysis of water-soluble organics in atmospheric aerosol: optimization of a solvent extraction procedure for simultaneous analysis of carboxylic acids and sugars*. Analytical Bioanalytical Chemistry 405, 1095-1104.

Pietrogrande M.C., Bacco D., Visentin M., Ferrari S., Poluzzi V., 2014a. *Polar organic marker compounds in atmospheric aerosol in the Po Valley during the Supersito campaigns d Part 1: Low molecular weight carboxylic acids in cold seasons*. Atmospheric Environment 85, 164-175.

Pietrogrande M.C., Bacco D., Visentin M., Ferrari S., Casali P., 2014b. *Polar organic marker compounds in atmospheric aerosol in the Po Valley during the Supersito campaigns d Part 2: Seasonal variations of sugars*. Atmospheric Environment 97, 215-225.

Pietrogrande M.C., Bacco D., Ferrari S., Kaipainen J., Ricciardelli I., Riekkola M.L., Trentini A., Visentin M., 2015. *Characterization of atmospheric aerosols in the Po valley during the supersito campaigns d Part 3: Contribution of wood combustion to wintertime atmospheric aerosols in Emilia Romagna region (Northern Italy)*. Atmospheric Environment 122, 291-305.

Pio C.A., Legrand M., Alves C.A., Oliveira T., Afonso J., Caseiro A., Puxbaum H., Sanchez-Ochoa A., Gelencser A., 2008. *Chemical composition of atmospheric aerosols during the 2003 summer intense forest fire period*. Atmospheric Environment 42, 7530-7543.

Pio C., Cerqueira M., Harrison R.M., Nunes T., Mirante F., Alves C., Oliveira C., Sanchez de la Campa A., Artíñano B., Matos M., 2011. *OC/EC ratio observations in Europe: Re-thinking the approach for apportionment between primary and secondary organic carbon.* Atmospheric Environment 45, 6121-6132.

Puxbaum H., Caseiro A., Sánchez-Ochoa A., Kasper-Giebl A., Claeys M., Gelencsér A., Legrand M., Preunkert S., Pio C., 2007. *Levoglucosan levels at background sites in Europe for assessing the impact of biomass combustion on the European aerosol background.* Journal of Geophysical Research 112, D23S05.

QUARG, 1993. *Urban air quality in the UK. The first report of the urban air review group.* Department of the Environment, London.

Ravindra K., Sokhi K., Van Grieken R., 2008. *Atmospheric polycyclic aromatic hydrocarbons: Source attribution, emission factors and regulation.* Atmospheric Environment 42, 2895-2921.

Ray J., McDow S.R., 2005. *Dicarboxylic acid concentration trends and sampling artifacts.* Atmospheric Environment 39, 7906-7919.

Rogge W. F., Mazurek M. A., Hildemann L. M., Cass G. R., Simoneit B. R. T., 1993. *Quantification of urban organic aerosols at a molecular level: identifications,abundance and seasona variation.* Atmospheric Environment 27, 1309-1330.

Rogge W.F., Hildemann L.M., Mazurek M.A., Cass G.R., 1998. *Sources of fine organic aerosol. 9. Pine, oak, and synthetic log combustion in residential fireplaces.* Environmental Science & Technology 32, 13-22.

Rogge W.F., Medeiros P.M., Simoneit B.R.T., 2006. *Organic marker compounds for surface soil and fugitive dust from open lot dairies and cattle feedlots.* Atmospheric Environment 40, 27-49.

Rogge W.F., Medeiros P.M., Simoneit B.R.T., 2007. *Organic marker compounds in surface soils of crop fields from the San Joaquin Valley fugitive dust characterization study.* Atmospheric Environment 41, 8183-8204.

Roginski V.A., Barsukova T.K., Stegmann H.B., 1999. *Kinetics of redox interaction between substitutes quinones and ascorbate under aerobic conditions.* Chemico-Biological Interactions 121, 177-197.

Rompp A., Winterhalter R., Moortgat G. K., 2006. *Oxodicarboxylic acid in atmospheric aerosol particles.* Atmospheric Environment 40, 6846-6862.

Ruiz-Jimenez J., Parshintsev J., Laitinen T., Hartonen K., Petäjä T., Kulmala M., Riekkola, M.L., 2012. *Influence of the sampling site, the season of the year, the particle size and the number of nucleation events on the chemical composition of atmospheric ultrafine and total suspended particles.* Atmospheric Environment 49, 60-68.

Saarnio K., Sillanpaa M., Hillamo R., Sandell E., Pennanen A.S., Salonen R.A., 2008. *Polycyclic aromatic hydrocarbons in size-segregated particulate matter from six urban sites in Europe.* Atmospheric Environment 42, 9087-9097.

Saffari A., Hasheminassab S., Wang D., Shafer M.M., Schauer J.J., Sioutas C., 2015. *Impact of primary and secondary organic sources on the oxidative potential of quasi-ultrafine particles (PM0.25) at three contrasting locations in the Los Angeles Basin.* Atmospheric Environment 120, 286-296.

Sánchez Ávila N., Priego Capote F., Luque de Castro M.D., 2007. *Ultrasound-assisted extraction and silylation prior to gas chromatography–mass spectrometry for the characterization of the triterpenic fraction in olive leaves.* Journal of Chromatography A 1165, 158-165.

Sandrini S., Fuzzi S., Piazzalunga A., Prati P., Bonasoni P., Cavalli F., Bove M.C., Calvello M., Cappelletti D., Colombi C., Contini D., De Gennaro G., Di Gilio A., Fermo P., Ferrero L., Gianelle V., Giugliano M., Ielpo P., Lonati G., Marinoni A. Massabò M., Molteni U., Moroni B., Pavese G., Perrino C., Perrone M.G., Perrone M.R., Putaud J.P., Sargolini T., Vecchi R., Gilardoni S., 2014. *Spatial and seasonal variability of carbonaceous aerosol across Italy.* Atmospheric Environment 99, 587-598.

Schafer, F.Q., Buettner, G.R. 2001. *Redox environment of the cell as viewed through the redox state of the glutathione disulfide/ glutathione couple.* Free Radical Biology & Medicine 30, 1191–1212.

Schauer J.J., Cass G.R., 2000. *Source apportionment of wintertime gas-phase and particle-phase air pollutants using organic compounds as tracers.* Environmental Science & Technology 34, 1821-1832.

Schauer J.J., Kleeman M.J., Cass G.R., Simoneit B.R.T., 2001. *Measurement of emissions from air pollution sources. 3. C1-C29 organic compounds from fireplace combustion of wood.* Environmental Science & Technology 35, 1716-1728.

Schmidl C., Marr L.L., Caseiro A., Kotianova P., Berner A., Bauer H., Kasper-Giebl A., Puxbaum H., 2008. *Chemical characterisation of fine particle emissions from wood stove combustion of common woods growing in mid-European Alpine regions*, Atmospheric Environment 42, 126–141.

Schummer C., Delhomme O., Appenzeller B.M.R., Wennig R., Millet M., 2009. *Comparison of MTBSTFA and BSTFA in derivatization reactions of polar compounds prior to GC/MS analysis.* Talanta 77, 1473-1482.

Schwartz J., 1994. *Air pollution and daily mortality: a review and meta analysis.* Environmental Research 64, 36–52.

Schwartz J., Laden F., Zanobetti A., 2002. *The concentration response relation between PM2.5 and daily deaths.* Environmental Health Perspective 110, 1025–1029.

Schwarze P.E., Øvrevik J., Lag M., Refsnes M., Nafstad P., Hetland R.B., Dybing E., 2006. *Particulate matter properties and health effects: consistency of epidemiological and toxicological studies*. Human & Experimental Toxicology 25, 559-579.

Shilling J. E., King S. M., Mochida M., Wornsnop D. R., Martin S. T., 2007. *Mass spectral evidence that small changes in composition caused by oxidative aging processes alter aerosol CCN properties*. Journal of Physical Chemistry A 111, 3358-3368.

Simoneit B.R.T., Schauer J.J., Nolte C.G., Oros D.R., Elias V.O., Fraser M.P., Rogge W.F., Cass G.R., 1999. *Levoglucosan, a tracer for cellulose in biomass burning and atmospheric particles*. Atmospheric Environment 33, 173-182.

Simoneit B.R.T., Rogge, W.F., Lang Q., Jaffè R., 2000. *Molecular characterization of smoke from campfire burning of pine wood (Pinus elliottii)*. Chemosphere: Global Change Science 2, 107-122.

Simoneit B.R.T., 2002. *Biomass burning — a review of organic tracers for smoke from incomplete combustion*. Applied Geochemistry 17, 129-162.

Simoneit B.R.T., Elias V.O., Kobayashi M., Kawamura, K., Rushdi A.I., Medeiros P M., Rogge W. F., Didyk B.M., 2004. *Sugars – Dominant water soluble organic compounds in soils and characterization as tracers in atmospheric particulate matter*. Environmental Science & Technology 38, 5939-5949.

Simoneit B.R.T., Bi X., Oros D.R., Medeiros P.M., Sheng G., Fu J., 2007. *Phenols and Hydroxy-PAHs (Arylphenols) as Tracers for Coal Smoke Particulate Matter: Source Tests and Ambient Aerosol Assessments*. Environmental Science & Technology 41, 7294-7302.

Standley L.J., Simoneit B.R.T., 1987. *Characterization of extractable plant wax, resin, and thermally matured components in smoke particles from prescribed burns*. Environmental Science and Technology 21, 163-169.

Strizhak P.E., 1994. *Effect of copper (II) ions on kinetics of ascorbic acid oxidation by methylene blue*. Theoretical and Experimental Chemistry 30, 239-244.

Suslick K.S., 1989. *The chemical effects of ultrasound*. Scientific American 260, 80-86.

Szidat S., Jenk T.M., Synal H.A., Kalberer M., Wacker L., Hajdas I., Kasper-Giebl A., Baltensperger U., 2006. *Contributions of fossil fuel, biomass-burning and biogenic emissions to carbonaceous aerosols in Zurich as traced by 14C*. Journal Geophysics Research 111, D07206.

Szmigielski R., Surratt J.D., Vermeylen R., Szmigielska K., Kroll J.H., Nga N.L., Murphy S.M., Sorooshian A., Seinfeld J.H., Claeys, M., 2007. *Characterization of 2-methylglyceric acid oligomers in secondary organic aerosol formed from the photooxidation of isoprene using trimethylsilylation and gas chromatography/ion trap mass spectrometry*. Journal of Mass Spectrometry 42, 101-116.

Taqui Khan M.M., Martell A.E., 1967. *Metal Ion and Metal Chelate Catalyzed Oxidation of Ascorbic Acid by Molecular Oxygen. I. Cupric and Ferric Ion Catalyzed Oxidation*. Journal of American Chemical Society 89, 4176-4185.

Tobiszewski M., Namieńśnik J., 2012. *PAH diagnostic ratios for the identification of pollution emission sources*. Environmental Pollution 162, 110-119.

Tominaga, S., Matsumoto, K., Kaneyasu, N., Shigihara, A., Katono, K., Igawa, M., 2011. *Measurements of particulate sugars at urban and forested suburban sites*. Atmospheric Environment 45, 2335-2339.

Tsai Y.I., Sopajaree K., Chotruksa A., Wu H.C., Kuo S.S., 2013. *Source indicators of biomass burning associated with inorganic salts and carboxylates in dry season ambient aerosol in Chiang Mai Basin, Thailand*. Atmospheric Environment 78, 93-104.

Todeschini R., 1998. *Introduzione alla chemiometria.* Edises.

Vallius M., 2005. *Characteristics and sources of fine particulate matter in urban air*. National Public Health Institute, Department of Environmental Health Kuopio, Finland.

Van Drooge B., Crusack M., Reche C., Mohr C., Alastuey A., Querol X., Prevot A., Douglas A., Day D.A., Jimenez J.L., Grimalt J.O., 2012. *Molecular marker characterization of the organic composition of submicron aerosols from Mediterranean urban and rural environments under contrasting meteorological conditions*. Atmospheric Environment 61, 482-489.

Vassura I., Venturini E., Marchetti S., Piazzalunga A., Bernardi E., Fermo P., Passarini F., 2014. *Markers and influence of open biomass burning on atmospheric particulate size and composition during a major bonfire event*. Atmospheric Environment 82, 218-225.

Viana M., Reche C., Amato F., Alastuey A., Querol X., Moreno T., Lucarelli F., Nava S., Cazolai G., Chiari M., Rico M., 2013. *Evidence of biomass burning aerosols in the Barcelona urban environment during winter time*. Atmospheric Environment 72, 81-88.

VIIAS: http://www.viias.it/pagine/impatto-sulla-salute

Virdis M.R., Gaeta M., Ciorba U., D'Elia I., 2015. *Gli impatti energetici e ambientali dei combustibili nel settore residenziale*. ENEA.

Visentin M., Pietrogrande M.C., 2014. *Determination of polar organic compounds in atmospheric aerosols by gas chromatography with ion trap tandem mass spectrometry*. Journal of Separation Science 37, 1561-1569.

Walgraeve C, Demeestere K, Dewulf J, Zimmermann R, Van Langenhove H., 2010. *Oxygenated polycyclic aromatic hydrocarbons in atmospheric particulate matter: Molecular characterization and occurrence*. Atmospheric Environment 44, 1831-1846.

Walser M.L, Desyaterik Y., Laskin J., Laskin A., Nizkorodov S.A., 2008. *High-resolution mass spectrometric analysis of secondary organic aerosol produced by ozonation of limonene*. Physical Chemistry Chemical Physics 21, 1009-1022.

Wang G., Niu S., Liu C., Wang L., 2002. *Identification of dicarboxylic acids and aldehydes of PM10 and PM2.5 aerosols in Nanjing, China*. Atmospheric Environment 36, 1941-1950.

Wang G., Chen C., Li J., Zhou B., Xie M., Hu S., Kawamura K., Chen C., 2011. *Molecular composition and size distribution of sugars, sugar-alcohols and carboxylic acids in airborne particles during a severe urban haze event caused by wheat straw burning*. Atmospheric Environment 40, 2473-2479.

Wang H., Shooter D., 2004. *Low molecular weight dicarboxylic acids in PM_{10} in a city with intensive solid fuel burning*. Chemosphere 56, 725-733.

Wang Z., Chen J., Yang P., Qiao X., Tian F., 2007. *Polycyclic aromatic hydrocarbons in Dalian soils: distribution and toxicity assessment*. Journal of Environmental Monitoring 9, 199-204.

Ward T.J., Hamilton R.F., Dixon R.W., Paulsen M., Simpson C.D., 2006. *Characterization and evaluation of smoke tracers in PM: results from the 2003 Montana wildfire season*. Atmospheric Environment 40, 7005–7017.

Wingfors H., Sjödin Å., Haglund P., Brorström-Lundén E., 2001. *Characterisation and determination of profiles of polycyclic aromatic hydrocarbons in a traffic tunnel in Gothenburg, Sweden*. Atmospheric Environment 35, 6361-6369.

Wold L.E., Simkhovich B.Z., Kleinman M.T.,Nordlie M.A., Dow J.S., Sioutas C., Kloner R.A., 2006. *In vivo and in vitro models to test the hypothesis of particle-induced effects on cardiac function and arrhythmias*. Cardiovascular Toxicology 6, 69-78.

Xie M., Wang G., Hu S., Han Q., Xu Y., Gao Z., 2009. *Aliphatic alkanes and polycyclic aromatic hydrocarbons in atmospheric PM $_{10}$ aerosols from Baoji, China: Implications for coal burning*. Atmospheric Research 93, 840-848.

Xu J., Jordan R.B., 1990. *Kinetics and Mechanism of the Reaction of Aqueous Copper(II) with Ascorbic Acid*. Inorganic Chemistry 29, 2933-2936.

Yang A., Jedynska A., Hellack B., Kooter I., Hoek G., Brunekreef B., Kuhlbusch T.A.J., Cassee F.R., Janssen N.A.H., 2014. *Measurement of the oxidative potential of PM2.5 and its constituents: the effect of extraction solvent and filter type*. Atmospheric Environment 83, 35-42.

Yang L., Ray M.B., Yu L.E., 2008. *Photooxidation of dicarboxylic acids – part I: effects of inorganic ions degradation of azelaic acid*. Atmospheric Environment 42, 856-867.

Yang L., Ray M.B., Yu L.E., 2008. *Photooxidation of dicarboxylic acids – part II: Kinetics, intermediates and field observations*. Atmospheric Environment 42, 868-880.

Yao X., Fang M., Chan C.K., 2002. *Size distributions and formation of dicarboxylic acids in atmospheric particles*. Atmospheric Environment 36, 2099–2107.

Yassaa N., Meklati B.Y., Cecinato A., Marino F., 2001. *Particulate n-alkanes, n-alkanoic acids and polycyclic aromatic hydrocarbons in the atmosphere of Algiers City Area*. Atmospheric Environment 35, 1843-1851.

Yttri K.E., Dye C., Kiss G., 2007. *Ambient aerosol concentrations of sugars and sugar-alcohols at four different sites in Norway*. Atmospheric Chemistry and Physics 7, 4267-4279.

Ytti K.E., Schnelle-Kreis J., Maenhaut W., Abbaszade G., Alves C., Bjerke A., Bonnier N., Bossi R., Claeys M., Dye C., Evtyugina M., García-Gacio D., HillanmoR., Hoffer A., Hyder M., Iiuma Y., Jaffrezo J.L., Kasper-Giebl A., Kiss G., López-Mahia P.L., Pio C., Piot C., Ramirez-Santa-Cruz C., Sciare J., Teinilä K., Vermeylen R., Vicente A., Zimmermann R., 2015. *An intercomparison study of analytical methods used for quantification of levoglucosano in ambient aerosol filter samples*. Atmospheric Measurement Techniques 8, 125-147.

Yunker M.B., Macdonald R.W., Vingarzan R., Mitchell R.H., Goyette D., Sylvestre S., 2002. *PAHs in the Fraser River basin: a critical appraisal of PAH ratios as indicators of PAH source and composition*. Organic Geochemistry 33,489-515.

Zangrando R., Barbaro E., Zennaro P., Rossi S., Kehrwald N.M., Gabrieli J., Barbante C., Gambaro A., 2013. *Molecular Markers of Biomass Burning in Arctic Aerosols*. Environmental Science & Technology 47, 8565-8574.

Zhang Q., Worsnop D.R., Canagaratna M.R., Jimenez J.L., 2005. *Hydrocarbon-like and oxygenated organic aerosols in Pittsburgh: insights into sources and processes of organic aerosols*. Atmospheric Chemistry and Physics 5, 3289-3311.

Zhang Y.Y., Müller L., Winterhalter R., Moortgat G.K., Hoffmann T., Pöschl U., 2010. *Seasonal cycle and temperature dependence of pinene oxidation products, dicarboxylic acids and nitrophenols in fine and coarse air particulate matter*. Atmospheric Chemistry and Physics 10, 7859-7873.

Zhao R., Mungall E.L., Lee A.K.Y., Aljawhary D., Abbatt J.P.D., 2014. *Aqueous-phase photooxidation of levoglucosan – a mechanistic study using aerosol time-of-flight chemical ionization mass spectrometry (Aerosol ToF-CIMS)*. Atmospheric Chemistry and Physics 14, 9695-9706.

Zheng M., Cass G.R., Schauer J.J., Edgerton E.S., 2002. *Source apportionment of PM2.5 in the southeastern United States using solvent-extractable organic compounds as tracers. n-alkanes*. Environmental Science and Technology 36, 2361-2371.

Zielinski H., Mudway I.S., Bérubé K.A., Murphy S., Richards R., Kelly F.J. 1999. *Modeling the interactions of particulates with epithelial lining fluid antioxidants*. The American Journal of Physiology 277, L719-L726.
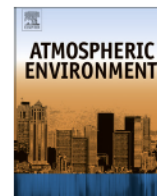
PUBLICATIONS

ELSEVIER LICENSE
TERMS AND CONDITIONS

Feb 07, 2016

This is an Agreement between Marco Visentin ("You") and Elsevier ("Elsevier"). It consists of your order details, the terms and conditions provided by Elsevier, and the payment terms and conditions.

All payments must be made in full to CCC. For payment instructions, please see information listed at the bottom of this form.

Supplier	Elsevier Limited The Boulevard,Langford Lane Kidlington,Oxford,OX5 1GB,UK
Registered Company Number	1982084
Customer name	Marco Visentin
Customer address	Via L. Borsari 46
	Ferrara, None 44121
License number	3803550610293
License date	Feb 07, 2016
Licensed content publisher	Elsevier
Licensed content publication	Atmospheric Environment
Licensed content title	Polar organic marker compounds in atmospheric aerosol in the Po Valley during the Supersito campaigns — Part 1: Low molecular weight carboxylic acids in cold seasons
Licensed content author	Maria Chiara Pietrogrande,Dimitri Bacco,Marco Visentin,Silvia Ferrari,Vanes Poluzzi
Licensed content date	April 2014
Licensed content volume number	86
Licensed content issue number	n/a
Number of pages	12
Start Page	164
End Page	175
Type of Use	reuse in a thesis/dissertation
Intended publisher of new work	other
Portion	full article
Format	both print and electronic
Are you the author of this Elsevier article?	Yes
Will you be translating?	No
Title of your thesis/dissertation	Chemical characterization of atmospheric aerosol for air quality evaluation in Emilia Romagna region
Expected completion date	Mar 2016
Estimated size (number of pages)	200
Elsevier VAT number	GB 494 6272 12
Price	0.00 EUR
VAT/Local Sales Tax	0.00 EUR / 0.00 GBP
Total	**0.00 EUR**
Terms and Conditions	

Polar organic marker compounds in atmospheric aerosol in the Po Valley during the Supersito campaigns — Part 1: Low molecular weight carboxylic acids in cold seasons

Maria Chiara Pietrogrande [a,*], Dimitri Bacco [a], Marco Visentin [a], Silvia Ferrari [b], Vanes Poluzzi [b]

[a] Department of Chemical and Pharmaceutical Sciences, University of Ferrara, Via Fossato di Mortara 17/19, I-44100 Ferrara, Italy
[b] Regional Agency of Prevention and Environment ARPA — Emilia-Romagna, Italy

HIGHLIGHTS

Dominant contributions of primary anthropogenic sources, such as traffic, domestic heating and biomass burning.
Minor contributions of in situ photo-chemical reactions.
Day-of-week trends of emission tracers indicate the main impact of vehicle traffic during fall.
Residential heating is predominant source in winter periods.
The urban and the rural background sites show homogeneous impact of the different sources.

ARTICLE INFO

ABSTRACT

In the framework of the "Supersito" project, three intensive experimental campaigns were conducted in the Po Valley (Northern Italy) in cold seasons, such as late autumn, pre-winter and deep-winter, over three years from 2011 to 2013. As a part of a study on polar marker compounds, including carboxylic acids, sugar derivatives and lignin phenols, the present study reports a detailed discussion on the atmospheric concentrations of 14 low molecular weight carboxylic acids, mainly dicarboxylic and oxo-hydroxy carboxylic acids, as relevant markers of primary and secondary organic aerosols.

$PM_{2.5}$ samples were collected in two monitoring sites, representing urban and rural background stations. The total quantities of carboxylic acids were 262, 167 and 249 ng m^{-3} at the urban site and 308, 115, 248 ng m^{-3} at the rural site in pre-winter, fall and deep-winter, respectively. These high concentrations can be explained by the large human emission sources in the urbanized region, combined with the stagnant atmospheric conditions during the cold seasons that accumulate the organic precursors and accelerate the secondary atmospheric reactions.

The distribution profiles of the investigated markers suggest the dominant contributions of primary anthropogenic sources, such as traffic, domestic heating and biomass burning. These results are confirmed by comparison with additional emission tracers, such as anhydro-saccharides for biomass burning and fatty acids originated from different anthropogenic sources. In addition, some secondary constituents were detected in both sites, as produced by in situ photo-chemical reactions from both biogenic (e.g. pinonic acid) and anthropogenic precursors (e.g. phthalic and adipic acids).

The impact of different sources from human activities was elucidated by investigating the week pattern of carboxylic and fatty acid concentrations. The weekly trends of analytes during the warmer campaign (fall 2012; mean temperature: 12 °C) may be related to emissions from motor vehicle traffic and industrial activities. Otherwise, the random pattern of the markers suggests the prevalent contribution of primary emissions from residential heating in the colder deep-winter (mean temperature: 5 °C).

© 2013 Elsevier Ltd. All rights reserved.

* Corresponding author.
  E-mail address: mpc@unife.it (M.C. Pietrogrande).

1. Introduction

Po Valley, which extends over a great part of Northern Italy and is the most industrialized and populated region of Italy, is recognized as one of the most worrying air pollution situations in Europe, where high air pollution may cause serious risks for human health. There is evidence that low wind speeds and stable atmospheric stratification are meteorological factors leading to air pollution episodes (Balducci and Cecinato, 2010; Bigi and Ghermandi, 2011; Squizzato et al., 2012; Larsen et al., 2012). This is particularly true in cold seasons, when enhanced anthropogenic emissions from residential heating combined with stagnant atmospheric conditions result into the accumulation of pollution near the source locations (Viana et al., 2008; Carbone et al., 2010; Perrone et al., 2013).

Under this complicated meteorological condition in Po Valley, it is worthy of interest to improve knowledge on chemical characteristics and sources of atmosphere particulate material and its effects on human health, in order to decide effective abatement strategies. This is one of the aims of the "Supersito" project, which was supported and financed by Emilia-Romagna Region and Regional Agency of Prevention and Environment (ARPA-ER), for a detailed study of some chemical, physical and toxicological parameters in the atmosphere of Emilia-Romagna Region and their assessments by epidemiological, environmental and health models (www.supersito-er.it).

In the framework of this project, this study is focused on the chemical characterization of polar organic compounds, including carboxylic acids (CAs), sugar derivatives and lignin phenols. Such polar species are emitted directly into the atmosphere by a multiplicity of sources including power plants, vehicular circulation, biomass burning and meat cooking operations (Ho et al., 2006; Rogge et al., 2006; Oliveira et al., 2007; Hsieh et al., 2008; Bi et al., 2008; Wang et al., 2011; Huang et al., 2012; Giannoni et al., 2012). They are also secondarily produced by photochemical reactions with volatile precursors including anthropogenic and biogenic hydrocarbons (Fisseha et al., 2004; Wang et al., 2006; Oliveira et al., 2007; Bi et al., 2008; Huang et al., 2012). Although constituting only a small fraction of the total aerosol mass, these highly water-soluble compounds may significantly enhance the hygroscopicity of aerosol particles and thereby influence cloud microphysical processes that affect the nucleation of clouds, acid precipitation and atmosphere optical properties, contributing to global climate change (Ruiz-Jimenez et al., 2012; Gierlus et al., 2012). In addition, studying polar compounds in atmospheric particulate matter (PM) may give additional insight into the effects of air pollution, since the increased polarity is thought to amplify the uptake and retention of fine particles within the respiratory system leading to undesirable effects (Perrone et al., 2013).

As the first part of this study, this paper presents a detailed discussion on atmospheric concentrations of 14 low molecular weight acids, mainly dicarboxylic (DCA) and oxo-hydroxy carboxylic acids (oxCA), that constitute a substantial fraction of polar organics. They have been proposed as useful markers to differentiate between primary emissions — including biomass burning, industrial activity and direct vehicle emissions — and secondary organic aerosol (SOA) production through photo-chemical reactions (Fisseha et al., 2004; Wang et al., 2006; Ho et al., 2006; Hsieh et al., 2008; Bi et al., 2008; Yang et al., 2008; Wang et al., 2011; Hyder et al., 2012). The study also includes characterization of anhydrosaccharides as specific tracers of biomass burning and n-fatty acids emitted from different anthropogenic sources (Rogge et al., 2006; Oliveira et al., 2007; Ho et al., 2011; Wang et al., 2011; Giannoni et al., 2012; Yang et al., 2013).

The atmospheric $PM_{2.5}$ samples were collected in two locations representing an urban (Main Site, MS) and a rural background (San Pietro Capofiume, SP) sites in the Po Valley. Three intensive field campaigns were carried out in cold seasons in subsequent years from 2011 to 2013. The obtained results were related to meteorological parameters in order to give insight into the emission sources and fate of organic components in atmospheric aerosol in the heavy polluted cold seasons.

2. Materials and methods

2.1. Aerosol sampling

The urban background site MS is located in the city of Bologna which is the most populous city in the region (~400,000 inhabitants) characterized by significant agricultural and industrial activities and the presence of main arterial roads. The field station of San Pietro Capofiume is a rural background site located about 30 km northeast from the city of Bologna (map shown in Fig. 1).

The present study concerns three sampling intensive campaigns in cold seasons to be representative of different meteorological scenarios in cold periods: late autumn, from 23rd October up to 10th November 2012, pre-winter, from 15th November up to 7th December 2011, and deep-winter from 30th January up to 19th February 2013.

Meteorological data were collected at the meteorological stations of San Pietro Capofiume and Bologna by Hydro-Meteo-Climate Service of ARPA-ER. Mixing layer height at both sites was estimated using the pre-processor CALMET by ARPA Emilia-Romagna (Scire et al., 2000; Deserti et al., 2001).

The $PM_{2.5}$ samples were collected on a quartz fiber filter (4.5 cm diameter) with low volume automatic outdoor samplers (Skypost PM, TCRTECORA Instruments, Corsico, Milan, Italy) operating at a flow rate of 38.3 Lmin^{-1} for 24 h. After sampling, the procedure outlined in European Standard EN 12341 (CEN, 1998) was applied for equilibration and weighing.

2.2. Analytical procedure

The analytical procedure has been described elsewhere (Pietrogrande et al., 2013) and briefly summarized in the following. PM samples were extracted for 15 min in an ultrasonication bath with 15 mL of methanol:dichloromethane, 9:1 solvent mixture. Then the extracts were filtered using a teflon filter (25 mm, 0.45 μm, Supelco, Bellefonte, PA) to remove insoluble particles and then the filtrates were evaporated to dryness in a centrifugal vacuum concentrator (miVac Duo Concentrator, Genevac Ltd, Ipswich, UK). Prior to GC/MS analysis, the sample extracts were submitted to a silylation reaction for 70 min at 75 °C: 40 μL of N,O-bis-(trimethylsilyl)trifluoroacetamide (BSTFA) containing 1% of trimethylchlorosilane (TMCS) and 15 μL of pyridine were added to 5 μL of Internal Standard (the deuterated $C_{12}H_{26}$, injected quantity: 127.5 ng) and 40 μL of iso-octane.

The GC/MS system was a Scientific Focus-GC (Thermo-Fisher Scientific, Milan, Italy) coupled to PolarisQ Ion Trap Mass Spectrometer (Thermo-Fisher Scientific, Milan, Italy). The column used was a DB-5MS column ($L = 30$ m, I.D. = 0.25 mm, df = 0.25 μm film thickness; J&W Scientific, Rancho Cordova, CA, USA). High purity helium was the carrier gas with a velocity of 1.5 ml min^{-1}. Temperature program conditions were optimized for analysis of a wide range of target polar organic compounds, including low molecular weight carboxylic acids: an initial temperature of 70 °C was raised to 125 °C at 2.5 °C min^{-1}, followed by an isothermal hold for 7 min; after that, the temperature was increased to 145 °C at 2 °C min^{-1}, an isothermal hold for 5 min; then further raised to 170 °C at
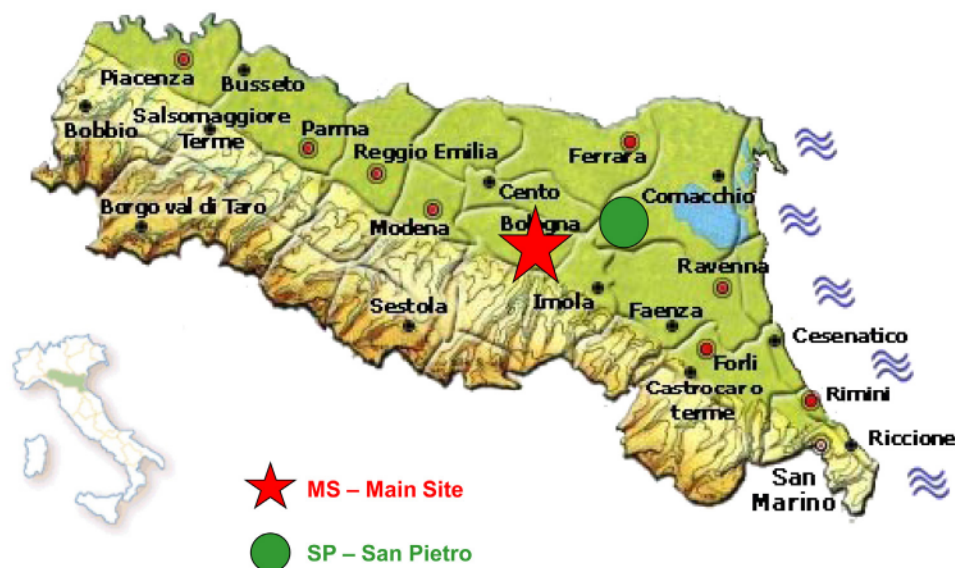
Fig. 1. Location of the sampling sites. Site symbols: MS: main site; SP: San Pietro.

2.5 °C min^{-1} and finally led to 300 °C at 7 °C min^{-1}; this temperature was maintained for 1 min. All samples were injected in splitless mode (splitless time: 60 s); the injector temperature was 250 °C.

The mass spectrometer operated in Electron Ionization mode (positive ion, 70 eV). Ion source and transfer-line temperatures were 250 °C and 280 °C, respectively. The mass spectra were acquired in full scan mode from 50 to 650 m/z in 0.58 s. For identification and quantification of the target analytes, the SIM (selected-ion monitoring) chromatograms were extracted from the acquired signal by selecting either the base peak ion or the most abundant characteristic fragments at $m/z = 147$ and $m/z = 149$ (Pietrogrande et al., 2010; Pietrogrande and Bacco, 2011). Chromatographic peaks of CAs were identified by comparison of the retention time and mass spectrum with standard compounds, literature and library data; quantitative analysis was performed using calibration curves determined using authentic standards.

Quality assurance and quality control were assessed by precision, accuracy and sensitivity for polar organic tracers. The procedure provides low detection limits (0.3–1 ng m^{-3}) and good reproducibility (RSD%   7%) suitable for applicability in environmental monitoring. Good procedure recoveries ranging from 78 to 104% were evaluated on PM samples spiked with surrogate standards (Pietrogrande et al., 2013).

3. Results and discussion

Six linear dicarboxylic acids with 3–9 carbon atoms as well as maleic and phthalic acids were analyzed in all the campaigns. In addition, four hydroxy carboxylic acids, namely glycolic, malic, and 3- and 4-hydroxy benzoic acids, and two oxo carboxylic acids, pinonic and 2-ketoglutaric acids, were investigated in this study. They have been found in the atmospheric aerosol as intermediate products of secondary photo-oxidation reactions (Kawamura and Yasui, 2005; Lee et at., 2006; Yang et al., 2008). It must be underlined that oxalic acid is not detectable with the used analytical procedure, and malonic acid may be somewhat underestimated because of the volatility of silyl derivatives (Pietrogrande et al., 2010; Pietrogrande and Bacco, 2011).

The results obtained for each campaign in the investigated sites are summarized in Table 1, which reports the observed concentration ranges, mean values and standard deviations (the term n.d.

indicates that less than 10% of the measured values are above the detection limit). In general, the data obtained in pre-winter 2011 and deep-winter 2013 show similar levels in comparison with results of the campaign in late fall 2012.

The total sum of acid concentrations (total carboxylic acid concentration, TCA) was computed from the values of each analyzed acid: the values (mean values   SD in Table 1 and Fig. 2) ranged from 167 ng m^{-3} in fall to 262 ng m^{-3} in pre-winter in MS site and from 115 ng m^{-3} in fall to 308 ng m^{-3} in pre-winter 2011 in rural SP site. These results were very similar with those found in Lombardia region (Milan and Oasi Bine) and comparable with those reported in atmospheric aerosols collected from different cities in the world (Rome, Algiers, Beijing and Helsinki) but significantly lower than those from other megacities (Tokio, Nanjing and Hong Kong), as listed in the literature overview reported in Table 2.

Another peculiarity of the obtained data is the close similarity between the PM composition of the urban and rural sites, reflecting the regional nature of the emission sources and photochemical processes and their similar impact across the airshed (see comparison between two sites in Fig. 2).

In the investigated cold seasons, PM$_{2.5}$ levels were close to 40 μg m^{-3} up to a maximum of 59 μg m^{-3} for urban site in winter 2011 (Table 1). These high values are consistent with other data found in the Po Valley in winter, because of the enhanced man-made emissions, mainly road traffic exhausts and domestic heating, combined with stagnant atmospheric conditions characterized by low vertical mixing and cold temperatures (Bigi and Ghermandi, 2011; Perrone et al., 2012; Larsen et al., 2012).

3.1. Molecular distributions of aliphatic/aromatic dicarboxylic acid

The concentration values of the target acids obtained in the 3 campaigns (Table 1) were compared with the levels found in urban and rural sites in the world (Table 3 reports an overview of literature data of selected CAs).

A detailed investigation of CA distribution profile may provide information on the origin and fate of organics in the atmosphere. In general, chain length distributions of dicarboxylic acids show a decrease of the concentration of the individual species with the increase in carbon chain length, as reported in most cities (Kawamura and Yasui, 2005; Ho et al., 2006; Ladji et al., 2009;

Table 1
Concentration values of each carboxylic acid measured in the three campaigns. The observed concentration ranges (ng m^{-3}), mean values and standard deviations are reported for the two sampling sites. Meteorological parameters were measured for each campaign in the investigated sites. The term 'n.d.' indicates the analytes showing less than 10% of the measured data values above the detection limit.

Pre-winter 2011	Main site				San Pietro			
Acids	Minimum (ng m^{-3})	Maximum (ng m^{-3})	Average (ng m^{-3})	S.D. (ng m^{-3})	Minimum (ng m^{-3})	Maximum (ng m^{-3})	Average (ng m^{-3})	S.D. (ng m^{-3})
Malonic	6.2	77.4	21.7	24.1	12.4	130.6	41.5	37.5
Succinic	60.9	162.5	112.1	36.6	44.1	218.1	110.7	44.1
Glutaric	8.8	31.6	18.4	7.2	6.3	30.3	17.4	7.8
Adipic	n.d.	n.d.	n.d.	n.d.	n.d.	n.d.	n.d.	n.d.
Pimelic	n.d.	n.d.	n.d.	n.d.	n.d.	n.d.	n.d.	n.d.
Azelaic	n.d.	n.d.	n.d.	n.d.	n.d.	n.d.	n.d.	n.d.
Maleic	9.6	107.3	30.3	27.4	10.1	661.5	90.8	182.4
Malic	5.4	92.5	40.9	24.2	6.4	63.3	33.8	17.3
Phthalic	2.6	4.6	3.3	0.5	2.6	5.1	4.3	0.7
Glycolic	7.6	42.6	20.1	8.3	5.9	37.0	19.0	8.1
2-ketoglutaric	0.7	15.4	8.7	3.4	3.4	13.3	8.9	3.2
3-OH benzoic	3.5	13.4	7.5	2.1	3.1	10.3	7.5	2.1
4-OH benzoic	4.3	25.7	9.7	4.8	4.3	12.1	7.6	2.8
Pinonic	n.d.	n.d.	n.d.	n.d.	n.d.	n.d.	n.d.	n.d.
Daily TCA	126.8	525.6	262.0	111.2	84.1	1010.0	308.3	220.2
Daily ToxCA	20.4	184.0	84.4	41.4	16.2	124.8	70.2	31.7
Burning Sugars	291	2807	1216	553	525	1833	1064	443
PM$_{2.5}$ (µg m^{-3})	33.1	91.3	59.0	17.4	22.2	84.9	46.2	18.0
C$_3$/C$_4$	0.07	0.45	0.17	0.14	0.15	0.74	0.33	0.24
ToxA/TCA %	12.2	36.6	31.7	6.0	7.8	37.1	25.8	8.4
Meteorological parameters								
Mixing height (m)	95	559	230	78	51	520	169	48
Daily solar radiation (W m^{-2})	16.4	88.9	61.0	23.0	17.5	117.5	64.7	30.2
Daily temperature (°C)	3.9	10.1	6.5	2.0	0.4	9.2	4.0	1.8
Precipitations (mm)			0.8				5.2	

Fall 2012	Main site				San Pietro			
ACIDS	Minimum (ng m^{-3})	Maximum (ng m^{-3})	Average (ng m^{-3})	S.D. (ng m^{-3})	Minimum (ng m^{-3})	Maximum (ng m^{-3})	Average (ng m^{-3})	S.D. (ng m^{-3})
Malonic	2.4	100.8	29.7	33.1	4.6	65.0	33.3	25.7
Succinic	5.7	49.9	26.8	14.3	6.2	49.8	22.2	12.6
Glutaric	3.9	35.9	17.1	9.0	0.5	13.2	5.9	3.9
Adipic	1.3	7.1	3.5	1.9	1.2	7.3	3.0	1.7
Pimelic	1.4	7.9	3.2	1.6	0.9	4.0	2.0	1.1
Azelaic	2.9	25.3	10.0	7.1	0.4	22.4	8.3	5.9
Maleic	n.d.	n.d.	n.d.	n.d.	n.d.	n.d.	n.d.	n.d.
Malic	3.4	66.9	25.7	22.5	5.2	56.1	22.1	17.1
Phthalic	1.7	11.4	5.3	3.0	1.0	5.0	3.2	1.2
Glycolic	3.7	43.4	16.3	12.4	3.9	42.9	13.6	11.7
2-ketoglutaric	4.8	67.7	27.4	19.2	5.9	91.8	22.3	22.4
3-OH benzoic	0.4	2.9	2.0	0.6	0.1	2.0	1.9	0.5
4-OH benzoic	0.4	5.3	2.2	1.3	0.6	3.1	2.2	0.6
Pinonic	1.3	5.1	2.6	0.9	2.5	3.4	2.8	0.4
Daily TCA	35.5	330.3	167.4	109.6	29.8	316.3	114.8	89.5
Daily ToxCA	15.1	147.4	74.8	50.4	16.3	165.7	61.1	47.8
Burning Sugars	69	676	382	199	96	550	304	153
Fatty acids	102	290	200	52	69	221	150	54
PM$_{2.5}$ (µg m^{-3})	6.2	70.7	31.0	17.2	10.2	64.4	27.7	16.2
ToxCA/TCA %	36.4	50.4	44.0	4.7	44.5	60.9	53.1	5.3
C$_3$/C$_4$	0.13	2.87	0.92	0.78	0.32	1.75	0.95	0.62
Phthalic/Adipic	0.93	3.12	1.58	0.53	0.64	2.07	1.07	0.44
C$_6$/C$_9$	0.20	0.78	0.40	0.15	0.26	3.04	0.65	0.73
Phthalic/C$_9$	0.93	3.13	1.58	0.53	0.22	2.27	0.61	0.54
Meteorological parameters								
Mixing height (m)	99	857	365	153	50	817	257	96
Daily solar radiation (W m^{-2})	5.3	121.0	70.6	37.7	5.7	148.5	85.4	46.0
Daily temperature (°C)	10.0	15.9	12.6	2.7	6.8	16.2	11.1	2.5
Precipitations (mm)			65.0				75.0	

Deep-winter 2013	Main site				San Pietro			
ACIDS	Minimum (ng m^{-3})	Maximum (ng m^{-3})	Average (ng m^{-3})	S.D. (ng m^{-3})	Minimum (ng m^{-3})	Maximum (ng m^{-3})	Average (ng m^{-3})	S.D. (ng m^{-3})
Malonic	4.3	63.6	26.8	21.1	2.9	92.0	32.7	25.7
Succinic	13.4	49.4	32.3	12.6	11.1	61.2	35.1	14.5
Glutaric	4.7	35.2	19.5	12.8	2.5	52.6	24.3	17.4
Adipic	0.9	9.6	4.7	1.9	1.7	8.5	4.6	1.8
Pimelic	3.3	4.7	4.1	0.5	1.4	7.6	5.3	2.3

Table 1 (*continued*)

Deep-winter 2013	Main site				San Pietro			
ACIDS	Minimum (ng m^{-3})	Maximum (ng m^{-3})	Average (ng m^{-3})	S.D. (ng m^{-3})	Minimum (ng m^{-3})	Maximum (ng m^{-3})	Average (ng m^{-3})	S.D. (ng m^{-3})
Azelaic	10.5	34.1	17.2	7.0	5.7	29.0	16.0	6.9
Maleic	14.3	158.6	67.8	37.8	8.4	134.2	57.4	39.3
Malic	3.9	38.8	20.3	11.5	2.9	46.2	22.5	15.0
Phthalic	2.3	28.5	11.8	6.7	2.3	35.5	11.8	8.5
Glycolic	5.9	32.0	14.2	6.5	4.3	34.4	16.9	9.5
2-ketoglutaric	11.1	97.0	46.8	28.4	2.3	137.8	45.4	33.7
3-OH benzoic	0.5	3.9	2.4	0.8	0.1	5.1	2.9	1.0
4-OH benzoic	0.9	5.3	3.1	1.4	0.6	7.5	3.7	1.7
Pinonic	n.d.	n.d.	n.d.	n.d.	2.9	6.4	3.9	1.2
Daily TCA	51.6	458.3	249.3	122.3	44.0	527.5	247.9	139.2
Daily ToxCA	15.5	149.0	83.4	43.0	15.6	161.2	87.7	55.7
Burning Sugars	169	598	355	133	149	637	346	151
Fatty acids	141	384	245	68	170	362	249	53
PM$_{2.5}$ (µg m^{-3})	12.5	71.7	32.8	13.7	14.7	86.5	34.6	19.4
ToxA/TCA %	12.7	54.9	34.4	9.9	18.7	50.2	34.1	9.2
C$_3$/C$_4$	0.14	1.99	0.81	0.51	0.15	2.30	0.87	0.64
Phthalic/Adipic	1.09	5.39	2.89	1.25	1.01	5.60	2.32	1.19
C$_6$/C$_9$	0.12	0.43	0.29	0.09	0.20	0.78	0.38	0.17
Phthalic/C$_9$	0.32	1.90	0.87	0.50	0.37	2.13	0.96	0.62
Meteorological parameters								
Mixing height (m)	102	1085	413	99	51	943	314	120
Daily solar radiation (W m^{-2})	13.7	130.0	80.8	34.5	9.2	160.3	92.0	48.4
Daily temperature (°C)	1.4	6.9	3.9	1.6	−0.8	7.5	2.6	1.0
Precipitations (mm)			48.6				40.6	

Hyder et al., 2012). Accordingly, the highest concentrations were observed for C$_3$–C$_4$ dicarboxylic acids with the most abundant succinic (32–112 ng m^{-3}), maleic (30–91 ng m^{-3}) and malic acids (20–41 ng m^{-3}) in winter 2011 and 2013 campaigns. In fall 2012 the most abundant species was malonic acid (30–33 ng m^{-3}), followed by 2-ketoglutaric, succinic and malic acids (each 22–27 ng m^{-3}).

3.2. Source attribution to the acidic contents of organic aerosol

To give insight into the origin of CAs, the correlation among carboxylic acids has been studied since strong correlation coefficients among these compounds may suggest a similar source or involvement in the same photo-oxidation processes (Ho et al., 2011; Hyder et al., 2012).

Table 4 shows a comprehensive picture of the correlation coefficients among the studied CAs (the study included only the analytes showing at least 50% of the measured values above the detection limit). If we look at the correlations among the CA concentrations, it is clear that most of the values obtained in fall 2012 (39 pairs) are nicely correlated ($r > 0.7$, values in bold), suggesting that the concentrations of these species are mainly controlled by the same atmospheric processes in this period (Table 4). Otherwise, only a limited number of acid pairs measured in 2011 and 2013 winter periods (14 and 12 pairs, respectively, Table 4a, c) show significant correlations ($r > 0.7$, values in bold), which strongly suggested the combined contribution of primary emissions and secondary reactions.

As a general trend, in the three campaigns, among the acids detected, succinic acid was the most correlated with the others, since it showed significant correlations with glycolic, malic, glutaric, adipic and phthalic acids: this result was consistent with the finding that succinic acid is originated from different sources, like the direct emissions from solid fuel burning (at least from wood burning) and the oxidation of unsaturated fatty acids, emitted from both anthropogenic and biogenic sources (Wang et al., 2006; Lee et al., 2006; Oliveira et al., 2007; Bi et al., 2008; Hsieh et al., 2008).

The limited correlation between succinic (C4) and malonic (C3) acids observed in all the campaigns ($r = 0.6–0.7$) suggested that malonic acid was only in part produced from oxidation atmospheric processes, with succinic as a precursor. These results were confirmed by computing the diagnostic ratio C3/C4 as indicator of photochemical production of dicarboxylic acids in the atmosphere: values ranging from 0.2 to 0.9 were obtained (Table 1). In comparison, the C3/C4 ratio was 0.35 for fresh emissions in Los Angeles, approximately 1.0 for urban Tokyo and 3.9 for the remote Pacific aerosol (Kawamura and Yasui, 2005; Li et al., 2006; Oliveira et al., 2007; Wang et al., 2011). This suggested that primary emissions largely control the atmospheric concentrations of diacids in cold seasons, yielding relatively fresh PM.

Significant amounts of pimelic (C7) and azelaic (C9) acids were detected in autumn 2012 (mean 3 and 9 ng m^{-3}, respectively) and in winter 2013 (mean 4 and 17 ng m^{-3}, respectively). These acids are believed to be produced from photo-oxidation of unsaturated carboxylic acids, such as oleic and linoleic acids having unsaturation at carbon 9 position (Ho et al., 2011; Hyder et al., 2012). The C7 and C9 concentrations are very nicely correlated each other, with $r \approx 0.84$, which strongly suggests the common involvement in the same photo-oxidation processes of biogenic precursors. In fact, pimelic is produced either directly from the same sources as those of azelaic acid or by further oxidation of azelaic acid down to lower carbon numbered dicarboxylic acids (Ho et al., 2011; Hyder et al., 2012). The presence of these acids is consistent with the emission of biogenic unsaturated fatty acids from the vegetation activity, although it is limited in the cold seasons. This hypothesis is confirmed by the presence of significant amount of pinonic acid in this period (≈ 3 ng m^{-3}) since this oxo carboxylic acid is one of the major products of the ozonolysis or OH-initiated oxidation of biogenic volatile organic compounds, like pinenes (Hyder et al., 2012; Ruiz-Jimenez et al., 2012).

Phthalic acid has been proposed as a surrogate for the contribution of SOA to an environmental sample, since it mainly derives from the oxidation of naphthalene and other polycyclic aromatic hydrocarbons or phthalates. In minor quantities, it may also have origin from primary sources like biomass burning or vehicle exhaust (Oliveira et al., 2007; Ho et al., 2011). If we look at its correlation with aliphatic dicarboxylic acids, we find a different
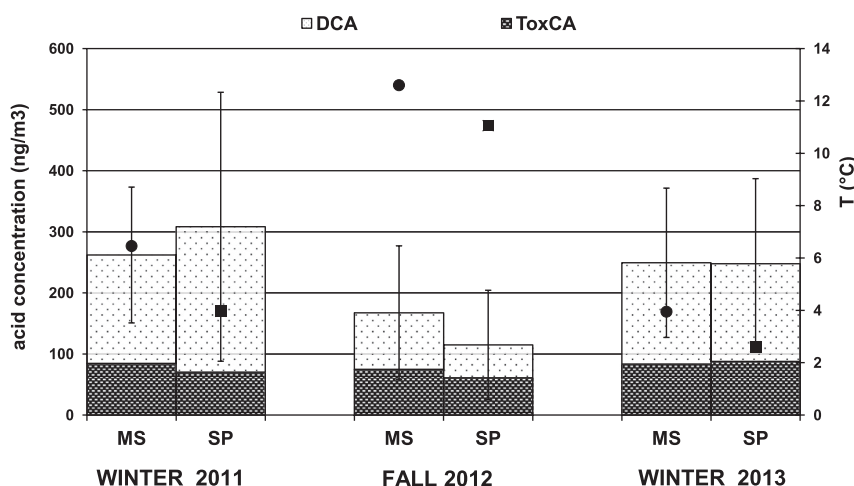
Fig. 2. Seasonal evolution of concentrations of dicarboxylic (empty bars) and oxo-hydroxy carboxylic acids (full bars) in monitoring campaigns: effect of the daily mean temperature, associated with the right axis (°C). A bar indicates 1 standard error.

pattern in winter campaigns in comparison with fall. In fall 2012 phthalic acid shows a good correlation with all C4–C9 dicarboxylic acids ($r \approx 0.8$), which suggests that it is mainly originated by the photo-oxidation of anthropogenic precursors. In winter phthalic acid is well correlated with the succinic acid ($r = 0.76–0.78$) but very poorly with other C6–C9 DCAs ($r < 0.6$), which is consistent with the concomitant contribution of primary emissions combined

Table 2
Total concentration values of carboxylic acids in atmospheric aerosols measured in different locations during autumn and winter (average concentrations, ng m^{-3}): comparison among literature data and this work.

Site	Total acids (ng m^{-3})	Season	References
Montelibretti (Italy), semi-rural	111	Winter	Balducci and Cecinato (2010)
Roma (Italy), urban	115	Winter	
Alpe san Colombano (Italy), remote	16	Winter	Perrone et al. (2012)
Oasi Bine (Italy), rural	152	Winter	
Milan (Italy), urban	240	Winter	
Melpitz (Germany), rural	34	Summer/ Autumn	Van Pinxteren and Herrman, 2007
Philadelphia (USA), urban	14	Winter	Li et al. (2006)
	22	Autumn	
Beijing (China), urban	42	Autumn	Huang et al. (2006)
	16	Winter	
Algiers (Algeria), urban	118	Autumn	Ladji et al. (2009)
	193	Winter	
Algiers (Algeria), suburban	63	Autumn	
	93		
Tokio (Japan), urban	438	Winter	Kawamura and Yasui (2005)
Beijing (China), urban	269	Autumn	Huang et al. (2005)
	231	Winter	
Hong Kong, urban	858	Winter	Ho et al. (2006)
Nanjing (China), urban	506	Autumn	Wang et al. (2011)
Shenzhen (China), urban	35	Autumn	Huang et al. (2012)
	31	Winter	
Vavihill (Sweden), background	33	One year	Hyder et al. (2012)
Hong Kong, urban	644	Winter	Ho et al. (2011)
Hong Kong, rural	656	Winter	
Guangzhou (China), urban	384	Winter	
Zhaoqing (China), semirural	490	Winter	
Bologna (Italy), urban	167	Autumn	This work
	266	Winter	
San Pietro Capofiume (Italy), rural	115	Autumn	
	278	Winter	

with photochemical processes in these colder seasons. These conclusions are also supported by the increase in phthalic acid quantities from fall and pre-winter (≈ 4 ng m^{-3}, similar to Toronto or Ljubljana, Table 3) to deep-winter 2013 (≈ 12 ng m^{-3}). Accordingly, the ratio of phthalic acid to adipic acid increases from fall (≈ 1.3) to deep-winter (≈ 2.5), which may be due to enhanced primary emissions of phthalic acid from motor vehicles and domestic heating using fossil fuels (Wang et al., 2006; Hyder et al., 2012).

As phthalic and adipic acids are produced by the atmospheric oxidation of anthropogenic hydrocarbons, their ratios to azelaic have been proposed as indicators of the impact of anthropogenic and biogenic precursors to SOA production (Wang et al., 2006). The phthalic/C9 and C6/C9 ratios were found to be lower to unity in either 2012 or 2013 campaigns: mean values were 0.6–1.6 and 0.3–0.6, respectively (Table 1). This result suggests that the photo-oxidation of anthropogenic precursors largely control the atmospheric reactions in cold seasons, that is consistent with the limited vegetation activity in wintertime (Wang et al., 2006; Li, et al., 2006; Oliveira et al., 2007; Huang et al., 2012).

Among the oxo and hydroxy acids, malic acid was found the dominant marker (41, 26 and 20 ng m^{-3} in pre-winter, fall and deep-winter, respectively in MS), followed by 2-ketoglutaric (9, 27 and 47 ng m^{-3} in pre-winter, fall and deep-winter, respectively in MS). The measured levels were in the range of concentrations found in suburban and urban sites reported elsewhere (Table 3). In particular, in addition to succinic acid, malic acid has been found as the most abundant C4 diacid during air pollution episodes (Hsieh et al., 2008; Van Drooge et al., 2012). In the three campaigns, the concentrations of malic and succinic acids were well correlated ($r \approx 0.8$, Table 4), indicating their involvement in common photochemical reactions. In fact, because of the similarity between their molecular structures, malic acid was thought to be produced by the hydroxylation reaction of succinic acid in the atmosphere (Kawamura and Yasui, 2005). Malonic acid is strongly correlated with malic acid only in the warmer period; suggesting that the higher temperature facilitates the conversion of oxidized acids into smaller dicarboxylic acids.

3.3. Relationship between carboxylic acids and meteorological conditions

In order to explain the trend of the obtained results, they were related to the weather conditions during the three campaigns,

Table 3
Concentration values of selected carboxylic acids in atmospheric aerosols measured in different locations during autumn and winter (average concentrations, ng m^{-3}): comparison among literature data and this work.

Acid	Site	Range (ng m^{-3})	Average (ng m^{-3})	Season	
Malonic	Tokio (Japan), urban	18–88	40	Winter	Kawamura and Yasui (2005)
	Toronto (Canada), urban	1–51	9	Winter	Dabek-Zlotorzynska (2005)
	Philadelphia (USA), urban		1.2	Winter	Li et al. (2006)
			0.7	Autumn	
	Tokio (Japan), urban	6–190	270	One year	Kawamura et al. (1993)
	Hong Kong, urban	10–145	68	One year	Ho et al. (2006)
			89	Winter	
	Ljubljana (Slovenia), semi rural	5.9–19	12	Winter	Kitanovski et al. (2011)
	Beijing (China), urban		34	Autumn	Huang et al. (2005)
			28	Winter	
	Bologna (Italy), urban	2.4–100.8	29.7	Autumn	This work
		4.3–77.4	24.2	Winter	
	San Pietro Capofiume (Italy), rural	4.6–65.0	33.3	Autumn	
		2.9–130.6	37.1	Winter	
Succinic	Tokio (Japan), urban	22–79	73	Winter	Kawamura and Yasui (2005)
	Toronto (Canada), urban	1–46	12	Winter	Dabek-Zlotorzynska (2005)
	Philadelphia (USA), urban		4.4	Winter	Li et al. (2006)
			7.7	Autumn	
	Taiwan, suburban		77	Autumn	Hsieh et al. (2008)
	Hong Kong, urban	13–121	52	One year	Ho et al. (2006)
			72	Winter	
	Nanjing (China), urban		87	Autumn	Wang et al. (2011)
	Ljubljana (Slovenia), semi rural	4.8–12	10	Winter	Kitanovski et al. (2011)
	Beijing (China), urban		40	Autumn	Huang et al. (2005)
			24	Winter	
	Algiers (Algeria), urban		11	Autumn	Ladji et al. (2009)
			113	Winter	
	Algiers (Algeria), suburban		123	Autumn	
			68	Winter	
	Bologna (Italy), urban	5.7–49.9	26.8	Autumn	This work
		13.4–162.5	72.2	Winter	
	San Pietro Capofiume (Italy), rural	6.2–49.8	22.2	Autumn	
		11.1–218.1	72.9	Winter	
Glutaric	Tokio (Japan), urban	9–26	18	Winter	Kawamura and Yasui (2005)
	Toronto (Canada), urban	2–9	4	Winter	Dabek-Zlotorzynska (2005)
	Philadelphia (USA), urban		1.5	Winter	Li et al. (2006)
			1.6	Autumn	
	Hong Kong, urban	2.8–28	13.5	One year	Ho et al. (2006)
			20	Winter	
	Nanjing (China), urban		40	Autumn	Wang et al. (2011)
	Ljubljana (Slovenia), semi rural	6–20	11.5	Winter	Kitanovski et al. (2011)
	Beijing (China), urban		9.2	Autumn	Huang et al. (2005)
			10	Winter	
	Algiers (Algeria), urban		3.9	Autumn	Ladji et al. (2009)
			9	Winter	
	Algiers (Algeria), suburban		12	Autumn	
			92	Winter	
	Bologna (Italy), urban	3.9–35.9	17.1	Autumn	This work
		4.7–35.2	18.9	Winter	
	San Pietro Capofiume (Italy), rural	0.5–13.2	5.9	Autumn	
		2.5–52.6	10.8	Winter	
Adipic	Tokio (Japan), urban	8–23	14	Winter	Kawamura and Yasui (2005)
	Toronto (Canada), urban	1–33	9	Winter	Dabek-Zlotorzynska (2005)
	Philadelphia (USA), urban		0.9	Winter	Li et al. (2006)
			1.7	Autumn	
	Hong Kong, urban	3.8–32	12	One year	Ho et al. (2006)
			11	Winter	
	Berlin (Germany), urban		1.7	One year	Wagener et al. (2012)
	Ljubljana (Slovenia), semi rural	3.1–9.2	5.8	Winter	Kitanovski et al. (2011)
	Algiers (Algeria), urban		13	Autumn	Ladji et al. (2009)
			80	Winter	
	Algiers (Algeria), suburban		48	Autumn	
			158	Winter	
	Bologna (Italy), urban	1.3–7.1	3.5	Autumn	This work
		0.9–9.6	4.7	Winter	
	San Pietro Capofiume (Italy), rural	1.2–7.3	3.0	Autumn	
		1.7–8.5	4.6	Winter	
Pimelic	Tokio (Japan), urban	2–14	10	Winter	Kawamura and Yasui (2005)

Table 3 (*continued*)

Acid	Site	Range (ng m^{-3})	Average (ng m^{-3})	Season	
	Hong Kong, urban	0.7–9.7	2.3	One year	Ho et al. (2006)
			3.2	Winter	
	Ljubljana (Slovenia), semi rural	1.3–5.1	2.9	Winter	Kitanovski et al. (2011)
	Bologna (Italy), urban	1.4–7.9	3.2	Autumn	This work
		3.3–4.7	4.1	Winter	
	San Pietro Capofiume (Italy), rural	0.9–4.0	2.0	Autumn	
		1.4–7.6	5.3	Winter	
Azelaic	Tokio (Japan), urban	11–36	21	Winter	Kawamura and Yasui (2005)
	Philadelphia (USA), urban		2.6	Winter	Li et al. (2006)
			5.1	Autumn	
	Hong Kong, urban	6–28	13	One year	Ho et al. (2006)
			17	Winter	
	Nanjing (China), urban		94	Autumn	Wang et al. (2011)
	Ljubljana (Slovenia), semi rural	1.6–9.4	4.4	Winter	Kitanovski et al. (2011)
	Bologna (Italy), urban	2.9–25.3	10.0	Autumn	This work
		10.5–34.1	17.2	Winter	
	San Pietro Capofiume (Italy), rural	0.4–22.4	8.3	Autumn	
		5.7–29.0	16.0	Winter	
Maleic	Tokio (Japan), urban	5–14	8	Winter	Kawamura and Yasui (2005)
	Taiwan, suburban		13	Autumn	Hsieh et al. (2008)
	Hong Kong, urban	2.2–37	16	One year	Ho et al. (2006)
			20	Winter	
	Nanjing (China), urban		2.2	Winter	Wang et al. (2011)
	Ljubljana (Slovenia), semi rural	2.9–6.9	4.6	Winter	Kitanovski et al. (2011)
	Bologna (Italy), urban	n.d.	n.d.	Autumn	This work
		9.6–158.6	49.0	Winter	
	San Pietro Capofiume (Italy), rural	n.d.	n.d.	Autumn	
		8.4–661.5	110.8	Winter	
Phthalic	Tokio (Japan), urban	13–36	24	Winter	Kawamura and Yasui (2005)
	Toronto (Canada), urban	2–9	3	Winter	Dabek-Zlotorzynska (2005)
	Hong Kong, urban	40–105	84	One year	Ho et al. (2006)
			78	Winter	
	Nanjing (China), urban		69	Winter	Wang et al. (2011)
	Ljubljana (Slovenia), semi rural	3.2–10	5.6	Winter	Kitanovski et al. (2011)
	Algiers (Algeria), urban		16	Autumn	Ladji et al. (2009)
			516	Winter	
	Algiers (Algeria), suburban		159	Autumn	Kitanovski et al. (2011)
			1020	Winter	
	Bologna (Italy), urban	1.7–11.4	5.3	Autumn	This work
		2.3–28.5	7.5	Winter	
	San Pietro Capofiume (Italy), rural	1.0–5.0	3.2	Autumn	
		2.6–34.4	8.0	Winter	
Malic	Tokio (Japan), urban	3–15	9	Winter	Kawamura and Yasui (2005)
	Toronto (Canada), urban	1–51	10	Winter	Dabek-Zlotorzynska (2005)
	Philadelphia (USA), urban		0.3	Winter	Li et al. (2006)
			1.1	Autumn	
	Taiwan, suburban		36	Autumn	Hsieh et al. (2008)
	Hong Kong, urban	1.1–10	4.5	One year	Ho et al. (2006)
			6.5	Winter	
	Berlin (Geramny), urban		50	One year	Wagener et al. (2012)
	Nanjing (China), urban		56	Autumn	Wang et al. (2011)
	Beijing (China), urban		20	Autumn	Huang et al. (2005)
			13	Winter	
	Bologna (Italy), urban	3.4–66.9	25.7	Autumn	This work
		3.9–92.5	30.6	Winter	
	San Pietro Capofiume (Italy), rural	5.6–52.1	26.1	Autumn	
		2.9–63.3	28.1	Winter	
Glycolic	Toronto (Canada), urban	1–10	4	Winter	Dabek-Zlotorzynska (2005)
	Ljubljana (Slovenia), semi rural	1.2–8.4	4.2	Winter	Kitanovski et al. (2011)
	Bologna (Italy), urban	3.7–43.2	16.3	Autumn	This work
		5.9–42.6	17.1	Winter	
	San Pietro Capofiume (Italy), rural	3.9–42.9	13.6	Autumn	
		4.3–37.0	17.9	Winter	
Pinonic	Berlin (Berlin), urban		9.4	One year	Wagener et al. (2012)
	Ljubljana (Slovenia), semi rural	1.6–2.4	1.9	Winter	Kitanovski et al. (2011)
	Toronto (Canada), urban		2.3	Autumn	Cheng et al. (2011)
			2.8	Winter	
	Bologna (Italy), urban	1.3–5.1	2.6	Autumn	This work
		n.d.	n.d.	Winter	
	San Pietro Capofiume (Italy), rural	2.5–3.4	2.8	Autumn	
		2.9–6.4	3.9	Winter	

Table 4

Correlation coefficients of carboxylic acid concentrations measured in the 3 monitoring campaigns at the MS site: pre-winter 2011, fall 2012 data and deep-winter 2013 data. Computations were performed only on the analytes showing at least 50% of the measured data above the detection limit. Bold values indicate significant correlations ($r > 0.7$).

Pre-winter 2011	Malonic	Succinic	Glutaric	Malic	Phthalic	Glycolic	Keto glutaric	3-OH benzoic	4-OH benzoic
Malonic	1	**0.734**	**0.772**	0.531	0.693	0.445	0.442	−0.006	0.001
Succinic		1	**0.946**	**0.747**	**0.780**	**0.721**	0.679	0.244	0.313
Glutaric			1	**0.853**	**0.724**	**0.790**	**0.725**	0.416	0.463
Malic				1	0.529	**0.812**	**0.852**	0.639	0.678
Phthalic					1	0.301	0.382	−0.086	−0.049
Glycolic						1	0.761	0.643	**0.732**
Ketoglutaric							1	0.675	0.648
3-OH benzoic								1	**0.913**
4-OH benzoic									1

Fall 2012	Malonic	Succinic	Glutaric	Adipic	Pimelic	Azelaic	Malic	Phthalic	Glycolic	Keto glutaric	3-OH benzoic	4-OH benzoic	Pinonic
Malonic	1	0.644	0.206	0.577	0.421	0.586	**0.900**	0.578	**0.898**	0.337	0.142	−0.038	0.058
Succinic		1	**0.729**	**0.916**	**0.825**	**0.859**	**0.856**	**0.764**	**0.860**	**0.877**	**0.722**	0.562	0.471
Glutaric			1	**0.748**	**0.854**	**0.730**	0.564	**0.812**	0.521	0.651	**0.808**	**0.794**	0.648
Adipic				1	**0.840**	**0.915**	**0.859**	0.758	**0.834**	**0.790**	**0.855**	0.662	0.647
Pimelic					1	**0.839**	**0.726**	**0.824**	0.699	**0.736**	**0.818**	**0.751**	0.677
Azelaic						1	**0.805**	**0.857**	**0.794**	**0.715**	**0.814**	0.650	0.587
Malic							1	**0.734**	**0.961**	0.652	0.600	0.403	0.418
Phthalic								1	0.689	0.599	0.661	0.595	0.507
Glycolic									1	0.641	0.545	0.363	0.343
Ketoglutaric										1	0.625	0.474	0.537
3OH benzoic											1	**0.863**	0.686
4OH benzoic												1	0.603
Pinonic													1

Deep-winter 2013	Malonic	Succinic	Glutaric	Adipic	Pimelic	Azelaic	Maleic	Malic	Phthalic	Glycolic	Keto glutaric	3-OH benzoic	4-OH benzoic	Pinonic
Malonic	1	0.581	0.675	0.482	0.407	0.452	0.347	0.693	0.619	0.662	0.528	0.492	0.498	−0.574
Succinic		1	0.543	**0.728**	0.283	0.121	0.263	**0.840**	**0.765**	**0.749**	**0.734**	0.428	0.461	−0.739
Glutaric			1	0.493	0.602	0.374	0.642	0.560	0.481	0.436	**0.761**	0.505	0.467	−0.084
Adipic				1	0.542	0.286	0.182	**0.816**	0.595	0.680	0.530	0.715	0.761	−0.400
Pimelic					1	0.543	−0.088	0.532	0.178	0.430	0.427	0.545	0.553	−0.682
Azelaic						1	−0.156	0.355	0.178	0.407	0.155	0.666	0.632	0.473
Maleic							1	0.140	0.219	−0.019	0.578	0.070	0.036	−0.032
Malic								1	**0.748**	**0.827**	0.687	0.592	0.667	**−0.833**
Phthalic									1	0.682	0.638	0.284	0.299	**−0.878**
Glycolic										1	0.511	0.657	0.703	−0.498
Keto glutaric											1	0.330	0.347	0.230
3-OH benzoic												1	**0.945**	−0.266
4-OH benzoic													1	−0.379
Pinonic														1

which were the typical atmospheric conditions in cold seasons in the Po Valley. The mixing layer heights were nearly continuously low, with mean values in the 169−314 m and 230−413 m ranges for the rural and urban sites, respectively: these are reduced heights in comparison with summer data (about 900 m during summer 2012). Also daily solar radiation was nearly constant in all the periods, characterized by low values (mean values of 61−81 Wm^{-2} and 65−92 $W\,m^{-2}$ in MS and SP, respectively) in comparison with summer values (i.e., nearly 300 $W\,m^{-2}$ during summer 2012). Precipitations were nearly absent (winter 2011) or present only in few days, yielding total precipitation values with the maximum of 75 mm in SP during fall 2012 (Table 1, last 4 lines).

These meteorological conditions might explain the high concentrations of carboxylic acids, since the low mixing layer height and weak amount of wet deposition confined vertical distribution of pollutants to the first hundred meters of the atmosphere, contributing to the accumulation of organic precursors and thereby promoting the secondary production of acids (Balducci and Cecinato, 2010; Carbone et al., 2010; Bigi and Ghermandi, 2011; Perrone et al., 2012; Pietrogrande et al., 2013). In addition, the organic pollutants emitted by specific local sources were homogenously accumulated and persist all over the investigated area, so that the PM$_{2.5}$ mass and CA concentrations showed background profiles slightly affected by the distance from source locations (see comparison between two sites in Fig. 2).

Temperature showed significant variation in the three periods ranging from 6.5 to 3.9 °C (mean values in Main Site in winter 2011 and 2013, respectively) to 12.6 °C in fall 2012. Consequently, it is possible to relate the higher amounts of acids with the lower temperature in the winter campaigns (Fig. 2, which reports the seasonal evolution of total concentrations of carboxylic acids in the three monitoring campaigns in both sites). This behavior may be likely attributed to the enhanced emission and accumulation of anthropogenic precursors associated with domestic heating in colder pre- and deep-winter in comparison with warmer autumn. This temperature dependence also explained the similarity between the data obtained during the pre- and deep-winter periods characterized by similar temperatures.

As consequence of the reduced solar radiation, limited photochemical processes are expected in all the investigated periods. The impact of the secondary photo-oxidation reactions can be estimated by the total amount of oxo and hydroxy carboxylic acids (ToxCA, in Table 1) (Kawamura and Yasui, 2005; Ho et al., 2006; Lee et al., 2006; Yang et al., 2008). Similar values were obtained in all the campaigns ranging from 61 ng m^{-3} in fall to 88 ng m^{-3} in winter (seasonal evolution of ToxCA is shown in Fig. 2). However, these data yield different values of their relative contribution to the total acids, estimated as the percent ratio of ToxCA to the total amount of CAs (ToxCA/TCA%, Table 1). They increased from about 30% in winter periods up to 44% and 53% in fall, in MS and SP,
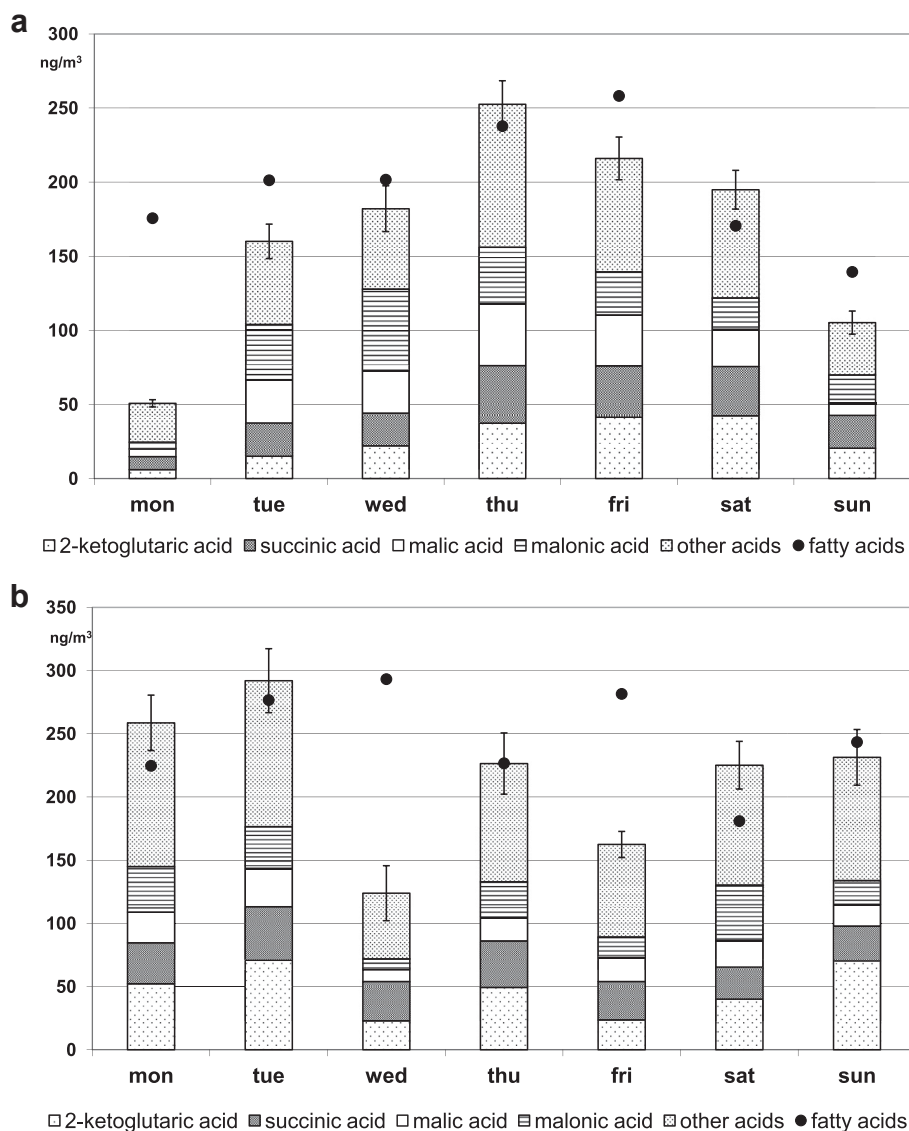
Fig. 3. Day-of-week pattern of carboxylic acid concentrations (ng m^{-3}) averaged by day of week for three weeks in the urban MS site: concentrations of 2-ketoglutaric, succinic, malic and malonic acids and total carboxylic acids are shown (a bar indicates 1 standard error). Points indicate concentrations of fatty acids. a: data of fall 2012 campaign; b: data of deep-winter 2013 campaign.

respectively: this trend may be likely due to the concomitant temperature increase in fall from 3.9 °C to 12.6 °C in MS and from 2.6 °C to 11.1 °C in SP.

3.3. Relationship between carboxylic acids and markers of primary emission sources

In addition to carboxylic acids, two relevant tracers of primary emissions were determined, in particular anhydro-sugars and n-fatty acids, that can be quantified by the used multi-residue GC/MS method (Pietrogrande et al., 2013).

Levoglucosan, mannosan and galactosan, are significant tracers for primary biomass burning (BB) emissions, as they are produced from cellulose and hemicellulose combustion (Oliveira et al., 2007; Wang et al., 2011; Giannoni et al., 2012; Yang et al., 2013). These burning sugars showed the highest concentration (total concentration in Table 1) in comparison with the other target markers, suggesting that wood burning is a major source for particulate matter in Emilia Romagna region in cold seasons. In fall 2012 and

winter 2013 anhydro-sugars had average total concentrations of ≈ 350 ng m^{-3}, similar to the levels generally found in European urban and rural areas (5–500 ng m^{-3}, Oliveira et al., 2007; Wang et al., 2011; Giannoni et al., 2012). In winter 2011 exceptionally high values of ≈ 1100 ng m^{-3} were found, indicating the large contribution of biomass burning in this period. It is difficult to explain this behavior that cannot be directly related to domestic heating, since the temperature in this period (≈ 5 °C) is similar with that in deep-winter (≈ 4 °C), when anhydro-sugar levels are lower. Direct emissions from wood burning may explain the enhanced TCA levels in pre-winter, mainly due to higher concentrations of succinic acid which has been found specifically originated from wood burning (Wang et al., 2006; Lee et al., 2006; Oliveira et al., 2007; Bi et al., 2008; Hsieh et al., 2008). This conclusion is supported by the excellent correlation ($r = 0.98$) found between succinic acid and BB sugars. However, the concentrations of BB sugars were not significantly correlated with the total CA concentration ($r \approx 0.3$), although literature papers report that biomass burning emissions are enriched in low molecular weight dicarboxylic acids

(Claeys et al., 2010; Yang et al., 2013). This result suggests that biomass burning contributes to emission of dicarboxylic acids only partially, in combination with other different sources. This point may be elucidated by a detailed investigation on the chemical composition of burning smoke (work in progress, forthcoming part 2).

In fall 2012 and winter 2013 campaigns also n-fatty acids were determined using an extension of the GC/MS method. Only palmitic (C16:0) and stearic (C18:0) acids were found, with dominant C16 acid (concentrations: 51–83 ng m^{-3}). The sum of their concentrations ranged from 85 to 134 ng m^{-3}, confirming that they are very abundant tracers in PM. These fatty acids are known to be emitted directly into the atmosphere by a multiplicity of sources, including power plants, vehicular circulation, combustion of fossil fuels, biomass burning and meat cooking operations (Rogge et al., 2006; Oliveira et al., 2007; Ho et al., 2011). The obtained values are strongly correlated with the total concentrations of carboxylic acids ($r = 0.98$), confirming the main contribution of emissions from primary sources of diacids in the investigated campaigns.

The ratio of C18/C16 has been used as a qualitative tool for source assessment. Ratios lower than 0.25 have been obtained in atmospheric PM$_{2.5}$ resulting from foliar vegetation combustion, waxy leaf surface abrasions, and wood smoke; values between 0.25 and 0.5 were registered for car and diesel truck exhausts; proportions in the interval 0.5–1 were achieved for paved and unpaved road dust and for hamburger charbroiling (Rogge et al., 2006). The C18/C16 ratio had average value of 0.6 in both the sites, indicating the dominant contribution of anthropogenic emissions, i.e., vehicular emissions and combustion of fossil fuels.

3.5. Day-of-week trends of dicarboxylic acids

The investigation of weekly trends in CA concentrations can help to elucidate the impact of various emission sources and photochemical transformations on atmospheric pollutant concentrations. In fact, day-of-week trends can be directly related to contributions of different sources from human activities, since no weekly trends were seen in meteorological properties, which usually played a major role in environment PM concentrations (Lough et al., 2006; Oliveira et al., 2007). Since each campaign went on in general for three weeks, samples were composited by day of week at each site and three-week averages were used to investigate day-of-week trends.

In fall 2012, the total CA concentration showed a significant dependence on the day of week at each site, since it increased from Monday through Friday and fell over the weekend to the lowest levels on Monday (e.g. bars in Fig. 3a shows the trend of TCA levels in fall 2012 in the urban site). This behavior might be a consequence of the accumulation throughout the weekdays of volatile organic precursors emitted from sources with weekly activity patterns, such as motor vehicle traffic, that are higher on weekdays (Lough et al., 2006; Oliveira et al., 2007; Bigi and Ghermandi, 2011). Accordingly, the highest levels of total CAs were mainly associated with the largest contributions of 2-ketoglutaric, succinic and malic acids (bars in Fig. 3a), which have been identified as specific tracers of secondary organic aerosol originated from traffic exhaust (Hsieh et al., 2008; Van Drooge et al., 2012).

This conclusion is supported by the same weekly trend showed by the concentration of C16 and C18 n-fatty acids throughout the week, with minimum on Monday and maximum on Friday (e.g. points in Fig. 3a shows the trend in fall 2012 in the urban site).

Total CAs show a random pattern during the week in either 2011 or 2013 winter seasons (e.g. Fig. 3b shows the trend of CA composition in winter 2013 in the urban site): this behavior suggested that in these colder winter periods the main contribution to CAs concentrations derived from civil heating, that is an anthropogenic source without clear weekly pattern. The strong impact of such sources was also suggested by the approximately two time increase in TCA levels in the colder weeks, pre-winter 2011 and deep-winter 2013, in comparison with fall 2012 (Table 1). Accordingly, also the concentration of C16 and C18 n-fatty acids showed a random pattern throughout the week (e.g. points in Fig. 3b shows the trend in winter 2013 in the urban site), confirming that the anthropogenic primary emissions are mainly dominated by the domestic heating in this period.

For each monitored periods, the same weekly trends were found in the urban and rural sites, which further confirmed the homogeneous impact of the different sources all over the investigated area.

4. Conclusions

Our study indicates that air pollution problems in Po Valley in wintertime were principally due to high anthropogenic emissions combined with stagnant atmospheric conditions, which favored pollutant accumulation.

The obtained results suggested that the molecular distributions of low molecular weight carboxylic acids provide essential information on emission sources and atmospheric chemical processes. Biomass burning appears to be the most important contributor to the aerosols in wintertime, followed by the emission from other anthropogenic sources, such as combustion of fossil fuels, residential heating and vehicular sources. In addition, it was observed that photo-oxidation is likely an important chemical process that contributes to SOA formation in the investigated area, although photochemical activity was limited due to low temperature and reduced solar radiation.

All these preliminary observations will be integrated by more detailed investigation of other polar and apolar organic tracers in atmospheric aerosol, provided by the measurement campaigns of the Supersito project. Further investigations focusing on Principal Component Analysis (PCA) and source apportionment studies by performing Positive Matrix Factorization (PMF) are planned to discuss the analytical results and study the in uence of potential sources, processes and meteorological conditions on the air quality of the investigated area.

References

Balducci, C., Cecinato, A., 2010. Particulate organic acids in the atmosphere of Italian cities: are they environmentally relevant? Atmos. Environ. 44, 652–659.

Bi, X., Simoneit, B.R.T., Sheng, G., Ma, S., Fu, J., 2008. Composition and major sources of organic compounds in urban aerosols. Atmos. Res. 88, 256–265.

Bigi, A., Ghermandi, G., 2011. Particle number size distribution and weight concentration of background urban aerosol in a Po Valley site. Water Air Soil. Pollut. 220, 265–278.

Carbone, C., Decesari, S., Mircea, M., Giulianelli, L., Finessing, E., Rinaldi, M., Fuzzi, S., Marinoni, A., 2010. Size-resolved aerosol chemical composition over the Italian Peninsula during typical summer and winter conditions. Atmos. Environ. 44, 5269–5278.

Claeys, M., Kourtchev, I., Pashynska, V., Vas, G., Vermeylen, R., Wang, W., Cafmeyer, J., Chi, X., Artaxo, P., Andreae, M.O., Maenhaut, W., 2010. Polar organic marker compounds in atmospheric aerosols during the LBA-SMOCC 2002 biomass burning experiment in Rondonia, Brazil: sources and source processes,

time series, diel variations and size distributions. Atmos. Chem. Phys. 19, 9319–9331.

Cheng, Y., Brook, J.R., Li, S.M., Leithead, A., 2011. Seasonal variation in the biogenic secondary organic aerosol tracers cis-pinonic acid: Enhancement due to emission from regional and local biomass burning. Atmos. Environ. 45, 7105–7112.

Dabek-Zlotorzynska, E., Aranda-Rodriguez, R., Graham, L., 2005. Capillary electrophoresis determinative and GC-MS confirmatory method for water-soluble organic acids in airborne particulate matter and vehicle emission. J. Sep. Sci. 28, 1520–1528.

Deserti, M., Savoia, E., Cacciamani, C., Golinelli, M., Kerschbaumer, A., Leoncini, G., Selvini, A., Paccagnella, T., Tibaldi, S., 2001. Operational meteorological preprocessing at Emilia-Romagna ARPA Meteorological Service as a part of a decision support system for Air Quality Management. Int. J. Environ. Pollut. 16, 571–582.

Fisseha, R., Dommen, M., Paulsen, D., Kalberer, M., Maurer, R., Ho er, F., Weingartner, E., Baltensperger, U., 2004. Identification of organic acids in secondary organic aerosol and the corresponding gas phase from chamber experiments. Anal. Chem. 76, 6535–6540.

Giannoni, M., Martellini, T., Del Bubba, M., Gambaro, A., Zangrando, R., Chiari, M., Lepri, M., Cincinelli, A., 2012. The use of levoglucosan for tracing biomass burning in PM2.5 samples in Tuscany (Italy). Environ. Pollut. 167, 7–15.

Gierlus, K.L., Laskina, O., Abernathy, T.L., Grassian, V.H., 2012. Laboratory study of the effect of oxalic acid on the cloud condensation nuclei activity of mineral dust aerosol. Atmos. Environ. 46, 125–130.

Ho, K.F., Lee, S.C., Cao, J.J., Kawamura, K., Watanabe, T., Cheng, Y., Chow, J.C., 2006. Dicarboxylic acids, ketocarboxylic acids and dicarbonyls in the urban roadside area of Hong Kong. Atmos. Environ. 40, 3030–3040.

Ho, K.F., Ho, S.S.H., Lee, S.C., Kawamura, K., Zou, S.C., Cao, J.J., Xu, H.M., 2011. Summer and winter variation of dicarboxylic acids, fatty acids and benzoic acid in PM2.5 in Pearl Delta River Region, China. Atmos. Chem. Phys. 11, 2197–2208.

Hsieh, L.Y., Chen, C.L., Wan, M.W., Tsai, C.H., Tsai, Y.I., 2008. Speciation and temporal characterization of dicarboxylic acids in PM2.5 during a PM episode and a period of non-episodic pollution. Atmos. Environ. 42, 6836–6850.

Huang, X.F., Hu, M., He, L.Y., Tang, X.T., 2005. Chemical characterization of water-soluble organic acids in PM2.5 in Beijing, China. Atmos. Environ. 39, 2819–2827.

Huang, X.F., He, L.Y., Hu, M., Zhang, Y.H., 2006. Annual variation of particulate organic compounds in PM2.5 in the urban atmosphere of Beijing. Atmos. Environ. 40, 2449–2458.

Huang, X.F., Cheng, D.L., Lan, Z.J., Feng, N., He, L.Y., Yu, G.H., Luan, S.J., 2012. Characterization of organic aerosol in fine particle in a mega-city of South China: molecular composition, seasonal variation and size distribution. Atmos. Res. 114–115, 28–37.

Hyder, M., Genberg, J., Sandahl, M., Swietlicki, E., Jonsson, J.A., 2012. Yearly trend of dicarboxylic acids in organic aerosols from south of Sweden and source attribution. Atmos. Environ. 57, 197–204.

Kawamura, K., Koulchi, I., 1993. Seasonal changes in the distribution of dicarboxylic acids, in the urban atmosphere. Environ. Sci. Technol. 27, 2227–2235.

Kawamura, K., Yasui, O., 2005. Diurnal changes in the distribution of dicarboxylic acids, ketocarboxylic acids and dicarbonyls in the urban Tokyo atmosphere. Atmos. Environ. 39, 1945–1960.

Kitanovski, Z., Grgic, I., Veber, M., 2011. Characterization of carboxylic acids in atmospheric aerosols using hydrophilic interaction liquid chromatography tandem mass spectrometry. J. Chromatogr. A 1218, 4417–4425.

Ladji, R., Yassaa, N., Calducci, C., Cecinato, A., Meklati, B.Y., 2009. Annual variation of particulate organic compounds in PM10 in the urban atmosphere of Algiers. Atmos. Res. 92, 258–269.

Larsen, B.R., Giraldoni, S., Stenstrom, K., Niedzialek, J., Jimenez, J., Belis, C.A., 2012. Sources for PM pollution in the Po Plain, Italy. II. Probabilistic uncertainty characterization and sensitivity analysis of secondary and primary sources. Atmos. Environ. 50, 203–213.

Lee, S.C., Cao, J.J., Kawamura, K., Watanabe, T., Cheng, T., Chow, J.C., 2006. Dicarboxylic acids, ketocarboxylic acids and dicarbonyls in the urban roadside area of Hong Kong. Atmos. Environ. 40, 3030–3040.

Li, M., McDow, S.R., Tollerud, D.J., Mazurek, M.A., 2006. Seasonal abundance of organic molecular markers in urban particulate matter from Philadelphia, PA. Atmos. Environ. 40, 2260–2273.

Lough, G.C., Schauer, J.J., Lawson, D.R., 2006. Day-of-week trends in carbonaceous aerosol composition in the urban atmosphere. Atmos. Environ. 40, 4137–4149.

Oliveira, C., Pio, C., Alves, C., Evtyugina, M., Santos, P., Goncalves, V., Nunes, T., Silvestre, A.J.D., Palmgren, F., Wahlin, P., Harrad, S., 2007. Seasonal distribution of polar organic compounds in the urban atmosphere of two large cities from the North and South of Europe. Atmos. Environ. 41, 5555–5570.

Perrone, M.G., Larsen, B.R., Ferrero, L., Sangiorgi, G., De Gennaro, G., Udisti, R., Zangrando, R., Gambaro, A., Bolzacchini, E., 2012. Sources of high PM2.5 concentrations in Milan, Northern Italy: molecular marker data and CMB modeling. Sci. Total Environ. 414, 343–355.

Perrone, M.G., Gualtieri, M., Consonni, V., Ferrero, L., Sangiorgi, G., Longhin, E., Ballabio, D., Bolzacchini, E., Camatini, M., 2013. Particle size, chemical composition, seasons of the year and urban, rural o remote size origins as determinants of biological effects of particulate matter on pulmonary cells. Environ. Pollut. 176, 215–227.

Pietrogrande, M.C., Bacco, D., 2011. GC–MS analysis of water-soluble organics in atmospheric aerosol: response surface methodology for optimizing silyl-derivatization for simultaneous analysis of carboxylic acids and sugars. Anal. Chim. Acta 689, 257–264.

Pietrogrande, M.C., Bacco, D., Mercuriali, M., 2010. GC–MS analysis of low-molecular-weight dicarboxylic acids in atmospheric aerosol: comparison between silylation and esterification derivatization procedures. Anal. Bioanal. Chem. 396, 877–885.

Pietrogrande, M.C., Bacco, D., Chiereghin, S., 2013. GC/MS analysis of water-soluble organics in atmospheric aerosol: optimization of a solvent extraction procedure for simultaneous analysis of carboxylic acids and sugars. Anal. Bioanal. Chem. 405, 1095–1104.

Rogge, W.F., Medeiros, P.M., Simoneit, B.R.T., 2006. Organic marker compounds for surface soil and fugitive dust from open lot dairies and cattle feedlots. Atmos. Environ. 40, 27–49.

Ruiz-Jimenez, J., Parshintsev, J., Laitinen, T., Hartonen, K., Petäjä, T., Kulmala, M., Riekkola, M.L., 2012. In uence of the sampling site, the season of the year, the particle size and the number of nucleation events on the chemical composition of atmospheric ultrafine and total suspended particles. Atmos. Environ. 49, 60–68.

Scire, J.S., Robe, F.R., Fernau, M.E., Yamartino, R.J., 2000. A User Guide for the CALMET Meteorological Model (Version 5). Earth Tech, Inc.

Squizzato, S., Masiol, M., Innocente, E., Pecorari, E., Ramazzo, G., Pavoni, B., 2012. A procedure to assess local and long-range transport contributions to PM2.5 and secondary inorganic aerosol. J. Aerosol Sci. 46, 64–76.

Van Drooge, B., Crusack, M., Reche, C., Mohr, C., Alastuey, A., Querol, X., Prevot, A., Douglas, A., Day, D.A., Jimenez, J.L., Grimalt, J.O., 2012. Molecular marker characterization of the organic composition of submicron aerosols from Mediterranean urban and rural environments under contrasting meteorological conditions. Atmos. Environ. 61, 482–489.

Van Pinxteren, D., Herrmann, H., 2007. Determination of functionalised carboxylic acids in atmospheric particles and cloud water using capillary electrophoresis/mass spectrometry. J. Chromatogr. A 1171, 112–123.

Viana, M., Kuhlbusch, T.A.J., Querol, X., Alastuey, A., Harrison, R.M., Hopke, P.K., Winiwarter, W., Vallius, M., Szidat, S., Prévôt, A.S.H., Hueglin, C., Bloemen, H., Wåhlin, P., Vecchi, R., Miranda, A.I., Kasper-Giebl, A., Maenhaut, W., Hitzenberger, R., 2008. Source apportionment of particulate matter in Europe: a review of methods and results. J. Aerosol Sci. 39, 827–849.

Wagener, S., Langner, M., Moriske, H.J., Endlicher, W.R., 2012. Spatial and seasonal variations of biogenic tracer compounds in ambient PM10 and PM1 samples in Berlin. Germany. Atmos. Environ 47, 33–42.

Wang, H., Kawamura, K., Ho, K.F., Lee, S.C., 2006. Low molecular weight dicarboxylic acids, ketoacids and dicarbonyls in the fine particles from a roadway tunnel: possible secondary production from the precursors. Environ. Sci. Technol. 40, 6255–6260.

Wang, G., Chen, C., Li, J., Zhou, B., Xie, M., Hu, S., Kawamura, K., Chen, C., 2011. Molecular composition and size distribution of sugars, sugar-alcohols and carboxylic acids in airborne particles during a severe urban haze event caused by wheat straw burning. Atmos. Environ. 40, 2473–2479.

Yang, L., Ray, M.B., Yu, L.E., 2008. Photooxidation of dicarboxylic acids – Part II: kinetics, intermediates and field observations. Atmos. Environ. 42, 868–880.

Yang, L., Nguyen, D.M., Jia, S., Reid, J.S., Yu, L.E., 2013. Impacts of biomass burning smoke on the distributions and concentrations of C2–C5 dicarboxylic acids and dicarboxylates in a tropical urban environment. Atmos. Environ. 78, 211–218.
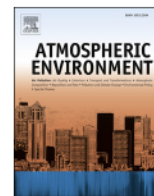
ELSEVIER LICENSE
TERMS AND CONDITIONS

Feb 07, 2016

This is an Agreement between Marco Visentin ("You") and Elsevier ("Elsevier"). It consists of your order details, the terms and conditions provided by Elsevier, and the payment terms and conditions.

All payments must be made in full to CCC. For payment instructions, please see information listed at the bottom of this form.

Supplier	Elsevier Limited The Boulevard,Langford Lane Kidlington,Oxford,OX5 1GB,UK
Registered Company Number	1982084
Customer name	Marco Visentin
Customer address	Via L. Borsari 46
	Ferrara, None 44121
License number	3803550843257
License date	Feb 07, 2016
Licensed content publisher	Elsevier
Licensed content publication	Atmospheric Environment
Licensed content title	Polar organic marker compounds in atmospheric aerosol in the Po Valley during the Supersito campaigns — Part 2: Seasonal variations of sugars
Licensed content author	Maria Chiara Pietrogrande,Dimitri Bacco,Marco Visentin,Silvia Ferrari,Patrizia Casali
Licensed content date	November 2014
Licensed content volume number	97
Licensed content issue number	n/a
Number of pages	11
Start Page	215
End Page	225
Type of Use	reuse in a thesis/dissertation
Intended publisher of new work	other
Portion	full article
Format	both print and electronic
Are you the author of this Elsevier article?	Yes
Will you be translating?	No
Title of your thesis/dissertation	Chemical characterization of atmospheric aerosol for air quality evaluation in Emilia Romagna region
Expected completion date	Mar 2016
Estimated size (number of pages)	200
Elsevier VAT number	GB 494 6272 12
Price	0.00 EUR
VAT/Local Sales Tax	0.00 EUR / 0.00 GBP
Total	**0.00 EUR**
Terms and Conditions	

Polar organic marker compounds in atmospheric aerosol in the Po Valley during the Supersito campaigns — Part 2: Seasonal variations of sugars

Maria Chiara Pietrogrande [a,*], Dimitri Bacco [a], Marco Visentin [a], Silvia Ferrari [b], Patrizia Casali [b]

[a] Department of Chemical and Pharmaceutical Sciences, University of Ferrara, Via Fossato di Mortara 17/19, I-44100 Ferrara, Italy
[b] Regional Agency of Prevention and Environment ARPA — Emilia-Romagna, Italy

HIGHLIGHTS

Saccharides are emitted from biomass burning and primary bio aerosol.
Emissions are dominated by biomass burning in the cold periods.
Primary biogenic emissions are dominant in summer and spring.

ARTICLE INFO

ABSTRACT

Four intensive experimental campaigns were conducted in the Po Valley (Northern Italy) in different seasons through the years 2012 and 2013, in the framework of the "Supersito" project. As a part of a study on polar tracers in atmospheric $PM_{2.5}$, the present paper describes the abundances and temporal variations of sugars, as primary biogenic biomarkers, being the major form of photosynthetically assimilated carbon in the biosphere. The study includes primary saccharides (glucose, sucrose, arabinose, galactose and mycose), sugar alcohols (arabitol and mannitol) and anhydrosugars (levoglucosan, galactosan and mannosan).

Strong seasonality was observed with total sugars concentration nearly 10 times higher in the cold seasons (mean 377 ng m^{-3}) than in summer/spring (mean 36 ng m^{-3}). Also sugar composition profiles varied seasonally, being dominated by anhydrosugars in fall and winter, i.e., levoglucosan (mean 271 ng m^{-3}), followed by mannosan (mean 53 ng m^{-3}) and galactosan (mean 29 ng m^{-3}). These data indicate that in the cold seasons the biomass combustion for domestic heating is the main sugar source representing nearly 94% of the total saccharides mass measured in $PM_{2.5}$. Accordingly, glucose, arabinose and galactose show the highest concentrations, since these saccharides are also emitted during the burning process as uncombusted biomass materials. In spring/summer the primary saccharides are dominant in $PM_{2.5}$, with mannitol as the most abundant, followed by mycose, glucose and ribitol that are emitted by the terrestrial biomass, reflecting the higher sugar production and utilization by the ecosystem in the warm seasons.

These results were confirmed by investigating other molecular markers, such as low-molecular-weight carboxylic acids and n-alkane homologs. Principal Component Analysis was applied to the data to extract three PCs that may be attributed to different saccharide sources, such as biomass burning and primary bio aerosol.

© 2014 Published by Elsevier Ltd.

1. Introduction

Several intensive experimental campaigns were conducted at an urban site (Bologna) and at a rural background station (San Pietro) in the Po Plain (Northern Italy) in the framework of the "Supersito" project, developed and financed by Emilia-Romagna Region and

Regional Agency of Prevention and Environment (ARPA-ER) (www.supersito-er.it). Po Valley, which is the most industrialized and populated region of Italy, is recognized as one of the most worrying air pollution situations in Europe, where high anthropogenic emissions and meteorological factors may cause air pollution episodes and serious risks for human health (Balducci and Cecinato, 2010; Carbone et al., 2010; Bigi and Ghermandi, 2011; Larsen et al., 2012; Perrone et al., 2013).

In the framework of this project, as the continuation of the previous study on carboxylic acids (Pietrogrande et al., 2014), this paper is focused on the chemical characterization of sugars, as relevant tracers for describing the contribution of biogenic sources (Simoneit et al., 2004; Medeiros et al., 2006).

These markers were found in substantial concentrations in atmospheric aerosols over the continental regions (Rogge et al., 2007; Bi et al., 2008; Jia et al., 2010; Wang et al., 2011; Tominaga et al., 2011; Wagener et al., 2012; Fu et al., 2012) and have a significant impact on climate effects by altering the cloud condensation nuclei activity of aerosol and playing an important role in the aqueous phase chemistry occurring within cloud droplet nucleated smoke (Fuzzi et al., 2007; Martin et al., 2010; Wang et al., 2011).

The saccharides present in aerosols are comprised of three main groups: (1) primary saccharides consisting of mono- and disaccharides, (2) saccharide polyols (reduced sugars), and (3) anhydrosaccharide derivatives, mainly levoglucosan. Their presence in aerosol particles derived from two major sources that are admixed depending on environmental conditions: natural biogenic detritus and biomass burning (natural and anthropogenic) (Simoneit et al., 2004; Medeiros et al., 2006; Jia et al., 2010; Holden et al., 2011; Tominaga et al., 2011; Fu et al., 2012; Li et al., 2013).

Levoglucosan − with minor quantities of its isomers mannosan, galactosan − is primarily produced during biomass combustion as the pyrolytic decomposition product of cellulose and hemicellulose. Therefore, it is the key tracer for biomass burning to estimate the contribution of both open and residential biomass combustion to fine particle (Simoneit et al., 2004; Wang et al., 2011; Giannoni et al., 2012; Li et al., 2013; Tsai et al., 2013; Sang et al., 2013).

The other sources of saccharides in aerosols are primary biological particles, including microorganisms, pollen, vegetative debris, bacteria and viruses, since sugars represent the major form of photosynthetically assimilated carbon in the biosphere (Simoneit et al., 2004; Medeiros et al., 2006). Glucose, sucrose and mycose (trehalose), as the most common saccharides present in vascular plants and microorganisms, have been proposed as source-specific tracers for soil biota released into the atmosphere by farmland soil suspension and natural soil erosion (Rogge et al., 2007; Jia et al., 2010; Tominaga et al., 2011; Fu et al., 2012; Tsai et al., 2013). Sugar alcohols, including mannitol and eritrytol, have been used as biomarkers to estimate atmospheric fungal spore abundance (Medeiros et al., 2006; Jia et al., 2010).

Size partitioning of sugars showed that the emissions from primary bio aerosols and soil resuspension are generally most associated with coarse fraction (Medeiros et al., 2006; Yttri et al., 2007; Bauer et al., 2008; Ma et al., 2009; Jia and Fraser, 2011; Wang et al., 2011; Tominaga et al., 2011), whereas those from biomass burning present higher concentrations in the fine mode range, with different size distributions depending on sampling sites and seasonality (Medeiros et al., 2006). Although the comprehensive apportionment of biogenic emissions would require investigation of coarse and fine PM samples (Medeiros et al., 2006; Bauer et al., 2008; Wang et al., 2011; Tominaga et al., 2011), the concentration and seasonal variation of major saccharides in PM$_{2.5}$

samples may give helpful information to track aerosols of biologically derived origin (Jia et al., 2010; Jia and Fraser, 2011).

Even if the atmospheric composition of sugars has been investigated in various regions and source profiles for open and residential biomass combustion have been characterized (Mazzoleni et al., 2007; Puxbaum et al., 2007; Holden et al., 2011), different sugar species were surveyed among these studies and seasonal and spatial distributions of the sugars have not yet been sufficiently clarified (Simoneit et al., 2004; Medeiros et al., 2006).

The main purpose of this study is to investigate the abundances and temporal variations of sugars and sugar alcohols in atmospheric PM$_{2.5}$, in order to isolate the sources of biological origins, as a part of the general study for characterize primary emissions and secondary processes that contribute to the ambient PM$_{2.5}$ levels in Emilia Romagna region (Pietrogrande et al., 2014).

Additional information were obtained by investigating other organic markers, such as low-molecular-weight carboxylic acids (CAs), to differentiate between primary emissions and secondary organic aerosol (Lee et al., 2006; Wang et al., 2006; Ho et al., 2011; Hsieh et al., 2008; Bi et al., 2008; Wang et al., 2011; Hyder et al., 2012; Yang et al., 2013; Pietrogrande et al., 2014), and n-alkane homologs to assess biogenic signatures of epicuticular plant waxes (Zheng et al., 2002; Jia et al., 2010; Pietrogrande et al., 2010).

Atmospheric PM$_{2.5}$ samples were collected in two locations representing an urban (Main Site, MS) and a rural background (San Pietro Capofiume, SP) site in the Po Valley. Four intensive field campaigns were carried out in all the seasons in 2012 and 2013 years (Pietrogrande et al., 2014).

2. Materials and methods

2.1. Aerosol sampling

The sampling protocol was described elsewhere (Pietrogrande et al., 2014). Briefly, the urban background site MS is located in the city of Bologna (~400,000 inhabitants) and the rural background station is located at San Pietro Capofiume about 30 km northeast from the city.

As part of the Supersito project, four sampling intensive campaigns were performed to represent different meteorological scenarios throughout the year: early-summer, from 14th June up to 11th July 2012, late-autumn, from 23rd October up to 10th November 2012, deep-winter from 30th January up to 19th February 2013 and late-spring from 7th up to 27th May 2013.

PM$_{2.5}$ samples were collected on quartz fiber filters (Whatman, 47 mm diameter) by low volume automatic outdoor samplers (Skypost PM, TCRTECORA Instruments, Corsico, Milan, Italy) at an airflow rate of 38.3 L min^{-1} for 24 h ($\approx$55 m^3 day^{-1}). In spring, higher air volumes ($\approx$283 m^3 day^{-1}) were sampled on quartz fiber filters (Munktell, 100 mm diameter) using an Hi-Vol sampler (Echo Hi-Vol, TECORA Instruments, Corsico, Milan, Italy) operating at a flow rate of 11.7 m^3 h^{-1} for 24 h. This choice was motivated by the need of assuring PM amounts compatible with the analytical sensitivity, since the target analytes are expected at low concentration levels in spring in the investigated region (Carbone et al., 2010; Bigi and Ghermandi, 2011; Perrone et al., 2013; Pietrogrande et al., 2013a).

After sampling, the procedure outlined in European Standard EN 12341 (CEN, 1998) was applied for equilibration and weighing. The filters were stored in a freezer at −20 °C before analysis.

Meteorological data were collected at the meteorological stations of San Pietro Capofiume and Bologna by Hydro-Meteo-Climate Service of ARPA-ER. Mixing layer height at both sites was estimated using the pre-processor CALMET by ARPA Emilia-Romagna (Scire et al., 2000; Deserti et al., 2001).

2.2. Analytical procedure for sugar analysis

The analytical procedure has been described elsewhere (Pietrogrande et al., 2013b, 2014). Briefly, PM samples were extracted with 15 mL of methanol:dichloromethane (9:1 solvent mixture) in an ultrasonication bath for 15 min and then filtered using a teflon filter (45 mm, 0.45 μm, Supelco, Bellefonte, PA). A solvent volume of 20 mL was used for extracting the larger quartz fiber filters (100 mm diameter) in the spring campaign. The filtrates were evaporated to dryness in a centrifugal vacuum concentrator (miVac Duo Concentrator, Genevac Ltd, Ipswich, UK). Then the sample extracts were submitted to silyl derivatization with N,O-bis-(trimethylsilyl)trifluoroacetamide (BSTFA) containing 1% of trimethylchlorosilane (TMCS) at 75 °C for 70 min: 40 μL of BSTFA-TMCS reagent and 15 μL of pyridine were added to 40 μL of iso-octane as solvent and 5 μL of Internal Standard (deuterated n-dodecane, $C_{12}D_{26}$, injected quantity: 127.5 ng).

The GC/MS system was a Scientific Focus-GC (Thermo-Fisher Scientific, Milan, Italy) coupled to PolarisQ Ion Trap Mass Spectrometer (Thermo-Fisher Scientific, Milan, Italy). The column used was a DB-5ms column ($L = 30$ m, I.D. = 0.25 mm, $d_f = 0.25$ μm film thickness; J&W Scientific, Rancho Cordova, CA, USA). High purity helium was the carrier gas with a linear flow rate of 1.5 mL min^{-1}. Temperature program conditions were optimized for analysis of a wide range of target polar organic compounds, including low molecular weight carboxylic acids: an initial temperature of 70 °C was raised to 125 °C at 2.5 °C min^{-1}, followed by an isothermal hold for 7 min; after that, the temperature was increased to 145 °C at 2 °C min^{-1}, an isothermal hold for 5 min; then further raised to 170 °C at 2.5 °C min^{-1} and finally led to 300 °C at 7 °C min^{-1}; this temperature was maintained for 1 min. All samples were injected in splitless mode (splitless time: 60 s); the injector temperature was 250 °C.

The mass spectrometer operated in Electron Ionization mode (positive ion, 70 eV). Ion source and transfer-line temperatures were 250 °C and 280 °C, respectively. The mass spectra were acquired in full scan mode from 50 to 650 m/z in 0.58 s. For identification and quantification of the target analytes, the SIM (selected-ion monitoring) chromatograms were extracted from the acquired signal by selecting either the base peak ion or the most abundant characteristic fragments (Pietrogrande et al., 2013b). Quality assurance and quality control were assessed by precision, accuracy and sensitivity for polar organic tracers. The procedure provides low detection limits (0.1–3 ng m^{-3} with low volume samplers, and 0.1–1 ng m^{-3} in spring, with higher air volume sampler, LOD in Table 1) and good reproducibility (RSD% 7%). The procedure recoveries were evaluated on PM samples spiked with surrogate standards submitted to extraction and derivatization prior to GC/MS analysis. Good recoveries ranging from 78% to 104% were obtained for the target analytes, assuring reliable results for the real samples (Pietrogrande et al., 2013b).

2.3. Analytical procedure for n-alkane analysis

The analysis of n-alkanes (C_{20}–C_{33}) was performed in the ARPA laboratory in Ravenna, as a part of the Supersito project activities (www.supersito.it). PM samples were extracted in an ultrasonic bath for 20 min with 15 mL of dichloromethane and then evaporated to dryness. Before extraction, 5-α-androstane ($C_{19}H_{32}$, 200 μl of a standard solution at 10 ng μl^{-1}) was spiked into all samples for recovery determination. Interfering compounds were removed by solid—liquid chromatography using a glass column (0.6 10 cm) packed with 3 g of deactivated silica gel and eluting with 25 mL of n-exane, following the procedure of the EPA 3630C method. The elution solvent was evaporated until dryness under a gentle stream

of nitrogen, then the residue was dissolved in 200 μL of isooctane containing 10 ng μl^{-1} of deuterated n-tetracosan ($C_{24}D_{50}$) as Internal Standard.

The extracts were analyzed by gas chromatography coupled with quadrupole mass spectrometry. An Agilent 6850 GC/MS (Agilent Technologies Italia, SpA, Milan, Italy) was used. The separation was performed on a DB-XLB capillary column ($L = 60$ m, I.D. = 0.25 mm, $d_f = 0.25$ μm film thickness; J&W Scientific, Rancho Cordova, CA, USA). Helium was used as carrier gas with a constant linear flow of 1 mL min^{-1}. An autosampler was installed with a split/splitless injector. The injector was kept at 300 °C and 2 μL of extract were injected in splitless mode. The n-alkane analysis was performed under the following temperature program: temperature ramp from 60°to 300 at 6 °C min^{-1}, then isothermal hold at 300 °C for 20 min. The transfer line was kept at 305 °C.

The MS operated at 70 eV in EI mode. The chromatograms were acquired in SIM (single ion monitoring) mode operating at 57, 71, and 85 m/z values during the whole chromatographic run.

The n-alkanes were identified by matching the retention times of each peak in the sample chromatogram with those of standard solutions and by comparing mass spectra of the samples with those of the standards as well as with those from the NIST mass spectra library (NIST MS Search r. 2.0).

The internal standard method was used for n-alkane quantification based on the GC/MS signal obtained from the sum of three m/z values (57, 71, and 85). For all the investigated n-alkanes the detection limits were 0.9 ng m^{-3} with low volume samplers, and 0.1 ng m^{-3} in spring, with higher air volume sampler (last column in Table 1).

2.4. PCA computation

The Principal Component Analysis was performed using the statistical program *MATLAB©* (The Mathworks, Inc. 2008) and run on a 1.53 GHz (256 RAM), AMD *Athlon* personal computer.

3. Results and discussion

12 saccharides were determined in PM$_{2.5}$ samples: they included 4 monosaccharides — glucose, arabinose, mannose and galactose — as well as 3 sugar polyols (ribitol, erythritol and mannitol), 2 disaccharides (sucrose and mycose) and 3 anhydrosugars (levoglucosan, galactosan and mannosan).

3.1. Ambient concentrations and seasonal variation

Table 1 reports the mean values of the concentrations observed for each campaign and integrated on ≈3 weeks: minimum, maximum and mean values ± standard deviation (SD) (the term n.d. indicates that more than 90% of the measured values were below the detection limit). These individual concentrations were summed to compute the total sugar concentrations (tot sugars), the sum of the 3 anhydrosugars (tot burning) and the total concentration of the primary biomass sugars emitted by the ecosystem (tot bio), computed by excluding anhydrosaccharides, that are independent of biota living cycle.

In general, total concentrations of sugars were one order of magnitude higher in the cold seasons than those in summer/spring (13th row in Table 1). In fact, total sugar concentrations ranged from 401 ng m^{-3} in fall to 378 ng m^{-3} in winter at MS site and from 335 ng m^{-3} in fall to 368 ng m^{-3} in winter at rural SP site. Minimum concentrations were observed in summer (6–39 ng m^{-3}) and spring (28–53 ng m^{-3}).

As expected, PM$_{2.5}$ levels were higher in the cold seasons (mean values close to 32 μg m^{-3}, 25th row in Table 1.) with respect to

Table 1

Concentration values of each sugar and marker and meteorological parameters measured in the four seasons. For each campaign, the observed minimum and maximum concentration values (ng m^{-3}), average values and standard deviations are reported for the two sampling sites. The term 'n.d.' indicates the analytes showing more than 90% of the measured data values below the detection limit (<LOD).

	Main site				San Pietro				LOD (ng m^{-3})
	Minimum (ng m^{-3})	Maximum (ng m^{-3})	Average (ng m^{-3})	S.D. (ng m^{-3})	Minimum (ng m^{-3})	Maximum (ng m^{-3})	Average (ng m^{-3})	S.D. (ng m^{-3})	
Summer 2012									
Erythritol	n.d.	n.d.	n.d.	n.d.	n.d.	n.d.	n.d.	n.d.	1.3
Arabinose	n.d.	n.d.	n.d.	n.d.	n.d.	n.d.	n.d.	n.d.	0.8
Galactosan	n.d.	n.d.	n.d.	n.d.	n.d.	n.d.	n.d.	n.d.	0.9
Mannosan	n.d.	n.d.	n.d.	n.d.	n.d.	n.d.	n.d.	n.d.	1.4
Levoglucosan	<LOD	5.3	2.2	1.9	n.d.	n.d.	n.d.	n.d.	0.5
Ribitol	<LOD	21.0	4.0	7.0	<LOD	22.7	4.3	7.0	1.4
Mannose	n.d.	n.d.	n.d.	n.d.	n.d.	n.d.	n.d.	n.d.	1.1
Galactose	n.d.	n.d.	n.d.	n.d.	n.d.	n.d.	n.d.	n.d.	1.7
Mannitol	<LOD	12.8	3.1	3.9	3.9	50.7	27.0	5.7	1.0
Glucose	<LOD	2.7	0.9	0.8	<LOD	22.2	3.3	4.6	1.5
Sucrose	n.d.	n.d.	n.d.	n.d.	n.d.	n.d.	n.d.	n.d.	0.6
Mycose	n.d.	n.d.	n.d.	n.d.	n.d.	n.d.	n.d.	n.d.	1.7
Tot sugars	0.6	16.4	6.2	5.3	0.9	200.4	38.8	52.7	
Tot burning	0.6	5.3	2.2	1.9	0	57.0	5.4	11.2	
Tot bio	0.2	14.5	4.0	4.4	0.3	187.9	33.4	45.1	
%Burning	11.7	89.3	46.2	26.5	0	61.7	17.2	18.1	
%Bio	10.7	88.3	53.8	26.5	38.3	96.3	82.8	18.1	
C$_{29}$	<LOD	2.6	0.9	0.6	1.5	19.9	4.2	3.6	0.9
C$_{20-27}$	0.9	5.0	2.1	1.8	0.9	16.4	11.5	9.2	
C$_{28-33}$	0.9	5.4	2.2	1.8	0.9	15.0	12.9	9.8	
Tot alkanes C$_{20-33}$	1.2	10.2	4.1	1.8	9.6	87.8	22.9	17.8	
CPI C$_{20-33}$	n.d.	n.d.	n.d.	n.d.	n.d.	n.d.	n.d.	n.d.	
Tot CA	n.d.	n.d.	n.d.	n.d.	n.d.	n.d.	n.d.	n.d.	
Tot oxoCA	n.d.	n.d.	n.d.	n.d.	n.d.	n.d.	n.d.	n.d.	
PM$_{2.5}$	8.4	26.6	15.1	4.3	9.5	29.0	17.7	4.4	
Mixing height(m)	816	1252	974	132	668	1120	854	109	
Daily temperature (°C)	20.4	31.9	27.5	2.6	18.6	29.6	25.7	2.6	
Daily solar radiation (W m^{-2})	213	328	295	27	246	366	324	32	
Malonic acid	n.d.	n.d.	n.d.	n.d.	n.d.	n.d.	n.d.	n.d.	0.2
Succinic acid	n.d.	n.d.	n.d.	n.d.	n.d.	n.d.	n.d.	n.d.	0.4
Glutaric acid	n.d.	n.d.	n.d.	n.d.	n.d.	n.d.	n.d.	n.d.	0.1
Adipic acid	n.d.	n.d.	n.d.	n.d.	n.d.	n.d.	n.d.	n.d.	0.7
Pimelic acid	n.d.	n.d.	n.d.	n.d.	n.d.	n.d.	n.d.	n.d.	0.6
Azelaic acid	n.d.	n.d.	n.d.	n.d.	n.d.	n.d.	n.d.	n.d.	0.9
Maleic acid	n.d.	n.d.	n.d.	n.d.	n.d.	n.d.	n.d.	n.d.	0.8
Malic acid	n.d.	n.d.	n.d.	n.d.	n.d.	n.d.	n.d.	n.d.	0.8
Phthalic acid	n.d.	n.d.	n.d.	n.d.	n.d.	n.d.	n.d.	n.d.	0.3
Glycolic acid	n.d.	n.d.	n.d.	n.d.	n.d.	n.d.	n.d.	n.d.	0.6
2-Ketoglutaric acid	n.d.	n.d.	n.d.	n.d.	n.d.	n.d.	n.d.	n.d.	0.7
3-OH benzoic acid	n.d.	n.d.	n.d.	n.d.	n.d.	n.d.	n.d.	n.d.	0.4
4-OH benzoic acid	n.d.	n.d.	n.d.	n.d.	n.d.	n.d.	n.d.	n.d.	0.6
Pinonic acid	n.d.	n.d.	n.d.	n.d.	n.d.	n.d.	n.d.	n.d.	0.3
Fall 2012									
Erythritol	<LOD	3.6	1.7	1.1	n.d.	n.d.	n.d.	n.d.	1.0
Arabinose	<LOD	5.9	2.4	1.6	n.d.	n.d.	n.d.	n.d.	4.2
Galactosan	3.4	62.1	29.8	18.3	6.7	49.4	23.7	13.8	2.0
Mannosan	15.2	152.7	63.5	38.4	14.8	103.6	47.0	25.6	2.0
Levoglucosan	57.4	498.1	288.9	143.9	75.1	454.1	233.2	114.6	2.4
Ribitol	n.d.	n.d.	n.d.	n.d.	n.d.	n.d.	n.d.	n.d.	3.0
Mannose	n.d.	n.d.	n.d.	n.d.	n.d.	n.d.	n.d.	n.d.	
Galactose	<LOD	5.1	2.8	1.2	<LOD	6.6	2.6	1.4	1.6
Mannitol	<LOD	10.4	3.4	3.8	<LOD	23.2	4.3	6.0	2.6
Glucose	<LOD	12.4	6.9	2.9	<LOD	8.6	4.9	1.9	2.3
Sucrose	<LOD	15.8	4.6	4.3	<LOD	46.1	6.2	11.0	1.9
Mycose	n.d.	n.d.	n.d.	n.d.	n.d.	n.d.	n.d.	n.d.	2.2
Tot sugars	84.7	718.2	400.6	205.7	104.5	654.9	335.2	165.0	
Tot burning	69.4	675.8	382.2	198.7	96.4	550.1	303.9	153.3	
Tot bio	6.2	42.3	18.4	9.6	7.9	64.5	31.3	16.8	
%Burning	81.9	97.9	94.5	3.6	78.8	93.8	90.4	4.2	
%Bio	2.1	18.1	5.5	3.6	6.2	21.2	9.6	4.2	
C$_{29}$	<LOD	10.0	4.2	3.5	1.0	277.3	13.9	60.9	0.9
C$_{20-27}$	2.8	32.2	16.4	8.2	3.8	33.7	23.54	33.4	
C$_{28-33}$	1.5	20.9	10.3	9.4	5.5	54.2	76.88	86.8	
Tot alkanes C$_{20-33}$	3.2	59.4	25.4	16.2	3.7	1598.3	105.0	351.9	
CPI C$_{20-33}$	1.2	3.1	1.8	0.44	1.6	3.5	2.2	0.61	
Tot CA	35.5	330.3	167.4	109.6	29.8	316.3	114.8	89.5	
Tot oxoCA	15.1	147.4	74.8	50.4	16.3	165.7	61.1	47.8	
PM$_{2.5}$	6.2	70.7	31.0	17.2	10.2	64.4	27.7	16.2	

Table 1 (*continued*)

	Main site				San Pietro				LOD (ng m^{-3})
	Minimum (ng m^{-3})	Maximum (ng m^{-3})	Average (ng m^{-3})	S.D. (ng m^{-3})	Minimum (ng m^{-3})	Maximum (ng m^{-3})	Average (ng m^{-3})	S.D. (ng m^{-3})	
Mixing height (m)	99	857	365	153	50	817	257	96	
Daily temperature (°C)	10.0	15.9	12.6	2.7	6.8	16.2	11.1	2.5	
Daily solar radiation (W m^{-2})	5.3	121	70.6	37.7	5.7	148	85.4	46.0	
Malonic acid	2.4	100.8	29.7	33.1	4.6	65.0	33.3	25.7	0.2
Succinic acid	5.7	49.9	26.8	14.3	6.2	49.8	22.2	12.6	0.4
Glutaric acid	3.9	35.9	17.1	9.0	0.5	13.2	5.9	3.9	0.1
Adipic acid	1.3	7.1	3.5	1.9	1.2	7.3	3.0	1.7	0.7
Pimelic acid	1.4	7.9	3.2	1.6	0.9	4.0	2.0	1.1	0.6
Azelaic acid	2.9	25.3	10.0	7.1	0.4	22.4	8.3	5.9	0.9
Maleic acid	n.d.	n.d.	n.d.	n.d.	n.d.	n.d.	n.d.	n.d.	0.8
Malic acid	3.4	66.9	25.7	22.5	5.2	56.1	22.1	17.1	0.8
Phthalic acid	1.7	11.4	5.3	3.0	1.0	5.0	3.2	1.2	0.3
Glycolic acid	3.7	43.4	16.3	12.4	3.9	42.9	13.6	11.7	0.6
2-ketoglutaric acid	4.8	67.7	27.4	19.2	5.9	91.8	22.3	22.4	0.7
3-OH benzoic acid	0.4	2.9	2.0	0.6	0.1	2.0	1.9	0.5	0.4
4-OH benzoic acid	0.4	5.3	2.2	1.3	0.6	3.1	2.2	0.6	0.6
Pinonic acid	1.3	5.1	2.6	0.9	2.5	3.4	2.8	0.4	0.3
Winter 2013									
Erythritol	<LOD	10.2	2.8	2.4	<LOD	7.3	2.1	1.9	1.0
Arabinose	<LOD	15.9	9.5	5.5	<LOD	21.6	8.9	6.1	4.2
Galactosan	7.9	50.9	31.6	12.3	8.7	57.0	32.0	15.4	2.0
Mannosan	29.8	104.6	63.6	23.7	23.2	110.7	61.5	27.2	2.0
Levoglucosan	125.5	438.1	259.4	98.9	114.4	427.2	252.9	110.7	2.4
Ribitol	n.d.	n.d.	n.d.	n.d.	n.d.	n.d.	n.d.	n.d.	3.0
Mannose	n.d.	n.d.	n.d.	n.d.	n.d.	n.d.	n.d.	n.d.	
Galactose	1.8	6.0	3.0	1.1	<LOD	4.8	3.1	1.3	1.6
Mannitol	n.d.	n.d.	n.d.	n.d.	n.d.	n.d.	n.d.	n.d.	2.6
Glucose	3.6	11.2	5.6	1.7	3.6	8.7	5.4	1.4	2.3
Sucrose	<LOD	14.0	3.1	3.0	<LOD	4.9	2.6	1.2	1.9
Mycose	n.d.	n.d.	n.d.	n.d.	n.d.	n.d.	n.d.	n.d.	2.2
Tot sugars	181.6	642.3	378.5	140.0	161.7	670.2	368.5	158.4	
Tot burning	169.5	598.2	355	133.3	149	637	346	151	
Tot bio	12.1	44.1	23.9	8.2	10.2	38.6	22.1	8.2	
%Burning	89.0	95.3	93.5	1.5	90.9	95.5	93.7	1.3	
%Bio	4.7	11.0	6.5	1.5	4.5	9.1	6.3	1.3	
C$_{29}$	1.2	8.1	4.5	1.8	<LOD	17.1	3.1	4.1	0.9
C$_{20-27}$	4.7	34.7	23.6	14.2	10.4	36.3	16.4	4.0	
C$_{28-33}$	4.2	17.7	14.9	8.2	5.6	25.4	9.9	3.7	
Tot alkanes C$_{20-33}$	9.7	68.2	37.4	17.1	4.4	91.0	23.9	21.9	
CPI C$_{20-33}$	1.1	1.7	1.32	0.26	1.2	1.7	1.4	0.23	
Tot CA	51.6	458.3	249.3	122.3	44.0	527.5	247.9	139.2	
Tot oxoCA	15.5	149.0	83.4	43.0	15.6	161.2	87.7	55.7	
PM$_{2.5}$	12.5	71.7	32.8	13.7	14.7	86.5	34.6	19.4	
Mixing height (m)	102	1085	413	99	51	943	314	120	
Daily temperature (°C)	1.4	6.9	3.9	1.6	−0.8	7.5	2.6	1.0	
Daily solar radiation (W m^{-2})	13.7	130	80.8	34.5	9.2	160	92.0	48.4	
Malonic acid	4.3	63.6	26.8	21.1	2.9	92.0	32.7	25.7	0.2
Succinic acid	13.4	49.4	32.3	12.6	11.1	61.2	35.1	14.5	0.4
Glutaric acid	4.7	35.2	19.5	12.8	2.5	52.6	24.3	17.4	0.1
Adipic acid	0.9	9.6	4.7	1.9	1.7	8.5	4.6	1.8	0.7
Pimelic acid	3.3	4.7	4.1	0.5	1.4	7.6	5.3	2.3	0.6
Azelaic acid	10.5	34.1	17.2	7.0	5.7	29.0	16.0	6.9	0.9
Maleic acid	14.3	158.6	67.8	37.8	8.4	134.2	57.4	39.3	0.8
Malic acid	3.9	38.8	20.3	11.5	2.9	46.2	22.5	15.0	0.8
Phthalic acid	2.3	28.5	11.8	6.7	2.3	35.5	11.8	8.5	0.3
Glycolic acid	5.9	32.0	14.2	6.5	4.3	34.4	16.9	9.5	0.6
2-Ketoglutaric acid	11.1	97.0	46.8	28.4	2.3	137.8	45.4	33.7	0.7
3-OH benzoic acid	0.5	3.9	2.4	0.8	0.1	5.1	2.9	1.0	0.4
4-OH benzoic acid	0.9	5.3	3.1	1.4	0.6	7.5	3.7	1.7	0.6
Pinonic acid	n.d.	n.d.	n.d.	n.d.	2.9	6.4	3.9	1.2	0.3
Spring 2013									
Erythritol	n.d.	n.d.	n.d.	n.d.	n.d.	n.d.	n.d.	n.d.	0.4
Arabinose	n.d.	n.d.	n.d.	n.d.	n.d.	n.d.	n.d.	n.d.	0.7
Galactosan	<LOD	10.6	1.3	2.7	n.d.	n.d.	n.d.	n.d.	0.3
Mannosan	0.4	12.4	2.0	3.0	<LOD	1.7	0.7	0.4	0.3
Levoglucosan	2.1	69.3	13.5	17.2	<LOD	8.1	3.8	2.5	0.8
Ribitol	n.d.	n.d.	n.d.	n.d.	n.d.	n.d.	n.d.	n.d.	0.6
Mannose	<LOD	35.6	4.0	9.2	<LOD	35.6	4.0	9.2	0.8
Galactose	<LOD	9.4	1.2	2.4	n.d.	n.d.	n.d.	n.d.	0.7
Mannitol	<LOD	72.1	14.7	17.6	<LOD	14.6	6.3	4.9	0.8
Glucose	<LOD	40.4	6.7	9.9	<LOD	29.0	7.3	9.2	0.7

Table 1 (_continued_)

	Main site				San Pietro				LOD (ng m^{-3})
	Minimum (ng m^{-3})	Maximum (ng m^{-3})	Average (ng m^{-3})	S.D. (ng m^{-3})	Minimum (ng m^{-3})	Maximum (ng m^{-3})	Average (ng m^{-3})	S.D. (ng m^{-3})	
Sucrose	<LOD	7.0	1.7	1.9	n.d.	n.d.	n.d.	n.d.	1.0
Mycose	2.0	15.8	7.3	5.1	<LOD	6.0	5.3	5.6	0.9
Tot sugars	10.0	253.2	52.9	60.2	7.0	73.8	28.3	21.0	
Tot burning	2.7	92.3	16.8	22.8	1.8	9.7	4.5	2.9	
Tot bio	1.4	160.9	36.2	38.3	6.0	66.5	23.8	20.1	
%Burning	12.2	66.3	32.5	14.4	4.7	55.6	20.4	13.9	
%Bio	33.7	27.8	67.5	14.4	44.4	95.3	79.6	13.9	
C$_{29}$	1.4	3.9	2.7	0.7	0.8	1.9	1.4	0.4	0.1
C$_{20-27}$	0.9	10.9	5.7	1.9	0.5	3.2	1.6	0.9	
C$_{28-33}$	4.0	14.4	9.1	5.1	2.0	4.9	3.1	1.4	
Tot alkanes C$_{20-33}$	9.1	20.1	14.5	3.1	2.4	4.8	4.3	1.1	
CPI C$_{20-33}$	2.2	9.5	5.6	2.2	2.4	9.7	6.9	2.69	
Tot CA	5.3	22.4	45.2	10.1	3.2	17.8	11.3	4.2	
Tot oxoCA	3.8	36.8	11.1	8.4	1.3	14.5	7.3	4.0	
PM$_{2.5}$	4.2	16.6	8.3	4.3	4.5	19.0	8.5	4.4	
Mixing height (m)	679	1348	955	197	566	1145	793	148	
Daily temperature (°C)	10.6	21.8	17.2	2.5	9.8	20.6	16.2	2.6	
Daily solar radiation (W m^{-2})	113	317	228	59.6	86.6	345	245	71.7	
Malonic acid	<LOD	2.0	0.9	0.6	<LOD	2.0	0.8	0.6	0.2
Succinic acid	<LOD	4.7	2.0	1.4	<LOD	5.3	2.8	1.5	0.4
Glutaric acid	<LOD	1.7	0.5	0.4	<LOD	1.4	0.5	0.4	0.1
Adipic acid	n.d.	n.d.	n.d.	n.d.	n.d.	n.d.	n.d.	n.d.	0.7
Pimelic acid	n.d.	n.d.	n.d.	n.d.	n.d.	n.d.	n.d.	n.d.	0.6
Azelaic acid	n.d.	n.d.	n.d.	n.d.	n.d.	n.d.	n.d.	n.d.	0.9
Maleic acid	n.d.	n.d.	n.d.	n.d.	n.d.	n.d.	n.d.	n.d.	0.8
Malic acid	<LOD	29.1	6.9	7.1	0.7	7.6	3.0	1.8	0.8
Phthalic acid	n.d.	n.d.	n.d.	n.d.	n.d.	n.d.	n.d.	n.d.	0.3
Glycolic acid	1.0	7.7	4.2	2.0	0.6	10.6	3.8	2.6	0.6
2-Ketoglutaric acid	n.d.	n.d.	n.d.	n.d.	n.d.	n.d.	n.d.	n.d.	0.7
3-OH benzoic acid	n.d.	n.d.	n.d.	n.d.	n.d.	n.d.	n.d.	n.d.	0.4
4-OH benzoic acid	n.d.	n.d.	n.d.	n.d.	n.d.	n.d.	n.d.	n.d.	0.6
Pinonic acid	n.d.	n.d.	n.d.	n.d.	n.d.	n.d.	n.d.	n.d.	0.3

those in spring/summer campaigns (8–18 μg m^{-3} range). In cold seasons, total sugars strongly contribute to the PM mass, comprising nearly 1.2% of the PM$_{2.5}$ mass (expressed as ratio tot sugars/PM%), while these percentages decreased to 0.3% during warmer seasons.

The increased level of atmospheric pollution during the cold seasons can be explained by the combination of higher anthropogenic emissions from domestic heating and weather conditions in the Po Valley (Balducci and Cecinato, 2010; Carbone et al., 2010; Bigi and Ghermandi, 2011; Perrone et al., 2012; Pietrogrande et al., 2013a, 2014). Temperature showed significant variation from the colder winter (3.9 and 2.6 °C mean values at MS and SP, respectively) to the warmer summer (≈26 °C) through intermediate fall and spring (≈12 and 17 °C, respectively). Also daily solar radiation showed strong seasonality with nearly constant low values in the cold periods (mean values of 71÷81 W m^{-2} and 85÷92 W m^{-2} at MS and SP, respectively) in comparison with high values in spring (≈230 W m^{-2}) and summer (≈310 W m^{-2}, 28th row in Table 1).

Fall/winter were characterized by low mixing layer with mean values in the 257–413 m range, and summer/spring by higher values, i.e., on average 964 m in MS and 823 in SP sites (26th row in Table 1). As a consequence, the stagnant conditions in fall/winter accumulate the pollutants that are confined to the first hundred meters of the atmosphere; otherwise the high mixing layer height promotes dispersion of the organic compounds in the atmosphere in the warmer seasons (Balducci and Cecinato, 2010; Carbone et al., 2010; Bigi and Ghermandi, 2011; Perrone et al., 2012; Pietrogrande et al., 2013a). This dependence is supported by the good correlation ($r = 0.94$) found between total sugar concentrations and mixing layer heights and may explain the similarity between the data obtained during the winter and fall periods, that are characterized by similar atmospheric conditions.

3.2. Contribution of biomass burning

The contribution of biomass burning was evaluated in the different seasons by computing the total concentrations of burning-sugars and investigating their seasonal evolution (Fig. 1).

Anhydrosugars were by far the dominant sugars in fall and winter, both on a relative and an absolute basis: higher levels were
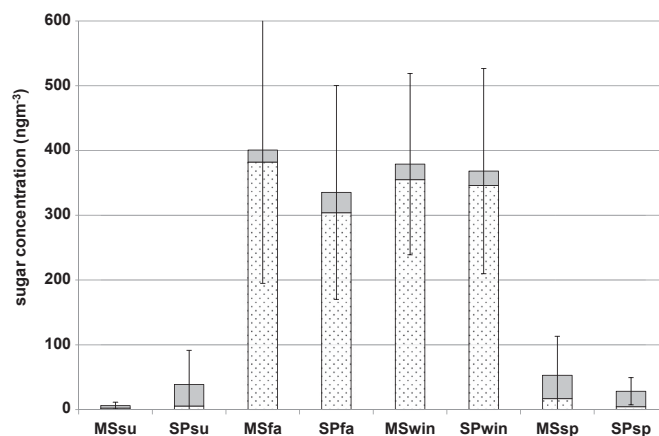
Fig. 1. Seasonal evolution of concentrations of total burning-sugars (dashed bars) and total biosystem sugars (gray bars) in monitoring campaigns: a bar indicates 1 standard deviation of the mean values.

found for levoglucosan in fall/winter (mean 271 ng m^{-3}), followed by mannosan (mean 53 ng m^{-3}) and galactosan (mean 29 ng m^{-3}). These data clearly indicate that biomass burning is nearly the only source for particulate saccharides in fall/winter, comprising nearly 94% of the total sugars at both sites (16th row in Table 1). At our knowledge, these data are the first results concerning the Emilia Romagna region, that is the Eastern part of the Po Plain as densely populated as the Lombardia region located at the Western side of the plain. This conclusion is consistent with other studies in Lombardia which demonstrated that wood burning for domestic heating is a diffuse regional source during fall and winter, that produces 25–30% of PM$_{2.5}$ (Perrone et al., 2012) and contributes with more than 75% of the benzo(a)pyrene pollution (Belis et al., 2011). Similar levels of burning-sugars (100–500 ng m^{-3}) were measured in urban and rural areas in Central and Northern Europe, where residential wood combustion has been identified as an important source of air pollution (Oliveira et al., 2007; Puxbaum et al., 2007; Caseiro et al., 2009; Wang et al., 2011; Giannoni et al., 2012; Yang et al., 2013). A strong season trend is evident, since the impact of biomass burning is strongly reduced in summer (nearly 32%) and spring (≈25%, Table 1 and Fig. 1). This trend was also observed in several urban and rural sites where the contribution of biomass burning to total sugars decreased form nearly 90% during winter to 10% during summer (Jia et al., 2010; Holden et al., 2011; Fu et al., 2012; Giannoni et al., 2012).

3.2.1. Relationship with low molecular weight carboxylic acids

To further investigate the contribution of biomass burning, low molecular weight carboxylic acids were studied as an extension of the previous paper concerning cold seasons (Pietrogrande et al., 2014). In fact, it has been reported that biomass burning emissions are enriched in carboxylic acids that can be directly emitted from the combustion process or secondarily produced by photochemical oxidation of organic precursors (Mazzoleni et al., 2007; Jia et al., 2010; Wang et al., 2011; Van Drooge et al., 2012; Yang et al., 2013). The investigated acids were C$_3$–C$_9$ linear dicarboxylic acids, maleic and phthalic acids, oxo-hydroxy carboxylic acids, namely glycolic, malic, and 3- and 4-hydroxy benzoic acids, pinonic and 2-ketoglutaric acids (29th–42nd rows in Table 1).

These acids were not detected in summer (more than 90% of the measured data values were below the detection limit) and showed low concentrations in spring (mean total concentration, tot CA ≈30 ng m^{-3}). This result may be explained by the high mixing layer that probably diluted the pollutants generated by the urban activities and therefore reduced secondary aerosol formation, despite the high solar radiation (≈250 W m^{-2}). On the other hand, the highest levels were observed in fall (mean tot CA: 141 ng m^{-3}) and winter (mean tot CA: 249 ng m^{-3}) when the stagnant atmospheric conditions and the high anthropogenic emissions favored accumulation of anthropogenic precursors that promoted their photooxidation. This finding of higher DCA concentrations in wintertime than in summer is inconsistent with the observations in most other cities in the world (Carvalho et al., 2003; Wang et al., 2006; Lee et al., 2006; Oliveira et al., 2007; Ho et al., 2011; Wang et al., 2011; Hyder et al., 2012; Yang et al., 2013).

Throughout the year, the total CA concentrations show good correlation (r ≈ 0.92) with those of burning-sugars, confirming the common involvement in emissions from wood burning (Mazzoleni et al., 2007; Jia et al., 2010; Wang et al., 2011; Van Drooge et al., 2012; Yang et al., 2013).

Among the measured carboxylic acids, malic and glycolic acids were the most abundant in the spring samples (≈2 ng m^{-3}), followed by succinic acid. On contrast, 2-ketoglutaric, malonic and maleic acids (≈30 ng m^{-3}) showed the highest concentration in fall/winter, followed by succinic acid. These most abundant C$_3$–C$_4$

acids are specific chemical markers of secondary photo-oxidation reactions in the atmosphere (Kawamura and Yasui, 2005; Lee et al., 2006). Therefore, their strong enrichment (>10 time) from spring to winter suggests strong contribution of photochemical oxidation of anthropogenic precursors. This conclusion is also supported by the excellent correlations (r 0.97) found throughout the year between burning-sugars and the individual acids that have been found the most abundant acids in biomass smoke, i.e., glycolic, malonic, malic and succinic acids (Wang et al., 2006; Lee et al., 2006; Oliveira et al., 2007; Bi et al., 2008; Hsieh et al., 2008; Tsai et al., 2013).

Accordingly, the concentrations of burning-sugars were very well correlated (r = 0.97) with the total concentrations of oxo-hydroxy carboxylic acids (tot oxoCA, 24th row in Table 1), which are intermediates in the oxidation of organic precursors originated from both biogenic and anthropogenic sources (Kawamura and Yasui, 2005; Lee et al., 2006; Li et al., 2013; Pietrogrande et al., 2014).

3.3. Season variation of primary biological sugars

The ambient concentration, seasonal variation, and urban/rural comparison of bio-sugars were separately investigated to single out the contribution of emissions associated with primary biological particles (Fig. 1). It must be underlined that these contributions could be influenced by the fact that bio-sugars are generally more represented by the coarse than by the fine particles of atmospheric aerosol, in variable fractions from 10% to 30% in PM$_{2.5}$ (Simoneit et al., 2004; Fuzzi et al., 2007; Yttri et al., 2007; Pio et al., 2008; Bauer et al., 2008), with the exception of some sugars displaying an enrichment in the fine mode over the coarse mode (Medeiros et al., 2006; Ma et al., 2009; Jia et al., 2010; Jia and Fraser, 2011; Wang et al., 2011; Fu et al., 2012). Therefore, their concentrations in the present study may represent only a fraction of the total primary biologically derived carbon present in atmospheric PM.

In general, the bio-sugars show nearly constant absolute abundance thought the year at both the sites (mean 24 ± 11 ng m^{-3}, 15th row in Table 1). However, the data clearly show that the relative contribution to PM$_{2.5}$ mass strongly varies with seasons increasing from nearly 0.1% in cold seasons to 0.3% in summer/spring. The low absolute values of sugar concentrations in warm season may be partially explained by the general contaminant dispersion into the atmosphere occurring during the warm seasons as a consequence of the high mixing layer heights (mean values 964 m at MS and 823 at SP, 26th row in Table 1).

Over all the sampling periods, mannitol was the major bio-sugar found in the aerosols with concentrations ranging from approximately 3 to 27 ng m^{-3} (9th row in Table 1). Glucose was the second most abundant saccharide (mean 5 ng m^{-3}, 10th row in Table 1), followed by the disaccharides sucrose and mycose (≈2 ng m^{-3}, 11th and 12th rows in Table 1). The monosaccharides galactose, mannose and arabinose and the polyols ribitol and erythritol were also present in lower concentrations in most samples (Table 1).

A detailed investigation of the distribution profile of bio-sugars shows clear seasonality to indicate the contribution of the different sources of the saccharides (Fig. 2a,b).

In the colder seasons, the sugar distribution profiles are dominated by monosaccharides, mainly glucose (≈6 ng m^{-3}), followed by arabinose and galactose (each ≈3 ng m^{-3}) (Fig. 2a). The prevalence of these compounds may be related to wood combustion, since they have been found in large quantity in wood smoke, as hemicellulose polysaccharides emitted as uncombusted material during the burning process (Medeiros et al., 2006; Wang et al., 2011). Glucose, in particular, is commonly present at higher levels in vascular plants, while arabinose and galactose are predominant
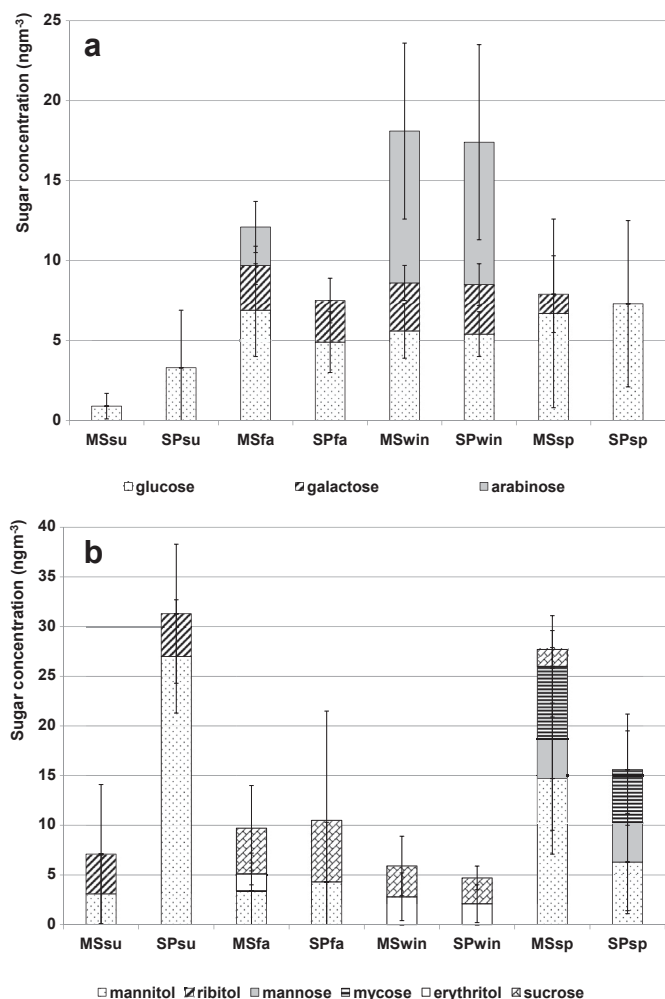
Fig. 2. Seasonal evolution of concentrations of primary bio-sugars in monitoring campaigns: a bar indicates 1 standard deviation of the mean values of each investigated sugar. 2a: concentrations of bio-saccharides related to wood burning: glucose, galactose and arabinose; 2b: concentrations of bio-saccharides related to primary biological aerosol particles: mannitol, ribitol, mannose, mycose, erythritol and sucrose.

sugars in pectin, a polysaccharide contained in nonwoody tissues, such as leaves and needles (Medeiros et al., 2006). Similar results were found in smoke-impacted samples in many other locations in the world (Simoneit et al., 2004; Medeiros et al., 2006; Pio et al., 2008; Jia et al., 2010).

The other sugars were nearly absent in fall/winter (Fig. 2b), that is consistent with the finding that the concentrations of sugar polyols and disaccharides are not significantly influenced by biomass burning (Medeiros et al., 2006). The exception is sucrose that is present at ≈ 5 ng m^{-3} level in late autumn (11th row in Table 1), likely reflecting the enhanced agricultural activities that release soil biota from farmland soils (Simoneit et al., 2004; Tsai et al., 2013). In fact, sucrose was found in some fungi and spores (Jia et al., 2010), though it is usually considered a tracer for airborne pollen in atmospheric PM (Fu et al., 2012). Also the reduced sugars mannitol and erythritol were detected in late autumn (≈ 1 ng m^{-3}), this result may be related with the contribution from microbially degraded materials during the period of leaf senescence and decay (Simoneit et al., 2004; Tsai et al., 2013).

In the warmer seasons, the sugar distribution profiles indicate the major contribution of bio-sugars than can be related to primary biological aerosol particles (Fig. 2b). In fact, the dominating sugar is

mannitol, with a maximum of 27 ng m^{-3} in summer at the rural site (9th row in Table 1). Mannitol has been found as the major sugar polyol in bacteria, fungi, lower plants and invertebrates, serving as storage or transport carbohydrate and cell protectant against external stresses (Elbert et al., 2007). The highest concentration of mannitol in summer has been explained by the increased emissions from vegetation detritus and fungal spores as a result of external stressors of heat (Medeiros et al., 2006; Burshtein et al., 2011).

Concentration of mannitol is strongly covaried with that of ribitol, the pentose alcohol formed by the reduction of ribose, with maximum values observed in summer (6th row in Table 1, Fig. 2b).

Glucose was found as the second most abundant species throughout the growing season, with higher abundance in spring (mean 7 ng m^{-3}, 10th row in Table 1), in comparison with summer (mean 2 ng m^{-3}). It is the most common monosaccharide present in vascular plants and is an important source of carbon for soil microorganisms (Tominaga et al., 2011; Fu et al., 2012). Since its presence in the atmospheric PM$_{2.5}$ can be originated from primary biological aerosol particles (fresh leaf surfaces, pollen, spores, fungi) and fugitive soil, the increase with the growing season parallels carbon cycling in plant growth and the enhanced agricultural activity that promotes exposure to the air of soil containing wheat root (Simoneit et al., 2004; Medeiros et al., 2006; Wang et al., 2011; Fu et al., 2012). It must be underlined that such a bio-sugar is also emitted as uncombusted material during wood combustion and for this reason it is abundant also in the colder seasons (Medeiros et al., 2006; Wang et al., 2011).

Mycose is one of the dominating sugars in spring (mean 7 ng m^{-3}, 12th row in Table 1): this may be related to the major synthesis of primary sugars early in the growing season. In fact, mycose, as the most common disaccharide in symbiotic fungal tissues, is present in a large variety of microorganisms (fungi, bacteria, yeast), higher plants and invertebrates (Simoneit et al., 2004). Also mannose, a monosaccharide present in hemicellulose polysaccharides, was found in spring (mean 4 ng m^{-3}, 7th row in Table 1) (Medeiros et al., 2006).

Finally, the urban and rural sites were compared by subjecting the measured concentrations to the Student's t test for verifying the statistically significant differences at confidence level of 95% (in Fig. 2a,b error bars are standard deviations of the mean values). In general, the sites show a close similarity in sugar concentrations, which indicates small influence of specific local sources yielding a common background regional profile homogenously distributed all over the investigated area. Such a similarity between the urban and rural sites has been already found in a previous study in a local area around Bologna (Pietrogrande et al., 2013a).

The only exception is summer, when the concentrations of mannitol and ribitol are significantly higher at the rural site, that is consistent with enhanced emissions from vegetation, soil dust and associated biota in the farmland (Simoneit et al., 2004; Rogge et al., 2007; Fu et al., 2012).

3.3.1. Relationship with n-alkanes

In order to further investigate the contribution of biogenic emissions, the study was extended to n-alkane homologous series, as biogenic biomarkers especially suited for discriminating between the contribution of biogenic and anthropogenic sources (Standley and Simoneit, 1987; Zheng et al., 2002; Jia et al., 2010; Pietrogrande et al., 2010; Van Drooge et al., 2012).

These compounds are emitted into the atmosphere by a large variety of sources, including biogenic sources from epicuticular waxes of vascular plants, anthropogenic combustion of fossil fuels and resuspension of deposited material from these sources. A specific bio signature can be identified for n-alkanes emitted from primary biogenic sources, since they reflect the biochemical

specificity of the biosystem metabolism characterized by higher concentrations of C_{29}–C_{31} terms with a strong odd carbon number predominance (Standley and Simoneit, 1987). Consequently, the carbon preference index (CPI, i.e., the relative abundance of odd versus even isomers) assumes high values for vegetation detritus and low values close to 1 for traffic emissions (Standley and Simoneit, 1987; Zheng et al., 2002; Jia et al., 2010; Pietrogrande et al., 2010; Van Drooge et al., 2012).

In this study the C_{20}–C_{33} terms of n-alkane series were investigated, as the most commonly found in atmospheric PM (e.g., Standley and Simoneit, 1987; Zheng et al., 2002; Jia et al., 2010). The concentrations of each C_{20}–C_{33} term were added together to obtain the total alkane content in $PM_{2.5}$ samples (tot alkanes, 21st row in Table 1). It must be underlined that the reported values measured in $PM_{2.5}$ samples may represent only a fraction of the total n-alkanes, since the n-alkanes emitted from biological sources may concentrate more in the coarse than in the fine fraction of atmospheric aerosol (Simoneit et al., 2004; Fuzzi et al., 2007; Yttri et al., 2007; Pio et al., 2008; Wang et al., 2011; Fu et al., 2012).

The n-alkane concentrations were low in the warmer seasons: most terms were below the detection limit in summer and the total concentration values were in the 4–14 ng m^{-3} range in spring. This behavior parallels the trend of the other pollutants, as a consequence of the general contaminant dispersion into the atmosphere due to the high mixing layer heights during the warm seasons (Table 1, 26th row). The concentrations increased in fall/winter, characterized by stagnant atmospheric conditions and enhanced anthropogenic emissions, to reach values ranging from 24 to 37 ng m^{-3} and a maximum of 105 ng m^{-3} in fall in the rural site.

In addition, a clear seasonal trend can be observed in the distribution profile of the series terms, described by the C_{29} concentration, total concentration of C_{20}–C_{27} and C_{28}–C_{33} n-alkanes (18th–20th rows in Table 1) and CPI values (22nd row).

In spring the most abundant term is C_{29} and the terms $C > C_{25}$ exhibit odd carbon number predominance, yielding elevated CPI values (≈ 6). This pronounced plant wax signature is a good indication of the predominance of biogenic sources from terrestrial higher plants and supports the above reported results on the dominating role of primary biogenic emissions, that parallels the vegetation activity in the ecosystem in warmer seasons.

In contrast, in fall/winter samples nearly 60% of the total measured n-alkanes was accounted by the n-alkanes with less than C_{27}, known mainly as emitted from fossil fuel combustion sources, particularly motor vehicle exhaust (≈ 4 ng m^{-3}, 19th row in Table 1) (Zheng et al., 2002). Accordingly, the measured CPI values were close to unity (1.3–2.2, 22nd row in Table 1), confirming the greater contribution from fossil carbon sources relative to biogenic sources.

3.4. Seasonal variation using Principal Component Analysis

The Principal Component Analysis was applied to the dataset in order to summarize the obtained results and make the differences and similarities in the sugar profiles more visible. In fact, the use of PCA could compress the original matrix and extract useful information by removing redundant information and determining the factors that account for the greatest variance (Vandeginste et al., 1998; Brinkman et al., 2009).

The data set comprised the concentrations of the quantified analytes in all the samples collected in the 4 seasons at the two sites ($n = 148$). 18 variables were chosen for the PCA model, including individual sugar concentrations, total quantities of carboxylic acids and n-alkanes, CPI values and meteorological parameters (Table 2).

In this study, the Varimax rotation was used to redistribute the variance in order to create more interpretable factor loadings and scores (Vandeginste et al., 1998). The PCA factor loadings, which

Table 2
Principal components' loading values and percentage of variance explained by three PCs explaining cumulative variance of 81%. The bold font refers to the loading (absolute) values 0.3 included in PC interpretations. Rotation method is Varimax with Kaiser normalization.

Variables	PCA1	PCA2	PCA3
Erythritol	0.20	−0.21	**−0.28**
Arabinose	**0.32**	−0.12	−0.02
Galactosan	**0.33**	−0.04	0.02
Mannosan	**0.32**	−0.02	0.03
Levoglucosan	**0.32**	−0.02	0.05
Ribitol	0.03	0.09	**−0.54**
Mannose	−0.14	**−0.58**	0.08
Galactose	**0.33**	−0.20	−0.07
Mannitol	−0.02	−0.22	**−0.43**
Glucose	**0.29**	−0.12	0.02
Sucrose	0.05	0.04	0.19
Mycose	−0.21	−0.19	**0.42**
Tot alkanes	**0.29**	0.16	0.01
CPI	**−0.31**	−0.18	0.03
Tot CA	**0.32**	0.05	0.15
Mixing height (m)	**−0.36**	−0.03	−0.16
Daily temperature (°C)	**−0.31**	0.03	−0.18
Daily solar radiation (W m^{-2})	**−0.32**	−0.03	−0.20
Variance (%)	58%	13	10%
Cumulative variance (%)		71	81%

represent the correlation between the factors and variables, are given in Table 2 for the main PCAs in descending order of the corresponding eigenvalues. Three components were retained for further interpretation, since they accounted for 81% of the variability in the original data. Only loading (absolute) values greater than or equal to ± 0.3 were included in PC interpretations (bold values in Table 2).

Component 1, explaining most of the variance (58%), clearly indicates biomass burning source, since it has high positive loadings of anhydrosugars, arabinose, galactose and glucose, total carboxylic acids and total alkanes, that are organic markers emitted during the burning process (Medeiros et al., 2006; Wang et al., 2011). In addition, PC1 has negative loadings of the meteorological parameters and CPI values (−0.3), that assume higher values in spring/summer. Therefore, this component may be associated to biomass burning in cold seasons.

Component 2 (explaining 12% of variance) is mainly loaded by mannose (≈ -0.6) that was found nearly exclusively in spring.

Component 3 (explaining 10% of variance) has high loadings of primary bio-sugars, namely ribitol and mannitol (≈ -0.5), which are the most abundant biogenic sugars in summer, and mycose (0.5) that is a dominant sugar in spring.

The two-dimensional score plot in the PC1 and PC3 coordinates clearly shows discrimination of the PM samples according to seasonality (Fig. 3): the main separation is along the PC1 axis based on the emissions from biomass burning, with fall/winter samples having high PC1 values and summer/spring samples located at the far left, negative end of PC1 axis. PC3 axis discriminates between summer and spring samples, since it reflects the seasonality of bio-sugar production, with greater contributions of ribitol and mannitol in summer and high levels of mycose in spring.

The samples collected at the two sites cluster closely in the score plot, indicating close similarity between their $PM_{2.5}$ composition that suggests a homogeneous impact of sugar sources all over the region. The only exceptions are summer samples that are somewhat separated, with SP samples characterized by lower PC3 values indicating higher levels of erythritol, ribitol and mannitol (Fig. 3): this behavior is consistent with the enhanced release from vegetation physiological activities and from farmland soils during the agricultural activities in the rural area.
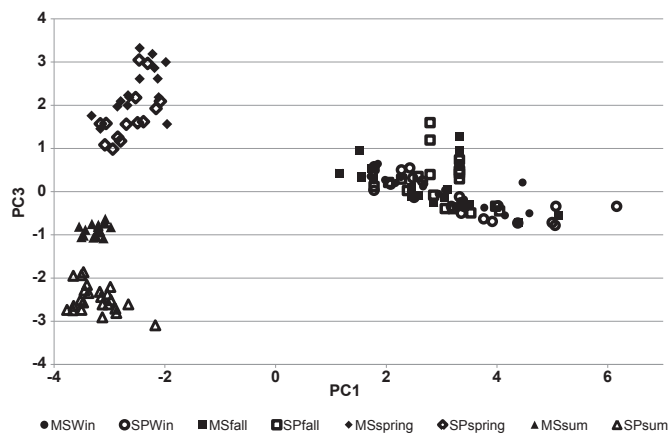
Fig. 3. Score plot of PC1 and PC3 components of the PCA model.

4. Conclusions

This study on the PM chemical composition of sugars indicates strong seasonality of emission sources with fall/winter aerosols being dominated by emissions from wood burning for domestic heating. The strong impact of biomass burning on air quality is further enhanced by the significant production of secondary organic aerosols from primary smoke precursors, as suggested by high concentrations of low molecular weight carboxylic acids.

Spring/summer samples are characterized by primary biological aerosols such as plant debris, fungal spores and biologically active surface soils due to enhanced sugar production and utilization by the ecosystem in the warm seasons.

The investigated saccharides by themselves cannot provide exhaustive information to differentiate biogenic inputs, since they can derive from primary emissions from the biosystem and from the burning processes as uncombusted material. Consequently, future research is needed to determine the concentration patterns of sugars and other compounds in order to obtain additional source-specific profiles that are needed for source receptor modeling for atmospheric samples. In particular, other polar and apolar organic tracers of primary combustion sources are under investigation in the framework of the Supersito project. They include lignin phenols, polycyclic aromatic hydrocarbons and aliphatic hydrocarbons to give more insight on local contributions from biomass burning on air quality of the polluted Po Plain (forthcoming part 3 of the present paper).

Acknowledgments

References

Balducci, C., Cecinato, A., 2010. Particulate organic acids in the atmosphere of Italian cities: are they environmentally relevant? Atmos. Environ. 44, 652–659.

Bauer, H., Schueller, E., Weinke, G., Berger, A., Hitzenberger, R., Marr, I.L., Puxbaum, H., 2008. Significant contributions of fungal spores to the organic carbon and to the aerosol mass balance of the urban atmospheric aerosol. Atmos. Environ. 42, 5542–5549.

Belis, C.A., Cancelinha, J., Duane, M., Forcina, V., Pedroni, V., Passarella, R., Tanet, G., Dous, K., Piazzalunga, A., Bolzacchini, E., Sangiorgi, G., Perrone, M.G., Ferrero, L.,

Fermo, P., Larsen, B.R., 2011. Sources for PM air pollution the Po Plain, Italy: I. Critical comparison of methods for estimating biomass burning contributions to benzo(a)pyrene. Atmos. Environ. 45, 7266–7275.

Bi, X., Simoneit, B.R.T., Sheng, G., Ma, S., Fu, J., 2008. Composition and major sources of organic compounds in urban aerosols. Atmos. Res. 88, 256–265.

Bigi, A., Ghermandi, G., 2011. Particle number size distribution and weight concentration of background urban aerosol in a Po Valley site. Water Air Soil Pollut. 220, 265–278.

Brinkman, G.L., Milford, J.B., Schauer, J.J., Shafer, M.M., Hannigan, M.P., 2009. Source identification of personal exposure to fine particulate matter using organic tracers. Atmos. Environ. 43, 1972–1981.

Burshtein, N., Lang-Yona, N., Rudich, Y., 2011. Ergosterol, arabitol and mannitol as tracers for biogenic aerosols in the eastern Mediterranean. Atmos. Chem. Phys. 11, 829–839.

Carbone, C., Decesari, S., Mircea, M., Giulianelli, L., Finessing, E., Rinaldi, M., Fuzzi, S., Marinoni, A., 2010. Size-resolved aerosol chemical composition over the Italian Peninsula during typical summer and winter conditions. Atmos. Environ. 44, 5269–5278.

Carvalho, A., Pio, C., Santos, C., 2003. Water-soluble hydroxylated organic compounds in German and Finnish aerosols. Atmos. Environ. 37, 1775–1783.

Caseiro, A., Bauer, H., Schmidl, C., Pio, C.A., Puxbaum, H., 2009. Wood burning impact on PM10 in three Austrian regions. Atmos. Environ. 43, 2186–2195.

Deserti, M., Savoia, E., Cacciamani, C., Golinelli, M., Kerschbaumer, A., Leoncini, G., Selvini, A., Paccagnella, T., Tibaldi, S., 2001. Operational meteorological preprocessing at Emilia-Romagna ARPA meteorological service as a part of a decision support system for air quality management. Int. J. Environ. Pollut. 16, 571–582.

Elbert, W., Taylor, P.E., Andreae, M.O., Poschl, U., 2007. Contribution of fungi to primary biogenic aerosols in the atmosphere: wet and dry discharged spores, carbohydrates, and inorganic ions. Atmos. Chem. Phys. 7, 4569–4588.

Fu, P., Kawamura, K., Kobayashi, M., Simoneit, B.R.T., 2012. Seasonal variations of sugars in atmospheric particulate matter from Gosan, Jeju Island: significant contributions of airborne pollen and Asian dust in spring. Atmos. Environ. 55, 234–239.

Fuzzi, S., Decesari, S., Facchini, M.C., Cavalli, F., Emblico, L., Mircea, M., Andreae, M.O., Trebs, I., Hoffer, A., Guyon, P., Artaxo, P., Rizzo, L.V., Lara, L.L., Pauliquevis, T., Maenhaut, W., Raes, N., Chi, X.G., Mayol-Bracero, O.L., Soto-Garcia, L.L., Claeys, M., Kourtchev, I., Rissler, J., Swietlicki, E., Tagliavini, E., Schkolnik, G., Falkovich, A.H., Rudich, Y., Fisch, G., Gatti, L.V., 2007. Overview of the inorganic and organic composition of size-segregated aerosol in Rondonia, Brazil, from the biomass-burning period to the onset of the wet season. J. Geophys. Res. 112, D01201. http://dx.doi.org/10.1029/2005JD006741.

Giannoni, M., Martellini, T., Del Bubba, M., Gambaro, A., Zangrando, R., Chiari, M., Lepri, M., Cincinelli, A., 2012. The use of levoglucosan for tracing biomass burning in PM2.5 samples in Tuscany (Italy). Environ. Pollut. 167, 7–15.

Ho, K.F., Ho, S.S.H., Lee, S.C., Kawamura, K., Zou, S.C., Cao, J.J., Xu, H.M., 2011. Summer and winter variation of dicarboxylic acids, fatty acids and benzoic acid in PM$_{2.5}$ in Pearl Delta River Region, China. Atmos. Chem. Phys. 11, 2197–2208.

Holden, A.S., Sullivan, A.P., Munchak, L.A., Kreidenweis, S.M., Schichtel, B.A., Malm, W.C., Collett Jr., J.L., 2011. Determining contributions of biomass burning and other sources to fine particle contemporary carbon in the western United States. Atmos. Environ. 45, 1986–1993.

Hsieh, L.Y., Chen, C.L., Wan, M.W., Tsai, C.H., Tsai, Y.I., 2008. Speciation and temporal characterization of dicarboxylic acids in PM$_{2.5}$ during a PM episode and a period of non-episodic pollution. Atmos. Environ. 42, 6836–6850.

Hyder, M., Genberg, J., Sandahl, M., Swietlicki, E., Jonsson, J.A., 2012. Yearly trend of dicarboxylic acids in organic aerosols from south of Sweden and source attribution. Atmos. Environ. 57, 197–204.

Jia, Y., Fraser, M.P., 2011. Characterization of saccharides in size-fractionated ambient particulate matter and aerosol sources: the contribution of primary biological aerosol particles (PBAPs) and soil to ambient particulate matter. Atmos. Environ. 45, 930–936.

Jia, Y., Bhat, S., Fraser, M.P., 2010. Characterization of saccharides and other organic compounds in fine particles and the use of saccharides to track primary biologically derived carbon sources. Atmos. Environ. 44, 724–732.

Kawamura, K., Yasui, O., 2005. Diurnal changes in the distribution of dicarboxylic acids, ketocarboxylic acids and dicarbonyls in the urban Tokyo atmosphere. Atmos. Environ. 39, 1945–1960.

Larsen, B.R., Giraldoni, S., Stenstrom, K., Niedzialek, J., Jimenez, J., Belis, C.A., 2012. Sources for PM pollution in the Po Plain, Italy. II. Probabilistic uncertainty characterization and sensitivity analysis of secondary and primary sources. Atmos. Environ. 50, 203–213.

Lee, S.C., Cao, J.J., Kawamura, K., Watanabe, T., Cheng, Y., Chow, J.C., 2006. Dicarboxylic acids, ketocarboxylic acids and dicarbonyls in the urban roadside area of Hong Kong. Atmos. Environ. 40, 3030–3040.

Li, L., Dai, D., Deng, S., Feng, J., Zhao, M., Wu, J., liu, L., Yang, X., Wu, S., Qi, H., Yang, G., Zhang, X., Wang, Y., Zhang, Y., 2013. Concentration, distribution and variation of polar organic aerosol tracers in Yaan, a middle-sized city in western China. Atmos. Res. 120-121, 29–42.

Ma, S.X., Wang, Z.Z., Bi, X.H., Sheng, G.Y., Fu, J.M., 2009. Composition and source of saccharides in aerosols in Guangzhou, China. Chin. Sci. Bull. 54, 4500–4506.

Martin, S.T., Andreae, M.O., Artaxo, P., Baumgardner, D., Chen, Q., Goldstein, A.H., Guenther, A., Heald, C.L., Mayol-Bracero, O.L., McMurry, P.H., Pauliquevis, T., Pöschl, U., Prather, K.A., Roberts, G.C., Saleska, S.R., Dias, M.A.S., Spracklen, D.V., Swietlicki, E., Trebs, I., 2010. Sources and properties of Amazonian aerosol particles. Rev. Geophys. 48, 2008RG000280.

Mazzoleni, L.R., Zielinska, B., Moosmüller, H., 2007. Emissions of levoglucosan, methoxy phenols, and organic acids from prescribed burns, laboratory combustion of wildland fuels, and residential wood combustion. Environ. Sci. Technol. 41, 2115—2122.

Medeiros, P.M., Conte, M.H., Weber, J.C., Simoneit, B.R.T., 2006. Sugars as source indicators of biogenic organic carbon in aerosols collected above the Howland Experimental Forest, Maine. Atmos. Environ. 40, 1694—1705.

Oliveira, C., Pio, C., Alves, C., Evtyugina, M., Santos, P., Goncalves, V., Nunes, T., Silvestre, A.J.D., Palmgren, F., Wahlin, P., Harrad, S., 2007. Seasonal distribution of polar organic compounds in the urban atmosphere of two large cities from the North and South of Europe. Atmos. Environ. 41, 5555—5570.

Perrone, M.G., Ferrero, L., Larsen, B.R., Sangiorgi, G., De Gennaro, G., Udisti, G., Zangrando, R., Gambaro, A., Bolzacchini, E., 2012. Sources of high PM2.5 concentrations in Milan, Northern Italy: molecular marker data and CMB modeling. Sci. Tot. Environ. 414, 343—355.

Perrone, M.G., Gualtieri, M., Consonni, V., Ferrero, L., Sangiorgi, G., Longhin, E., Ballabio, D., Bolzacchini, E., Camatini, M., 2013. Particle size, chemical composition, seasons of the year and urban, rural or remote size origins as determinants of biological effects of particulate matter on pulmonary cells. Environ. Pollut. 176, 215—227.

Pietrogrande, M.C., Mattia Mercuriali, M., Perrore, M.G., Ferrero, L., Sangiorgi, G., Bolzacchini, E., 2010. Distribution of n-alkanes in the northern Italy aerosols: data handling of GC-MS signals for homologous series characterization. Environ. Sci. Technol. 44, 4232—4240.

Pietrogrande, M.C., Bacco, D., Rossi, M., 2013a. Chemical characterization of polar organic markers in aerosols in a local area around Bologna, Italy. Atmos. Environ. 75, 279—286.

Pietrogrande, M.C., Bacco, D., Chiereghin, S., 2013b. GC/MS analysis of water-soluble organics in atmospheric aerosol: optimization of a solvent extraction procedure for simultaneous analysis of carboxylic acids and sugars. Anal. Bioanal. Chem. 405, 1095—1104.

Pietrogrande, M.C., Bacco, D., Visentin, M., Ferrari, S., Poluzzi, V., 2014. Polar organic marker compounds in atmospheric aerosol in the Po Valley during the Supersito campaigns — part 1: low molecular weight carboxylic acids in cold seasons. Atmos. Environ. 86, 164—175.

Pio, C.A., Legrand, M., Alves, C.A., Oliveira, T., Afonso, J., Caseiro, A., Puxbaum, H., Sanchez-Ochoa, A., Gelencser, A., 2008. Chemical composition of atmospheric aerosols during the 2003 summer intense forest fire period. Atmos. Environ. 42, 7530—7543.

Puxbaum, H., Caseiro, A., Sanchez-Ochoa, A., Kasper-Giebl, A., Claeys, M., Gelencser, A., Legrand, M., Preunkert, S., Pio, C., 2007. Levoglucosan levels at background sites in Europe for assessing the impact of biomass combustion on the European aerosol background. J. Geophys. Res. Atmos. 112 http://dx.doi.org/10.1029/2006JD008114.

Rogge, W.F., Medeiros, P.M., Simoneit, B.R.T., 2007. Organic marker compounds in surface soils of crop fields from the San Joaquin Valley fugitive dust characterization study. Atmos. Environ. 41, 8183—8204.

Sang, X., Zhang, Z., Chan, C., Engling, G., 2013. Source categories and contribution of biomass smoke to organic aerosol over the southeastern Tibetan Plateau. Atmos. Environ. 78, 113—123.

Scire, J.S., Robe, F.R., Fernau, M.E., Yamartino, R.J., 2000. A User Guide for the CALMET Meteorological Model (Version 5). Earth Tech, Inc.

Simoneit, B.R.T., Elias, V.O., Kobayashi, M., Kawamura, K., Rushdi, A.I., Medeiros, P.M., Rogge, W.F., Didyk, B.M., 2004. Sugars dominant water-soluble organic compounds in soils and characterization as tracers in atmospheric particulate matter. Environ. Sci. Technol. 38, 5939—5949.

Standley, L.J., Simoneit, B.R.T., 1987. Characterization of extractable plant wax, resin, and thermally matured components in smoke particles from prescribed burns. Environ. Sci. Technol. 21, 163—169.

Tominaga, S., Matsumoto, K., Kaneyasu, N., Shigihara, A., Katono, K., Igawa, M., 2011. Measurements of particulate sugars at urban and forested suburban sites. Atmos. Environ. 45, 2335—2339.

Tsai, Y.I., Sopajaree, K., Chotruksa, A., Wu, H.C., Kuo, S.S., 2013. Source indicators of biomass burning associated with inorganic salts and carboxylates in dry season ambient aerosol in Chiang Mai Basin, Thailand. Atmos. Environ. 78, 93—104.

Van Drooge, B., Crusack, M., Reche, C., Mohr, C., Alastuey, A., Querol, X., Prevot, A., Douglas, A., Day, D.A., Jimenez, J.L., Grimalt, J.O., 2012. Molecular marker characterization of the organic composition of submicron aerosols from Mediterranean urban and rural environments under contrasting meteorological conditions. Atmos. Environ. 61, 482—489.

Vandeginste, B.G.M., Massart, D.L., Buydens, L.M.C., 1998. Handbook of Chemometrics and Qualimetrics (Part B). Elsevier Science, Amsterdam, NL.

Wagener, S., Langner, M., Moriske, H.J., Endlicher, W.R., 2012. Spatial and seasonal variations of biogenic tracer compounds in ambient PM10 and PM1 samples in Berlin, Germany. Atmos. Environ. 47, 33—42.

Wang, H., Kawamura, K., Ho, K.F., Lee, S.C., 2006. Low molecular weight dicarboxylic acids, ketoacids and dicarbonyls in the fine particles from a roadway tunnel: possible secondary production from the precursors. Environ. Sci. Technol. 40, 6255—6260.

Wang, G., Chen, C., Li, J., Zhou, B., Xie, M., Hu, S., Kawamura, K., Chen, C., 2011. Molecular composition and size distribution of sugars, sugar-alcohols and carboxylic acids in airborne particles during a severe urban haze event caused by wheat straw burning. Atmos. Environ. 40, 2473—2479.

Yang, L., Nguyen, D.M., Jia, S., Reid, J.S., Yu, L.E., 2013. Impacts of biomass burning smoke on the distributions and concentrations of C2—C5 dicarboxylic acids and dicarboxylates in a tropical urban environment. Atmos. Environ. 78, 211—218.

Yttri, K.E., Dye, C., Kiss, G., 2007. Ambient aerosol concentrations of sugars and sugar-alcohols at four different sites in Norway. Atmos. Chem. Phys. 7, 4267—4279.

Zheng, M., Cass, G.R., Schauer, J.J., Edgerton, E.S., 2002. Source apportionment of PM2.5 in the southeastern United States using solvent-extractable organic compounds as tracers. n-alkanes. Environ. Sci. Technol. 36 (11), 2361—2371.

<div align="center">

ELSEVIER LICENSE
TERMS AND CONDITIONS

Feb 07, 2016

</div>

This is a License Agreement between Marco Visentin ("You") and Elsevier ("Elsevier") provided by Copyright Clearance Center ("CCC"). The license consists of your order details, the terms and conditions provided by Elsevier, and the payment terms and conditions.

All payments must be made in full to CCC. For payment instructions, please see information listed at the bottom of this form.

Supplier	Elsevier Limited The Boulevard,Langford Lane Kidlington,Oxford,OX5 1GB,UK
Registered Company Number	1982084
Customer name	Marco Visentin
Customer address	Via L. Borsari 46
	Ferrara, 44121
License number	3803550288347
License date	Feb 07, 2016
Licensed content publisher	Elsevier
Licensed content publication	Atmospheric Environment
Licensed content title	Characterization of atmospheric aerosols in the Po valley during the supersito campaigns — Part 3: Contribution of wood combustion to wintertime atmospheric aerosols in Emilia Romagna region (Northern Italy)
Licensed content author	Maria Chiara Pietrogrande,Dimitri Bacco,Silvia Ferrari,Jussi Kaipainen,Isabella Ricciardelli,Marja-Liisa Riekkola,Arianna Trentini,Marco Visentin
Licensed content date	December 2015
Licensed content volume number	122
Licensed content issue number	n/a
Number of pages	15
Start Page	291
End Page	305
Type of Use	reuse in a thesis/dissertation
Portion	full article
Format	both print and electronic
Are you the author of this Elsevier article?	Yes
Will you be translating?	No
Title of your thesis/dissertation	Chemical characterization of atmospheric aerosol for air quality evaluation in Emilia Romagna region
Expected completion date	Mar 2016

Characterization of atmospheric aerosols in the Po valley during the supersito campaigns — Part 3: Contribution of wood combustion to wintertime atmospheric aerosols in Emilia Romagna region (Northern Italy)

Maria Chiara Pietrogrande [a], [*], Dimitri Bacco [a], [b], Silvia Ferrari [b], Jussi Kaipainen [c], Isabella Ricciardelli [b], Marja-Liisa Riekkola [c], Arianna Trentini [b], Marco Visentin [a]

[a] Department of Chemical and Pharmaceutical Sciences, University of Ferrara, Via Fossato di Mortara 17/19, I-44100 Ferrara, Italy
[b] Regional Centre for Urban Areas, Regional Agency for Prevention and Environment ARPA- Emilia-Romagna, Italy
[c] Department of Chemistry, Laboratory of Analytical Chemistry, P.O. Box 55, 00014 University of Helsinki, Finland

HIGHLIGHTS

Nearly 650 daily $PM_{2.5}$ samples were collected at 2 sampling sites in cold months.
58 organic compounds related to biomass burning were determined.
Wood burning contributed nearly 77% to BaP concentration in the winter months.
Wood burning contributed roughly 35% to OC during the cold November–February.

ARTICLE INFO

ABSTRACT

This paper investigates the influence of wood combustion on PM in fall/winter that are the most favorable seasonal periods with presumed intense biomass burning for residential heating due to low temperatures. As a part of the Supersito project, nearly 650 $PM_{2.5}$ samples were daily collected at urban and rural sites in Emilia Romagna (Northern Italy) in five intensive experimental campaigns throughout the years from 2011 to 2014.

From specific compounds related to wood combustion a set of 58 organic compounds was determined, such as anhydrosugars, primary biological sugars, low-molecular-weight carboxylic acids, methoxylated phenols, PAHs and carbonaceous components (EC/OC).

Levoglucosan was by far the most dominant anhydrosugar, both on a relative and an absolute basis (35–1043 ng m^{-3}), followed by mannosan (7–121 ng m^{-3}) and galactosan (4–52 ng m^{-3}), indicating that wood burning for domestic heating is a diffuse regional source during the seasons studied. Different diagnostic ratios between anhydrosugars and methoxylated phenols were computed to discriminate the prevalent contribution of hardwood as combustion fuel.

The investigated 19 high molecular weight PAHs were more abundant at the urban than at the rural site, with mean total value of 4.3 and 3.2 ng m^{-3} at MS and SP, respectively. The strong contribution of wood combustion to atmospheric PAHs was indicated by the positive correlation between levoglucosan and the most abundant PAHs ($R^2 = 0.71 \div 0.79$) and individually with benzo(a)pyrene ($R^2 = 0.79$). By using this correlation, it was estimated that wood burning contributed nearly 77% to BaP concentration in the winter months.

Based on the ratio between levoglucosan and OC data, it could be concluded that the wood burning contributed about 35% to OC during the cold November–February periods and the contribution was similar at both sampling sites.

* Corresponding author.
E-mail address: mpc@unife.it (M.C. Pietrogrande).

1. Introduction

There is general consensus that the impact of residential wood combustion is globally much higher than assumed in the past, especially during winter season, when the domestic burning of wood logs, briquettes, chips and pellet represents an important renewable energy source (Bernardoni et al., 2011; Caseiro and Oliviera, 2012; Perrone et al., 2012; Calvo et al., 2013; Viana et al., 2013; Herich et al., 2014; Fountoukis et al., 2014). In fact, numerous studies have demonstrated that emissions from biomass combustion in domestic appliances are significant contributors of the total $PM_{2.5}$ and PM_{10} emitted, and these particles may contain numerous toxic/carcinogenic components with a potentially high impact on human health (Oliveira et al., 2007; Puxbaum et al., 2007; Caseiro et al., 2009; Giannoni et al., 2013; Perrone et al., 2013; Piazzalunga et al., 2013). In addition, the budget of the organic compounds emitted by combustion sources often includes a non-negligible fraction of secondary products formed in the plume by photoreactions (Simoneit, 2002; Hallquist et al., 2009; Paglione et al., 2014).

For these reasons, the primary and secondary contribution of biomass burning to organic aerosols has been investigated in Emilia Romagna region (Po Valley, Northern Italy), as a part of the Supersito project developed by ARPA-ER (Emilia-Romagna Region and Regional Agency for Prevention and Environment, www.supersito-er.it). To extend the previous studies (Pietrogrande et al., 2014a, 2014b), the aim of the present paper was to exploit a larger data set of samples collected during four years period and characterized by a larger number of analytes.

By knowing that the molecular composition of organic matter in smoke particles is highly complex, the emphasis of this study was put mainly on the determination of specific tracer compounds of biomass burning caused by degradation of biopolymers, such as sugar derivatives — which have been identified as major products of cellulose and hemicellulose pyrolysis (e.g. Simoneit, 2002; Wang et al., 2011; Giannoni et al., 2012) — and substituted methoxyphenols, as primary products of lignin breakdown (Mazzoleni et al., 2007; Schmid et al., 2008; Kuo et al., 2011; Caseiro and Oliviera, 2012). In addition, the study includes other solvent-extractable compounds related to biomass burning, such as low-molecular-weight carboxylic acids, to help the differentiation between primary emissions and secondary organic aerosols (Ho et al., 2011; Hsieh et al., 2008; Wang et al., 2011; Hyder et al., 2012; Yang et al., 2013; Pietrogrande et al., 2013a, 2014a), and polycyclic aromatic hydrocarbons (PAHs), that are typical thermal degradation products of fuels (Fabbri et al., 2009). Further, the carbonaceous components were characterized and quantified as organic and elemental carbon.

To our knowledge, though the impact of biomass burning to aerosol composition has been quite extensively investigated in the Western part of the Po Valley in recent years — Lombardia region (i.e., Bernardoni et al., 2011; Perrone et al., 2012; Belis et al., 2011; Larsen et al., 2012; Perrone et al., 2013; Piazzalunga et al., 2013) — there are actually no papers providing such a detailed study in other locations of the same valley, such as Emilia Romagna region.

2. Materials and methods

2.1. Aerosol sampling

The sampling protocol was developed for the Supersito project, as described elsewhere (Pietrogrande et al., 2014a, 2014b). Briefly, the $PM_{2.5}$ samples were collected in two locations representing an urban site (Main Site, MS) located in the city of Bologna (~400,000 inhabitants) and a rural background station located at San Pietro Capofiume (SP) about 30 km northeast from the city, on a flat, homogeneous terrain of harvested fields.

As part of the Supersito project, five sampling intensive campaigns were performed from 2011 to 2014 to represent different meteorological scenarios in cold seasons: from 18th November up to 6th December 2011 (November 2011), from 23rd October up to 10th November 2012 (November 2012), from 30th January up to 17th February 2013 (February 2013), from 27th September up to 25th October 2013 (October 2013) and from 28th January up to 27th February 2014 (February 2014).

$PM_{2.5}$ samples were collected by automatic outdoor samplers (Skypost PM, TCRTECORA Instruments, Corsico, Milan, Italy) on quartz fiber filters (Whatman, 47 mm diameter) at an airflow rate of 38.3 $Lmin^{-1}$ for 24 h ($\approx$ 55 m^3 day^{-1}). After sampling, the procedure outlined in European Standard EN 12341 (CEN, 1998) was applied for equilibration and weighing.

Meteorological data were collected at the meteorological stations of San Pietro Capofiume and Bologna by Hydro-Meteo-Climate Service of ARPA-ER. Mixing layer height at both sites was estimated using the pre-processor CALMET by ARPA Emilia-Romagna (Deserti et al., 2001).

2.2. Analytical procedure for polar organic compounds

The analytical procedure has been described elsewhere (Pietrogrande et al., 2013b, 2014a, 2014b). Briefly, $PM_{2.5}$ samples were extracted for 15 min in an ultrasonication bath with 15 mL of methanol:dichloromethane (9:1) solvent mixture and then filtered using a teflon filter (25 mm, 0.45 μm, Supelco, Bellefonte, PA). The filtrates were evaporated to dryness in a centrifugal vacuum concentrator (miVac Duo Concentrator, Genevac Ltd, Ipswich, UK). Then the sample extracts were submitted to silyl derivatization with N,O-bis-(trimethylsilyl)trifluoroacetamide (BSTFA) containing 1% of trimethylchlorosilane (TMCS) at 75 C for 70 min: 40 μL of BSTFA-TMCS reagent and 15 μL of pyridine were added to 40 μL of isooctane and 5 μL of Internal Standard (deuterated $C_{12}H_{26}$, injected quantity: 127.5 ng).

The GC/MS system was a Scientific Focus-GC (Thermo-Fisher Scientific, Milan, Italy) coupled to PolarisQ Ion Trap Mass Spectrometer (Thermo-Fisher Scientific, Milan, Italy). The column used was a DB-5MS column (L = 30 m, I.D. = 0.25 mm, df = 0.25 μm film thickness; J&W Scientific, Rancho Cordova, CA, USA). High purity helium was the carrier gas with a flow rate of 1.5 ml min^{-1}. Temperature program conditions were optimized for analysis of a wide range of target polar organic compounds, including low molecular weight carboxylic acids.

The mass spectrometer operated in Electron Ionization mode (positive ion, 70 eV). Ion source and transfer-line temperatures were 250 C and 280 C, respectively. The mass spectra were acquired in full scan mode from 50 to 650 m/z in 0.58 s. For identification and quantification of the target analytes, the extracted-ion chromatograms (EICs) were recovered from the entire data set for each chromatographic run by selecting the most abundant characteristic fragments (Pietrogrande et al., 2013b). The procedure provides low detection limits (0.1–3 ng m^{-3}, LOD in Table 1) and good reproducibility (RSD% 7%) suitable for applicability in environmental monitoring.

In addition, a tandem MS/MS analysis was applied for target analytes present at lower concentration, i.e., low-molecular-weight carboxylic acids and methoxyphenols (Visentin and Pietrogrande, 2014). The multiple reaction monitoring mode was applied, by setting the isolation window at 1.5 m/z. Precursor ions were stored with a Paul stability parameter (qz) of 0.30 and fragmented by collision-induced dissociation (CID) using the resonant excitation mode. This method reduces detection limits for standard solutions

Table 1

Concentration values of each marker measured and parameters computed in the five monitoring campaigns. For each campaign the average values and standard deviations ($ng\ m^{-3}$) are reported for the two sampling sites. Meteorological parameters were measured for each campaign in the investigated sites. The term 'n.d.' indicates the analytes showing more than 90% of the measured data values below the detection limit.

November 2011	Main site		San Pietro	
	Average ($ng\ m^{-3}$)	S.D. ($ng\ m^{-3}$)	Average ($ng\ m^{-3}$)	S.D. ($ng\ m^{-3}$)
Levoglucosan	1042.9	490.4	916.0	389.3
Mannosan	120.7	45.1	105.7	39.6
Galactosan	52.0	20.0	42.8	16.5
Arabinose	5.0	0.8	6.4	2.4
Galactose	4.8	1.7	4.4	0.9
Glucose	10.0	12.3	6.6	1.6
Sucrose	35.4	16.6	36.1	12.2
Tot sugars	1287.9	559.6	1129.8	452.1
Lev/Man	8.5	1.1	8.6	0.9
Lev/Gal + Man	6.0	0.7	6.1	0.6
tot Burning Sugars, Tot_{BB}	1215.6	552.8	1064.5	443.4
tot Bio Sugars, Tot_{BS}	72.2	24.1	65.3	18.9
spruce%	58.0	6.3	63.4	19.8
Vanillin	0.7	0.3	0.6	0.4
Acetosiringone	1.3	1.1	0.8	0.6
Syringaldeide	n.d.		n.d.	
Vanillic acid + acetovanillone	8.6	3.9	6.4	3.3
Syringic acid	2.1	0.9	1.5	0.8
Tot phenols	13.3	6.2	9.2	5.3
Tot syringic phenols, Syr	3.4	2.0	1.7	1.5
Tot vanillic phenols, Van	9.3	4.1	5.1	4.4
Syr/Van	0.36	0.08	0.35	0.09
Malonic acid	21.7	24.1	41.5	37.5
Maleic acid	30.3	27.4	90.8	182.4
Succinic acid	112.1	36.6	110.7	44.1
Malic acid	40.9	24.2	33.8	17.3
Glyoxylic acid	n.d.		n.d.	
3-hydroxy benzoic acid	7.5	2.1	7.5	2.1
4-hydroxy benzoic acid	9.7	4.8	7.6	2.8
2-ketoglutaric acid	8.7	3.4	8.9	3.2
Tot CAs	262.0	111.2	308.3	220.2
chrysene	1.18	0.52	0.62	0.36
benzo[b]fluoranthene	2.36	0.77	1.82	0.95
benzo[k]fluoranthene	0.58	0.19	0.400	0.21
benzo[e]pyrene	1.01	0.37	0.72	0.36
benzo[a]pyrene	1.12	0.48	0.72	0.45
indeno[1,2,3−c,d]pyrene	1.15	0.50	0.65	0.33
benzo[g,h,i]perylene	1.44	0.58	0.75	0.36
Tot PAHs	12.98	4.68	7.80	4.26
BaP_{BB}	0.83	0.39	0.73	0.31
BaP_{BB}%	61.6	23.5	89.0	31.2
OC ($\mu g\ m^{-3}$)				
EC ($\mu g\ m^{-3}$)				
TC ($\mu g\ m^{-3}$)	11.9	3.1	8.6	3.2
OC/EC				
Lev/OC				
OC_{BB}	6.5	3.6	6.1	2.6
OC_{BB}%				
$PM_{2.5}$ ($\mu g\ m^{-3}$)	59.1	17.3	46.2	18.0
$Tot_{BB}/PM_{2.5}$%	2.2	1.6	2.5	1.1
$TC/PM_{2.5}$%	20.4	5.8	18.4	4.7
Meteorological parameters				
Mixing height (m)	230	78	169	48
Daily temperature (°C)	6.5	2.0	4.0	1.8
Daily solar radiation ($W\ m^{-2}$)	61.0	23.0	64.7	30.2
Precipitations (mm)	0.8		5.2	
November 2012	Main site		San Pietro	
	Average ($ng\ m^{-3}$)	S.D. ($ng\ m^{-3}$)	Average ($ng\ m^{-3}$)	S.D. ($ng\ m^{-3}$)
Levoglucosan	288.9	143.9	233.2	114.6
Mannosan	63.5	38.4	47.0	25.6
Galactosan	29.8	18.3	23.7	13.8
Arabinose	2.4	1.6	n.d.	
Galactose	2.8	1.2	2.6	1.4
Glucose	6.9	2.9	4.9	1.9
Sucrose	4.6	4.3	6.2	11.0
Tot sugars	400.6	205.7	335.2	165.0

(continued on next page)

Table 1 (*continued*)

November 2012	Main site		San Pietro	
	Average (ng m^{-3})	S.D. (ng m^{-3})	Average (ng m^{-3})	S.D. (ng m^{-3})
Lev/Man	4.9	0.8	5.1	0.5
Lev/Gal + Man	3.4	0.6	5.1	0.6
tot Burning Sugars, Tot$_{BB}$	382.2	198.7	303.9	153.3
tot Bio Sugars, Tot$_{BS}$	18.4	9.6	31.3	16.8
spruce%	72.3	10.8	70.5	6.3
Vanillin	1.8	0.3	1.2	0.2
Acetosiringone	n.d.		n.d.	
Syringaldeide	4.2	1.5	3.4	0.9
Vanillic acid	2.3	1.1	1.1	0.1
Acetovanillone	1.9	2.1	1.5	0.8
Syringic acid	3.6	1.2	3.2	1.0
Tot phenols	13.8	4.8	8.0	4.0
Tot syringic phenols, Syr	7.8	2.6	5.6	2.7
Tot vanillic phenols, Van	6.0	2.7	3.0	1.1
Syr/Van	1.4	0.3	1.9	0.6
Malonic acid	29.7	33.1	33.3	25.7
Maleic acid	n.d.		n.d.	
Succinic acid	26.8	14.3	22.2	12.6
Malic acid	25.7	22.5	22.1	17.1
Glyoxylic acid	n.d.		n.d.	
3-hydroxy benzoic acid	2.0	0.6	1.9	0.5
4-hydroxy benzoic acid	2.2	1.3	2.2	0.6
2-ketoglutaric acid	27.4	19.2	22.3	22.4
Tot CAs	167.4	109.6	114.8	89.5
chrysene	0.28	0.19	0.13	0.08
benzo[b]fluoranthene	0.79	0.47	0.48	0.34
benzo[k]fluoranthene	0.23	0.13	0.13	0.09
benzo[e]pyrene	0.37	0.20	0.24	0.16
benzo[a]pyrene	0.40	0.26	0.22	0.19
indeno[1,2,3–c,d]pyrene	0.32	0.17	0.082	0.12
benzo[g,h,i]perylene	0.44	0.23	0.18	0.12
Tot PAHs	3.68	2.10	1.94	1.31
BaP$_{BB}$	0.25	0.13	0.20	0.10
BaP$_{BB}$%	67.0	21.9	77.0	19.6
OC (μg m^{-3})	6.4	4.2	4.9	1.2
EC (μg m^{-3})	2.4	1.4	1.1	0.2
TC (μg m^{-3})	9.0	4.6	6.0	1.4
OC/EC	2.7	1.7	4.7	1.1
Lev/OC	0.07	0.04	0.04	0.02
OC$_{BB}$	2.1	1.1	1.7	0.8
OC$_{BB}$%	43.9	27.7	25.1	11.2
PM$_{2.5}$ (μg m^{-3})	31.0	17.2	27.7	16.2
Tot$_{BB}$/PM$_{2.5}$%	1.5	0.6	1.2	0.6
TC/PM$_{2.5}$%	30.2	5.9	25.5	5.6
Meteorological parameters				
Mixing height (m)	365	153	257	96
Daily temperature (C)	12.6	2.7	11.1	2.5
Daily solar radiation (W m^{-2})	70.6	37.7	85.4	46.0
Precipitations (mm)	65.0		75.0	

February 2013	Main site		San Pietro	
	Average (ng m^{-3})	S.D. (ng m^{-3})	Average (ng m^{-3})	S.D. (ng m^{-3})
Levoglucosan	259.4	98.9	252.9	110.7
Mannosan	63.6	23.7	61.5	27.2
Galactosan	31.6	12.3	32.0	15.4
Arabinose	9.5	5.5	8.9	6.1
Galactose	3.0	1.1	3.1	1.3
Glucose	5.6	1.7	5.4	1.4
Sucrose	3.1	3.0	2.6	1.2
Tot sugars	378.5	140.0	368.5	158.4
Lev/Man	4.1	0.4	4.2	0.5
Lev/Gal + Man	2.7	0.3	2.8	0.5
tot Burning Sugars, Tot$_{BB}$	354.6	133.3	346.3	151.3
tot Bio Sugars, Tot$_{BS}$	23.9	8.2	22.1	8.2
spruce%	85.5	8.3	84.6	10.1
Vanillin	0.6	0.6	1.0	0.5
Acetosiringone	n.d.		n.d.	
Syringaldeide	4.2	4.3	4.5	4.8
Vanillic acid	4.2	1.9	4.5	2.9
Acetovanillone	2.2	2.1	2.6	3.3
Syringic acid	5.8	2.8	5.3	3.1
Tot phenols	17.0	9.5	17.9	11.3

Table 1 (*continued*)

February 2013	Main site		San Pietro	
	Average (ng m^{-3})	S.D. (ng m^{-3})	Average (ng m^{-3})	S.D. (ng m^{-3})
Tot syringic phenols, Syr	10.0	6.3	9.8	6.8
Tot vanillic phenols, Van	7.0	3.9	8.1	6.2
Syr/Van	1.52	0.81	1.33	0.58
Malonic acid	26.8	21.1	32.7	25.7
Maleic acid	67.8	37.8	57.4	39.3
Succinic acid	32.3	12.6	35.1	14.1
Malic acid	20.3	11.5	22.1	17.1
Glyoxylic acid	n.d.		n.d.	
3-hydroxy benzoic acid	2.4	0.8	2.0	1.9
4-hydroxy benzoic acid	3.1	1.4	3.1	2.2
2-ketoglutaric acid	46.8	28.4	45.4	33.7
Tot CAs	249.3	122.3	247.9	139.2
chrysene	0.42	0.32	0.32	0.32
benzo[b]fluoranthene	0.84	0.62	0.98	0.69
benzo[k]fluoranthene	0.22	0.17	0.28	0.20
benzo[e]pyrene	0.39	0.29	0.44	0.31
benzo[a]pyrene	0.39	0.48	0.47	0.41
indeno[1,2,3−c,d]pyrene	0.27	0.14	0.30	0.22
benzo[g,h,i]perylene	0.36	0.18	0.37	0.27
Tot PAHs	3.51	2.41	4.15	2.81
BaP$_{BB}$	0.21	0.08	0.20	0.09
BaP$_{BB}$%	74.2	35.7	60.2	34.3
OC (µg m^{-3})	7.2	2.2	8.3	3.6
EC (µg m^{-3})	2.0	0.8	1.4	0.3
TC (µg m^{-3})	9.2	2.9	10.2	3.9
OC/EC	3.7	1.0	5.9	1.6
Lev/OC	0.03	0.02	0.03	0.01
OC$_{BB}$	1.8	0.7	1.7	0.7
OC$_{BB}$%	22.5	11.9	20.2	10.1
PM$_{2.5}$ (µg m^{-3})	32.8	13.7	34.6	19.4
Tot$_{BB}$/PM$_{2.5}$%	1.2	0.4	1.1	0.5
TC/PM$_{2.5}$%	19.1	14.0	32.0	10.8
Meteorological parameters				
Mixing height (m)	413	99	314	120
Daily temperature (C)	3.9	1.6	2.6	1.0
Daily solar radiation (W m^{-2})	80.8	34.5	94.2	48.4
Precipitations (mm)	48.6		40.6	
October 2013	Main site		San Pietro	
	Average (ng m^{-3})	S.D. (ng m^{-3})	Average (ng m^{-3})	S.D. (ng m^{-3})
Levoglucosan	34.6	23.8	38.8	25.9
Mannosan	8.3	8.5	6.9	5.6
Galactosan	5.0	3.1	4.3	2.9
Arabinose	0.6	0.6	0.7	0.6
Galactose	n.d.		n.d.	
Glucose	4.1	1.7	4.3	2.3
Sucrose	4.1	6.0	2.9	1.9
Tot sugars	75.9	29.7	75.7	32.0
Lev/Man	7.1	5.1	7.4	3.8
Lev/Gal + Man	3.5	2.1	4.0	1.5
tot Burning Sugars, Tot$_{BB}$	47.1	31.1	50.1	33.0
tot Bio Sugars, Tot$_{BS}$	28.0	18.4	25.6	12.5
spruce%	57.1	17.0	65.2	33.9
Vanillin	n.d.		n.d.	
Acetosiringone	n.d.		n.d.	
Syringaldeide	n.d.		n.d.	
Vanillic acid	n.d.		n.d.	
Acetovanillone	n.d.		n.d.	
Syringic acid	n.d.		n.d.	
Tot phenols	n.d.		n.d.	
Tot syringic phenols, Syr	n.d.		n.d.	
Tot vanillic phenols, Van	n.d.		n.d.	
Syr/Van	n.d.		n.d.	
Malonic acid	10.3	8.8	10.6	9.5
Maleic acid	3.6	6.6	3.1	4.6
Succinic acid	8.6	5.3	9.9	6.9
Malic acid	9.5	4.4	11.2	6.0
Glyoxylic acid	0.9	0.8	0.7	0.8
3-hydroxy benzoic acid	n.d.		n.d.	
4-hydroxy benzoic acid	0.7	1.1	n.d.	
2-ketoglutaric acid	1.8	1.7	2.7	2.0
Tot CAs	52.6	27.7	55.5	34.3

Table 1 (*continued*)

October 2013	Main site		San Pietro	
	Average (ng m^{-3})	S.D. (ng m^{-3})	Average (ng m^{-3})	S.D. (ng m^{-3})
chrysene	0.04	0.03	0.03	0.02
benzo[b]fluoranthene	0.15	0.15	0.13	0.07
benzo[k]fluoranthene	0.04	0.03	0.03	0.02
benzo[e]pyrene	0.07	0.05	0.06	0.03
benzo[a]pyrene	0.07	0.07	0.05	0.03
indeno[1,2,3–c,d]pyrene	0.04	0.03	0.04	0.02
benzo[g,h,i]perylene	0.06	0.03	0.04	0.02
Tot PAHs	0.59	0.48	0.56	0.33
BaP$_{BB}$	0.03	0.02	0.03	0.02
BaP$_{BB}$%	53.6	33.5	56.0	28.8
OC (µg m^{-3})	4.3	1.9	4.9	1.3
EC (µg m^{-3})	1.3	0.3	0.8	0.2
TC (µg m^{-3})	7.1	2.6	5.7	1.4
OC/EC	3.3	0.7	6.1	0.9
Lev/OC	0.009	0.006	0.007	0.002
OC$_{BB}$	0.3	0.2	0.3	0.2
OC$_{BB}$%	6.0	4.1	5.0	1.4
PM$_{2.5}$ (µg m^{-3})	20.2	10.0	16.5	10.3
Tot$_{BB}$/PM$_{2.5}$%	0.3	0.1	0.6	0.7
TC/PM$_{2.5}$%	32.9	10.0	41.5	28.7
Meteorological parameters				
Mixing height (m)	468	188	402	133
Daily temperature (°C)	16.0	2.6	15.3	2.5
Daily solar radiation (W m^{-2})	81.4	47.2	89.0	57.0
Precipitations (mm)	4.5		4.1	

February 2014	Main site		San Pietro	
	Average (ng m^{-3})	S.D. (ng m^{-3})	Average (ng m^{-3})	S.D. (ng m^{-3})
Levoglucosan	300.8	117.8	341.9	129.6
Mannosan	26.4	16.8	32.1	18.8
Galactosan	14.9	6.2	16.3	6.4
Arabinose	1.5	1.0	1.8	0.9
Galactose	n.d.		n.d.	
Glucose	8.2	4.6	8.0	2.4
Sucrose	8.5	9.6	9.6	9.4
Tot sugars	372.9	147.4	421.4	165.6
Lev/Man	15.0	7.9	12.4	4.3
Lev/Gal + Man	8.2	2.1	7.9	2.1
tot Burning Sugars, Tot$_{BB}$	342.1	140.4	390.4	154.3
tot Bio Sugars, Tot$_{BS}$	30.9	14.9	31.1	15.4
spruce%	34.6	16.4	36.5	16.7
Vanillin	1.8	0.5	1.8	0.5
Acetosiringone	1.1	0.3	1.1	0.3
Syringaldeide	4.2	1.2	4.4	1.5
Vanillic acid	0.7	0.6	0.9	1.0
Acetovanillone	1.6	0.6	1.8	1.2
Syringic acid	1.8	1.6	2.3	2.2
Tot phenols	11.3	4.2	12.4	6.5
Tot syringic phenols, Syr	7.1	2.6	7.7	3.9
Tot vanillic phenols, Van	4.1	1.6	4.5	2.6
Syr/Van	1.8	0.3	1.8	0.2
Malonic acid	2.0	3.1	2.9	2.4
Maleic acid	34.6	45.2	15.1	6.3
Succinic acid	22.4	13.6	25.3	15.2
Malic acid	22.5	12.6	25.9	12.2
Glyoxylic acid	n.d.		n.d.	
3-hydroxy benzoic acid	0.5	0.4	0.6	0.6
4-hydroxy benzoic acid	0.8	0.9	1.1	1.0
2-ketoglutaric acid	9.2	13.4	6.3	8.2
Tot CAs	118.0	72.4	103.6	34.0
chrysene	0.22	0.23	0.09	0.10
benzo[b]fluoranthene	0.39	0.28	0.42	0.28
benzo[k]fluoranthene	0.11	0.08	0.11	0.07
benzo[e]pyrene	0.22	0.11	0.20	0.13
benzo[a]pyrene	0.21	0.14	0.15	0.14
indeno[1,2,3–c,d]pyrene	0.18	0.09	0.15	0.15
benzo[g,h,i]perylene	0.27	0.14	0.21	0.17
Tot PAHs	2.07	1.14	1.68	1.06
BaP$_{BB}$	0.24*	0.10	0.27*	0.10
BaP$_{BB}$%	100*		100*	
OC (µg m^{-3})	4.7	2.1	4.6	1.8
EC (µg m^{-3})	1.3	0.5	0.8	0.4
TC (µg m^{-3})	6.0	2.5	5.7	1.4

Table 1 (*continued*)

February 2014	Main site		San Pietro	
	Average (ng m^{-3})	S.D. (ng m^{-3})	Average (ng m^{-3})	S.D. (ng m^{-3})
OC/EC	3.6	1.0	5.8	1.9
Lev/OC	0.06	0.02	0.08	0.03
OC$_{BB}$	2.0	0.9	2.3	0.9
OC$_{BB}$%	38.1	17.6	52.3	19.4
PM$_{2.5}$ (μg m^{-3})	19.1	11.3	15.9	8.3
Tot$_{BB}$/PM$_{2.5}$%	2.0	0.9	2.6	1.0
TC/PM$_{2.5}$%	34.0	9.3	36.8	11.6
Meteorological parameters				
Mixing height (m)	417	142	309	94
Daily temperature (°C)	8.2	2.2	7.2	1.9
Daily solar radiation (W m^{-2})	71.1	43.8	78.7	52.6
Precipitations (mm)	4.3		3.9	

from 1 to 2.6 to 0.1–0.4 ng μL^{-1} ranges (concentrations in the injected solution).

The procedure provides good reproducibility (RSD% 7%) and recovery (78–104%) useful for environmental monitoring (Pietrogrande et al., 2013a).

2.3. Analytical procedure for polycyclic aromatic hydrocarbons

The analysis of polycyclic aromatic hydrocarbons was performed in the ARPA laboratory in Ravenna, as a part of the Supersito project activities (www.supersito.it).

The PAHs were analyzed on Thermo Scientific DFS High Resolution GC/MS system formed by a gas chromatograph equipped with a capillary column (TR-5MS-Thermo 60 m, 0.25 mm, 0.25 μm) coupled with a Magnetic Sector high resolution mass spectrometer. Each extract (1 μL) was injected in splitless mode with a 10 min solvent delay time. High purity helium was used as the carrier gas, with a flow rate of 1.2 mL min^{-1}. The temperature of the injector and transfer line was 280 °C and 300 °C, respectively. The initial oven temperature was set at 100 °C for 1 min, raised to 300 °C at a rate of 10 °C min^{-1} and then held for 50 min.

Isotope labeled (deuterated) PAH standards were used for quantification.

2.4. Analytical procedure for carbonaceous aerosol

The carbonaceous aerosol fractions (OC and EC) were quantified in the ARPA laboratory in Ferrara as a part of the Supersito project activities (www.supersito.it). A thermo-optical-transmission analyzer by Sunset (Laboratory Inc.) was used. The punched filters (1.5 cm^2) were submitted to volatilization using the EUSAAR2 thermal protocol (Cavalli et al., 2010; Sandrini et al., 2014).

3. Results and discussion

3.1. Meteorological conditions

The fall and winter seasons with low temperatures with presumed intense biomass burning for residential heating were selected for the present study as the most favorable periods for the clarification of the impact of residential wood burning on the concentrations of organic compounds studied.

During the monitoring campaigns, typical winter meteorological conditions of Po Valley occurred, characterized by atmospheric stability with shallow Planetary Boundary Layer (PBL) depths (H$_{mix}$ mean values in the 169–468 m ranges), low temperature (3–16 °C), weak amount of wet deposition (maximum precipitations $\approx$ 70 mm during fall 2012) and low wind velocity.

Such atmospheric conditions favored the accumulation of pollutants to the first hundred meters of the atmosphere and condensation of semi-volatile species, causing high PM episodes. In addition, the low solar radiation (61–94 W m^{-2}) limited atmospheric photochemical processing of the accumulated organic precursors (Balducci and Cecinato, 2010; Belis et al., 2011; Bigi and Ghermandi, 2011; Perrone et al., 2012; Pietrogrande et al., 2013a, 2014b; Paglione et al., 2014).

Among the investigated seasonal periods, the atmospheric conditions of October 2013 were more typical for late summer than fall, with the highest Hmix (468 m), solar radiation (89 W m^{-2}) and temperature (16 °C).

3.2. Concentrations of organic markers impacted by biomass burning

A set of 58 different tracers of biomass burning was investigated in order to provide useful information on emissions from wood combustion, although it is known that chemical composition of wood smoke depends largely on fuel composition and burning conditions. The investigated indicators included anhydrosugars, primary biological sugars, low-molecular-weight carboxylic acids, phenols, PAHs and carbonaceous components (Simoneit, 2002; Szidat et al., 2006; Schmid et al., 2008; Alves et al., 2010; Holden et al., 2011; Katsoyiannis et al., 2011; Wang et al., 2011; Morville et al., 2011; Maenhaut et al., 2012; Viana et al., 2013; Sandrini et al., 2014).

For each investigated indicator the concentration values were averaged over the campaign duration of $\approx$ 3 weeks and reported in Table 1 (mean values and standard deviations; the term n.d. indicates that more than 90% of the measured values are below the detection limit).

In general, all the parameters demonstrated the presence of high level of atmospheric pollution, as indicated by high PM$_{2.5}$ close to 35 μg m^{-3} measured in all the monitoring campaigns, with the exception of October 2013 (PM$_{2.5}$, Table 1). The results of Table 1 are in agreement with those obtained earlier for the Po Valley in cold seasons (Balducci and Cecinato, 2010; Bigi and Ghermandi, 2011; Perrone et al., 2012; Giannoni et al., 2012; Perrone et al., 2013; Pietrogrande et al., 2013a, 2014a; Perrino et al., 2014).

3.2.1. Anhydrosugars

Levoglucosan - with minor quantities of its isomers mannosan and galactosan - has been commonly used as an excellent source-specific tracer for both open and residential biomass burning, since it is exclusively produced during biomass combustion as the thermal alteration product of cellulose and hemicellulose, and it highly resists to degradation in the atmosphere (Simoneit, 2002; Puxbaum et al., 2007; Munchak et al., 2011; Wang et al., 2011; Giannoni et al., 2012; Sang et al., 2013).

Table 1 reports the concentrations of each anhydrosugar and their sum (Tot$_{BB}$, total biomass burning) at the investigated sites, as average values of each campaign. As expected, levoglucosan was by far the most dominant anhydrosugar, evaluated both on a relative and an absolute basis (35–1043 ng m^{-3}), followed by mannosan (7–121 ng m^{-3}) and galactosan (4–52 ng m^{-3}). In general, a total anhydrosugar mean value close to 450 ng m^{-3} was found at the both sites, with the exception of high values in fall 2011 (1216 and 1064 ng m^{-3} at MS and SP, respectively) and low values in fall 2013 (48 and 50 ng m^{-3} MS and SP, respectively). These results prove that wood burning for domestic heating is a diffuse regional source during fall and winter, since the total amount of BB sugars represents on average $\approx$ 1.5% of the total PM$_{2.5}$ mass (expressed as ratio Tot$_{BB}$/PM%, Table 1), with similar contribution at both sites.

These burning sugar levels (300–500 ng m^{-3}) are consistent with the results obtained in other studies dealing with anhydrosugars measured in urban and rural areas in Central and Northern Europe, where residential wood combustion has been identified as an important source of air pollution (Oliveira et al., 2007; Puxbaum et al., 2007; Schmid et al., 2008; Caseiro et al., 2009; Maenhaut et al., 2012; Van Drooge et al., 2012; Viana et al., 2013). As to Italy, levoglucosan levels close to 400 ng m^{-3} have been found in the same seasonal periods at other urban-background sites located in the plains (Florence, Mantova) (Piazzalunga et al., 2010; Giannoni et al., 2012), while higher levoglucosan concentrations close to 1000 ng m^{-3} have been measured during winter in Milan and at other sites in Northern Italy closest to the Alps (Schmidl et al., 2008; Perrone et al., 2012; Piazzalunga et al., 2011; Belis et al., 2011; Larsen et al., 2012; Piazzalunga et al., 2013; Herich et al., 2014).

In this study both the urban and the rural background sites showed similar levels of burning sugars, indicating a homogeneous impact of wood combustion in all the investigated regions. The reason may be the use of wood for residential and domestic heating in both the areas in combination with the homogenous distribution of organic pollutants due to atmospheric stratification.

Then the effect of meteorological conditions on the levoglucosan levels was elucidated. A significant negative correlation (although quite scattered R^2 $\approx$ 0.6) was found with the boundary layer depth, suggesting that accumulation of BB sugars is related to the stagnant atmospheric situation. In addition, a significant negative correlation was seen with solar radiation (R^2 $\approx$ 0.6), indicating a significant effect of photo-oxidation atmospheric processes that deplete anhydrosugars primarily emitted by biomass burning (Hallquist et al., 2009; Saarikoski et al., 2012; Paglione et al., 2014).

The correlation between the concentrations of the 3 anhydrosugars was exploited in order to give insights into the composition of wood fuels. In general, the concentrations of all the anhydrosugars were very highly correlated with each other (0.87 < R^2 < 0.96) at both sites in each campaign, indicating that residential wood burning was always the common source. The ratios between the concentrations of anhydrosugars (Lev/Man and Man/Gal) were utilized as useful diagnostic indicators for the possible biomass burning categories (Puxbaum et al., 2007; Fabbri et al., 2009; Alves et al., 2010; Kuo et al., 2011; Kourtchev et al., 2011; Munchak et al., 2011; Piazzalunga et al., 2011; Giannoni et al., 2012; Sang et al., 2013).

As an example, the scatter plots of mannosan versus levoglucosan (Fig. 1) may be valuable indicators to distinguish the smoke emissions from different wood types. Although the overall correlation between levoglucosan and mannosan data is strong (R^2 = 0.83), Fig. 1 demonstrates that the measured data are largely scattered in the Lev/Man space yielding a wide range of Lev/Man ratio values (Lev/Man, Table 1), suggesting a large variability in

wood categories and burning conditions. It has been found that generally smoke samples from conifer wood have an average Lev/Man ratios in the range of 2–5, while emissions from hardwood exhibit ratio values higher than 15 (Schmidl et al., 2008; Caseiro et al., 2009; Fabbri et al., 2009; Alves et al., 2010; Kuo et al., 2011; Giannoni et al., 2012; Herich et al., 2014). The measured Lev/Man ratios cover a wide range from 4 to 15 (shown by the lines in Fig. 1) with a mean value of $\approx$ 8 (Lev/Man, Table 1). These are intermediate values from which we can infer that in the investigated region wood smoke is produced by combustion of a mixture of hard- and softwood. The limit cases are maximum values (on average 15) measured in winter 2014 indicating nearly exclusive combustion of hard wood type (oak, beech and walnut), and minimum values in winter 2013 (on average 4) suggesting an increased contribution of soft wood.

The proportion of soft- and hardwood to ambient wood smoke level can be estimated from the Lev/Man ratios in ambient PM by applying a simple equation derived by Schmidl on the basis of the data obtained for the combustion of common hardwoods (beech and oak) and softwoods (spruce and larch) in wood stoves in Austria (Schmidl et al., 2008). When the Austrian approach is transferred to Emilia Romagna region, it can be estimated that wood fuel used in the investigated seasonal periods is generally formed by a 70% softwood − 30% hardwood mixture, with lower percentages of softwood in winter 2014 (spruce% in Table 1).

As to our knowledge, information on the wood types burnt in the region is lacking. The only available information is an inventory of the wood consumption, compiled in 2010 by the Emilia Romagna Regional Agency for Environmental and Sustainable Development (Deserti and Tugnoli, 2010). They reported that 90% of the wood burnt in domestic heating systems is common firewood collected in the local woodland and only 10% consists of logs or pellets. As a consequence, the prevalence of hardwood combustion would be likely expected, due to the highest local availability of these kinds of wood types in Emilia Romagna, such as poplar, beech, hornbeam, black locust, ash, oak.

However, caution should be taken when anhydrosugar ratios are exploited in the interpretations, since the strong dependence of anhydrosugar yields on combustion condition limits the comparability of values obtained across diverse studies (Simoneit, 2002; Kuo et al., 2011; Orasche et al., 2012). Thus, the conclusions made should take into consideration a more complex suite of parameters, such as the combination with galactosan and mannosan, that has been suggested as an even more discriminating markers (Simoneit, 2002 and citations therein; Fabbri et al., 2009; Kuo et al., 2011; Maenhaut et al., 2012).

Accordingly, the Lev/(Man + Gal) ratio is another diagnostic ratio that has been suggested to distinguish the smoke emissions caused by different fuel types: the diagnostic values are 1.5 $\pm$ 0.3 for softwood and 3.9 $\pm$ 2.1 for hardwood (Fabbri et al., 2009; Kuo et al., 2011; Kourtchev et al., 2011). The values computed for the investigated samples ranged from 3 to 8 (Lev/Man + Gal, Table 1), that suggest the prevalence of hardwood in the mixed wood fuel.

However, further arguments or data must be provided for substantiating this conclusion.

3.2.2. Methoxylated phenols

In addition to the most abundant anhydrosaccharides, a number of aromatic species carrying hydroxyl, carbonyl and carboxyl functional groups have been identified as lignin breakdown products and proposed as tracers for wood smoke pollution. They are mostly constituted by methoxyphenols arising from pyrolysis of wood lignin that is an important constituent of the macromolecular matter in wood. In addition, functionalized aromatic compounds − phthalic acid, 3-hydroxybenzoic acid, 4-hydroxy benzoic acid − are
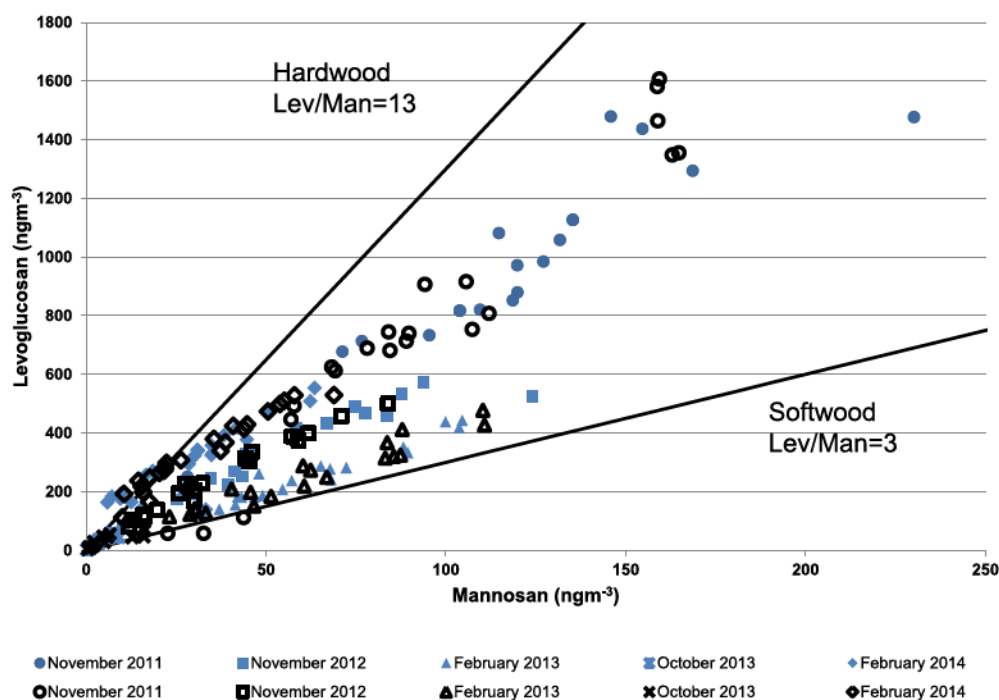
Fig. 1. Levoglucosan versus mannosan concentrations during 5 monitoring campaigns at MS (full symbols) and SP (empty symbols) sites.

also known to be produced during the pyrolysis of polysaccharides (Simoneit, 2002; Fine et al., 2004; Mazzoleni et al., 2007; Fabbri et al., 2009; Alves et al., 2010).

In the present study 11 lignin derivatives were determined, including three products derived from coniferyl alcohol – vanillin, acetovanillone and vanillic acid –, four compounds derived from sinapyl alcohol – syringaldehyde, acetosyringone, syringol and syringic acid – and four compounds derived from coumaryl alcohol – catecol, pyrogallol, coumaryc and ferrulic acids. The concentrations of individual compounds were added together to obtain the total concentration of all the investigated phenols (Tot phenols, Table 1). Overall, each methoxylated phenol occurred at low level in the 0.1–5.8 ng m^{-3} range, yielding a total average level of ≈ 13 ng m^{-3}, with the exception of low values close to 1 ng m^{-3} in Fall 2013. It must be underlined that the concentration levels of several target phenols were close to the detection limit of the analytical procedure, yielding large measurement uncertainties. For this reason the more sensible GC/MS/MS method was applied during the last campaign in February 2014 to assure the accurate quantification of the less abundant target tracers (Visentin and Pietrogrande, 2014).

Although with much lower concentration values, the methoxylated phenol data resembles closely those of sugars, even if relative abundances of methoxy phenols were not found to correlate with those of BB sugars. This observation is not surprising since the two classes of biomarkers originate from distinct biopolymers — hemicellulose/cellulose and lignin — with different combustion processes (Mazzoleni et al., 2007; Kuo et al., 2011). On the contrary, hydroxyl aromatic compounds – 3-OH and 4-OH benzoic acids – correlated very well with BB sugars ($R^2 \approx 0.9$) since they are produced during the pyrolysis of polysaccharides (Medeiros et al., 2006).

The lignin derivatives may be categorized into syringyls (Syr) and vanillyls (Van), according to the relative distribution of OH/OCH$_3$ substituents: the total concentration of each class was computed, from which the syringyls to vanillyls ratio was estimated (Syr/Van, Table 1).

Such Syr/Van ratios have been shown to be a useful indicator for the class of plant that is burnt. Gymnosperms (softwood) give rise to vanillyl compounds, whilst angiosperms (hardwood) yield predominantly syringyl compounds. Thus, high Syr/Van ratio values in burning smoke prove the presence of angiosperms (Mazzoleni et al., 2007; Kuo et al., 2011). The measured Syr/Van values cover the range from 0.4 to 4, indicating that these smoke particles were emitted from a heterogeneous mix of combustion conditions. However, for the most of the samples Syr/Van ratios fall in range 0.4–2.5 yielding a general mean value of 1.1 that is characteristic for chars from hardwood. This is confirmed by the average values computed for each campaign that are 1, (Syr/Van, Table 1), thus confirming the predominant contribution of smoke from hardwood combustion, with the only exception of unexpected lower value in November 2011 (Syr/Van ≈ 0.3, Table 1).

Finally, this data was combined with anhydrosugar ratios in a dual-biomarker approach that has been demonstrated to provide more reliable source discrimination in comparison with single diagnostic ratio, since it is less affected by diverse combustion conditions (Kuo et al., 2011). In this study property–property plots, drawn by plotting the levoglucosan to mannosan (Lev/Man) vs. syringyl to vanillyl phenols (Syr/Van) ratios (Fig. 2) clearly shows that almost all the samples are confined in the range of 5–14 for Lev/Man and that of 1–2 for Syr/Van that are diagnostic of emissions from hardwood combustion.

3.2.3. Primary biological sugars: saccharides and sugar alcohols

In addition to anhydrosaccharides, nine primary saccharides (glucose, sucrose, arabinose, galactose, mannose and mycose) and sugar alcohols (erythritol, ribitol and mannitol) were included in the study, since they have been found abundant in PM samples impacted by wood smoke (Pietrogrande et al., 2014b). These sugars are primary products of combustion, either emitted through direct volatilization from vascular plant saccharides or formed from the breakdown of polysaccharides. Some of the sugars may also be produced by hydrolysis of the corresponding anhydrosugars under the acidic atmospheric conditions created by biomass burning
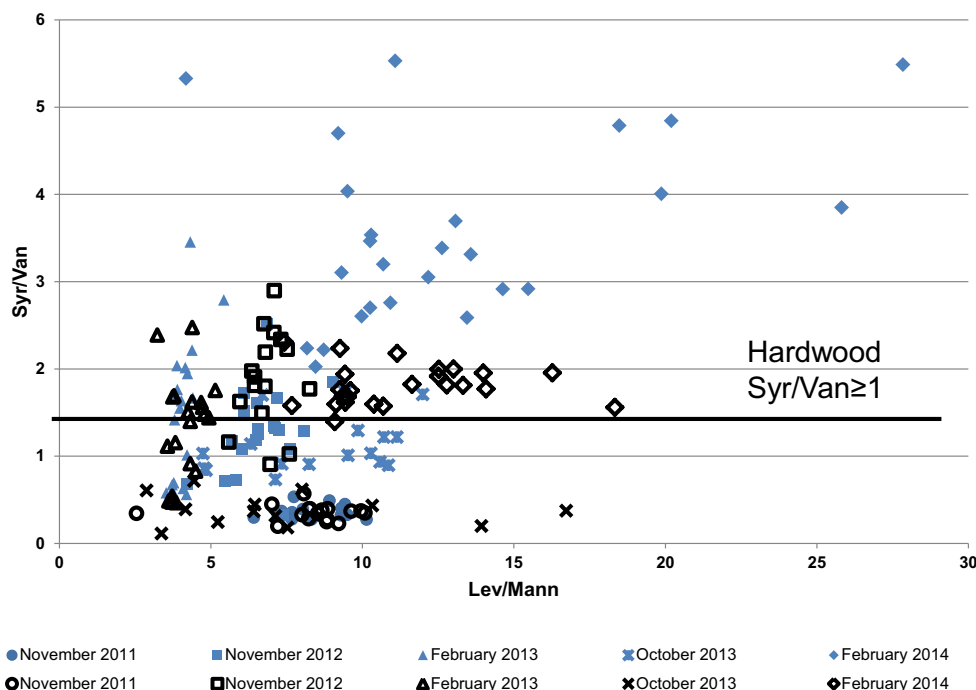
Fig. 2. Property–property plot of diagnostic ratios: levoglucosan to mannosan (Lev/Man) ratio vs. syringyl to vanillyl phenols (Syr/Van) ratios. Data of 5 monitoring campaigns at MS (full symbols) and SP (empty symbols) sites.

(Simoneit et al., 2004; Medeiros et al., 2006; Wang et al., 2011).

Table 1 lists the sum of nine primary sugars studied (total bio sugars, Tot_{BS}) and the individual concentration of the most abundant ones, i.e., arabinose, galactose, glucose and sucrose (mean values $\pm$ SD). Average values of total biosugar concentrations were close to 35 ng m^{-3} during all the campaigns, with the exception of the highest values of ≈ 70 ng m^{-3} in the first campaign in November 2011.

In most of the samples, the most abundant saccharides were sucrose and glucose (mean ≈ 10 ng m^{-3}) and the other sugars had concentrations of approximately 2 ng m^{-3}. The prevalence of these sugars may be related to direct volatilization during the combustion, since they are predominant sugars present at higher levels in vascular plants (Medeiros et al., 2006; Wang et al., 2011). This conclusion is supported by the good correlation found for the total concentrations of BB sugars and those of biological sugars ($R^2 = 0.8$) and sucrose in particular ($R^2 = 0.82$). Similar results have been found in smoke-impacted samples in many other locations in the world (Simoneit et al., 2004; Medeiros et al., 2006; Pio et al., 2008; Jia et al., 2010).

3.2.4. Carboxylic acids

High concentrations of carboxylic acids have been found in biomass burning smoke, as they can be directly generated by biomass combustion or secondary formed via photo-oxidation of biogenic gases or volatile combustion products (Simoneit, 2002; Mazzoleni et al., 2007; Jia et al., 2010; Alves et al., 2010; Wang et al., 2011; Van Drooge et al., 2012; Yang et al., 2013; Pietrogrande et al., 2013a, 2014a).

In the present study 16 carboxylic acids were investigated, including seven linear dicarboxylic acids with 3–9 carbon atoms and maleic and phthalic acids and 7 hydroxy/oxo carboxylic acids, namely glycolic, malic, glyoxylic, pinonic, 3- and 4-hydroxy benzoic and 2-ketoglutaric acids. At both the sites the total amount of the analyzed acids were ≈ 190 ng m^{-3}, with exceptionally lower data of nearly 55 ng m^{-3} in October 2013 (Tot CAs, mean values $\pm$ SD in

Table 1). In most of the analyzed samples, succinic acid was present in the highest concentration (≈ 45 ng m^{-3}, Table 1) among the measured carboxylic acids, followed by other C3–C4 dicarboxylic acids, i.e., malonic, maleic and malic (≈ 25 ng m^{-3}, Table 1). This may be related to the strong impact of emissions from wood burning, since succinic acid has been found specifically originated from wood burning, as well as the other C3–C4 diacids with similar molecular structures that are involved in common photochemical reactions of the burning products (Lee et al., 2006; Oliveira et al., 2007; Mazzoleni et al., 2007; Hsieh et al., 2008; Alves et al., 2010; Wang et al., 2011; Ho et al., 2011; Hyder et al., 2012). This hypothesis is supported by the excellent correlation of BB sugars with succinic acid ($R^2 = 0.96$) as well as with malic acid ($R^2 = 0.85$).

The data is in a good agreement with the results recently obtained by Paglione at the same site San Pietro indicating that biomass burning aerosol includes a non-negligible fraction of secondary origin, rich of carbonylic compounds and acids, in addition to a primary oxygenated component, rich of phenols and polyols (Paglione et al., 2014).

Overall, only a scattered correlation ($R^2 \approx 0.6$) was found between the concentrations of BB sugars and the total CA concentrations. This suggests that acids are emitted by a combination of different sources and are involved in secondary oxidation of several biogenic gases or volatile precursors, in addition to those related to biomass burning (Lee et al., 2006; Oliveira et al., 2007; Hsieh et al., 2008; Hallquist et al., 2009; Ho et al., 2011; Hyder et al., 2012; Saarikoski et al., 2012).

The results agreed well with those found in Lombardia region (Milan and Oasi Bine) and they were comparable with those reported in atmospheric aerosols of different cities in the world, i.e., Rome, Algiers, and Helsinki (Oliveira et al., 2007; Balducci and Cecinato, 2010; Hyder et al., 2012; Perrone et al., 2012) but significantly lower than those of other megacities, i.e., Tokio, Nanjing and Hong Kong (Lee et al., 2006; Ho et al., 2011; Wang et al., 2011; Huang et al., 2012).

3.2.5. Polycyclic aromatic hydrocarbons

To give further insights into the impact of wood combustion on air quality, high molecular weight PAHs were investigated in $PM_{2.5}$ samples, as they have been frequently found in Northern Italy during the cold seasons, as emitted from residential heating, including wood and coal combustion and natural gas-fired home appliance or their mix (van Drooge and Ballesta, 2010; Belis et al., 2011; Van Drooge et al., 2012; Perrone et al., 2012; Piazzalunga et al., 2013; Vassura et al., 2014; Gianelle et al., 2014). 19 individual PAHs were quantified, including the US EPA PAH priority pollutants: naphthalene, acenaphthene, acenaphthylene, fluorene, phenanthrene, anthracene, fluoranthene, pyrene, benzo[a]anthracene, cyclopenta(cd)pyrene, chrysene (Chr), benzo[b]fluoranthene (BbF), benzo[k]fluoranthene (BkF), benzo[e]pyrene (BeP), benzo[a]pyrene (BaP), perylene, indeno[1,2,3−c,d]pyrene (Ind123P), dibenzo[a,h]anthracene and benzo[g,h,i]perylene (BghiP). Table 1 reports the concentrations of the most abundant compounds – Chr, BbF, BkF, BeP, BaP, Ind 123P and BghiP – and the total PAH mass (tot PAHs, Table 1).

In general, PAHs were more abundant at the urban than at the rural site (mean value of tot PAHs are 4.3 and 3.2 ng m^{-3} at MS and SP, respectively). For the both sites, the seasonal variability was characterized by upper values in November 2011 (≈ 13 ng m^{-3} and ≈ 8 ng m^{-3} at MS and SP, respectively) and lower values in October 2013 (≈ 1 ng m^{-3} at the both sites), accordingly to the pattern observed for the other organic tracers. The measured data provided increased PAH levels at lower temperatures (rough negative correlation, $R^2 \approx 0.6$), that may be explained by the strengthening of emissions related to domestic heating in combination with factors related to the PAH physicochemical properties, such as volatility and reactivity with oxidants (Belis et al., 2011; Perrone et al., 2012; Piazzalunga et al., 2013; Vassura et al., 2014).

In the present dataset, the particulate PAHs were dominated by five− to six−ring compounds, such as by benzo[b] and benzo[k] fluoranthenes, followed by benzo[ghi]perylene and benzo[a], benzo[e] and indeno[1,2,3-cd] pyrenes. Also crysene was one of the most abundant PAHs in several samples. Such PAH distribution profiles indicate that the major emission sources in the studied area are wood combustion and traffic, in agreement with similar figures found in wintertime at other sites in Northern Italy (Larsen et al., 2012; Van Drooge and Ballesta, 2010; Perrone et al., 2012; Vassura et al., 2014). It is relatively difficult to identify PAH source profiles in ambient air, as the chemical composition and emissions rates of PAHs from sources depend largely on the nature of the fuel (i.e., gasoline, diesel, and type of wood) and the combustion conditions (i.e., temperature, humidity, availability of oxygen) (Ravindra et al., 2008; Katsoyiannis et al., 2011; Morville et al., 2011; Jedynska et al., 2014).

The set of individual PAHs showed a strong collinearity with intercorrelation values ranging from 0.7 to 0.9, which indicated a single dominant source for these compounds. In order to relate such a local emission source to wood combustion, the PAH levels were compared with levoglucosan data. A scattered but significant positive correlation was found with the total PAHs concentration ($R^2 = 0.78$), as well as with the most abundant PAHs – Chr, BbF, BkF, BeP, BaP, Ind123P and BghiP – with $R^2 = 0.71-0.79$, indicating that wood burning is a very important source for the measured PAHs in the studied area.

Among the target PAHs, benzo(a)pyrene (BaP) was investigated in detail, as it is regulated in the European Union (EU) by the 4th Air Quality Daughter Directive (2004/107/EC). The average concentrations ranged from 0.1 ng m^{-3} in October 2013 to 1.1 ng m^{-3} in November 2011. In general, BaP levels were lower than those detected in cold seasons at other urban sites in Northern Italy (Van Drooge and Ballesta, 2010; Perrone et al., 2012).

The measured BaP data showed a linear increase with levoglucosan concentrations, following a statistically significant correlation ($R^2 = 0.79$ for the whole data set and 0.7−0.8 for each sampling campaign, Fig. 3). This relationship is the basis for computing the BaP to Lev ratio giving the estimation for the source contribution of BB to the measured BaP concentration (BaP_{BB}), using the levoglucosan-BaP tracer method (Van Drooge and Ballesta, 2010; Belis et al., 2011; Piazzalunga et al., 2013). From our experimental data, a mean BaP/Lev value of 0.8 10^{-3} was found, similar to what has been reported by Belis et al. (Belis et al., 2011) as a ratio value representative of wood combustion in Lombardia region. The relative contribution of wood combustion to BaP ($BaP_{BB}/BaP\%$, Table 1) was estimated to be close to 70% for most of the campaigns, nearly 50% in warmer October 2013 (T = 15 C), but unrealistically close to 100% in February 2014 campaign. This may be due to the low accuracy of this single tracer method associated with the intrinsic uncertainty of the emission factors, since emissions of BaP and levoglucosan in wood smoke are largely influenced by several experimental conditions (Szidat et al., 2006; Orasche et al., 2012; Gianelle et al., 2014; Viana et al., 2013). Although the approximation of the present approach, the obtained results clearly prove that wood burning for residential heating is the main source for ambient BaP during the colder months (T 12 C). Such a contribution is lower ($\approx 70\%$) at the urban site MS, that is strongly impacted also by traffic source, and more relevant ($\approx 85\%$) at the rural site, where BaP emissions from traffic are lower.

The conclusions are comparable to those made from the data of recent monitoring results and emissions inventories in the Lombardy Region, that identified wood burning for residential heating as the major source of BaP, responsible almost completely (75%) for the total emissions in cold seasons (Belis et al., 2011; Gianelle et al., 2014). Similar results have been reported for different cities, where high proportion of the PAH air concentration in fall and winter has been associated with the predominant contribution of coal, wood, and peat burning (Van Drooge and Ballesta, 2010; Yin et al., 2010; Jedynska et al., 2014).

3.3. Composition of the carbonaceous aerosol

The characterization of the carbonaceous aerosol into organic (OC) and elemental carbon (EC) was performed, as generic indicator of air quality and source apportionment since it is related to several sources in urban and rural environments. In particular, there is actually general consensus that residential wood combustion is globally a very important source of the carbonaceous particulates, contributing up to 30% of the global particulate organic carbon (OC) budget (Holden et al., 2010; Herich et al., 2014; Philip et al., 2014; Fountoukis et al., 2014; Jedynska et al., 2014).

3.3.1. Carbonaceous aerosol loads

Each $PM_{2.5}$ filter was analyzed for EC, OC and their sum (total carbon, TC) was computed (averaged values and standard deviations for each campaign in Table 1). For the first campaign in November 2011, only TC values were available, since an unbiased discrimination between OC and EC was not obtained (Costa et al., 2016). In general, similar TC levels were measured in all the investigated periods, with TC mean values close to 7 μg m^{-3}, with the exception of high values (11.8 μg m^{-3}) at MS in November 2011. Overall, a constant contribution of TC to $PM_{2.5}$ mass close to 30% was found throughout the investigated periods at the both sites (TC/PM%, Table 1).

Although the spatial homogeneity of OC data with mean value of 5 μg m^{-3} at both sampling sites, significant differences were found for EC values with higher levels at the urban site MS (mean value 1.7 μg m^{-3}) in comparison with rural SP (mean value 1.0 μg m^{-3}).
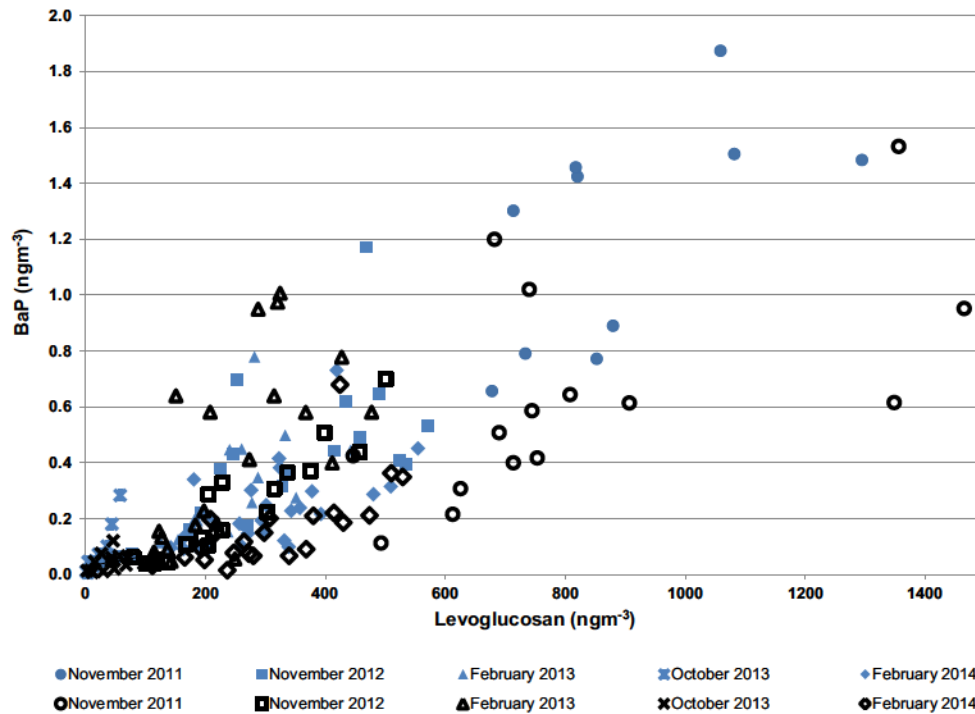
Fig. 3. Scatter plot of BaP versus levoglucosan concentrations: data of 5 monitoring campaigns at MS (full symbols) and SP (empty symbols) sites.

Such a higher spatial variability of EC compared to that of OC reflects the strong impact on EC of primary emissions from local traffic or residential heating, in contrast to OC, which is emitted by a much larger number of source types and also produced by secondary formation processes (Szidat et al., 2006; Kourtchev et al., 2011; Sandrini et al., 2014; Philip et al., 2014; Jedynska et al., 2014).

The results of this study are comparable with those observed during the cold period (October–March) at other urban background and rural sites in Po Valley, characterized by very high regional background, due to strength of anthropogenic emission sources (Piazzalunga et al., 2011; Belis et al., 2011; Perrone et al., 2012). In particular, the same urban/rural discrimination of EC levels was observed, with high levels encountered at urban background sites (≈ 2 μg m^{-3}) decreasing when moved to rural areas (≈ 1.0 μg m^{-3}) (Sandrini et al., 2014).

The ratio between OC and EC values was computed as an useful parameter in source apportionment studies, being influenced by primary emission sources and secondary organic aerosol formation. The measured OC to EC ratios were ≈ 3 at MS and ≈ 5 at SP (OC/EC; Table 1), that are values frequently found in polluted environments in winter. This data suggests that the primary sources of both OC and EC are combination of fossil fuels burning, characterized by OC/EC values frequently lower than 1, and residential wood burning, which is expected to release an enriched OC fraction (Gilardoni et al., 2011a; Piazzalunga et al., 2011; Sandrini et al., 2014; Jedynska et al., 2014). Consistently, the measured ratios are higher at the rural site, where the fraction of residential wood burning is larger in comparison with the traffic source.

Similar values ranging from 3 to 9 have been reported for ground-level rural and urban sites located in the Po Valley (Piazzalunga et al., 2011; Sandrini et al., 2014), consistent to what observed at other rural sites in Europe (Jedynska et al., 2014). However, it must be noted that the values of this study were lower than those (≈ 10) measured during cold seasons in other sites in the Eastern part of the Po Valley (Piazzalunga et al., 2011; Perrone et al., 2012; Piazzalunga et al., 2013) and even at the San Pietro site

(Gilardoni et al., 2014) and at Cassana, located at close distance (ca. 50 km) from it (Perrino et al., 2014).

3.3.2. Contribution of wood combustion to the carbonaceous fraction

In order to give insight into the relative contribution of wood combustion to OC, the scatter plots of levoglucosan versus OC were investigated, using levoglucosan as the key tracer for biomass combustion (Fig. 4). The obtained plots suggest a wide impact of wood combustion for domestic heating, in comparison with literature data (Szidat et al., 2006; Mazzoleni et al., 2007; Alves et al., 2010; Piazzalunga et al., 2011; Munchak et al., 2011; Holden et al., 2011; Maenhaut et al., 2012; Giannoni et al., 2012; Herich et al., 2014; Paglione et al., 2014; Vassura et al., 2014). The only exception is warmer October 2013 (mean temperature 15 C) characterized by lower levoglucosan concentration. Indeed, largely scattered data was obtained, that indicates a large variability of levoglucosan and OC concentrations in wood smoke. Such variations are potentially explained by differences in the type of wood combusted and stove used as well as in the burning conditions, i.e., rates, air dilution, and moisture content in the fuel (Szidat et al., 2006; Mazzoleni et al., 2007; Piazzalunga et al., 2011; Holden et al., 2011; Maenhaut et al., 2012; Herich et al., 2014).

From this data the levoglucosan to OC emission factors were computed (Lev/OC, Table 1) providing data ranging from 0.01 to 0.13 (indicated by the lines in Fig. 4). Although the large variability of such Lev/OC ratios, most of the results are included in the value range 0.06–0.2 reported in literature for the residential burning of softwood-hardwood mixtures (Szidat et al., 2006; Schimdl et al., 2008; Bari et al., 2010; Holden et al., 2011; Herich et al., 2014).

Based on the ambient concentrations of levoglucosan, the mono-tracer approach was applied for estimating the impact of wood burning on aerosol OC (OC$_{WB}$) in Emilia Romagna region (Puxbaum et al., 2007; Piazzalunga et al., 2011; Gilardoni et al., 2011; Herich et al., 2014). As suggested by Caseiro et al. (2009), an accurate estimate of such contribution in a region could be
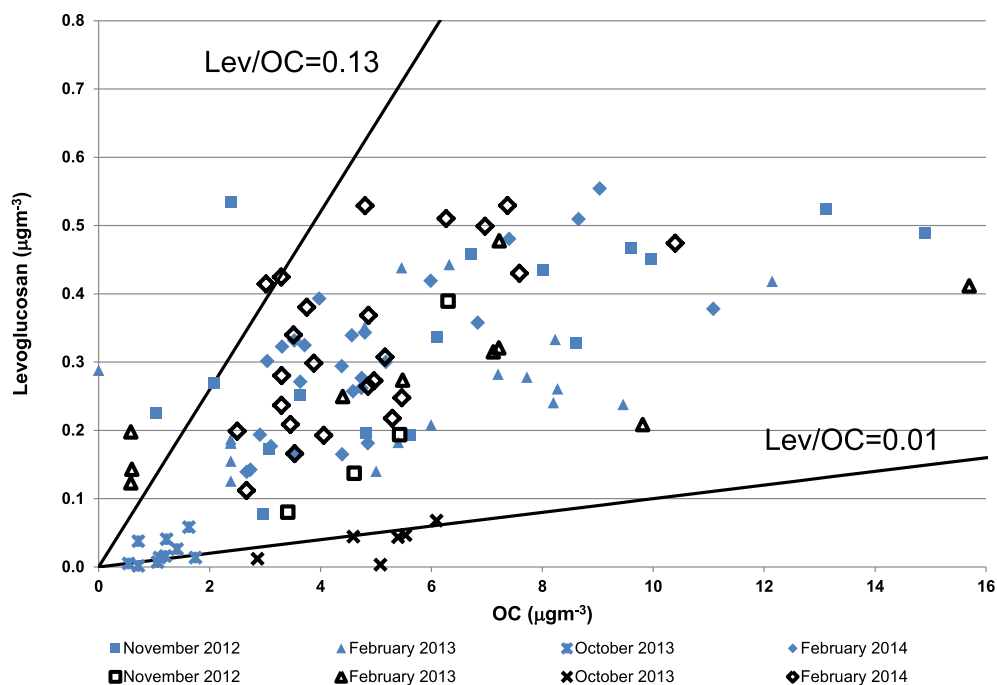
Fig. 4. Scatter plot of levoglucosan versus OC: data of 4 monitoring campaigns at MS (full symbols) and SP (empty symbols) sites.

achieved using site-specific emission factors, taking into account both the wood species actually burnt and the type of appliances in use. As this information was unknown, we utilized results from published field studies (Szidat et al., 2006; Puxbaum et al., 2007; Caseiro et al., 2009; Sang et al., 2013; Herich et al., 2014). In particular, we used the emission factor of 0.15 proposed by Szidat, as suitable for European areas. Such a factor has been calculated from literature data considering combustion for domestic heating of a wood fuel consisting of a mixture of hard and softwood that is consistent with our results from diagnostic ratios, as reported in Sections 3.2.1 and 3.2.2. This factor has been recently used in a study carried out at another Emilia Romagna site (Perrino et al., 2014).

With this assumption, we estimated the amount of OC derived from wood smoke as absolute concentrations (OC_{wb}) as well as relative contributions of OC_{wb} to total OC (OC_{wb}%) (mean values $\pm$ SD in Table 1). The absolute concentrations of OC_{wb} at both the sites were on average ≈ 3 μg m^{-3} in all the campaigns, excluding the exceptionally low values of ≈ 0.2 μg m^{-3} in October 2013. Consequently, we can estimate that the wood burning contribution to OC concentrations is about 33% in the November–February periods and only 5% in October 2013 (OC_{wb}%, Table 1). However, it must be underlined that these results may be affected by the relatively large uncertainty of the approach, as a consequence of the lack of specific emission factors based on the domestic heating systems in Emilia Romagna region (Caseiro et al., 2009; Schmidl et al., 2008; Munchak et al., 2011).

The results reported in Table 1 indicate that the use of wood stoves for domestic heating is a predominant source of organic carbon in atmospheric aerosol during the cold season at rural and urban sites in Emilia Romagna. These estimates are comparable with those found in cold seasons at other sites in the Po valley, such as in Lombardia region (Gilardoni et al., 2011) and Torino (Piazzalunga et al., 2013), which represent common background conditions of the densely populated plain characterized by agricultural and industrial activities (Bernardoni et al., 2011; Piazzalunga et al., 2011; Belis et al., 2011; Perrone et al., 2012). On the contrary, higher OC_{wb}% contributions close to 50% were

estimated at the industrial site of Cantù and Alpine locations (Piazzalunga et al., 2011, 2013; Herich et al., 2014). Similar wood burning impact on OC of about 35–40% is reported in the literature for other European locations in winter (Szidat et al., 2006; Caseiro et al., 2009; Bari et al., 2010; Puxbaum et al., 2007; Maenhaut et al., 2012; Fountoukis et al., 2014).

4. Conclusions

The large dataset measured in five monitoring campaigns during three years in two sites in Emilia Romagna region gave helpful insight into the contribution of wood burning to the ambient PM$_{2.5}$ in the regional area.

The distribution profiles of organic tracers and carbonaceous components indicated that in fall/winter air quality is strongly impacted by emissions from wood burning for domestic heating and also by secondary organic aerosols produced from primary smoke precursors, as suggested by high concentrations of low molecular weight carboxylic acids.

Besides the most abundant anhydrosaccharides, also methoxylated phenols were measured in all the samples and their diagnostic ratios were used to estimate the differentiation between the use of softwood and hardwood as combustion fuel. It was found that contribution from hardwood was dominating with little variation with campaign or with site.

The mono-tracer approach based on the levoglucosan content was applied to get a preliminary assessment of the wood burning impact to air quality in Emilia Romagna. The results demonstrated that wood smoke is one of the major contributors to organic particulate matter responsible for roughly 35% of OC at both sites. In addition, wood combustion is the dominating emission source of BaP, accounting for ≈ 85% of BaP ambient concentration at the rural site and for ≈ 70% at the urban site, the latter mostly influenced by the traffic source.

The uncertainty of the reported results based on wood burning profiles from literature can be reduced by more detailed information on the emission inventory that identifies the real impact of biomass burning source, as well as the real contribution of wood

and peat as burning fuels.

The importance of the contribution of wood burning to PM emission in Emilia Romagna region highlights the need of focused policies to control the use of wood burning for domestic heating as an efficient PM abatement strategy. As an example, recent simulation studies have predicted that the replacement of current residential wood combustion technologies with pellet stoves may provide a large decrease of organic aerosols in urban and suburban areas during winter (Fountoukis et al., 2014).

References

Alves, C.A., Gonçalves, C., Mirante, F., Nunes, T., Evtyugina, M., Sánchez de la Campa, A., Rocha, A.C., Marques, M.C., 2010. Organic speciation of atmospheric particles in Alvão Natural Park (Portugal). Environ. Monit. Assess. 168, 321—337.

Balducci, C., Cecinato, A., 2010. Particulate organic acids in the atmosphere of Italian cities: are they environmentally relevant? Atmos. Environ. 44, 652—659.

Bari, M.A., Baumbach, G., Kuch, B., Scheffknecht, G., 2010. Temporal variation and impact of wood smoke pollution on a residential area in southern Germany. Atmos. Environ. 44, 3823—3832.

Belis, C.A., Cancelinha, J., Duane, M., Forcina, V., Pedroni, V., Passarella, R., Tanet, G., Dous, K., Piazzalunga, A., Bolzacchini, E., Sangiorgi, G., Perrone, M.G., Ferrero, L., Fermo, P., Larsen, B.R., 2011. Sources for PM air pollution in the Po Plain, Italy: I. Critical comparison of methods for estimating biomass burning contributions to benzo(a)pyrene. Atmos. Environ. 45, 7266—7275.

Bernardoni, V., Vecchi, R., Valli, G., Piazzalunga, A., Fermo, P., 2011. PM10 source apportionment in Milan (Italy) using time-resolved data. Sci. Total Environ. 409, 4788—4795.

Bigi, A., Ghermandi, G., 2011. Particle number size distribution and weight concentration of background urban aerosol in a Po Valley site. Water Air Soil Pollut. 220, 265—278.

Calvo, A.I., Alves, C., Castro, A., Pont, V., Vicente, A.M., Fraile, R., 2013. Research on aerosol sources and chemical composition: past, current and emerging issues. Atmos. Environ. 44, 652—659.

Caseiro, A., Bauer, H., Schmidl, C., Pio, C.A., Puxbaum, H., 2009. Wood burning impact on PM10 in three Austrian regions. Atmos. Environ. 43, 2186—2195.

Caseiro, A., Oliviera, C., 2012. Variations in wood burning organic marker concentrations in the atmospheres of four European cities. J. Environ. Monit. 14, 2261—2269.

Cavalli, F., Viana, M., Yttri, K.E., Genberg, J., Putaud, J.P., 2010. Toward a standardized thermal-optical protocol for measuring atmospheric organic and elemental carbon: the EUSAAR protocol. Atmos. Meas. Tech. 3, 79—89.

Costa, V., Bacco, D., Castellazzi, S., Ricciardelli, I., Vecchietti, R., Zigola, C., Pietrogrande, M.C., 2016. Characterization of Carbonaceous Aerosol in Emilia-romagna during the Supersito Project: Influences of the Thermal-Optical Measurement Protocols. Atmos. Res. http://dx.doi.org/10.1016/j.atmosres.2015.07.020.

Deserti, M., Savoia, E., Cacciamani, C., Golinelli, M., Kerschbaumer, A., Leoncini, G., Selvini, A., Paccagnella, T., Tibaldi, S., 2001. Operational meteorological pre-processing at Emilia-Romagna ARPA Meteorological service as a part of a decision support system for Air Quality Management. Int. J. Environ. Pollut. 16, 571—582.

Deserti, M., Tugnoli, S., 2010. Inventory of the wood consumption in Emilia Romagna Region. Regional Agency Environ. Sustain. Dev. 11—16.

Fabbri, D., Torri, C., Simoneit, B.R.T., Marynowski, L., Rushdi, A.I., Fabianska, M.J., 2009. Levoglucosan and other cellulose and lignin markers in emissions from burning of Miocene lignites. Atmos. Environ. 43, 2286—2295.

Fine, P.M., Cass, G.R., Simoneit, B.R.T., 2004. Chemical characterization of fine particle emissions from the fireplace combustion of wood types grown in the Midwestern and Western United States. Environ. Eng. Sci. 21, 387—409.

Fountoukis, C., Butler, T., Lawrence, M.G., Denier van der Gon, H.A.C., Visschedijk, A.J.H., Charalampidis, P., Pilinis, C., Pandis, S.N., 2014. Impacts of controlling biomass burning emissions on wintertime carbonaceous aerosol in Europe. Atmos. Environ. 87, 175—182.

Gianelle, V., Colombi, C., Caserini, S., Ozgen, S., Galante, S., Marongiu, A., Lanzani, G., 2014. Benzo(a)pyrene air concentrations and emission inventory in Lombardy region Italy. Atmos. Pollut. Res. 4, 257—266.

Giannoni, M., Martellini, T., Del Bubba, M., Gambaro, A., Zangrando, R., Chiari, M., Lepri, M., Cincinelli, A., 2012. The use of levoglucosan for tracing biomass burning in PM2.5 samples in Tuscany (Italy). Environ. Pollut. 167, 7—15.

Gilardoni, S., Vignati, E., Cavalli, F., Putaud, J.P., Larsen, B.R., Karl, M., Stenström, K., Genberg, J., Henne, S., Dentener, F., 2011. Better constraints on sources of carbonaceous aerosols using a combined ^{14}C macro tracer analysis in a European rural background site. Atmos. Chem. Phys. 11, 5685—5700.

Gilardoni, S., Massoli, P., Giulianelli, L., Rinaldi, M., Paglione, M., Pollini, F., Lanconelli, C., Poluzzi, V., Carbone, S., Hillamo, R., Russell, L.M., Facchini, M.C., Fuzzi, S., 2014. Fog scavenging of organic and inorganic aerosol in the Po Valley. Atmos. Chem. Phys. Discuss. 14, 4787—4826.

Hallquist, M., Wenger, J.C., Baltensperger, U., Rudich, Y., Simpson, D., Claeys, M., Dommen, J., Donahue, N.M., George, C., Goldstein, A.H., Hamilton, J.F., Herrmann, H., Hoffmann, T., Iinuma, Y., Jang, M., Jenkin, M.E., Jimenez, J.L., Kiendler-Scharr, A., Maenhaut, W., McFiggans, G., Mentel, T.F., Monod, A., Prevot, A.S.H., Seinfeld, J.H., Surratt, J.D., Szmigielski, R., Wildt, J., 2009. The formation, properties and impact of secondary organic aerosol: current and emerging issues. Atmos. Chem. Phys. 9, 5155—5236.

Herich, H., Gianini, M.F.D., Piot, C., Mocnik, G., Jaffrezo, J.L., Besombes, J.L., Prévôt, A.S.H., Hueglin, C., 2014. Overview of the impact of wood burning emissions on carbonaceous aerosols and PM in large parts of the Alpine region. Atmos. Environ. 89, 64—75.

Ho, K.F., Ho, S.S.H., Lee, S.C., Kawamura, K., Zou, S.C., Cao, J.J., Xu, H.M., 2011. Summer and winter variation of dicarboxylic acids, fatty acids and benzoic acid in PM2.5 in Pearl Delta River Region, China. Atmos. Chem. Phys. 11, 2197—2208.

Holden, A.S., Sullivan, A.P., Munchak, L.A., Kreidenweis, S.M., Schichtel, B.A., Malm, W.C., Collett Jr., J.L., 2011. Determining contributions of biomass burning and other sources to fine particle contemporary carbon in the western United States. Atmos. Environ. 45, 1986—1993.

Hsieh, L.Y., Chen, C.L., Wan, M.W., Tsai, C.H., Tsai, Y.I., 2008. Speciation and temporal characterization of dicarboxylic acids in PM2.5 during a PM episode and a period of non-episodic pollution. Atmos. Environ. 42, 6836—6850.

Huang, X.F., Cheng, D.L., Lan, Z.J., Feng, N., He, L.Y., Yu, G.H., Luan, S.J., 2012. Characterization of organic aerosol in fine particle in a mega-city of South China: molecular composition, seasonal variation and size distribution. Atmos. Res. 114—115, 28—37.

Hyder, M., Genberg, J., Sandahl, M., Swietlicki, E., Jonsson, J.A., 2012. Yearly trend of dicarboxylic acids in organic aerosols from south of Sweden and source attribution. Atmos. Environ. 57, 197—204.

Jedynska, A., Hoek, G., Eeftens, M., Cyrys, J., Keukena, M., Ampe, C., Beelen, R., Cesaroni, G., Forastiere, F., Cirachg, M., Van de Hoogh, K., De Nazelle, A., Madsen, C., Declercq, C., Eriksen, K.T., Katsouyanni, K., Akhlaghi, H.M., Lanki, T., Meliefste, K., Nieuwenhuijsen, M., Oldenweningb, M., Pennanen, A., Raaschou-Nielsen, O., Brunekreef, B., Kooter, I.M., 2014. Spatial variations of PAH, hopanes/steranes and EC/OC concentrations within and between European study areas. Atmos. Environ. 87, 239—248.

Jia, Y., Bhat, S., Fraser, M.P., 2010. Characterization of saccharides and other organic compounds in fine particles and the use of saccharides to track primary biologically derived carbon sources. Atmos. Environ. 44, 724—732.

Katsoyiannis, A., Sweetman, A.J., Jones, K.C., 2011. PAH molecular diagnostic ratios applied to atmospheric sources: a critical evaluation using two decades of source inventory and air concentration data from the UK. Environ. Sci. Technol. 45, 8897—8906.

Kourtchev, I., Hellebust, S., Bell, J.M., O'Connor, I.P., Healy, R.M., Allanic, A., Healy, D., Wenger, J.C., Sodeau, J.R., 2011. The use of polar organic compounds to estimate the contribution of domestic solid fuel combustion and biogenic sources to ambient levels of organic carbon and PM2.5 in Cork Harbor, Ireland. Sci. Total Environ. 409, 2143—2155.

Kuo, L.-J., Louchouarn, P., Herbert, P.L., 2011. Influence of combustion conditions on yields of solvent-extractable anhydrosugars and lignin phenols in chars: implications for characterizations of biomass combustion residues. Chemosphere 85, 797—805.

Larsen, B.R., Giraldoni, S., Stenstrom, K., Niedzialek, J., Jimenez, J., Belis, C.A., 2012. Sources for PM pollution in the Po Plain, Italy. II. Probabilistic uncertainty characterization and sensitivity analysis of secondary and primary sources. Atmos. Environ. 50, 203—213.

Lee, S.C., Cao, J.J., Kawamura, K., Watanabe, T., Cheng, Y., Chow, J.C., 2006. Dicarboxylic acids, ketocarboxylic acids and dicarbonyls in the urban roadside area of Hong Kong. Atmos. Environ. 40, 3030—3040.

Maenhaut, W., Vermeylen, R., Claeys, M., Vercauteren, J., Matheeussen, C., Roekens, E., 2012. Assessment of the contribution from wood burning to the PM10 aerosol in Flanders, Belgium. Sci. Total Environ. 437, 226—236.

Mazzoleni, L.R., Zielinska, B., Moosmüller, H., 2007. Emissions of levoglucosan, methoxy phenols, and organic acids from prescribed burns, laboratory combustion of wildland fuels, and residential wood combustion. Environ. Sci. Technol. 41, 2115—2122.

Medeiros, P.M., Conte, M.H., Weber, J.C., Simoneit, B.R.T., 2006. Sugars as source indicators of biogenic organic carbon in aerosols collected above the Howland Experimental Forest, Maine. Atmos. Environ. 40, 1694—1705.

Morville, S., Delhomme, O., Millet, M., 2011. Seasonal and diurnal variations of atmospheric PAH concentrations between rural, suburban and urban areas. Atmos. Pollut. Res. 2, 366—373.

Munchak, L.A., Bret, A., Schichtel, B.A., Sullivan, A.P., Holden, A.S., Kreidenweis, S.M., Malm, W.C., Collett Jr., J.L., 2011. Development of wildland fire particulate smoke marker to organic carbon emission ratios for the conterminous United States. Atmos. Environ. 45, 395—403.

Oliveira, C., Pio, C., Alves, C., Evtyugina, M., Santos, P., Goncalves, V., Nunes, T.,

Silvestre, A.J.D., Palmgren, F., Wahlin, P., Harrad, S., 2007. Seasonal distribution of polar organic compounds in the urban atmosphere of two large cities from the North and South of Europe. Atmos. Environ. 41, 5555–5570.

Orasche, J., Torben Seidel, T., Hartmann, H., Schnelle-Kreis, J., Chow, J.C., Ruppert, H., Zimmermann, R., 2012. Comparison of emissions from Wood combustion. Part 1: emission factors and characteristics from different small-scale residential heating appliances considering particulate matter and Polycyclic Aromatic Hydrocarbon (PAH)-related toxicological potential of particle-bound organic species. Energy Fuels 26, 6695–6704.

Paglione, M., Saarikoski, S., Carbone, S., Hillamo, R., Facchini, M.C., Finessi, E., Giulianelli, L., Carbone, C., Fuzzi, S., Moretti, F., Tagliavini, E., Swietlicki, E., Stenstrom, K.E., Prevot, A.S.H., Massoli, P., Canaragatna, M., Worsnop, D., Decesari, S., 2014. Primary and secondary biomass burning aerosols determined by proton nuclear magnetic resonance (H-1-NMR) spectroscopy during the 2008 EUCAARI campaign in the Po Valley (Italy). Atmos. Chem. Phys. 14, 5089–5110.

Perrino, C., Catrambone, M., Dalla Torre, S., Rantica, E., Sargolini, T., Canepari, S., 2014. Seasonal variations in the chemical composition of particulate matter: a case study in the Po Valley. Part I: macro-components and mass closure. Environ. Sci. Pollut. Environ. Res. 21, 3999–4009.

Perrone, M.G., Ferrero, L., Larsen, B.R., Sangiorgi, G., De Gennaro, G., Udisti, G., Zangrando, R., Gambaro, A., Bolzacchini, E., 2012. Sources of high $PM_{2.5}$ concentrations in Milan, Northern Italy: molecular marker data and CMB modeling. Sci. Total Environ. 414, 343–355.

Perrone, M.G., Gualtieri, M., Consonni, V., Ferrero, L., Sangiorgi, G., Longhin, E., Ballabio, D., Bolzacchini, E., Camatini, M., 2013. Particle size, chemical composition, seasons of the year and urban, rural o remote size origins as determinants of biological effects of particulate matter on pulmonary cells. Environ. Pollut. 176, 215–227.

Philip, S., Martin, R.V., Pierce, J.R., Jimenez, J.L., Zhang, Q., Canagaratna, M.R., Spracklen, D.V., Nowlan, C.R., Lamsal, L.N., Cooper, M.J., Krotkov, N.A., 2014. Spatially and seasonally resolved estimate of the ratio of organic mass to organic carbon. Atmos. Environ. 87, 34–40.

Piazzalunga, A., Belis, C., Bernardoni, V., Cazzuli, O., Fermo, P., Valli, G., Vecchi, R., 2011. Estimates of wood burning contribution to PM by the macro-tracer method using tailored emission factors. Atmos. Environ. 45, 6642–6649.

Piazzalunga, A., Anzano, M., Collina, M., Lasagni, M., Lollobrigida, F., Pannocchia, A., Fermo, P., Pitea, D., 2013. Contribution of wood combustion to PAH and PCDD/F concentrations in two urban sites in Northern Italy. J. Aerosol Sci. 56, 30–40.

Pietrogrande, M.C., Bacco, D., Rossi, M., 2013a. Chemical characterization of polar organic markers in aerosols in a local area around Bologna, Italy. Atmos. Environ. 75, 279–286.

Pietrogrande, M.C., Bacco, D., Chiereghin, S., 2013b. GC/MS analysis of water-soluble organics in atmospheric aerosol: optimization of a solvent extraction procedure for simultaneous analysis of carboxylic acids and sugars. Anal. Bioanal. Chem. 405, 1095–1104.

Pietrogrande, M.C., Bacco, D., Visentin, M., Ferrari, S., Poluzzi, V., 2014a. Polar organic marker compounds in atmospheric aerosol in the Po Valley during the Supersito campaigns – Part 1: low molecular weight carboxylic acids in cold seasons. Atmos. Environ. 86, 164–175.

Pietrogrande, M.C., Bacco, D., Visentin, M., Ferrari, S., Casali, P., 2014b. Polar organic marker compounds in atmospheric aerosol in the Po Valley during the Supersito campaigns – Part 2: seasonal variations of sugars. Atmos. Environ. 97, 215–225.

Pio, C.A., Legrand, M., Alves, C.A., Oliveira, T., Afonso, J., Caseiro, A., Puxbaum, H., Sanchez-Ochoa, A., Gelencser, A., 2008. Chemical composition of atmospheric aerosols during the 2003 summer intense forest fire period. Atmos. Environ. 42, 7530–7543.

Puxbaum, H., Caseiro, A., Sanchez-Ochoa, A., Kasper-Giebl, A., Claeys, M., Gelencsér, A., Legrand, M., Preunkert, S., Pio, C., 2007. Levoglucosan levels at background sites in Europe for assessing the impact of biomass combustion on the European aerosol background. J. Geophys. Res. Atmos. 112 http://dx.doi.org/

10.1029/2006JD008114.

Ravindra, K., Sokhi, R., Van Grieken, R., 2008. Atmospheric polycyclic aromatic hydrocarbons: source attribution, emission factors and regulation. Atmos. Environ. 42, 2895–2921.

Saarikoski, S., Carbone, S., Decesari, S., Giulianelli, L., Angelini, F., Canagaratna, M., Ng, N.L., Trimborn, A., Facchini, M.C., Fuzzi, S., Hillamo, R., Worsnop, D., 2012. Chemical characterization of springtime submicrometer aerosol in Po Valley, Italy. Atmos. Chem. Phys. 12, 8401–8421.

Sandrini, S., Fuzzi, S., Piazzalunga, A., Prati, P., Bonasoni, P., Cavalli, F., Bove, M.C., Calvello, M., Cappelletti, D., Colombi, C., Contini, D., de Gennaro, G., Di Gilio, A., Fermo, P., Ferrero, L., Gianelle, V., Giugliano, M., Ielpo, P., Lonati, G., Marinoni, A., Massabò, M., Molteni, U., Moroni, B., Pavese, G., Perrino, C., Perrone, M.G., Perrone, M.R., Putaud, J.P., Sargolini, T., Vecchi, R., Gilardoni, S., 2014. Spatial and seasonal variability of carbonaceous aerosol across Italy. Atmos. Environ. 99, 587–598.

Sang, X., Zhang, Z., Chan, C., Engling, G., 2013. Source categories and contribution of biomass smoke to organic aerosol over the southeastern Tibetan Plateau. Atmos. Environ. 78, 113–123.

Schmidl, C., Marr, I.L., Caseiro, A., Kotianova, P., Berner, A., Bauer, H., Kasper-Giebl, A., Puxbaum, H., 2008. Chemical characterization of fine particle emissions from wood stove combustion of common woods growing in mid-European Alpine regions. Atmos. Environ. 42, 126–141.

Simoneit, B.R.T., 2002. Biomass burning—a review of organic tracers for smoke from incomplete combustion. Appl. Geochem. 17, 129–162.

Simoneit, B.R.T., Elias, V.O., Kobayashi, M., Kawamura, K., Rushdi, A.I., Medeiros, P.M., Rogge, W.F., Didyk, B.M., 2004. Sugars dominant water-soluble organic compounds in soils and characterization as tracers in atmospheric particulate matter. Environ. Sci. Technol. 38, 5939–5949.

Szidat, S., Jenk, T.M., Synal, H.-A., Kalberer, M., Wacker, L, Hajdas, I., Kasper-Giebl, A., Baltensperger, U., 2006. Contributions of fossil fuel, biomass-burning and biogenic emissions to carbonaceous aerosols in Zurich as traced by 14C. J. Geophys. Res. 111, D07206. http://dx.doi.org/10.1029/2005JD006590.

Vassura, I., Venturini, E., Marchetti, S., Piazzalunga, A., Bernardi, E., Fermo, P., Passarini, F., 2014. Markers and influence of open biomass burning on atmospheric particulate size and composition during a major bonfire event. Atmos. Environ. 82, 218–225.

Van Drooge, B., Ballesta, P.P., 2010. The influence of the North-Föhn on tracer organic compounds in ambient air PM10 at a pre-alpine site in Northern Italy. Environ. Pollut. 158, 2880–2887.

Van Drooge, B., Crusack, M., Reche, C., Mohr, C., Alastuey, A., Querol, X., Prevot, A., Douglas, A., Day, D.A., Jimenez, J.L., Grimalt, J.O., 2012. Molecular marker characterization of the organic composition of submicron aerosols from Mediterranean urban and rural environments under contrasting meteorological conditions. Atmos. Environ. 61, 482–489.

Viana, M., Reche, C., Amato, F., Alastuey, A., Querol, X., Moreno, T., Lucarelli, F., Nava, S., Cazolai, G., Chiari, M., Rico, M., 2013. Evidence of biomass burning aerosols in the Barcelona urban environment during winter time. Atmos. Environ. 72, 81–88.

Visentin, M., Pietrogrande, M.C., 2014. Determination of polar organic compounds in atmospheric aerosols by gas chromatography with ion trap tandem mass spectrometry. J. Sep. Sci. 37, 1561–1569.

Wang, G., Chen, C., Li, J., Zhou, B., Xie, M., Hu, S., Kawamura, K., Chen, C., 2011. Molecular composition and size distribution of sugars, sugar-alcohols and carboxylic acids in airborne particles during a severe urban haze event caused by wheat straw burning. Atmos. Environ. 40, 2473–2479.

Yang, L., Nguyen, D.M., Jia, S., Reid, J.S., Yu, L.E., 2013. Impacts of biomass burning smoke on the distributions and concentrations of C2-C5 dicarboxylic acids and dicarboxylates in a tropical urban environment. Atmos. Environ. 78, 211–218.

Yin, J., Harrison, R.M., Chen, Q., Rutter, A., Schauer, J.J., 2010. Source apportionment of fine particles at urban background and rural sites in the UK atmosphere. Atmos. Environ. 44, 841–851.

JOHN WILEY AND SONS LICENSE
TERMS AND CONDITIONS

Feb 07, 2016

This Agreement between Marco Visentin ("You") and John Wiley and Sons ("John Wiley and Sons") consists of your license details and the terms and conditions provided by John Wiley and Sons and Copyright Clearance Center.

License Number	3803551062824
License date	Feb 07, 2016
Licensed Content Publisher	John Wiley and Sons
Licensed Content Publication	Journal of Separation Science
Licensed Content Title	Determination of polar organic compounds in atmospheric aerosols by gas chromatography with ion trap tandem mass spectrometry
Licensed Content Author	Marco Visentin,Maria Chiara Pietrogrande
Licensed Content Date	May 14, 2014
Pages	9
Type of use	Dissertation/Thesis
Requestor type	Author of this Wiley article
Format	Print and electronic
Portion	Full article
Will you be translating?	No
Title of your thesis / dissertation	Chemical characterization of atmospheric aerosol for air quality evaluation in Emilia Romagna region
Expected completion date	Mar 2016
Expected size (number of pages)	200
Requestor Location	Marco Visentin Via L. Borsari 46 Ferrara, Italy 44121 Attn: Marco Visentin
Billing Type	Invoice
Billing Address	Marco Visentin Via L. Borsari 46 Ferrara, Italy 44121 Attn: Marco Visentin
Total	0.00 EUR
Terms and Conditions	

TERMS AND CONDITIONS

Marco Visentin
Maria Chiara Pietrogrande

Department of Chemical and
Pharmaceutical Sciences,
University of Ferrara, Ferrara,
Italy

Research Article

Determination of polar organic compounds in atmospheric aerosols by gas chromatography with ion trap tandem mass spectrometry

A gas chromatography with ion trap mass spectrometry method has been developed and validated for the analysis of 27 polar organic compounds in atmospheric aerosols. The target analytes were low-molecular-weight carboxylic acids and methoxyphenols, as relevant markers of source emissions and photochemical processes of organic aerosols. The operative parameters were optimized in order to achieve the best sensitivity and selectivity for the analysis. In comparison with the previous gas chromatography with mass spectrometry procedure based on single ion monitoring detection, the tandem mass spectrometry technique increased the analytical sensitivity by reducing detection limits for standard solutions from 1–2.6 to 0.1–0.4 ng/μL ranges (concentrations in the injected solution). In addition, it enhanced selectivity by reducing matrix interferences and chemical noise in the chromatogram. The applicability of the developed method in air quality monitoring campaigns was effectively checked by analyzing environmental samples collected in the Po Valley (Northern Italy) in different seasons. The obtained results indicate that the ion trap mass spectrometer may be an ideal alternative to high-resolution mass spectrometers for the user-friendly and cost-effective determination of a wide range of molecular tracers in airborne particulate matter.

1 Introduction

In recent years, there is increasing interest in chemical speciation of atmospheric particulate material (PM) since it is known to play an important role in local and regional air quality and to cause adverse effects on human health [1–3]. A substantial fraction of the organic component of atmospheric particles consists of polar, possibly multifunctional, compounds including carboxylic acids, sugars, and methoxyphenols. Although these organics are typically present in ambient air at low concentration levels, they have been used as reliable molecular markers to trace emission sources and environmental processes of the atmospheric PM [4, 5].

Among the different organic tracers, this work is focused on polar organic compounds, namely, low-molecular-

weight (LMW) carboxylic acids and methoxyphenols, that are mainly used as atmospheric markers to determine the contribution of wood smoke to ambient atmospheric PM [4, 6–9].

Organic acids are an important class of ubiquitous organic components that have been identified as molecular markers of a variety of primary sources, such as biomass burning, vehicular exhausts, cooking, and natural marine sources [4, 9–11]. In addition, they are mainly produced from the atmospheric photo-oxidation of various organic precursors [12, 13]. It is noteworthy that, although constituting only a small fraction of the total aerosol mass, these hydrophilic and hygroscopic compounds affect the earth's radiation budget and global climate, since they may modify cloud condensation nuclei, acid precipitation, and atmosphere optical properties [14, 15]. The more relevant tracers are C_2–C_9 dicarboxylic acids—with oxalic, malonic, or succinic acids being the most abundant species—and oxo-hydroxy carboxylic acids, as intermediate products of secondary photo-oxidation reactions [8, 10, 11, 16].

Methoxyphenols have been suggested as reliable molecular markers of biomass combustion, as they are specifically produced by lignin pyrolysis [4, 9, 17–20]. In addition to the most abundant anhydrosaccharides [21, 22], methoxyphenols are unique markers of biomass burning since the relative

---

Correspondence: Professor Maria Chiara Pietrogrande, Department of Chemical and Pharmaceutical Sciences, University of Ferrara, Via Fossato di Mortara 17/19, I-44100 Ferrara, Italy
E-mail: mpc@unife.it
Fax: +39-0532-240709

Abbreviations: CID, collision-induced dissociation; **IS**, internal standard; **LMW**, low-molecular-weight; **PM**, particulate material; **SIM**, selected-ion monitoring

distribution of OH/OCH substituents on their molecules can be related to the class of plant that is burnt [7, 23]. Therefore, diagnostic ratios of syringic/vanillic compounds (S/V) and cinnamic/vanillic compounds (C/V) have been proposed to identify emissions from specific plant tissue combustion, i.e. hard woods (oak, beech, and walnut) or soft woods (conifers) and grass and soft plant tissues.

In light of the normally low-concentration levels of these polar organic tracers in aerosols and the complexity of the environmental matrix [8,10,11,21,24], the reliable quantification of these compounds represents an analytical challenge, also because they are polar, semivolatile, and somewhat reactive. LC–MS or GC–MS are the typically used techniques because they provide high separation resolution, identification capability, and sensitivity compatible with PM monitoring. In this context, the GC–MS method remains the technique of choice complementary to LC–MS because it provides higher separation power and is much less affected by matrix effects, such as matrix ion suppression and isobaric interference [4, 25, 26].

Detection and quantification of GC–MS methods can be greatly improved in terms of specificity and sensitivity by using MS/MS that decreases LODs and improves S/Ns due to the effective exclusion of interfering matrix compounds [27–37]. To date, a tandem-in-space MS approach with triple quadrupole or sector MS/MS instruments is used in the majority of analytical applications to environmental samples, since it provides excellent quantification and unambiguous identification of the detected analytes [27–29]. In addition, the tandem-in-time technique with ion trap detector MS/MS (ITD-MS/MS) system has been shown to be a valuable user-friendly and cost-effective alternative, in particular instruments with internal source that allow switching between full-scan and MS/MS detection modes during the same chromatographic run [12, 30–37]. Although several reports have been published over the last years describing IT-MS applications in environmental analysis [12, 30, 31, 33–36], to our best knowledge, no work has been reported using GC–ITD-MS/MS method for the systematic analysis of polar organics in ambient particles, after the pioneering paper of Andalò on lignin monomers [38].

In this work, we investigated the potential of GC–MS/MS using ion trap for the sensitive and reliable determination of 27 polar organic compounds, namely, LMW carboxylic acids and methoxyphenols, in atmospheric PM samples. This is an improvement of the GC–MS procedure previously described [24, 39].

For this purpose, special attention was devoted to the investigation of ion trap MS/MS operating parameters in order to select precursor and product ions and optimize collision energy of each target compound. The developed procedure was applied exemplarily to examine the presence of the target compounds in real $PM_{2.5}$ samples collected in Bologna, a large urban center in the Po Valley (Northern Italy) that is recognized to have one of the most worrying air pollution situations in Europe [40–42].

2 Materials and methods

2.1 Chemicals

Dicarboxylic acid and methoxyphenols standards with purity higher than 99% were purchased from Fluka/Aldrich/Sigma (Sigma Aldrich, Milan, Italy). Deuterated *n*-dodecane was purchased from CDN Isotopes (Quebec, Canada). Individual standard stock solutions were prepared for each dicarboxylic acid and methoxyphenol investigated at concentrations varying from 1 to 2 $\mu g/\mu L$ in methanol and then diluted serially to prepare standard solutions at lower concentration levels. Derivatization was performed using *N,O*-bis(trimethylsilyl)trifluoroacetamide containing 1% trimethylchlorosilane and pyridine (silylation grade), both from Aldrich Chemical (Milan, Italy). The derivatizing agents, as well as the individual and composite standard solutions, were stored at 4°C.

2.2 GC–ITD-MS/MS analysis

The GC–MS system was a Scientific Focus-GC (Thermo-Fisher Scientific, Milan, Italy) coupled to PolarisQ Ion Trap Mass Spectrometer (Thermo-Fisher Scientific). The column used was a DB-5ms column (L = 30 m, I.D. = 0.25 mm, d_f = 0.25 μm film thickness; J&W Scientific, Rancho Cordova, CA, USA). High-purity helium was the carrier gas with constant flow of 1.5 mL/min. Temperature program conditions were optimized for analysis of a wide range of target polar organic compounds: an initial temperature of 70°C was raised to 125°C at 2.5°C/min, followed by an isothermal hold for 7 min; after that, the temperature was increased to 145°C at 2°C/min, an isothermal hold for 5 min; then further raised to 170°C at 2.5°C/min and finally led to 300°C at 7°C/min; this temperature was maintained for 1 min. All samples were injected in splitless mode (splitless time: 60 s); the injector temperature was 250°C.

Ion source and transfer-line temperatures were 250 and 280°C, respectively. The mass spectrometer operated in electron ionization mode (positive ion, 70 eV) and the mass spectra were acquired in full-scan mode from 50 to 650 *m/z* in 0.58 s. For identification and quantification of the target analytes, the selected-ion monitoring (SIM) chromatograms were extracted from the acquired signal by selecting either the base peak ion or the most abundant characteristic fragments [39].

In the multiple reaction monitoring mode, the isolation window was set at 1.5 *m/z*. Precursor ions were stored with a Paul stability parameter (qz) of 0.30 and fragmented by collision-induced dissociation (CID) using a resonant excitation mode.

2.3 Aerosol sampling and preparation

$PM_{2.5}$ samples were collected and handled following the procedure outlined in European Standard EN 12341 (CEN, 1998),

in accordance with Quality Assurance and Quality Control procedures, as reported in detail elsewhere [24]. Aerosols were collected on quartz fiber filters (Whatman, 47 mm diameter) using a low-volume sampler (Skypost PM, TECORA Instruments, Corsico, Milan, Italy) operating at a flow rate of 2.3 m^3/h for 24 h ($\approx$55 m^3/day). In spring, aerosols were collected on quartz fiber filters (Munktell, 100 mm diameter) using a high-volume air sampler (Echo Hi-Vol, TECORA Instruments) at the flow rate of 11.7 m^3/h for 24 h ($\approx$283 m^3/day). The collected samples were protected against light and temperature between the sampling and the analysis, in conformity with EN15549 (CEN, 2008).

The analytical procedure has been described elsewhere [43] and briefly summarized in the following. PM samples were extracted for 15 min in an ultrasonication bath with 15 mL of methanol/dichloromethane 9:1 solvent mixture. Then the extracts were filtered using a Teflon filter (25 mm, 0.45 μm, Supelco, Bellefonte, PA, USA) to remove insoluble particles and then the filtrates were evaporated to dryness in a

centrifugal vacuum concentrator (miVac Duo Concentrator, Genevac, Ipswich, UK).

Due to their high polarity, lignin phenols and carboxylic acids have to be converted into volatilizable and stable derivatives prior to GC analysis. The analytical protocol is based on a silylation reaction at 75°C: the sample evaporated to dryness was added to 40 μL of *N,O*-bis(trimethylsilyl) trifluoroacetamide containing 1% of trimethylchlorosilane and 15 μL of pyridine, in addition to 5 μL of internal standard (IS). After 70 min, the derivatives were cooled to room temperature and 2 μL of solution were injected for GC–MS analysis [43].

2.4 Method development and validation

Quantitative analysis was performed by the IS calibration method. Stock standard solution of deuterated $C_{12}H_{26}$ was prepared in *iso*-octane at 1275 ng/μL concentration to be used as injection IS.

Table 1. GC retention times and operative conditions of MS and MS/MS methods

Compound	Retention time (min)	SIM Monitoring ion(s) (*m/z*)	MS/MS Precursor ion (*m/z*)	CID voltage (V)	Product ions (*m/z*)	Ion intensity ratio
Acids						
Malonic acid	11.5	73, 147, 149	233	1.00	147, 149, 217	1:1:3.9
Glyoxylix acid	13.4	191, 221 265, 133	191	1.00	149, 73, 147	1:1.3:1.6
Maleic acid	15.7	73, 147, 149	245	1.00	217, 149, 147	1:1.3:2.6
succinic acid	16.3	73, 147, 149	247	1.00	149, 147	1:2.2
glutaric acid	20.5	73, 147, 149	233	1.25	149, 147	1:1.8
malic acid	24.9	73, 147, 149	245	1.25	149, 217, 147	1:1.5:2.5
pyruvic acid	25.1	215, 258, 281	215	1.25	149, 147	1:1.9
adipic acid	25.9	141, 185, 111	141	0.75	99, 75	1:32
pinonic acid	26.6	171, 109, 83, 125	109	1.00	91, 81, 79	1:1.7:3.2
3-hydroxybenzoic acid	29.8	267, 223, 193	267	1.25	193, 225, 223	1:2.1:3.2
pimelic acid	33.4	125, 155, 199	125	1.00	97, 69, 79	1:1.1:3.3
2-ketoglutaric acid	34	113, 347, 291	113	1.25	85, 95, 69	1:1.1:1.3
4-hydroxybenzoic acid	34.3	267, 223, 193	267	1.25	193, 225, 223	1:6:17.2
phthalic acid	38.3	295, 219, 265	295	1.00	149, 147	1:2.7
suberic acid	39.7	169, 303, 187	169	1.00	141, 93, 75	1:1.1:21
azelaic acid	47.4	317, 225, 133	225	1.25	169, 143, 167	1:2.7:7.8
Phenols						
Catechol	16.6	239, 254, 327, 166	254	1.00	166, 239	1:49
Syringol	20.6	181, 211, 196	196	1.25	167, 153, 181	1:2.2:3.5
Vanillin	26.7	193, 194, 209	194	1.50	165, 137	1:1
Pyrogallol	27.2	239, 240, 342	239	1.25	151, 133, 211	1:3.4:4.6
Acetosyringone	33.1	193, 208, 223	193	1.25	137, 165	1:1.3
Syringaldehyde	38.6	223, 224, 239	224	1.25	167, 137, 195	1:1.4:1.5
Acetovanillone	43.6	238, 223, 253	238	1.00	238, 223	1:18
Vanillic acid	44.1	223, 267, 297	267	1.25	225, 223	1:2.9
Syringic acid	53	253, 297, 327, 312	297	1.50	223, 253	1:5.8
p-Coumaric acid	54.8	219, 249, 293	293	1.50	219, 233, 249	1:1.1:6.3
Ferulic acid	59.3	249, 293, 323	293	1.50	219, 233, 249	1:1.1:5.5

MS detection: *m/z* values of characteristic fragments in full-scan spectrum; MS/MS detection: *m/z* values of ion retained as precursor ion, optimized CID voltage (V), *m/z* values of characteristic product ions used for identification, ratio values between intensities of the quantifier and qualifiers ions.
Underlined values indicate fragment ions used for quantitation in MS/SIM and MS/MS modes.

Five-point calibration curves were computed using working standard solutions composed of the 27 target analytes in the 0.2–3 ng/μL concentration range (corresponding to 0.4–5.4 ng/m^3 concentration in the air with the aerosol sampling protocol of 55 m^3/day). The selected concentration range is representative of trace levels at which the target analytes are most widely found in atmospheric aerosol [6–9, 11, 16, 18]. Each point of the curve was obtained as the average of three replicated measurements.

3   Results and discussion

In this paper, 27 target analytes were selected as representative of polar markers that are usually present in PM samples at trace levels. They include 16 LMW acids, namely, dicarboxylic (C$_3$–C$_9$ *n*-alkanoic, maleic, and phthalic dicarboxylic acids, DCAs) and oxo- (glyoxylic, pyruvic, pinonic, and 2-ketoglutaric acids) and hydroxy carboxylic acids (malic, OH-benzoic acids). Eleven alkoxyphenols were also investigated as molecular markers of biomass burning: cathecol, pyrogallol, *p*-coumaric, and ferulic acids; vanillic compounds, such

as vanillin, vanillic acid, acetovanillone; and syringic compounds, i.e. syringol, syringaldehyde, syringic acid, and acetosyringone.

GC–MS analysis using full-scan detection mode was used to optimize the separation conditions of all the target analytes (retention times in Table 1, 2nd column) and to obtain the EI mass spectra of each analyte from which the most abundant and/or characteristic ions were selected for extracting the monitored signal (underlined values in Table 1, 3rd column).

3.1 Optimization of IT-MS/MS conditions

An IT-MS/MS multiple reaction monitoring method was developed by investigating the operative key parameters, in order to select proper precursor and product ions and to optimize collision energies for the best responses.

One precursor ion was selected for each compound from EI full-scan spectra at 70 eV and an emission current of 40 mA. The choice was based on selectivity rather than on signal intensity: among the potential precursor ions,
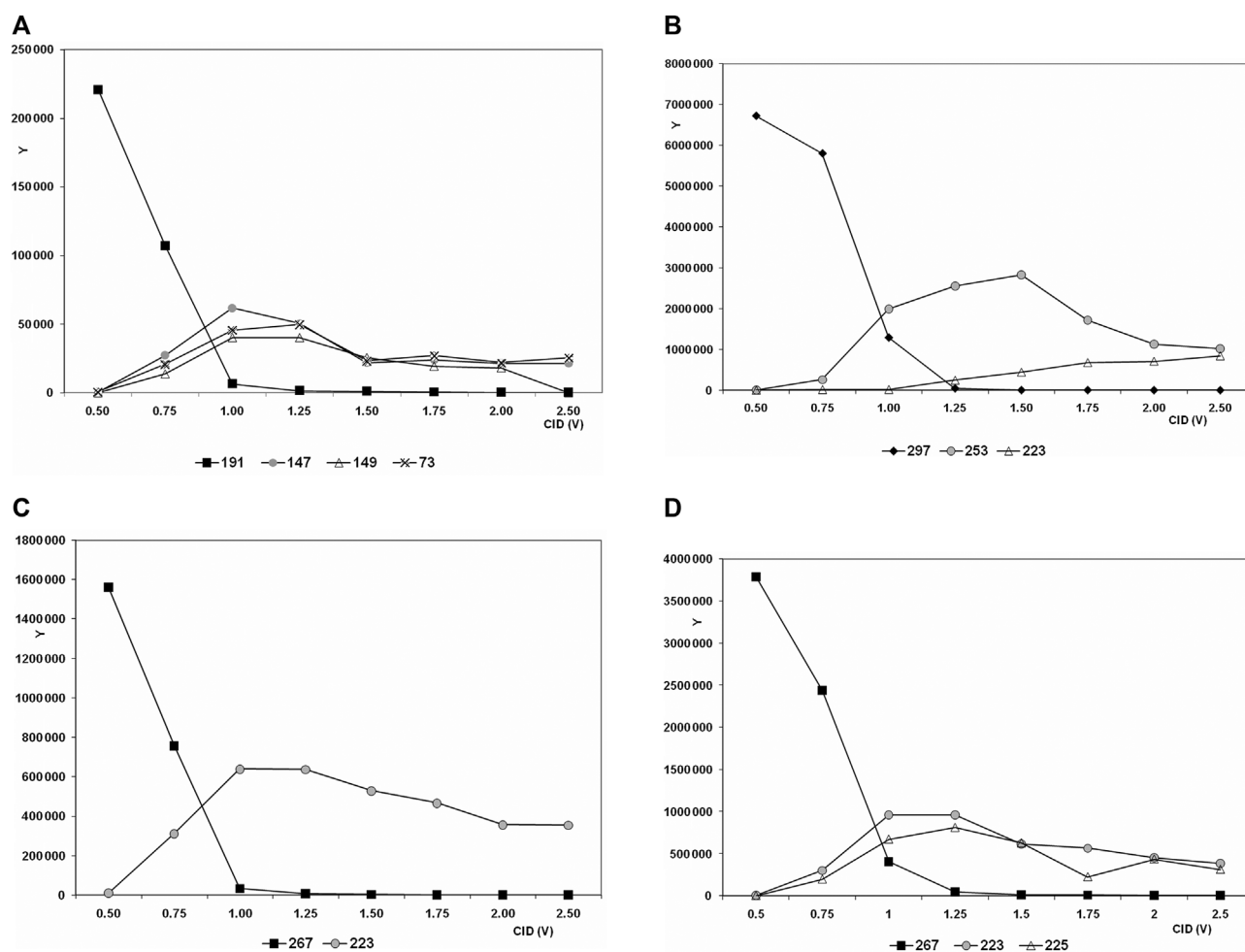
Figure 1. Optimization of the ion trap resonant excitation voltage for four selected organic polar compounds: (A) glyoxilic acid; (B) syringic acid; (C) vanillic acid; (D) 3-OH-benzoic acid.

preferably ions at the higher mass range ($m/z > 100$) were chosen because this usually afforded the highest S/Ns for the obtained product ions (the selected precursor ions are listed in Table 1, 4th column).

For each analyte, the precursor ion was subjected to further fragmentation under different collision energies to give different fragments in product scan mode. Product ions were selected from such fragment ions on the criteria of peak sensitivity and the likelihood of potential interference from other compounds in real samples [44]. At least two product ions with high responses were chosen for each target analyte (listed in Table 1, 6th column); among them, product ions with lower abundance were used for qualification and those with higher abundance for quantitation (ratio values between quantifier and qualifier ions for each analyte are reported in Table 1, 7th column).

The next step for MS/MS method development was the optimization of the CID value that produces the highest abun-

dance of product ions and minimizes interference during the analysis. So a series of different collision energies (0.5–2.5 V) were applied and the responsiveness (peak area) for different voltage was measured for each analyte. As a general pattern, the abundance of the parent ion was at the highest when the applied voltage was lower. The parent ion gradually fragmented, and peak area of the product ion obtained increased with the voltage. However, when the voltage was too high, the product ion intensity sharply reduced.

Figure 1A–D illustrates the change in the abundance of precursor and product ions with the CID voltage for glyoxilic, syringic, vanillic, and 3-OH-benzoic acids, respectively (other parameters as default values). The plots show that the CID optimum values were 1.0 V for glyoxilic acid, 1.25 V for vanillic and 3-OH-benzoic acids, and 1.5 V for syringic acid, since these voltages yield the highest intensity of the product ions used for quantification. The optimized CID voltages for each analyte are summarized in Table 1 (4th column).

Table 2. Statistical parameters of the calibration curves (2nd−4th columns) and sensitivity (LOD values, 5th−7th columns) of the developed MS/MS detection procedure. Sensitivity for MS detection (SIM mode, 8th−10th columns) is reported for comparison

	R^2	b1	b0	X_{LOD} MS/MS (ng/μL)	X_{LOD} MS/MS 55 m^3 (ng/m^3)	X_{LOD} MS/MS 283 m^3 (ng/m^3)	X_{LOD} SIM (ng/μL)	X_{LOD} SIM 55 m^3 (ng/m^3)	X_{LOD} SIM 283 m^3 (ng/m^3)
Acids									
Malonic acid	0.996	0.0074 ± 0.0001	−0.0003 ± 0.0001	0.25	0.46	0.09	0.69	1.25	0.24
Glyoxylix acid	0.998	0.044 ± 0.0010	0.0017 ± 0.0016	0.18	0.32	0.06	1.65	3.01	0.58
Maleic acid	0.999	0.016 ± 0.0003	0.0001 ± 0.0005	0.15	0.27	0.05	2.14	3.89	0.75
Succinic acid	0.999	0.0210 ± 0.0003	0.0009 ± 0.0005	0.12	0.22	0.04	1.23	2.23	0.43
Glutaric acid	0.998	0.0911 ± 0.0021	−0.0038 ± 0.0033	0.18	0.33	0.06	0.40	0.73	0.14
Malic acid	0.994	0.029 ± 0.0011	0.0021 ± 0.0018	0.30	0.55	0.11	2.31	4.21	0.82
Pyruvic acid	0.997	0.0791 ± 0.0023	−0.0044 ± 0.0034	0.21	0.39	0.08	2.36	4.28	0.83
Adipic acid	0.999	0.147 ± 0.0026	−0.0039 ± 0.0041	0.14	0.25	0.05	1.91	3.47	0.67
pinonic acid	0.997	0.0160 ± 0.0004	−0.0014 ± 0.0007	0.20	0.37	0.07	0.97	1.76	0.34
3-OH-benzoic acid	0.999	1.019 ± 0.020	−0.073 ± 0.031	0.15	0.28	0.05	1.12	2.03	0.39
Pimelic acid	0.994	0.0316 ± 0.0013	−0.0018 ± 0.0020	0.32	0.59	0.11	1.67	3.03	0.59
2-Keto-glutaric acid	0.998	0.0038 ± 0.0001	−0.0001 ± 0.0001	0.18	0.32	0.06	2.02	3.67	0.71
4-OH-benzoic acid	0.992	0.908 ± 0.040	−0.036 ± 0.063	0.35	0.64	0.12	1.62	2.95	0.57
Phthalic acid	0.999	0.0350 ± 0.0006	−0.0024 ± 0.0009	0.13	0.25	0.05	0.98	1.79	0.35
Suberic acid	0.996	0.0494 ± 0.0015	−0.0043 ± 0.0024	0.24	0.44	0.08	2.46	4.48	0.87
Azelaic acid	0.995	0.0074 ± 0.0003	−0.0010 ± 0.0004	0.28	0.52	0.10	2.65	4.82	0.93
Phenols									
Catechol	0.998	0.0661 ± 0.0014	−0.0029 ± 0.0024	0.18	0.33	0.06	1.53	2.72	0.53
Syringol	0.997	0.452 ± 0.012	−0.017 ± 0.023	0.26	0.47	0.09	2.35	4.27	0.83
Vanillin	0.994	0.2196 ± 0.0087	−0.024 ± 0.013	0.30	0.54	0.10	2.59	4.71	0.91
Pyrogallol	0.998	1.138 ± 0.028	0.002 ± 0.041	0.18	0.33	0.06	2.04	3.70	0.72
Acetosyringone	0.992	0.2200 ± 0.0098	−0.023 ± 0.016	0.37	0.68	0.13	2.01	3.66	0.71
Syringaldehyde	0.991	0.1510 ± 0.0074	−0.014 ± 0.011	0.38	0.70	0.14	1.26	2.28	0.44
Acetovanillone	0.991	0.553 ± 0.026	−0.067 ± 0.039	0.36	0.65	0.13	1.89	3.43	0.67
Vanillic acid	0.995	0.623 ± 0.023	−0.079 ± 0.036	0.29	0.53	0.10	2.31	4.21	0.82
Syringic acid	0.993	0.694 ± 0.028	−0.093 ± 0.043	0.32	0.57	0.11	1.93	3.50	0.68
p-Coumaric acid	0.997	0.479 ± 0.012	−0.053 ± 0.022	0.23	0.42	0.08	1.56	2.83	0.55
Ferulic acid	0.995	0.567 ± 0.020	−0.078 ± 0.034	0.30	0.54	0.10	1.72	3.12	0.61

X_{LOD} values are computed as concentration in the injected solution (ng/μL, 5th and 8th columns) or in the sampled air (ng/m^3) using low-volume (55 m^3, 6th and 9th columns) or high-volume (283 m^3, 7th and 10th columns) air sampling protocols.

3.2 Method validation

Using these IT-MS-optimized operating conditions, the method was validated by determining the linearity and LODs on standard solutions of the target compounds.

The calibration curves were developed using working solutions composed of mixed 27 target standards. The statistical parameters were computed by least-square fit between the peak areas of the chromatographic signals. In general, all the obtained calibration curves show good linearity in the exploited range, with a coefficient of determination $R^2 \geq 0.98$ (Table 2, 2nd column). From such curves, the LODs of the procedure, X_{LOD}, were calculated as the concentration that produces signals with S/Ns equal to or greater than 3. As the blank values were outside the noise of the instrument, the effective X_{LOD} was calculated as $X_{LOD} = 3b_0/b_1$, where b_0 is the intercept and b_1 is the slope of the calibration line (Table 2, 3rd–5th columns). X_{LOD} was computed as concentration in the injected solution (ng/μL) and additionally as concentration in the air volume sampled using low-volume (55 m^3, 6th column) or high-volume (283 m^3, 7th column) air sampling protocols. The obtained X_{LOD} values were in the range 0.1–0.4 ng/μL, corresponding to air concentration of 0.2–0.7 ng/m^3 using a low-volume air sampler. This sensibility is comparable with that provided by more advanced systems that require high capital and operating costs, such as

high-resolution mass spectrometers (GC–HRMS) [14, 29, 45] or direct thermal desorption method followed by GC and TOF MS [22].

In order to evaluate the effective improvement of the MS/MS procedure, the detection limits were also computed for the same standard solutions using the GC—MS method with SIM detection (Table 2, 8th–10th columns). The obtained X_{LOD} values varied from 0.7 to 2.7 ng/μL in the injected solution (corresponding to 1.3–4.9 ng/m^3 in the air, sampling air volume of 55 m^3), in agreement with the data previously reported for carboxylic acids and sugars [43]. This sensitivity is comparable with that of some literature methods using solvent extraction ranging from 0.5 to 1.1 ng/m^3 [6, 11, 16, 18, 19, 43].

These results clearly show that the hyphenation with MS/MS method effectively improves method sensitivity by a factor of six in comparison with the same analytical procedure with SIM detection (compare 5th versus 8th columns in Table 2).

3.3 Method feasibility in analysis of real-life samples

Finally, to further illustrate the potential of the developed method, it was applied to PM$_{2.5}$ real samples and its performance was compared with that of GC–MS with SIM detection.
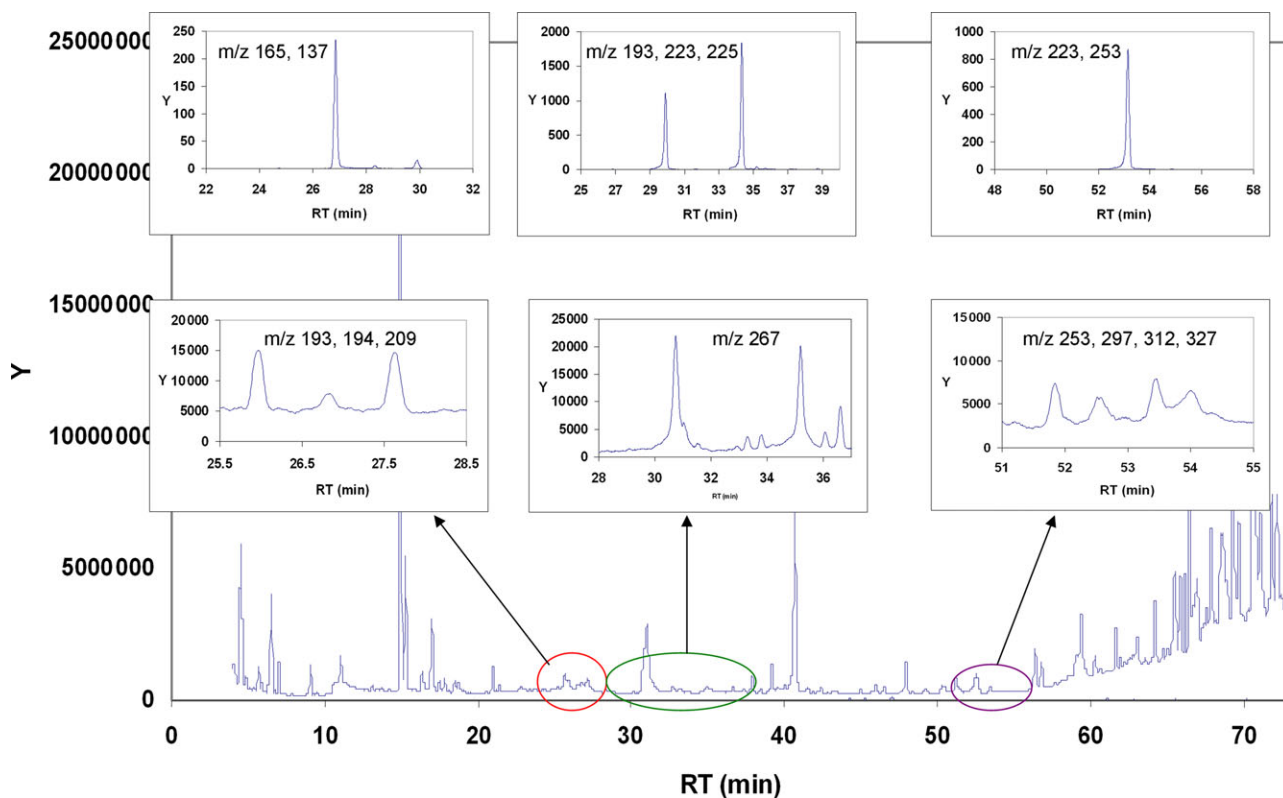
Figure 2. GC–MS chromatogram (TIC signal) of the real PM sample collected in winter. Enlarged details: signals for four selected compounds using SIM detection (bottom) and MS/MS detection (top). *m/z* 165, 137: Vanillin, *m/z* 193, 223, 225: 3-OH- and 4-OH-benzoic acids, *m/z* 223, 253: syringic acid.

The PM$_{2.5}$ filter samples were collected in winter 2011 and spring 2013 in an urban site (Bologna) in the Emilia Romagna region (Northern Italy).

Figure 2 shows the GC–MS chromatogram (total ion current, TIC signal) of the real PM sample collected in winter. As expected, the complex TIC signal contains several visible peaks due to original and derivatized components of the real sample that may interfere the GC–MS analysis. The plots clearly show that the SIM detection (lower enlarged detail) strongly enhances selectivity of each target analyte and the MS/MS method (upper enlarged detail) further improves detection performance due to the effective exclusion of interfering matrix compounds.

The results obtained revealed that the implementation with MS/MS detection permits the quantification of nearly all the target tracers at concentration level below the detection limits of the SIM detection (Table 3). Although some pairs of the target compounds show very close retention times,

they can be quantified by using SIM detection for the more abundant component and MS/MS method with specific precursor ion for the less abundant, i.e. succinic acid/catechol at ≈16.5 min, vanillin/pirogallol at ≈27 min, 2-ketoglutaric/pimelic acid at ≈34 min, phthalic acid/syringaldehyde at ≈38.6 min. The exception was the acetovanillone/vanillic acid pair, which were both present at low levels: in this case, two distinct MS/MS acquisition runs were required with proper precursor ion for each compounds, i.e. *m/z* 238 and 267, respectively.

The winter sample shows a PM composition strongly impacted by maleic and succinic acids (≈30 ng/m^3, each) followed by glycolic acid (≈ 12 ng/m^3, Table 3, 4th column). These markers are mainly related to anthropogenic activities, since they are either emitted from primary sources (power plants, vehicular circulation, biomass burning) or produced by *in situ* photochemical reactions of such emissions. In addition, other specific tracers were identified

Table 3. Concentrations of the polar markers in the real PM$_{2.5}$ samples collected in winter (2nd−4th columns) and spring (5th−7th columns)

	Winter 2011			Spring 2013		
	SIM (ng/μL)	MS/MS (ng/μL)	ng/m^3 (55 m^3)	SIM (ng/μL)	MS/MS (ng/μL)	ng/m^3 (283 m^3)
Acids						
Glycolic acid	6.9		12.4	19.2		6.8
Malonic acid	n.d.	1.1	2.1	n.d.	4.6	1.6
Glyoxylix acid	n.d.	n.d.	n.d.	n.d.	1.4	0.5
Maleic acid	15.2		27.6	n.d.	1.2	0.4
Succinic acid	18.1		32.8	7.4		2.6
Glutaric acid	1.4		2.6	2.0		0.7
Malic acid	n.d.	n.d.		21.5		7.6
Pyruvic acid	n.d.	<X_{LOD}		n.d.	0.6	0.2
Adipic acid	<X_{LOD}	1.6	0.3	1.9		0.7
Pinonic acid	n.d.	n.d.		2.0		0.7
3-OH-benzoic acid	<X_{LOD}	0.4	0.7	<X_{LOD}	0.3	0.1
Pimelic acid	n.d.	n.d.		n.d.	2.5	0.9
2-Ketoglutaric acid	n.d.	0.7	1.2	2.1		0.7
4-OH-benzoic acid	<X_{LOD}	0.6	1.1	<X_{LOD}	0.7	0.2
Phthalic acid	2.8		5.0	2.5		0.9
Suberic acid	n.d.	n.d.		3.7	n.d.	1.3
Azelaic acid	n.d.	2.1	3.9	4.2	n.d.	1.5
Phenols						
Catechol	<X_{LOD}	<X_{LOD}		n.d.	0.3	0.1
Syringol	n.d.	<X_{LOD}		n.d.	<X_{LOD}	
Vanillin	n.d.	0.3	0.6	<X_{LOD}	<X_{LOD}	
Pyrogallol	n.d.	<X_{LOD}		n.d.	<X_{LOD}	
Acetosyringone	n.d.	n.d.		n.d.	n.d.	
Syringaldehyde	<X_{LOD}	0.7	1.3	n.d.	<X_{LOD}	
Acetovanillone	<X_{LOD}	<X_{LOD}		n.d.	n.d.	
Vanillic acid	n.d.	<X_{LOD}		<X_{LOD}	0.5	0.2
Syringic acid	n.d.	0.4	0.7	<X_{LOD}	<X_{LOD}	
p-Coumaric acid	n.d.	<X_{LOD}		n.d.	<X_{LOD}	
Ferulic acid	n.d.	n.d.		n.d.	<X_{LOD}	

Analyses were performed using GG–MS method with SIM detection (2nd and 5th columns) and MS/MS method (3rd and 6th columns). Concentration values (expressed as ng/μL in the injected solutions) were transformed into air concentrations (ng/m^3, 4th and 7th columns) considering volume of the sampled air, i.e. 55 and 283 m^3 in winter and spring campaigns, respectively.
n.d: not detected analyte; <X_{LOD}: detected but not quantified analyte, since below the detection limit.

(≈ 2 ng/m^3, each, Table 3, 3rd column) produced by oxidation of anthropogenic (adipic acid) or biogenic (azelaic acid) precursors [8–11, 13, 16, 46].

Several methoxyphenols emitted from wood burning were detected at low concentration levels (total concentration ≈ 2.5 ng/m^3), but only three of them could be quantified since they are above the detection limit with the used sampling protocol (low-volume collection, 55 m^3/day) [7, 18, 20]. The diagnostic ratio between syringyl and vanillic compounds (S/V ≈ 3) indicates predominant syringyl-type compounds that can be used to diagnose the contribution of smoke from hard wood combustion [23, 47]. This finding confirms the results of several studies indicating that biomass combustion in household stoves is becoming a relevant potential to contribute to atmospheric pollution in Northern Italy, especially in winter [40–42].

Since spring in the investigated region is characterized by high mixing heights that disperse contaminants in the atmosphere and anthropogenic emissions are reduced, low abundances of the target analytes are expected in spring samples [3, 24, 48]. For this reason, a high-volume air sampler (283 m^3/day) was used to collect enough PM quantity to assure the quantification of several tracers. Nearly all the target tracers were detected in the spring sample at low levels (total abundance 28 ng/m^3), most of them in the 0.2–0.7 ng/m^3 range (Table 3, 7th column). Among the measured carboxylic acids, malic and glycolic acids showed highest concentrations (≈ 7 ng/m^3), followed by succinic acid (≈ 3 ng/m^3). These results are expected in the warm season, since these acids are mainly produced by *in situ* photochemical reactions of anthropogenic precursors [8, 13, 16]. A significant contribution of pinonic acid (≈ 0.7 ng/m^3) was also identified, as a specific marker of photochemical oxidation of biogenic compounds consistent with high vegetation activity in spring [11, 46]. Some methoxyphenols were detected in this sample but their concentration was below the detection limit.

4 Concluding remarks

In this study, a GC–MS method was extended to methoxyphenols analysis and upgraded with ion trap MS/MS detection to permit the simultaneous determination of several polar organic compounds at trace levels in atmospheric particles.

The MS/MS technique proved to have several advantages compared with single-stage MS, in terms of the qualification and quantification of a large range of compounds in complicated environmental matrices. Namely, detection limits were reduced to 0.1 ng/μL for standard solutions, matrix interferences and chemical noise were reduced in the chromatogram and selectivity was enhanced provided by the product ions in mass spectra for a more reliable confirmation of the target compounds in the samples.

The GC–IT-MS has the advantage of being a user-friendly and low-cost instrument, in comparison with high-resolution MS, with the possibility of combining full-spectrum mode to MS/MS detection in a single chromatographic acquisition run.

This indicates that IT-MS is an ideal alternative method for cost-effective analyses of a wide range of polar tracers in atmospheric aerosol to give information on contribution of primary emission sources and secondary processes on air quality of the investigated sites.

The authors have declared no conflict of interest.

5 References

[1] Schwarze, P. E., Øvrevik, J., Lag, M., Refsnes, M., Nafstad, P., Hetland, R. B., Dybing, E., *Human Experim. Toxicol.* 2006, *25*, 559–579.

[2] Perez, I. R., Alfaro-Moreno, J. S. E., Baumgardner, D., Garcıa-Cuellar, C., Martın del Campo, J. M., Raga, G. B., Castillejosg, M., Drucker, C. R., Osornio Vargas A. R., *Chemosphere* 2007, *67*, 1218–1228.

[3] Perrone, M. G., Gualtieri, M., Consonni, V., Ferrero, L, Sangiorgi, G., Longhin, M., Ballabio, D., Bolzacchini, E., Camatin, M., *Environ. Pollut.* 2013, *176*, 215–227.

[4] Simoneit, B. R. T., *Mass Spectrom. Rev.* 2005, *24*, 719–765.

[5] Viana, M., Kuhlbusch, T. J., Querol, X., Alastuey, Harrison, R. M., Hopke, P. K., Winiwarter, W., Vallius, M., Szidat, S., Prévôt, A. S., Hueglin, C., Bloemen, A., Wåhli, P., Vecchi, R., Miranda, A. I., Kasper-Giebl, A., Maenhaut, W., Hitzenberger, R., *J. Aerosol Sci.* 2008, *39*, 827–849.

[6] Nolte, C. G., Schauer, J. J., Cass, G., Simoneit, B. R. T., *Environ. Sci. Technol.* 2001, *35*, 1912–1919.

[7] Graham, B., Mayol-Bracero, O. L., Guyon, P, Roberts, G. C., Decesari, S., Facchini, M. C., Artaxo, P., Maenhaut, W., Koll, P, Andreae, M. O., *J. Geophys. Res.* 2002, *107*, 8047–8050.

[8] Bi, X., Simoneit, B. R. T., Sheng, G., Ma, S., Fu, J., *Atmos. Res.* 2008, *88*, 256–265.

[9] Yang, L., Nguyen, D. M., Shiguo, J. S., Reid, J. S., Yu, L. E., *Atmos. Environ.* 2013, *78*, 211–218.

[10] Ho, K. F., Ho, S. S. H., Lee, S. C., Kawamura, K., Zo, S. C., Cao, J. J, Xu, H. M., *Atmos. Chem. Phys.* 2011, *11*, 2197–2208.

[11] Hyder, M., Genberg, J., Sandahl, M., Swietlicki, E., Jönsson, J. A., *Atmos. Environ.* 2012, *57*, 197–204.

[12] Szmigielski, R., Surratt, J. D., Vermeylen, R., Szmigielska, K., Kroll, J. H., Ng, N. L., Murphy, S. M., Sorooshian, A., Seinfeld, J. H., Claeys, M., *J. Mass Spectrom.* 2007, *42*, 101–116.

[13] Yang, L., Ray, M. B., Yu, L. E., *Atmos. Environ.* 2008, *42*, 868–880.

[14] Ruiz-Jimenez, J., Parshintse, J., Laitinen, T., Hartonen, K., Petäjä, T., Kulmala, M., Riekkola, M. L., *Atmos. Environ.* 2012, *49*, 60–68.

[15] Gierlus, K. M., Laskina, O., Abernathy, T. L., Grassian, V. H., *Atmos. Environ.* 2012, *46*, 125–130.

[16] Wagener, S., Langner, M., Hansen, U., Moriske, H. J., Endlicher, W. R., *Atmos. Environ.* 2012, *47*, 33–42.

[17] Reale, S., Di Tullio, A., Spreti, N., De Angelis, F., *Mass Spectrom. Rev.* 2004, *23*, 87–126.

[18] Simpson, C. D., Paulsen, M., Dills, R. L., Liu, L. J. S., Kalman, D. A., *Environ. Sci. Technol.* 2005, *39*, 631–637.

[19] Ward, T., Hamilton, J. Jr., Dixon, R. F., Paulsen, R. W., Simpson, C. D., *Atmos. Environ.* 2006, *40*, 7005–7017.

[20] Zhang, Y., Obrist, D., Zielinska, B., Gertler, A., *Atmos. Environ.* 2013, *72*, 27–35.

[21] Wang, G., Chen, C., Li, J., Zhou, B., Xie, M., Hu, S., Kawamura, K., Chen, Y., *Atmos. Environ.* 2011, *45*, 2473–2479.

[22] Orasche, J., Schnelle-Kreis, J., Abbaszade, G., Zimmermann, R., *Atmos. Chem. Phys.* 2011, *11*, 8977–8993.

[23] Kuo, L. J., Louchouarn, P., Herbert, B. E., *Chemosphere* 2011, *85*, 797–805.

[24] Pietrogrande, M. C., Bacco, D., Rossi, M., *Atmos. Environ.* 2013, *75*, 279–286.

[25] Pratt, K. A., Prather, K. A., *Mass Spectrom. Rev.* 2012, *31*, 1–16.

[26] Medeiros, P. M., Simoneit, B. R. T., *J. Sep. Sci.* 2007, *30*, 1516–1536.

[27] Garrido Frenich, A., Plaza-Bolaños, P., Vidal, J. L. M., *J. Chromatogr. A* 2008, *1203*, 229–238.

[28] Medina, C. M., Pitarch, E., Portolés, T., López, F. J., Hernández, F., *J. Sep. Sci.* 2009, *32*, 2090–2102.

[29] Dong, J., Pan, U. X., Lv, J. X., Sun, J., Gong, X. M., Li, K., *Chromatographia* 2011, *74*, 109–119.

[30] Hernando, M. D., Mezcua, M., Gomez, M. J., Malato, O., Agueera, A., Fernandez-Alba, A. R., *J. Chromatogr. A* 2004, *1047*, 129–135.

[31] Wang, D., Cai, Z., Jiang, G., Wong, M. H., Wong, W. K., *Rapid Commun. Mass Spectrom.* 2005, *19*, 83–89.

[32] Gómara, B., Herrero, L., Borjadandi, L. R., González, M. J., *Rapid Comm. Mass Spectrom.* 2006, *20*, 69–74.

[33] Walser, M. L., Desyaterik, Y., Laskin, J., Laskin, A., Nizkorodo, S. A., *Phys. Chem. Chem. Phys.* 2007, *10*, 1009–1022.

[34] Zhu, L., Ma, B., Liang, X., *Rapid Commun. Mass Spectrom.* 2008, *22*, 394–400.

[35] Kinani, A., Bouchonnet, S., Bourcier, S., Creusot, N., Porcher, J. M., Selim Aıt-Aıss, S., *Rapid Commun. Mass Spectrom.* 2008, *22*, 3651–3661.

[36] Botitsi, H. V., Garbis, S. D., Economou, A., Despina, F., Tsipi, D. F., *Mass Spectrom. Rev.* 2011, *30*, 907–939.

[37] Lv, Q., Zhang, Q., Li, W., Li, H., Li, P., Ma, Q., Meng, X., Qi, M., Bai, H., *J. Sep. Sci.* 2013, *36*, 3534–3549.

[38] Andalò, C., Galletti, G. C., Bocchini, P., *Rapid Commun. Mass Spectrom.* 1998, *12*, 1777–1782.

[39] Pietrogrande, M. C., Bacco, D., Chiereghin, S., *Anal. Bioanal. Chem.* 2013, *405*, 1095–1104.

[40] Giannoni, M., Martellini, T., Del Bubba, M., Gambaro, A., Zangrando, R., Chiari, M., Lepri, L., Cincinelli, A., *Environ. Poll.* 2012, *167*, 7–15.

[41] Caserini, S., Galante, S., Ozgen, S., Cucco, S., Gregorio, K., Moretti, M., *Sci. Tot. Environ.* 2013, *450–451*, 22–30.

[42] Piazzalunga, A., Anzano, M., Collina, E., Lasagni, M., Lollobrigida, F., Pannocchia, A., Fermo, P., Pitea, D., *J. Aerosol Sci.* 2013, *56*, 30–40.

[43] Pietrogrande, M. C., Bacco, D., *Anal. Chim. Acta* 2011, *689*, 257–264.

[44] Kawanaka, Y., Kazuhiko, S., Wang, N., Sun-Ja, Y., *J. Chromatogr. A* 2007, *1163*, 312–317.

[45] Zangrando, R., Barbaro, E., Zennaro, P., Rossi, S., Kehrwald, N. M., Gabrieli, J., Barbante, C., Gambaro, A., *Environ. Sci. Technol.* 2013, *47*, 8565–8574.

[46] Cheng, Y., Brook, J. R., Li, S. M., Leithead, A., *Atmos. Environ.* 2011, *45*, 7105–7112.

[47] Gonçalves, C., Evtyugina, M., Alves, C., Monteiro, C., Pio, C., Tomé, M., *Atmos. Res.* 2011, *101*, 666–680.

[48] Carbone, C., Decesari, S., Mircea, M., Giulianelli, L., Finessin, E., Rinaldi, M., Fuzzi, S., Marinoni, A., *Atmos. Environ.* 2010, *44*, 5269–5278.

Q1 # Characteristics and major sources of carbonaceous aerosols in PM2.5 in Emilia Romagna Region (Northern Italy) from four-year observations

Q2 Maria Chiara Pietrogrande [a,*], Dimitri Bacco [a,b], Silvia Ferrari [b], Isabella Ricciardelli [b], Fabiana Scotto [b], Arianna Trentini [b], Marco Visentin [a]

[a] Department of Chemical and Pharmaceutical Sciences, University of Ferrara, Via Fossato di Mortara 17/19, I-44100 Ferrara, Italy
[b] Regional Agency for Prevention and Environment—ARPA, Emilia-Romagna, Italy

HIGHLIGHTS

- Carbonaceous levels show strong seasonality with the highest OC and EC concentrations during the cold periods and the lowest in the warm months
- Vehicle emissions and biomass burning are the dominant sources of carbonaceous aerosols
- Wood burning for domestic heating is the predominant emission source in fall/winter contributing ≈ 33% to OC
- PAHs emission profiles confirmed combined emissions from vehicle traffic and wood burning, with relative contribution varying with the season
- The urban and the rural background sites show nearly homogeneous impact of the different sources and processes.

GRAPHICAL ABSTRACT
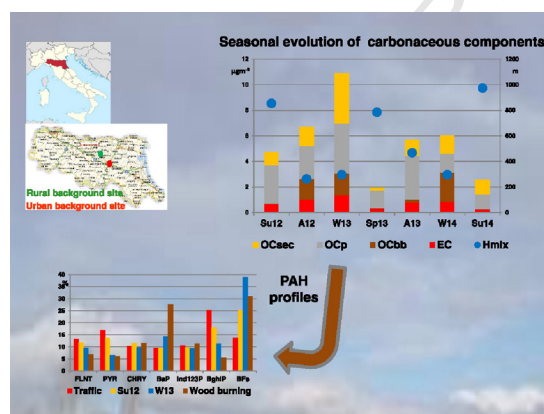
ABSTRACT

The concentrations of organic and elemental carbon in PM$_{2.5}$ aerosol samples were measured in two sites of Emilia Romagna (Po Valley, Northern Italy) in eight campaigns during different seasons from 2011 to 2014. Strong seasonality was observed with the highest OC concentrations during the cold periods ($\approx 5.5\ \mu g\ m^{-3}$) and the lowest in the warm months ($\approx 2.7\ \mu g\ m^{-3}$) as well as with higher EC levels in fall/winter ($\approx 1.4\ \mu g\ m^{-3}$) in comparison with spring/summer ($\approx 0.6\ \mu g\ m^{-3}$). Concerning spatial variability, there were no statistically significant difference ($p < 0.05$) between OC concentrations at the two sampling sites in each campaign, while the EC values were nearly twofold higher levels at the urban site than those at the rural one.

Specific molecular markers were investigated to attempt the basic apportionment of OC by discriminating between the main emission sources of primary OC, such as fossil fuels burning – including traffic vehicle emission – residential wood burning, and bio-aerosol released from plants and microorganisms, and the atmospheric photo-oxidation processes generating OC$_{sec}$. The investigated markers were low-molecular-weight carboxylic acids – to describe the contribution of secondary organic aerosol – anhydrosugars – to quantify primary emissions from biomass burning – bio-sugars – to qualitatively estimate biogenic sources – and Polycyclic Aromatic Hydrocarbons – to differentiate among different combustion emissions.

Using the levoglucosan tracer method, contribution of wood smoke to atmospheric OC concentration was computed. Wood burning accounts for 33% of OC in fall/winter and for 3% in spring/summer. A clear seasonal trend is

* Corresponding author.
  E-mail address: mpc@unife.it (M.C. Pietrogrande).

also observed for the impact of secondary processes with higher contribution in the warm seasons ($\approx 63\%$) in comparison with that in colder months ($\approx 33\%$), that is consistent with enhanced solar radiation in spring/summer.

1. Introduction

Carbonaceous species are known to be a very important part of the atmospheric aerosol accounting typically for 20–45% of PM$_{2.5}$ with concentration ranging from few to hundreds ngm^{-3}. It is comprised of myriad of individual species with vastly different chemical and thermodynamic properties and it is known to contain high amount of light absorbing carbon compounds (black carbon), which significantly influence the aerosol radiative forcing and the atmospheric photochemistry (Yttri et al., 2007; Saarikoski et al., 2008; Putaud et al., 2010; Pio et al., 2011; Valipour et al., 2012; Valipour et al., 2013; Calvo et al., 2013; Bautista et al., 2014; Jedynska et al., 2014; Sandrini et al., 2014). The carbonaceous aerosol is broadly classified into two main fractions: elemental carbon (EC) and organic carbon (OC). EC is a highly polymerized dark fraction that is generated by incomplete combustion of organic material from traffic, residential heating, industrial activities and energy production using heavy oil, coal or biofuels. OC is a complex mixture of several organic compounds, that can be both primarily emitted (OC$_{prim}$) and formed in the atmosphere through condensation and oxidation processes (OC$_{sec}$) (Sillanpää et al., 2005; Gelencser et al., 2007; Saarikoski et al., 2008; Pio et al., 2011). The main emission sources producing OC$_{prim}$ are fossil fuel combustion from mobile and stationary sources, biomass burning (OC$_{bb}$) and biological particles (OC$_{bio}$) (Pio et al., 2011). A complete characterization of OC and EC composition is a major issue for all the receptor models currently in use, which would identify the PM sources, their emission profile and loading (Bautista et al., 2014).

In this paper the apportionment of the carbonaceous aerosol was attempted with the main objective to generate baseline knowledge on OC and EC concentrations and their different fractions. The study was conducted in Emilia Romagna region located in the Eastern Po Valley (Northern Italy), in the framework of the Supersito project (www.supersito-er.it). This area is recognized as one of the most worrying air pollution situations in Europe, since high anthropogenic emissions and meteorological factors may cause air pollution episodes and serious risks for human health (Balducci and Cecinato, 2010; Bigi et al., 2012; Carbone et al., 2010; Perrone et al., 2012, 2013; Perrino et al., 2014; Decesari et al., 2014). As a part of the Supersito project, our previous studies on PM$_{2.5}$ chemical composition have shown an high pollution level generated by different sources from human activities, such as traffic, domestic heating and biomass burning, and produced by in situ photo-chemical reactions from both biogenic and anthropogenic precursors (Pietrogrande et al., 2014a, 2014b, 2015). Given that studies regarding the OC/EC speciation and chemical characterization of the carbonaceous aerosol are still very limited in the region, in this paper the study has been extended to nearly 1000 PM$_{2.5}$ samples daily collected in eight intensive experimental campaigns throughout the years from 2011 to 2014, in urban and rural settings in the studied region.

Qualitative or quantitative estimate of the different contributions to carbonaceous PM were attempted by quantifying molecular tracers of specific emissions sources and atmospheric processes. In particular, low-molecular-weight carboxylic acids were quantified to differentiate between primary emissions and secondary organic aerosol, sugars to discriminate between primary emissions from biomass burning and from the ecosystem and polycyclic aromatic hydrocarbons (PAHs) to differentiate among different combustion emissions.

The spatial and temporal variations of the parameters were observed to obtain inferences relating to the possible sources of carbonaceous particulate matter. The relationship between carbonaceous species, concentration of specific organic components (acids, sugars and PAHs) and meteorological variables are also investigated within the studied region. Data obtained were compared to existing OC and EC measurements from neighboring locations in Po Plain to give perspective to the understanding of the carbonaceous aerosol composition in the region.

2. Materials and methods

2.1. Aerosol sampling

Sampling protocol was described elsewhere (Pietrogrande et al., 2014a, 2014b). Briefly, the urban background site MS is located in the city of Bologna (~400,000 inhabitants) and the rural background station SP is located at San Pietro Capofiume about 30 km northeast from the city.

As part of the Supersito project, eight sampling intensive campaigns were performed to represent different meteorological scenarios throughout the year: 14th November up to 6th December 2011 (late-autumn), from 14th June up to 11th July 2012 (early-summer), from 23rd October up to 10th November 2012 (deep-autumn), from 30th January up to 19th February 2013 (deep-winter), from 7th up to 27th May 2013 (late-spring), from 27th September up to 18th October 2013 (early-autumn), from 28th January up to 27th February 2014 (deep-winter), from 13th May up to 11th June 2014 (late-spring).

A low volume automatic outdoor sampler (Skypost PM, TCRTECORA Instruments, Corsico, Milan, Italy) operated at the standard airflow rate of 38.3 L min^{-1} for 24 h to collect an air volume of 55 m^3 per day was used. PM$_{2.5}$ samples were collected on 47 mm diameter quartz fiber filters provided from Whatman (Whatman® QM-A quartz filters) for GC/MS analysis (Pietrogrande et al., 2014a, 2014b) and from Pall (Pall Tissu Quartz 2500 QAO-UP 2500 filters) for TOT analysis (Costa et al., 2016).

In spring/summer, higher air volumes (≈ 283 m^3 per day) were sampled on quartz fiber filters (Munktell, 100 mm diameter) using an Hi-Vol sampler (Echo Hi-Vol, TECORA Instruments, Corsico, Milan, Italy) operating at a flow rate of 11.7 m^3 h^{-1} for 24 h. This choice was motivated by assuring PM$_{2.5}$ amounts compatible with the analytical sensitivity due to low abundances of the target analytes expected during spring/summer in the investigated region (Carbone et al., 2010; Bigi et al., 2012; Perrone et al., 2013; Pietrogrande et al., 2013, 2014a, 2014b, 2015).

The quartz fiber filters were heated for 3 h at 800 °C in air before use, to reduce their carbon blank. After sampling, the procedure outlined in European Standard EN 12341 (CEN, 1998) was applied for equilibration and weighing the collected samples.

Meteorological data were collected at the meteorological stations of San Pietro Capofiume and Bologna by Hydro-Meteo-Climate Service of ARPA-ER. Mixing layer height at both sites was estimated using the pre-processor CALMET by ARPA Emilia-Romagna (Deserti et al., 2001).

2.2. Analytical procedure

2.2.1. Analytical procedure for carbonaceous aerosol

The carbonaceous aerosol fractions (OC and EC) were quantified in the ARPA laboratories in Ferrara and Ravenna, as a part of the Supersito project activities (www.supersito.it; Costa et al., 2016).

A Sunset Laboratory Thermal/Optical Carbonaceous Aerosol Analyzer (Laboratory Inc.) was used, as the thermal-optical transmission method (CEN, 2011) is a common procedure widely used for the

determination of OC/EC content in Po Valley (Lonati et al., 2007; Perrino et al., 2014; Sandrini et al., 2014; Vassura et al., 2014) as well as in other European urban sites (e.g., Szidat et al., 2006; Pio et al., 2011; Viana et al., 2013). The instrument was calibrated prior to use with injections of sucrose standard solution (concentration of 10 g L^{-1} corresponding to 42 µg cm^{-2} of organic carbon on the filter surface) (Costa et al., 2016).

The punched filters (1.5 cm^2) were submitted to volatilization using the EUSAAR2 thermal protocol (Cavalli et al., 2010; Chiappini et al., 2014). According to this protocol, the carbonaceous material (OC) is initially thermally desorbed in an inert atmosphere (99.999% pure He) at relatively low temperature in four steps (200 °C for 120 s; 300 °C for 150 s; 450 °C for 180 s; 650 °C for 180 s). Then desorption is performed to evolve the EC component at higher temperature in four steps (500 °C for 120 s; 550 °C for 120 s; 700 °C for 70 s; 850 °C for 80 s) in an oxidizing atmosphere (2% oxygen/98% helium final mixture in the sample oven).

2.2.2. Analytical procedure for polar organic compounds

Polar organic compounds, including carboxylic acids and sugars, were determined using a GC/MS analytical procedure described elsewhere (Pietrogrande et al., 2014a, 2014b). Briefly, PM$_{2.5}$ samples were extracted for 15 min in an ultrasonication bath with 15 mL of methanol:dichloromethane mixture (9:1) and then submitted to silyl derivatization with *N,O*-bis-(trimethylsilyl) trifluoroacetamide (BSTFA) containing 1% of trimethylchlorosilane (TMCS) at 75 °C for 70 min.

The GC/MS system was a Scientific Focus-GC (Thermo-Fisher Scientific, Milan, Italy) coupled to PolarisQ Ion Trap Mass Spectrometer (Thermo-Fisher Scientific, Milan, Italy). The column used was a DB-5MS column (L = 30 m, I.D = 0.2 5 mm, d$_f$ = 0.25 µm film thickness; J&W Scientific, Rancho Cordova, CA, USA). The mass spectrometer operated in Electron Ionization mode (positive ion, 70 eV). The mass spectra were acquired in full scan mode from 50 to 650 *m/z* in 0.58 s. For identification and quantification of the target analytes, the extracted-ion chromatograms (EICs) were recovered from the entire data set of each chromatographic run by selecting either the base peak ion or the most abundant characteristic fragments (Pietrogrande et al., 2014a).

2.2.3. Analytical procedure for polycyclic aromatic hydrocarbons

The analysis of polycyclic aromatic hydrocarbons were performed in the ARPA laboratory in Ravenna, as a part of the Supersito project activities (www.supersito.it; Pietrogrande et al., 2015). The PAHs were analyzed on a DFS High Resolution GC/MS system (Thermo-Fisher Scientific, Milan, Italy) formed by a gas chromatograph equipped with a capillary column a TR-5MS column (L = 60 m, I.D. = 0.2 5 mm, df = 0.25 µm film thickness; Thermo Scientific, USA) coupled with a Magnetic Sector high resolution mass spectrometer. The initial oven temperature was set at 100 °C for 1 min, raised to 300 °C at a rate of 10 °C min^{-1} and then held for 50 min. Isotope labelled (deuterated) PAH standards were used for quantification. The procedure provides analytical reproducibility (RSD% ≤10%) and accuracy (recovery: 70 ÷ 115%) suitable for applicability in environmental monitoring.

3. Results and discussion

The ambient concentrations of OC and EC were measured and summed to compute TC. In addition, 40 specific chemical markers were quantified, namely low-molecular-weight carboxylic acids, sugars and polycyclic aromatic hydrocarbons. Data are reported in Table 1, as mean values and standard deviations of the concentrations measured at each site for each campaign and integrated on ≈3 weeks (the term n.d. indicates that more than 90% of the measured values are below the detection limit).

3.1. Meteorological condition

During the monitoring campaigns, typical season meteorological conditions of Po Valley occurred (Table 1, last 3 lines). Fall/winter periods are characterized by atmospheric stability with shallow Planetary Boundary Layer (PBL) depths (H$_{mix}$ mean values ≈ 300 m), low temperature (3–12 °C), low solar radiation (mean values ≈ 75 W m^{-2}), weak amount of wet deposition (maximum precipitations ≈ 142 mm during winter 2014) and low wind velocity. On the contrary, spring/summer periods are characterized by high Planetary Boundary Layer (PBL) depths (H$_{mix}$ mean values ≈ 920 m), high temperature (16–28 °C), strong solar radiation (mean values ≈ 270 W m^{-2}), weak amount of wet deposition (maximum precipitations ≈ 65 mm during May 2013).

Among the investigated periods, the atmospheric conditions of October 2013 were intermediate between cold/warm seasons, closer to late summer than to fall, with H$_{mix}$ of 430 m, solar radiation of ≈ 100 Wm^{-2} and temperature of 15 °C. For this reason, in general the data collected in this campaign were excluded from calculation of mean values of cold/warm periods.

3.2. Concentration levels of OC and EC

The OC, EC and TC values measured during the eight campaigns at MS and SP sites were compared in order to highlight the spatial and season variability. For the first campaign in November 2011, only TC values were available, since the used method prevented unbiased discrimination between OC and EC (Costa et al., 2016).

As expected, at both sites, the carbonaceous components show the highest levels during the November–March periods and the lowest in the May–June months. In fall/winter TC values ranged from a high of 11.8 µg m^{-3} in November 2011 at MS to a low of 5.5 µg m^{-3} in February 2014 at SP, with an average of 9.1 µg m^{-3} and 7.6 µg m^{-3} at MS and SP, respectively. In spring/summer TC values ranged from 4.8 µg m^{-3} in June 2012 at MS to 1.8 µg m^{-3} in May 2013 at SP, with an average of 3.6 µg m^{-3} and 2.9 µg m^{-3} at MS and SP, respectively (Table 1).

Accordingly, OC and EC concentrations exhibit the same seasonality. The highest concentrations of OC are in all cases observed during the cold periods (an average of 6.2 µg m^{-3} and 5.9 µg m^{-3} at MS and SP, respectively) and the lowest in the warm months (an average of ≈2.7 µg m^{-3} at both sites). The highest EC levels were in fall/winter (average values of 1.9 µg m^{-3} and 1.1 µg m^{-3} at MS and SP, respectively) in comparison with spring/summer winter (average values of 0.8 µg m^{-3} and 0.4 µg m^{-3} at MS and SP, respectively). In agreement with intermediate atmospheric conditions, TC, OC and EC levels in October 2013 show halfway values, i.e., 6.0, 4.3 and 1.0 µgm^{-3}, respectively (Table 1).

This trend may be related to the seasonal cycle of Planetary Boundary Layer (PBL) dynamics, since in the Po Valley the dispersion of primary emissions has been found largely dependent on vertical mixing, in the absence of strong wind throughout the year (Carbone et al., 2010; Bigi et al., 2012; Sandrini et al., 2014; Decesari et al., 2014; Pietrogrande et al., 2015; Khana et al., 2016). During winter, the stable **Q6** atmospheric conditions (H$_{mix}$ ≈ 300 m) promote the accumulation of pollutants that are confined to the first hundred meters of the atmosphere and the ageing of the air masses with a relevant increase in the concentration of secondary pollutants. Instead, during summer, the strong thermal convective activity increases PBL height and H$_{mix}$ reaches ≈1000 m favoring dispersion of the organic compounds in the atmosphere. This hypothesis may be supported by the significant negative correlation (although quite scattered R^2 ≈ 0.6) found between TC, OC and EC concentrations and the boundary layer depth.

In addition, larger anthropogenic emissions are expected in fall/winter, in particular wood combustion for domestic heating, which is a frequent practice in cold seasons in the Po Plain. This leads to a sharp increase in the wood–related carbonaceous emission yielding nearly twofold higher concentrations of each carbonaceous component (cold/

Table 1

Mean values ± standard deviation (SD) of the concentrations observed for each campaign and integrated on ≈3 weeks: the term n.d. indicates that more than 90% of the measured values were below the detection limit).

	Fall11	Sum12	Fall12	Win13	Sp13	Fall13	Win14	Sum14
MS								
OC (μgm^{-3})		3.73 ± 0.75	6.94 ± 3.84	7.23 ± 2.00	2.02 ± 0.58	3.71 ± 0.88	4.57 ± 2.06	2.55 ± 1.52
EC (μgm^{-3})		1.02 ± 0.43	2.43 ± 1.25	1.89 ± 0.78	0.90 ± 0.41	1.14 ± 0.40	1.30 ± 0.46	0.60 ± 0.26
TC (μgm^{-3})	11.9 ± 2.9	4.77 ± 0.96	9.58 ± .19	9.24 ± 2.66	2.92 ± 0.92	6.32 ± 2.88	5.87 ± 2.42	3.15 ± 1.70
OC/EC		4.01 ± 1.46	2.87 ± 1.51	3.80 ± 0.91	2.55 ± 1.07	3.18 ± 0.75	3.55 ± 0.97	s4.42 ± ± 1.82
OC/EC$_{min}$		1.62	0.77	2.53	1.47	2.17	1.94	1.96
OC$_{sec}$ (μgm^{-3})		1.99 ± 0.71	3.97 ± 3.34	3.97 ± 1.22	0.58 ± 0.33	1.66 ± 1.30	2.45 ± 1.58	1.48 ± 1.27
OC$_{sec}$%		52.6 ± 14.7	44.0 ± 21.0	54.9 ± 0.5	29.5 ± 18.8	40.5 ± 13.0	50.9 ± 12.5	3.3 ± 17.3
CA$_{tot}$ (ngm^{-3})	262.0 ± 111.2	n.d.	167.4 ± 109.6	249.3 ± 122.3	17.4 ± 11.9	50.0 ± 25.9	117.9 ± 72.4	93.0 ± 120.8
CA$_{oxo}$ (ngm^{-3})	84.4 ± 41.4	n.d.	74.8 ± 50.4	83.4 ± 43.0	11.6 ± 8.6	18.3 ± 8.8	41.4 ± 22.4	58.2 ± 79.2
CAoxo%	31.7 ± 6.0	n.d.	4.0 ± 4.7	34.4 ± 9.9	9.0 ± 9.7	38.7 ± 10.1	36.8 ± 9.2	60.9 ± 14.3
Levoglucosan (ngm^{-3})	1042.9 ± 490.4	2.07 ± 1.93	288.9 ± 143.9	259.4 ± 98.9	12.6 ± 16.9	34.6 ± 23.8	300.7 ± 117.8	6.53 ± 3.65
Mannosan (ngm^{-3})	120.7 ± 45.1	0.14 ± 0.24	63.5 ± 38.4	63.6 ± 23.7	1.85 ± 2.97	8.34 ± 8.51	26.3 ± 16.7	1.07 ± 0.56
Galactosan (ngm^{-3})	52.0 ± 20.0	n.d.	29.7 ± 18.3	31.5 ± 12.2	1.26 ± 2.61	4.98 ± 3.15	14.9 ± 6.1	1.07 ± 0.32
Lev/Mann	8.54 ± 1.09	14.7 ± 4.9	4.91 ± 0.77	4.09 ± 0.41	6.98 ± 2.84	7.12 ± 5.14	14.9 ± 7.9	6.24 ± 2.19
S$_{tot}$ (ngm^{-3})	1287.9 ± 559.6	6.71 ± 6.01	406.1 ± 208.2	374.5 ± 139.8	50.2 ± 60.2	77.2 ± 29.7	372.9 ± 147.4	58.5 ± 28.2
S$_{bb}$ (ngm^{-3})	1215.6 ± 552.8	2.33 ± 2.15	382.2 ± 198.6	354.6 ± 133.3	15.7 ± 22.3	47.9 ± 31.1	342.1 ± 140.3	8.66 ± 4.34
S$_{bio}$ (ngm^{-3})	72.3 ± 24.1	4.38 ± 5.04	23.9 ± 12.9	19.96 ± 7.48	34.5 ± 38.6	29.3 ± 18.7	30.8 ± 14.7	49.7 ± 27.5
S$_{bb}$%	93.7 ± 2.5	46.0 ± 27.3	93.1 ± 4.4	94.6 ± 0.9	30.7 ± 14.1	57.8 ± 23.2	91.1 ± 5.3	18.4 ± 14.7
S$_{bio}$%	6.3 ± 2.5	54.0 ± 27.3	6.9 ± 4.4	5.4 ± 0.9	69.3 ± 14.1	42.2 ± 23.2	8.9 ± 5.3	81.6 ± 14.7
Lev/OC		0.00 ± 0.00	0.05 ± 0.04	0.03 ± 0.02	0.01 ± 0.01	0.01 ± 0.01	0.07 ± 0.02	0.00 ± 0.00
OC$_{bb}$ (ngm^{-3})	6.94 ± 3.27	0.01 ± 0.01	1.92 ± 0.96	1.73 ± 0.66	0.08 ± 0.11	0.23 ± 0.16	2.00 ± 0.78	0.04 ± 0.02
OC$_{bb}$%		0.4 ± 0.4	36.1 ± 24.2	26.2 ± 12.4	4.4 ± 5.6	5.2 ± 3.6	43.7 ± 12.4	2.2 ± 1.84
S$_{bio}$/OC%		0.13 ± 0.13	0.43 ± 0.24	0.30 ± 0.17	1.77 ± 1.81	1.16 ± 0.79	0.72 ± 0.46	2.29 ± 1.6
Fluorantene (ngm^{-3})	0.73 ± 0.32	0.02 ± 0.01	0.15 ± 0.09	0.09 ± 0.09	0.53 ± 0.24	0.04 ± 0.02	0.09 ± 0.06	0.01 ± 0.01
Pirene (ngm^{-3})	0.67 ± 0.40	0.02 ± 0.01	0.15 ± 0.12	0.05 ± 0.05	0.58 ± 0.16	0.03 ± 0.02	0.10 ± 0.07	0.01 ± 0.01
Chrysene (ngm^{-3})	1.18 ± 0.52	0.02 ± 0.01	0.28 ± 0.19	0.42 ± 0.32	0.33 ± 0.20	0.04 ± 0.03	0.22 ± 0.23	0.01 ± 0.01
Benzo[b + j]fluoranthene (ngm^{-3})	2.36 ± 0.77	0.03 ± 0.02	0.79 ± 0.47	0.84 ± 0.62	0.98 ± 0.30	0.15 ± 0.15	0.39 ± 0.28	0.02 ± 0.01
Benzo[k]fluoranthene (ngm^{-3})	0.58 ± 0.19	0.01 ± 0.01	0.23 ± 0.13	0.22 ± 0.17	0.40 ± 0.29	0.03 ± 0.03	0.11 ± 0.08	0.01 ± 0.00
Benzo[a]pyrene (ngm^{-3})	1.12 ± 0.48	0.02 ± 0.01	0.40 ± 0.26	0.39 ± 0.48	0.31 ± 0.26	0.07 ± 0.07	0.21 ± 0.14	0.01 ± 0.01
Indeno[1,2,3–c,d]pyrene (ngm^{-3})	1.15 ± 0.50	0.02 ± 0.01	0.32 ± 0.17	0.27 ± 0.14	0.34 ± 0.25	0.04 ± 0.03	0.18 ± 0.09	0.01 ± 0.00
Benzo[g,h,i]perylene (ngm^{-3})	1.44 ± 0.58	0.03 ± 0.01	0.44 ± 0.23	0.36 ± 0.18	0.34 ± 0.14	0.06 ± 0.03	0.27 ± 0.14	0.02 ± 0.01
tot PAHs (ngm^{-3})	11.5 ± 4.1	0.20 ± 0.09	3.37 ± 1.91	3.31 ± 2.36	0.26 ± 0.11	0.56 ± 0.45	1.92 ± 1.08	0.11 ± 0.07
BaP/BeP	1.10 ± 0.20	0.73 ± 0.14	1.02 ± 0.20	0.85 ± 0.31	0.71 ± 0.18	0.91 ± 0.18	0.90 ± 0.21	0.57 ± 0.16
BaP/BaP + BeP	0.52 ± 0.05	0.42 ± 0.04	0.50 ± 0.05	0.45 ± 0.09	0.40 ± 0.06	0.47 ± 0.05	0.47 ± 0.06	0.36 ± 0.06
IcdP/IcdP + BghiP	0.44 ± 0.03	0.34 ± 0.05	0.42 ± 0.03	0.43 ± 0.02	0.32 ± 0.04	0.38 ± 0.05	0.40 ± 0.03	0.33 ± 0.03
$\sum$ Benzofluoranthenes/BghiP	2.19 ± 0.65	1.42 ± 0.39	2.37 ± 0.64	2.81 ± 0.62	2.25 ± 0.35	2.91 ± 1.06	1.98 ± 0.68	1.92 ± 0.48
Meteorological parameters								
H$_{mix}$ (m)	230 ± 81	974 ± 32	376 ± 107	398 ± 83	954 ± 204	468 ± 188	411 ± 140	974 ± 171
Temperature (°C)	6.5 ± 1.8	27.5 ± 2.6	12.0 ± 2.6	3.9 ± 1.6	17.6 ± 2.2	15.7 ± 2.5	8.3 ± 2.1	21.0 ± 3.3
Solar radiation (W m^{-2})	61 ± 23	295 ± 27	71 ± 35	78 ± 33	228 ± 64	97 ± 52	72 ± 44	258 ± 57
Precipitations (mm)	1.0	3.8	65.0	49.4	64.6	131.6	141.6	24.4
SP								
OC (μgm^{-3})		3.80 ± 1.00	4.94 ± 1.23	8.29 ± 3.57	1.52 ± 0.35	4.90 ± 1.26	4.62 ± 1.76	2.28 ± 1.03
EC (μgm^{-3})		0.68 ± 0.23 ±	1.06 ± 0.23	1.38 ± 0.30	0.33 ± 0.12	0.80 ± 0.19	0.86 ± 0.36	0.26 ± 0.10
TC (μgm^{-3})	8.61 ± 3.23	4.40 ± 1.03	5.99 ± 1.37	10.21 ± 3.87	1.85 ± 0.46	5.69 ± 1.42	5.48 ± 2.07	2.54 ± 1.11
OC/EC		5.86 ± 1.19	4.73 ± 1.08	5.91 ± 1.62	4.89 ± 81.22	6.15 ± 0.86	5.63 ± 1.35	9.11 ± 3.11
OC/EC$_{min}$		3.63	3.28	4.00	3.47	5.15	3.92	6.06
OC$_{sec}$ (μgm^{-3})		1.02 ± 0.55	1.48 ± 0.37	3.92 ± 2.92	0.23 ± 0.13	1.26 ± 0.67	1.42 ± 0.92	1.11 ± 0.72
OC$_{sec}$%		25.3 ± 9.5	27.8 ± 8.5	38.1 ± 13.9	18.1 ± 12.3	24.3 ± 10.5	30.7 ± 14.0	45.9 ± 13.4
CA$_{tot}$ (ngm^{-3})	308.3 ± 220.1	n.d.	114.8 ± 89.53	247.8 ± 139.1	13.9 ± 4.7	55.4 ± 34.2	103.5 ± 33.9	98.8 ± 74.4
CA$_{oxo}$ (ngm^{-3})	70.2 ± 31.7	n.d.	61.0 ± 47.8	7.75 ± 55.66	8.55 ± 4.13	22.9 ± 12.1	41.2 ± 14.4	62.2 ± 57.1
CAoxo%	25.8 ± 8.4	n.d.	53.1 ± 5.3	34.2 ± 9.3	59.4 ± 14.8	45.1 ± 8.8	39.9 ± 5.7	59.9 ± 15.1
Levoglucosan (ngm^{-3})	916.0 ± 389.3	5.40 ± 11.49	233.1 ± 114.5	252.9 ± 110.7	3.77 ± 2.49	38.8 ± 25.8	341.9 ± 129.5	6.20 ± 2.57
Mannosan (ngm^{-3})	105.6 ± 39.6	0.90 ± 2.26	47.0 ± 25.6	61.4 ± 27.1	0.66 ± 0.39	6.90 ± 5.58	32.1 ± 18.7	0.96 ± 0.54
Galactosan (ngm^{-3})	42.7 ± 16.4	n.d.	23.7 ± 13.8	31.9 ± 15.4	0.44 ± 0.22	4.35 ± 2.92	16.3 ± 6.4	1.55 ± 2.04
Lev/Mann	8.59 ± 0.87	7.66 ± 2.18	5.09 ± 0.46	4.18 ± 0.52	5.40 ± 1.58	7.43 ± 3.82	15.5 ± 18.1	8.32 ± 7.50
S$_{tot}$ (ngm^{-3})	1129.7 ± 452.1	41.8 ± 59.2	326.9 ± 158.7	364.7 ± 155.9	30.5 ± 22.3	75.7 ± 32.0	421.4 ± 165.5	75.7 ± 79.6
S$_{bb}$ (ngm^{-3})	1064.4 ± 443.4	6.86 ± 4.23	303.9 ± 153.3	346.3 ± 151.3	4.86 ± 3.04	50.1 ± 32.9	390.3 ± 154.3	7.13 ± 5.04
S$_{bio}$ (ngm^{-3})	65.3 ± 18.9	35.5 ± 49.7	23.01 ± 13.82	18.37 ± 5.33	25.6 ± 21.2	25.6 ± 12.5	31.0 ± 15.4	67.0 ± 76.4
S$_{bb}$%	93.7 ± 2.0	19.1 ± 18.5	92.3 ± 4.6	94.6 ± 1.2	20.4 ± 13.5	59.8 ± 23.0	92 ± 2.4	15.7 ± 8.2
S$_{bio}$%	6.3 ± 2.0	80.9 ± 18.5	7.7 ± 4.6	5.4 ± 1.2	79.6 ± 13.5	40.2 ± 23.0	7.5 ± 2.4	84.3 ± 8.2
Lev/OC		0.00 ± 0.00	0.03 ± 0.01	0.03 ± 0.01	0.00 ± 0.00	0.01 ± 0.00	0.08 ± 0.03	0.00 ± 0.00
OC$_{bb}$ (ngm^{-3})	6.10 ± 2.59	0.04 ± 0.08	1.55 ± 0.76	1.68 ± 0.74	0.03 ± 0.02	0.26 ± 0.17	2.28 ± 0.86	0.04 ± 0.02
OC$_{bb}$%		0.5 ± 0.5	23.0 ± 10.0	20.3 ± 7.1	1.5 ± 1.9	5.0 ± 1.4	52.7 ± 21.3	2.1 ± 1.7
S$_{bio}$/OC%		1.19 ± 1.56	0.42 ± 0.22	0.24 ± 0.09	1.62 ± 1.43	0.63 ± 0.50	0.73 ± 0.38	2.17 ± 1.41
Fluorantene (ngm^{-3})	0.41 ± 0.29	0.01 ± 0.01	0.01 ± 0.01	0.08 ± 0.09	n.d.	0.01 ± 0.01	0.01 ± 0.01	n.d.
Pirene (ngm^{-3})	0.34 ± 0.27	0.01 ± 0.01	0.03 ± 0.02	0.21 ± 0.12	n.d.	0.04 ± 0.03	0.09 ± 0.06	0.02 ± 0.05
Chrysene (ngm^{-3})	0.62 ± 0.36	0.01 ± 0.00	0.13 ± 0.08	0.32 ± 0.32	n.d.	0.03 ± 0.02	0.09 ± 0.10	0.01 ± 0.02
Benzo[b + j]fluoranthene (ngm^{-3})	1.82 ± 0.95	0.02 ± 0.02	0.48 ± 0.34	0.98 ± 0.69	0.02 ± 0.03	0.13 ± 0.07	0.42 ± 0.28	0.02 ± 0.01
Benzo[k]fluoranthene (ngm^{-3})	0.40 ± 0.21	0.01 ± 0.00	0.12 ± 0.09	0.28 ± 0.20	0.01 ± 0.01	0.03 ± 0.02	0.11 ± 0.07	0.01 ± 0.01
Benzo[a]pyrene (ngm^{-3})	0.72 ± 0.45	0.01 ± 0.00	0.21 ± 0.19	0.47 ± 0.41	0.01 ± 0.01	0.05 ± 0.03	0.15 ± 0.14	0.01 ± 0.01
Indeno[1,2,3c,d]pyrene (ngm^{-3})	0.65 ± 0.33	0.01 ± 0.01	0.18 ± 0.12	0.30 ± 0.22	0.00 ± 0.00	0.04 ± 0.02	0.15 ± 0.15	0.01 ± 0.01

Table 1 (*continued*)

	Fall11	Sum12	Fall12	Win13	Sp13	Fall13	Win14	Sum14
Benzo[*g,h,i*]perylene (ngm^{-3})	0.75 ± 0.36	0.01 ± 0.01	0.22 ± 0.14	0.37 ± 0.27	0.01 ± 0.00	0.04 ± 0.02	0.21 ± 0.17	0.01 ± 0.01
tot PAHs (ngm^{-3})	7.18 ± 3.82	0.11 ± 0.05	1.76 ± 1.21	3.93 ± 2.63	0.07 ± 0.07	0.50 ± 0.28	1.58 ± 0.99	0.11 ± 0.16
BaP/BeP	0.93 ± 0.23	0.63 ± 0.15	0.83 ± 0.29	0.89 ± 0.31	0.54 ± 0.11	0.73 ± 0.14	0.68 ± 0.20	0.59 ± 0.15
BaP/BaP + BeP	0.47 ± 0.07	0.38 ± 0.07	0.44 ± 0.11	0.46 ± 0.10	0.35 ± 0.05	0.42 ± 0.05	0.40 ± 0.07	0.40 ± 0.15
IcdP/IcdP + BghiP	0.46 ± 0.04	0.41 ± 0.05	0.45 ± 0.02	0.46 ± 0.06	0.41 ± 0.03	0.48 ± 0.03	0.41 ± 0.02	0.41 ± 0.14
∑ Benzofluoranthenes/BghiP	3.05 ± 0.60	1.42 ± 0.52	2.93 ± 1.83	3.54 ± 0.73	4.91 ± 5.81	3.53 ± 0.72	2.91 ± 1.15	2.48 ± 1.55
Meteorological parameters								
H$_{mix}$ (m)	169 ± 43	854 ± 109	263 ± 77	296 ± 103	786 ± 160	402 ± 133	302 ± 86	974 ± 171
Temperature (°C)	3.9 ± 1.8	25.7 ± 2.6	10.6 ± 2.7	2.6 ± 0.9	16.5 ± 2.4	15.0 ± 2.5	7.3 ± 1.8	19.4 ± 2.8
Solar radiation (W m^{-2})	65 ± 30	324 ± 32	86 ± 44	89 ± 47	240 ± 79	105 ± 62	80 ± 52	286 ± 55
Precipitations (mm)	5.2	12.4	74.8	40.4	53.0	118.6	117.0	49.0

warm ratios ≈ 2). This explanation is proved by the significant negative correlation of TC values with temperature ($R^2 \approx 0.6$).

The results of this study are comparable with those observed at other urban and rural sites in Po Valley, characterized by very high regional background in the cold seasons, due to strength of anthropogenic emission sources (Piazzalunga et al., 2011; Belis et al., 2011; Perrone et al., 2012; Perrino et al., 2014), in agreement with similar seasonal differences found in Italy (Sandrini et al., 2014; Khana et al., 2016) and Europe (Yttri et al., 2007; Pio et al., 2011; Jedynska et al., 2014; Vodička et al., 2015).

The spatial variability of OC and EC values were evaluated by applying the *t*-Test at the significance level $p < 0.05$ on the values measured for each campaign. The OC concentrations at the two sampling sites show no statistically significant difference, while the EC concentrations exhibit a larger variability, with nearly double levels at the urban site MS compared with rural SP: the mean enrichment range from 1.6 in fall/winter up to 2.1 in spring/summer. This behavior reflects the strong impact on EC of primary emissions from local traffic or residential heating, in contrast to OC, which is emitted by a much larger number of source types and also produced by secondary formation processes (Szidat et al., 2006; Gelencser et al., 2007; Kourtchev et al., 2011). The same urban/rural discrimination of EC levels was observed in other locations in Northern Italy, with high levels at urban background sites (≈2 µgm^{-3}) that decrease moving to rural areas (≈1.0 µg m^{-3}) (Sandrini et al., 2014).

3.2.1. OC/EC concentration ratios

The relationship between OC and EC was evaluated to give useful information to discriminate between different sources and processes of PM (Fig. 1a, b). In fact, significant correlation of OC vs. EC commonly indicates dominance of the primary carbon emissions compared with photochemical activity, since EC is mainly representative of OC$_{prim}$ (Alves et al., 2010; Pio et al., 2011; Bautista et al., 2014).

In general, the whole dataset show significant correlation between OC and EC measured values, with good correlation for the data collected at the rural site ($R^2 \approx 0.75$), but only weak ($R^2 \approx 0.5$) for those at the urban site. These scattered data may be related to the occurrence of concomitant contribution of different local emission sources and also to the low accuracy of the OC/EC discrimination using the TOT measurement that is limited by the high EC loading on PM filters (EC ≥ 2 µg m^{-3}) (Costa et al., 2016). The slopes of the computed lines differ significantly with nearly double value at rural SP in comparison with urban MS (5 vs. 2, see inset in Fig. 1a, b). This spatial discrimination can be interpreted by a joint impact of local emissions and regional transport, in particular as a consequence of larger EC fractions locally emitted from fossil fuel combustion at the more populated urban site (Jones and Harrison, 2005; Saylor et al., 2006; Sandrini et al., 2014).

To give deeper insight into these findings, the ratio of particulate OC to EC was computed (mean value for each campaign and site reported in Table 1). A clear OC/EC seasonality was found with OC/EC ratios typically higher in spring/summer (mean values 3.7 and 6.6 at MS and SP,

respectively) in comparison with fall/winter (mean values 3.3 and 5.6 at MS and SP, respectively). This increase during summer may be ascribed to the enhanced production of secondary OC through photochemical activity and to the increased emission of biogenic precursors of SOA. During winter, the ratio is influenced by primary emissions such as fossil fuels burning, characterized by an OC/EC ratio frequently lower than 1 (OC/EC ratio ≈ 0.3–0.4) and residential wood burning, which is expected to release more organics (OC/EC ≥ 9) (Alves et al., 2010; Pio et al., 2011; Giannoni et al., 2012; Bautista et al., 2014).

In addition, a clear spatial discrimination is observed, with OC/EC values in general higher at the rural site, which is less impacted by EC emission sources, in particular related to traffic.

These results are similar to what observed at other ground-level rural sites located in the Po Valley characterized by OC/EC ratios ranging from 3 to 9 (Piazzalunga et al., 2011; Perrino et al., 2014; Sandrini et al., 2014), similar to what observed at other rural sites in Europe (i.e., Yttri et al., 2007; Saarikoski et al., 2008; Pio et al., 2011; Jedynska et al., 2014). At these sites the enrichment in OC during the warm months is consistent with the increased photochemical activity due to higher temperature and solar radiation (Pio et al., 2011; Perrino et al., 2014; Sandrini et al., 2014), while in winter it can be attributed to wood burning for residential heating (Szidat et al., 2006; Schmidl et al., 2008; Pio et al., 2011; Caseiro and Oliviera, 2012; Giannoni et al., 2012; Viana et al., 2013; Herich et al., 2014).

3.3. Contribution of secondary OC to carbonaceous matter

3.3.1. Estimation of secondary OC concentrations

The direct discrimination between primary (OC$_{prim}$) and secondary OC (OC$_{sec}$) is a difficult task, because of the still limited knowledge of OC molecular composition, atmospheric processes and characteristic emission profiles (Gelencser et al., 2007; Gentner et al., 2012). With the current lack of an experimental method to directly measure OC$_{prim}$ and OC$_{sec}$ fractions, indirect methods are usually employed based on the observed concentrations of total OC and EC.

In this study we applied the common EC tracer method, which calculates OC$_{sec}$ using an estimated OC_{prim}/EC_{prim} ratio, since it has the advantage of simplicity and low cost (Cabada et al., 2004; Pio et al., 2011; Xu et al., 2015; Day et al., 2015). This approach is based on the assumption that the minimum OC/EC ratio of the dataset, $(OC/EC)_{min}$, represents samples containing nearly exclusively primary OC and only negligible secondary OC. $(OC/EC)_{min}$ is then multiplied with individual EC value, entirely emitted from primary source, to get OC$_{prim}$, and this value is then subtracted from the total OC to determine OC$_{sec}$ value, according to the following equation:

$$OC_{sec} = OC - EC(OC/EC)_{min} \tag{1}$$

It seems to be a reasonable hypothesis that the minimum OC/EC ratio measured in urban areas strongly impacted by traffic represents the ratio between the OC and EC components resulting from road
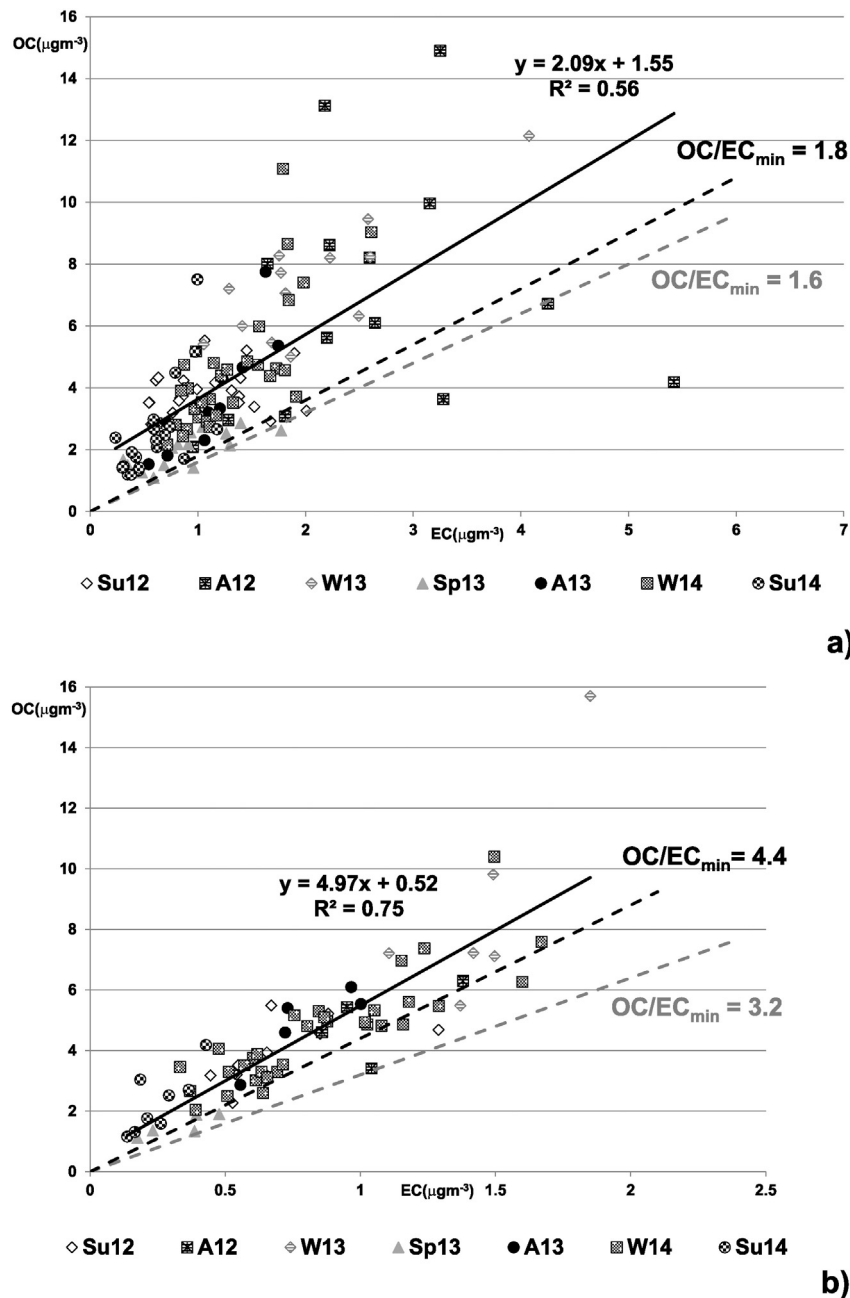
Fig. 1. Scatter plot of OC versus EC values measured in each monitoring campaign. Full black line: best fitting straight line of the whole dataset (equation parameters in the inset); dashed grey line: straight line corresponding to OC/EC$_{min}$ values estimated from spring/summer data; dashed black line: straight line corresponding to OC/EC$_{min}$ values estimated from fall/winter data; **2a**: data at MS site; **2b**: data at SP site.

transport fossil fuel combustion (Robert et al., 2007; El Haddad et al., 2009; Pio et al., 2011).

To compensate for individual imprecision in analytical measurements, $(OC/EC)_{min}$ ratios were estimated for each sampling campaign through visual inspection of OC versus EC scatter charts, by drawing a best fit line through the origin and including points aligned in the lower edge of the chart, as shown in Fig. 1a, b. In this work, in order to reduce subjectivity in the fitting and to remove outliers, data are grouped by seasons and location. At the urban site the computed $(OC/EC)_{min}$ values were 1.6 and 1.8 in cold and warm periods, respectively (Fig. 1a) and at the rural SP were 3.2 and 4.4 in the two periods (Fig. 1b).

It is noteworthy that the computed values are higher than the ratio of 0.7 found by Pio as characteristic of fossil fuel combustion in urban background, on the basis of a large set of measurements (Pio et al., 2011). This result may indicate that in the investigates atmosphere

there is a constant input of OC added to the fossil fuel transport emission, presumably generated by biomass burning. This may likely explain higher values in cold months, when larger emissions of wood burning for domestic heating are expected, as well as at the rural site that is less impacted by vehicle traffic (Cabada et al., 2004; Pio et al., 2011; Day et al., 2015; Vodička et al., 2015).

Using the computed $(OC/EC)_{min}$ ratios, OC$_{sec}$ concentrations were estimated for every campaign, as absolute OC$_{sec}$ and relative OC$_{sec}$% values (Table 1). The absolute OC$_{sec}$ values show the same seasonal trend of the other carbonaceous components with higher values in fall/winter than in spring/summer (on average, ≈ 2.9 μg m^{-3} and ≈ 1 μg m^{-3}, respectively, Table 1). Otherwise, the percentage contribution OC$_{sec}$ % is nearly constant across the year: 47% at MS and 30% at SP (Table 1). However, a seasonal trend would be expected with higher OC$_{sec}$% contribution in spring/summer, as a consequence of a stronger photochemical

oxidation promoted by the increasing of solar radiation from $\approx 75 \, Wm^{-2}$ in November/February up to $\approx 270 \, Wm^{-2}$ in May/August (Table 1). One likely reason of this unexpected result may be that in the cold seasons the limited photochemical oxidation is compensated by the condensation or adsorption of VOCs in aerosols, which are facilitated by the stable atmosphere and the low temperature (Gelencser et al., 2007; Lonati et al., 2007; Xu et al., 2015; Khana et al., 2016). Another surprising result concerns spatial distribution, since secondary processes are presumed stronger at the rural site, that is less impacted by local emission sources, mainly traffic. It is noteworthy that the computed values may be affected by the large uncertainty of the used approach, that was found to overestimate the OC_{prim} from vehicle emissions and underestimates OC_{sec} components, as a consequence of bias in estimating $(OC/EC)_{min}$ ratios from open air measurements of OC and EC (Cabada et al., 2004; Pio et al., 2011; Day et al., 2015).

Despite the weakness of the used approach, the estimated OC_{sec} values $\approx 40\%$ are very close to those found at other urban and rural and locations in Northern Italy (Lonati et al., 2007; Bernardoni et al., 2011; Bigi et al., 2012; Saarikoski et al., 2012; Paglione et al., 2014; Khana et al., 2016).

3.3.2. Concentration of carboxylic acids

To avoid the limitations of the $(OC/EC)_{min}$ method, the contribution of secondary OC was estimated with another independent approach. With this aim the concentration of carboxylic acids was measured, as they are useful molecular markers to help the differentiation between primary emissions and secondary organic aerosols. These acids have been found in the atmospheric aerosol as directly emitted by a multiplicity of sources — including power plants, vehicular circulation, biomass burning and meat cooking operations – and secondarily produced through photo-chemical reactions with volatile precursors including anthropogenic and biogenic hydrocarbons. In particular, hydroxy/oxo carboxylic acids have been identified as intermediate products of such secondary photo-oxidation reactions (Mazzoleni et al., 2007; Oliveira et al., 2007; Schmidl et al., 2008; Balducci and Cecinato, 2010; Wang et al., 2011; Holden et al., 2011; Kourtchev et al., 2011; Saarikoski et al., 2012; Pietrogrande et al., 2014a).

In all the campaigns, 16 low-molecular-weight carboxylic acids were investigated, namely seven linear dicarboxylic acids with 3–9 carbon atoms and maleic and phthalic acids, five hydroxy carboxylic acids, namely glycolic, malic, glyoxylic and 3- and 4-hydroxy benzoic acid, and two oxo carboxylic acids, pinonic and 2-ketoglutaric acid.

The total amount of the analyzed acids follows the same seasonal trend of other markers, with concentrations ≈ 5 times higher in fall/winter (mean value $\approx 200 \, ngm^{-3}$) in comparison with spring/summer (mean value $\approx 40 \, ngm^{-3}$) (CA_{tot}, mean values $\pm$ SD in Table 1). In June 2012 acid concentrations were $\leq$ LOD since low-volume air sampler ($55 \, m^3$ in a day) was used.

Such a season trend can be likely explained with the enhanced emission from wood combustion for domestic heating expected in the cold seasons combined with pollutants accumulation promoted by atmospheric stagnant conditions in fall/winter (Pietrogrande et al., 2014a). In fact, some acids, mainly succinic acid, have been found abundant in biomass smoke as well as involved in photochemical reactions of the burning products (Mazzoleni et al., 2007; Oliveira et al., 2007; Wang et al., 2011; Caseiro and Oliviera, 2012; Saarikoski et al., 2012; Viana et al., 2013; Paglione et al., 2014). This statement is supported by the good correlations found between total concentrations of carboxylic acids and burning sugars ($R^2 \approx 0.76$) as well as temperature (negative correlation, $R^2 \approx 0.78$).

As useful marker to discriminate between primary and secondary origin of the investigated carboxylic acids, the separated contribution of hydroxy/oxo carboxylic acids was computed as absolute (CA_{oxo} in Table 1) and relative to CA_{tot} values ($CA_{oxo}\%$ in Table 1). Although the absolute data are ≈ 2 times higher in fall/winter (mean value $\approx 68 \, ngm^{-3}$) in comparison with spring/summer (mean value

$\approx 35 \, ngm^{-3}$), the relative values are higher in the warm seasons ($CA_{oxo}\% \approx 62\%$) in comparison with those in colder months ($CA_{oxo}\% \approx 38\%$), with similar values at both sites. This clear seasonal trend is consistent with enhanced photochemical oxidation in spring/summer with increasing solar radiation, as supported by the significant positive correlation ($R^2 = 0.83$) between $CA_{oxo}\%$ and solar radiation. Therefore, $CA_{oxo}\%$ seems a more suitable parameter for estimating the relative contribution of SOA in comparison with $OC_{sec}\%$ based on $(OC/EC)_{min}$ procedure.

3.4. Sugars as markers of primary biogenic carbon

Sugars were determined in $PM_{2.5}$ samples to give insight into the relative contribution of biogenic emissions to OC, being the major form of photosynthetically assimilated carbon in the biosphere (Simoneit et al., 2004; Medeiros et al., 2006; Jia and Fraser, 2011; Tominaga et al., 2011; Fu et al., 2012; Calvo et al., 2013). As an extension of pervious work (Pietrogrande et al., 2014b), the study concerns 12 saccharides: 3 anhydrosugars — levoglucosan, galactosan and mannosan — as specific markers of biomass burning (biomass burning sugars) and 9 primary saccharides — glucose, sucrose, arabinose, galactose and mycose — and sugar alcohols — erythritol and mannitol — that are mainly emitted from biological particles, namely, microorganisms, pollen, vegetative debris, bacteria and viruses (bio sugars) (Puxbaum et al., 2007; Mazzoleni et al., 2007; Jia and Fraser, 2011; Fu et al., 2012; Giannoni et al., 2012).

The individual sugar concentrations were overall summed to compute the total sugars concentrations (S_{tot}) and separately to compute the contribution of the sugars emitted by biomass burning (3 anhydrosugars, S_{bb}) and by the ecosystem (S_{bio}) (Table 1).

In general, total sugar concentrations are nearly 10 times higher in the cold seasons (mean $580 \, ngm^{-3}$) than in warm periods (mean $50 \, g \, m^{-3}$) (Table 1). In fact, the highest levels were found in November/February ranging from $1288 \, ng \, m^{-3}$ in November 2011 at MS to $327 \, ng \, m^{-3}$ in October 2012 at SP site, while the lowest concentrations were observed in summer/spring ranging from $76 \, ng \, m^{-3}$ in May 2014 at SP to $7 \, ng \, m^{-3}$ in June 2012 at MS.

Seasonality is evident also in sugar concentration profiles ($S_{bb}\%$ and $S_{bio}\%$), providing information on the relative contributions of different emission sources. Anhydrosugars were by far the dominant sugars in fall and winter, both on a relative and an absolute basis: higher levels were found for levoglucosan in fall/winter ($1043–233 \, ng \, m^{-3}$, mean $454 \, ng \, m^{-3}$), followed by mannosan ($121–26 \, ngm^{-3}$, mean $65 \, ngm^{-3}$) and galactosan ($52–15 \, ng \, m^{-3}$, mean $31 \, ng \, m^{-3}$). These data specifically indicate that anhydrosugars are nearly the only source for particulate saccharides in fall/winter, comprising nearly 94% of the total sugars at both sites, while their impact strongly decreases in spring/summer ($\approx 25\%$, $S_{bb}\%$ in Table 1).

The obtained data are comparable with those observed at several urban and rural sites, where burning sugars contributed nearly 90% of total sugars during winter, but only 10% during summer (Jia et al., 2010; Holden et al., 2011; Fu et al., 2012; Giannoni et al., 2012).

As anhydrosugars are key tracers for smoke emissions from both open and residential biomass combustion, these results indicate the relevance of BB emissions as a source of atmospheric particles. This may be mainly related to wood combustion occurring in household stoves, since the use of biomass as a fuel for residential purposes is increasing in recent years, not only in rural areas but also in urban environments, as a consequence of increasing oil prices. This hypothesis is supported by a nearly linear negative dependence of burning sugar concentration with temperature ($R^2 \approx 0.73$), that is consistent with increased BB emissions for residential heating experienced with decreasing temperature.

Similar anhydrosugars levels ($300–500 \, ngm^{-3}$) were measured in urban and rural areas in Central and Northern Europe, where residential wood combustion has been identified as an important source of air

pollution (Oliveira et al., 2007; Schmidl et al., 2008; Caseiro and Oliviera, 2012; Van Drooge et al., 2012; Viana et al., 2013). As to Italy, levoglucosan levels close to 400 ngm^{-3} have been found in cold seasons at other urban-background sites (Florence, Mantova) (Piazzalunga et al., 2011; Giannoni et al., 2012), while higher concentrations close to 1000 ngm^{-3} have been measured during winter in Milan and at other sites in Northern Italy closest to the Alps (Schmidl et al., 2008, Perrone et al., 2012; Belis et al., 2011; Piazzalunga et al., 2013; Herich et al., 2014).

In this study both the urban and the rural background sites showed similar levels of burning sugars, indicating a homogeneous impact of wood combustion in all the investigated regions. The reason may be the widespread use of wood combustion for residential heating in the area combined with the atmospheric stratification that homogenizes spatial distribution of organic pollutants.

In the warm seasons anhydrosugars show low levels and homogeneous distribution between urban and rural sites (≈ 8 ng m^{-3} at both sites): this likely excludes a significant contribution of smoke emissions from open fires (Mazzoleni et al., 2007; Gelencser et al., 2007; Kourtchev et al., 2011; Munchak et al., 2011; Vassura et al., 2014).

3.4.1. Contribution of wood combustion to carbonaceous matter

The mono-tracer approach based on the ambient concentrations of levoglucosan was used in this paper to estimate the contribution of OC generated by wood burning (Puxbaum et al., 2007; Schmidl et al., 2008, Piazzalunga et al., 2011; Giannoni et al., 2012; Herich et al., 2014). Therefore, the relationship between levoglucosan and OC was studied for each campaign to represent wood combustion contribution to organic particulate (Fig. 2). The obtained plots show clear season discrimination with spring/summer data, including October 2013, closely grouped near to OC axis (levoglucosan concentration $0.02 \le \mu gm^{-3}$, full symbols in the figure).

Otherwise, the fall/winter values are rather scattered in the levoglucosan/OC space between straight lines with slope 0.02–0.15, as indicated by the lines in Fig. 2. The measured values yield highly variable levoglucosan to OC emission factors (Lev/OC, Table 1) which are mostly included in the 0.06–0.2 range reported in literature for the residential burning of softwood-hardwood mixtures (Szidat et al., 2006; Schmidl et al., 2008; Bari et al., 2010; Holden et al., 2011; Kourtchev et al.,

2011; Herich et al., 2014). Such a large differentiation may be ascribed to the variability of factors that influence emissions from wood combustion, meanly the type of wood combusted, the appliance used and the burning operative conditions, i.e., burning rates, air dilution, and moisture content in the fuel (Szidat et al., 2006; Mazzoleni et al., 2007; Alves et al., 2010; Piazzalunga et al., 2011; Holden et al., 2011; Munchak et al., 2011; Caseiro and Oliviera, 2012; Herich et al., 2014). Therefore, an accurate estimate of OC$_{bb}$ using the mono-tracer approach would require site-specific emission factors, actually presentative of the different types of appliances in use on the territory and the different wood species actually burnt. Given the lack of this information for Emilia Romagna region, we used the emission factor of 0.15 proposed by Szidat as the average value of the data present in the literature (Szidat et al., 2006).

This value has been computed for combustion of a wood fuel consisting of a mixture of hard and softwood, that adequately describe wood burning profiles in Emilia Romagna region, as supported by a previous study based on diagnostic ratios of anhydrosugars and methoxylated phenols (Pietrogrande et al., 2015). The suitability of such a factor has been proved by its widespread use in different studies in European areas (i.e., Puxbaum et al., 2007; Piazzalunga et al., 2011; Caseiro and Oliviera, 2012; Herich et al., 2014; Perrino et al., 2014).

With this assumption, we estimated the amount of OC derived from wood smoke as absolute concentrations (OC$_{bb}$) as well as relative contributions of OC$_{bb}$ to total OC (OC$_{bb}$%) (mean values $\pm$ SD in Table 1). The absolute concentrations of OC$_{bb}$ at both the sites were on average ≈ 3 µg m^{-3} in November/February and decrease to ≈ 0.1 µg m^{-3} in warm periods, including October 2013.

Not surprisingly, primary organic aerosol emission from wood burning established a significant contribution (OC$_{bb}$% ≈ 33%) at both sites in fall/winter, and a small impact in spring/summer (OC$_{bb}$% ≈ 3%) (OC$_{wb}$%, Table 1). However, it has to be underlined that these results may be affected by the relatively large uncertainty of the approach, as a consequence of the lack of site-specific emission factors in Emilia Romagna region (Caseiro and Oliviera, 2012; Schmidl et al., 2008; Munchak et al., 2011; Piazzalunga et al., 2013). Despite such an uncertainty, the obtained results are in agreement with the data found in neighboring Lombardia region (Gilardoni et al., 2011) and Torino (Piazzalunga et al., 2013). This demonstrates that a mass of wood is diffusely used
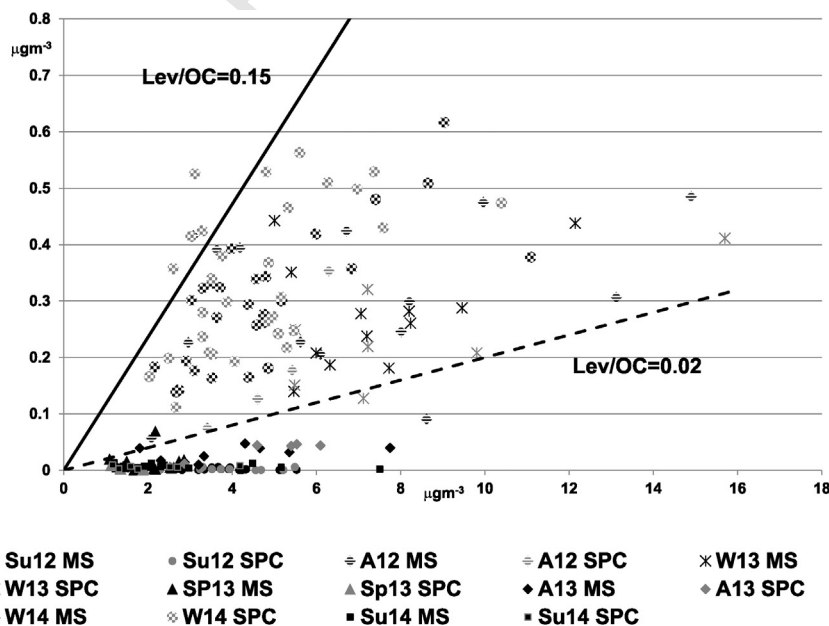

Fig. 2. Scatter plot of levoglucosan versus OC concentrations measured in each monitoring campaign. Black symbols: data at MS site; grey symbols: data at SP site. Full symbols: spring/summer data, including October 2013. Dashed symbols: fall/winter data. Dashed black line: straight line corresponding to Lev/OC ratio value of 0.02; full black line: straight line corresponding to Lev/OC ratio value of 0.15.

in Po Plain as fuel for domestic heating in the coldest months (November–February) which leads to a sharp increase in the wood–related carbonaceous emission contributing nearly 30% of OC. Otherwise, even higher OC_{bb}% contributions close to 50% were estimated in the same region at the industrial site of Cantù and Alpine locations (Piazzalunga et al., 2011, 2013; Herich et al., 2014).

3.4.2. Contribution of biosystem emission to carbonaceous matter

The most common saccharides present in vascular plants and microorganisms were measured in all the sampling campaigns (S_{bio}, Table 1). They have been proposed as source-specific tracers for soil biota released into the atmosphere by farmland soil suspension and natural soil erosion — glucose, sucrose and mycose — and for atmospheric fungal spore abundance, i.e., mannitol and erithrytol (Medeiros et al., 2006; Jia et al., 2010; Tominaga et al., 2011; Fu et al., 2012). In addition, these sugars are emitted as uncombusted materials from the biomass burning processes, i.e., glucose is commonly present at higher levels in vascular plants, while arabinose and galactose are predominant sugars in pectin, a polysaccharide contained in nonwoody tissues (Szidat et al., 2006; Medeiros et al., 2006; Wang et al., 2011).

In general, these bio-sugars show nearly constant value close to 35 ng m^{-3} through the year at both the urban and rural sites (S_{bio}, Table 1). This may indicate a common background regional profile reflecting bio-aerosol released from plants and microorganisms, in particular from farmland soils related to the agricultural activities (Simoneit et al., 2004; Tsai et al., 2013; Pietrogrande et al., 2014b). However, the relative contribution of bio-sugars shows strong seasonality, since they dominate sugar distribution profiles, comprising ≈65% of total sugars in warmer seasons when biomass burning is nearly absent. On the contrary, they contribute nearly 8% to sugar levels in fall/winter (S_{bio}%, in Table 1).

These data on bio-sugars can be used in the apportionment of the carbonaceous aerosol to isolate the contribution of primary biological sources to aerosol OC (OC_{bio}). Even if a quantitative computation is impossible, the relative concentration of bio-sugars, expressed as the ratio S_{bio}/OC%, may be an estimation of the impact of bio-aerosol (Table 1). On average, such a ratio is close to 0.5% in fall/winter at both the sites and increases up to 1.4% in spring/summer with the highest value of 2.2% in summer 2014. This pattern reasonably reflects the life cycle of vegetation, with the higher activity in the warmer seasons, and the agricultural activities prevailing in the farmland in spring to fall periods (Simoneit et al., 2004; Medeiros et al., 2006; Jia and Fraser, 2011; Fu et al., 2012; Pietrogrande et al., 2014b).

3.5. Polycyclic aromatic hydrocarbons as markers for apportionment of organic carbon

Finally, high molecular weight PAHs were investigated in PM$_{2.5}$ samples in order to elucidate the composition of the combustion emission sources of OC_{prim}, as they are emitted into the atmosphere from incomplete combustion of different fuels, such as fossil (e.g. traffic emission) as well as biomass (e.g. wood combustion emissions). Once emitted into the atmosphere PAHs distribute between gas– and particle phases, depending on their volatile properties, with five– and six–ring PAHs mainly adsorbed in the particulate matter, depending on ambient temperatures (El Haddad et al., 2009; Belis et al., 2011; Van Drooge et al., 2012; Calvo et al., 2013; Piazzalunga et al., 2013; Jedynska et al., 2014; Vassura et al., 2014).

In the present study 12 individual PAHs were quantified, including the US EPA PAH priority pollutants: phenanthrene (PHE), anthracene (ANT), fluoranthene (FLNT), pyrene (PYR), benzo[a]anthracene (BaA), chrysene (CRY), benzo[b + j]fluoranthene (BbF), benzo[k]fluoranthene (BkF), benzo[e]pyrene (BeP), benzo[a]pyrene (BaP), indeno[1,2,3–c,d]pyrene (Ind123P) and benzo[g,h,i]perylene (BghiP). Table 1 reports the measured values of the total PAH mass (PAH$_{tot}$) and the

concentrations of the most abundant compounds, i.e., FLNT, PYR, CRY, BbF, BkF, BaP, Ind123P and BghiP.

As expected, PAHs showed the strong seasonal trend experienced by the other trace organics with higher atmospheric levels during colder periods in comparison with the warmer months. This increase is nearly 100 times with the total PAH mass increasing from 0.11 ng m^{-3} in Summer 2014–11.5 ng m^{-3} in Fall 2011 at the urban site, and from 0.07 ng m^{-3} in Spring 2013–7.2 ng m^{-3} in Fall 2011 at the SP site Table 1). The higher PAH levels in the colder seasons could be explained by higher PAH emissions related to domestic heating and more stagnant atmospheric conditions supporting atmospheric PAH accumulation. In addition, besides these ambient factors, the PAH concentrations are influenced by physicochemical properties, such as volatility related to the gas/particle partitioning, and reactivity with oxidants (Saarnio et al., 2008; Jedynska et al., 2014; Rybak and Olejniczak, 2014).

In all the campaigns PAH levels were higher at Main Site than at site San Pietro, that is consistent with larger direct emissions in the more populated urban location.

In the present dataset, the particulate-phase PAHs distribution profiles are similar for all the samples. They are dominated by five– to six–ring compounds, such as benzo[b] and benzo[k]fluoranthenes and benzo[ghi]perylene followed by BaP, Ind123P and CRY. In addition, fluoranthene and pyrene were among the most abundant PAHs in the warmer seasons. Such PAHs have been found in airborne particulate emitted from road transport and biomass burning, as found in other sites in the Po valley (Belis et al., 2011; Perrone et al., 2012; Van Drooge et al., 2012; Perrone et al., 2013; Piazzalunga et al., 2013; Pietrogrande et al., 2014c; Vassura et al., 2014).

3.5.1. Profile-based source apportionment of PAHs

In order to identify the most important pollution emissions in the studied area, the PAH relative molecular concentration ratios were investigated (Alves, 2008; Tobiszewski and Namienśnik, 2012; Agudelo-Castaneda and Teixeira, 2014). In particular, BaP/BeP and BaP/BaP + BeP ratios were computed, as they have been proposed as indicators of aerosol age, since both compounds are normally emitted in similar amounts by combustion sources. As BaP is more reactive than BeP in the atmosphere, a BaP/BeP ratio < 1 and a BaP/BeP + BaP ratio < 0.5 indicate an aged aerosol (Oliveira et al., 2011). The values obtained during sampling campaigns are usually lower than the reference values especially during spring/summer (minimum value 0.16 in spring 2013, Table 1). This highlights that a certain fraction of SOA is always present in atmospheric PM$_{2.5}$, even in wintertime.

Other ratios were computed in order to obtain more specific information about combustion processes that originate PAHs. In particular, the ratio IcdP/IcdP + BghiP may be useful to discriminate between fossil fuels and biomass burning. In fact, values above 0.50 have been reported for grass combustion, wood soot, creosote, while ratios below 0.50 were found for combustion products of gasoline, kerosene, diesel and crude oil, with values falling between 0.24 and 0.40 for vehicle emissions (Yunker et al., 2002; Tobiszewski and Namienśnik, 2012). In all sampling campaigns the calculated values are around 0.4 (Table 1), a value that indicates mainly a contribution from fossil fuel combustion.

On the other hand, the ratio $\sum$ Benzofluoranthenes/BghiP, also proposed for discriminating combustion sources, indicates that wood burning is the major source of aerosol. In fact the ratios computed in the sampling campaigns are in most part higher than 2 (lowest value 1.4 in summer 2012, Table 1), which are values close to 2.2 characteristic for wood burning, while ratios of 1.6 and 0.3 are indicative for diesel and gasoline combustion respectively (Li and Kamens, 1993; Alves, 2008). In conclusion, the PAHs ratio approach provides conflicting results, that confirms the weakness of the method, although its simplicity and ease of application (Yunker et al., 2002; Tobiszewski and Namienśnik, 2012; Agudelo-Castaneda and Teixeira, 2014; Clément et al., 2015).

Therefore, in the present study, also a profile-based source apportionment was applied by comparing the abundance distributions of the measured PAHs to those of the dominant emissions, i.e., traffic and wood combustion (Szidat et al., 2006; Mazzoleni et al., 2007; Saarikoski et al., 2008; Saarnio et al., 2008; Holden et al., 2011; Orasche et al., 2012; Pietrogrande et al., 2014c; Jedynska et al., 2014; Herich et al., 2014). However, uncertainty may affect also the results of this approach, since PAHs relative distribution can be greatly modified by atmospheric removal and transformation processes.

Concerning the contribution of traffic source, the chemical profiles of emissions from gasoline-powered and diesel-powered vehicles have been found largely influenced by several factors, including different fleet compositions, driving patterns, climate conditions and fuel compositions (Saarikoski et al., 2008; Saarnio et al., 2008; Pietrogrande et al., 2014c; Jedynska et al., 2014). Therefore, a traffic profile that closely describes actual fleets of on-road vehicles in the investigated area is needed. Given the lack of such experimental profiles for Emilia Romagna region, in the present study we assumed a traffic source profile derived from studies performed in several urban areas, including cities in Northern Italy (Wingfors et al., 2001; Saarnio et al., 2008; Oliveira et al., 2011; Perrone et al., 2012; Pietrogrande et al., 2014c; Rybak and Olejniczak, 2014) (data reported in Fig. 3, full black bars). Such a traffic profile, with a prevailing diesel contribution, is characterized by high amount of lighter PAHs — FLNT, PYR, CRY — and BghiP. Similar profiles were found in other EU countries, where the contribution of diesel vehicles is relevant, as also reported by El Haddad for a tunnel study in France (El Haddad et al., 2009).

Concerning PAH profiles from biomass combustion sources, a large variability was found potentially related to differences in the type of wood combusted and stove used as well as in the burning conditions, i.e., rates, air dilution, and moisture content in the fuel (Szidat et al., 2006; Mazzoleni et al., 2007; Holden et al., 2011; Orasche et al., 2012; Herich et al., 2014). Therefore, site-specific source profiles are needed for an accurate description of local emissions, taking into account both the wood species actually burnt and the type of appliances in use. As this information was unknown for Emilia Romagna region, we utilized a representative profile derived from several literature sources (Hays et al., 2003; Fine et al., 2004; Orasche et al., 2012; Perrone et al., 2012; Pietrogrande et al., 2014c: Vassura et al., 2014). They concern different combustion systems, mainly including those most commonly used in Northern Italy, that are wood stoves fired with wood logs originated from spruce and beech (Pietrogrande et al., 2015). The burning profile is dominated by benzofluoranthenes BFs: BbF + BjF + BkF — and benzo[a]pyrene, followed by indeno[123 cd]pyrene and chrysene (data reported in Fig. 3, full grey bars).

In order to investigate the impact of the two main sources to ambient PAHs, the correspondence between the experimental PAH distribution and source profile was estimated by intercorrelation values. The PAHs more specifically related to traffic source — FLNT, PYR, CHRY and BghiP — show collinearity ($R^2 \sim 0.7$) between source profile and values measured in warm seasons, mainly in July 2012 and June 2014 values ($R^2 > 0.9$, Fig. 3, dashed black bars). Such a correlation was found only for the data collected at the urban site, that is consistent with the direct impact of traffic emissions, associated with vehicle transport inside Bologna city and close to major roads. The contribution of such a local source decreases and combines with other emission sources by moving away from the city to SP (30 km far).

In most campaigns, all the measured PAHs show a significant collinearity ($R^2 \geq 0.6$) with wood burning emissions profile (Fig. 3, dashed grey bars), excluding July 2012 and June 2014 data (no correlation) and May 2013 ($R^2 \sim 0.5$). These findings suggest that measured PAHs distributions are composite profiles of the 2 investigated sources, with higher contribution of biomass burning in cold seasons. This result may explain the approximation of the OC_{sec} values computed with the $(OC/EC)_{min}$ method: the assumption that OC_{prim} is mainly generated by fossil emission is not fulfilled, in particular at SP site, where biased $OC_{sec}\%$ values more different from $CA_{oxo}\%$ estimates were computed (Table 1).

Similar results have been reported from recent monitoring studies in the Po Plain, that identified wood burning for residential heating as a predominant source of the PAHs air concentration in fall and winter (Belis et al., 2011; Piazzalunga et al., 2013; Gianelle et al., 2013; Perrino et al., 2014; Pietrogrande et al., 2015).   **Q19**

4. Conclusions

In summary, the obtained results indicate high level of carbonaceous particulate matter, specifically in cold seasons with elevated OC and EC levels. An OC–dominated profile is in general measured, as demonstrated by high OC/EC ratios. The spatial and temporal variations of OC and EC concentrations provided information on their different fractions in urban and rural settings in Emilia Romagna region.

The carbonaceous particulate was mainly generated from vehicular traffic and residential heating emissions combined with secondary formation, accounting nearly 40%, even in cold months.

Results on background levoglucosan indicate that wood burning for domestic heating is the dominating emission source at both the investigated sites in cold seasons during fall/winter. Its strong impact is further enhanced by the significant production of secondary organic aerosols from primary smoke precursors, as suggested by high concentrations of low molecular weight carboxylic acids.

The information obtained about OC and EC would lead to increased understanding and better management of emissions in both urban and rural areas of the region. In particular, the dangerous implications of biomass combustion sources highlight the need for the regulation of the emissions of such particulates.
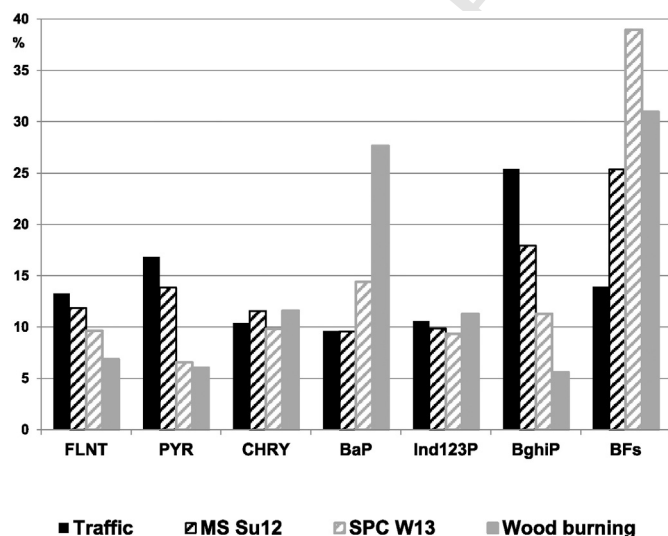
Acknowledgements

Fig. 3. PAH distribution profiles: correspondence between the source emission profiles derived from literature (full bars) and the experimental PAH distributions (dashed bars). Full black bars: traffic emission profile; full grey bars: wood burning emission profile.

References

Agudelo-Castaneda, D.M., Teixeira, E.C., 2014. Seasonal changes, identification and source apportionment of PAH in PM1.0. Atmos. Environ. 96, 186–200.

Alves, C.A., 2008. Characterisation of solvent extractable organic constituent in atmospheric matter: an overview. An. Acad. Bras. Cienc. 80, 21–82.

Alves, C.A., Gonçalves, C., Mirante, F., Nunes, T., Evtyugina, M., Sánchez de la Campa, A., Rocha, A.C., Marques, M.C., 2010. Organic speciation of atmospheric particles in Alvão Natural Park (Portugal). Environ. Monit. Assess. 168, 321–337.

Balducci, C., Cecinato, A., 2010. Particulate organic acids in the atmosphere of Italian cities: are they environmentally relevant? Atmos. Environ. 44, 652–659.

Bari, M.A., Baumbach, G., Kuch, B., Scheffknecht, G., 2010. Temporal variation and impact of wood smoke pollution on a residential area in Southern Germany. Atmos. Environ. 44, 3823–3832.

Bautista, A.T.V.II., Pabroa, P.C.B., Santos, F.L., Racho, J.M.D., Quirit, L.L., 2014. Carbonaceous particulate matter characterization in an urban and a rural site in the Philippines. Atmos. Pollut. Res. 5, 245–252.

Belis, C., Cancelinha, J., Duane, M., Forcina, V., Pedroni, V., Passarella, R., Tanet, G., Douglas, K., Piazzalunga, A., Bolzacchini, E., 2011. Sources for PM air pollution in the Po plain, Italy: I. Critical comparison of methods for estimating biomass burning contributions to benzo(a)pyrene. Atmos. Environ. 45, 7266–7275.

Bernardoni, V., Vecchi, R., Valli, G., Piazzalunga, A., Fermo, P., 2011. PM10 source apportionment in Milan (Italy) using time-resolved data. Sci. Total Environ. 409, 4788–4795.

Bigi, A., Ghermandi, G., Harrison, R.M., 2012. Analysis of the air pollution climate at a background site in the Po valley. J. Environ. Monit. 14, 552–563.

Cabada, J.C., Pandis, S.N., Subramanian, R., Robinson, A.L., Polidori, A., Turpin, B., 2004. Estimating the secondary organic aerosol contribution to PM2.5 using the EC tracer method. Aerosol Sci. Technol. 38, 140–155.

Calvo, A.I., Alves, C., Castro, A., Pont, V., Vicente, A.M., Fraile, R., 2013. Research on aerosol sources and chemical composition: Past, current and emerging issues. Atmos. Environ. 44, 652–659.

Carbone, C., Decesari, S., Mircea, M., Giulianelli, L., Finessi, E., Rinaldi, M., Fuzzi, S., Marinoni, A., Duchi, R., Perrino, C., 2010. Size-resolved aerosol chemical composition over the Italian peninsula during typical summer and winter conditions. Atmos. Environ. 44, 5269–5278.

Caseiro, A., Oliviera, C., 2012. Variations in wood burning organic marker concentrations in the atmospheres of four European cities. J. Environ. Monit. 14, 2261–2269.

Cavalli, F., Viana, M., Yttri, K., Genberg, J., Putaud, J., 2010. Toward a standardised thermal-optical protocol for measuring atmospheric organic and elemental carbon: the EUSAAR protocol. Atmos. Meas. Tech. 3, 79–89.

CEN, 1998. Cen 12341: Air quality-determination of the PM10 fraction of suspended particulate matter-reference method and field test procedure to demonstrate reference equivalence of measurement methods. European Committee for Standardization, Brussels, Belgium.

CEN, 2011. Cen/tr 16243: Ambient air quality - guide for the measurement of elemental carbon (EC) and organic carbon (OC) deposited on filters. European Committee for Standardization, Brussels, Belgium.

Chiappini, L., Verlhac, S., Aujay, R., Maenhaut, W., Putaud, J.P., Sciare, J., Jaffrezo, J.L., Liousse, C., Galy-Lacaux, C., Alleman, L.Y., Panteliadis, P., Leoz, E., Favez, O., 2014. Clues for a standardised thermal-optical protocol for the assessment of organic and elemental carbon within ambient air particulate matter. Atmos. Meas. Tech. 7, 1649–1661.

Clément, N., Muresan, B., Hedde, M., François, D., 2015. PAH dynamics in roadside environments: influence on the consistency of diagnostic ratio values and ecosystem contamination assessments. Sci. Total Environ. 538, 997–1009.

Costa, V., Bacco, D., Castellazzi, S., Ricciardelli, I., Vecchietti, R., Zigola, C., Pietrogrande, M.C., 2016. Characterization of carbonaceous aerosol in Emilia-Romagna during the Supersito Project: influences of the Thermal-Optical measurement protocols. 2016. Atmos. Res. 10, 100–107. http://dx.doi.org/10.1016/j.atmosres.2015.07.020.

Day, M.C., Zhang, M., Pandis, S.N., 2015. Evaluation of the ability of the EC tracer method to estimate secondary organic carbon. Atmos. Environ. 112, 317–325.

Decesari, S., Allan, J., Plass-Duelmer, C., Williams, B.J., Paglione, M., Facchini, M.C., O'Dowd, C., Harrison, R.M., Gietl, J.K., Coe, H., Giulianelli, L., Gobbi, G.P., Lanconelli, C., Carbone, C., Worsnop, D., Lambe, A.T., Ahern, A.T., Moretti, F., Tagliavini, E., Elste, T., Gilge, S., Zhang, Y., Dall'Osto, M., 2014. Measurements of the aerosol chemical composition and mixing state in the Po Valley using multiple spectroscopic techniques. Atmos. Chem. Phys. 14, 12109–12132.

Deserti, M., Savoia, E., Cacciamani, C., Golinelli, M., Kerschbaumer, A., Leoncini, G., Selvini, A., Paccagnella, T., Tibaldi, S., 2001. Operational meteorological pre-processing at Emilia-Romagna ARPA Meteorological Service as a part of a decision support system for Air Quality Management. Int. J. Environ. Pollut. 16, 571–582.

El Haddad, I., Marchand, N., Dron, J., Temime-Roussel, B., Quivet, E., Wortham, H., Jaffrezo, J.L., Baduel, C., Voisin, D., Besombes, J.L., Gille, G., 2009. Comprehensive primary particulate organic characterization of vehicular exhaust emissions in France. Atmos. Environ. 43, 6190–6198.

Fine, P.M., Cass, G.R., Simoneit, B.R.T., 2004. Chemical characterization of fine particle emissions from the wood stove combustion of prevalent United States tree species. Environ. Eng. Sci. 21, 387–409.

Fu, P., Kawamura, K., Kobayashi, M., Simoneit, B.R.T., 2012. Seasonal variations of sugars in atmospheric particulate matter from gosan, Jeju Island: significant contributions of airborne pollen and Asian dust in spring. Atmos. Environ. 55, 234–239.

Gelencser, A., May, B., Simpson, D., Sanchez-Ochoa, A., Kasper-Giebl, A., Puxbaum, H., Caseiro, A., Pio, C., Legrand, M., 2007. Source apportionment of PM2.5 organic aerosol over Europe: primary/secondary, natural/anthropogenic, and fossil/biogenic origin. J. Geophys. Res. Atmos. 112, D23S04.

Gentner, D.R., Isaacman, G., Worton, D.R., Chan, A.W.H., Dallmann, T.R., Davis, L., Liu, S., Day, D.A., Russell, L.M., Wilson, K.R., Weber, R., Guha, A., Harley, R.A., Goldstein, A.H., 2012. Elucidating secondary organic aerosol from diesel and gasoline vehicles through detailed characterization of organic carbon emissions. Proc. Natl. Acad. Sci. U. S. A. 109, 18318–18323.

Gianelle, V., Colombi, C., Caserini, S., Ozgen, S., Galante, S., Marongiu, A., Lanzani, G., 2013. Benzo(a)pyrene air concentrations and emission inventory in Lombardy region, Italy. Atmos. Pollut. Res. 4, 257–266.

Giannoni, M., Martellini, T., Del Bubba, M., Gambaro, A., Zangrando, R., Chiari, M., Lepri, M., Cincinelli, A., 2012. The use of levoglucosan for tracing biomass burning in PM2.5 samples in Tuscany (Italy). Environ. Pollut. 167, 7–15.

Gilardoni, S., Vignati, E., Cavalli, F., Putaud, J., Larsen, B., Karl, M., Stenström, K., Genberg, J., Henne, S., Dentener, F., 2011. Better constraints on sources of carbonaceous aerosols using a combined 14C–macro tracer analysis in a european rural background site. Atmos. Chem. Phys. 11, 5685–5700.

Hays, M.D., Smith, N.D., Kinsey, J., Dong, Y., Kariher, P., 2003. Polycyclic aromatic hydrocarbon size distributions in aerosols from appliances of residential wood combustion as determined by direct thermal desorption-GC/MS. J. Aerosol Sci. 34, 1061–1084.

Herich, H., Gianini, M.F.D., Piot, C., Mocnik, G., Jaffrezo, J.L., Besombes, J.L., Prévôt, A.S.H., Hueglin, C., 2014. Overview of the impact of wood burning emissions on carbonaceous aerosols and PM in large parts of the alpine region. Atmos. Environ. 89, 64–75.

Holden, A.S., Sullivan, A.P., Munchak, L.A., Kreidenweis, S.M., Schichtel, B.A., Malm, W.C., Collett Jr., J.L., 2011. Determining contributions of biomass burning and other sources to fine particle contemporary carbon in the Western United States. Atmos. Environ. 45, 1986–1993.

Jedynska, A., Hoek, G., Eeftens, M., Cyrys, J., Keuken, M., Ampe, C., Beelen, R., Cesaroni, G., Forastiere, F., Cirach, M., 2014. Spatial variations of PAH, hopanes/steranes and EC/OC concentrations within and between European study areas. Atmos. Environ. 87, 239–248.

Jia, Y., Fraser, M.P., 2011. Characterization of saccharides in size-fractionated ambient particulate matter and aerosol sources: the contribution of primary biological aerosol particles (PBAPs) and soil to ambient particulate matter. Atmos. Environ. 45, 930–936.

Jones, A.M., Harrison, R.M., 2005. Interpretation of particulate elemental and organic carbon concentrations at rural, urban and kerbside sites. Atmos. Environ. 39, 7114–7126.

Khana, M.B., Masiol, M., Formenton, G., Di Gilio, A., de Gennaro, G., Agostinelli, C., Pavoni, B., 2016. Carbonaceous PM2.5 and secondary organic aerosol across the Veneto region (NE Italy). Sci. Total Environ. 542, 172–181.

Kourtchev, I., Hellebust, S., Bell, J.M., O'Connor, I.P., Healy, R.M., Allanic, A., Healy, D., Wenger, J.C., Sodeau, J.R., 2011. The use of polar organic compounds to estimate the contribution of domestic solid fuel combustion and biogenic sources to ambient levels of organic carbon and PM2.5 in Cork Harbor, Ireland. Sci. Total Environ. 409, 2143–2155.

Li, C.K., Kamens, R.M., 1993. The use of polycyclic aromatic hydrocarbons as source signature in receptor modelling. Atmos. Environ. 27, 523–532.

Lonati, G., Ozgen, S., Giugliano, M., 2007. Primary and secondary carbonaceous species in PM2.5 samples in Milan (Italy). Atmos. Environ. 41, 4599–4610.

Mazzoleni, L.R., Zielinska, B., Moosmüller, H., 2007. Emissions of levoglucosan, methoxy phenols, and organic acids from prescribed burns, laboratory combustion of wildland fuels, and residential wood combustion. Environ. Sci. Technol. 41, 2115–2122.

Medeiros, P.M., Conte, M.H., Weber, J.C., Simoneit, B.R.T., 2006. Sugars as source indicators of biogenic organic carbon in aerosols collected above the Howland experimental Forest, Maine. Atmos. Environ. 40, 1694–1705.

Munchak, L.A., Bret, A., Schichtel, B.A., Sullivan, A.P., Holden, A.S., Kreidenweis, S.M., Malm, W.C., Collett, J.L.J., 2011. Development of wildland fire particulate smoke marker to organic carbon emission ratios for the conterminous United States. Atmos. Environ. 45, 395–403.

Oliveira, C., Pio, C., Alves, C., Evtyugina, M., Santos, P., Goncalves, V., Nunes, T., Silvestre, A.J.D., Palmgren, F., Wahlin, P., Harrad, S., 2007. Seasonal distribution of polar organic compounds in the urban atmosphere of two large cities from the north and south of Europe. Atmos. Environ. 41, 5555–5570.

Oliveira, C., Martins, N., Tavares, J., Pio, C., Cerqueira, M., Matos, M., Silva, H., Oliveira, C., Camões, F., 2011. Size distribution of polycyclic aromatic hydrocarbons in a roadway tunnel in Lisbon, Portugal. Chemosphere 83, 1588–1596.

Orasche, J., Seidel, T., Hartmann, H., Schnelle-Kreis, J., Chow, J.C., Ruppert, H., Zimmermann, R., 2012. Comparison of emissions from wood combustion. part 1: emission factors and characteristics from different small-scale residential heating appliances considering particulate matter and polycyclic aromatic hydrocarbon (PAH)-related toxicological potential of particle-bound organic species. Energy Fuel 26, 6695–6704.

Paglione, M., Saarikoski, Carbone, S., Hillamo, R., Facchini, M.C., Finessi, E., Giulianelli, L., Carbone, C., Fuzzi, S., Moretti, F., Tagliavini, E., Swietlicki, E., Eriksson Stenström, K., Prévôt, A.S.H., Massoli, P., Canaragatna, M., Worsnop, D., Decesari, S., 2014. Primary and secondary biomass burning aerosols determined by proton nuclear magnetic resonance (^{1}H NMR) spectroscopy during the 2008 EUCAARI campaign in the Po Valley (Italy). Atmos. Chem. Phys. 14, 5089–5110.

Perrino, C., Catrambone, M., Dalla Torre, S., Rantica, E., Sargolini, T., Canepari, S., 2014. Seasonal variations in the chemical composition of particulate matter: a case study in the Po valley. Part I: macro-components and mass closure. Environ. Sci. Pollut. Res. 21, 3999–4009.

Perrone, M., Larsen, B., Ferrero, L., Sangiorgi, G., De Gennaro, G., Udisti, R., Zangrando, R., Gambaro, A., Bolzacchini, E., 2012. Sources of high PM2.5 concentrations in Milan, Northern Italy: molecular marker data and CMB modelling. Sci. Total Environ. 414, 343–355.

Perrone, M., Gualtieri, M., Consonni, V., Ferrero, L., Sangiorgi, G., Longhin, E., Ballabio, D., Bolzacchini, E., Camatini, M., 2013. Particle size, chemical composition, seasons of

the year and urban, rural or remote site origins as determinants of biological effects of particulate matter on pulmonary cells. Environ. Pollut. 176, 215–227.

Piazzalunga, A., Belis, C., Bernardoni, V., Cazzuli, O., Fermo, P., Valli, G., Vecchi, R., 2011. Estimates of wood burning contribution to PM by the macro-tracer method using tailored emission factors. Atmos. Environ. 45, 6642–6649.

Piazzalunga, A., Anzano, M., Collina, E., Lasagni, M., Lollobrigida, F., Pannocchia, A., Fermo, P., Pitea, D., 2013. Contribution of wood combustion to PAH and PCDD/F concentrations in two urban sites in Northern Italy. J. Aerosol Sci. 56, 30–40.

Pietrogrande, M.C., Bacco, D., Rossi, M., 2013. Chemical characterization of polar organic markers in aerosols in a local area around Bologna, Italy. Atmos. Environ. 75, 279–286.

Pietrogrande, M.C., Bacco, D., Visentin, M., Ferrari, S., Poluzzi, V., 2014a. Polar organic marker compounds in atmospheric aerosol in the Po valley during the Supersito campaigns-part 1: low molecular weight carboxylic acids in cold seasons. Atmos. Environ. 86, 164–175.

Pietrogrande, M.C., Bacco, D., Visentin, M., Ferrari, S., Casali, P., 2014b. Polar organic marker compounds in atmospheric aerosol in the Po valley during the Supersito campaigns-part 2: seasonal variations of sugars. Atmos. Environ. 97, 215–225.

Pietrogrande, M.C., Perrone, M.G., Sangiorgi, G., Ferrero, L., Bolzacchini, E., 2014c. Data handling of GC/MS signals for characterization of PAH sources in Northern Italy aerosols. Talanta 120, 283–288.

Pietrogrande, M.C., Bacco, D., Ferrari, S., Kaipainen, J., Ricciardelli, I., Riekkola, M.-J., Trentini, A., Visentin, M., 2015. Polar organic marker compounds in atmospheric aerosol in the Po valley during the Supersito campaigns — Part 3: contribution of wood combustion to wintertime atmospheric aerosols in Emilia Romagna region (Northern Italy). Atmos. Environ. 122, 291–305.

Pio, C., Cerqueira, M., Harrison, R.M., Nunes, T., Mirante, F., Alves, C., Oliveira, C., Sanchez de la Campa, A., Artíñano, B., Matos, M., 2011. OC/EC ratio observations in Europe: Re-thinking the approach for apportionment between primary and secondary organic carbon. Atmos. Environ. 45, 6121–6132.

Putaud, J.P., Van Dingenen, R., Alastuey, A., Bauer, H., Birmili, W., Cyrys, J., Flentje, H., Fuzzi, S., Gehrig, R., Hansson, H.C., Harrison, R.M., Herrmann, H., Hitzenberger, R., Hueglin, C., Jones, A.M., Kasper-Giebl, A., Kiss, G., Kousa, A., Kuhlbusch, T.A.J., Loeschau, G., Maenhaut, W., Molnar, A., Moreno, T., Pekkanen, J., Perrino, C., Pitz, M., Puxbaum, H., Querol, X., Rodriguez, S., Salma, I., Schwarz, J., Smolik, J., Schneider, J., Spindler, G., Ten Brink, H., Tursic, J., Viana, M., Wiedensohler, A., Raes, F., 2010. A European aerosol phenomenology-3: physical and chemical characteristics of particulate matter from 60 rural, urban, and kerbside sites across Europe. Atmos. Environ. 44, 1308–1320.

Puxbaum, H., Caseiro, A., Sanchez-Ochoa, A., Kasper-Giebl, A., Claeys, M., Gelencsér, A., Legrand, M., Preunkert, S., Pio, C., 2007. Levoglucosan levels at background sites in Europe for assessing the impact of biomass combustion on the European aerosol background. J. Geophys. Res. Atmos. 112. http://dx.doi.org/10.1029/2006JD008114.

Robert, M.A., VanBergen, S., Kleeman, M.J., Jakober, C.A., 2007. Size and composition distributions of particulate matter emissions: part 1-light duty gasoline vehicles. J. Air Waste Manage. Assoc. 57, 1414–1428.

Rybak, J., Olejniczak, T., 2014. Accumulation of polycyclic aromatic hydrocarbons (PAHs) on the spider webs in the vicinity of road traffic emissions. Environ. Sci. Pollut. Res. 21, 2313–2324.

Saarikoski, S., Timonen, H., Saarnio, K., Aurela, M., Jarvi, L., Keronen, P., Kerminen, V.M., Hilmo, R., 2008. Sources of organic carbon in fine particulate matter in Northern European urban air. Atmos. Chem. Phys. 8, 6281–6295.

Saarikoski, S., Carbone, S., Decesari, S., Giulianelli, L., Angelini, F., Canagaratna, M., Ng, N.L., Trimborn, A., Facchini, M.C., Fuzzi, S., Hillamo, R., Worsnop, D., 2012. Chemical characterization of springtime submicrometer aerosol in Po Valley, Italy. Atmos. Chem. Phys. 12, 8401–8421.

Saarnio, K., Sillanpaa, M., Hillamo, R., Sandell, E., Pennanen, A.S., Salonen, R.A., 2008. Polycyclic aromatic hydrocarbons in size-segregated particulate matter from six urban sites in Europe. Atmos. Environ. 42, 9087–9097.

Sandrini, S., Fuzzi, S., Piazzalunga, A., Prati, P., Bonasoni, P., Cavalli, F., Bove, M.C., Calvello, M., Cappelletti, D., Colombi, C., Contini, D., De Gennaro, G., Di Gilio, A., Fermo, P., Ferrero, L., Gianelle, V., Giugliano, M., Ielpo, P., Lonati, A., Marinoni, A., Massabò, D., Molteni, U., Moroni, B., Pavese, G., Perrino, C., Perrone, M.G., Perrone, M.R., Putaud, J.P., Sargolini, T., Vecchi, R., Gilardoni, S., 2014. Spatial and seasonal variability of carbonaceous aerosol across Italy. Atmos. Environ. 99, 587–598.

Saylor, R.D., Edgerton, E.S., Hartsell, B.E., 2006. Linear regression techniques for use in the EC tracer method of secondary organic aerosol estimation. Atmos. Environ. 40, 7546–7556.

Schmidl, C., Marr, I.L., Caseiro, A., Kotianova, P., Berner, A., Bauer, H., Kasper-Giebl, A., Puxbaum, H., 2008. Chemical characterization of fine particle emissions from wood stove combustion of common woods growing in mid-European Alpine regions. Atmos. Environ. 42, 126–141.

Sillanpää, M., Frey, A., Hillamo, R., Pennanen, A., Salonen, R., 2005. Organic, elemental and inorganic carbon in particulate matter of six urban environments in Europe. Atmos. Chem. Phys. 5, 2869–2879.

Simoneit, B.R.T., Elias, V.O., Kobayashi, M., Kawamura, K., Rushdi, A.I., Medeiros, P.M., Rogge, W.F., Didyk, B.M., 2004. Sugars dominant water-soluble organic compounds in soils and characterization as tracers in atmospheric particulate matter. Environ. Sci. Technol. 38, 5939–5949.

Szidat, S., Jenk, T.M., Synal, H.-A., Kalberer, M., Wacker, L., Hajdas, I., Kasper-Giebl, A., Baltensperger, U., 2006. Contributions of fossil fuel, biomass-burning and biogenic emissions to carbonaceous aerosols in Zurich as traced by 14C. J. Geophys. Res. 111, D07206.

Tobiszewski, M., Namieśnik, J., 2012. PAH diagnostic ratios for the identification of pollution emission sources. Environ. Pollut. 162, 110–119.

Tominaga, S., Matsumoto, K., Kaneyasu, N., Shigihara, A., Katono, K., Igawa, M., 2011. Measurements of particulate sugars at urban and forested suburban sites. Atmos. Environ. 45, 2335–2339.

Tsai, Y.I., Sopajaree, K., Chotruksa, A., Wu, H.C., Kuo, S.S., 2013. Source indicators of biomass burning associated with inorganic salts and carboxylates in dry season ambient aerosol in Chiang Mai Basin, Thailand. Atmos. Environ. 78, 93–104.

Valipour, M.M., Seyyed, M., Valipour, R., Rezaei, E., 2012. Air, water, and soil pollution study in industrial units using environmental flow diagram. J. Basic. Appl. Sci. Res. 2, 12365–12372.

Valipour, M.M., Seyyed, M., Valipour, R., Rezaei, E., 2013. A new approach for environmental crises and its solutions by computer modeling. The 1st international conference on environmental crises and its solutions, Kiseh Island, Iran.

Van Drooge, B., Crusack, M., Reche, C., Mohr, C., Alastuey, A., Querol, X., Prevot, A., Douglas, A., Day, D.A., Jimenez, J.L., Grimalt, J.O., 2012. Molecular marker characterization of the organic composition of submicron aerosols from Mediterranean urban and rural environments under contrasting meteorological conditions. Atmos. Environ. 61, 482–489.

Vassura, I., Venturini, E., Marchetti, S., Piazzalunga, A., Bernardi, E., Fermo, P., Passarini, F., 2014. Markers and influence of open biomass burning on atmospheric particulate size and composition during a major bonfire event. Atmos. Environ. 82, 218–225.

Viana, M., Reche, M., Amato, C., Alastuey, F., Querol, A., Moreno, X., Lucarelli, T., Nava, F., Cazolai, S., Chiari, G., Rico, M., 2013. Evidence of biomass burning aerosols in the Barcelona urban environment during winter time. Atmos. Environ. 72, 81–88.

Vodička, P., Schwarz, J., Cusack, M., Ždímal, V., 2015. Detailed comparison of OC/EC aerosol at an urban and a rural Czech background site during summer and winter. Sci. Total Environ. 518–519, 424–433.

Wang, G., Chen, C., Li, J., Zhou, B., Xie, M., Hu, S., Kawamura, K., Chen, C., 2011. Molecular composition and size distribution of sugars, sugar-alcohols and carboxylic acids in airborne particles during a severe urban haze event caused by wheat straw burning. Atmos. Environ. 40, 2473–2479.

Wingfors, H., Sjödin, Å., Haglund, P., Brorström-Lundén, E., 2001. Characterization and determination of profiles of polycyclic aromatic hydrocarbons in a traffic tunnel in Gothenburg, Sweden. Atmos. Environ. 35, 6361–6369.

Xu, Z., Wen, T., Li, X., Wang, J., Yuesi Wang, Y., 2015. Characteristics of carbonaceous aerosols in Beijing based on two-year observation. Atmos. Poll. Res. 6, 202–208.

Yttri, K., Aas, W., Bjerke, A., Cape, J., Cavalli, F., Ceburnis, D., Dye, C., Emblico, L., Facchini, M.C., Forster, C., Hanssen, J.E., Hansson, H.C., Jennings, S.G., Maenhaut, W., Putaud, J.P., Tørseth, K., 2007. Elemental and organic carbon in PM10: a one year measurement campaign within the European monitoring and evaluation programme EMEP. Atmos. Chem. Phys. 7, 5711–5725.

Yunker, M.B., Macdonald, R.W., Vingarzan, R., R.H., Mitchell, Goyette, D., Sylvestre, S., 2002. PAHs in the Fraser River basin: a critical appraisal of PAH ratios as indicators of PAH source and composition. Org. Geochem. 33, 489–515.